New Applications of Cyclobutadiene Cycloadditions: Diversity and Target Oriented Synthesis

Author: Jason Joseph Marineau

Boston College

The Graduate School of Arts and Sciences

Department of Chemistry

NEW APPLICATIONS OF CYCLOBUTADIENE CYCLOADDITIONS: DIVERSITY AND TARGET ORIENTED SYNTHESIS

a dissertation

by

JASON JOSEPH MARINEAU

submitted in partial fulfillment of the requirements

for the degree of

Doctor of Philosophy

December 2010

New Applications of Cyclobutadiene Cycloadditions: Diversity and Target Oriented Synthesis

Jason J. Marineau

Thesis Advisor: Professor Marc. L. Snapper

Abstract

Cyclobutadiene cycloadditions provide rapid access to rigid polycyclic systems with high strain energy and unusual molecular geometries. Further functionalization of these systems allows entry into unexplored chemical space. A tricarbonylcyclobutadiene iron complex on solid support enables exploration of these cycloadditions in a parallel format amenable to diversity oriented synthesis. Modeling of the cycloaddition transition states with density functional calculations provides a theoretical basis for analysis of the regioselectivity observed in generation of these substituted bicyclo[2.2.0]hexene derivatives.

The high strain energy accessible in cyclobutadiene cycloadducts and their derivatives renders them useful synthons for access to medium-ring natural products through ring expansion. Torilin, a guaiane sesquiterpene isolated from extracts of the fruits of *Torilis japonica*, exhibits a range of biological activities including testosterone 5α-reductase inhibition, hKv1.5 channel blocking, hepatoprotective, anti-inflammatory and anti-cancer effects. These activities are reviewed and analyzed from the perspective of a common biochemical target.

Tandem oxidation and acid-catalyzed rearrangement of a highly strained tetracyclo[5.3.0.$0^{1,5}$.$0^{2,4}$]decane in the presence of tetrapropylammonium

perruthenate provides the bicyclo[5.3.0]decane core of this natural product with complete control of relevant stereochemistry. The complex precursor required for this rearrangement is rapidly accessed by cyclopropanation of an intramolecular cyclobutadiene cycloadduct. Synthetic studies are reported which provide preliminary access to 8-deoxytorilolone.

Acknowledgements

I would like to thank everyone who has supported me on this long journey and made it all possible. I could not have done it without my family and their patience, understanding and encouragement.

I would first and foremost like to thank my wife Sara Marineau. You've been there through everything, enjoyed the highs with me when things were working and pulled me back out of the lows when things failed. You endured the long hours in the lab and were always ready to listen. We make a great team, you and I. You did your best to learn the in's and out's of cyclobutadiene, NMR, cyclopropanation and other things that were barely in English and even proof read a thesis about them. You never stopped believing in me, even when I doubted myself. Thank you so much, I would not have made it here without you. I love you!

To my parents, Sue and Joe Marineau, I obviously would not be where I am today without you. Thank you for teaching me to work hard and always strive for the best. I could not have done it without your patient words of encouragement and constant support.

I'd like to thank the Campbells. Sue, Jerry, Lindsey, Mary. You cared so much about what I was doing and listened to all the stories. Thank you so much for all your prayers and support.

I'd like to thank Marc for some very interesting projects and the freedom to pursue them in the ways I saw fit. I may not have always understood what you

were doing at the time, but in the end I know that my research turned out better because of it. Thank you for the opportunity to grow as a scientist and learn to solve some good problems.

The Snapper lab has been a great place to work and I have made a lot of good friends along the way. It has been a fun and supportive environment in which to do chemistry. I'd like to thank all of the members, past and present who I've been lucky enough to work with. In particular, I'd like to thank Michael Williams for stepping in to share some hood space with me that first year and along with Andy Leyhane, teaching me the ins and outs of the Iron project. To Dave Finnegan, my fellow WPI alum, thanks for all the interesting and wide ranging discussions and for helping to pass down your share of lab lore. I had the pleasure of sharing my time in lab with two other Jasons, Gavenonis and Rodrigo. We certainly had some great times while giving Marc less names to remember. Thanks for all the discussions over coffee and always being there to bounce ideas off. Thanks too for helping proof read this thesis. I'd like to thank Jing He, for generous donations of iron compound to my cause when I was trying to get everything wrapped up and for doing a great job taking on most of the group responsibilities as the remaining senior member. Best of luck, I'm sure you'll do very well! I'd also like to thank two talented undergraduates whom I was fortunate enough to work with, Michael Millonig and Doug Rioux. I had a great time mentoring you guys and all your hard work certainly helped me move the project forward. While perhaps not a group member in the traditional sense, I'd

like to thank Deb Lynch. You were always there with conversation (and candy) and it seems like you could fix just about any non-chemistry problem in the department.

The BC Chemistry Department is a wonderful group of people and a great place to do graduate work. I've made so many friends over the years and always appreciated the collaborative nature of all the groups. It was a rare problem that could not be solved by talking to the right person, and in that case, they were there to commiserate. I'd like to thank Ross Kelly for reading my progress reports over the years, you always had helpful suggestions and I enjoyed those discussions. I also enjoyed getting to teach with you and preparing all the exciting demonstrations. My teaching also would not be where it is today without Christine Goldman. We had the pleasure of teaching together for a number of years and I learned a ton, especially from the excitement and innovation you brought to every class. Getting to help you design and implement a brand new lab class was also one of my best teaching experiences. Finally, I'd like to thank my thesis committee, Dr. Scott, Kian, Jason, Marc, I really appreciate the time you spent working with me on this document and the helpful suggestions and discussions that really made it all come together.

Table of Contents

Chapter 1: Studies on the Biological Activity of Torilin

INTRODUCTION

Figure 1.1: Flowers and Seeds of *Torilis japonica*[1]

Torilin is a guaiane natural product (Figure 1.2) that was first isolated from the widely distributed East Asian biennial plant *Torilis japonica (Figure 1.1)*.[2] The crude extract of this plant's fruits also includes other sesquiterpene components (germacrane, eudesmane, humulene and oppositane) along with flavonoids as major components. This extract has a rich history in Asian folk medicine and is known as *Qie-yi* in China, *Yabujirami* in Japan and *Sa-sang-ja* in Korea. The decoction is usually administered either orally or topically and has been used to

[1] Public Domain Image by Leo Michels. http://www.imagines-plantarum.de accessed via http://luirig.altervista.org/schedeit/pz/torilis_japonica.htm, March 29, 2010.
[2] (a) Nakazaki, M.; Chikamatsu, H.; Maeda, M. *Tetrahedron Lett.* **1966**, *37*, 4499-4504. (b) Chikamatsu, H.; Maeda, M.; Nakazaki, M. *Tetrahedron* **1969**, *25*, 4751-4765.

treat parasite infections such as *Trichomonas vaginalis*, ascariasis, and scabies, skin conditions including carbuncle and pruritus, chronic diarrhea, impotence, and infertility.[3] Torilin and its free-alcohol congener torilolone (Figure 1.2) have also been subsequently isolated from the stems and root bark of *Ulmus davidiana*[4] and the fruit of *Cnidium monnieri*[5], two plants commonly used in similar folk medicines.[6]

Figure 1.2: Guaiane Sesquiterpenes

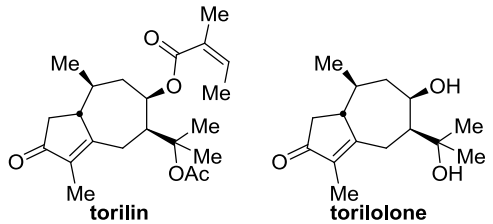

The long history of traditional medical treatments on human patients using these extracts has generated great interest in their biological study. Refinement of the crude preparations and identification of their active constituents holds promise for new herbal therapeutics and potential drug leads with an improved safety profile. Indeed, *Torilis japonica* has appeared as a component in a number of recently reported herbal preparations. “Pana Wang” contains a dose of 30 mg per day of the dried fruits of *Torilis japonica* (2% of the preparation),

---

[3] (a) Sung, C. K.; Kimura, T.; But, Paul, P. H.; Guo, J. X. *International Collation of Traditional and Folk Medicine* 3, **1998**, 101-102. (b) Lee, S. J. *Korean Folk Medicine*, Seoul National University Press, **1966**.

[4] (a) Kim, Y. C.; Lee, M., K.; Sung, S. H; Kim, S. H. *Fitoterapia* **2007**, *78*, 196-199. (b) Choi, Y.; Lee, M. K.; Lim, S. Y.; Sung, S. H.; Kim, Y. C. *British J. Pharmacology* **2009**, *156*, 933-940.

[5] (a) Oh, H.; Kim, J. S.; Song, E. K.; Cho, H.; Kim, D. H.; Park, S. E.; Lee, H. S.; Kim, Y. C. *Planta Med.* **2002**, *68*, 748-749. (b) Kitajima, J.; Suzuki, N.; Satoh, M.; Watanabe, M. *Phytochemistry* **2002**, *59*, 811-815.

[6] *Ulmus davidiana* is used in the Korean medicine Neu-Reup-Na-Mu (see Ref. 3b) and *Cnidium monnieri* in the Chinese medicine She chuang zi (see Ref. 5b).

along with 10 other herbs, and is reported to enhance interferon-γ production and the proliferation of splenic lymphocytes, which may inhibit tumor growth and metastasis and reduce the impact of infectious diseases.[7] The traditional Korean prescription *Paeng-Jo-Yeon-Nyeon-Baek-Ja-In-Hwan* (PJBH) contains 6.3 g (12% of the preparation) of the dried fruits of *Torilis japonica*. This mixture was found to exhibit a reduction of hydroxyl radical induced toxicity in rat pheochromocytoma PC12 cells and an increase in glutathione peroxidase activity. This antioxidant activity is suggested to have neuroprotective applications in Alzheimer's disease treatment.[8] A patented formulation invented by Pangenomics of Korea and involved in human clinical trials includes *Torilis japonica* extract and is reported to reduce inflammation and arthritis symptoms.[9]

Anti-Inflammatory

Primarily as a result of their traditional medical applications, the crude extracts of *Torilis japonica* have also been examined for anti-inflammatory activity *in vitro* and *in vivo*. Torilin has furthermore been isolated from these extracts and shown to be the likely anti-inflammatory component.

---

[7] Tega, E.; Kiga, C.; Chino, A.; Sakurai, H.; Koizumi, K.; Tani,T.; Saiki, I. *Biol. Pharm. Bull.* **2005**, *28*, 1869-1872.
[8] Koo, B. S.; Kim, Y. K.; Park, K. S.; Chung, K. H.; Kim, C. H. *Phytother. Res.* **2004**, *18*, 488-493.
[9] Cho, B. W.; Jin, M.; Jung, H. J.; Shin, S. S.; Kim, S.; Jeon, H.; Oh, J. H.; Eo, H. K.; Kim, B. Crude Drug Compositions for Treating or Preventing Arthritic Diseases and the Preparation Process. U. S. Patent 7,074,435 B2, July 11, 2006.

In a study[10] aimed at developing herbal mixtures to treat skin wrinkles, the water extract of the fruit of *Torilis japonica* were applied to human dermal fibroblast cells. These extracts triggered an increase in procollagen biosynthesis at 5 μg/mL and also displayed a slight decrease in matrix-metalloproteinase activity and some antioxidant effects. The torilin in these extracts was quantified and found to be 0.238 mg/g of dry extract weight.

Lee[11] and co-workers examined the crude extracts of the fruit in rats with carrageenan-induced paw edema. The crude methanol extract displayed a significant decrease in paw swelling at doses of 500 or 1000 mg/kg *p.o.* Further fractionation resulted in a hexane fraction that displayed potent anti-edemateous effects at 237 mg/kg *p.o.* This activity was comparable to that of the non-steroidal anti-inflammatory drug Piroxicam dosed at 9 mg/kg. The hexane fraction further resulted in a 35.2% inhibition of vascular permeability when dosed at 77 mg/kg *p.o.* Comparitively, aspirin resulted in 59.5% inhibition at 200 mg/kg. Finally, the hexane fraction inhibited leukocyte emigration in a carboxymethylcellulose (CMC) air pouch inflammation model and significantly decreased rat's paw swelling in an adjuvant arthritis model at 120 mg/kg *p.o.,* which compared favorably to peroxicam at 4.5 mg/kg *p.o.* Taken together, these results suggest the presence of an anti-inflammatory component in the hexane fraction.

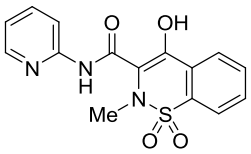

Piroxicam

---

[10] So, S. H.; Lee, S. K.; Hwang, E. I.; Koo, B. S.; Han, G. H.; Kim, N. M. *J. Ginseng. Res.* **2007**, *31*, 196-202.
[11] Lee, E. B.; Kim, S. M.; and Kim, T. H. *Kor. J. Pharmacogn.* **1998**, *29*, 384-390.

Indeed, in a follow-up study,[12] purification of the hexane fraction afforded torilin. The purified compound showed strong anti-edemateous activity in carrageenan induced rats at 90 and 270 mg/kg *p.o.* It also inhibited vascular permeability in mice at doses of 30 mg/kg (27.4%) and 90 mg/kg (36.5%) *p.o.,* performing comparably to aspirin at 200 mg/kg (44.4%), and reduced leukocyte emigration in the CMC pouch assay. These effects are all similar to those of the crude extract and seem to confirm that torilin is responsible for the observed anti-inflammatory effects. Torilin was shown to inhibit acetic acid or phenylquinone-induced writhing syndrome in mice and increase the pain threshold (measured via tail pressure or Randall-Selitto paw pressure methods) at a dose of 90 mg/kg. These effects were demonstrated to be comparable to aminopyrine at a dose of 200 to 250 mg/kg *p.o*. In addition to the anti-inflammatory effects, torilin was demonstrated to have a low acute toxicity with an LD_{50} value of 2000 mg/kg *i.p.* and >5000 mg/kg *p.o.* in male mice. These results suggest that torilin may have potential as an analgesic and anti-inflammatory lead compound.

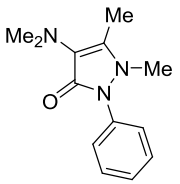

Aminopyrine

Nitric oxide (NO) is an important biological mediator and marker of inflammation that is produced by two types of nitric oxide synthases (NOS). Constitutive NOS produces the low levels of NO that are required by normal biological processes. Inducible NOS produces greater quantities of NO in

---

[12] Lee, E. B.; Cho, S. I.; Kang, S. S.; Kim, K. R.; Kim, T. H. *Kor. J. Pharmacogn.* **1999**, *30*, 137-144.

response to stimuli like lipopolysaccharide (LPS) or proinflammatory cytokines (TNF-α, IL-1β, IFN-γ, etc.). This increase in NO is indicative of inflammation and may also be linked to carcinogenesis.[13] Perhaps owing to the importance of inflammatory processes in human disease, a number of groups have studied the effects of torilin on nitric oxide production.

The crude methanolic extracts of T*orilis japonica* were identified in a screen of medicinal herbs[13] and identified as inhibitors of NO production in RAW 264.7 murine macrophage cells that had been treated with LPS to activate the release of NO. The crude extract was fractionated into hexane, ethyl acetate and butanol and these fractions all retained most of their activity. The hexane fraction performed the best, completely inhibiting NO production at 50 μg/mL and reducing production by 50% at a concentration of 10 μg/mL. Western blot analysis further indicated that the ethyl acetate fraction from *Torilis japonica* reduced the expression of inducible NOS (iNOS) by 20%.

Kim[4a] reported the isolation of torilin from the stem and root bark of the Asian deciduous tree *Ulmus davidiana* along with two oxidized derivatives, 1-hydroxytorilin[14] and another diastereomer that they named 1-hydroxytorilin A[15] (Figure 1.3). These compounds were evaluated for their effects on NO production by LPS stimulated murine microglial BV2 cells as a model of

---

[13] Lee, H. J.; Kim, J. S.; Jin, C.; Ryu, J. H. *Nat. Prod. Sci.* **2005**, *11*, 16-21.
[14] 1-Hydroxytorilin was previously isolated from *Cnidium monieri* in reference 5a.
[15] 1-β-hydroxytorilin (1-hydroxytorilin A) was actually previously reported. Park, H. W.; Choi, S. U.; Baek, N. I.; Kim, S. H.; Eun, J. S.; Yang, J. H.; Kim, D. K. *Arch. Pharm. Res.* **2006**, *29*, 131-134.

neuroinflammation. 1-Hydroxytorilin A was found to be the most active with a 70.4% inhibition of NO production at 10 μM. Torilin and 1-hydroxytorilin were considerably less active at this concentration, producing 53.1% and 36.3% inhibition respectively.

Figure 1.3: Oxygenated Torilin Derivatives

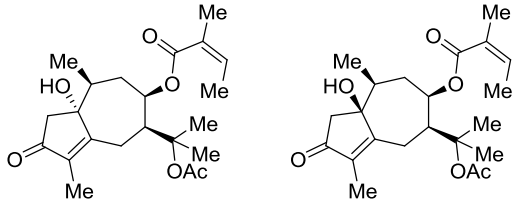

1-hydroxytorilin
(1-α-hydroxytorilin)

1-hydroxytorilin A
(1-β-hydroxytorilin)

COX-1 and constituitive NOS are widely distributed across various tissue types and regulate many important physiological processes. COX-2 and iNOS generate prostaglandins (PG) and NO, respectively during cellular inflammation. Microglia are the immune cells in the central nervous system and are known to secrete IL-1β under neuroinflammatory conditions. This pro-inflammatory cytokine stimulates NO and PG production, which can increase neurodegeneration. Increases in NO and PG levels are also involved with inflammation, pain, arthritis, multiple sclerosis, brain ischemia and cancer. COX-1 and iNOS are transcriptionally regulated and have binding sites for a shared set of transcription factors. These factors include CCAT enhancer binding protein (C/EBP), cyclic AMP-responsive element-binding protein (CREB) and nuclear factor-κB (NF-κB), all of which are involved in LPS and cytokine-based induction of NO and PG production. Activation of iNOS is also

believed to involve the Janus kinase/signal transducer and activator of transcription (JAK/STAT), while PG biosynthesis can involve the mitogen activated protein kinase (MAPK) cascade. These activation pathways and the specific effects of iNOS/COX-2 vary between cell types and environments. [16]

MAPK kinase cascades, of which the Ras/Raf system is exemplary, are important in eliciting cellular response to stimuli and regulating processes such as cell proliferation and differentiation.[17] Many MAPK cascades exist within a cell and each kinase is a single member of a family of related proteins. The general form of such a cascade is shown in Figure 1.4.[18] An environmental stimulus or a signaling molecule, such as a growth factor or cytokine, interacts with a membrane bound receptor. Activation of the receptor can eventually trigger the phosphorylation of a G protein, such as RAS, which activates a mitogen activated protein kinase kinase kinase (MAPKKK), such as Raf. Raf in turn phosphorylates a MAP kinase kinase (MAPKK) such as MAPK/ERK kinase (MEK). MEK activates a MAPK such as the extracellular signal-regulated kinases (ERK-1 and ERK-2). The p38 MAPK is another member of this family that is known to be involved in inflammation.[16] These activated kinases can then move to the nucleus and act upon a number of substrates including transcription factors to exert their effects on gene expression and other cellular processes.

---

[16] Choi, Y.; Lee, M. K.; Lim, S. Y.; Sung, S.H.; Kim, Y. C. *Br. J. Pharmacol.* **2009**, *156*, 933-940.
[17] Karp, G. *Cell and Molecular Biology*, 5th ed.; Wiley, Hoboken, NJ, 2008, pp 638-641.
[18] Figure adapted from Reference 17.

Figure 1.4: Generalized Schematic of MAPK Pathway

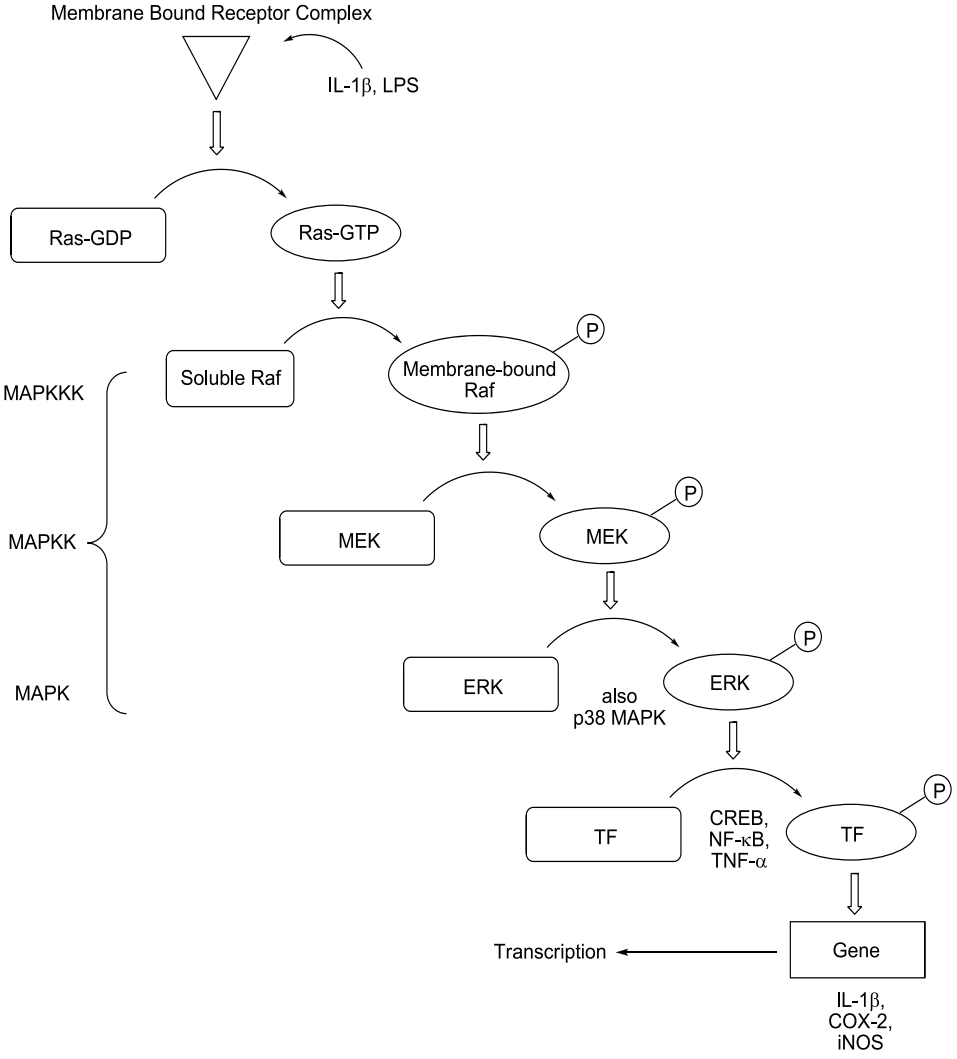

The Kim group further examined the effects of torilin,[16] the major guaiane sesquiterpene constituent of *Ulmus davidiana*, in microglial BV2 cells. They expanded the previous work to include the constitutive cyclooxygenase-1 (COX-1) and proinflammatory COX-2, as well as the cytokine interleukin-1β (IL-1β). Treatment of LPS stimulated microglial BV2 cells with torilin reduced the production of NO concentration-dependantly. Torilin also led to a significant

reduction in the levels of iNOS mRNA, COX-2 mRNA, IL-1β mRNA and iNOS protein, at 10, 30 and 50 μM by RT-PCR and Western blot analysis. At 50 μM the levels return essentially to that of the untreated controls. Expression of IL-1β and COX-mediated production of prostaglandin E_2 (PGE_2) were monitored by ELISA and decreased in a concentration-dependant fashion over the same concentration range with levels matching the control by 50 μM. Torilin treatment restored the degradation of inhibitor of κB-α (IκB-α) to normal levels after treatment with LPS. This would reduce the amount of activated NF-κB and suggests that the anti-inflammatory effects of torilin likely involve the NF-κB pathway. Torilin was shown to reduce observed phosphorylation in the MAPK pathway. Activated P38 MAPK was significantly reduced by 30 and 50 μM of torilin while ERK1 was reduced at 10, 30 and 50 μM. The ultimate substrate of the mitogen- and stress-activated protein kinases-1 (MSK1) pathway (downstream of P38 MAPK and ERK1) is the transcription factor CREB and reduced phosphorylation of CREB was also observed at all concentrations of torilin.

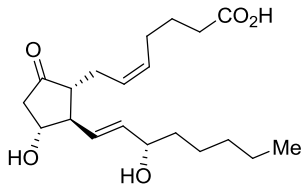

Prostaglandin E_2

Based on these results,[16] it appears that torilin may be inhibiting activation of the p38 MAPK and ERK signaling pathways. Downstream of this inhibition, the activation of NF-κB by this pathway in response to treatment with LPS is reduced, which leads to a decrease in transcriptional activation of iNOS and COX-2 expression. CREB is a transcription factor activated by the p38 MAPK

pathway. It regulates expression of COX-2 and IL-1β and its activation is reduced by treatment with torilin. The cytokine IL-1β is believed to increase NO production by iNOS and to up-regulate COX-2 through a MAPK pathway. Inhibition of IL-1β expression suggests a secondary pathway by which torilin can reduce NO and PG production during the inflammatory response.

Yun[19] and co-workers recently isolated torilin and three new ester congeners (Figure 1.8) through preparative HPLC of the methanol extract of the fruits of *Torilis japonica*. These guaiane esters were tested for inhibition of NO production in LPS-stimulated RAW 264.7 murine microglial cells. Torilin and 11-acetoxy-8-methacryloyl-4-guaien-3-one showed the most potent inhibition of NO production. This suggests that the α,β-unsaturated ester moiety may be important for this activity. As in previous studies,[12,16] no cellular toxicity was observed at the concentrations needed for inhibition of NO production.

---

[19] Lee, I. K.; Lee, J. H.; Hwang, E. I.; Yun, B.S. *Chem. Pharm. Bull.* **2008**, *56*, 1483-1485.

Figure 1.5: 11-acetoxy-4-guaien-3-one Esters

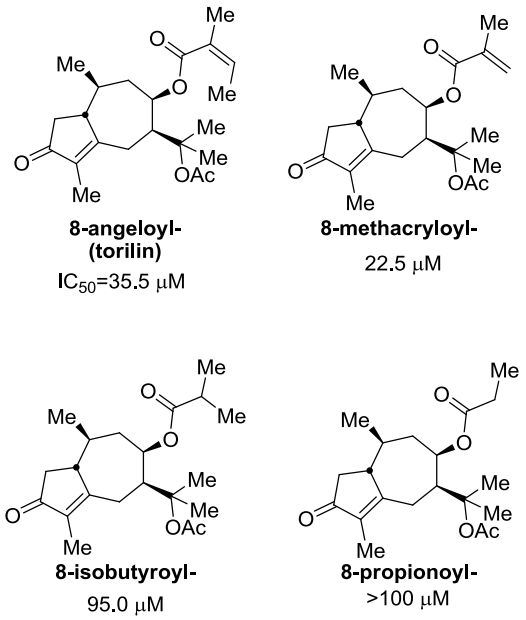

Anti-Cancer Activity

Isolated torilin and the crude extracts of *Torilis japonica* have shown promising anti-cancer activity. This includes reversal of multi-drug resistance (MDR), anti-angiogenic and matrix metalloproteinase 9 (MMP-9) inhibitiory activities. These effects may reduce the metastatic ability of tumor cells.[20]

The Lee group[21] identified the crude methanol extracts of *Torilis japonica* as having strong MDR reversing activity during a screen of 450 medicinal plants. These extracts were applied to human oral epidermoid carcinoma KB-3-1 cells and the KB-V1 vinblastine-resistant cell lines derived from them. The inhibition of

---

[20] Review: Modzelewska, A.; Sur, S.; Kumar, S. K.; Khan, S. R. *Curr. Med. Chem. – Anti-Cancer Agents*, **2005**, *5*, 477-499.
[21] Kim, S. E.; Hwang, B. Y.; Kim, Y. H.; Kim, Y. C, Lee, K. S.; Lee, J. J. *Kor. J. Pharmacogn.* **1997**, *28*, 174-178.

cell growth of these extracts were similar for sensitive (KB-3-1, IC_{50}=38.35 μg/mL) and resistant cells (KB-V1, IC_{50}=30.98 μg/mL) indicating that the effect does not arise from differential toxicity. The IC_{50} for KB-V1 cells in the presence of 100 nM vinblastine sulfate decreased by a factor of 39 in the presence of torilin indicating a reversal of drug resistance.

Figure 1.6: Chemotherapeutic Agents

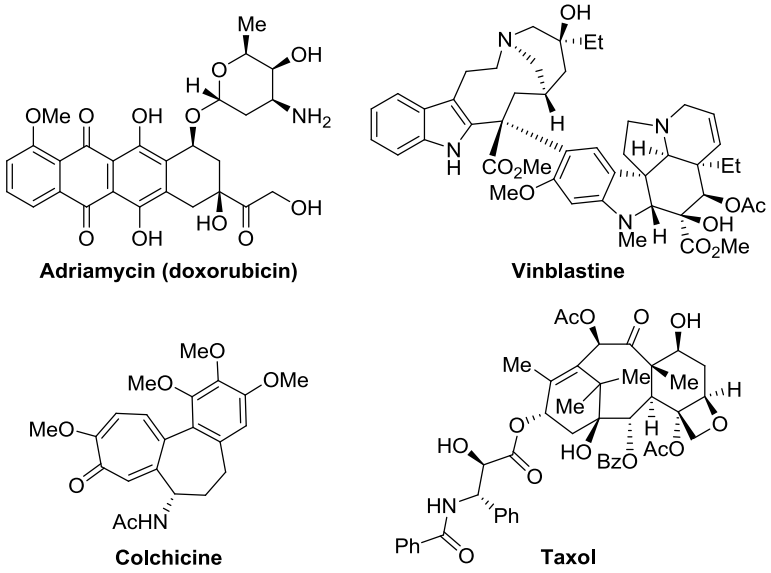

Lee next identified[22] torilin as the active principle in the methanol extract of *Torilis japonica.* In what was the first report of biological activity for torilin, it was tested for MDR reversing activity in KB-3-1 and KB-V1 cell lines as well as in human breast cancer cell line MCF7 and an adriamycin-resistant derivative, the MCF7/ADR line. Torilin was found to be minimally cytotoxic with IC_{50} values between

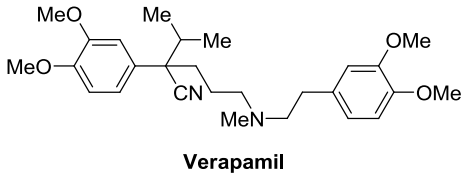

[22] Kim, S. E.; Kim, Y. H.; Kim, Y. C.; Lee, J. J. *Planta Med.* **1998**, *64*, 332-334.

40 and 60 μM for these cell lines. It also showed little effect on the toxicity of these chemotherapeutics (Figure 1.6) to sensitive cell lines. The relative resistance (ratio of IC_{50} in resistant cells to IC_{50} in sensitive cells) to adriamycin (doxorubicin), vinblastine, colchicine and taxol in resistant cell lines (KB-V1, MCF7/ADR) however, decreased in a concentration dependent fashion for torilin concentrations of 0, 3, 10 and 30 μM. As an example (Table 1.1), 10 μM torilin exhibited a strong reversal of MDR which was in most cases, comparable to verapamil (a known MDR reversing agent). The effect was somewhat weaker for adriamycin and colchicine.

Table 1.1: Factor Reduction in Relative Resistance[23]

	Adriamycin	**Vinblastine**	**Colchicine**	**Taxol**
KB-V1				
10 μM torilin	8.3	58.1	6.0	91.5
10 μM verapamil	136.7	74.4	1.4	74.1
MCF7/ADR				
10 μM torilin	8.2	60.6	4.6	61.4
10 μM Verapamil	9.4	19.8	1.1	39.6

Tumor cells can readily mutate to develop MDR, which decreases the effectiveness of cancer chemotherapeutics. This resistance is commonly believed to arise from increased expression of P-glycoprotein in their cell membranes. P-glycoprotein then acts as a drug efflux pump and removes the

[23] Based on Data from Reference 22.

cytotoxic drug from the cell. These pumps tend to have limited specificity and often resistance will develop to multiple chemotherapeutics, even those with unrelated molecular structures. Along with some alkaloids and other drugs, calcium channel blockers, such as verapamil, are known to competitively inhibit P-glycoprotein binding with the chemotherapeutic agents and prevent drug efflux. Toxicity issues, however, have prevented widespread use of many of these compounds.[22] Torilin could provide an important lead for alternative MDR reducing compounds.

In order to further probe the potential utility of torilin in this context, Lee studied the mechanism of MDR reversal by torilin.[24] KB-3-1 and KB-V1 cells were treated with [^{3}H]-vinblastine and the drug accumulation measured based on the radioactivity. The concentration reaches a steady-state in resistant (KB-V1) cells after 4 hours that is 10% of that found in sensitive cells (KB-3-1). KB-3-1 cells retained 60% of the vinblastine after 2 hrs while KB-V1 cells only retained 17% of the initial concentration due to the action of their efflux pumps. When treated with 30 μM torilin, 75% of the vinblastine remained in these resistant cells, a result that is similar to that obtained from treatment with verapamil. This appears to suggest that torilin inhibits the drug efflux pumps in KB-V1 cells. The amount of mdr1 mRNA was measured by Northern blot analysis and found to be unchanged in the presence of torilin indicating that expression of the P-glycoprotein drug efflux pumps (encoded by *mdr1*) is not affected. These

---

[24] Kim, S. E.; Hong, Y. S.; Kim, Y. C.; Lee, J. J. *Planta Med.* **1998**, *64*, 335-338.

pumps depend upon adenosine triphosphate (ATP) and therefore exhibit ATPase activity. In fact, the membrane ATPase activity of the resistant KB-V1 cells is 3.45 fold higher than the sensitive KB-3-1. Both torilin and verapamil exhibit a similar profile, increasing the ATPase activity at concentrations from 0.1 to 100 μM with a decrease at 1000 μM. This behavior is typical of ATPase activators and is shared by daunomycin (structurally similar to adriamycin) and vinblastine, two drugs that are substrates for the MDR drug efflux pumps. From these observations, it is likely that torilin is a competitive inhibitor of P-glycoprotein drug efflux pumps. Lee suggests that comparable hydrophobicity to known MDR drugs (i.e. verapamil) may be responsible for its transport despite the lack of a planar aromatic ring and tertiary amine usually found in this class of molecules.

Kim and co-workers isolated torilin and its oxygenated congeners 1α-hydroxytorilin and 1β-hydroxytorilin (Figure 1.3) from the methanol extract of T*orilis japonica* and measured the cytotoxity of these compounds in a small panel of cancer cell lines.[15] In A549 human lung cancer, SK-OV-3 human ovarian cancer, SK-MEL-2 human skin cancer and HCT15 human colon cancer cell lines, torilin was found to have ED_{50} (50% inhibition of cell growth) values ranging from 5.16 to 14.75 μg/mL. Both diastereomers of 1-hydroxytorilin displayed similar results with ED_{50} values from 14.74 to 42.54 μg/mL. These results can be compared with doxorubicin, which exhibited ED_{50} values from 0.008 to 0.101 μg/mL. As might be expected from a compound generally described to

have minimal toxicity,[12] the cytotoxicity in these cancer cell lines was moderate at best.

Angiogenesis is an important process that must take place to provide sufficient oxygen and nutrients for the growth and metastasis of solid tumors.[25] Hypoxia in the center of these tumors triggers the expression of vascular endothelial growth factor (VEGF) and insulin-like growth factor (IGF-II), which lead to an increase in new blood vessels during tumor angiogenesis. Kim reported[26] the measurement of anti-angiogenic activity for torilin isolated from *Torilis japonica*. Torilin (50 μg/egg) was found to reduce neovascularization of chick eggs induced with basic fibroblast growth factor (bFGF) from 33% to 11% in a chorioallantoic membrane (CAM) assay. This effect was comparable to that of the known anti-angiogenic compound retinoic acid at 1 μg/egg. Importantly, existing vessels were not affected and there was little evidence of egg lethality and no thrombosis or hemorrhage due to malformed vessels.

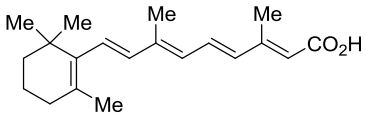

Retinoic Acid

An *in vivo* Matrigel plug assay in mice[26] measured the growth of human umbilical vein endothelial cells (HUVECs) in response to the angiogenic factor bFGF. Torilin (25 μM) was found to inhibit tube formation over 72 hours and the tubes that did form were typically broken, shortened, or thinner. The IC_{50} values

---

[25] Karp, G. *Cell and Molecular Biology*, 5th ed.; Wiley: Hoboken, NJ, 2008, pp 685-686.
[26] Kim, M. S.; Lee, Y. M.; Moon, E. J.; Kim, S. E.; Lee, J. J.; Kim, K. W. *Int. J. Cancer* **2000**, 269-275.

of torilin in HUVECs and bovine aortic endothelial cells (BAECs) were found to be 15 μM and 8 μM, respectively for the inhibition of tube formation.

Cell proliferation was measured[26] for a number of cell lines using a [^{3}H]-methylthymidine incorporation assay. Torilin was found to inhibit HUVEC (and to a similar extent BAEC) proliferation to 27% of the control over 72 hours. Torilin did not, however, inhibit proliferation of other cell lines including NIH3T3, HepG2, HT1080, and Chang liver cells under these conditions. This suggests that torilin may be selective for vascular endothelial cells.

Tumor cells are known to express angiogenic factors such as VEGF and IGF-II and release them into the extracellular medium in response to hypoxia. The concentrated conditioned medium (CCM) from HepG2 (immortalized human hepatoma) cells induced significant angiogenesis as observed in a CAM assay with a small increase seen using medium from cells kept under hypoxic conditions.[26] When the HepG2 cells were treated with 25 μM torilin, the activation of angiogenesis was reduced by 75% for normoxic medium and 67% for hypoxic medium. This suggests that torilin is interfering with the function, production or release of angiogenic factors by tumor cells. In fact, torilin treatment (25 μM) was found to greatly reduce the expression of VEGF and IGF-II mRNA in hypoxic HepG2 cells and even to cause a slight decrease of their expression in normoxic cells. This suggests that the effect of torilin is caused by either direct inhibition of VEGF expression along with IGF-II, or by the regulation

of VEGF expression through upstream inhibition of IGF-II or hypoxia inducible factor-1α (HIF-1α).

Anti-Microbial Activity

Bacterial and parasite infections can cause many practical problems beyond human health. Bacteria, particularly those that form endospores can cause problems with food contamination and spoilage. The endospores are often more stable to the common sterilization conditions than the cells of the food product, and harsh conditions can limit packaging, alter food properties, and risk the generation of toxic byproducts.[27] Parasites (such as protozoa and helminthes) can cause particular problems for agriculture where infected livestock can be costly to treat and there can be a concern of antibiotic resistance and residual traces of drugs in the meat. Chickens, for example, can develop diseases of the digestive tract, such as avian coccidiosis.[28] Both types of infections would be well served by safe, natural antimicrobial agents.

Youn has studied the anti-parasitic potential of *Torilis japonica* extracts. The boiling water extract of the fruits of *Torilis japonica* was evaluated as part of a screen of 15 medicinal herbs.[28] The water extract was found to cause a moderate increase in survival rate of the broiler chicks employed in the study after infection with the bacterium *Eimeria tenella* (a typical cause of coccidiosis),

---

[27] Cho, W. I.; Choi, J. B.; Lee, K.; Cho, S. C.; Park, E. J.; Chung, M. S. *Food Sci. Biotechnol.* **2007**, *16*, 1072-1077.
[28] Youn, H. J.; Noh, J. W. *Vet. Parasitol.* **2001**, *96*, 257-263.

and to decrease the number of excreted oocysts. Treatment with this extract, however, produced little decrease in bloody diarrhea or lesion scores and resulted in an initial decrease in weight gain.

Youn also examined the effects of the ethanol extract of *Torilis japonica* against two other important protozoan parasites.[29] These were *Toxoplasmosa gondii,*[30] which commonly infects cats (toxoplasmosis), but also has detrimental effects in humans (particularly pregnant women and immunocompromised individuals) and the related *Neospora caninum,*[31] which can cause spontaneous abortion in livestock. Growth of these parasites in equine dermal cell culture, was determined by the uptake of [^{3}H]-uracil. The extract inhibited the growth of *T. gondii* by 99.3 to 54% over the concentration range of 156 to 19.5 ng/mL and *N. caninum* by 97.8 to 46.4% at the same concentrations.

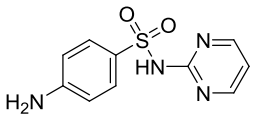

Sulfadiazine

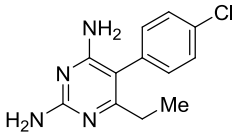

Pyrimethamine

Inhibition was stronger than for pyrimethamine and sulfadiazine (two drugs typically used in conjunction to treat toxoplasmosis) at similar concentrations, and toxicity to the host cells was only observed at concentrations higher than 625 ng/mL.[29a] Youn further investigated this result by purifying the extract by reverse-phase HPLC. The two major fractions both retained some activity, with the least polar fraction being the most active. This fraction inhibited growth of *T. gondii* by

---

[29] (a) Youn, H. J.; Lakritz, J.; Kim, D. Y.; Rottinghaus, G. E.; Marsh, A. E. *Vet. Parasitol.* **2003**, *116*, 7-14. (b) Youn, H. J.; Lakritz, J.; Rottinghaus, G. E.; Seo, H. S.; Kim, D. Y.; Cho, M. H.; Marsh, A. E. *Vet. Parasitol.* **2004**, *125*, 409-414.

[30] Ryan, K. J., Ray, C. G., Eds. *Sherris Medical Microbiology*, 4th ed.; McGraw Hill: New York, 2004; pp. 722-7.

[31] Dubey, J. P. *Int. J. Parasitol.* **1999**, *29*, 1485-1488.

99.2 to 27% over the concentration range of 2.85 to 0.356 ng/mL and *N. caninum* by 98.3 to 30.6% over the same range suggesting that it may contain the active anti-protozoal component.[29b]

Chung[27] investigated the antibacterial activity of the crude ethanol extract of the fruits of *Torilis japonica* against the bacterial endospores of the gram-positive *Bacillus subtilis*. This bacterium is a common food contaminant and while it is not generally considered a human pathogen, it can cause food spoilage. *B. subtilis* endospores are surrounded by a tough peptidoglycan matrix that can prevent the passage of small molecules and makes the bacterium resistant to sterilization by heat or ultraviolet irradiation. A 1% concentration of this extract reduced the number of colony forming units of *B. subtilis* ATCC 6633 by 99.9%, the strongest inhibition of the 79 plant extracts screened. Even a 0.1% concentration was sufficient to inactivate 99% of spores.

Chung[32] further fractionated the crude extract and identified torilin from the hexane fraction as the active antibacterial component. The fruit of *Torilis japonica* afforded 2.68 g torilin from 400 g fruit. At a concentration of 0.1%, torilin reduced the spore count by a factor of ten and the vegetative cells by 5 to 6 orders of magnitude even at a concentration of 50 to 100 ppm. The mechanism of spore inactivation was studied and Chung suggests that torilin may be acting as a surfactant. Analysis of the hydrophilic-lipophilic balance (based on its functional groups) of torilin indicated that its HLB value of 10.5 fell within the

---

[32] Cho, W. I.; Choi, J. B.; Lee, K.; Chung, M. S.; Pyun, Y. R. *J. Food. Sci.* **2008**, *73*, M37-M46.

range (9.6 to 16.7) typically observed for surfactants. As with many terpenoids, torilin may act through denaturization of the bacterial protein coat. Torilin, however, is also active on genetically-modified strains that do not express a spore coat. It is therefore likely that torilin may also be active through a different mechanism, which results in these bactericidal effects once denaturation has allowed the spore coat to be penetrated.

Other Activities

Testosterone 5α-Reductase Inhibition

Testosterone 5α-reductase is a Δ^4-3-oxo-steroid-5α-oxidoreductase that catalyzes the reduction of the male hormone testosterone into the more active androgen 5α-dihydrotestosterone (DHT) (Scheme 1.1). Inhibitors of testosterone 5α-reductase are useful in the treatment of androgen-dependant diseases. These include benign prostate hyperplasia, prostate cancer and alopecia. The inhibitors are usually based on a steroid ring structure, though some non-steroidal inhibiters are known.[33] Many of these have been isolated from natural sources.[34]

---

[33] Park, W. S.; Son, E. D.; Nam, G. W.; Kim, S. H.; Noh, M. S.; Lee, B. G; Jang, I. S.; Kim, S. E.; Lee, J. J.; Lee, C. H. *Planta Med.* **2003**, *69*, 459-461.
[34] Li, Y.; Yang, Y.; Kong, D. *Zhong Cao Yao* **2006**, *37*, 1740-1744.

Scheme 1.1: Action of Testosterone 5α-reductase

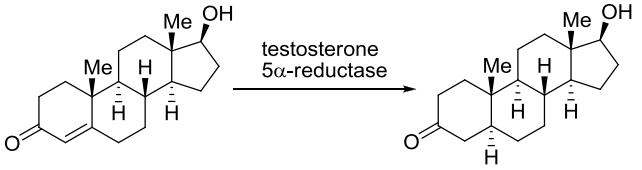

Testosterone **5α-Dihydrotestosterone**

The methanolic extract of the fruits of *Torilis japonica* was found to inhibit testosterone 5α-reductase up to 40% at 25 μg/mL. It also reduced sebum production in a fuzzy rat model. Lee and co-workers[33] then purified the extract and identified torilin as the active component. Torilin displayed dose-dependent inhibition of testosterone 5α-reductase with an IC_{50} value of 31.7 μM. Various inhibitors were compared with torilin (Figure 1.7) to determine some basic structure-activity relationship (SAR). Torilin was found to be more potent than the known acyclic inhibitor α-linoleic acid, but was not as potent as the aza-steroid finasteride. The guaiane structure was found to be an important component for activity, as the less substituted compound guaiol retained some potency. The fully unsaturated guaiane skeleton in guaiazulene, however, showed a further reduction and azulene was inactive. The previously reported inhibitor epigallocatechin 3-gallate (ECGC) was also shown to be inactive in this assay.

Figure 1.7: Testosterone 5α-reductase Inhibitors

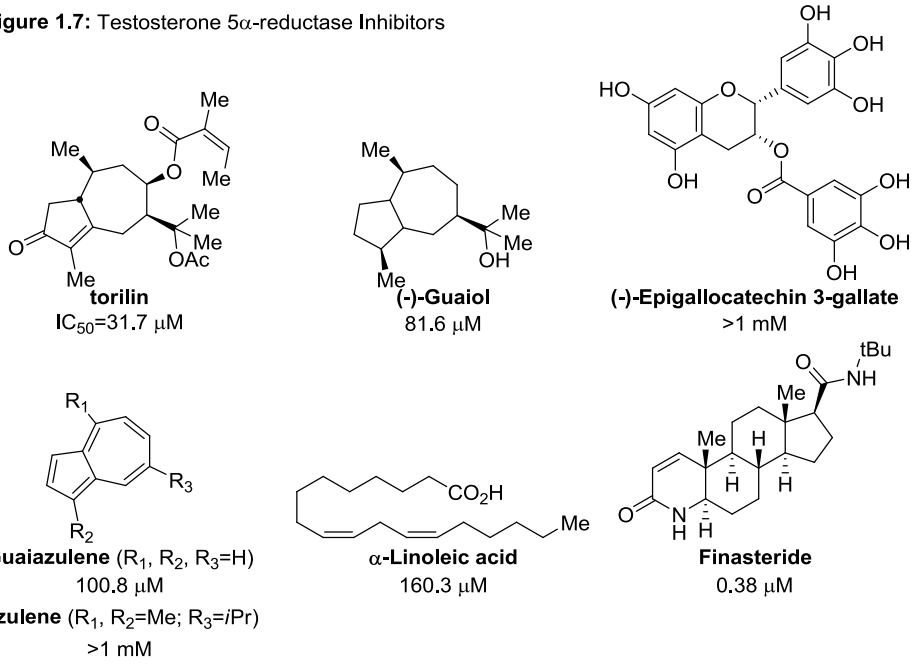

Lee[33] rationalizes this pattern by suggesting that the bulky, non-polar acetate and angelate esters of torilin may act as a substitute for the C and D rings of testosterone. They also likely provide similar contacts to the bulky *tert*-butyl amide of finasteride. The ketone and unsaturation in the 5-membered ring combine to mimic the A ring of the steroid much like the unsaturated amide in finasteride. Torilin may represent a new non-steroidal lead structure for the development of testosterone 5α-reductase inhibitors. (Figure 1.8)

Figure 1.8: B3LYP/6-31G* Geometries for Torilin and Testosterone[35]

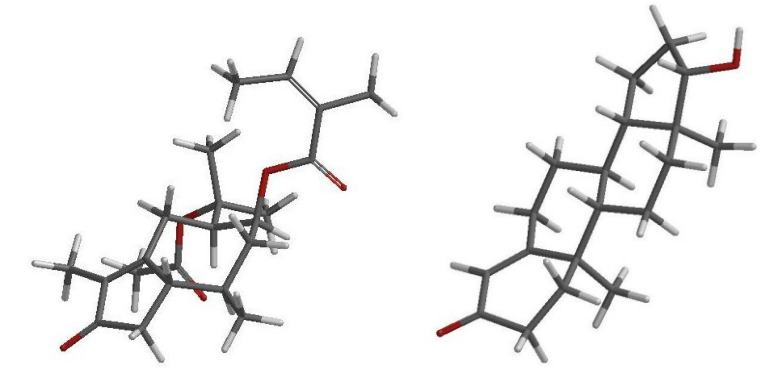

Torilin **Testosterone**

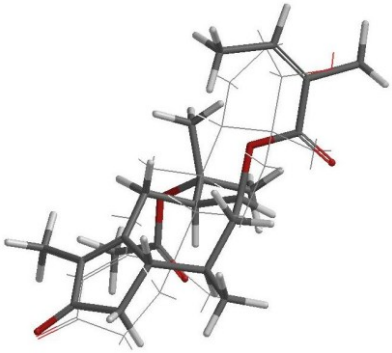

Overlaid Geometries

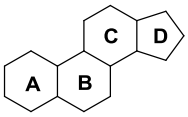

Steroid Ring-System

[35] Gas-phase equilibrium geometries calculated and images generated using Spartan '04, Wavefuntion, Inc. Irvine, CA. as described in Kong, J.; White, C. A.; Krylov, A. I.; Sherrill, C. D.; Adamson, R. D.; Furlani, T. R.; Lee, M. S.; Lee, A. M.; Gwaltney, S. R.; Adams, T. R.; Ochsenfeld, C.; Gilbert, A. T. B.; Kedziora, G. S.; Rassolov, V. A.; Maurice, D. R.; Nair, N.; Shao, Y.; Besley, N. A.; Maslen, P. E.; Dombroski, J. P.; Daschel, H.; Zhang, W.; Korambath, P. P.; Baker, J.; Byrd, E. F. C.; Van Voorhis, T.; Oumi, M.; Hirata, S.; Hsu, C.-P.; Ishikawa, N.; Florian, J.; Warshel, A.; Johnson, B. G.; Gill, P. M. W.; Head-Gordon, M.; Pople, J. A. *J. Computational Chem.*, **2000**, *21*, 1532-1548.

Hepatoprotective Activity

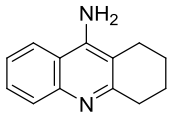

Tacrine

Tacrine is an acetylcholinesterase inhibitor with potential as an Alzheimer's disease treatment. Tacrine causes reversible hepatotoxicity in 30-50% of patients at therapeutic doses, which decreases its clinical utility. The crude ethanolic extract of *Cnidium monnieri* was found to inhibit toxicity at 254 μg/mL. This prompted Kim[5a] and co-workers to purify the active components from this extract. They isolated three guaiane natural products, torilin, torilolone, and 1α-hydroxytorilin. Torilin was moderately effective (EC_{50}=20.5 μM) at protecting Hep G2 cells from tacrine-induced toxicity and torilolone proved even more active (3.6 μM). 1α-hydroxytorilin showed no hepatoprotective properties in this assay. In the absence of tacrine, torilin and torilolone displayed no cytotoxicity over the concentration range from 1-100 μM.

hKv1.5 Channel Blockade

Voltage–gated potassium ion channels are important trans-membrane pores that modulate cellular potential gradients and are present in most cell types. The delayed rectifier K^+ channel hKv1.5 is a cardiac-specific isoform that is important in determining the length of the cardiac action potential and is therefore a potential antiarrhythmic target. Blocking this channel results in a prolongation

of the action potential. The Eun group[36] isolated torilin from *Torilis japonica* and studied its effects on hKv1.5 channels expressed in mouse Ltk cells. Torilin blocks this channel at +60 mV with an IC_{50} value of 2.51 μM. The kinetics of the channel blockade were determined. Torilin causes rapid decline of the hKv1.5 current during depolarization and delays the deactivating current, causing a tail crossover of the pulses. The effects were found to be dose, voltage and use dependant. This pattern suggests that torilin binds to the open hKv1.5 channel and is typical of that found in antiarrythmic drugs for atrial fibrillation.

Inhibition of Melanin Production

Melanin refers to a class of tyrosine-based pigments that determine the color of human skin. They are synthesized in cells called melanocytes and transferred to the keratinocytes. This process can be activated by α–melanocyte stimulating hormone (α-MSH), which binds to a G protein-coupled receptor (GPCR) called the melanocortin 1 receptor (MC1R). This transmembrane receptor activates adenylate cyclase to increase the production of cAMP. This, in turn, continues the cascade by activating tyrosinase to increase melanin biosynthesis. Increased activation of MC1R is implicated in McCune-Albright syndrome in which it causes hyperpigmented patches on the skin.

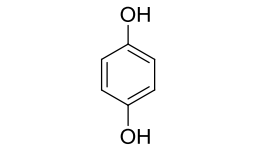

Hydroquinone

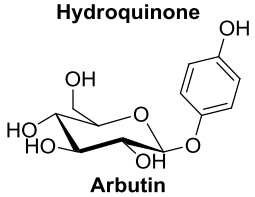

Arbutin

[36] Kwak, Y. G.; Kim, D. K.; Ma, T. Z.; Park, S. A.; Park, H.; Jung, Y. H.; Yoo, D. J.; Eun, J. S. *Arch. Pharm. Res.* **2006**, *29*, 834-839.

Excess melanin accumulation is also responsible for melasma, freckles and senile lentigines. Treatment of these conditions typically involves administration of tyrosinase inhibitors like arbutin or hydroquinone.[37]

Kim[37] recently discovered that the crude methanolic extract of *Torilis japonica* inhibited melanin production in α–MSH activated B16 murine melanoma cells by 64% at 50 μg/mL compared to 55% for arbutin at the same concentration. The ethyl acetate fraction of this extract displayed increased inhibition of 79% compared with just 7% for the aqueous layer. The extract was purified by bioassay-guided fractionation to afford torilin, which was identified as the active component. Torilin inhibited melanin production in a dose-dependant manner between 10 μM and 40 μM with an IC_{50} value of 25 μM. In comparison, arbutin, a known skin-whitening agent,

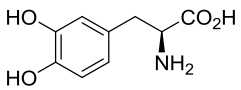

***L*-DOPA**

inhibits melanin production with an IC_{50} value of 170 μM. Treatment with torilin at these concentrations did not cause any cytotoxicity. Western blot analysis further indicated that torilin down-regulated the α–MSH induced levels of tyrosinase. Torilin was not, however, found to inhibit the DOPA oxidation activity of tyrosinase directly and therefore does not share the same mechanism as arbutin.

---

[37] Yun, C. Y.; Kim, D.; Lee, W. H.; Park, Y. M.; Lee, S. H.; Na, M.; Jahng, Y.; Hwang, B. Y.; Lee, M. K.; Han, S. B.; Kim, Y. *Planta Med.* **2009**, *75*, 1505-1508.

CONCLUSIONS

Given the long history of *Torilis japonica* in traditional medicine, it is not surprising that this material should be found to contain bioactive natural products. Indeed, inspired by these folk medicine practices, a number of researchers have found useful pharmacological activity in its crude extracts. Purification of these extracts has often resulted in the identification of torilin as the active principle. This guaiane sesquiterpene and its congeners display a number of promising activities including anti-inflammatory, antimicrobial and anti-cancer among others. They have also been isolated from other medicinal plants including *Cnidium monnieri* and *Ulmus davidiana* suggesting a phytochemical link between these traditional medicines.

Torilin may provide a promising lead compound in a number of therapeutic areas. It has very low reported toxicity in a number of cell lines and animal models. It displays low micromolar activities in a number of *in vitro* assays including those for important inflammation markers and processes related to the cancer growth and metastasis. The molecular properties of torilin (molecular weight, Log P[38], etc.) are typical of those for an orally bioavailable drug with a favorable pharmacokinetic profile.[39]

---

[38] Calculated Log P values were generated with Advanced Chemistry Development ACD/Labs Software V9.04 ©1994-2010 (ACD/Labs)

[39] Lipinski, C. A.; Lombardo, F.; Dominy, B. W.; Feeney, P. J. *Adv. Drug Delivery Rev.* **1997**, *23*, 3-25.

Figure 1.9: "Rule of Five" Properties

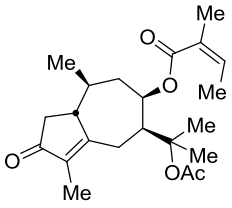

torilin

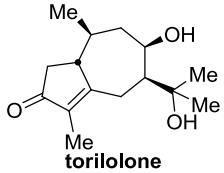

torilolone

	torilin	torilolone
Molecular Weight:	376.49	252.35
Log P:	4.23	0.85
Hydrogen Bond Donors:	0	2
Hydrogen Bond Acceptors:	5	3

It is likely that the apparently disparate activities reported for torilin could be rationalized and potentially optimized through further study and the synthesis of appropriate analogs. Its hydrophobicity and geometric similarity with the steroid ring system along with its reported antimicrobial surfactant activity suggest that torilin could be cell permeable and may be membrane localized. Many of the suggested mechanisms of inhibition involve the action of G protein coupled receptors[40] and other membrane-bound proteins including ion channels, testosterone 5α-reductase and P-glycoprotein. Activation of tyrosinase for the production of melanin relies on α–MSH binding to a GPCR. Activation of the ERK/MAPK also requires activation of a G protein such as Ras. Inhibition of this pathway reduces the activation of the cell signaling molecule NF-κB as part of its anti-inflammatory mechanism. NF-κB is known to be activated in certain tumors that over express VEGF,[41] which suggests the MAPK pathway as a potential link between the anti-inflammatory and anti-angiogenic activities of torilin. It is

---

[40] Karp, G. *Cell and Molecular Biology*, 5th ed.; Wiley: Hoboken, NJ, 2008, pp 620-621.
[41] Bancroft, C. C.; Chen, Z.; Yeh, J.; Sunwoo, J. B.; Yeh, N. T.; Jackson, S.; Jackson, C.; Van Waes, C. *Int. J. Cancer.* **2002**, *99*, 538-548.

possible that torilin is binding to one or more GPCRs and either blocking their activation or the binding of the G-protein. Further study into the specific cellular targets of torilin may make it possible to take advantage of the therapeutic potential described by these reports.

Chapter 2: Cycloadditions of Solid-Supported Cyclobutadiene

Introduction

General Introduction

The generation of chemical diversity is an important concept in such fields as materials science, catalysis and medicinal chemistry. As new reactions and technologies are developed, untapped regions of chemical space can be explored in the quest for a desired set of properties.[42] Particularly in medicinal chemistry, unusual presentations of hydrogen bond donors and acceptors can access novel pharmacophores and provide the opportunity to discover new drugs and useful biological tools. As an example of the power of this concept, a recent successful diversity-oriented synthesis campaign resulted in the synthesis of emmacin, a new lead compound that displays activity against methicillin-resistant *Staphylococcus aureus*.[43]

Molecular transformations that form multiple bonds in a single operation allow the rapid generation of molecular complexity. If such transformations can occur between wide ranges of reactive partners, there is the potential to generate diversity and produce chemical libraries. Cycloadditions are one class of

---

[42] (a) Schreiber, S. L. *Science* **2000**, *287*, 1964-1969. (b) Lipinski, C.; Hopkins, A. *Nature*, **2004**, *432*, 855-861.
[43] (a) Wyatt, E. E.; Galloway, W. R. J. D.; Thomas, G, L.; Welch, M; Loiseleur, O.; Plowright, A. T.; Spring, D. R. *Chem. Commun.* **2008**, 4962-4964. (b) Galloway, W. R. J. D.; Bender, A.; Welch, M.; Spring, D. R. *Chem. Commun.* **2009**, 2446-2448.

reactions that have proven to be a versatile means of generating diverse cyclic molecular skeletons.[44]

One popular technology used in the generation of combinatorial libraries is solid phase organic synthesis (SPOS).[45] Since the compound of interest is tethered to a polystyrene bead, this technique allows for rapid purification of intermediates during a synthetic sequence. This technique allows multi-step synthetic procedures to be more easily carried out in parallel. The advent of tagging technologies to track individual beads that carry a unique chemical structure has allowed for the rapid generation of diversity through combinatorial split-pool synthesis.[46]

Background

Cyclobutadiene, with its antiaromatic four electron π-system has long been studied for theoretical insight.[47] The discovery of its stable iron tricarbonyl complex by Pettit[48] made it available as a reagent for the synthetic chemist. This laboratory has contributed to the development of synthetic methodologies utilizing the cyclobutenes generated upon oxidative degradation of these

---

[44] Review: Yli-Kauhaluoma, J. *Tetrahedron* **2001**, *57*, 7053-7071.
[45] Gordon, E. M.; Barrett, R. W.; Dower, W. J.; Fodor, S. P. A.; Gallop, M. A. *J. Med. Chem.* **1994**, *37*, 1385-1401.
[46] Swartz, M. E. "*Analytical Techniques in Combinatorial Chemistry*" **2000**, *Deker*, New York.
[47] Review: Seyferth, D. *Organometallics*, **2003**, *22*, 2-20.
[48] (a) Emerson, G. F.; Watts, L.; Pettit, R. *J. Am. Chem. Soc.,* **1965**, *87*, 131-133. (b) Review: Efraty, A. *Chem. Rev.* **1977**, *77*, 691-744.

complexes.[49] These methodologies have been applied in the synthesis of medium-ring containing natural products.[50] These routes have relied on the use of tethered dienes and dienophiles for intramolecular cycloadditions. Previous studies exploring the synthetic utility[51] of intermolecular cyclobutadiene cycloadditions have involved the synthesis of cubane,[52] ladderane-type cyclobutadiene oligomers[53] and other theoretically interesting molecules.[54]

Interestingly, polystyrene supports were important in the early studies on the nature of these cyclobutadiene complexes as part of Rebek's three-phase test.[55] A cyclobutadiene complex was coordinated through iron to a polystyrene bound phenanthroline ligand and upon oxidative decomplexation, cyclobutadiene

---

[49] (a) Tallarico, J. A.; Randall, M. L.; Snapper, M. L. *J. Am. Chem. Soc.* **1996,** *118*, 9196-9197. (b) Limanto, J.; Snapper, M. L. *J. Org. Chem.* **1998**, *63*, 6440-6441. (c) Randall, M. L.; Lo, P. C-K.; Bonitatebus, P. J; Snapper, M. L. *J. Am. Chem. Soc.* **1999**, *121*, 4534-4535. (c) Limanto, J.; Tallarico, J. A.; Porter, J. R; Khuong, K. S.; Houk, K. N.; Snapper, M. L. *J. Am. Chem. Soc.* **2002**, *124*, 14748-14758. (d) Deak, H. L.; Stokes, S. S.; Snapper, M. L. *J. Am. Chem. Soc.* **2001**, *123*, 5152-5153. (e) Lo, P. C-K.; Snapper, M. L. *Org. Lett.* **2001**, *3*, 2819-2821. (f) Limanto, J.; Khuong, K. S.; Houk, K. N.; Snapper, M. L. *J. Am. Chem. Soc.* **2003**, *125*, 16310-16321. (g) Seigal, B. A.; An, M. H.; Snapper, M. L.; *Angew. Chem. Int. Ed.* **2005**, *44*, 4929-4932. (h) Bader, S. J.; Snapper, M. L. *J. Am. Chem. Soc.* **2005**, *127*, 1201-1205. (i) Deak, H. L.; Williams, M. J.; Snapper, M. L. *Org. Lett.* ***2005,*** 7, 5785-5788. (j) Leyhane, A. J.; Snapper, M. L. *Org. Lett.* **2006**, *8*, 5183-5186.

[50] (a) Limanto, J.; Snapper, M. L. *J. Am. Chem. Soc.* **2000**, *122*, 8071-8072. (b) Williams, M. J.; Deak, H. L.; Snapper, M. L. *J. Am. Chem. Soc.* **2007**, *129*, 486-487.

[51] Intermolecular trapping experiments have also appeared in mechanistic studies: (a) Watts, L.; Fitzpatrick, J. D.; Pettit, R. *J. Am. Chem. Soc.* **1966**, *88*, 624-625. (b) Reeves, P.; Henery, J.; Pettit, R. *J. Am. Chem. Soc.* **1969**, *91*, 5888-5890. (c) Reeves, P.; Devon, T.; Pettit, R. *J. Am. Chem. Soc.* **1969**, *91*, 5890-5891. see also references 55 and 56.

[52] Barborak, J. C.; Watts, L.; Pettit, R. *J. Am. Chem. Soc.* **1966**, *88*, 1328.

[53] (a) Martin, H-D.; Hekman, M. *Tetrahedron Lett.* **1978**, 1183-1186. (b) Mehta, G.; Viswanath, M. B.; Sastry, G. N.; Jemmis, E. D.; Reddy, D. S. K.; Kunwar, A. C. *Angew. Chem. Int. Ed. Engl.* **1992**, *31*, 1488-1490. (c) Warrener, R. N.; Abbenante, G.; Kennard, C. H. L. *J. Am. Chem. Soc.* **1994**, *116*, 3645-3646. (d) Mehta, G.; Viswanath, M. B.; Kunwar, A. C. *J. Org. Chem*. **1994**, *59*, 6131-6132. (e) Fox, M. A.; Li, W. *J. Am. Chem. Soc.* **1996**, *118*, 11752-11758.

[54](a) Paquette, L. A.; Leichter, L. M. *J. Am. Chem. Soc.* **1971**, *93*, 5128-5136. (b) Paquette, L. A.; Stowell, J. C. *J. Am. Chem. Soc.* **1971,** *93*, 5735-5740. (c) Miki, S.; Kobayashi, O.; Kagawa, H.; Yoshida, Z.; Nakatsuji, H. *Chem. Lett.* **1992**, *21*, 65-68.

[55] (a) Rebek, J.; Gaviña, F. *J. Am. Chem. Soc.* **1974**, *96*, 7112-7114. (b) Rebek, J.; Gaviña, F. *J. Am. Chem. Soc.* **1975**, *97*, 3453-3456.

was shown to pass into solution and react with a solid supported dienophile. This information, along with stereochemical experiments by Grubbs and Schmidt,[56] was used to show that cyclobutadiene must exist in solution free of the iron complex during these cycloadditions.

A solid supported cyclobutadiene methodology promises to simplify separation of the intermolecular cyclobutadiene cycloadducts from the oxidants and excess dienophile, as well as facilitating multi-step sequences to generate daughter libraries. A solid support should also help to slow dimerization of the liberated cyclobutadiene.

Scheme 2.1: Solid Supported Cyclobutadiene Cycloaddition

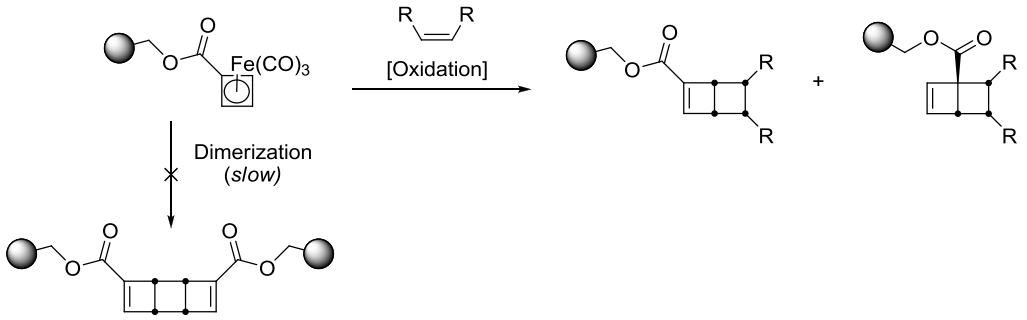

The cycloadducts generated from these reactions possess multiple strained cyclobutane rings in a stereochemically well-defined, rigid skeleton. This enables access to unusual, compact molecular geometries for the presentation of heteroatom functionalities. Such compounds may therefore

[56] (a) Grubbs, R. H.; Grey, R. A. *J. Am. Chem. Soc.* **1973**, *95*, 5765-5767. (b) Schmidt, E. K. G. *Chem. Ber.* **1975,** *108, 1599*. (c) Schmidt, E. K. G. *Chem. Ber.* **1975,** *108, 1609*. (d) Schmidt, E. K. G. *Angew. Chem. Int. Ed.* **1973**, *12*, 777-778.

display interesting biological activities and useful metabolic properties and thereby provide leads for new drug-like molecules and biological tools.[57]

RESULTS AND DISCUSSION

Preparation of Iron Cyclobutadiene Functionalized Polystyrene

Tethering of the cyclobutadieneiron tricarbonyl complex to a polystyrene support limits the dimerization of the free cyclobutadiene and provides convenient reaction monitoring via the infrared absorptions of the carbonyl ligands. The commercially available Wang Resin[58] was chosen due to the acid lability of its benzyl alcohol tether. This tether was esterified with the previously reported (cyclobutadienecarboxylic acid)iron tricarbonyl complex **2.2**[59] to provide the solid-supported cyclobutadiene ester **2.3** in good yield.[60]

Scheme 2.2: Preparation of Solid-Supported Cyclobutdiene Complex **2.3**

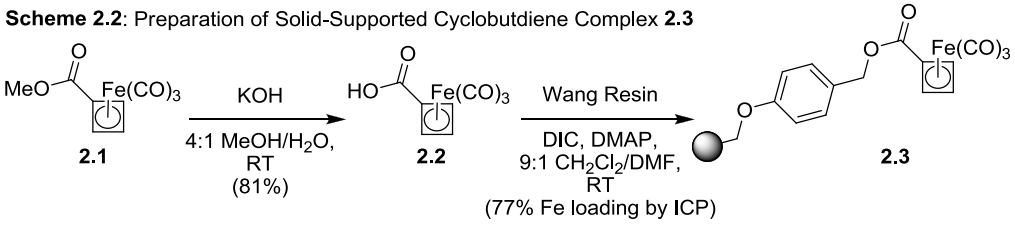

---

[57] Schreiber, S. L., *Chem. & Eng. News*, March 3, 2003, 51-61.
[58] Wang, S.-S. *J. Am. Chem. Soc.* **1973**, *95*, 1328-1333.
[59] Agar, J.; Kaplan, F.; Roberts, B. W. *J. Org. Chem*. **1974**, *39*, 3451-3452.
[60] Iron content of the polystyrene resin was determined by atomic emission spectroscopy using an inductively coupled plasma instrument and found to be 77% of the theoretically predicted value.

Intermolecular Cycloadditions

With the cyclobutadieneiron tricarbonyl functionalized polystyrene resin in hand, its cycloaddition chemistry could be explored. Symmetrically-substituted dienophiles were chosen to limit the formation of regioisomeric products. A range of dienophiles were examined to provide diverse functionalization and to test the impact of sterics on the course of the reaction.

Solution Phase Cycloadditions

As a point of comparison for the new methodology, the reactions were examined in typical solution phase conditions (Table 2.1). Solution phase yields were generally moderate to good with the exception of entries 3 and 7. In entry 3, the desired maleic anhydride adduct was not isolated under any attempted workup conditions. This was likely due to the aqueous solubility of the compound and potential sensitivity of the anhydride products. In entry 7, only a mixture of cyclobutadiene dimers (tricyclooctadiene diesters) was isolated, likely indicating that the more hindered dienophile could not efficiently approach the cyclobutadiene.

The cycloadducts were isolated as mixtures of two regioisomers in which the methyl ester was either present at the bridgehead of the bicyclic system or in conjugation with the olefin of the cyclobutene. In almost all cases, the conjugated regioisomer formed preferentially except for the cycloaddition with N-phenylmaleimide in entry 5, which showed no regioselectivity.

Table 2.1: Solution Phase Cycloadditions

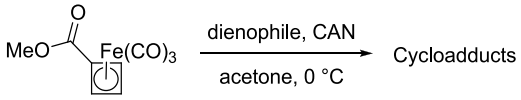

2.1

Entry	Dienophile	Cycloadducts A	Cycloadducts B	Yield (Ratio A:B)
(1)	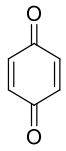	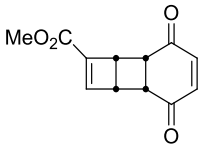	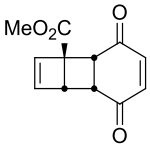	59% (2.5:1)
(2)	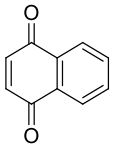	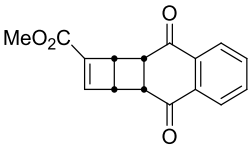	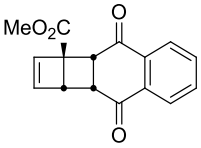	93% (1.9:1)
(3)	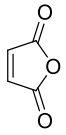	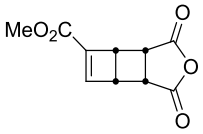	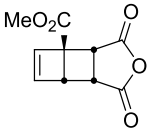	-[a]
(4)	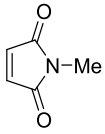	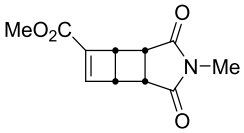	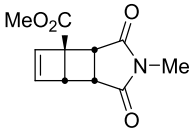	63% (2.9:1)
(5)	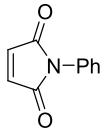	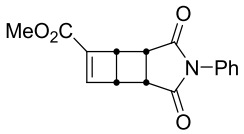	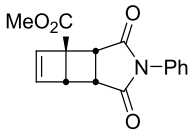	56% (1:1)
(6)	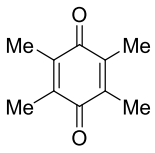	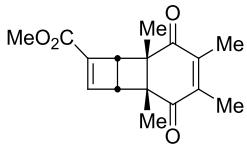	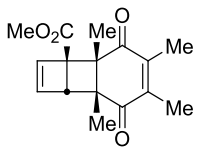	98% (4.3:1)
(7)	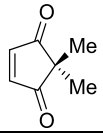	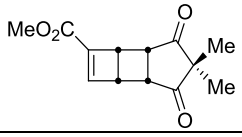	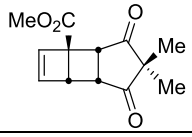	0% cyclobutadiene dimers (14%)

[a] Desired products were observed by crude ^{1}H-NMR, but could not be isolated free from cerium and iron salts even after esterification using $TMSCHN_2$.

Solid-Supported Cycloadditions

Cyclobutadieneiron tricarbonyl functionalized resin **3** was oxidized with ceric ammonium nitrate in the presence of excess dienophile (Table 2.2). Trimethylamine N-oxide was also examined as an oxidant, but the resin proved unstable to these conditions. The cycloadducts were then cleaved from the solid-support under standard acidic conditions. The crude cyclobutene carboxylic acids proved difficult to purify and were instead esterified directly using trimethylsilyldiazomethane.[61]

For each reaction, a pair of regioisomeric cycloadducts was isolated in low to moderate overall yield. The yields are likely lowered as they encompass not only the cycloaddition, but the overall four step sequence beginning with functionalization of the Wang resin. The ratios of regioisomers differed from those obtained in the analogous solution phase reactions. The same general trend existed favoring the conjugated esters; however, in general, the selectivities were not as high. Entries 3 and 5 provided an apparent reversal of selectivity to favor the bridgehead ester. Although the yield in entry 3 is low, it is important to note that this compound could not be isolated in the solution phase reaction. In entry 7 the desired product was again not observed for the sterically encumbered dienophiles. Also, as expected for the solid support,[62] no

---

[61] Aoyama, T.; Shioiri, T. *Chem. Pharm. Bull.* **1981**, *29*, 3249-3255.

[62] Immobilization of benzyne on polystyrene has been shown to prevent dimerization and prolong the lifetime of this reactive intermediate. Jayalekshmy, P.; Mazur, S. *J. Am. Chem. Soc.* **1976**, *98*, 6710-6711. For reactions not approaching the limit of diffusion control, however, the reactive

cyclobutadiene dimers were isolated in a control experiment in which the resin was oxidized in the absence of dienophile. Attempted trapping of the cyclobutadiene after completion of the oxidation proved inconclusive. Oxidation of the resin in an inert atmosphere, followed by addition of a solution of benzoquinone provided the expected cycloadducts along with (Methylcyclobutadienoate)iron tricarbonyl indicating that the rate of oxidation had been reduced. The reaction had not proceeded to completion in the usual time and was still occurring during addition of the dienophile.[63] To rule out this possibility, the oxidation was conducted in a Schlenk filter and the resin was washed with degassed acetone to remove the oxidant and stop the reaction.[64] Subsequent addition of benzoquinone solution, followed by standard work up and isolation afforded no cycloadducts. However, the low-resolution mass spectrum of the crude reaction mixture did indicate the presence of a molecular ion at 219.19 which might indicate the presence of this species in trace amounts. Given the time required (2 hours) for the oxidation and washing steps, it is still possible that the resin lengthens the lifetime of cyclobutadiene; however, it is

---

sites have been shown to interact. Scott, L. T.; Rebek, J.; Ovsyanko, L.; Sims, C. L. *J. Am. Chem. Soc.* **1976**, *99*, 625-626.

[63] The FT-IR spectrum of the KBr pellet of a sample of beads removed before addition of the dienophile also indicated the presence of the carbonyl absorbance bands from the starting iron complex.

[64] A sample of beads was removed at this point for analysis. The FT-IR spectrum of this KBr pellet displayed a weak band at 1241 cm^{-1} which indicates the possible presence of free cyclobutadiene. A band at 1240 cm-1 was reported for this reactive intermediate when isolated within a hemicarcerand. Cram, D. J.; Tanner, M. E.; Thomas, R. *Angew. Chem. Int. Ed.* **1991**, *30*, 1024-1027.

destroyed by other unidentified reactions during this interval before it can undergo productive cycloaddition and be observed.

Table 2.2: Solid-Supported Cycloaddition

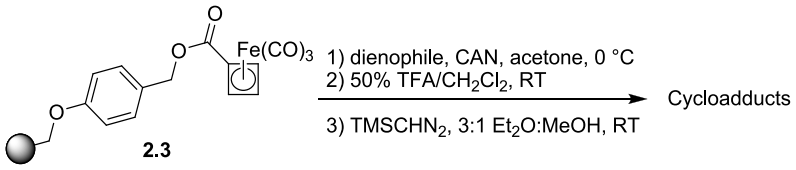

2.3

Entry	Dienophile	Cycloadducts A	Cycloadducts B	Yield (Ratio A:B)
(1)	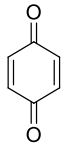	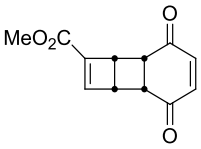	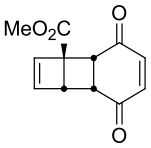	36% (1.1:1)
(2)	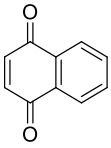	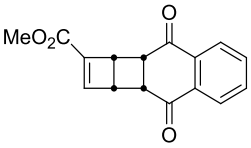	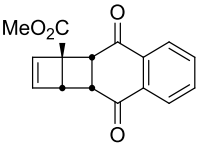	40% (1.7:1)
(3)	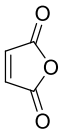	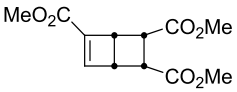	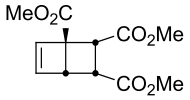	14% (1:1.3)
(4)	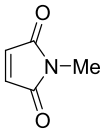	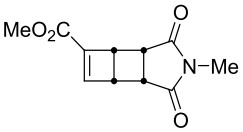	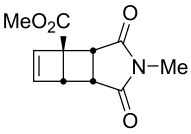	29% (1.6:1)
(5)	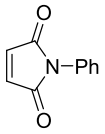	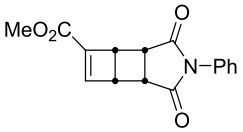	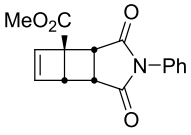	61% (1:1.8)
(6)	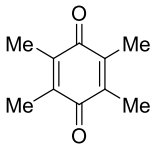	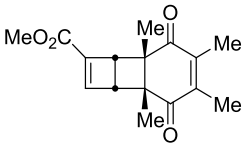	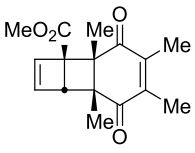	24% (3:1)
(7)	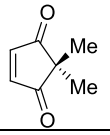	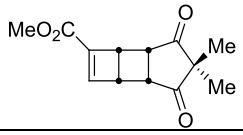	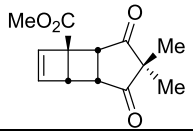	0%

Density Functional Calculations

Regioselectivity in the cycloaddition of diester-substituted cyclobutadiene species has been examined.[65] Cyclobutadiene derivatives with a single ester substituent, however, have not been explored. It is apparent from the product ratios that these cycloadditions display some regioselectivity. This selectivity appears to vary slightly based on the structure of the dienophile and between solution and solid-supported reactions.

Density functional calculations have proved to be a powerful tool for the examination of organic reaction mechanisms.[66] A computational study was undertaken to gain a better understanding of the factors controlling regioselectivity in these cycloadditions. Calculated free-energy values (Table 2.3) appeared to provide the best correlation with experimental product ratios;[67] however, they still fell short of providing a predictive model.

---

[65] Mehta, G.; Viswanath, M. B.; Jemmis, E. D.; Sastry, G. N. *J. Chem. Soc. Perkin Trans. 2*, **1994**, 433-436.
[66] Koch, W.; Holthausen, M. C. "A Chemist's Guide to Density Functional Theory" **2000**, Wiley-VCH, New York.
[67] In most cases, the solution phase results were used for comparison due to the higher yields. For the cycloaddition with maleic anhydride, a comparison was made to the solid-supported result since no product was recovered from the solution phase reaction.

Table 2.3: Calculated Transition State Energies

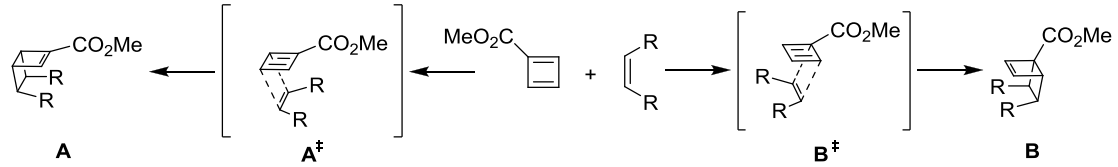

Entry	Dienophile	$\Delta\Delta G^{\ddagger}$ (kcal/mol)[a] (**B**‡ - **A**‡)	Calculated Ratio **A**:**B**	Solution Ratio **A**:**B**	Supported Ratio **A**:**B**
(1)	benzoquinone	0.30	1.7:1	2.4:1	1.1:1
(2)	naphthoquinone	0.28	1.7:1	1.9:1	1.7:1
(3)	maleic anhydride	0.14	1.3:1	n/a	1:1.3
(4)	N-methyl maleimide	-0.62	1:3.3	3.1:1	1.6:1
(5)	N-phenyl maleimide	0.40	2.1:1	1:1	1:1.8
(6)	duroquinone	-0.18	1:1.4	4.3:1	3:1
(8)	dimethylcyclopentenedione	-0.01	1:1	n/a	n/a
(7)	ethylene	0.45	2.3:1	n/a	n/a

[a] Free energy of activation at 0 °C calculated from vibrational analysis of transition state (RB3LYP 6-31G*)

The model case of ethylene suggests a preference for the conjugated cyclobutene ester product **A**, which would be expected to be favored by both steric and electronic factors. The model performed best for the flat quinone-type dienophiles; however, the alkyl substituted maleimide and tetrasubsituted olefins of duroquinone predicted a reversal in selectivity and exhibited further deviance from the calculated ratios. As these ratios represent very small energy differences in the transition state, it is possible that the deviation is due to a limitation[68] of the computational methodology.[69] Since these geometries are

---

[68] It has been noted (Wodrich, M. D.; Corminboeuf, C.; Schreiner, P. R.; Fokin, A. A.; Schleyer, P. R. *Org. Lett*. **2007**, *9*, 1851-1854) that density functional theory may not be ideal for accurate prediction of transition state energies. While previous studies of cyclobutadiene cycloadditions[49c,f] successfully employed B3LYP/6-31G* to model the transition states, it is possible that the small energy differences responsible for these regioselectivities are significantly distorted by these effects.

[69] Optimization of the transition state at higher levels of theory including B3LYP/6-311+G** and MP2, refinement of single point energies including hybrid M06-2X functional and inclusion of a dielectric based solvent model for acetone in the optimization failed to improve the correlation with experimental ratios for the benzoquinone cycloaddition.

calculated in the gas phase, is also possible that a solvent effect involving the dynamics of diffusion control is intervening through modification of the cycloaddition trajectories and providing the actual regiochemical control element. A clear example of the limited predictive power of this computational methodology lies in the cycloaddition with 2,2-dimethylcyclopent-4-en-1,3-dione. Neither solution phase nor solid-supported cycloadditions with this sterically encumbered dienophile (the only non-planar dienophile tested) afforded any of the desired cycloadducts. However, the calculated free energy of activation (Table 2.4) lies within the limits of successful cycloadditions reported in this and other[65,49c,f] work. The solid-supported cycloadditions show a general trend of being more selective for the ring-junction substituted regioisomer **B** than the reactions in solution. The variation in selectivity between solution phase and solid-supported cycloadditions is difficult to explain. This difficulty lies mostly in the reduced yields in the supported case. While it is possible that the resin provides a more hindered environment around the cyclobutadiene, it is also possible that there is a subtle electronic effect. Contrary to what might be expected, the preferred isomer in the solid-supported cycloadditions results from what appears to be the more sterically encumbered transition state $\mathbf{B}^{\ddagger}$ (Table 2.4). The low yields, however, present the possibility that one product (likely the α,β-unsaturated ester) is simply less stable to the conditions of subsequent cleavage and esterification reactions as a viable explanation for the apparent

change in regioselectivity.[52,65,70]

[70] A few experiments have been conducted with regard to product stability. The benzoquinone cycloadducts were subjected to a 50% solution of TFA in dichloromethane and showed no decomposition as judged by ^{1}H-NMR after 12 hours. There was some indication that the α,β-unsaturated ester or ketone moieties in some cycloadducts could participate in dipolar cycloadditions with trimethylsilyldiazomethane (Aoyama, T., Iwamoto, Y., Nishigaki, S., Shioiri, T. *Chem. Pharm. Bull.* **1989**, *37*, 253-256.). Cycloadducts of cyclobutadiene with benzoquinones have also been shown to undergo photochemical cycloaddition to provide caged compounds (see reference 52). Activating substituents on the cyclobutene allow this process to occur under irradiation by sunlight (see reference 65). Decomposition of the duroquinone cycloadducts by this pathway has been observed and may lead to preferential consumption of one regioisomer.

Table 2.4: Transition State Geometries[71]

Dienophile	$\Delta G^{\ddagger}$ (kcal/mol) at 0 °C		Transition States	
	$A^{\ddagger}$	$B^{\ddagger}$	$A^{\ddagger}$	$B^{\ddagger}$
1,4-Benzoquinone	12.65	12.95	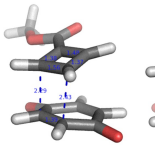	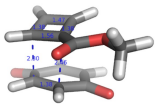
1,4-Naphthoquinone	12.84	13.13	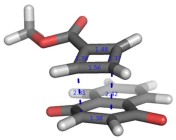	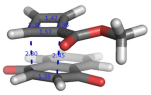
Maleic Anhydride	12.72	12.85	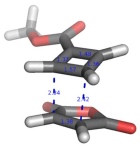	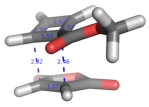
N-Methyl Maleimide	14.25	13.63	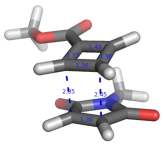	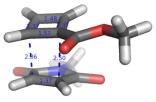
N-Phenyl Maleimide	11.51	11.91	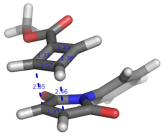	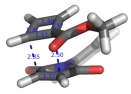
Duroquinone	15.23	15.05	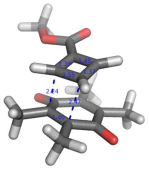	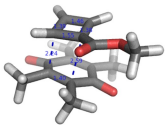
Ethylene	12.14	12.58	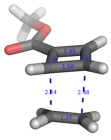	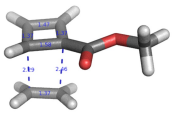
Dimethylcyclopentenedione	13.46	13.44	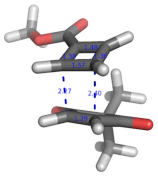	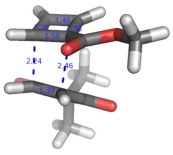

[71] DeLano, W. L. **The PyMOL Molecular Graphics System** (2002) DeLano Scientific, Palo Alto, CA, USA. **http://www.pymol.org**

SUMMARY

A new solid-supported cyclobutadieneiron tricarbonyl complex has been developed, providing a convenient polystyrene bound source of the highly-reactive diene. Cycloadditons with this reagent have been examined, which provide a small library of bicyclohexene-derivatives substituted with various functionalities. Analogous solution phase cycloadditions have also been examined and the mechanistic explanation for the observed regioselectivity has been explored using density functional calculations. While the origin of regiocontrol is not entirely understood, some general trends have emerged.

Scheme 2.3: Potential Daughter Libraries

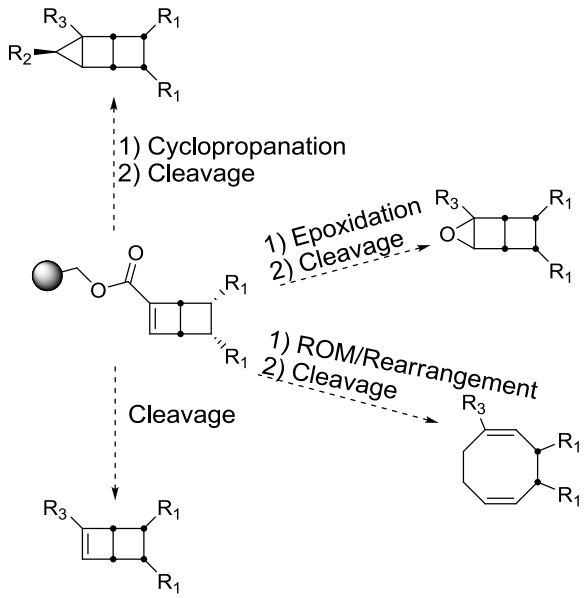

The bicyclohexene scaffold produced by these cycloadditions provides a compact, rigid ring system with unique bond angles due to the high ring strain. (Figure 2.1) These highly strained compounds and the versatile ester tether that attaches them to the polystyrene support provide opportunities for further

functionalization and the generation of polycyclic and medium-ring containing daughter libraries (Scheme 2.2). Further investigation of these compounds and library generation coupled with biological study provides the opportunity for discovery of biologically interesting compounds.

Figure 2.1: ORTEP for *N*-Methylmaleimide Cycloadducts

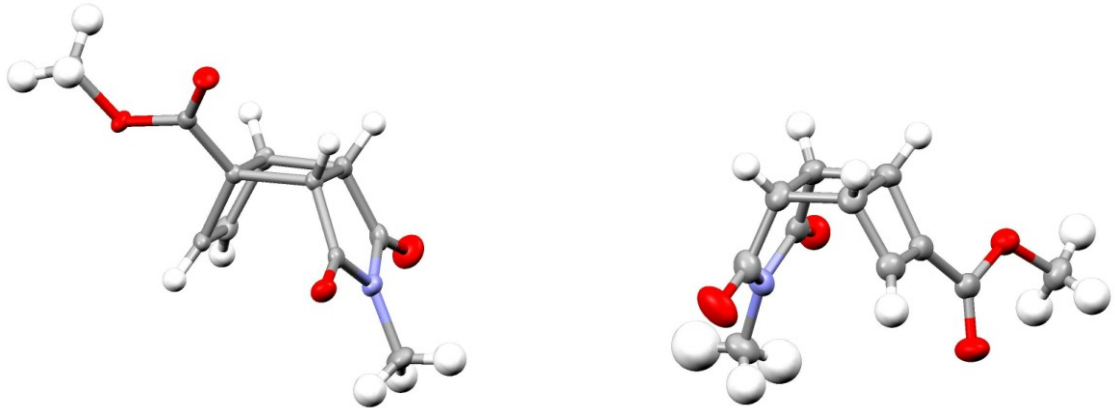

EXPERIMENTAL

General Information

Proton nuclear magnetic resonance spectra (^{1}H-NMR) were measured on either a Gemini-400 instrument (400 MHz) or a Gemini-500 instrument (500 MHz). Chemical shifts are reported in ppm downfield from tetramethylsilane with the solvent reference as the internal standard ($CHCl_3$: δ 7.26 ppm). Data is reported as follows: chemical shift, multiplicity (s = singlet, d = doublet, t = triplet, q = quartet, br = broad, m = multiplet), coupling constants (Hz), and integration. ^{13}C-NMR spectra were recorded on either a Gemini-400 instrument (100 MHz), or a Gemini-500 instrument (125 MHz) with complete proton decoupling. Chemical shifts are reported in ppm downfield from tetramethylsilane with the solvent as the internal reference ($CDCl_3$: δ 77.23 ppm). Infrared spectra (IR) were reported in wave numbers (cm^{-1}). Bands are characterized as broad (br), strong (s), medium (m), or weak (w). Elemental analyses (ICP) were performed by Robertson Microlit Laboratories, Inc., Madison, NJ and are reported in percent atomic abundance. High resolution mass spectral analyses (HRMS) were performed by the Mass Spectrometry Laboratory, University of Illinois at Urbana-Champaign or at Boston College. Melting points (mp) were reported uncorrected.

Starting materials and reagents were purchased from commercial suppliers and used without further purification except the following:

Dichloromethane and diethyl ether were used from a solvent purification system.[72] N,N-dimethylformamide was dried over 4 Å molecular sieves. Methanol was distilled from magnesium methoxide. Hexanes and Et_2O used in chromatography were distilled before use. Molecular sieves were dried in a 250 °C oven overnight before use. (Methylcyclobutadienoate)iron tricarbonyl,[50a] (cyclobutadienal)iron tricarbonyl,[50b] (cyclobutadienecarboxylic acid)iron tricarbonyl[59] and 2,2-dimethylcyclopenten-1,3-dione[73] were prepared as reported in the literature and displayed satisfactory spectral data. [Please note potential hazards: Iron carbonyls complexes can be a source of carbon monoxide.] Benzoquinone and naphthoquinone were purified by sublimation prior to use. All oxygen- or moisture-sensitive reactions were carried out under N_2 atmosphere in oven-dried (140 °C, > 4 h) or flame-dried glassware. Air- or moisture-sensitive liquids were transferred by syringe and were introduced into the reaction flasks through rubber septa or through a stopcock under N_2 positive pressure. Unless otherwise stated, reactions were stirred with a Teflon covered stir bar. Concentration refers to the removal of solvent using a rotary evaporator followed by use of a vacuum pump at approximately 1 torr. Silica gel column chromatography refers to flash chromatography[74] and was performed using 60 Å

---

[72] Pangborn, A. B.; Giardello, M. A.; Grubbs, R. H.; Rosen, R. K.; Timmers. F. J. *Organometallics* **1996**, *15*, 1518.
[73] Preparation: Kreiser, W.; Wiggermann, A.; Krief, A.; Swinnen, D. *Tetrahedron Lett.* **1996**, *39*, 7119-7122. Spectral Data: Agosta, W. C.; Smith, A. B. III *J. Org. Chem.* **1970**, *35*, 3856-3860.
[74] Still, W.C.; Kahn, M.; Mitra, A. *J. Org. Chem.* **1978**, *43*, 2923.

(230-400 Mesh ASTM) silica gel. Thin layer chromatography was performed on glass backed 60 Å (250 μm thickness) silica gel plates.

X-ray data were collected using a Bruker SMART APEX CCD (charge coupled device) based diffractometer with Mo (λ=0.71073 Å) radiation equipped with an LT-3 low-temperature apparatus operating at 100 K (**V**) or 193 (**VI**). A stable crystal was chosed and mounted on a glass fiber using grease. Data were measured using omega scans of 0.3° per frame for 30 s, such that a hemisphere was collected. A total of 12737 (**V**) or 6730 (**VI**) frames were collected with a maximum resolution of 0.90 Å. Cell parameters were retrieved using SMART[75] software and refined using SAINT on all observed reflections. The structures are solved by the direct method using the SHELXS-97[76] program and refined by least squares method on F2, SHELXTL-97,[77] incorporated in SHELXTL-PC V 5.10.[78] The crystals used for diffraction studies showed no decomposition during data collection. The drawing was displayed at 50% ellipsoids. The structures were solved by Dr. Stephanie Ng or Dr. Bo Li at Boston College.

---

[75] SMART V 5.050 (NT) Software for the CCD Detector System; Bruker Analystical X-ray Systems, Madison, WI (1998).
[76] Sheldrick, G. M. SHELXS-90, Program for the Solution of Crystal Structure, University of Gottingen, Germany, 1990.
[77] Sheldrick, G. M. SHELXS-97, Program for the Refinement of Crystal Structure, University of Gottingen, Germany, 1997.
[78] SHELXTL 5.10 (PC-Version), Program Library for Structure Solution and Molecular Graphics, Bruker Analytical X-ray Systems, Madison, WI (1998).

Experimental Procedures

Cyclobutadieneiron tricarbonyl Wang Resin (2.3)

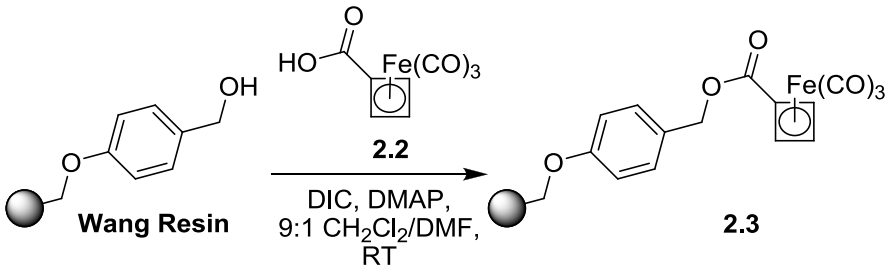

An oven-dried 25 mL schlenk flask was charged with 1.13 g Wang Resin (0.9 mmol/g, 1 equiv., 1.02 mmol) and 600 mg **2.2** (2.5 equiv., 2.54 mmol) under a nitrogen atmosphere and the beads suspended in 15 mL 9:1 CH_2Cl_2/DMF. The resin was allowed to swell for 1.5 h. Diisopropylcarbodiimide (5 equiv., 5.1 mmol, 199 μL) was added via syringe, followed by a solution of dimethylaminopyridine (0.1 equiv., 0.102 mmol, 12.5 mg) in DMF (500 μL). The flask was sealed with a glass stopper and stirred at ambient temperature for 12 h. Resin was collected by filtration and washed successively with DMF, CH_2Cl_2 and methanol (3 portions of 10 mL each per solvent) and dried under high vacuum for 12 h. Recovered 1.45 g red/orange resin.

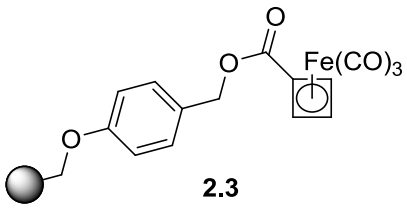

2.3

^{13}C NMR (101 MHz, $CDCl_3$, gel phase[79]) δ 211.79, 166.71, 145.08, 130.07, 127.73, 114.71, 69.88, 67.69, 65.05, 62.34, 40.53. **IR** (KBr pellet) 3466 (br), 3399 (br), 3063 (m), 3033 (m), 2940 (m) 2918 (m), 2901 (m), 2886 (m),

[79] Jones, A.J., Leznof, C. C., Svirskaya, P. I. *Org. Mag. Res.* **1982**, *18*, 236-240.

2856 (m), 2058 (s), 1977 (s), 1711 (s), 1609 (m), 1511 (m), 1440 (m), 1368 (w), 1307 (w), 823 (w), 764 (w), 752 (w), 694 (w), 611 (m), 586 (m), 538 (m). **ICP-Fe Anal:** Found: 4.25% Calc'd: 5.52% (indicates 77% loading of resin hydroxyl groups)

General Solution Phase Cycloaddition Procedure

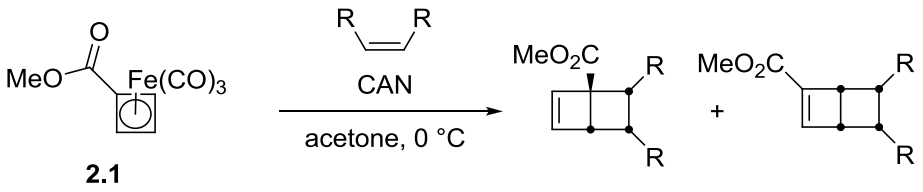

2.1

To a stirring solution of (methylcyclobutadienoate)iron tricarbonyl (**2.1**, 250 mg, 1 mmol, 1 equiv.) and dienophile (3 mmol, 3 equiv.) in acetone (10 mM, 100 mL) at 0 °C, was added ceric ammonium nitrate (2.7 g, 5 mmol, 5 equiv.). The reaction was stirred loosely capped for 3 hours[80] and then quenched with 7 mL saturated aqueous $NaHCO_3$. Solution was decanted from the precipitated salts and the salts washed three times with CH_2Cl_2. Combined organics were then concentrated and the residue purified by gradient silica gel flash chromatography.

Benzoquinone Cycloaddition

Purification by silica gel flash chromatography (eluting with a gradient from hexanes to 30% then 50% diethyl ether in hexanes and finally 100% diethyl

[80] CAUTION: Cycloaddition reactions of cyclobutadieneiron tricarbonyl complexes result in the evolution of carbon monoxide and should be performed in a well-ventilated fume hood.

ether) afforded two regioisomeric cycloadducts in a combined yield of 59% (76.4 mg **I** as a pale yellow solid and 183 mg **II** as a pale yellow solid (1:2.4 ratio **I**:**II**)).

7,10-Dioxo-tricyclo[4.4.0.0^{2,4}]deca-3,8-diene-2-carboxylic acid methyl ester (I)

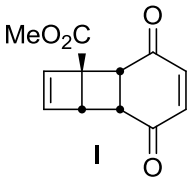

I

(**mp** 51-57 °C). **^{1}H NMR** (400 MHz, $CDCl_3$) δ 6.78 (s, 2H), 6.31 (d, *J* = 2.5 Hz, 1H), 6.25 (t, *J* = 2.4 Hz, 1H), 4.11 (d, *J* = 10.0 Hz, 1H), 3.94 (dd, *J* = 2.2, 9.0 Hz, 1H), 3.76 (s, 3H), 3.75 – 3.68 (m, 1H). **^{13}C NMR** (101 MHz, $CDCl_3$) δ 197.29, 196.30, 170.55, 144.10, 143.96, 140.35, 138.31, 56.92, 52.86, 49.88, 43.37, 41.12. **IR** (KBr, thin film) 2955 (m), 2892 (w), 2870 (w), 1727 (s), 1676 (s) 1599 (w), 1459 (w), 1436 (m), 1377 (w), 1318 (w), 1275 (s), 1241 (m), 1199 (m), 1180 (m), 1129 (m), 1103 (w), 1072 (w), 1060 (w), 1021 (w), 864 (w), 779 (w), 410 (w). **DART-HRMS (m/z):** Calc'd for [M+H]+: 219.06573; Found: 219.06552.

7,10-Dioxo-tricyclo[4.4.0.0^{2,4}]deca-3,8-diene-3-carboxylic acid methyl ester (II)

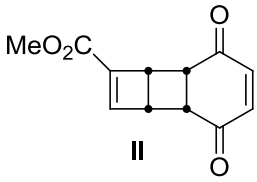

II

(**mp** 109-112 °C). **^{1}H NMR** (400 MHz, $CDCl_3$) δ 6.85 (d, *J* = 2.4 Hz, 1H), 6.73 (s, 2H), 4.13 – 4.00 (m, 1H), 3.82 (t, *J* = 5.5 Hz, 1H), 3.75 – 3.64 (m, 5H). **^{13}C NMR** (101 MHz, $CDCl_3$) δ 197.36, 196.26, 161.31, 147.28, 144.33, 144.07, 141.17, 51.94, 45.63,

43.09, 42.34, 41.29. **IR** (KBr, thin film) 3081 (w), 3059 (m), 3029 (s), 1722 (m), 1674 (m), 1600 (w), 1447 (w), 1316 (w), 1291 (w), 1251 (m), 1252 (w), 1127 (w), 1101 (w), 750 (m), 697 (m). **DART-HRMS (m/z):** Calc'd for [M+H]+: 219.06573; Found: 219.06561.

Duroquinone Cycloaddition

Purification by silica gel flash chromatography (eluting with 30% diethyl ether in hexanes) afforded two regioisomeric cycloadducts in a combined yield of 98% (51mg of **III** as a white powder and 217 mg of **IV** as a yellow powder (1:4.3 ratio **III**:**IV**)).

1,6,8,9-Tetramethyl-7,10-dioxo-tricyclo[4.4.0.$0^{2,4}$]deca-3,8-diene-2-carboxylic acid methyl ester (III)

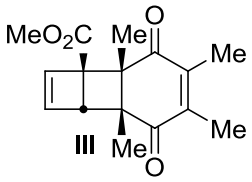

(**mp** 90-93 °C). **^{1}H NMR** (400 MHz, $CDCl_3$) δ 6.11 (t, *J* = 2.3 Hz, 1H), 6.07 (d, *J* = 2.1 Hz, 1H), 3.74 (s, 3H), 3.37 (d, *J* = 1.9 Hz, 1H), 1.98 (s, 3H), 1.97 (s, 3H), 1.41 (s, 3H), 1.34 (s, 3H). **^{13}C-NMR** (101 MHz, $CDCl_3$) 200.60, 199.53, 170.04, 148.45, 148.28, 140.13, 139.83, 58.65, 53.51, 52.34, 52.12, 48.18, 19.87, 17.02, 13.83, 13.71. **IR** (KBr, thin film) 3067 (w), 3041 (m), 2958 (m), 2872 (w), 1728 (s), 1664 (m), 1461 (m), 1436 (m), 1379 (m), 1313 (m), 1261 (m), 1218 (m), 1199 (m), 1159 (m), 1123 (m), 1092 (m), 1037 (m). **DART-HRMS (m/z):** Calc'd for [M+H]+: 275.12833; Found: 275.12739.

1,6,8,9-Tetramethyl-7,10-dioxo-tricyclo[4.4.0.0^{2,4}]deca-3,8-diene-3-carboxylic acid methyl ester (IV)

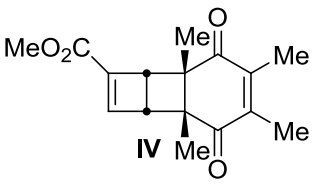

(**mp** 45-55 °C dec.). **^{1}H-NMR** (400 MHz, $CDCl_3$) δ 6.65 (dd, *J* = 2.1, 0.7 Hz, 1H), 3.61 (s, 3H), 3.32 (dd, *J* = 2.9, 2.2 Hz, 1H), 3.14 (dd, *J* = 2.9, 0.6 Hz, 1H), 1.89 (q, *J* = 1.0 Hz, 3H), 1.86 (q, J=1.0 Hz, 3H), 1.38 (s, 3H), 1.35 (s, 3H). **^{13}C NMR** (101 MHz, $CDCl_3$) δ 200.48, 199.06, 161.70, 148.79, 148.341, 147.95, 141.04, 51.65, 50.19, 49.92, 48.24, 47.77, 19.68, 19.16, 13.63, 13.50. **IR** (KBr, thin film) 3059 (m) 3027 (s), 2915 (s), 1727 (s), 1661 (m), 1447 (m), 1379 (w), 1262 (m), 1221 (m), 1126 (m), 755 (s) 697 (s), 540 (m). **DART-HRMS (m/z):** Calc'd for [M+H]+: 275.12833; Found: 275.12731.

N-Methyl Maleimide Cycloaddition

Purification by silica gel flash chromatography (eluting with a gradient from diethyl ether to 10% methanol in ethyl acetate) afforded two regioisomeric cycloadducts in a combined yield of 63% (33.3 mg **V** as a clear oil which solidified to white solid in the freezer at -20 °C and 106.2 mg **VI** as a white powder (1:3.1 ratio **V**:**VI**)). Crystals for x-ray diffraction were grown by slow evaporation from benzene for **V** and from 10% methanol in ethyl acetate for **VI**.

8-Methyl-7,9-dioxo-8-aza-tricyclo[4.3.0.0^{2,4}]non-3-ene-2-carboxylic acid methyl ester (V)

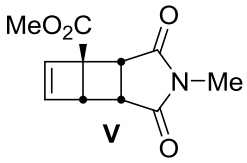

V

(**mp** 41-43 °C). **^{1}H NMR** (400 MHz, $CDCl_3$) δ 6.30 (dd, *J* = 9.5, 11.8 Hz, 2H), 3.90 (d, *J* = 7.7 Hz, 1H), 3.81 (d, *J* = 8.7 Hz, 1H), 3.75 (s, 3H), 3.49 (t, *J* = 8.2 Hz, 1H), 2.98 (s, 3H). **^{13}C NMR** (101 MHz, CDCl3) δ 176.09, 175.45, 170.27, 139.78, 137.97, 53.32, 52.69, 46.33, 39.07, 36.56, 24.90. **IR** (KBr, thin film), 3059 (m), 3026 (s), 2926 (s), 1725 (m), 1698 (m), 1448 (w), 1430 (w), 1294 (w), 1126 (w), 710 (w), 697 (w). **ESI-HRMS (m/z):** Calc'd for [M+Na]: 244.0586; Found: 244.0578.

8-Methyl-7,9-dioxo-8-aza-tricyclo[4.3.0.0^{2,4}]non-3-ene-3-carboxylic acid methyl ester (VI)

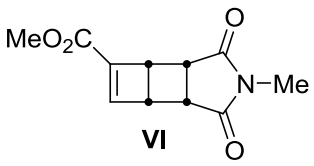

VI

(**mp** 128-132 °C). **^{1}H NMR** (300 MHz, $CDCl_3$) δ 6.85 (d, *J* = 2.4, 1H), 3.90 (m, 1H), 3.73 (s, 3H), 3.66 (m, 1H), 3.57 – 3.44 (m, 2H), 2.91 (s, 3H). **^{13}C- NMR (101 MHz, $CDCl_3$)** δ 176.23, 175.77, 160.91, 146.39, 141.06, 52.08, 41.60, 39.01, 37.79, 37.11, 25.11. **IR** (KBr pellet) 3059 (w), 3025 (w), 2929 (m), 1760 (s), 1728 (s), 1690 (s), 1585 (w), 1433 (m), 1375 (m), 1332 (m), 1294 (m), 1272 (w), 1261 (w), 1240 (m), 1192 (w), 1166 (w), 1113 (m), 1083 (w), 1060 (w), 993 (w), 965 (m), 847 (w), 752 (w), 646 (m). **EI-HRMS (m/z):** Calc'd for [M]+: 221.0688 ; Found: 221.0688.

N-Phenyl Maleimide Cycloaddition

Purification by silica gel flash chromatography (eluting with a gradient from diethyl ether to ethyl acetate) afforded two regioisomeric cycloadducts in a combined yield of 56% (77.7 mg **VII** as a white solid and 79.9 mg **VIII** as a white solid (1:1 ratio of **VII**:**VIII**)).

8-Phenyl-7,9-dioxo-8-aza-tricyclo[4.3.0.0^{2,4}]non-3-ene-2-carboxylic acid methyl ester (VII)

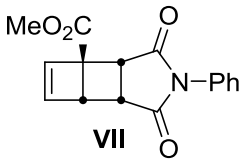

VII

(**mp** 131-133 °C). **^{1}H NMR** (400 MHz, $CDCl_3$) δ 7.43 (m, 4H), 7.21 (d, *J* = 7.2 Hz, 2H), 6.50 (d, *J* = 2.5 Hz, 1H), 6.45 (t, *J* = 2.4 Hz, 1H), 4.06 (d, *J* = 7.8 Hz, 1H), 3.92 (dd, *J* = 2.2, 8.7 Hz, 1H), 3.78 (s, 3H), 3.66 (t, *J* = 8 Hz, 1H). **^{13}C NMR** (101 MHz, $CDCl_3$) δ 175.39, 174.66, 170.30, 139.97, 138.26, 132.10, 129.40, 129.06, 126.87, 54.04, 53.93, 47.05, 39.09, 36.60. **IR** (KBr, thin film) 3058 (w), 3026 (m), 2924 (m), 2912 (w), 1709 (s), 1498 (w), 1435 (w), 1377 (m), 1320 (w), 1292 (m), 1229 (w), 1176 (m), 1112 (w), 1060 (w), 703 (w). **DART-HRMS (m/z):** Calc'd for $[M+H]^+$: 284.09228; Found: 284.09198.

8-Phenyl-7,9-dioxo-8-aza-tricyclo[4.3.0.0^{2,4}]non-3-ene-3-carboxylic acid methyl ester (VIII)

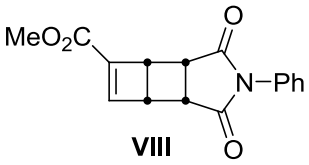

VIII

(**mp** 130-132 °C). **^{1}H NMR** (300 MHz, $CDCl_3$) δ 7.50 – 7.32 (m, 4H), 7.16 – 7.10 (m, 2H), 7.03 (dd, *J* = 2.4, 0.7

Hz, 1H), 4.09-4.03 (m, 1H), 3.84 – 3.77 (m, 1H), 3.76 (s, 3H), 3.72 – 3.66 (m, 2H). **^{13}C NMR** (101 MHz, $CDCl_3$) δ 175.56, 175.02, 161.12, 146.79, 141.21, 132.14, 129.45, 129.04, 126.93, 52.08, 42.15, 39.56, 37.84, 36.86. **IR** (KBr pellet) 3029 (w), 2921 (m), 1702 (s), 1596 (w), 1498 (w), 1434 (w), 1377 (m), 1286 (m), 1250 (m), 1173 (m), 1156 (m), 1110 (w), 733 (w), 629 (w). **DART-HRMS (m/z):** Calc'd for [M+H]+: 284.09228; Found: 284.09118.

Naphthoquinone Cycloaddition

Purification by silica gel flash chromatography (eluting with a gradient from 30% diethyl ether in hexanes to ethyl acetate) afforded two regioisomeric cycloadducts in a combined yield of 93% (86 mg **IX** as an off-white powder and 163 mg **X** as a white powder (1:1.9 ratio **IX**:**X**)).

8-Benzo-7,10-dioxo-tricyclo[4.4.0.0^{2,4}]dec-3-ene-2-carboxylic acid methyl ester (IX)

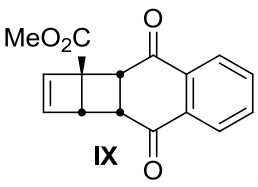

IX

(**mp** 80-83 °C dec.). **^{1}H NMR** (500 MHz, $CDCl_3$) δ 8.13 – 7.99 (m, 2H), 7.78 – 7.66 (m, 2H), 6.25 (d, *J* = 2.5 Hz, 1H), 6.21 (t, *J* = 2.4 Hz, 1H), 4.29 (d, *J* = 10.3 Hz, 1H), 4.01 (dd, *J* = 2.2, 9.0 Hz, 1H), 3.93 – 3.87 (m, 1H), 3.77 (s, 3H). **^{13}C NMR** (126 MHz, $CDCl_3$) δ 196.16, 195.11, 170.98, 140.67, 138.58, 137.32, 137.25, 134.55, 134.48, 127.46, 127.27, 56.78, 52.80, 49.84, 44.59, 42.34. **IR** (KBr, thin film) 2953 (w), 1726 (s), 1680 (s), 1592 (m), 1435 (w), 1318 (m), 1268 (s), 1197 (m), 1180 (m),

1124 (w), 1102 (w), 965 (w), 814 (w), 715 (m). **DART-HRMS (m/z):** Calc'd for [M+H]+: 269.08138; Found: 269.08043.

8-Benzo-7,10-dioxo-tricyclo[4.4.0.0^{2,4}]dec-3-ene-3-carboxylic acid methyl ester (X)

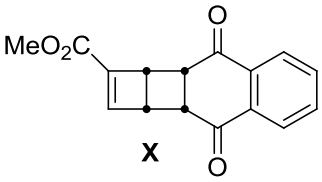

X

(**mp** 154-156 °C dec.). **^{1}H NMR** (400 MHz, $CDCl_3$) δ 8.10 – 7.98 (m, 2H), 7.77 – 7.65 (m, 2H), 6.75 (d, *J* = 2.3 Hz, 1H), 4.18 – 4.07 (m, 1H), 3.98 – 3.86 (m, 3H), 3.59 (s, 3H). **^{13}C NMR** (101 MHz, $CDCl_3$) δ 195.89, 194.71, 161.08, 147.42, 140.92, 137.19, 137.11, 134.29, 134.20, 127.13, 127.01, 51.58, 45.41, 43.33, 43.01, 42.23. **IR** (KBr pellet) 2980 (w), 2953 (w), 2915 (w), 1707 (s), 1674 (s), 1590 (m), 1440 (w), 1287 (s), 1253 (s), 1195 (w), 1147 (m), 1103 (m), 1006 (w), 986 (w), 969 (w), 858 (w), 796 (w), 748 (w), 723 (m), 706 (w). **DART-HRMS (m/z):** Calc'd for [M+H]+: 269.08138; Found: 269.08096.

Cyclobutadiene Dimerization

Attempted cycloadditon with 2,2-dimethylcyclopenten-1,3-dione

resulted in the isolation of 14% yield of a mixture of isomeric cyclobutadiene dimerization products and with their cyclooctatetraene fragmentation products.[81,82] The major isomer was isolated sufficiently pure for

---

[81] Two of the isomers have been previously prepared. 1,4-disubstituted: Maier, G.; Sayrac, T.; Kalinowski, H. O.; Askani, R. *Chem. Ber.* **1982**, *115*, 2214-2220. 1,5-disubstituted: Figeys, H. P.; Van Lommen, G.; Belladone, M.; Destrebecq, M. *Tetrahedron Lett.* **1960**, *21*, 2365-2368.

characterization after flash chromatography on silica gel eluting with a gradient from 30% diethyl ether in hexanes to 100% diethyl ether.

Tricyclo[4.2.0.0^{2,4}]octa-3,7-diene-3,7-dicarboxylic acid dimethyl ester (XIII)

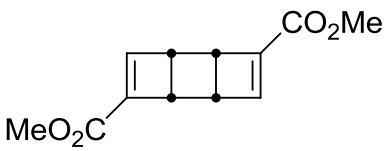

XIII

^{1}H NMR (400 MHz, $CDCl_3$) δ 6.73 (s, 2H), 3.67 (s, 6H), 3.50 (dd, *J* = 1.8, 1.0 Hz, 2H), 3.22 – 3.16 (m, 2H). **^{13}C NMR** (101 MHz, $CDCl_3$) δ 162.18, 144.63, 138.06, 51.46, 37.90, 35.85, 34.91, 31.83, 22.90, 14.34. **IR** (KBr, thin film) 3060.5 (w), 3026.7 (s), 2940.0 (w), 2931.3 (w), 2924.5 (w), 2913.9 (w), 2894.6 (m), 1725.0 (s), 1595.8 (w), 1282.43 (s), 1249.7 (m), 1197.6 (w), 1157.1 (m), 1128.2 (w). **DART-HRMS (m/z):** Calc'd for [M+H]+: 221.08135; Found: 221.08138.

General Solid-Supported Cycloaddition Procedure

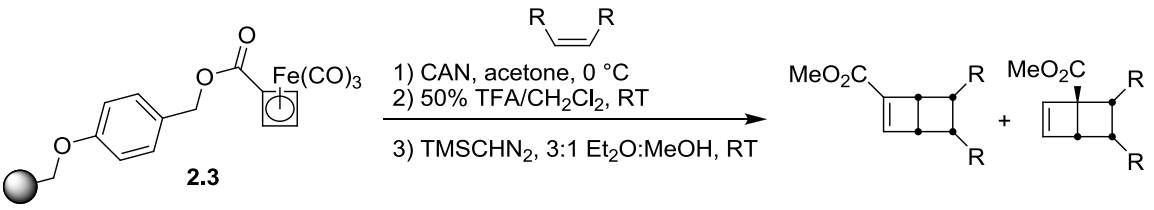

2.3

Cyclobutadiene resin **2.3** (400 mg, 0.36 mmol, 1 equiv.) was suspended in wet acetone (10 mL) in a loosely capped scintillation vial. The suspension was agitated via magnetic stirring at ambient temperature for 1 hour to allow swelling of the resin and then cooled to 0 °C. The dienophile was added to the

---

[82] For this highly-strained "*cis-syn-cis*" ring system, this rearrangement appears to occur slowly even at ambient temperature.

suspension (3.6 mmol, 10 equiv.), followed by ceric ammonium nitrate (990 mg, 1.8 mmol, 5 equiv.) and the reaction was stirred for 2 hours at 0 °C.[80] The resin was then collected by filtration in a fritted 4 cm Bio-Rad Poly-Prep chromatography column and washed successively with water, acetone, dichloromethane, and methanol (3 portions of 5 mL each) and dried under high vacuum for 12 hours. Infrared spectroscopy (KBr pellet) of the resin indicated complete consumption of the cyclobutadiene complex as monitored by the iron carbonyl absorbances.

Cleavage of the cycloadduct from the resin was accomplished by suspending the resin in a 50% v/v solution of trifluoroacetic acid in dichloromethane and agitating the Poly-Prep column on a rotary shaker for 1 hr at room temperature. The resin was removed by filtration and washed with dichloromethane (3 portions of 5 mL). Combined filtrates were concentrated.

The crude residue from product cleavage was dissolved in a 3:1 mixture of anhydrous diethyl ether and methanol and cooled to 0 ºC under a nitrogen atmosphere. A 2.0 M solution of trimethylsilyldiazomethane in diethyl ether (200 μL, 0.40 mmol, 1.1 equiv.) was added dropwise and the solution was stirred while warming to room temperature over 12 hours.

Products were purified as for the solution phase cycloadditions and spectral data matched that for previously reported compounds. (*vide supra*)

Maleic Anhydride Cycloadditon

Purified by silica gel flash chromatography eluting with diethyl ether to afford 22.4 mg (14%) of a 1:1.3 mixture (**XI**:**XII**) of regioisomeric cycloadducts (by ^{1}H-NMR) which was then separated by preparative normal phase HPLC (10 mm Varian Dynamax 100Å Si column, step gradient (10 min. per step) hexane:1% isopropanol: 5% isopropanol: 10% isopropanol, 2.3 mL/min) to afford analytically pure samples of each regioisomer as a clear, colorless oil (retention times 24.6 min and 28.2 min respectively).

Bicyclo[2.2.0]hex-5-ene-1,2,3-tricarboxylic acid trimethyl ester (XI)

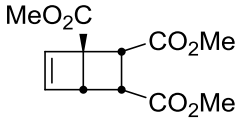

XI

^{1}H NMR (400 MHz, $CDCl_3$) δ 6.48-6.36 (m, 2H), 4.09 (d, *J* = 11.4 Hz, 1H), 3.75-3.70 (m, 4H), 3.67 (s, 3H) 3.66 (s, 3H), 3.60 – 3.55 (m, 1H). **^{13}C NMR** (101 MHz, $CDCl_3$) δ 171.40, 170.84, 170.45, 139.12, 137.21, 53.46, 52.61, 52.04, 51.97, 46.24, 42.70, 40.80. **IR** (KBr, thin film) 3059 (m), 3026 (m), 2999 (w), 2953 (m), 2932 (m), 2923 (m), 2914 (m), 1729 (s), 1490 (w), 1435 (m), 1359 (m), 1277 (s), 1204 (s), 1174 (m), 1090 (w), 1054 (m), 849 (w), 801 (w), 765 (w). **DART-HRMS (m/z):** Calc'd for [M+H]+: 255.08686; Found: 255.08746.

Bicyclo[2.2.0]hex-5-ene-2,3,5-tricarboxylic acid trimethyl ester (XII)

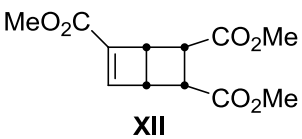

XII

^{1}H NMR (400 MHz, $CDCl_3$) δ 7.14 (dd, *J* = 2.1, 0.8 Hz, 1H), 3.79 (dd, *J* = 11.4, 7.7 Hz, 2H), 3.74 (s, 3H), 3.70 (dt, *J* = 11.7, 3.2 Hz, 2H), 3.66 (s, 3H), 3.61 (s, 3H), 3.40 (dd, *J* = 7.8, 2.9 Hz, 1H). **^{13}C NMR** (126 MHz, $CDCl_3$) δ 171.37, 171.09, 162.37, 147.72, 138.81, 51.96, 51.86, 51.66, 41.34, 41.19, 40.80, 38.83. **IR** (KBr,thin film) 3060 (w), 3027 (m), 2926 (s), 1728 (m), 1681 (m), 1436 (w), 1325 (w), 1267 (m), 1200 (m), 1167 (m), 1126 (w), 1108 (w). **DART-HRMS (m/z):** Calc'd for [M+H]+: 255.08686; Found: 255.08706.

Calculation Details

Transition states were optimized using the Becke-3 Lee-Yang-Parr functional[83] and the 6-31G* basis set as implemented in Gaussian '04.[84] Previous density functional treatments of intramolecular cyclobutadiene cycloadditions were used as a model for these studies.[49c,f] Transition state geometries were located using the QST2 algorithm as in Gaussian '04. Stationary points (Table 4) were characterized as transition states by analysis of

---

[83] Stevens, P. J.; Devlin, J. F.; Chabalowski, C. F.; Frisch, M. J. *J. Phys. Chem.*, **1994**, *98*, 11623-11627.

[84] *Gaussian 03, Revision D.01*, Frisch, M. J.; Trucks, G. W.; Schlegel, H. B.; Scuseria, G. E.; Robb, M. A.; Cheeseman, J. R.; Montgomery, J. A., Jr.; Vreven, T.; Kudin, K. N.; Burant, J. C.; Millam, J. M.; Iyengar, S. S.; Tomasi, J.; Barone, V.; Mennucci, B.; Cossi, M.; Scalmani, G.; Rega, N.; Petersson, G. A.; Nakatsuji, H.; Hada, M.; Ehara, M.; Toyota, K.; Fukuda, R.; Hasegawa, J.; Ishida, M.; Nakajima, T.; Honda, Y.; Kitao, O.; Nakai, H.; Klene, M.; Li, X.; Knox; H. P. Hratchian; J. B. Cross; V. Bakken; C. Adamo; J. Jaramillo; R. Gomperts; R. E. Stratmann, J. E.; Yazyev, O.; Austin, A. J.; Cammi, R.; Pomelli, C.; Ochterski, J. W.; Ayala, P. Y.; Morokuma, K.; Voth, G. A.; Salvador, P.; Dannenberg, J. J.; Zakrzewski, V. G.; Dapprich, S.; Daniels, A. D.; Strain, M. C.; Farkas, O.; Malick, D. K.; Rabuck, A. D.; Raghavachari, K.; Foresman, J. B.; Ortiz; Q. Cui; A. G. Baboul; S. Clifford; J. Cioslowski; B. B. Stefanov; G. Liu; A. Liashenko; P. Piskorz, J. V.; Komaromi, I.; Martin, R. L.; Fox, D. J.; Keith, T.; Al-Laham, M. A.; Peng, C. Y.; Nanayakkara, A.; Challacombe, M.; Gill, P. M. W.; Johnson, B.; Chen, W.; Wong, M. W.; Gonzalez, C.; Pople, J. A. Gaussian, Inc., Wallingford CT, 2004.

the vibrational frequencies and found to have one imaginary vibrational mode. Frequency analysis was used to calculate the free energy values for use in the determination of predicted product ratios.[85] Selected bond lengths (in angstroms) are presented in the transition state figures.

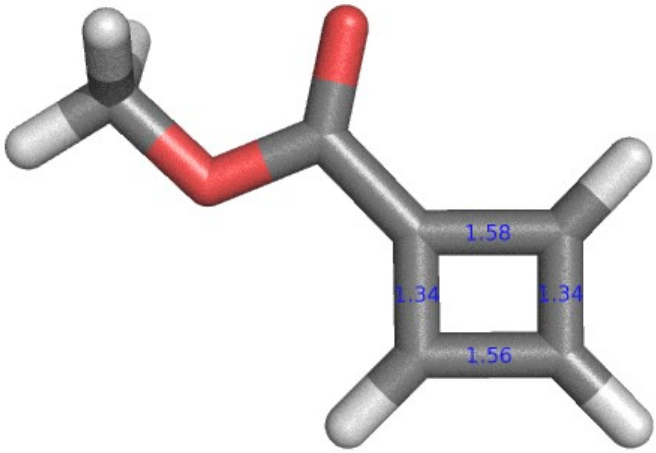

Methylcyclobutadienoate
UB3LYP/6-31G (d)
SCF Done: E(UB+HF-LYP) = -382.560612481
Zero-point correction= 0.105114 (Hartree/Particle)
Thermal correction to Energy= 0.113204
Thermal correction to Enthalpy= 0.114148
Thermal correction to Gibbs Free Energy= 0.072145
Sum of electronic and zero-point Energies= -382.455499
Sum of electronic and thermal Energies= -382.447408
Sum of electronic and thermal Enthalpies= -382.446464
Sum of electronic and thermal Free Energies= -382.488467

	E (Thermal)	CV	S

[85] $\Delta\Delta G^{\ddagger}=-RT\ln(k_b/k_a)$

	KCal/Mol	Cal/Mol-Kelvin	Cal/Mol-Kelvin
Total	71.037	27.945	88.402

Center Number	Atomic Number	Atomic Type	Coordinates (Angstroms) X	Y	Z
1	6	0	0.768401	-0.003178	0.000000
2	6	0	1.486488	-1.139110	0.000001
3	6	0	2.810686	-0.317614	0.000000
4	6	0	2.110811	0.821398	-0.000001
5	1	0	1.236211	-2.194025	0.000003
6	1	0	3.860564	-0.581944	0.000000
7	1	0	2.341823	1.879374	-0.000002
8	6	0	-0.637707	0.364535	0.000000
9	8	0	-1.046025	1.513206	0.000001
10	8	0	-1.447494	-0.726520	-0.000001
11	6	0	-2.852110	-0.436631	0.000000
12	1	0	-3.350861	-1.406643	0.000001
13	1	0	-3.129501	0.136670	0.889204
14	1	0	-3.129503	0.136669	-0.889204

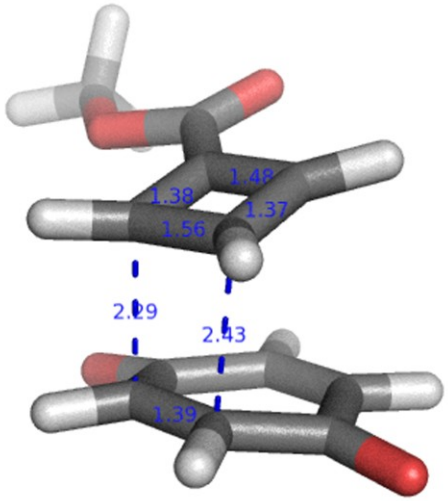

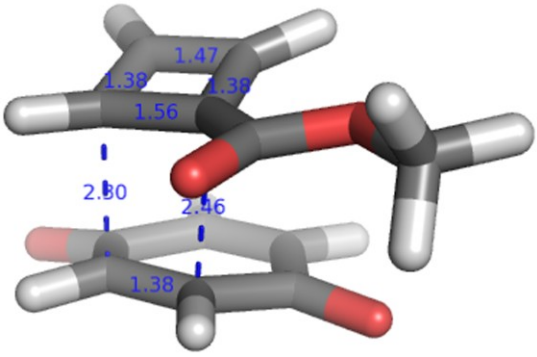

CBBQe-ts **CBBQi-ts**

CBBQe-ts
RB3LYP/6-31G (d)
SCF Done: E(RB+HF-LYP) = -764.010424075
Zero-point correction= 0.192017 (Hartree/Particle)
Thermal correction to Energy= 0.206765

Thermal correction to Enthalpy= 0.207709
Thermal correction to Gibbs Free Energy= 0.149185
Sum of electronic and zero-point Energies= -763.818407
Sum of electronic and thermal Energies= -763.803659
Sum of electronic and thermal Enthalpies= -763.802715
Sum of electronic and thermal Free Energies= -763.861239

	E (Thermal)	CV	S
	KCal/Mol	Cal/Mol-Kelvin	Cal/Mol-Kelvin
Total	129.747	54.021	123.173

Center Number	Atomic Number	Atomic Type	Coordinates (Angstroms) X	Y	Z
1	6	0	0.575240	1.769189	-0.406002
2	6	0	2.274226	-0.081051	-0.859551
3	6	0	2.686683	-0.054535	0.570113
4	6	0	1.205336	0.785947	-1.333390
5	8	0	-0.239343	2.610928	-0.786907
6	8	0	3.595140	-0.763583	1.009561
7	6	0	0.844224	-1.970129	-1.054250
8	1	0	1.297525	-2.776040	-1.631516
9	6	0	-0.906942	-1.230923	-0.259863
10	6	0	0.088005	-2.136982	0.139138
11	1	0	0.244068	-2.706872	1.047770
12	1	0	1.347969	1.203681	-2.334515
13	1	0	3.120979	-0.226745	-1.534640
14	6	0	-2.114928	-0.739976	0.417989
15	8	0	-2.478419	-1.095770	1.529238
16	8	0	-2.774798	0.157687	-0.352623
17	6	0	-3.962839	0.739145	0.231806
18	1	0	-4.714656	-0.033942	0.411224
19	1	0	-4.315570	1.464182	-0.500179
20	1	0	-3.719148	1.229230	1.177388
21	6	0	-0.283167	-0.941157	-1.520946
22	1	0	-0.817776	-0.932355	-2.472893
23	6	0	0.980793	1.698565	1.020080
24	1	0	0.464583	2.384207	1.686951
25	6	0	1.949581	0.872734	1.463186
26	1	0	2.254123	0.855597	2.506387

CBBQi-ts

RB3LYP/6-31G (d)

SCF Done: E(RB+HF-LYP) = -764.011738605

Zero-point correction= 0.192236 (Hartree/Particle)

Thermal correction to Energy= 0.206957

Thermal correction to Enthalpy= 0.207901

Thermal correction to Gibbs Free Energy= 0.149692

Sum of electronic and zero-point Energies= -763.819502

Sum of electronic and thermal Energies= -763.804782

Sum of electronic and thermal Enthalpies= -763.803838

Sum of electronic and thermal Free Energies= -763.862047

Center Number	Atomic Number	Atomic Type	Coordinates (Angstroms) X	Y	Z
1	1	0	-1.581887	-0.930462	-2.131569
2	6	0	-1.481099	-0.273886	-1.272328
3	6	0	-0.409473	0.593762	-1.162430
4	6	0	-0.470463	-1.865928	0.047295
5	6	0	0.730956	-0.929869	0.397880
6	1	0	-0.613960	-2.628271	-0.706591
7	1	0	0.395964	0.579633	-1.889501
8	6	0	-0.919531	-1.702123	1.339418
9	1	0	-1.775122	-2.070493	1.891136
10	6	0	0.209401	-0.824245	1.667249
11	1	0	0.534151	-0.309817	2.564324
12	6	0	-0.395704	1.694714	-0.183334
13	6	0	-2.700153	-0.097651	-0.448564
14	8	0	0.479557	2.557052	-0.162925
15	8	0	-3.737601	-0.717792	-0.658991
16	6	0	2.042471	-0.697627	-0.203240
17	8	0	2.402058	-1.163287	-1.270148
18	8	0	2.794130	0.109970	0.575364
19	6	0	4.070392	0.478631	0.026551
20	1	0	4.684710	-0.408333	-0.149114
21	1	0	4.530725	1.125452	0.773379
22	1	0	3.936441	1.017122	-0.915114
23	6	0	-2.593005	0.892564	0.653526
24	1	0	-3.449531	0.951812	1.320685
25	6	0	-1.531503	1.716256	0.775681
26	1	0	-1.480384	2.478214	1.549733

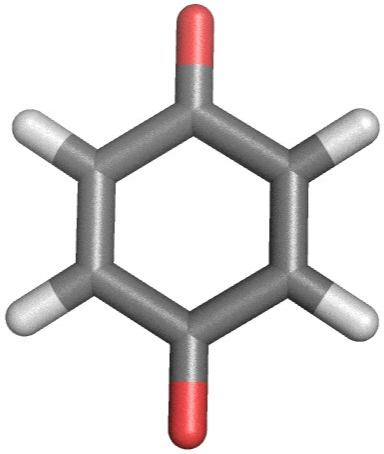

Benzoquinone
RB3LYP/6-31G(d)
SCF Done: E(RB+HF-LYP) = -381.451687350
Zero-point correction= 0.085361 (Hartree/Particle)
Thermal correction to Energy= 0.091592
Thermal correction to Enthalpy= 0.092536
Thermal correction to Gibbs Free Energy= 0.056156
Sum of electronic and zero-point Energies= -381.366327
Sum of electronic and thermal Energies= -381.360095
Sum of electronic and thermal Enthalpies= -381.359151
Sum of electronic and thermal Free Energies= -381.395531

	E (Thermal) KCal/Mol	CV Cal/Mol-Kelvin	S Cal/Mol-Kelvin
Total	57.475	23.264	76.568

Center Number	Atomic Number	Atomic Type	Coordinates (Angstroms) X	Y	Z
1	6	0	0.000000	1.269343	0.671513
2	6	0	0.000000	1.269343	-0.671513
3	6	0	0.000000	0.000000	-1.445316
4	6	0	0.000000	-1.269343	-0.671513
5	6	0	0.000000	-1.269343	0.671513
6	6	0	0.000000	0.000000	1.445316
7	1	0	0.000000	2.182778	1.259834
8	1	0	0.000000	2.182778	-1.259834
9	1	0	0.000000	-2.182778	-1.259834
10	1	0	0.000000	-2.182778	1.259834
11	8	0	0.000000	0.000000	-2.670228
12	8	0	0.000000	0.000000	2.670228

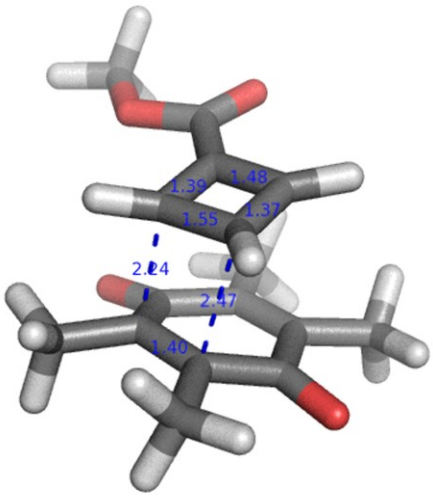

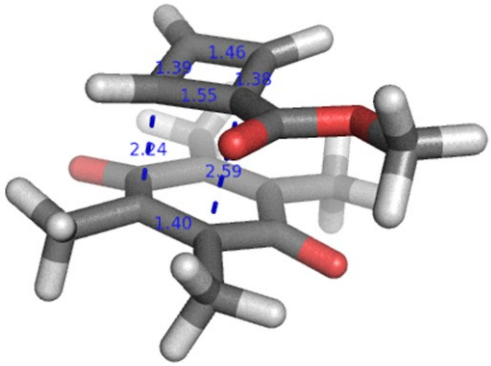

CBDQts-e **CBDQts-i**

CBDQts-e
RB3LYP/6-31G (d)
SCF Done: E(RB+HF-LYP) = -921.289592409
Zero-point correction= 0.304097 (Hartree/Particle)
Thermal correction to Energy= 0.325255
Thermal correction to Enthalpy= 0.326199
Thermal correction to Gibbs Free Energy= 0.254679
Sum of electronic and zero-point Energies= -920.985496
Sum of electronic and thermal Energies= -920.964338
Sum of electronic and thermal Enthalpies= -920.963394
Sum of electronic and thermal Free Energies= -921.034913

	E (Thermal) KCal/Mol	CV Cal/Mol-Kelvin	S Cal/Mol-Kelvin
Total	204.100	77.162	150.525

Center Number	Atomic Number	Atomic Type	Coordinates (Angstroms) X	Y	Z
1	6	0	-0.014053	-0.336920	-1.413703
2	6	0	2.071706	-0.767869	-0.103803
3	6	0	2.281801	0.694411	0.013581
4	6	0	0.930927	-1.276788	-0.738893
5	8	0	-0.860651	-0.757618	-2.200067
6	8	0	3.345671	1.153809	0.437145
7	6	0	0.875541	-0.721478	2.053787

8	1	0	1.778842	-1.057563	2.542488
9	6	0	-0.996254	-0.282364	1.367116
10	6	0	0.053309	0.363431	2.178816
11	1	0	0.128386	1.325553	2.670466
12	6	0	-2.340174	0.114916	0.960565
13	8	0	-2.838972	1.200502	1.208082
14	8	0	-2.959284	-0.871135	0.275209
15	6	0	-4.265417	-0.548567	-0.226615
16	1	0	-4.943361	-0.303195	0.595394
17	1	0	-4.603106	-1.441807	-0.752087
18	1	0	-4.211744	0.300152	-0.913142
19	6	0	-0.203840	-1.410561	1.184291
20	1	0	-0.457795	-2.446592	1.001332
21	6	0	0.104433	1.116228	-1.109690
22	6	0	1.182473	1.597047	-0.428469
23	6	0	-0.974940	2.011944	-1.655443
24	1	0	-1.652914	2.332657	-0.853125
25	1	0	-0.555732	2.914574	-2.112436
26	1	0	-1.561457	1.472160	-2.401294
27	6	0	1.377159	3.066232	-0.161972
28	1	0	1.589236	3.608667	-1.093377
29	1	0	0.476724	3.514750	0.271587
30	1	0	2.224449	3.216699	0.508735
31	6	0	0.865361	-2.709130	-1.218953
32	1	0	-0.160232	-2.969041	-1.487272
33	1	0	1.477284	-2.830966	-2.122713
34	1	0	1.241648	-3.414574	-0.472676
35	6	0	3.236118	-1.645871	0.267724
36	1	0	2.922201	-2.544164	0.810824
37	1	0	3.759371	-1.989142	-0.635758
38	1	0	3.949182	-1.080611	0.870069

CBDQts-i

RB3LYP/6-31G (d)

E(RB+HF-LYP) = -921.289147602

Zero-point correction= 0.304085 (Hartree/Particle)

Thermal correction to Energy= 0.325278

Thermal correction to Enthalpy= 0.326222

Thermal correction to Gibbs Free Energy= 0.254364

Sum of electronic and zero-point Energies= -920.985063

Sum of electronic and thermal Energies= -920.963870

Sum of electronic and thermal Enthalpies= -920.962926

Sum of electronic and thermal Free Energies= -921.034783

	E (Thermal) KCal/Mol	CV Cal/Mol-Kelvin	S Cal/Mol-Kelvin
Total	204.115	77.069	151.237

Center Number	Atomic Number	Atomic Type	Coordinates (Angstroms) X	Y	Z
1	6	0	0.908638	-1.382475	0.578367
2	6	0	0.005751	-0.514776	1.207444
3	6	0	-0.040730	-1.290148	-1.444562
4	6	0	-1.113379	-0.214448	-1.112874
5	1	0	-0.090854	-2.369525	-1.499645
6	6	0	0.595824	-0.341516	-2.233002
7	1	0	1.483268	-0.351920	-2.852523
8	6	0	-0.404542	0.667951	-1.900006
9	1	0	-0.563406	1.701773	-2.185191
10	6	0	0.245722	0.947275	1.211778
11	6	0	2.211059	-0.852763	0.076918
12	8	0	-0.480948	1.717162	1.845189
13	8	0	3.133371	-1.612484	-0.212776
14	6	0	-2.484663	-0.287453	-0.639323
15	8	0	-3.047615	-1.324842	-0.323843
16	8	0	-3.064647	0.934433	-0.600330
17	6	0	-4.419956	0.955255	-0.126810
18	1	0	-5.065976	0.361188	-0.779306
19	1	0	-4.717132	2.004061	-0.143609
20	1	0	-4.477639	0.557773	0.889806
21	6	0	2.359356	0.624176	-0.059238
22	6	0	1.431005	1.467638	0.472338
23	6	0	0.870313	-2.868960	0.851486
24	1	0	1.520868	-3.399975	0.154148
25	1	0	1.243072	-3.075581	1.863791
26	1	0	-0.145874	-3.267595	0.788614
27	6	0	-1.085474	-1.025200	2.105030
28	1	0	-1.751644	-1.725743	1.591587
29	1	0	-0.648511	-1.554643	2.963271
30	1	0	-1.672180	-0.186259	2.482296
31	6	0	1.591078	2.964138	0.443949
32	1	0	1.892272	3.320233	-0.547400
33	1	0	0.659322	3.446178	0.743603
34	1	0	2.371473	3.284743	1.147786
35	6	0	3.625785	1.117008	-0.709874
36	1	0	3.411987	1.814005	-1.529066

37	1	0	4.252721	1.659012	0.010095
38	1	0	4.202217	0.273901	-1.093916

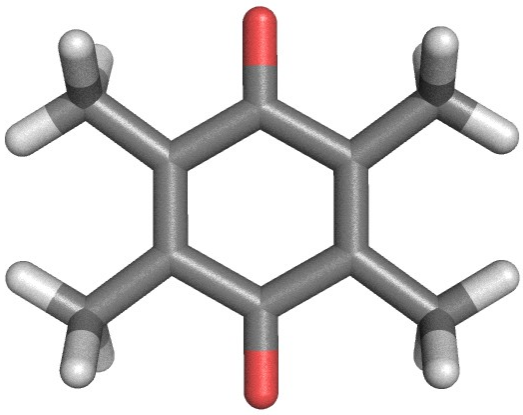

duroquinone

RB3LYP/6-31G (d)

SCF Done: E(RB+HF-LYP) = -538.733148669

Zero-point correction= 0.196911 (Hartree/Particle)

Thermal correction to Energy= 0.210250

Thermal correction to Enthalpy= 0.211194

Thermal correction to Gibbs Free Energy= 0.157128

Sum of electronic and zero-point Energies= -538.536238

Sum of electronic and thermal Energies= -538.522898

Sum of electronic and thermal Enthalpies= -538.521954

Sum of electronic and thermal Free Energies= -538.576020

	E (Thermal) KCal/Mol	CV Cal/Mol-Kelvin	S Cal/Mol-Kelvin
Total	131.934	46.671	113.792

Center Number	Atomic Number	Atomic Type	Coordinates (Angstroms) X	Y	Z
1	6	0	1.301282	0.000003	0.676860
2	6	0	1.301282	-0.000003	-0.676860
3	6	0	0.000000	0.000000	-1.414370
4	6	0	0.000000	0.000000	1.414370
5	6	0	-1.301282	0.000003	-0.676860
6	6	0	-1.301282	-0.000003	0.676860
7	8	0	0.000000	0.000000	-2.642976
8	8	0	0.000000	0.000000	2.642976

9	6	0	-2.514634	0.000008	-1.565756
10	1	0	-2.501499	-0.874569	-2.225715
11	1	0	-2.501428	0.874523	-2.225796
12	1	0	-3.448767	0.000070	-1.003524
13	6	0	-2.514634	-0.000008	1.565756
14	1	0	-2.501428	-0.874523	2.225796
15	1	0	-3.448767	-0.000070	1.003524
16	1	0	-2.501499	0.874569	2.225715
17	6	0	2.514634	-0.000008	-1.565756
18	1	0	2.501428	-0.874523	-2.225796
19	1	0	3.448767	-0.000070	-1.003524
20	1	0	2.501499	0.874569	-2.225715
21	6	0	2.514634	0.000008	1.565756
22	1	0	2.501499	-0.874569	2.225715
23	1	0	2.501428	0.874523	2.225796
24	1	0	3.448767	0.000070	1.003524

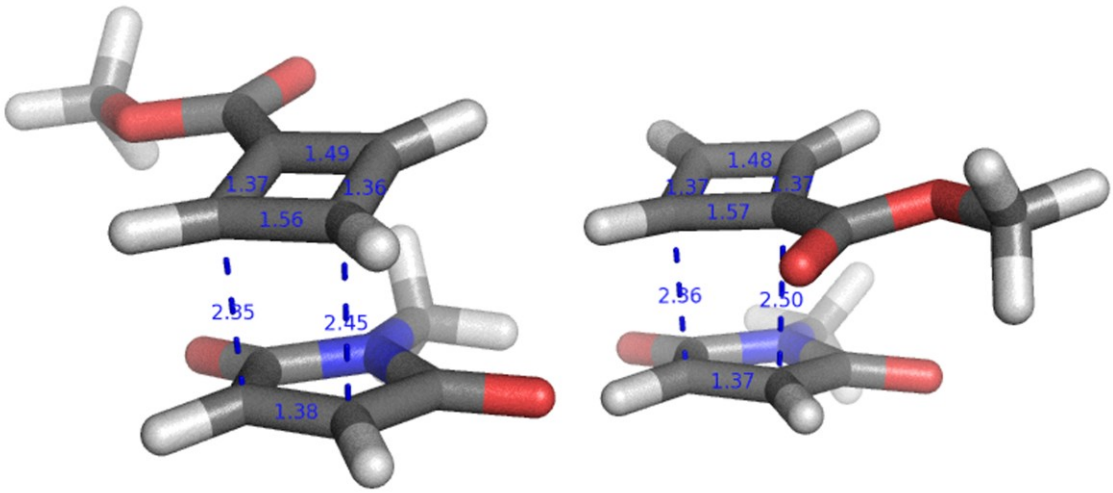

CBMMts-e **CBMMts-i**

CBMMts-e

RB3LYP/6-31G (d)

SCF Done: E(RB+HF-LYP) = -781.303109592

Zero-point correction= 0.203557 (Hartree/Particle)

Thermal correction to Energy= 0.219031

Thermal correction to Enthalpy= 0.219975

Thermal correction to Gibbs Free Energy= 0.160366

Sum of electronic and zero-point Energies= -781.099552

Sum of electronic and thermal Energies= -781.084079

Sum of electronic and thermal Enthalpies= -781.083135

Sum of electronic and thermal Free Energies= -781.142744

	E (Thermal) KCal/Mol	CV Cal/Mol-Kelvin	S Cal/Mol-Kelvin
Total	137.444	55.950	125.458

Center Number	Atomic Number	Atomic Type	Coordinates (Angstroms) X	Y	Z
1	6	0	0.485173	-0.959841	1.093074
2	6	0	2.252328	0.546587	0.990466
3	6	0	2.340138	-0.373243	-0.176072
4	6	0	1.142506	0.215972	1.732579
5	8	0	-0.455198	-1.627391	1.484304
6	8	0	3.209758	-0.462906	-1.022587
7	6	0	1.028155	2.302048	-0.199639
8	1	0	1.829607	3.019649	-0.089361
9	6	0	-0.722858	1.264397	-0.404539
10	6	0	0.424761	1.683948	-1.253157
11	1	0	0.677673	1.530036	-2.294749
12	1	0	0.900413	0.519348	2.742308
13	1	0	3.067038	1.206207	1.256756
14	6	0	-1.891923	0.417151	-0.652375
15	8	0	-2.080913	-0.186754	-1.693992
16	8	0	-2.704524	0.372021	0.420273
17	6	0	-3.786228	-0.571538	0.334365
18	1	0	-4.412421	-0.361226	-0.536230
19	1	0	-4.352539	-0.448044	1.257474
20	1	0	-3.387666	-1.586489	0.263630
21	6	0	-0.173359	1.865171	0.702161
22	1	0	-0.575475	2.199202	1.649190
23	7	0	1.189011	-1.178609	-0.099296
24	6	0	0.867544	-2.238641	-1.039238
25	1	0	1.691661	-2.305526	-1.751351
26	1	0	0.751910	-3.186918	-0.506926
27	1	0	-0.063691	-2.007813	-1.565395

CBMMts-i

RB3LYP/6-31G (d)

SCF Done: E(RB+HF-LYP) = -781.303100336

Zero-point correction= 0.203427 (Hartree/Particle)

Thermal correction to Energy= 0.219145

Thermal correction to Enthalpy= 0.220089

Thermal correction to Gibbs Free Energy= 0.159287

Sum of electronic and zero-point Energies= -781.099674
Sum of electronic and thermal Energies= -781.083956
Sum of electronic and thermal Enthalpies= -781.083011
Sum of electronic and thermal Free Energies= -781.143814

	E (Thermal) KCal/Mol	CV Cal/Mol-Kelvin	S Cal/Mol-Kelvin
Total	137.515	55.971	127.969

Center Number	Atomic Number	Atomic Type	Coordinates (Angstroms) X	Y	Z
1	1	0	-1.178626	-1.618233	-2.078594
2	6	0	-1.171555	-0.790918	-1.382193
3	6	0	-0.307513	0.273400	-1.342481
4	6	0	0.042320	-2.002967	0.241656
5	6	0	1.025304	-0.800036	0.478115
6	1	0	0.080861	-2.876167	-0.395273
7	1	0	0.568729	0.442177	-1.952301
8	6	0	-0.538841	-1.714526	1.446854
9	1	0	-1.367344	-2.132698	2.004484
10	6	0	0.387218	-0.584566	1.671964
11	1	0	0.529969	0.131650	2.473171
12	6	0	-0.887533	1.326067	-0.466215
13	6	0	-2.369285	-0.459526	-0.554299
14	8	0	-0.484610	2.449165	-0.229469
15	8	0	-3.403584	-1.084156	-0.414237
16	6	0	2.313529	-0.431735	-0.097749
17	8	0	2.803135	-0.962817	-1.080219
18	8	0	2.894494	0.576436	0.592723
19	6	0	4.149098	1.035880	0.066046
20	1	0	4.886287	0.228420	0.066895
21	1	0	4.462994	1.844001	0.727046
22	1	0	4.025495	1.403920	-0.956139
23	7	0	-2.074244	0.774270	0.049364
24	6	0	-3.011286	1.519099	0.869801
25	1	0	-3.865169	0.868642	1.065971
26	1	0	-2.541547	1.816582	1.811120
27	1	0	-3.346166	2.421761	0.348688

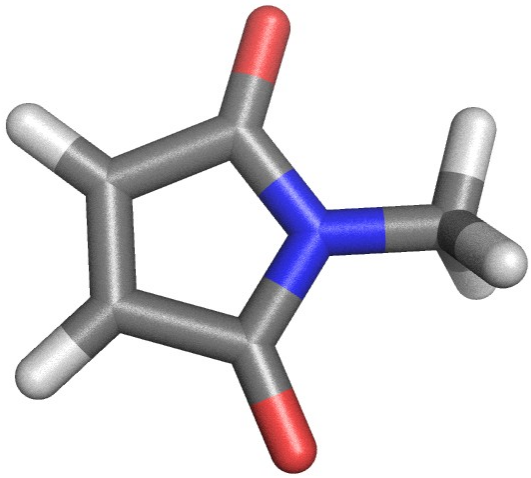

***N*-Methylmaleimide**
RB3LYP/6-31G (d)
SCF Done: E(RB+HF-LYP) = -398.744261305
Zero-point correction= 0.096652 (Hartree/Particle)
Thermal correction to Energy= 0.103856
Thermal correction to Enthalpy= 0.104800
Thermal correction to Gibbs Free Energy= 0.064553
Sum of electronic and zero-point Energies= -398.647610
Sum of electronic and thermal Energies= -398.640405
Sum of electronic and thermal Enthalpies= -398.639461
Sum of electronic and thermal Free Energies= -398.679709

	E (Thermal) KCal/Mol	CV Cal/Mol-Kelvin	S Cal/Mol-Kelvin
Total	65.171	25.178	84.709

Center Number	Atomic Number	Atomic Type	Coordinates (Angstroms) X	Y	Z
1	6	0	0.669540	-1.627024	0.000000
2	1	0	1.359607	-2.461123	0.000000
3	6	0	-0.666574	-1.628002	0.000000
4	1	0	-1.355806	-2.462787	0.000000
5	6	0	-1.150264	-0.204114	0.000000
6	6	0	1.149392	-0.201550	0.000000
7	8	0	-2.295414	0.198371	0.000000
8	8	0	2.291562	0.209495	0.000000
9	7	0	0.000000	0.591820	0.000000
10	6	0	0.003902	2.043199	0.000000
11	1	0	0.513666	2.425183	0.889296
12	1	0	-1.036293	2.372821	0.000000

13	1	0	0.513666	2.425183	-0.889296

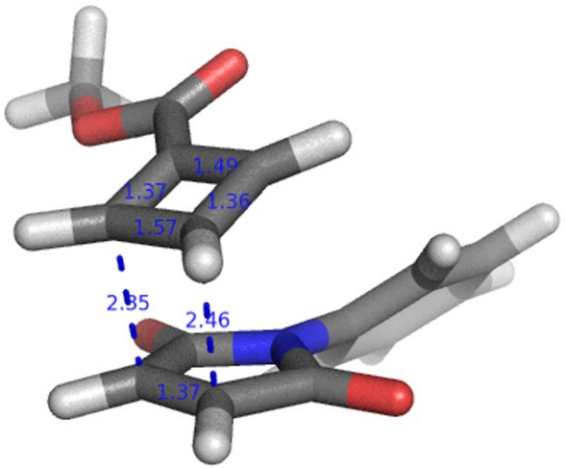

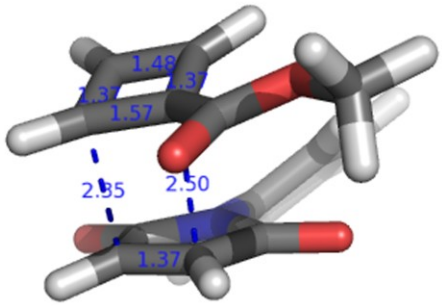

CBPMts-e **CBPMts-i**

CBPMts-e

RB3LYP/6-31G (d)

SCF Done: E(RB+HF-LYP) = -973.035446195

Zero-point correction= 0.255727 (Hartree/Particle)

Thermal correction to Energy= 0.274313

Thermal correction to Enthalpy= 0.275257

Thermal correction to Gibbs Free Energy= 0.206792

Sum of electronic and zero-point Energies= -972.779719

Sum of electronic and thermal Energies= -972.761133

Sum of electronic and thermal Enthalpies= -972.760189

Sum of electronic and thermal Free Energies= -972.828654

	E (Thermal) KCal/Mol	CV Cal/Mol-Kelvin	S Cal/Mol-Kelvin
Total	172.134	69.609	144.098

Center Number	Atomic Number	Atomic Type	Coordinates (Angstroms) X	Y	Z
1	6	0	0.326597	-0.502026	1.513384
2	6	0	0.961535	-2.609957	0.767508
3	6	0	-0.330297	-2.259256	0.127129
4	6	0	1.361662	-1.569459	1.566172
5	8	0	0.275974	0.525161	2.160679
6	8	0	-1.028552	-2.946179	-0.590637
7	6	0	2.413668	-1.846444	-1.069204
8	1	0	2.774522	-2.848678	-1.255340

9	6	0	2.092904	0.162191	-0.841878
10	6	0	1.715590	-0.925398	-1.787776
11	1	0	1.112964	-0.952994	-2.687014
12	1	0	2.119442	-1.569107	2.337937
13	1	0	1.355699	-3.615810	0.720558
14	6	0	1.776595	1.592457	-0.790396
15	8	0	1.109332	2.167483	-1.629171
16	8	0	2.316637	2.175027	0.299151
17	6	0	1.974325	3.557721	0.489263
18	1	0	2.314029	4.158305	-0.358830
19	1	0	2.483116	3.859190	1.404837
20	1	0	0.892489	3.665977	0.599148
21	6	0	2.818136	-0.710327	-0.069361
22	1	0	3.616653	-0.579925	0.648827
23	7	0	-0.623891	-0.934317	0.554214
24	6	0	-1.814038	-0.227573	0.204097
25	6	0	-2.522264	0.491057	1.174978
26	6	0	-2.275985	-0.266511	-1.116602
27	6	0	-3.684279	1.172549	0.814962
28	1	0	-2.158376	0.525874	2.193664
29	6	0	-3.446304	0.407483	-1.459501
30	1	0	-1.728560	-0.829054	-1.862552
31	6	0	-4.153281	1.131846	-0.498543
32	1	0	-4.226855	1.732977	1.571468
33	1	0	-3.800600	0.370096	-2.485874
34	1	0	-5.061799	1.661315	-0.771901

CBPMts-i

RB3LYP/6-31G (d)

SCF Done: E(RB+HF-LYP) = -973.037919674

Zero-point correction= 0.255995 (Hartree/Particle)

Thermal correction to Energy= 0.274547

Thermal correction to Enthalpy= 0.275492

Thermal correction to Gibbs Free Energy= 0.207473

Sum of electronic and zero-point Energies= -972.781925

Sum of electronic and thermal Energies= -972.763372

Sum of electronic and thermal Enthalpies= -972.762428

Sum of electronic and thermal Free Energies= -972.830447

	E (Thermal) KCal/Mol	CV Cal/Mol-Kelvin	S Cal/Mol-Kelvin
Total	172.281	69.452	143.158

Center Number	Atomic Number	Atomic Type	Coordinates (Angstroms) X	Y	Z
1	1	0	-0.957706	2.978967	-1.111503
2	6	0	-0.557778	1.991464	-0.926712
3	6	0	-1.025454	0.788725	-1.385074
4	6	0	-1.672946	1.793363	1.133863
5	6	0	-2.150424	0.333672	0.799396
6	1	0	-2.131675	2.766021	1.018430
7	1	0	-1.926980	0.593556	-1.948219
8	6	0	-0.766135	1.254461	2.007332
9	1	0	0.000532	1.667040	2.650827
10	6	0	-1.217501	-0.117168	1.697585
11	1	0	-0.940600	-1.103163	2.052732
12	6	0	0.024401	-0.240610	-1.200722
13	6	0	0.840512	1.810071	-0.447293
14	8	0	0.010179	-1.405153	-1.543278
15	8	0	1.613681	2.663978	-0.060463
16	6	0	-3.357696	-0.211001	0.188160
17	8	0	-4.202091	0.460627	-0.379918
18	8	0	-3.418922	-1.555147	0.327254
19	6	0	-4.555288	-2.183289	-0.287217
20	1	0	-5.485077	-1.807981	0.148644
21	1	0	-4.440261	-3.249090	-0.089091
22	1	0	-4.563974	-1.992768	-1.363830
23	7	0	1.105615	0.420920	-0.546977
24	6	0	2.339004	-0.208776	-0.201811
25	6	0	2.329411	-1.513909	0.307880
26	6	0	3.554281	0.466567	-0.373105
27	6	0	3.531382	-2.136272	0.639322
28	1	0	1.390520	-2.041061	0.421974
29	6	0	4.748075	-0.164405	-0.024350
30	1	0	3.560631	1.477199	-0.759042
31	6	0	4.744853	-1.465202	0.479809
32	1	0	3.515078	-3.151192	1.027201
33	1	0	5.686209	0.368031	-0.155178
34	1	0	5.679027	-1.952580	0.744743

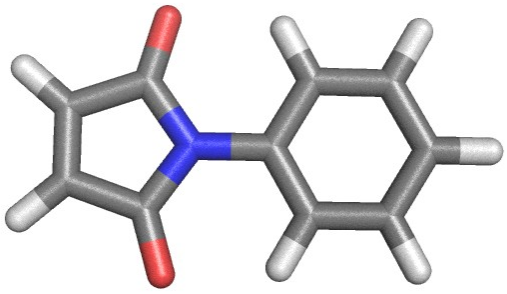

***N*-Phenylmaleimide**
RB3LYP/6-31G (d)
SCF Done: E(RB+HF-LYP) = -590.476515413
Zero-point correction= 0.149646 (Hartree/Particle)
Thermal correction to Energy= 0.158596
Thermal correction to Enthalpy= 0.159541
Thermal correction to Gibbs Free Energy= 0.115797
Sum of electronic and zero-point Energies= -590.326869
Sum of electronic and thermal Energies= -590.317919
Sum of electronic and thermal Enthalpies= -590.316975
Sum of electronic and thermal Free Energies= -590.360719

	E (Thermal) KCal/Mol	CV Cal/Mol-Kelvin	S Cal/Mol-Kelvin
Total	99.521	36.535	92.067

Center Number	Atomic Number	Atomic Type	Coordinates (Angstroms) X	Y	Z
1	7	0	0.000000	0.000000	0.758124
2	6	0	0.000000	1.149216	1.591404
3	6	0	0.000000	0.665629	3.007455
4	6	0	0.000000	-0.665629	3.007455
5	6	0	0.000000	-1.149216	1.591404
6	1	0	0.000000	1.364572	3.833804
7	1	0	0.000000	-1.364572	3.833804
8	8	0	0.000000	2.312837	1.249092
9	8	0	0.000000	-2.312837	1.249092
10	6	0	0.000000	0.000000	-0.681184
11	6	0	0.000000	0.000000	-3.495785
12	6	0	0.000000	1.211720	-1.392220

13	6	0	0.000000	-1.211720	-1.392220
14	6	0	0.000000	-1.199550	-2.786403
15	6	0	0.000000	1.199550	-2.786403
16	1	0	0.000000	2.152211	-0.863199
17	1	0	0.000000	-2.152211	-0.863199
18	1	0	0.000000	-2.148437	-3.316205
19	1	0	0.000000	2.148437	-3.316205
20	1	0	0.000000	0.000000	-4.582161

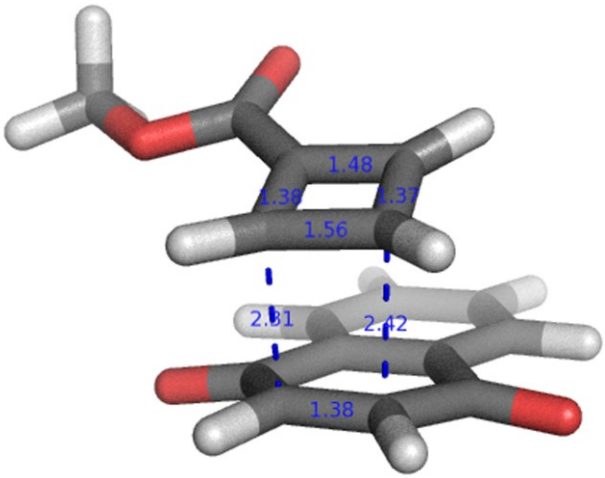

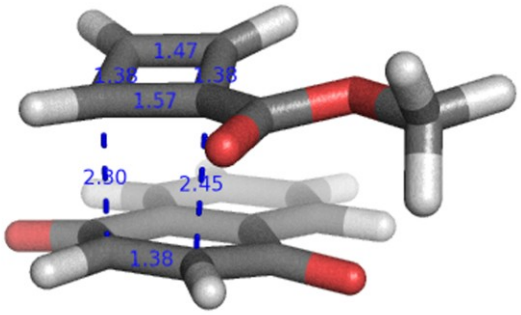

CBNQts-e **CBNQts-i**

CBNQts-e

RB3LYP/6-31G (d)

SCF Done: E(RB+HF-LYP) = -917.671737991

Zero-point correction= 0.239583 (Hartree/Particle)

Thermal correction to Energy= 0.256870

Thermal correction to Enthalpy= 0.257815

Thermal correction to Gibbs Free Energy= 0.193207

Sum of electronic and zero-point Energies= -917.432155

Sum of electronic and thermal Energies= -917.414868

Sum of electronic and thermal Enthalpies= -917.413923

Sum of electronic and thermal Free Energies= -917.478531

	E (Thermal) KCal/Mol	CV Cal/Mol-Kelvin	S Cal/Mol-Kelvin
Total	161.189	65.166	135.978

Center Number	Atomic Number	Atomic Type	Coordinates (Angstroms) X	Y	Z

1	6	0	-0.089525	-0.123504	1.720135
2	6	0	-1.683891	-1.831513	0.822645
3	6	0	-2.430026	-0.818901	0.053324
4	6	0	-0.571064	-1.515761	1.582601
5	8	0	0.769227	0.182289	2.541420
6	8	0	-3.489918	-1.086477	-0.507993
7	6	0	-0.305666	-2.524816	-1.036093
8	1	0	-0.928688	-3.394274	-1.193572
9	6	0	1.189618	-1.136822	-0.896493
10	6	0	0.057167	-1.451643	-1.798226
11	1	0	-0.323227	-0.991964	-2.701762
12	6	0	2.239278	-0.115024	-0.928041
13	8	0	2.361303	0.709043	-1.814621
14	8	0	3.053666	-0.216913	0.144097
15	6	0	4.098441	0.765315	0.219545
16	1	0	4.781344	0.665161	-0.628826
17	1	0	4.616475	0.566820	1.157621
18	1	0	3.675826	1.773323	0.219766
19	6	0	0.882162	-2.199129	-0.073341
20	1	0	1.469961	-2.781131	0.624194
21	1	0	-2.163252	-2.802634	0.905601
22	1	0	-0.179915	-2.214822	2.316287
23	6	0	-1.834613	0.550974	0.016118
24	6	0	-0.717905	0.883718	0.812920
25	6	0	-2.426850	1.530910	-0.791518
26	1	0	-3.294838	1.253843	-1.381244
27	6	0	-0.213630	2.190891	0.788829
28	1	0	0.633409	2.426182	1.425252
29	6	0	-1.907391	2.820531	-0.820537
30	1	0	-2.365142	3.575360	-1.454086
31	6	0	-0.798931	3.151312	-0.028800
32	1	0	-0.399217	4.161375	-0.050859

CBNQts-i

RB3LYP/6-31G (d)

SCF Done: E(RB+HF-LYP) = -917.673812326

Zero-point correction= 0.239800 (Hartree/Particle)

Thermal correction to Energy= 0.257072

Thermal correction to Enthalpy= 0.258017

Thermal correction to Gibbs Free Energy= 0.193681

Sum of electronic and zero-point Energies= -917.434013

Sum of electronic and thermal Energies= -917.416740

Sum of electronic and thermal Enthalpies= -917.415796

Sum of electronic and thermal Free Energies= -917.480131

	E (Thermal) KCal/Mol	CV Cal/Mol-Kelvin	S Cal/Mol-Kelvin
Total	161.315	65.044	135.405

Center Number	Atomic Number	Atomic Type	Coordinates (Angstroms) X	Y	Z
1	6	0	0.260021	1.605139	-1.216599
2	6	0	-0.472825	0.451739	-1.430187
3	6	0	-0.788245	2.034279	0.788378
4	6	0	-1.560235	0.669062	0.758979
5	1	0	-1.051891	3.035929	0.476675
6	6	0	-0.013550	1.522906	1.804128
7	1	0	0.817772	1.905585	2.382574
8	6	0	-0.736511	0.246361	1.776711
9	1	0	-0.670528	-0.673090	2.346823
10	6	0	0.054959	-0.889209	-1.128345
11	6	0	1.654802	1.563608	-0.723535
12	8	0	-0.557103	-1.910322	-1.433570
13	8	0	2.362046	2.566234	-0.702144
14	6	0	-2.866905	0.259400	0.252546
15	8	0	-3.590753	0.961357	-0.432114
16	8	0	-3.160857	-1.003200	0.633652
17	6	0	-4.384642	-1.535258	0.101261
18	1	0	-5.237930	-0.928199	0.415035
19	1	0	-4.461043	-2.545288	0.504169
20	1	0	-4.343224	-1.561815	-0.990711
21	1	0	-0.050159	2.549532	-1.653821
22	1	0	-1.413851	0.484938	-1.969388
23	6	0	2.151001	0.232862	-0.257114
24	6	0	1.384891	-0.937538	-0.445447
25	6	0	1.895475	-2.174514	-0.029838
26	1	0	1.293500	-3.061064	-0.202224
27	6	0	3.415307	0.146354	0.341453
28	1	0	3.992014	1.058542	0.457575
29	6	0	3.145325	-2.247288	0.576130
30	1	0	3.536100	-3.208373	0.899439
31	6	0	3.907101	-1.084893	0.761438
32	1	0	4.886760	-1.147321	1.227513

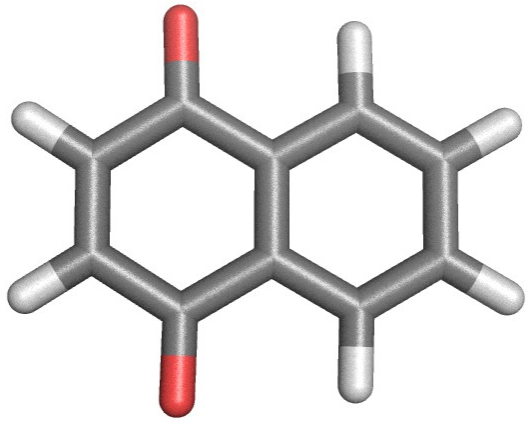

1,4-Naphthoquinone
RB3LYP/6-31G (d)
SCF Done: E(RB+HF-LYP) = -535.115946612
Zero-point correction= 0.133157 (Hartree/Particle)
Thermal correction to Energy= 0.141789
Thermal correction to Enthalpy= 0.142733
Thermal correction to Gibbs Free Energy= 0.099824
Sum of electronic and zero-point Energies= -534.982790
Sum of electronic and thermal Energies= -534.974158
Sum of electronic and thermal Enthalpies= -534.973214
Sum of electronic and thermal Free Energies= -535.016123

	E (Thermal) KCal/Mol	CV Cal/Mol-Kelvin	S Cal/Mol-Kelvin
Total	88.974	34.304	90.310

Center Number	Atomic Number	Atomic Type	Coordinates (Angstroms) X	Y	Z
1	1	0	0.000000	2.485169	1.447453
2	6	0	0.000000	1.400181	1.472770
3	6	0	0.000000	-1.400181	1.472770
4	6	0	0.000000	0.704424	0.260020
5	6	0	0.000000	0.699646	2.677524
6	6	0	0.000000	-0.699646	2.677524
7	6	0	0.000000	-0.704424	0.260020
8	1	0	0.000000	1.242217	3.618819
9	1	0	0.000000	-1.242217	3.618819
10	1	0	0.000000	-2.485169	1.447453
11	6	0	0.000000	1.462995	-1.024668
12	6	0	0.000000	-1.462995	-1.024668

13	6	0	0.000000	0.671749	-2.281510
14	1	0	0.000000	1.253978	-3.199048
15	6	0	0.000000	-0.671749	-2.281510
16	1	0	0.000000	-1.253978	-3.199048
17	8	0	0.000000	2.688118	-1.061506
18	8	0	0.000000	-2.688118	-1.061506

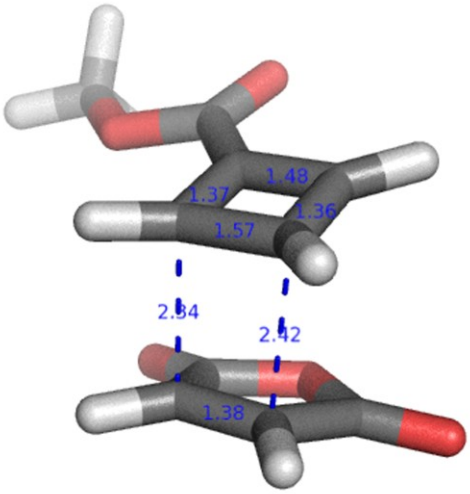

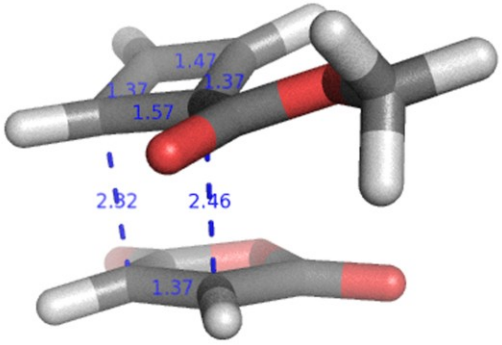

CBMAts-e **CBMAts-i**

CBMAts-e

RB3LYP/6-31G(d)

SCF Done: E(RB+HF-LYP) = -761.846248649

Zero-point correction= 0.162463 (Hartree/Particle)

Thermal correction to Energy= 0.176182

Thermal correction to Enthalpy= 0.177126

Thermal correction to Gibbs Free Energy= 0.120625

Sum of electronic and zero-point Energies= -761.683786

Sum of electronic and thermal Energies= -761.670067

Sum of electronic and thermal Enthalpies= -761.669123

Sum of electronic and thermal Free Energies= -761.725624

	E (Thermal) KCal/Mol	CV Cal/Mol-Kelvin	S Cal/Mol-Kelvin
Total	110.556	49.513	118.917

Center Number	Atomic Number	Atomic Type	Coordinates (Angstroms) X	Y	Z
1	6	0	-0.687733	1.540270	0.133122
2	6	0	-2.397064	0.154189	0.828919

3	6	0	-2.431272	0.276897	-0.641923
4	6	0	-1.338128	0.897603	1.296437
5	8	0	0.197530	2.350048	0.076061
6	8	0	-3.221307	-0.135348	-1.447487
7	6	0	-1.090180	-1.885553	0.870883
8	1	0	-1.895998	-2.446386	1.324464
9	6	0	0.697287	-1.123258	0.230075
10	6	0	-0.391032	-1.984430	-0.295866
11	1	0	-0.554651	-2.475607	-1.246983
12	1	0	-1.143689	1.229151	2.307205
13	1	0	-3.217784	-0.277451	1.384765
14	6	0	1.960916	-0.647201	-0.348807
15	8	0	2.369479	-0.984997	-1.442020
16	8	0	2.593848	0.195974	0.489662
17	6	0	3.805559	0.777535	-0.022784
18	1	0	4.534172	-0.002241	-0.259638
19	1	0	4.175147	1.424614	0.772374
20	1	0	3.591933	1.359143	-0.922802
21	8	0	-1.313806	1.038232	-1.014359
22	6	0	0.056088	-0.973968	1.436006
23	1	0	0.398271	-0.715001	2.429379

CBMAts-i

RB3LYP/6-31G (d)

SCF Done: E(RB+HF-LYP) = -761.848910616

Zero-point correction= 0.162586 (Hartree/Particle)

Thermal correction to Energy= 0.176335

Thermal correction to Enthalpy= 0.177279

Thermal correction to Gibbs Free Energy= 0.120853

Sum of electronic and zero-point Energies= -761.686324

Sum of electronic and thermal Energies= -761.672576

Sum of electronic and thermal Enthalpies= -761.671632

Sum of electronic and thermal Free Energies= -761.728058

	E (Thermal) KCal/Mol	CV Cal/Mol-Kelvin	S Cal/Mol-Kelvin
Total	110.652	49.416	118.758

Center Number	Atomic Number	Atomic Type	Coordinates (Angstroms) X	Y	Z
1	1	0	-1.693988	-0.851069	-2.162231
2	6	0	-1.539894	-0.218226	-1.299180

3	6	0	-0.555730	0.719959	-1.098281
4	6	0	-0.412787	-1.849149	-0.086548
5	6	0	0.716780	-0.831632	0.320446
6	1	0	-0.501482	-2.571325	-0.887150
7	1	0	0.291729	0.944751	-1.729769
8	6	0	-0.867211	-1.792336	1.207157
9	1	0	-1.696543	-2.245283	1.735997
10	6	0	0.191199	-0.845044	1.589842
11	1	0	0.467463	-0.353886	2.515838
12	6	0	-0.969636	1.589179	0.019261
13	6	0	-2.627846	0.051321	-0.330405
14	8	0	-2.182597	1.075652	0.511022
15	8	0	-0.459540	2.569821	0.488602
16	8	0	-3.712904	-0.449726	-0.210918
17	6	0	2.014835	-0.499903	-0.263372
18	8	0	2.377165	-0.862337	-1.369136
19	8	0	2.752164	0.261821	0.573081
20	6	0	4.032549	0.671880	0.063724
21	1	0	4.661176	-0.198995	-0.140098
22	1	0	4.471737	1.288977	0.847452
23	1	0	3.912049	1.248689	-0.857096

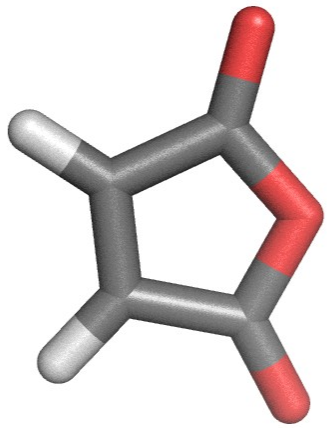

Maleic Anhydride
RB3LYP/6-31G (d)
SCF Done: E(RB+HF-LYP) = -379.289544696
Zero-point correction= 0.055888 (Hartree/Particle)
Thermal correction to Energy= 0.061072
Thermal correction to Enthalpy= 0.062016
Thermal correction to Gibbs Free Energy= 0.027469
Sum of electronic and zero-point Energies= -379.233657

Sum of electronic and thermal Energies= -379.228473
Sum of electronic and thermal Enthalpies= -379.227529
Sum of electronic and thermal Free Energies= -379.262076

	E (Thermal) KCal/Mol	CV Cal/Mol-Kelvin	S Cal/Mol-Kelvin
Total	38.323	18.571	72.710

Center Number	Atomic Number	Atomic Type	Coordinates (Angstroms) X	Y	Z
1	6	0	0.000000	0.667808	-1.258272
2	1	0	0.000000	1.360863	-2.089475
3	6	0	0.000000	-0.667808	-1.258272
4	1	0	0.000000	-1.360863	-2.089475
5	6	0	0.000000	-1.131930	0.158826
6	6	0	0.000000	1.131930	0.158826
7	8	0	0.000000	-2.245573	0.599809
8	8	0	0.000000	2.245573	0.599809
9	8	0	0.000000	0.000000	0.971919

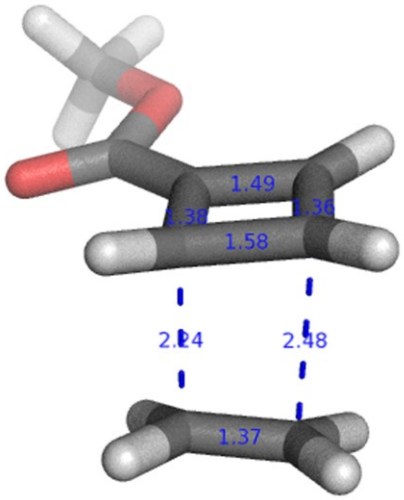

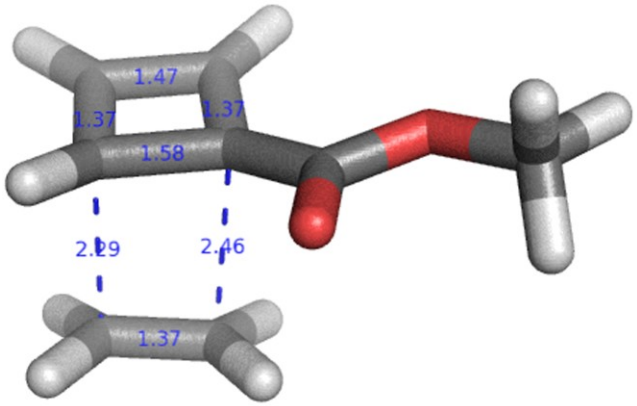

CBETHts-e **CBETHts-i**

CBETHts-e
RB3LYP/6-31G (d)
SCF Done: E(RB+HF-LYP) = -461.136403104
Zero-point correction= 0.158787 (Hartree/Particle)
Thermal correction to Energy= 0.169562
Thermal correction to Enthalpy= 0.170507
Thermal correction to Gibbs Free Energy= 0.121934

Sum of electronic and zero-point Energies= -460.977616
Sum of electronic and thermal Energies= -460.966841
Sum of electronic and thermal Enthalpies= -460.965897
Sum of electronic and thermal Free Energies= -461.014469

	E (Thermal) KCal/Mol	CV Cal/Mol-Kelvin	S Cal/Mol-Kelvin
Total	106.402	38.384	102.229

Center Number	Atomic Number	Atomic Type	Coordinates (Angstroms) X	Y	Z
1	6	0	1.054567	1.672175	-0.085537
2	6	0	2.026075	1.022736	0.605542
3	6	0	0.977343	-0.102869	0.949827
4	6	0	0.050560	0.620731	0.230109
5	1	0	1.011063	2.585758	-0.667186
6	1	0	2.994594	1.288973	1.006683
7	1	0	0.871904	-0.779191	1.789234
8	6	0	1.950058	-1.655187	-0.337930
9	1	0	2.103631	-2.356549	0.477318
10	1	0	1.094413	-1.855635	-0.972676
11	6	0	2.963359	-0.827886	-0.743662
12	1	0	2.913555	-0.277109	-1.675934
13	1	0	3.908921	-0.788844	-0.211366
14	6	0	-1.352361	0.449373	-0.108999
15	8	0	-2.032039	1.269182	-0.702602
16	8	0	-1.831694	-0.751083	0.323168
17	6	0	-3.219000	-0.981056	0.046942
18	1	0	-3.411716	-0.949030	-1.029346
19	1	0	-3.437066	-1.973436	0.444258
20	1	0	-3.843046	-0.227830	0.536742

CBETHts-i
RB3LYP/6-31G (d)
SCF Done: E(RB+HF-LYP) = -461.137861038
Zero-point correction= 0.159036 (Hartree/Particle)
Thermal correction to Energy= 0.169748
Thermal correction to Enthalpy= 0.170692
Thermal correction to Gibbs Free Energy= 0.122595
Sum of electronic and zero-point Energies= -460.978825
Sum of electronic and thermal Energies= -460.968113
Sum of electronic and thermal Enthalpies= -460.967169

Sum of electronic and thermal Free Energies= -461.015266

	E (Thermal) KCal/Mol	CV Cal/Mol-Kelvin	S Cal/Mol-Kelvin
Total	106.518	38.199	101.228

Center Number	Atomic Number	Atomic Type	Coordinates (Angstroms) X	Y	Z
1	6	0	0.788899	-1.605735	-0.552779
2	6	0	0.304177	-0.483316	0.073068
3	6	0	1.681698	-0.417132	0.849779
4	6	0	2.067920	-1.542543	0.164355
5	1	0	0.367557	-2.285360	-1.286385
6	1	0	1.948534	-0.000630	1.812295
7	1	0	2.973822	-2.136325	0.137717
8	6	0	2.348550	1.471924	-0.254762
9	1	0	2.522397	2.016325	0.668471
10	1	0	3.230600	1.065956	-0.737997
11	6	0	1.162084	1.595053	-0.924139
12	1	0	1.044201	1.247920	-1.944855
13	1	0	0.342949	2.169662	-0.505455
14	6	0	-1.018716	0.036867	0.363091
15	8	0	-1.285444	0.814575	1.265898
16	8	0	-1.948961	-0.442349	-0.510905
17	6	0	-3.283293	0.031240	-0.291892
18	1	0	-3.891239	-0.436543	-1.067770
19	1	0	-3.642027	-0.258047	0.700140
20	1	0	-3.329461	1.121085	-0.376420

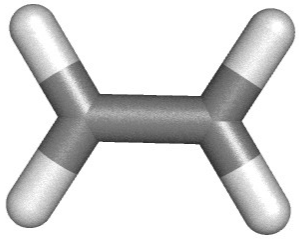

Ethylene
RB3LYP/6-31G (d)
SCF Done: E(RB+HF-LYP) = -78.5874583000
Zero-point correction= 0.051229 (Hartree/Particle)
Thermal correction to Energy= 0.054271
Thermal correction to Enthalpy= 0.055215
Thermal correction to Gibbs Free Energy= 0.030353
Sum of electronic and zero-point Energies= -78.536230
Sum of electronic and thermal Energies= -78.533188
Sum of electronic and thermal Enthalpies= -78.532244
Sum of electronic and thermal Free Energies= -78.557105

	E (Thermal) KCal/Mol	CV Cal/Mol-Kelvin	S Cal/Mol-Kelvin
Total	34.055	8.089	52.325

Center Number	Atomic Number	Atomic Type	Coordinates (Angstroms) X	Y	Z
1	6	0	0.000000	0.000000	0.665462
2	1	0	0.000000	0.923584	1.239565
3	1	0	0.000000	-0.923584	1.239565
4	6	0	0.000000	0.000000	-0.665462
5	1	0	0.000000	0.923584	-1.239565
6	1	0	0.000000	-0.923584	-1.239565

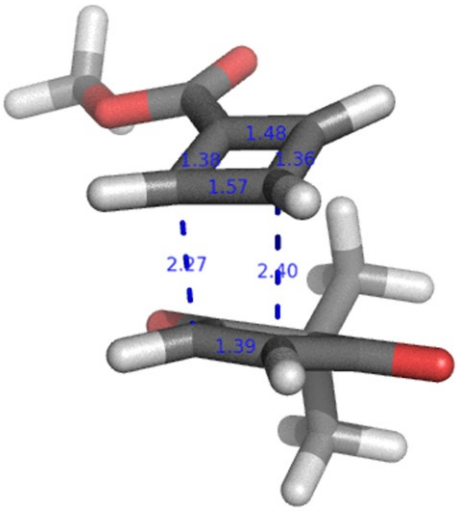

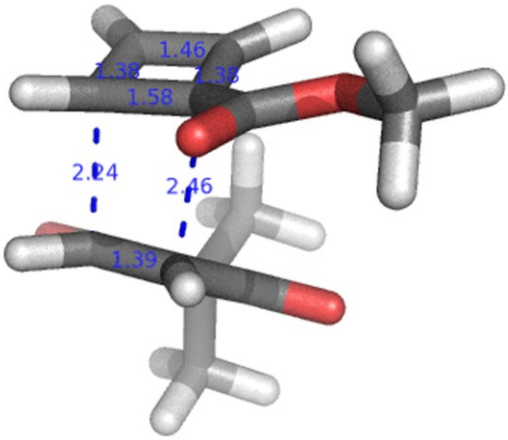

CBDMts-e **CBDMts-i**

CBDMts-e

RB3LYP/6-31G (d)

SCF Done: E(RB+HF-LYP) = -804.541174600

Zero-point correction= 0.242306 (Hartree/Particle)

Thermal correction to Energy= 0.259502

Thermal correction to Enthalpy= 0.260446

Thermal correction to Gibbs Free Energy= 0.196820

Sum of electronic and zero-point Energies= -804.298869

Sum of electronic and thermal Energies= -804.281672

Sum of electronic and thermal Enthalpies= -804.280728

Sum of electronic and thermal Free Energies= -804.344354

	E (Thermal) KCal/Mol	CV Cal/Mol-Kelvin	S Cal/Mol-Kelvin
Total	162.840	62.840	133.912

Center Number	Atomic Number	Atomic Type	Coordinates (Angstroms) X	Y	Z
1	6	0	-0.752897	-0.977301	-0.921793
2	6	0	-1.899646	1.080217	-1.008478
3	6	0	-2.371896	0.398276	0.223055
4	6	0	-0.958008	0.300535	-1.664784
5	8	0	-0.008654	-1.884933	-1.243969
6	8	0	-3.199206	0.821993	1.010818
7	6	0	-0.192886	2.546352	-0.181759
8	1	0	-0.782259	3.425590	-0.403052
9	6	0	1.312747	1.200534	0.151434
10	6	0	0.406206	2.060792	0.943687

11	1	0	0.276318	2.224188	2.006567
12	1	0	-0.663791	0.389621	-2.704495
13	1	0	-2.422404	1.939037	-1.413458
14	6	0	2.352131	0.238214	0.527804
15	8	0	2.616791	-0.051124	1.680687
16	8	0	2.962439	-0.282981	-0.554809
17	6	0	3.933869	-1.306164	-0.279918
18	1	0	4.741358	-0.911682	0.342614
19	1	0	4.312702	-1.615704	-1.253858
20	1	0	3.461515	-2.147870	0.232712
21	6	0	0.764251	1.633089	-1.035794
22	1	0	1.164348	1.699551	-2.039022
23	6	0	-1.704404	-0.988881	0.289857
24	6	0	-2.793413	-2.059347	0.041085
25	1	0	-3.526009	-2.031003	0.853731
26	1	0	-3.323638	-1.889466	-0.903175
27	1	0	-2.331213	-3.050597	0.000636
28	6	0	-0.996718	-1.264294	1.624722
29	1	0	-1.718887	-1.182878	2.443459
30	1	0	-0.578379	-2.275844	1.618315
31	1	0	-0.176640	-0.568698	1.822489

CBDMts-i

RB3LYP/6-31G (d)

SCF Done: E(RB+HF-LYP) = -804.542513254

Zero-point correction= 0.242365 (Hartree/Particle)

Thermal correction to Energy= 0.259612

Thermal correction to Enthalpy= 0.260556

Thermal correction to Gibbs Free Energy= 0.196785

Sum of electronic and zero-point Energies= -804.300149

Sum of electronic and thermal Energies= -804.282901

Sum of electronic and thermal Enthalpies= -804.281957

Sum of electronic and thermal Free Energies= -804.345728

	E (Thermal) KCal/Mol	CV Cal/Mol-Kelvin	S Cal/Mol-Kelvin
Total	162.909	62.739	134.218

Center Number	Atomic Number	Atomic Type	Coordinates (Angstroms) X	Y	Z
1	1	0	0.894346	1.458746	-2.193940
2	6	0	0.958619	0.772861	-1.356974

3	6	0	0.196363	-0.372424	-1.182022
4	6	0	-0.437042	2.070447	-0.170882
5	6	0	-1.333385	0.856776	0.294641
6	1	0	-0.549229	2.784615	-0.975949
7	1	0	-0.652652	-0.669384	-1.784943
8	6	0	-0.015243	2.192868	1.134419
9	1	0	0.678488	2.853215	1.639991
10	6	0	-0.851820	1.070049	1.565036
11	1	0	-1.051342	0.599076	2.521293
12	6	0	0.861684	-1.300399	-0.236409
13	6	0	2.211078	0.674671	-0.549219
14	8	0	0.449263	-2.390389	0.120544
15	8	0	3.099952	1.503904	-0.496677
16	6	0	-2.543256	0.245556	-0.247161
17	8	0	-2.988914	0.473215	-1.359160
18	8	0	-3.103767	-0.608752	0.638547
19	6	0	-4.272872	-1.298861	0.168574
20	1	0	-5.064668	-0.588157	-0.082943
21	1	0	-4.580928	-1.942256	0.992935
22	1	0	-4.035529	-1.896598	-0.715604
23	6	0	2.220239	-0.690877	0.163632
24	6	0	3.348201	-1.555698	-0.442246
25	1	0	3.243020	-1.655753	-1.528679
26	1	0	4.319179	-1.095390	-0.233893
27	1	0	3.317606	-2.557957	-0.003391
28	6	0	2.402796	-0.575381	1.683319
29	1	0	1.623580	0.037507	2.147267
30	1	0	2.362034	-1.571216	2.135969
31	1	0	3.371668	-0.117775	1.907600

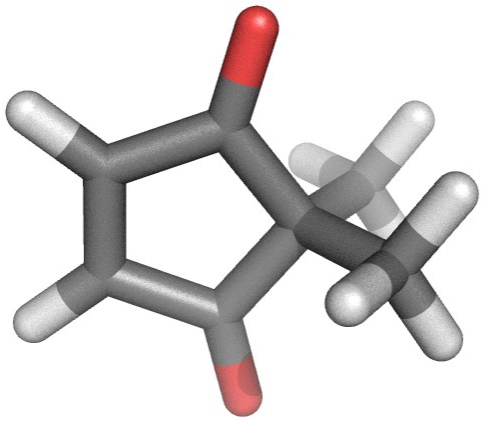

2,2-Dimethylcyclopent-4-ene-1,3-dione

RB3LYP/6-31G (d)

SCF Done: E(RB+HF-LYP) = -421.991654245

Zero-point correction= 0.135670 (Hartree/Particle)

Thermal correction to Energy= 0.144384

Thermal correction to Enthalpy= 0.145328

Thermal correction to Gibbs Free Energy= 0.102373

Sum of electronic and zero-point Energies= -421.855984

Sum of electronic and thermal Energies= -421.847270

Sum of electronic and thermal Enthalpies= -421.846326

Sum of electronic and thermal Free Energies= -421.889282

	E (Thermal) KCal/Mol	CV Cal/Mol-Kelvin	S Cal/Mol-Kelvin
Total	90.602	32.051	90.407

Center Number	Atomic Number	Atomic Type	Coordinates (Angstroms) X	Y	Z
1	6	0	0.672337	1.760375	0.000036
2	1	0	1.332926	2.621317	0.000073
3	6	0	-0.672444	1.760336	-0.000036
4	1	0	-1.333077	2.621242	-0.000074
5	6	0	-1.196701	0.362498	-0.000032
6	6	0	1.196672	0.362564	0.000031
7	6	0	0.000011	-0.601716	0.000000
8	8	0	-2.370228	0.046977	-0.000007
9	8	0	2.370215	0.047105	0.000006
10	6	0	0.000006	-1.474637	1.268323
11	1	0	0.892201	-2.108305	1.281785
12	1	0	-0.892238	-2.108236	1.281811
13	1	0	0.000042	-0.865407	2.179238
14	6	0	0.000101	-1.474638	-1.268322
15	1	0	0.892439	-2.108103	-1.281841
16	1	0	-0.000079	-0.865411	-2.179239
17	1	0	-0.891994	-2.108448	-1.281747

X-ray Crystal Structures

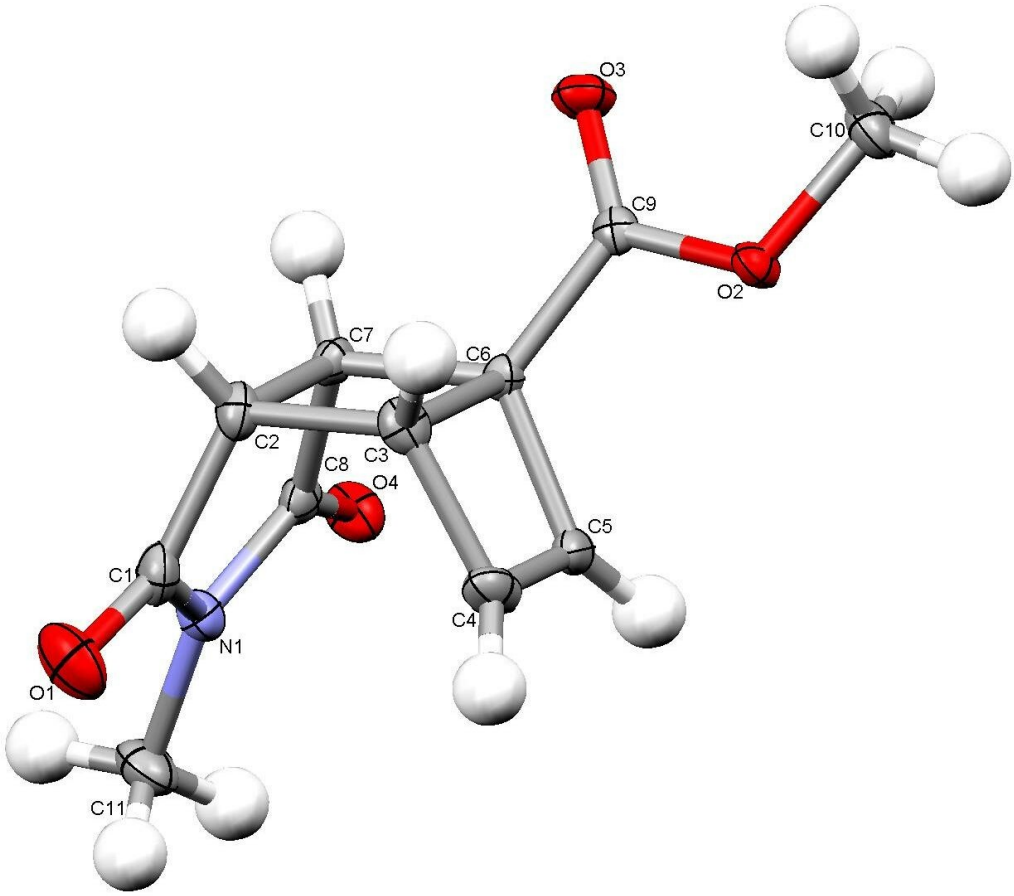

Table 2.5. Crystal data and structure refinement for **V**.

Identification code	C11H11NO4	
Empirical formula	C11 H11 N O4	
Formula weight	221.21	
Temperature	100(2) K	
Wavelength	0.71073 Å	
Crystal system	Orthorhombic	
Space group	P 21 21 21	
Unit cell dimensions	a = 6.3827(18) Å	α= 90°.
	b = 7.269(2) Å	β= 90°.
	c = 22.991(7) Å	γ = 90°.
Volume	1066.7(5) Å^3	

Z	4
Density (calculated)	1.377 Mg/m^3
Absorption coefficient	0.106 mm^{-1}
F(000)	464
Crystal size	0.12 x 0.08 x 0.01 mm^3
Theta range for data collection	2.94 to 28.30°.
Index ranges	-8<=h<=8, -9<=k<=9, -30<=l<=30
Reflections collected	12737
Independent reflections	1554 [R(int) = 0.0572]
Completeness to theta = 28.30°	99.3 %
Absorption correction	Semi-empirical from equivalents
Max. and min. transmission	0.9989 and 0.9874
Refinement method	Full-matrix least-squares on F^2
Data / restraints / parameters	1554 / 0 / 147
Goodness-of-fit on F^2	1.069
Final R indices [I>2sigma(I)]	R1 = 0.0451, wR2 = 0.1001
R indices (all data)	R1 = 0.0549, wR2 = 0.1046
Extinction coefficient	na
Largest diff. peak and hole	0.348 and -0.184 $e.Å^{-3}$

Table 2.6: Atomic coordinates (x 10^4) and equivalent isotropic displacement parameters ($Å^2$x 10^3) for **V**. U(eq) is defined as one third of the trace of the orthogonalized U^{ij} tensor.

	x	y	z	U(eq)
O(1)	6058(3)	13473(3)	-2129(1)	35(1)
O(2)	4286(3)	9820(2)	336(1)	16(1)
O(3)	4904(3)	7356(2)	-226(1)	22(1)
O(4)	890(3)	9377(3)	-1702(1)	22(1)
N(1)	3206(3)	11585(3)	-2002(1)	19(1)
C(1)	5244(4)	12155(4)	-1894(1)	21(1)
C(2)	6165(4)	10916(4)	-1441(1)	18(1)
C(3)	6093(4)	11700(3)	-806(1)	17(1)
C(4)	4476(5)	13174(3)	-703(1)	22(1)
C(5)	2943(4)	12012(3)	-586(1)	17(1)
C(6)	4264(4)	10304(3)	-661(1)	13(1)
C(7)	4421(4)	9542(3)	-1298(1)	15(1)
C(8)	2601(4)	10071(4)	-1682(1)	16(1)
C(9)	4502(4)	8967(3)	-173(1)	14(1)
C(10)	4610(5)	8694(4)	846(1)	25(1)
C(11)	1828(4)	12499(4)	-2414(1)	28(1)

Table 2.7: Bond lengths [Å] and angles [°] for **V**.

O(1)-C(1)	1.216(3)
O(2)-C(9)	1.332(3)
O(2)-C(10)	1.445(3)
O(3)-C(9)	1.205(3)
O(4)-C(8)	1.204(3)
N(1)-C(8)	1.379(3)
N(1)-C(1)	1.388(3)
N(1)-C(11)	1.453(3)
C(1)-C(2)	1.497(4)
C(2)-C(7)	1.532(3)
C(2)-C(3)	1.568(3)
C(2)-H(2)	1.0000
C(3)-C(4)	1.507(4)
C(3)-C(6)	1.582(3)
C(3)-H(3)	1.0000
C(4)-C(5)	1.320(4)
C(4)-H(4)	0.9500
C(5)-C(6)	1.510(3)
C(5)-H(5)	0.9500
C(6)-C(9)	1.492(3)
C(6)-C(7)	1.569(3)
C(7)-C(8)	1.510(3)
C(7)-H(7)	1.0000
C(10)-H(10A)	0.9800
C(10)-H(10B)	0.9800
C(10)-H(10C)	0.9800
C(11)-H(11A)	0.9800
C(11)-H(11B)	0.9800
C(11)-H(11C)	0.9800
C(9)-O(2)-C(10)	115.76(19)
C(8)-N(1)-C(1)	113.9(2)

C(8)-N(1)-C(11)	122.9(2)
C(1)-N(1)-C(11)	123.2(2)
O(1)-C(1)-N(1)	123.8(3)
O(1)-C(1)-C(2)	127.9(3)
N(1)-C(1)-C(2)	108.2(2)
C(1)-C(2)-C(7)	104.9(2)
C(1)-C(2)-C(3)	114.7(2)
C(7)-C(2)-C(3)	90.87(17)
C(1)-C(2)-H(2)	114.6
C(7)-C(2)-H(2)	114.6
C(3)-C(2)-H(2)	114.6
C(4)-C(3)-C(2)	115.2(2)
C(4)-C(3)-C(6)	85.24(17)
C(2)-C(3)-C(6)	89.17(17)
C(4)-C(3)-H(3)	119.3
C(2)-C(3)-H(3)	119.3
C(6)-C(3)-H(3)	119.3
C(5)-C(4)-C(3)	94.8(2)
C(5)-C(4)-H(4)	132.6
C(3)-C(4)-H(4)	132.6
C(4)-C(5)-C(6)	95.1(2)
C(4)-C(5)-H(5)	132.4
C(6)-C(5)-H(5)	132.4
C(9)-C(6)-C(5)	120.47(19)
C(9)-C(6)-C(7)	117.70(19)
C(5)-C(6)-C(7)	115.59(18)
C(9)-C(6)-C(3)	120.09(19)
C(5)-C(6)-C(3)	84.77(17)
C(7)-C(6)-C(3)	88.97(16)
C(8)-C(7)-C(2)	105.50(19)
C(8)-C(7)-C(6)	114.05(19)
C(2)-C(7)-C(6)	90.97(17)
C(8)-C(7)-H(7)	114.6
C(2)-C(7)-H(7)	114.6

C(6)-C(7)-H(7)	114.6
O(4)-C(8)-N(1)	124.6(2)
O(4)-C(8)-C(7)	127.9(2)
N(1)-C(8)-C(7)	107.5(2)
O(3)-C(9)-O(2)	124.3(2)
O(3)-C(9)-C(6)	125.3(2)
O(2)-C(9)-C(6)	110.27(19)
O(2)-C(10)-H(10A)	109.5
O(2)-C(10)-H(10B)	109.5
H(10A)-C(10)-H(10B)	109.5
O(2)-C(10)-H(10C)	109.5
H(10A)-C(10)-H(10C)	109.5
H(10B)-C(10)-H(10C)	109.5
N(1)-C(11)-H(11A)	109.5
N(1)-C(11)-H(11B)	109.5
H(11A)-C(11)-H(11B)	109.5
N(1)-C(11)-H(11C)	109.5
H(11A)-C(11)-H(11C)	109.5
H(11B)-C(11)-H(11C)	109.5

Symmetry transformations used to generate equivalent atoms:

Table 2.8: Anisotropic displacement parameters ($Å^2 x\ 10^3$) for **V**. The anisotropic displacement factor exponent takes the form: $-2\pi^2[\ h^2\ a^{*2}U^{11} + ...\ + 2\ h\ k\ a^*\ b^*\ U^{12}\ ]$

	U^{11}	U^{22}	U^{33}	U^{23}	U^{13}	U^{12}
O(1)	35(1)	36(1)	33(1)	13(1)	2(1)	-13(1)
O(2)	23(1)	15(1)	11(1)	1(1)	-3(1)	0(1)
O(3)	30(1)	13(1)	24(1)	0(1)	-3(1)	3(1)
O(4)	18(1)	27(1)	22(1)	3(1)	-4(1)	-4(1)
N(1)	21(1)	22(1)	14(1)	2(1)	-1(1)	2(1)
C(1)	21(1)	24(1)	18(1)	-2(1)	7(1)	-4(1)
C(2)	15(1)	24(1)	15(1)	-2(1)	2(1)	-1(1)
C(3)	17(1)	18(1)	16(1)	-1(1)	-3(1)	-6(1)
C(4)	35(1)	13(1)	18(1)	-2(1)	-3(1)	2(1)
C(5)	22(1)	18(1)	12(1)	0(1)	0(1)	6(1)
C(6)	13(1)	13(1)	12(1)	-1(1)	0(1)	-1(1)
C(7)	16(1)	16(1)	13(1)	-4(1)	0(1)	2(1)
C(8)	18(1)	18(1)	12(1)	-3(1)	1(1)	1(1)
C(9)	11(1)	17(1)	14(1)	0(1)	-1(1)	-2(1)
C(10)	30(1)	29(1)	16(1)	7(1)	-2(1)	0(1)
C(11)	28(1)	31(2)	23(1)	11(1)	-4(1)	2(1)

Table 2.9: Hydrogen coordinates (x 10^4) and isotropic displacement parameters ($Å^2$x 10^3) for **V**.

	x	y	z	U(eq)
H(2)	7531	10341	-1553	21
H(3)	7396	11685	-565	20
H(4)	4537	14479	-717	26
H(5)	1510	12188	-490	21
H(7)	4845	8221	-1325	18
H(10A)	3683	7621	830	37
H(10B)	4295	9415	1196	37
H(10C)	6071	8283	859	37
H(11A)	1974	11924	-2797	41
H(11B)	2207	13803	-2440	41
H(11C)	374	12386	-2282	41

Table 2.10: Torsion angles [°] for **V**.

C(8)-N(1)-C(1)-O(1)	-179.3(2)
C(11)-N(1)-C(1)-O(1)	0.6(4)
C(8)-N(1)-C(1)-C(2)	-0.8(3)
C(11)-N(1)-C(1)-C(2)	179.1(2)
O(1)-C(1)-C(2)-C(7)	178.6(2)
N(1)-C(1)-C(2)-C(7)	0.2(3)
O(1)-C(1)-C(2)-C(3)	80.6(3)
N(1)-C(1)-C(2)-C(3)	-97.8(2)
C(1)-C(2)-C(3)-C(4)	21.5(3)
C(7)-C(2)-C(3)-C(4)	-85.3(2)
C(1)-C(2)-C(3)-C(6)	105.9(2)
C(7)-C(2)-C(3)-C(6)	-0.93(18)
C(2)-C(3)-C(4)-C(5)	86.3(2)
C(6)-C(3)-C(4)-C(5)	-0.51(18)
C(3)-C(4)-C(5)-C(6)	0.53(19)
C(4)-C(5)-C(6)-C(9)	121.5(2)
C(4)-C(5)-C(6)-C(7)	-86.9(2)
C(4)-C(5)-C(6)-C(3)	-0.51(18)
C(4)-C(3)-C(6)-C(9)	-121.9(2)
C(2)-C(3)-C(6)-C(9)	122.7(2)
C(4)-C(3)-C(6)-C(5)	0.45(16)
C(2)-C(3)-C(6)-C(5)	-114.90(17)
C(4)-C(3)-C(6)-C(7)	116.26(17)
C(2)-C(3)-C(6)-C(7)	0.91(17)
C(1)-C(2)-C(7)-C(8)	0.4(2)
C(3)-C(2)-C(7)-C(8)	116.26(19)
C(1)-C(2)-C(7)-C(6)	-114.92(19)
C(3)-C(2)-C(7)-C(6)	0.94(18)
C(9)-C(6)-C(7)-C(8)	127.8(2)
C(5)-C(6)-C(7)-C(8)	-24.7(3)
C(3)-C(6)-C(7)-C(8)	-108.4(2)
C(9)-C(6)-C(7)-C(2)	-124.8(2)

C(5)-C(6)-C(7)-C(2)	82.8(2)
C(3)-C(6)-C(7)-C(2)	-0.93(18)
C(1)-N(1)-C(8)-O(4)	178.6(2)
C(11)-N(1)-C(8)-O(4)	-1.3(4)
C(1)-N(1)-C(8)-C(7)	1.1(3)
C(11)-N(1)-C(8)-C(7)	-178.8(2)
C(2)-C(7)-C(8)-O(4)	-178.3(2)
C(6)-C(7)-C(8)-O(4)	-80.0(3)
C(2)-C(7)-C(8)-N(1)	-0.9(3)
C(6)-C(7)-C(8)-N(1)	97.3(2)
C(10)-O(2)-C(9)-O(3)	1.3(3)
C(10)-O(2)-C(9)-C(6)	-176.4(2)
C(5)-C(6)-C(9)-O(3)	154.7(2)
C(7)-C(6)-C(9)-O(3)	3.7(4)
C(3)-C(6)-C(9)-O(3)	-102.6(3)
C(5)-C(6)-C(9)-O(2)	-27.7(3)
C(7)-C(6)-C(9)-O(2)	-178.70(18)
C(3)-C(6)-C(9)-O(2)	75.0(3)

Symmetry transformations used to generate equivalent atoms:

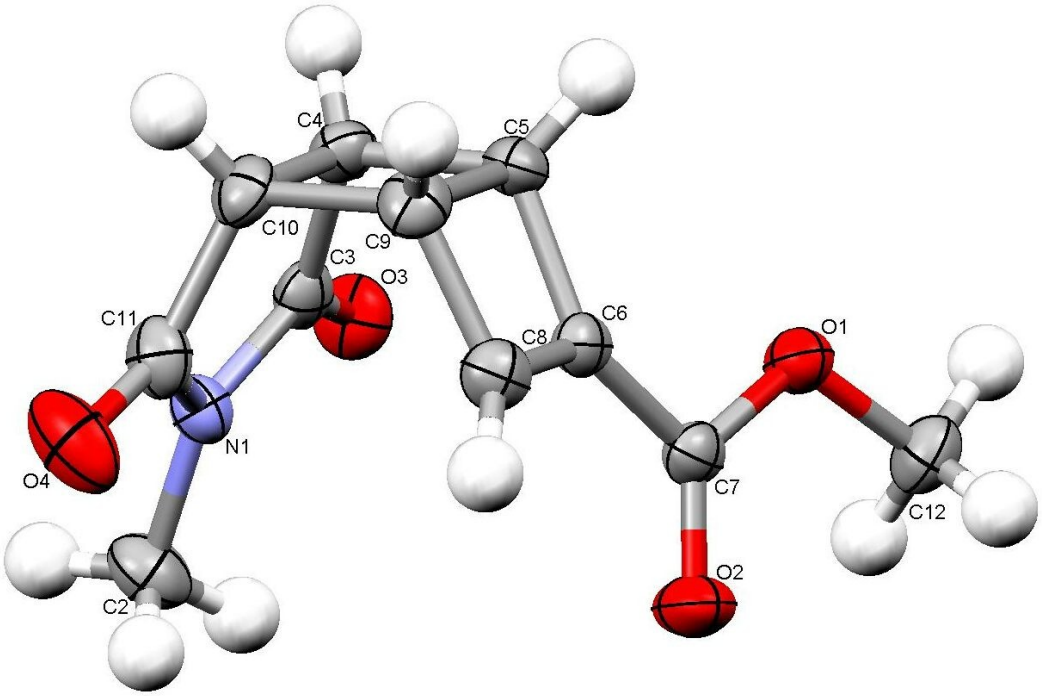

Table 2.11: Crystal data and structure refinement for **VI**.

Identification code	jm02t	
Empirical formula	C11 H11 N O4	
Formula weight	221.21	
Temperature	193(2) K	
Wavelength	0.71073 Å	
Crystal system	Monoclinic	
Space group	P2(1)/n	
Unit cell dimensions	a = 7.303(2) Å	α= 90°.
	b = 7.345(2) Å	β= 99.013(5)°.
	c = 18.369(5) Å	γ = 90°.
Volume	973.2(5) $Å^3$	
Z	4	
Density (calculated)	1.510 Mg/m^3	
Absorption coefficient	0.116 mm^{-1}	
F(000)	464	
Crystal size	0.20 x 0.10 x 0.10 mm^3	
Theta range for data collection	2.25 to 28.41°.	

Index ranges	-7<=h<=9, -9<=k<=9, -24<=l<=23
Reflections collected	6730
Independent reflections	2424 [R(int) = 0.0434]
Completeness to theta = 28.41°	99.3 %
Absorption correction	Empirical
Refinement method	Full-matrix least-squares on F^2
Data / restraints / parameters	2424 / 0 / 189
Goodness-of-fit on F^2	0.982
Final R indices [I>2sigma(I)]	R1 = 0.0509, wR2 = 0.1063
R indices (all data)	R1 = 0.0858, wR2 = 0.1182
Largest diff. peak and hole	0.237 and -0.265 e.$Å^{-3}$

Table 2.12: Atomic coordinates (x 10^4) and equivalent isotropic displacement parameters ($Å^2$x 10^3) for **VI**. U(eq) is defined as one third of the trace of the orthogonalized U^{ij} tensor.

	x	y	z	U(eq)
O(1)	3364(2)	2837(2)	10198(1)	31(1)
O(3)	1182(2)	5956(2)	8692(1)	37(1)
O(2)	4306(2)	1396(2)	9272(1)	43(1)
C(3)	121(3)	4768(2)	8494(1)	27(1)
N(1)	84(2)	3860(2)	7847(1)	27(1)
C(4)	-1291(3)	3958(3)	8883(1)	29(1)
C(9)	-1568(3)	1033(3)	8944(1)	32(1)
C(6)	1148(2)	1557(2)	9339(1)	26(1)
C(7)	3097(3)	1907(2)	9580(1)	27(1)
O(4)	-1480(2)	1600(2)	7202(1)	53(1)
C(8)	291(3)	311(3)	8901(1)	31(1)
C(5)	-577(3)	2486(3)	9462(1)	29(1)
C(2)	1380(4)	4198(4)	7356(1)	40(1)
C(12)	5248(3)	3114(3)	10522(1)	37(1)
C(11)	-1254(3)	2557(3)	7730(1)	33(1)
C(10)	-2219(3)	2537(3)	8372(1)	31(1)

Table 2.13: Bond lengths [Å] and angles [°] for **VI**.

O(1)-C(7)	1.312(2)
O(1)-C(12)	1.426(2)
O(3)-C(3)	1.186(2)
O(2)-C(7)	1.183(2)
C(3)-N(1)	1.358(2)
C(3)-C(4)	1.469(3)
N(1)-C(11)	1.361(2)
N(1)-C(2)	1.429(3)
C(4)-C(10)	1.494(3)
C(4)-C(5)	1.549(3)
C(4)-H(4)	0.93(2)
C(9)-C(8)	1.471(3)
C(9)-C(5)	1.534(3)
C(9)-C(10)	1.547(3)
C(9)-H(6)	0.92(2)
C(6)-C(8)	1.311(3)
C(6)-C(7)	1.446(3)
C(6)-C(5)	1.481(2)
O(4)-C(11)	1.189(2)
C(8)-H(8)	0.96(2)
C(5)-H(7)	0.942(18)
C(2)-H(1)	0.99(3)
C(2)-H(2)	0.94(3)
C(2)-H(3)	0.91(3)
C(12)-H(11)	0.96(2)
C(12)-H(10)	1.00(2)
C(12)-H(9)	0.95(2)
C(11)-C(10)	1.465(3)
C(10)-H(5)	0.890(19)
C(7)-O(1)-C(12)	116.01(16)
O(3)-C(3)-N(1)	123.49(18)

O(3)-C(3)-C(4)	128.58(18)
N(1)-C(3)-C(4)	107.89(16)
C(3)-N(1)-C(11)	113.51(16)
C(3)-N(1)-C(2)	122.88(17)
C(11)-N(1)-C(2)	123.56(17)
C(3)-C(4)-C(10)	105.15(15)
C(3)-C(4)-C(5)	115.48(16)
C(10)-C(4)-C(5)	90.79(15)
C(3)-C(4)-H(4)	113.1(12)
C(10)-C(4)-H(4)	117.1(12)
C(5)-C(4)-H(4)	113.3(11)
C(8)-C(9)-C(5)	86.25(15)
C(8)-C(9)-C(10)	114.16(16)
C(5)-C(9)-C(10)	89.38(15)
C(8)-C(9)-H(6)	119.7(13)
C(5)-C(9)-H(6)	124.6(12)
C(10)-C(9)-H(6)	116.1(13)
C(8)-C(6)-C(7)	131.62(18)
C(8)-C(6)-C(5)	94.56(16)
C(7)-C(6)-C(5)	133.77(17)
O(2)-C(7)-O(1)	123.95(18)
O(2)-C(7)-C(6)	124.74(18)
O(1)-C(7)-C(6)	111.30(16)
C(6)-C(8)-C(9)	94.08(17)
C(6)-C(8)-H(8)	133.7(13)
C(9)-C(8)-H(8)	132.2(13)
C(6)-C(5)-C(9)	85.11(14)
C(6)-C(5)-C(4)	114.87(15)
C(9)-C(5)-C(4)	89.13(14)
C(6)-C(5)-H(7)	117.6(11)
C(9)-C(5)-H(7)	125.5(11)
C(4)-C(5)-H(7)	117.8(11)
N(1)-C(2)-H(1)	109.4(14)
N(1)-C(2)-H(2)	109.9(18)

H(1)-C(2)-H(2)	114(2)
N(1)-C(2)-H(3)	110.6(16)
H(1)-C(2)-H(3)	103(2)
H(2)-C(2)-H(3)	109(2)
O(1)-C(12)-H(11)	108.1(14)
O(1)-C(12)-H(10)	105.5(13)
H(11)-C(12)-H(10)	111.2(18)
O(1)-C(12)-H(9)	108.4(14)
H(11)-C(12)-H(9)	112.2(19)
H(10)-C(12)-H(9)	111.2(18)
O(4)-C(11)-N(1)	123.31(18)
O(4)-C(11)-C(10)	128.94(18)
N(1)-C(11)-C(10)	107.69(16)
C(11)-C(10)-C(4)	105.69(16)
C(11)-C(10)-C(9)	114.72(17)
C(4)-C(10)-C(9)	90.68(14)
C(11)-C(10)-H(5)	111.1(12)
C(4)-C(10)-H(5)	117.7(12)
C(9)-C(10)-H(5)	115.3(12)

Symmetry transformations used to generate equivalent atoms:

Table 2.14: Anisotropic displacement parameters ($Å^2 x\ 10^3$) for **VI**. The anisotropic displacement factor exponent takes the form: $-2\pi^2[\ h^2\ a^{*2}U^{11} + ...\ + 2\ h\ k\ a^*\ b^*\ U^{12}\ ]$

	U^{11}	U^{22}	U^{33}	U^{23}	U^{13}	U^{12}
O(1)	27(1)	34(1)	32(1)	-5(1)	4(1)	2(1)
O(3)	39(1)	28(1)	42(1)	-5(1)	2(1)	-7(1)
O(2)	31(1)	57(1)	41(1)	-11(1)	11(1)	7(1)
C(3)	29(1)	22(1)	29(1)	1(1)	0(1)	6(1)
N(1)	31(1)	25(1)	25(1)	0(1)	5(1)	-3(1)
C(4)	28(1)	27(1)	32(1)	0(1)	7(1)	6(1)
C(9)	28(1)	30(1)	39(1)	5(1)	8(1)	-5(1)
C(6)	29(1)	24(1)	26(1)	6(1)	7(1)	4(1)
C(7)	30(1)	24(1)	28(1)	4(1)	6(1)	5(1)
O(4)	70(1)	54(1)	36(1)	-15(1)	8(1)	-27(1)
C(8)	35(1)	25(1)	34(1)	2(1)	8(1)	0(1)
C(5)	29(1)	32(1)	26(1)	0(1)	10(1)	4(1)
C(2)	49(2)	38(1)	35(1)	1(1)	16(1)	-6(1)
C(12)	29(1)	38(1)	41(1)	0(1)	-2(1)	1(1)
C(11)	35(1)	32(1)	30(1)	0(1)	-1(1)	-7(1)
C(10)	22(1)	34(1)	36(1)	3(1)	1(1)	-2(1)

Table 2.15: Hydrogen coordinates (x 10^4) and isotropic displacement parameters ($Å^2$x 10^3) for **VI**.

	x	y	z	U(eq)
H(4)	-2050(30)	4820(30)	9056(10)	31(5)
H(6)	-2470(30)	270(30)	9060(11)	36(6)
H(7)	-750(30)	2690(20)	9952(10)	26(5)
H(5)	-3440(30)	2620(30)	8236(10)	29(5)
H(1)	2580(40)	4590(40)	7643(14)	73(8)
H(8)	700(30)	-680(30)	8630(11)	44(6)
H(11)	5780(30)	1950(30)	10665(12)	57(7)
H(10)	5200(30)	3910(30)	10962(12)	52(7)
H(2)	870(40)	5020(40)	6989(16)	95(10)
H(9)	5870(30)	3700(30)	10172(13)	52(7)
H(3)	1670(30)	3150(40)	7139(14)	65(8)

Table 2.16: Torsion angles [°] for **VI**.

O(3)-C(3)-N(1)-C(11)	-179.66(18)
C(4)-C(3)-N(1)-C(11)	2.6(2)
O(3)-C(3)-N(1)-C(2)	2.8(3)
C(4)-C(3)-N(1)-C(2)	-174.91(19)
O(3)-C(3)-C(4)-C(10)	179.67(19)
N(1)-C(3)-C(4)-C(10)	-2.7(2)
O(3)-C(3)-C(4)-C(5)	-82.0(2)
N(1)-C(3)-C(4)-C(5)	95.60(18)
C(12)-O(1)-C(7)-O(2)	-4.2(3)
C(12)-O(1)-C(7)-C(6)	174.41(16)
C(8)-C(6)-C(7)-O(2)	20.8(3)
C(5)-C(6)-C(7)-O(2)	-155.9(2)
C(8)-C(6)-C(7)-O(1)	-157.80(19)
C(5)-C(6)-C(7)-O(1)	25.4(3)
C(7)-C(6)-C(8)-C(9)	-177.21(19)
C(5)-C(6)-C(8)-C(9)	0.43(15)
C(5)-C(9)-C(8)-C(6)	-0.42(15)
C(10)-C(9)-C(8)-C(6)	87.21(18)
C(8)-C(6)-C(5)-C(9)	-0.42(15)
C(7)-C(6)-C(5)-C(9)	177.1(2)
C(8)-C(6)-C(5)-C(4)	-87.18(18)
C(7)-C(6)-C(5)-C(4)	90.4(2)
C(8)-C(9)-C(5)-C(6)	0.37(13)
C(10)-C(9)-C(5)-C(6)	-113.89(14)
C(8)-C(9)-C(5)-C(4)	115.42(14)
C(10)-C(9)-C(5)-C(4)	1.16(14)
C(3)-C(4)-C(5)-C(6)	-24.2(2)
C(10)-C(4)-C(5)-C(6)	83.01(18)
C(3)-C(4)-C(5)-C(9)	-108.43(17)
C(10)-C(4)-C(5)-C(9)	-1.20(15)
C(3)-N(1)-C(11)-O(4)	-178.6(2)
C(2)-N(1)-C(11)-O(4)	-1.2(3)

C(3)-N(1)-C(11)-C(10)	-1.3(2)
C(2)-N(1)-C(11)-C(10)	176.19(19)
O(4)-C(11)-C(10)-C(4)	176.6(2)
N(1)-C(11)-C(10)-C(4)	-0.5(2)
O(4)-C(11)-C(10)-C(9)	78.4(3)
N(1)-C(11)-C(10)-C(9)	-98.7(2)
C(3)-C(4)-C(10)-C(11)	1.9(2)
C(5)-C(4)-C(10)-C(11)	-114.76(16)
C(3)-C(4)-C(10)-C(9)	117.90(16)
C(5)-C(4)-C(10)-C(9)	1.19(14)
C(8)-C(9)-C(10)-C(11)	20.8(2)
C(5)-C(9)-C(10)-C(11)	106.45(17)
C(8)-C(9)-C(10)-C(4)	-86.80(19)
C(5)-C(9)-C(10)-C(4)	-1.20(15)

Symmetry transformations used to generate equivalent atoms:

Spectra

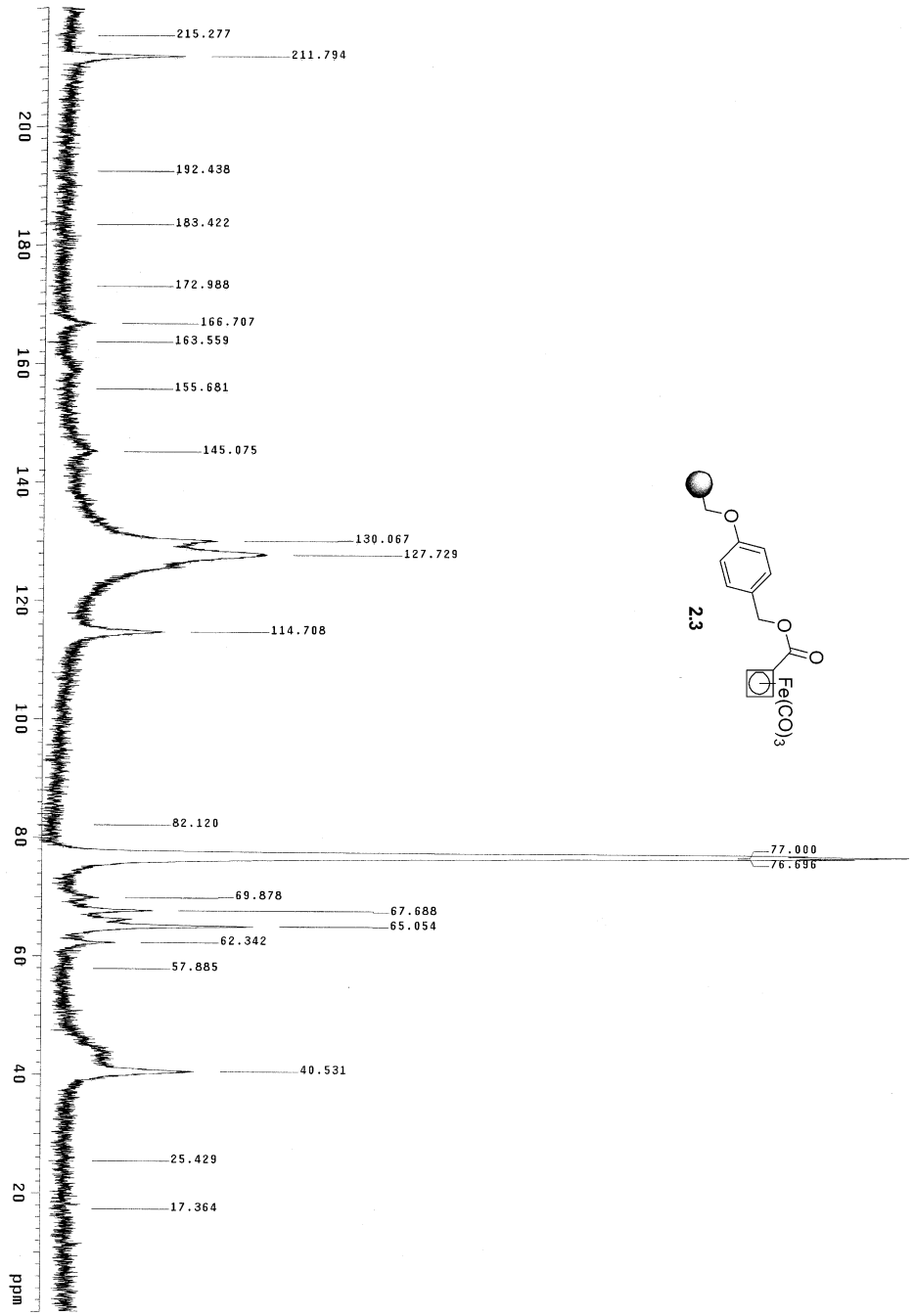
215.277
211.794
192.438
183.422
172.988
166.707
163.559
155.681
145.075
130.067
127.729
114.708
82.120
77.000
76.696
69.878
67.688
65.054
62.342
57.885
40.531
25.429
17.364
ppm
200
180
160
140
120
100
80
60
40
20
2.3
Fe(CO)3

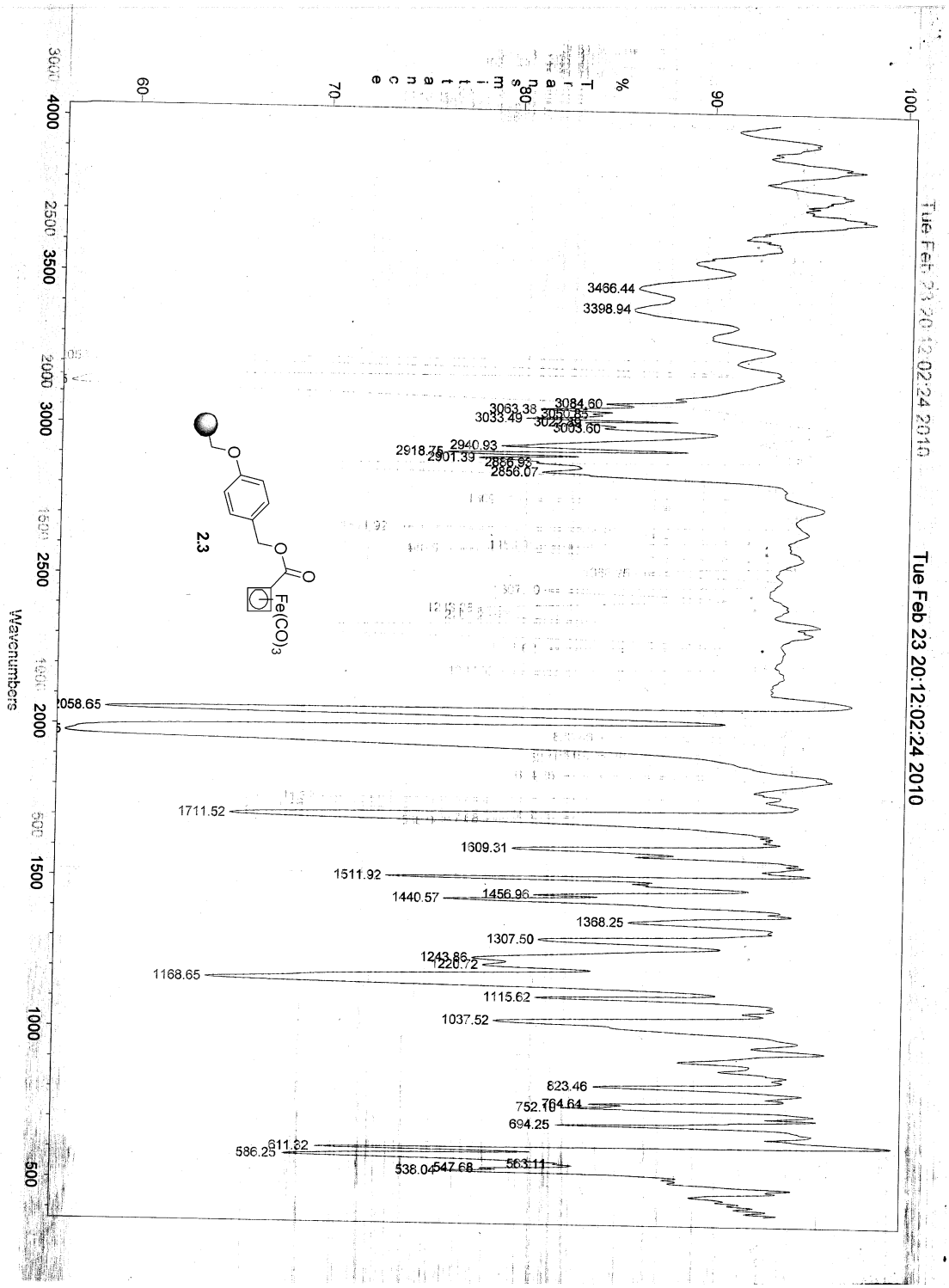
Transmittance %
Wavenumbers
Tue Feb 23 20:12:02:24 2010
3466.44
3398.94
3084.60
3063.38
3033.49
3003.60
2940.93
2918.75
2901.39
2856.07
2058.65
1711.52
1609.31
1511.92
1440.57
1456.96
1368.25
1307.50
1243.86
1220.72
1168.65
1115.62
1037.52
823.46
764.64
694.25
611.82
586.25
547.68
563.11
538.04
2.3
Fe(CO)3

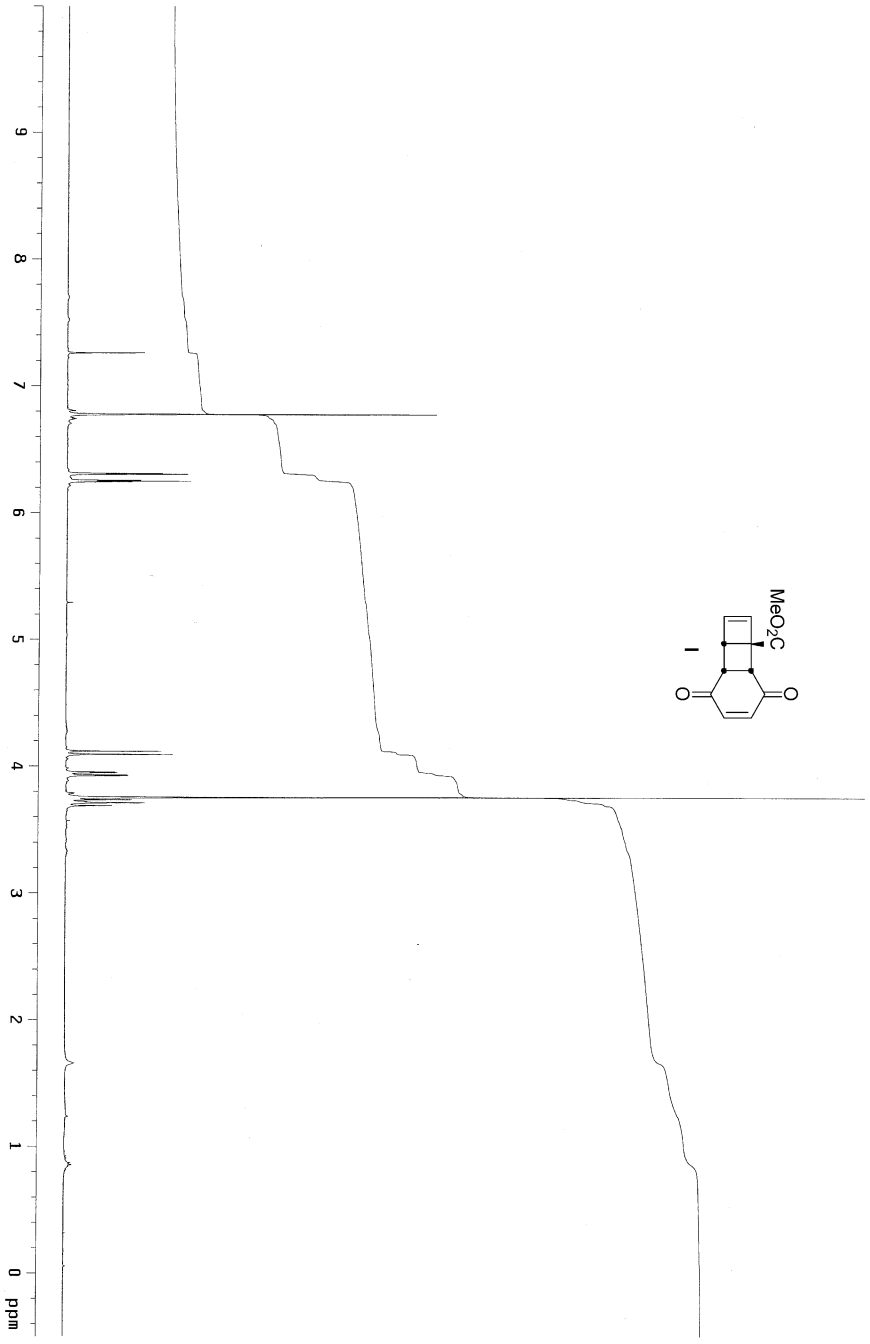
9
8
7
6
5
4
3
2
1
0
ppm
MeO2C
I
O
O

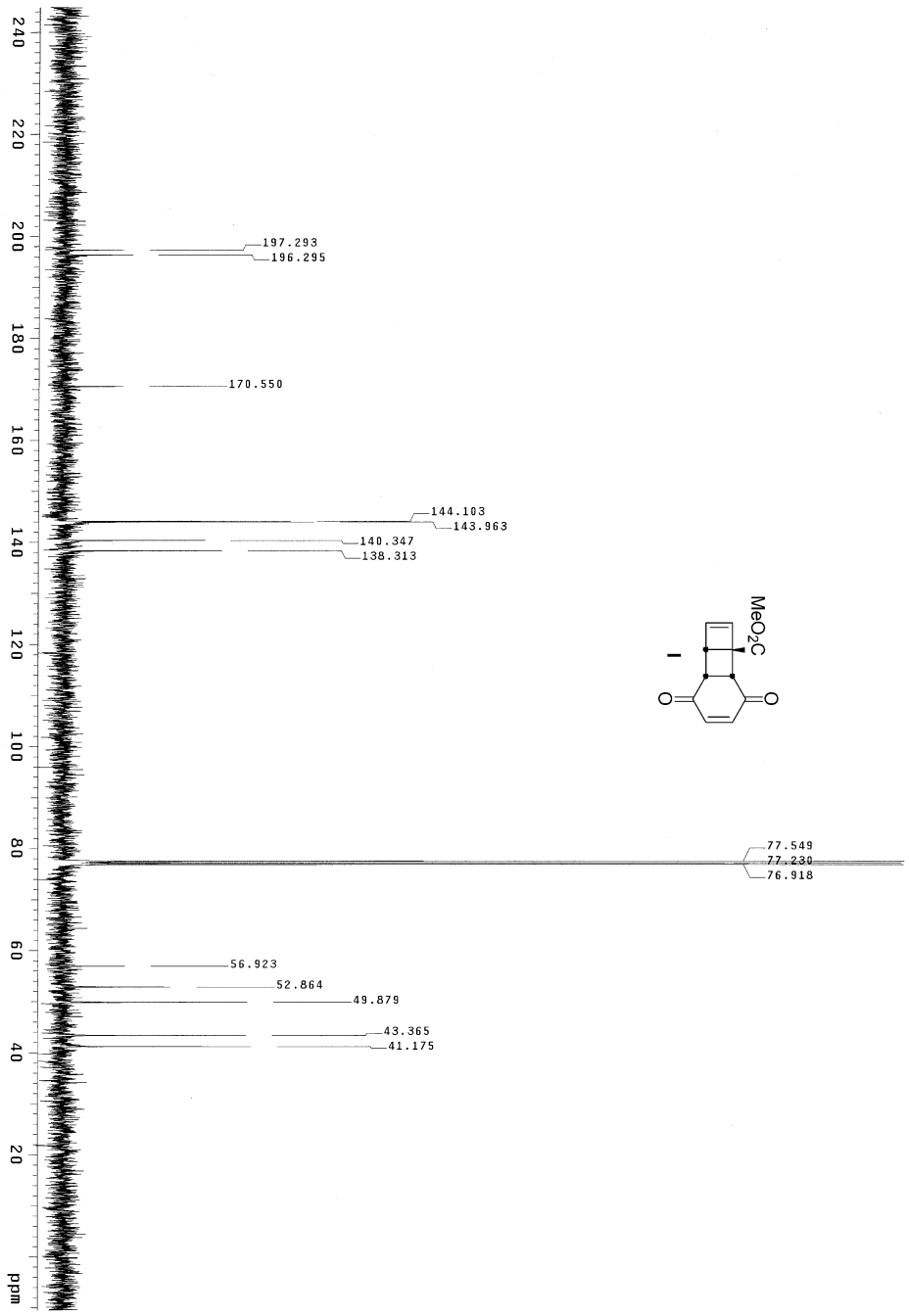
240
220
200
180
160
140
120
100
80
60
40
20
ppm
197.293
196.295
170.550
144.103
143.963
140.347
138.313
77.549
77.230
76.918
56.923
52.864
49.879
43.365
41.175
I
MeO2C
O
O

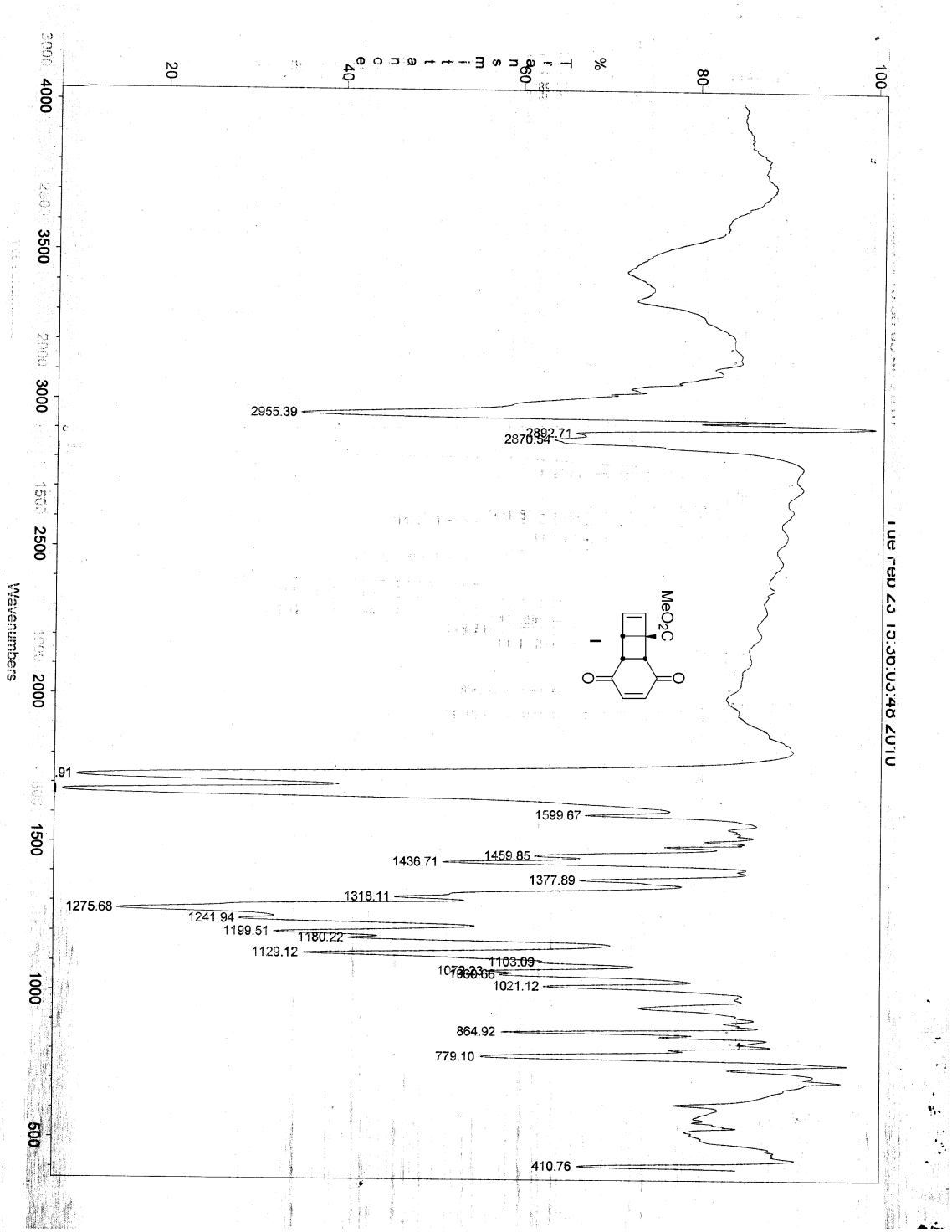
% Transmittance
Wavenumbers
4000
3500
3000
2500
2000
1500
1000
500
20
40
60
80
100
2955.39
2882.71
2870.54
1599.67
1459.85
1436.71
1377.89
1318.11
1275.68
1241.94
1199.51
1180.22
1129.12
1103.09
1021.12
864.92
779.10
410.76
MeO2C
O
O

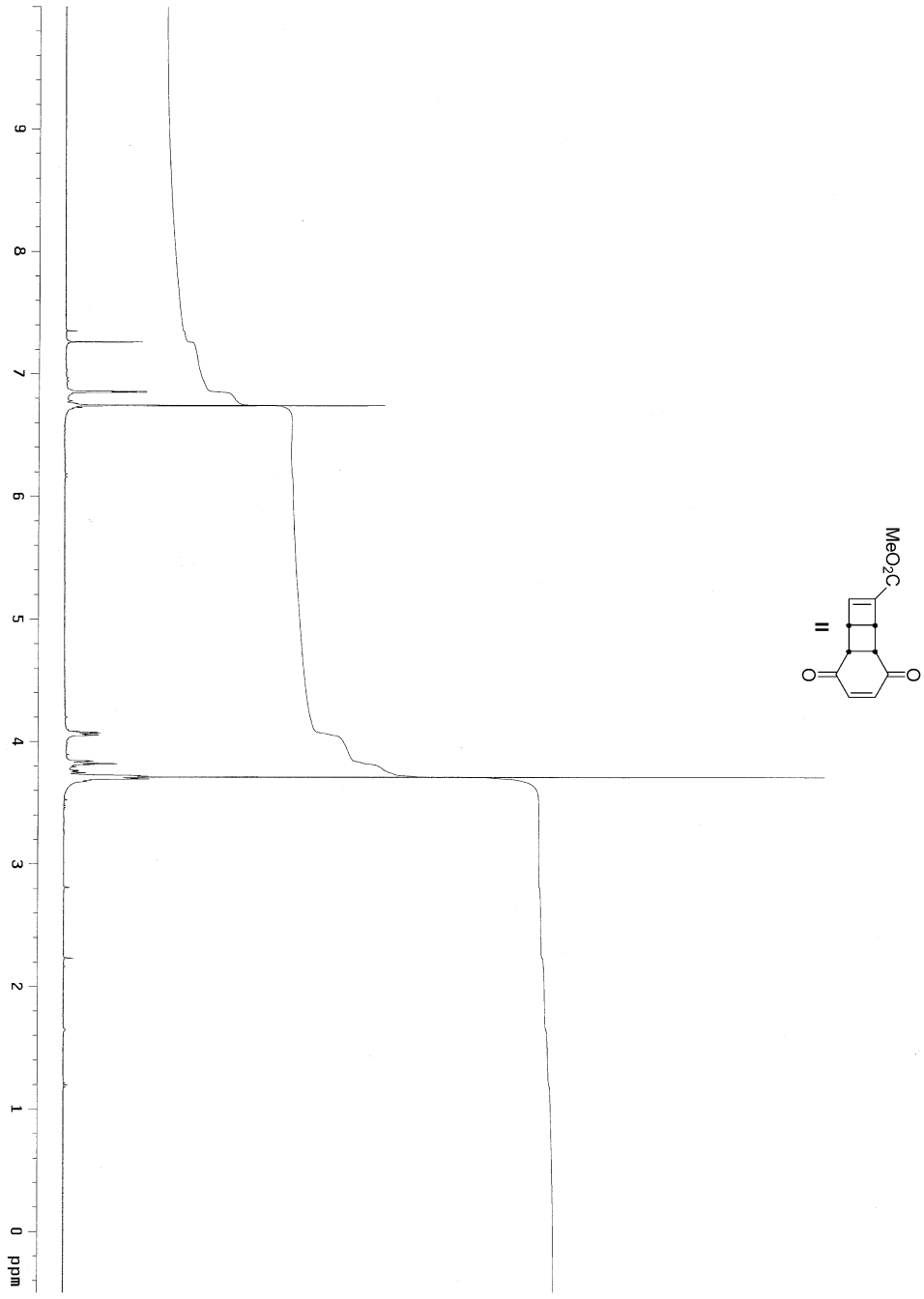
9
8
7
6
5
4
3
2
1
0
ppm
MeO2C
O
O

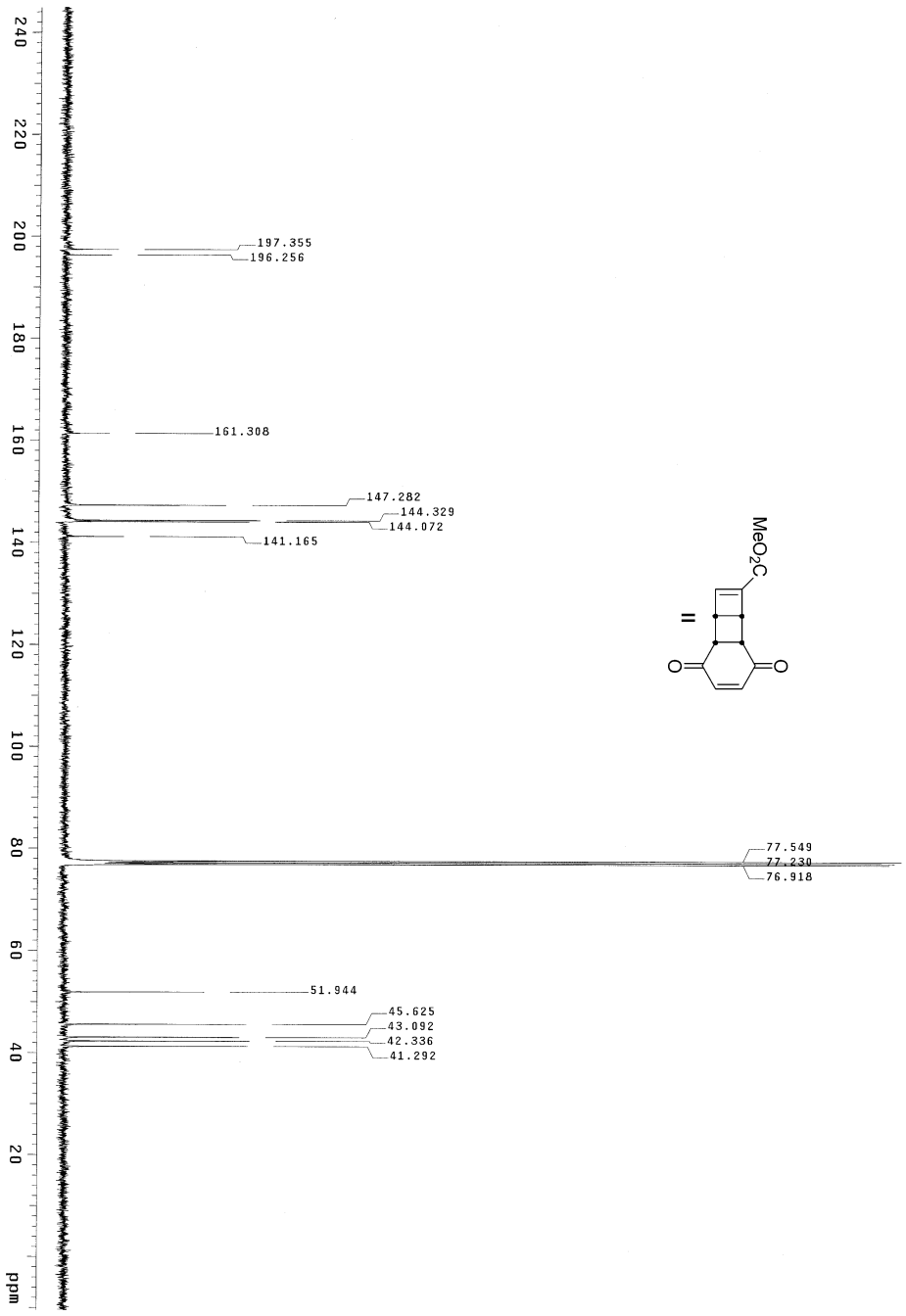
240
220
200
180
160
140
120
100
80
60
40
20
ppm
197.355
196.256
161.308
147.282
144.329
144.072
141.165
77.549
77.230
76.918
51.944
45.625
43.092
42.336
41.292
MeO2C
II
O
O

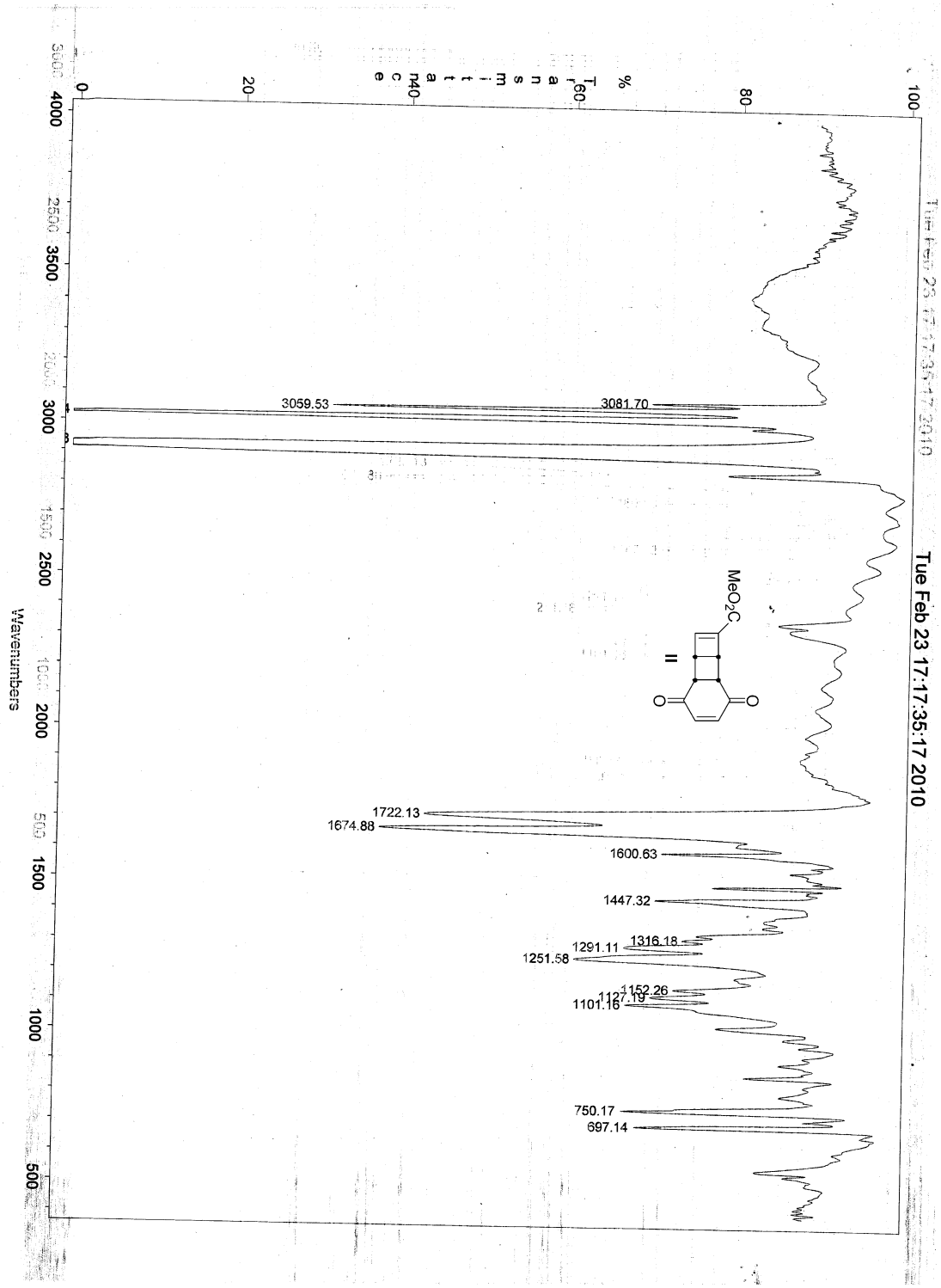
Tue Feb 23 17:17:35:17 2010
% Transmittance
Wavenumbers
4000
3500
3000
2500
2000
1500
1000
500
3059.53
3081.70
1722.13
1674.88
1600.63
1447.32
1316.18
1291.11
1251.58
1152.26
1127.19
1101.16
750.17
697.14
MeO2C

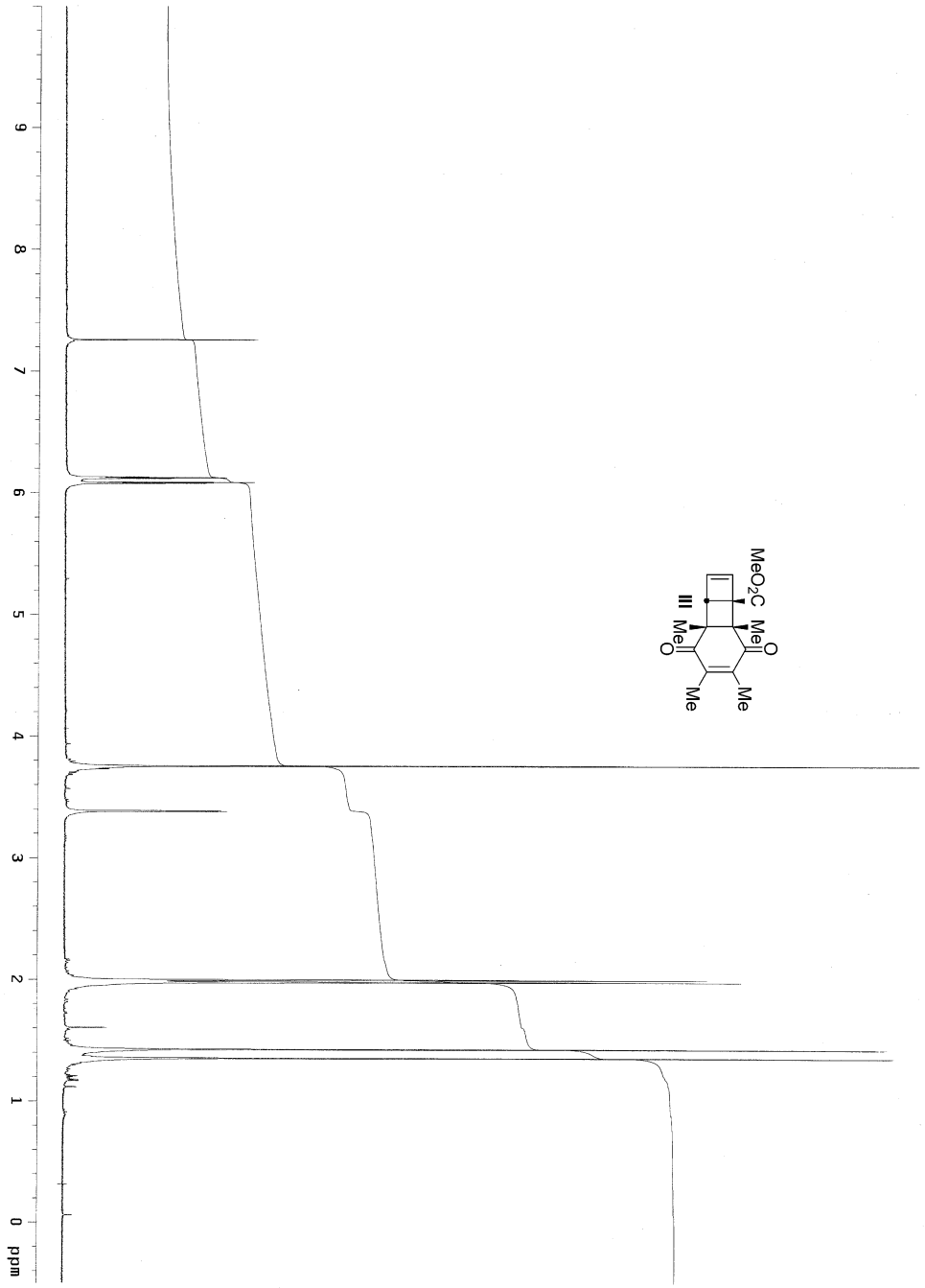
9
8
7
6
5
4
3
2
1
0
ppm
MeO2C
Me
O
Me
Me
O
Me
Me

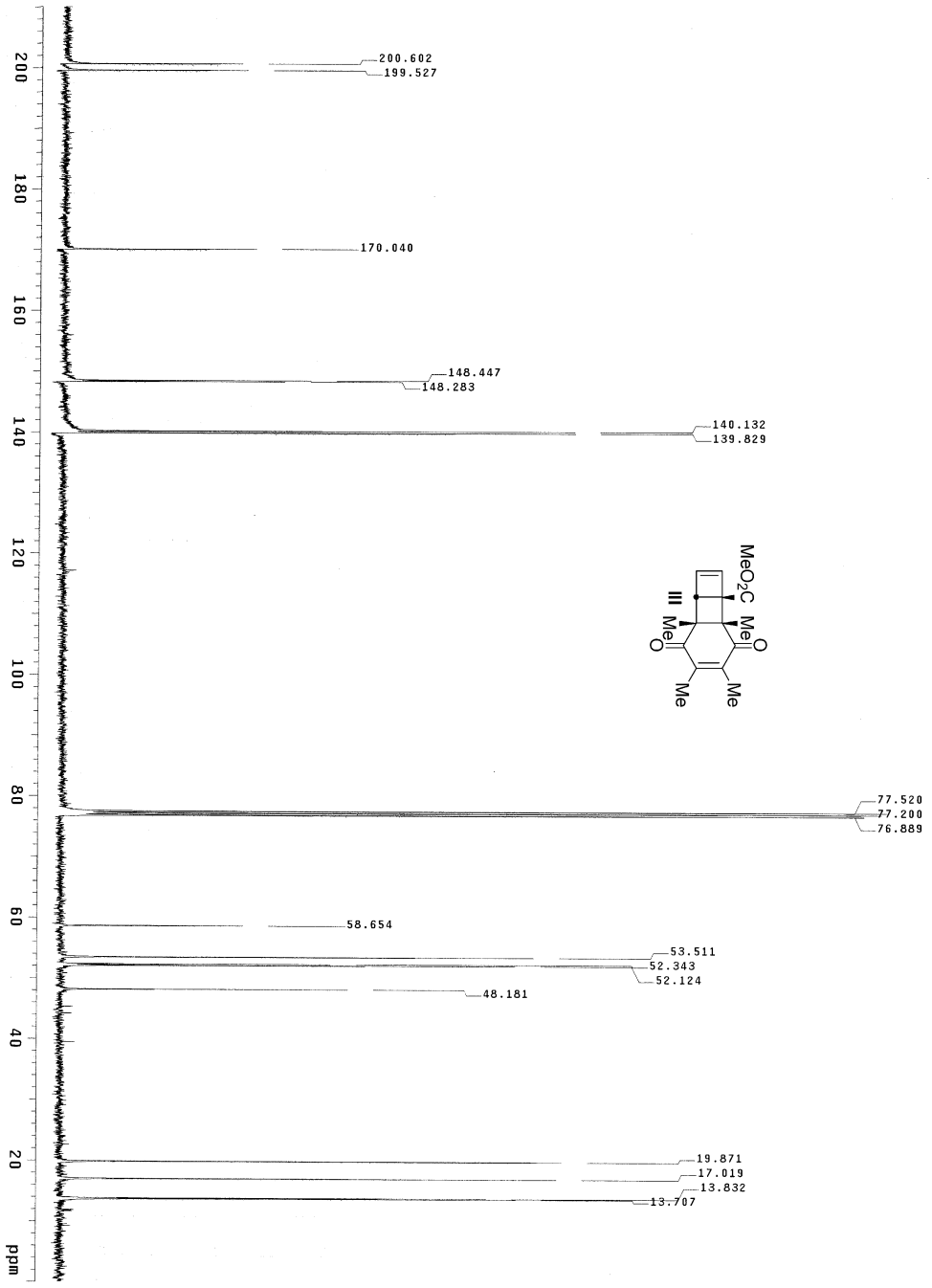
200.602
199.527
170.040
148.447
148.283
140.132
139.829
77.520
77.200
76.889
58.654
53.511
52.343
52.124
48.181
19.871
17.019
13.832
13.707
200
180
160
140
120
100
80
60
40
20
ppm
MeO2C
Me
O
Me
Me
Me
O
Me

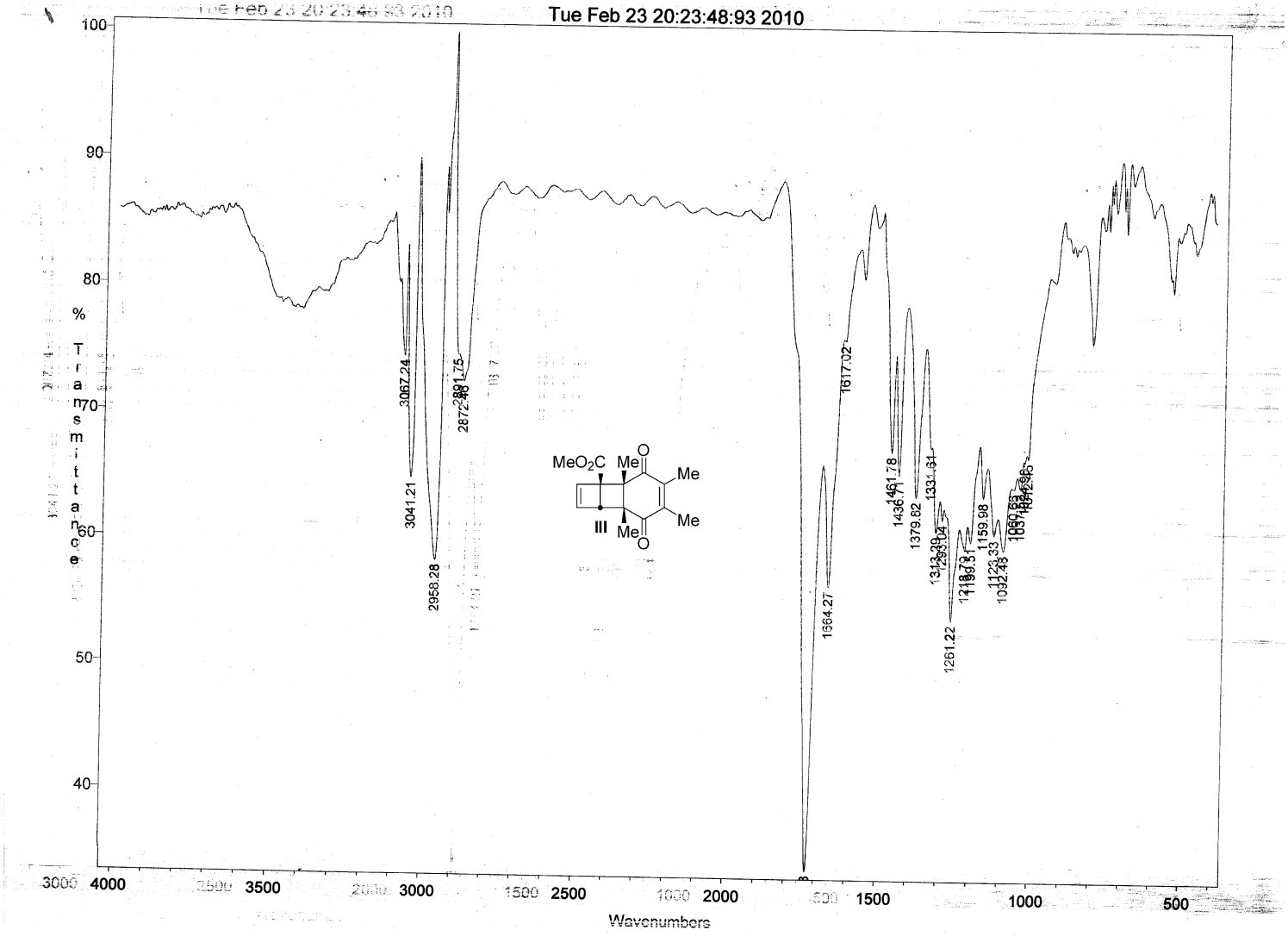
Tue Feb 23 20:23:48:93 2010
% Transmittance
Wavenumbers
3067.24
3041.21
2958.28
2891.75
2872.48
1617.02
1564.27
1461.78
1436.71
1379.82
1331.61
1261.22
1159.98
MeO2C
Me
O
Me
Me
Me
O
III

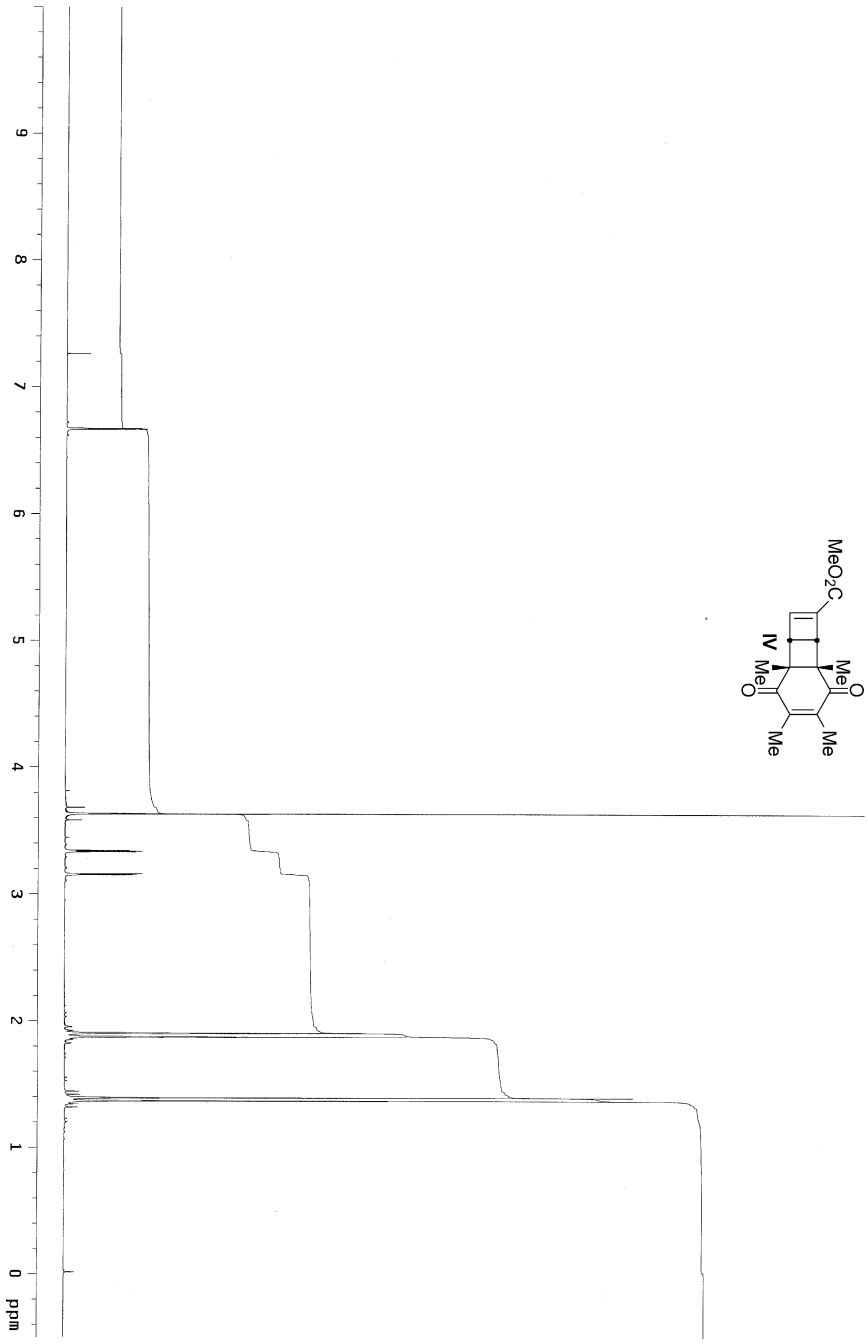
MeO2C
IV
Me
Me
O
Me
Me
O
9
8
7
6
5
4
3
2
1
0
ppm

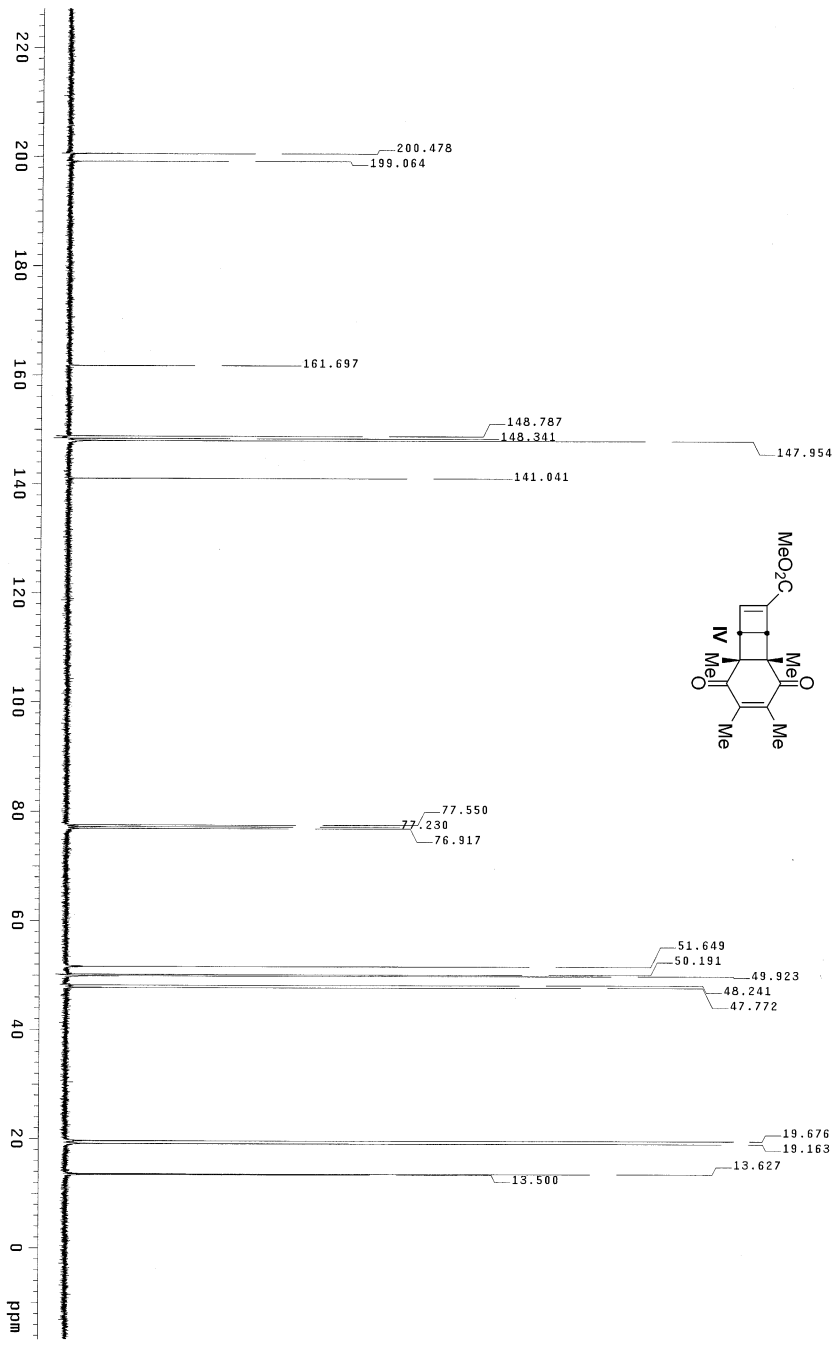
220
200
180
160
140
120
100
80
60
40
20
0
ppm
200.478
199.064
161.697
148.787
148.341
147.954
141.041
77.550
77.230
76.917
51.649
50.191
49.923
48.241
47.772
19.676
19.163
13.627
13.500
IV
MeO2C
Me
Me
Me
Me
O
O

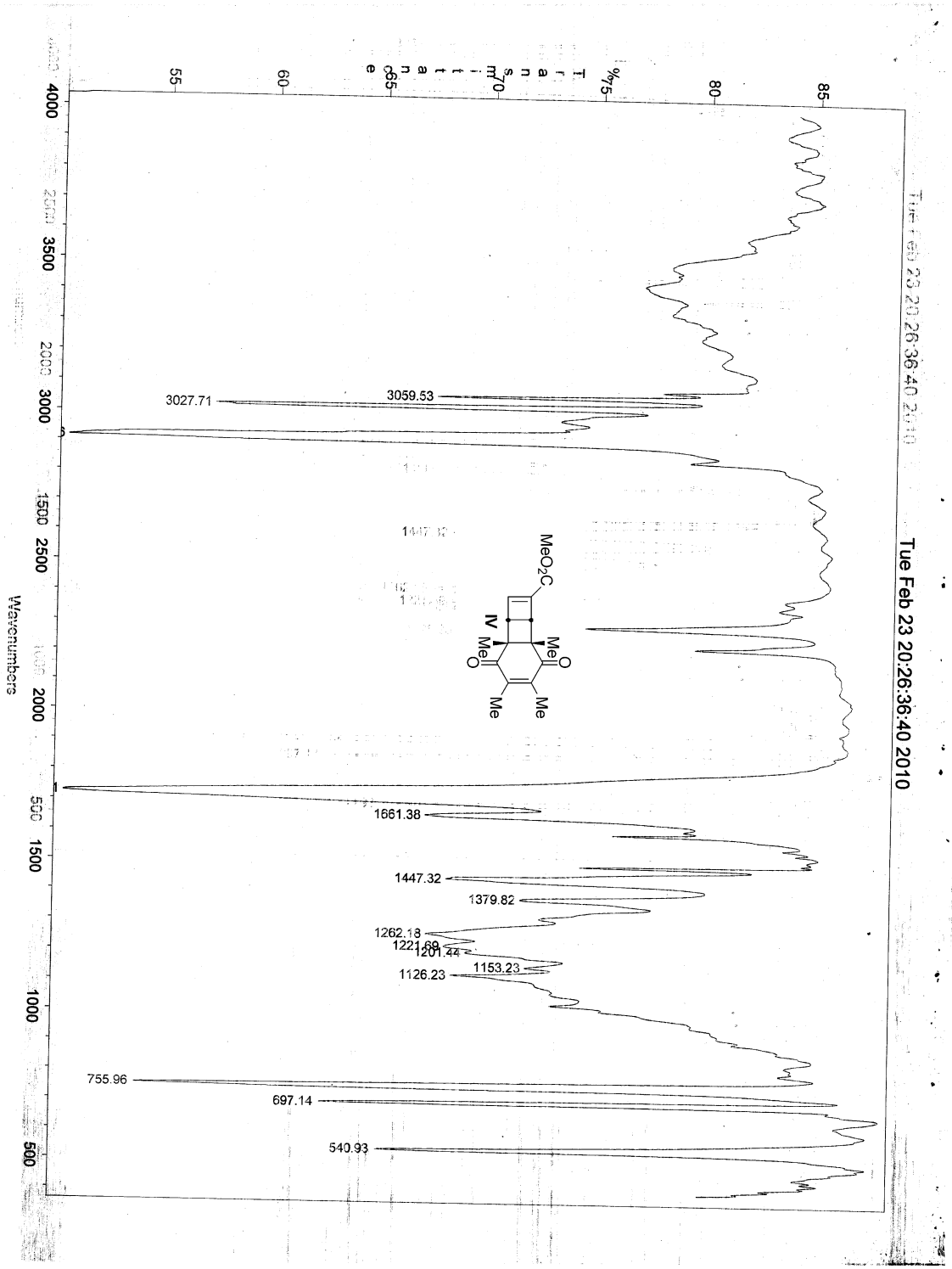
Tue Feb 23 20:26:36:40 2010
%T
Transmittance
Wavenumbers
4000
3500
3000
2500
2000
1500
1000
500
55
60
65
70
75
80
85
3027.71
3059.53
1661.38
1447.32
1379.82
1262.18
1221.69
1201.44
1153.23
1126.23
755.96
697.14
540.93
IV
MeO2C
Me
Me
Me
Me
O
O

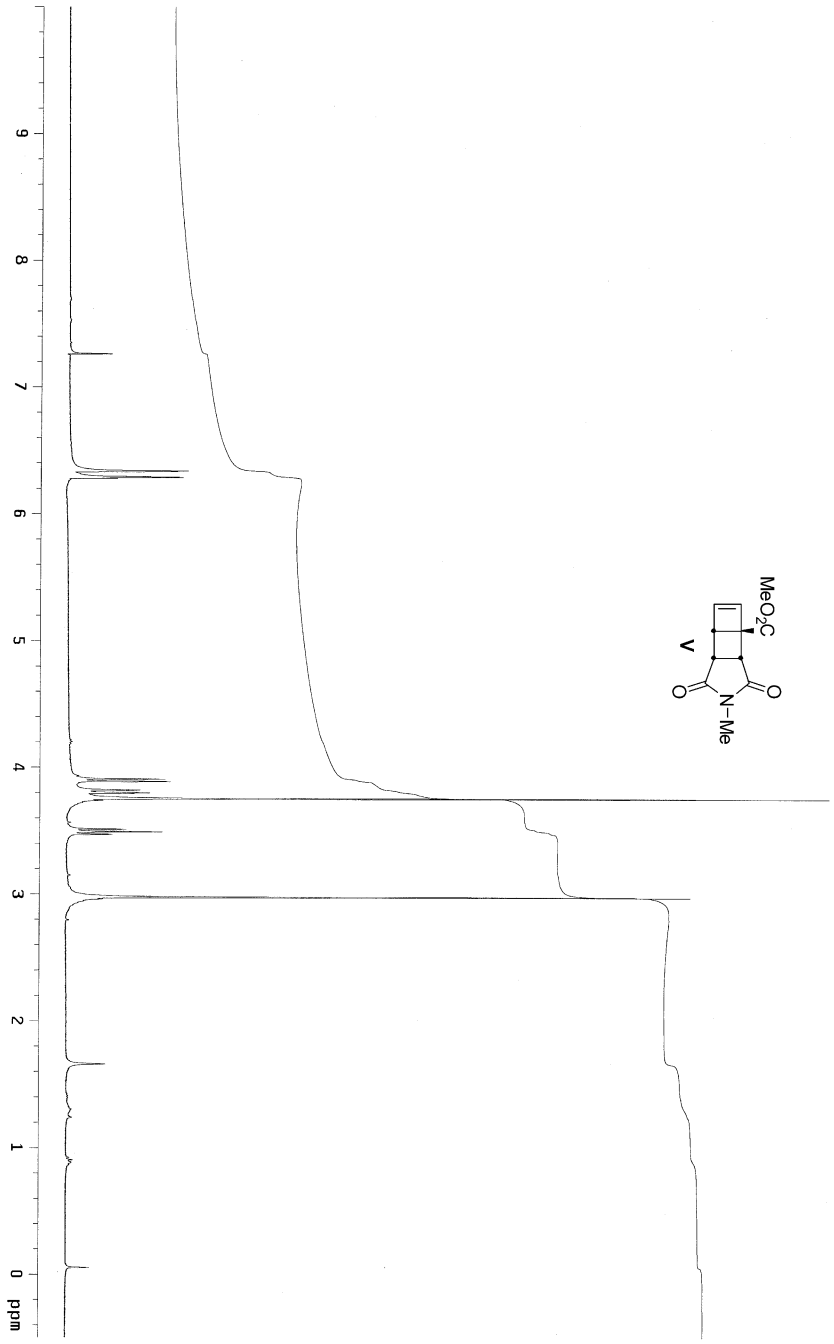
MeO2C
V
O
O
N–Me
9
8
7
6
5
4
3
2
1
0
ppm

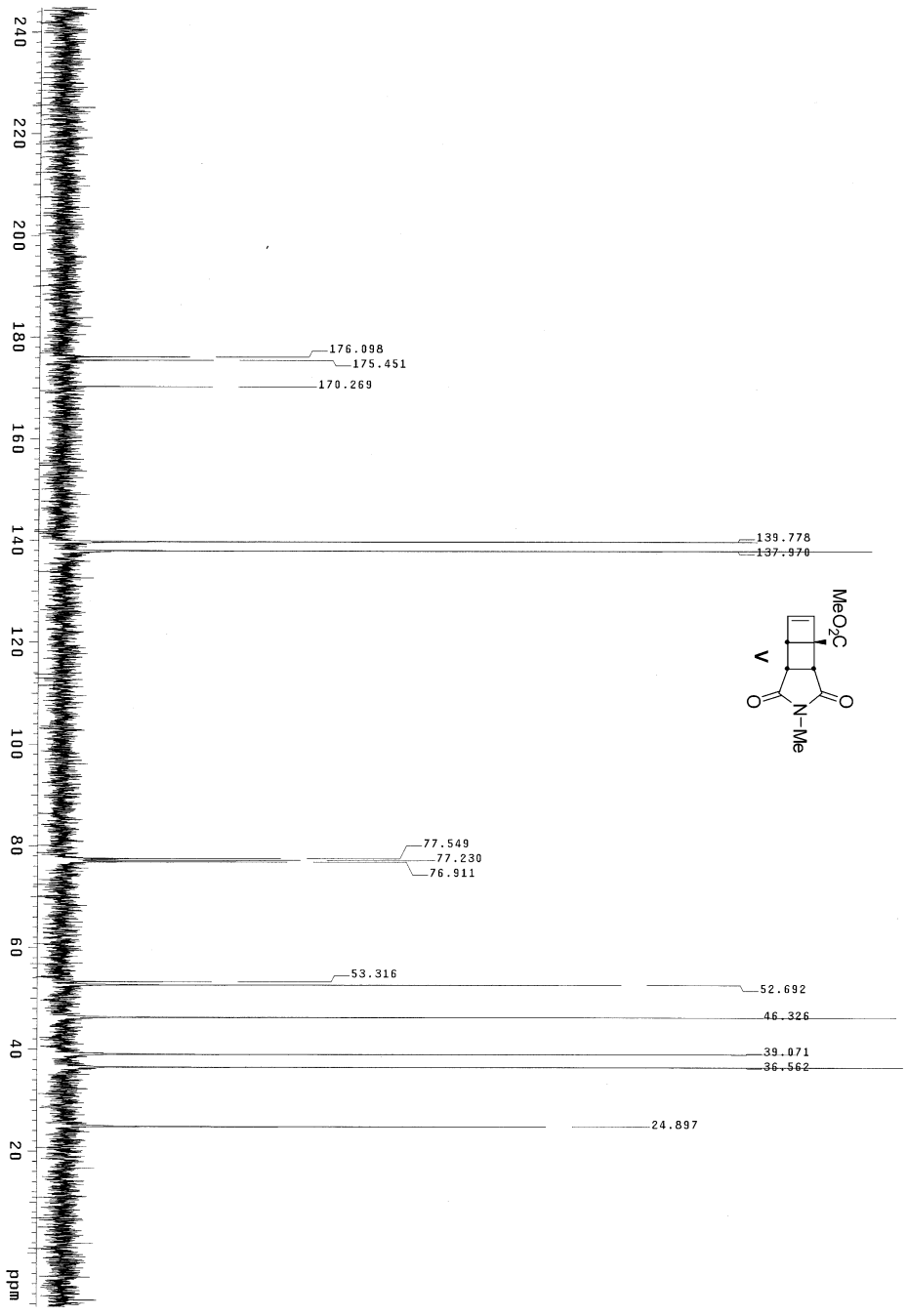
240
220
200
180
160
140
120
100
80
60
40
20
ppm
176.098
175.451
170.269
139.778
137.970
77.549
77.230
76.911
53.316
52.692
46.326
39.071
36.562
24.897
V
MeO2C
O
O
N–Me

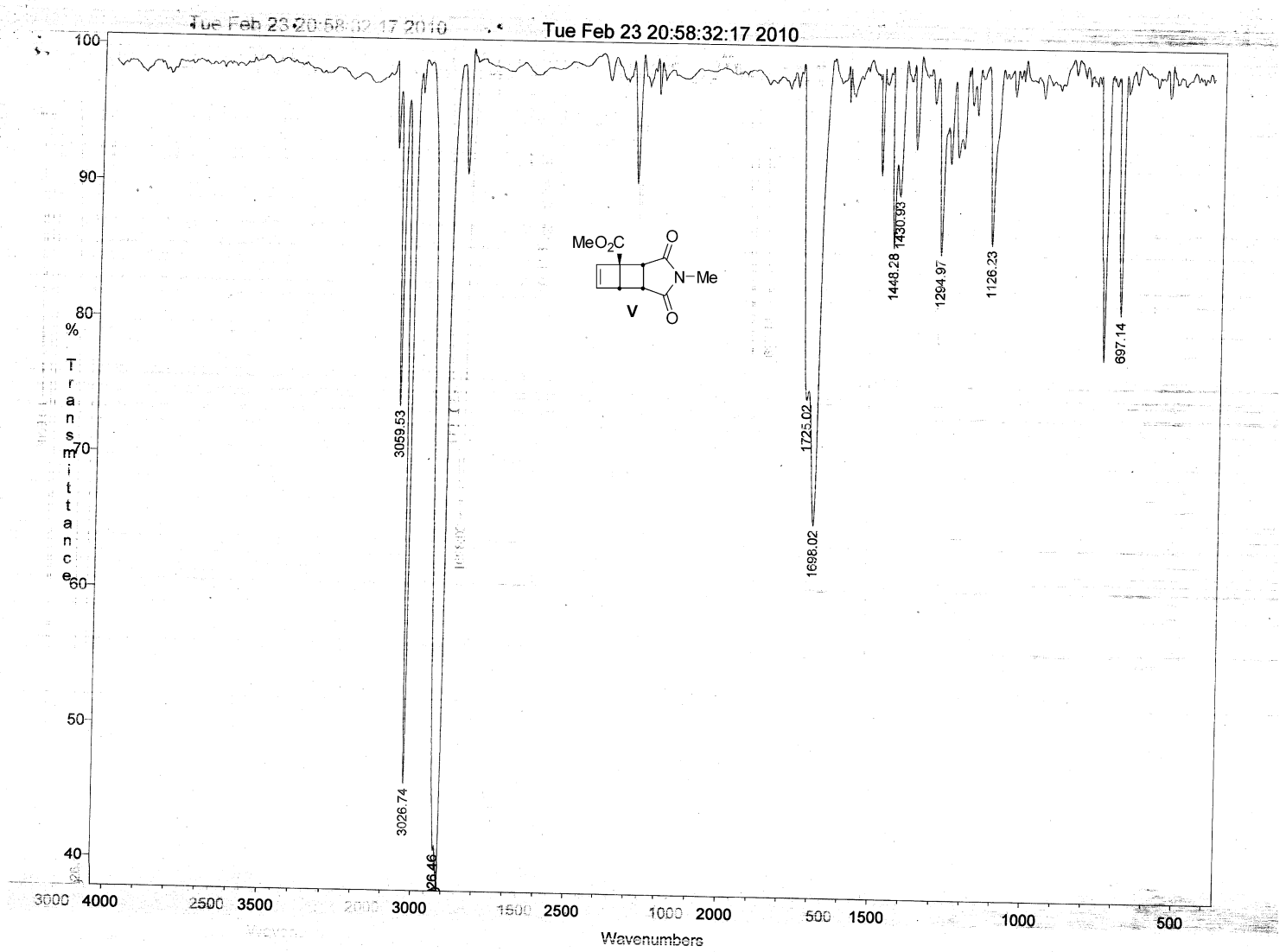
Tue Feb 23 20:58:32:17 2010
Tue Feb 23 20:58:32:17 2010
100
90
80
70
60
50
40
% Transmittance
3059.53
3026.74
2926.46
1725.02
1698.02
1448.28
1430.83
1294.97
1126.23
697.14
MeO2C
O
N–Me
O
V
4000
3500
3000
2500
2000
1500
1000
500
Wavenumbers

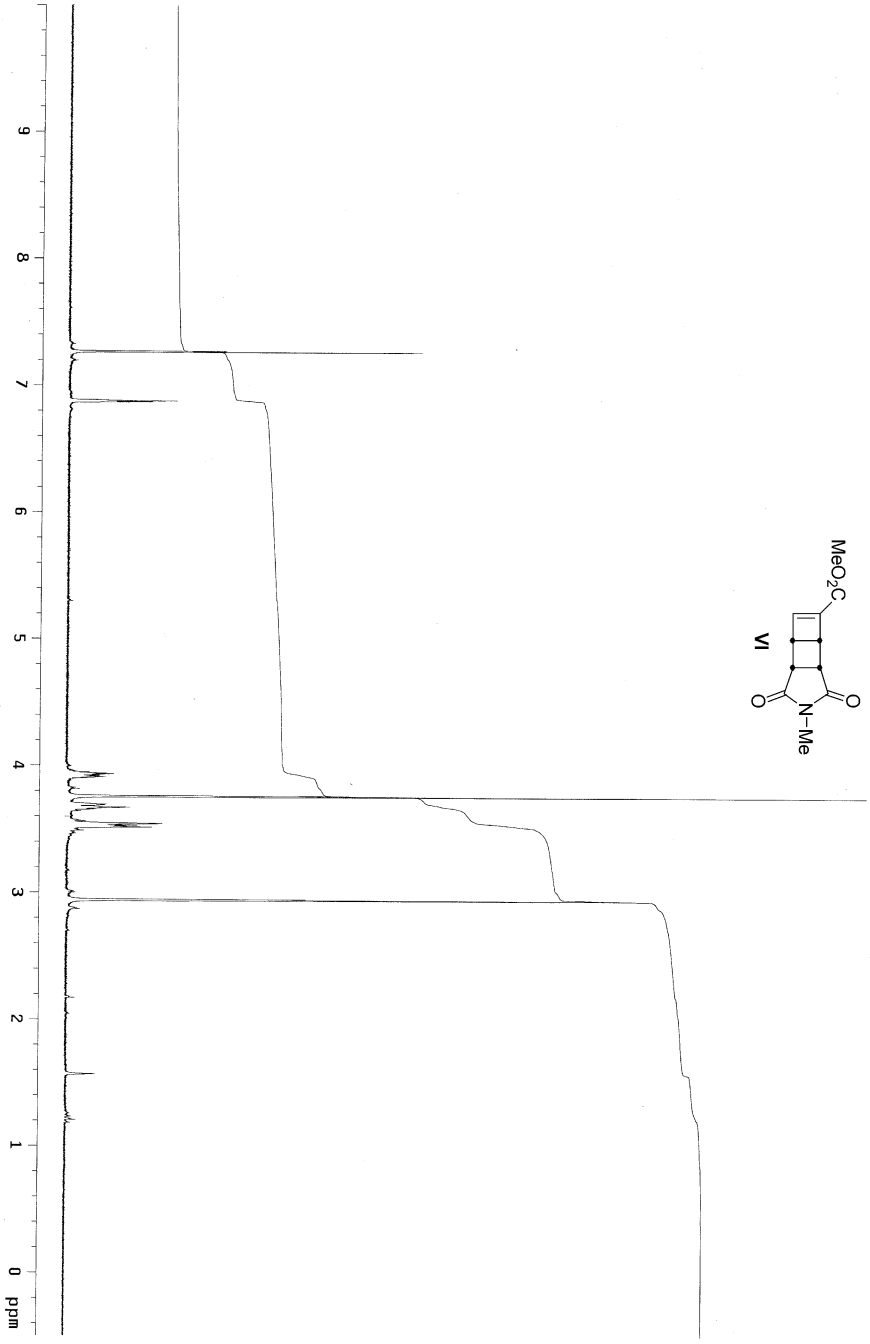
MeO2C
VI
O
O
N–Me
9
8
7
6
5
4
3
2
1
0
ppm

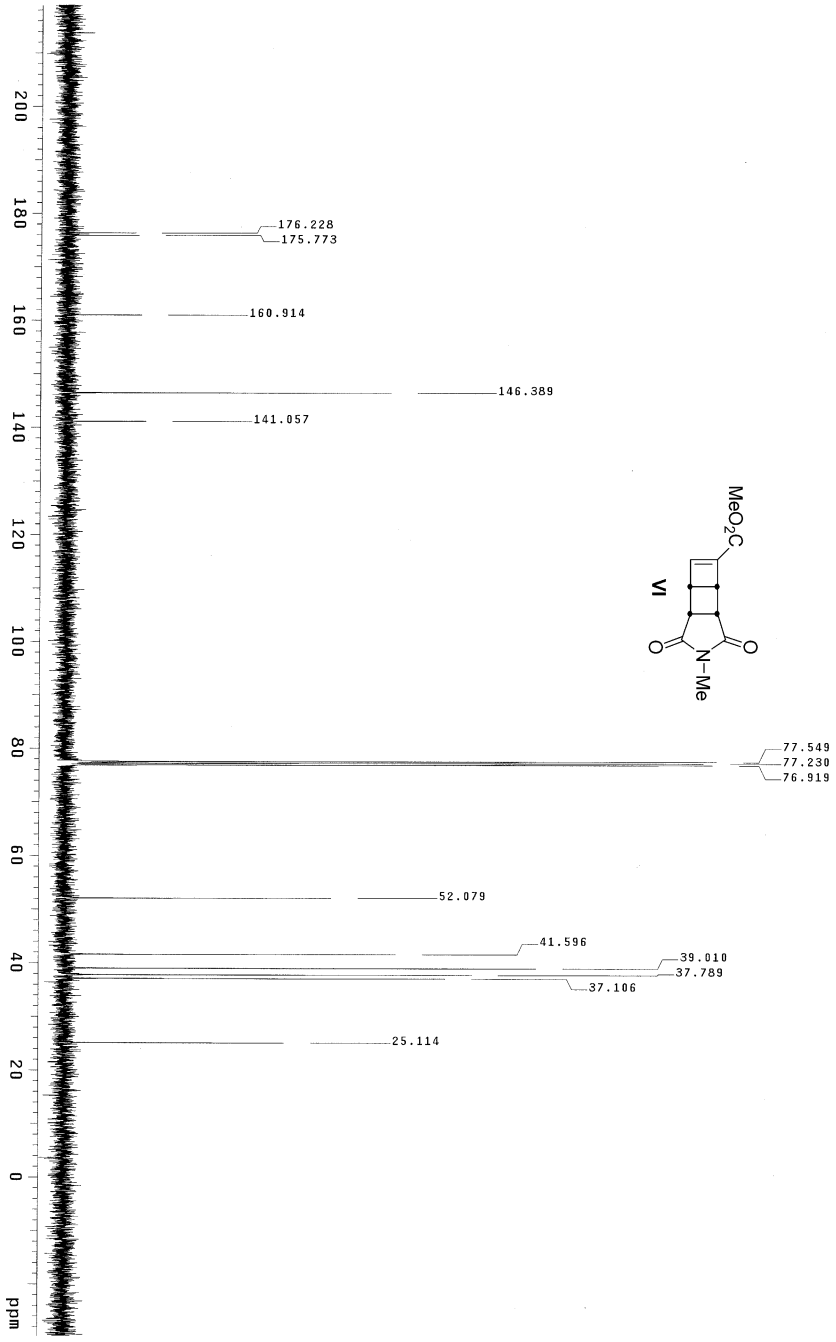
176.228
175.773
160.914
146.389
141.057
77.549
77.230
76.919
52.079
41.596
39.010
37.789
37.106
25.114
200
180
160
140
120
100
80
60
40
20
0
ppm
VI
MeO2C
N-Me
O
O

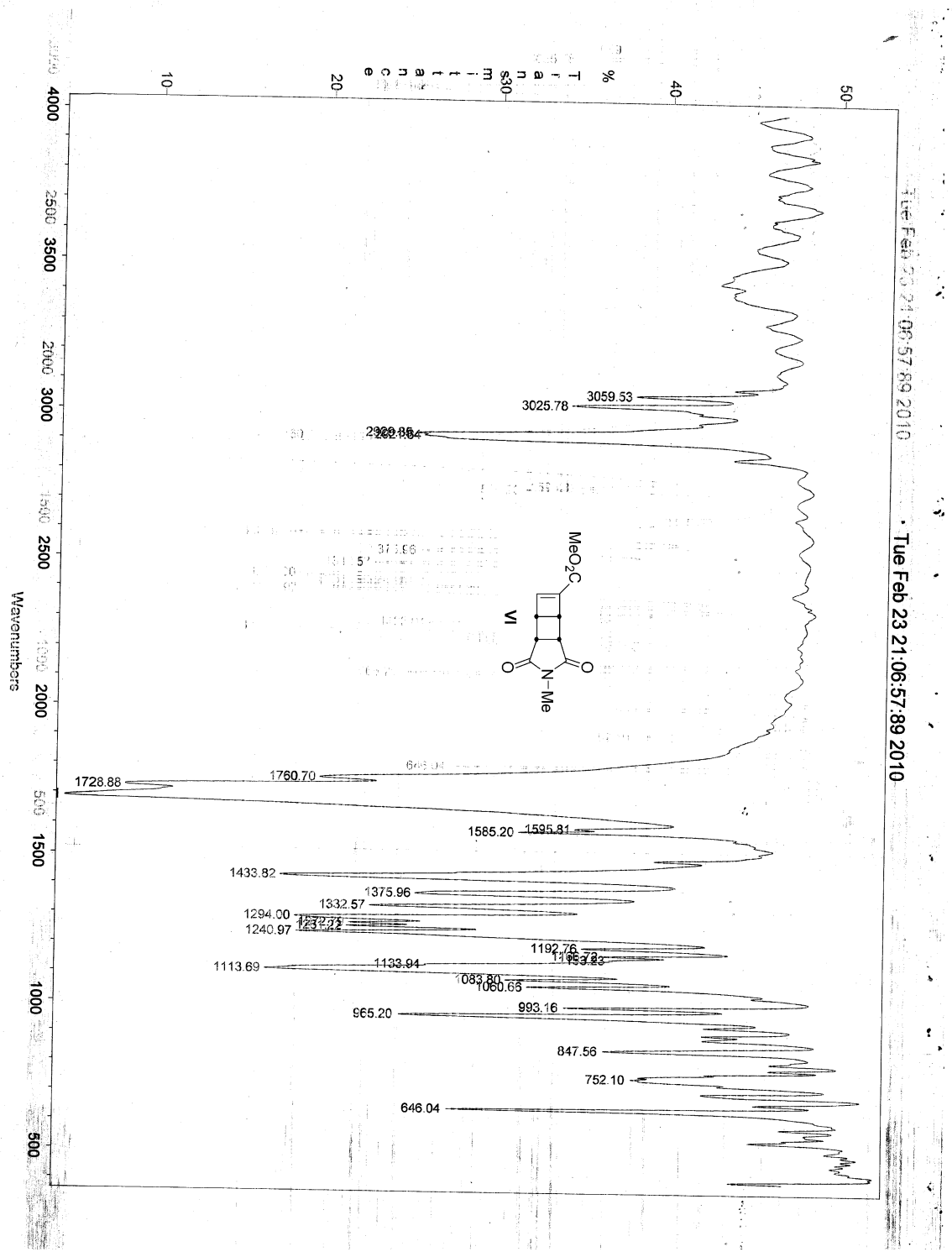
Tue Feb 23 21:06:57:89 2010
Transmittance %
Wavenumbers
4000
3500
3000
2500
2000
1500
1000
500
3059.53
3025.78
1728.88
1760.70
1585.20
1595.81
1433.82
1375.96
1332.57
1294.00
1240.97
1192.76
1133.94
1113.69
1083.80
1060.65
993.16
965.20
847.56
752.10
646.04
VI
MeO2C
N–Me
O
O

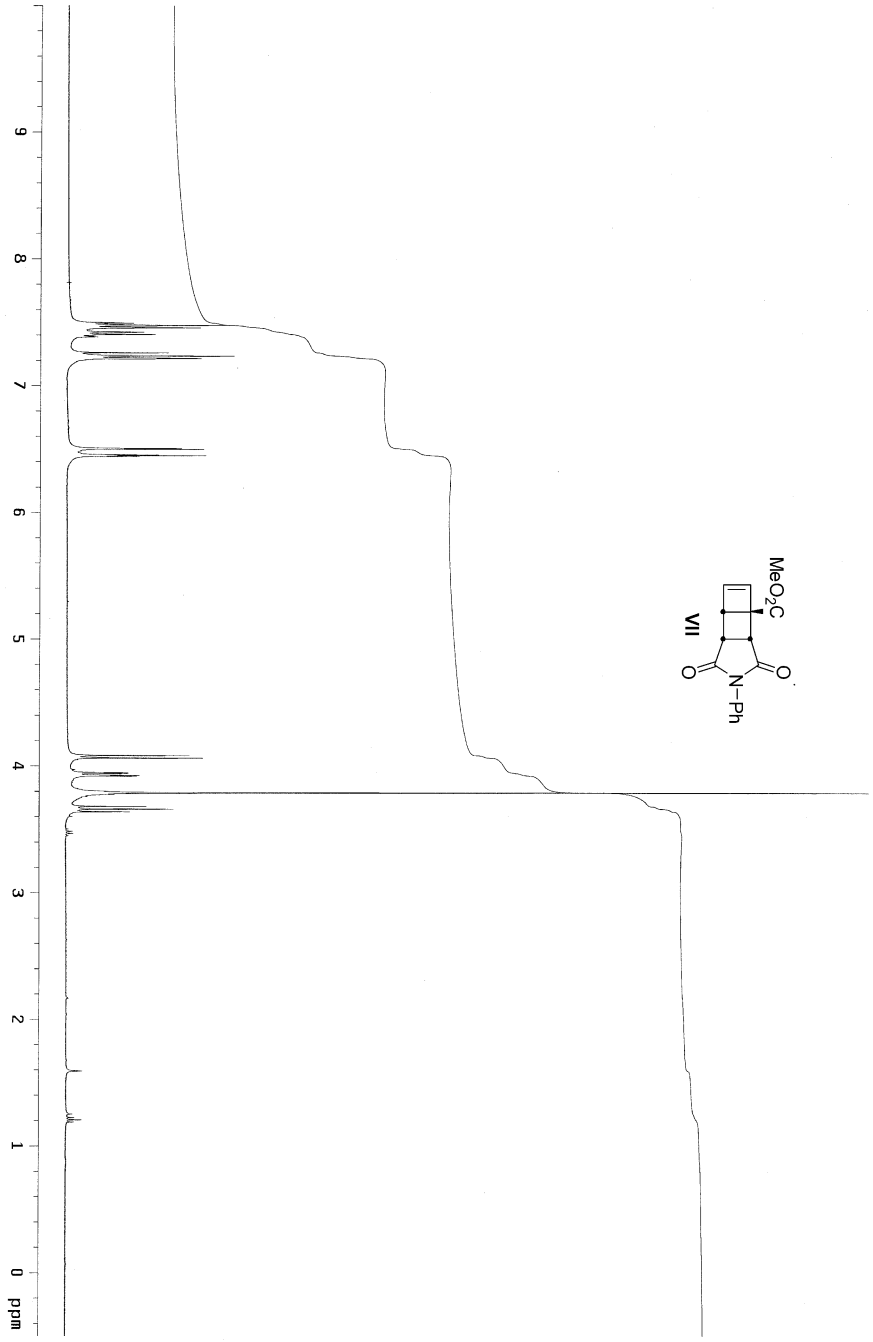
MeO2C
VII
O
O
N–Ph
9
8
7
6
5
4
3
2
1
0
ppm

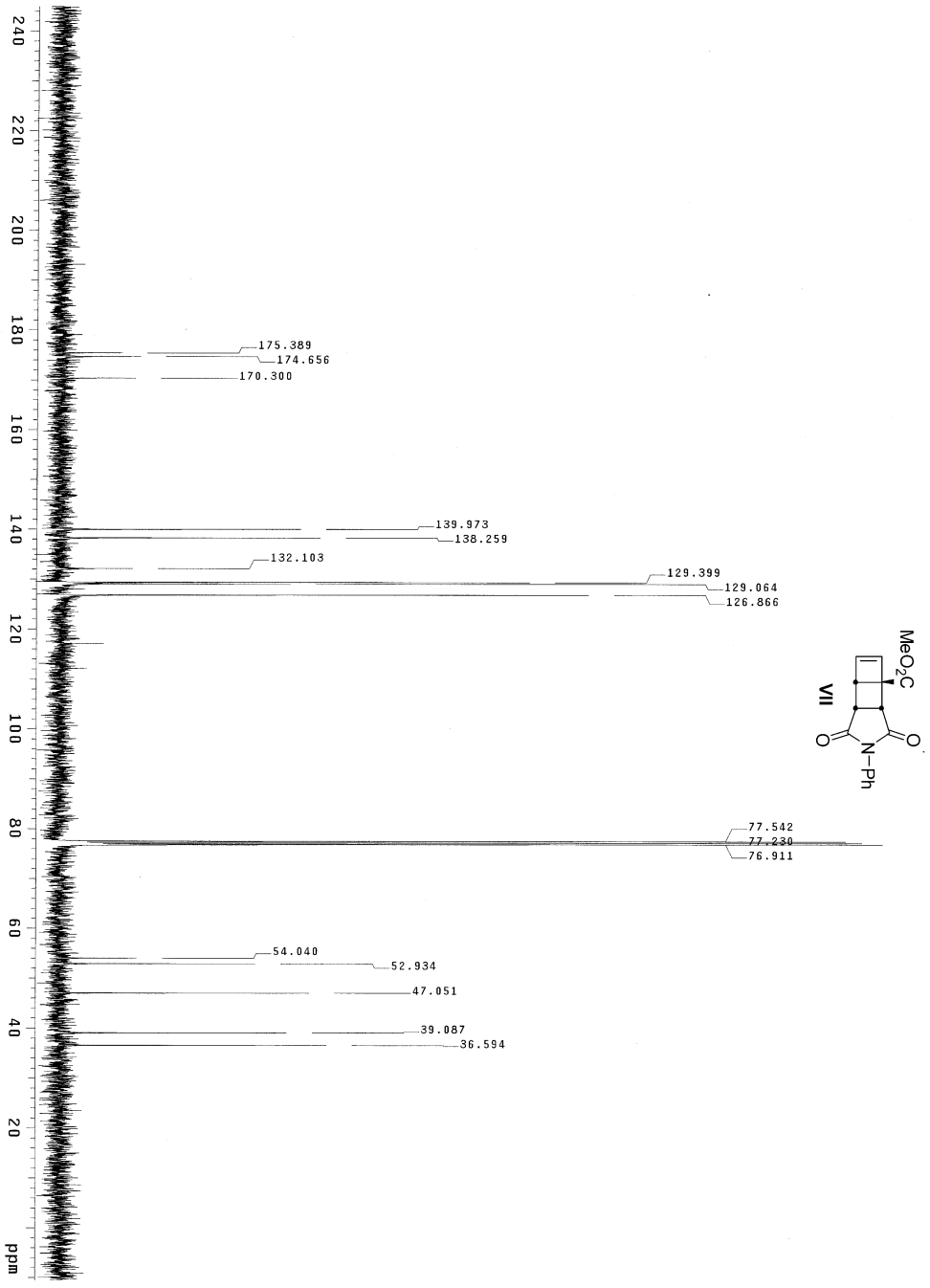
240
220
200
180
160
140
120
100
80
60
40
20
ppm
175.389
174.656
170.300
139.973
138.259
132.103
129.399
129.064
126.866
77.542
77.230
76.911
54.040
52.934
47.051
39.087
36.594
VII
MeO2C
O
N–Ph
O

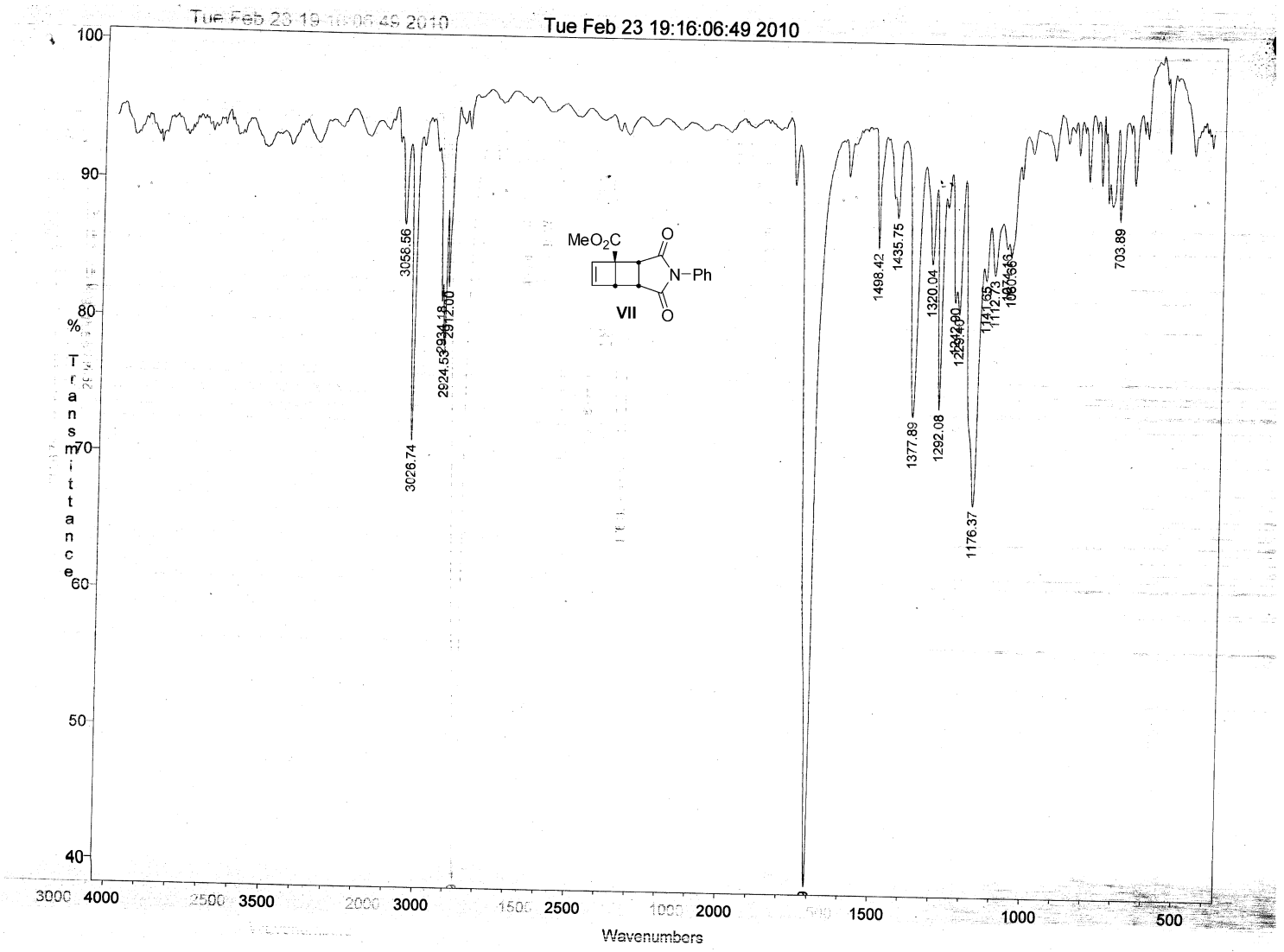
Tue Feb 23 19:16:06:49 2010
Tue Feb 23 19:16:06:49 2010
100
90
80
70
60
50
40
% Transmittance
3058.56
3026.74
2924.53
2934.18
2912.00
1498.42
1435.75
1377.89
1320.04
1292.08
1223.90
1176.37
1141.95
1112.23
1080.66
703.89
MeO2C
O
N–Ph
O
VII
3000
4000
2500
3500
2000
3000
1500
2500
1000
2000
1500
1000
500
Wavenumbers

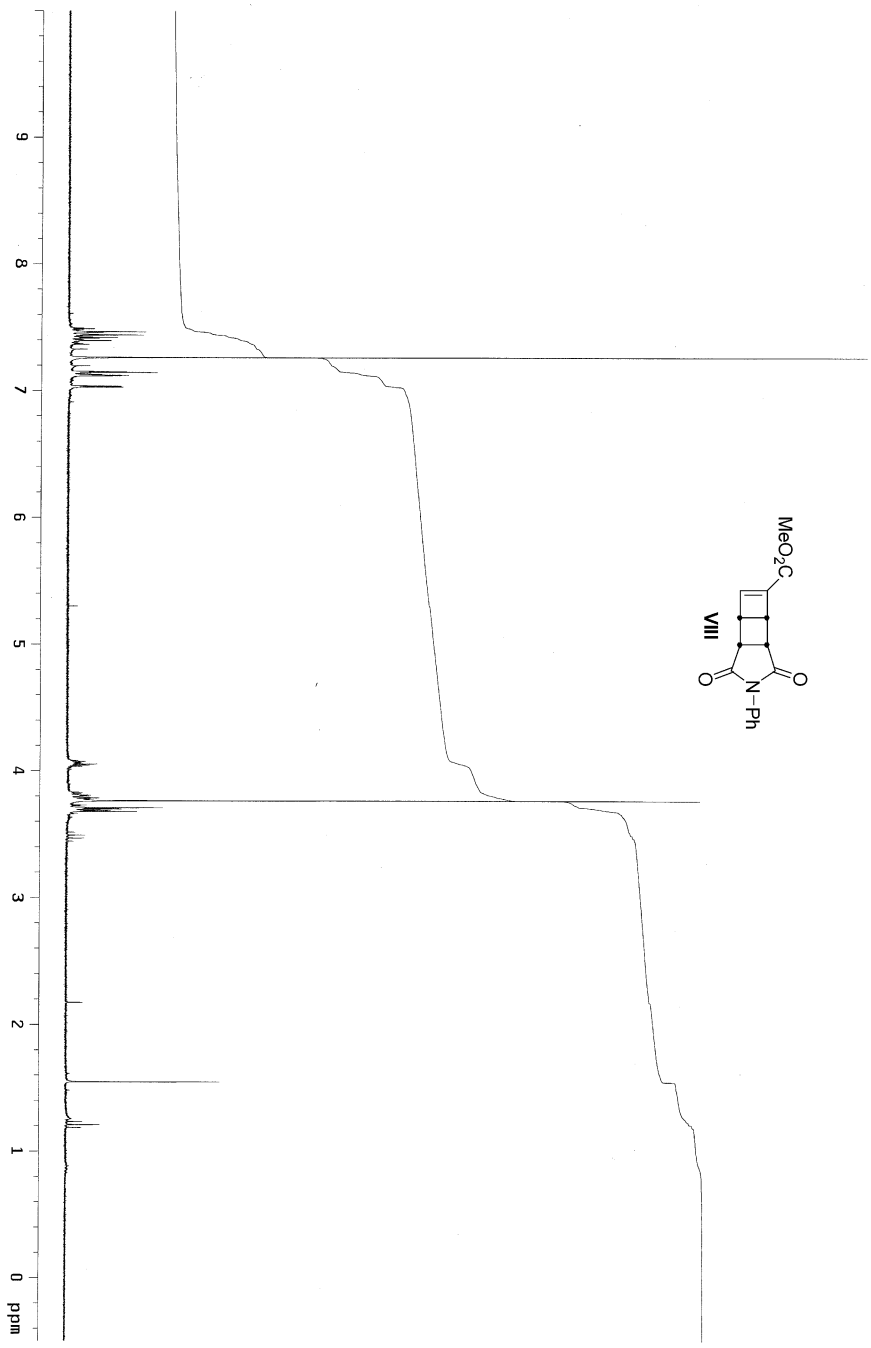
MeO2C
VIII
O
O
N–Ph
9
8
7
6
5
4
3
2
1
0
ppm

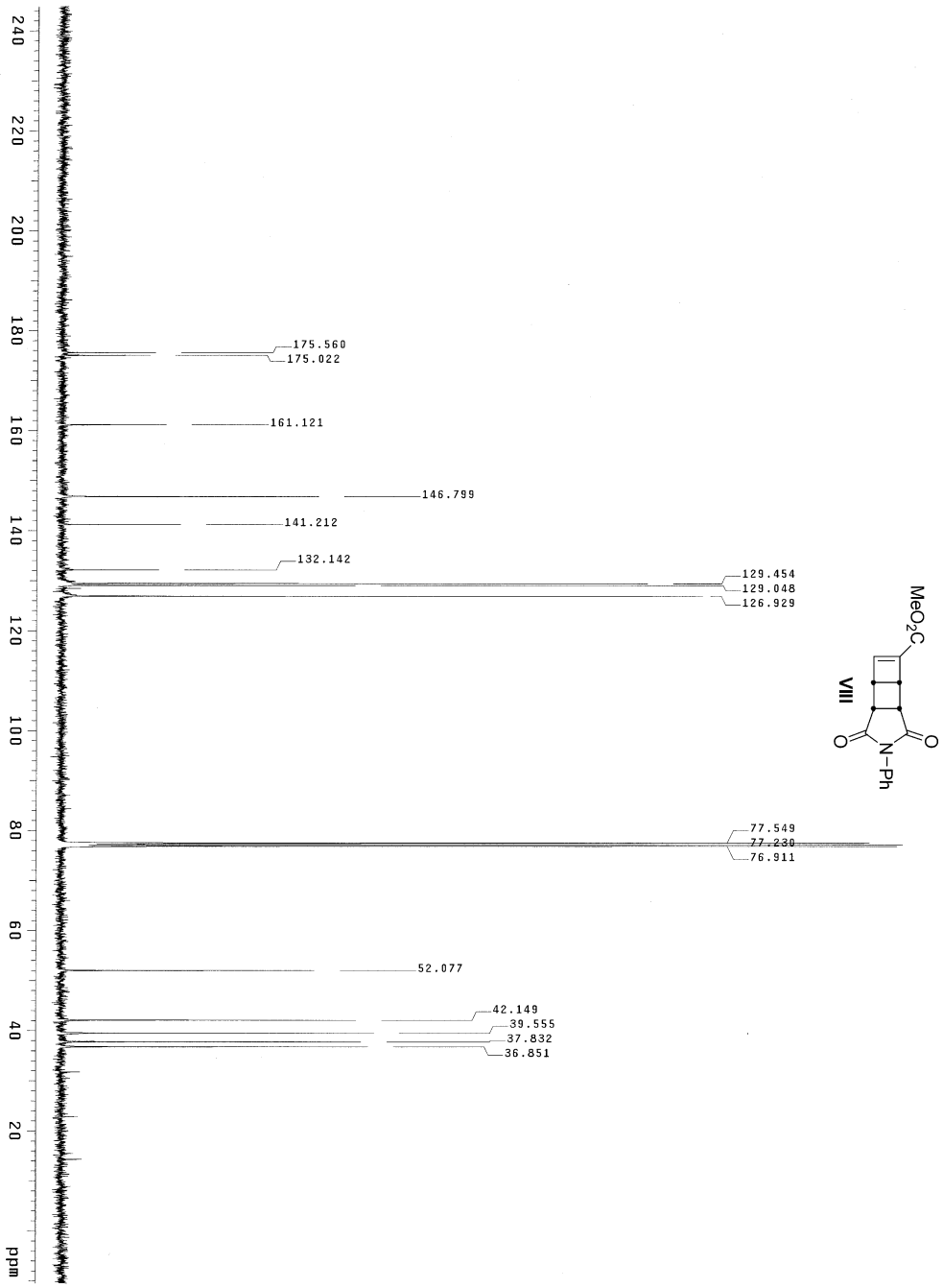
175.560
175.022
161.121
146.799
141.212
132.142
129.454
129.048
126.929
77.549
77.230
76.911
52.077
42.149
39.555
37.832
36.851
ppm
MeO2C
VIII
N-Ph
O
O

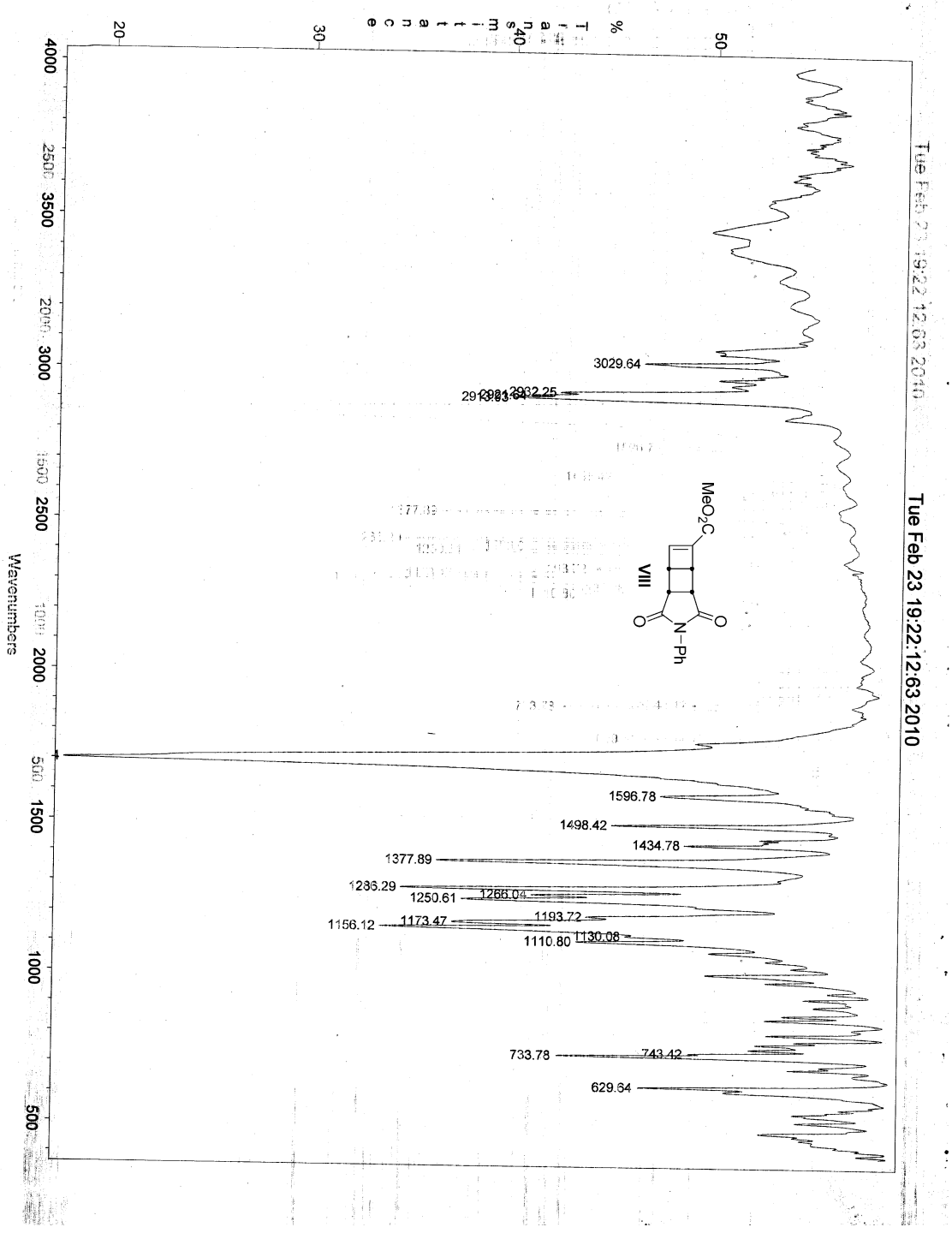
Tue Feb 23 19:22:12:63 2010
%
Transmittance
Wavenumbers
4000
3500
3000
2500
2000
1500
1000
500
20
30
40
50
3029.64
2962.25
1596.78
1498.42
1434.78
1377.89
1286.29
1250.61
1266.04
1193.72
1173.47
1156.12
1130.08
1110.80
743.42
733.78
629.64
MeO2C
N–Ph
O
O
VIII

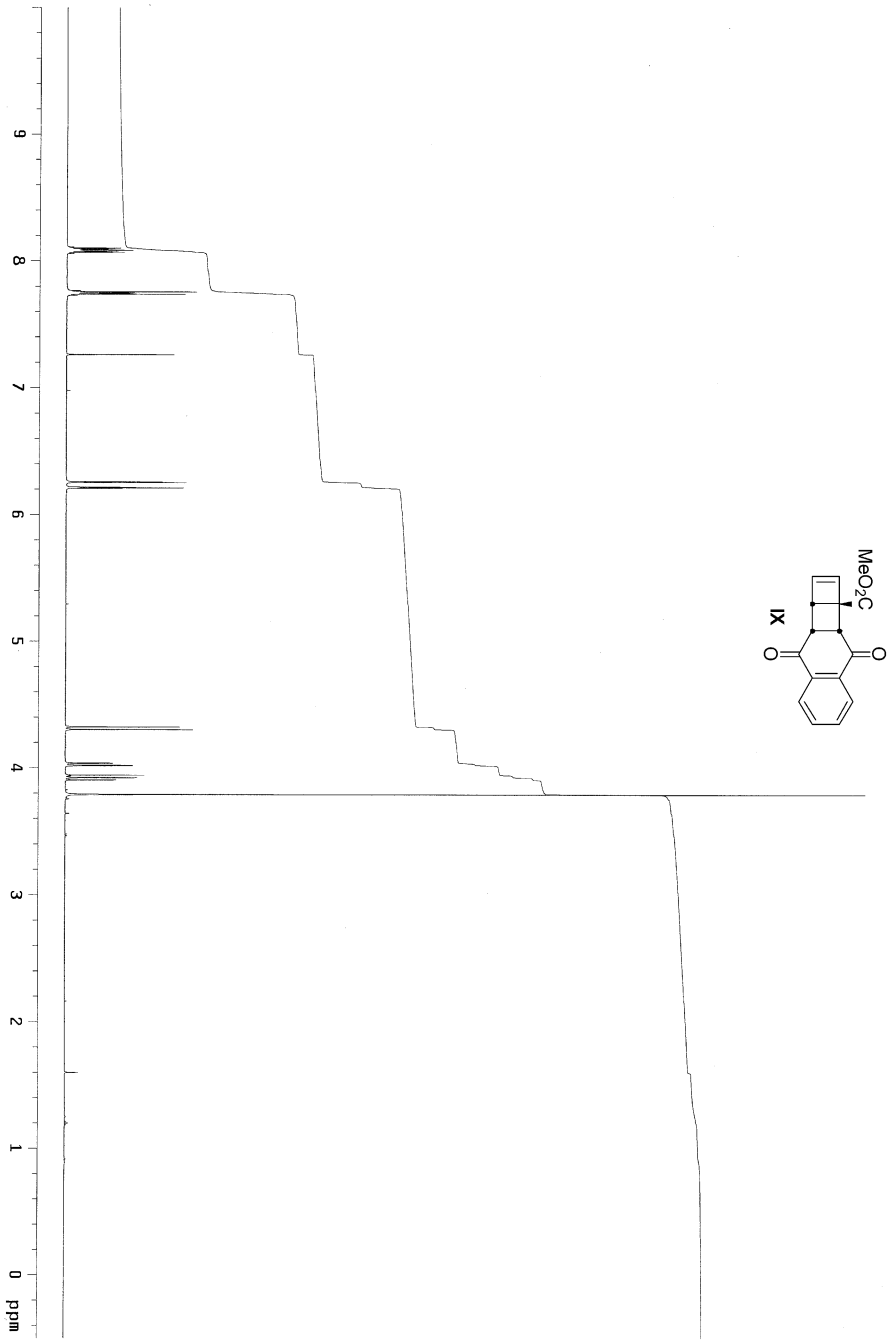

XI

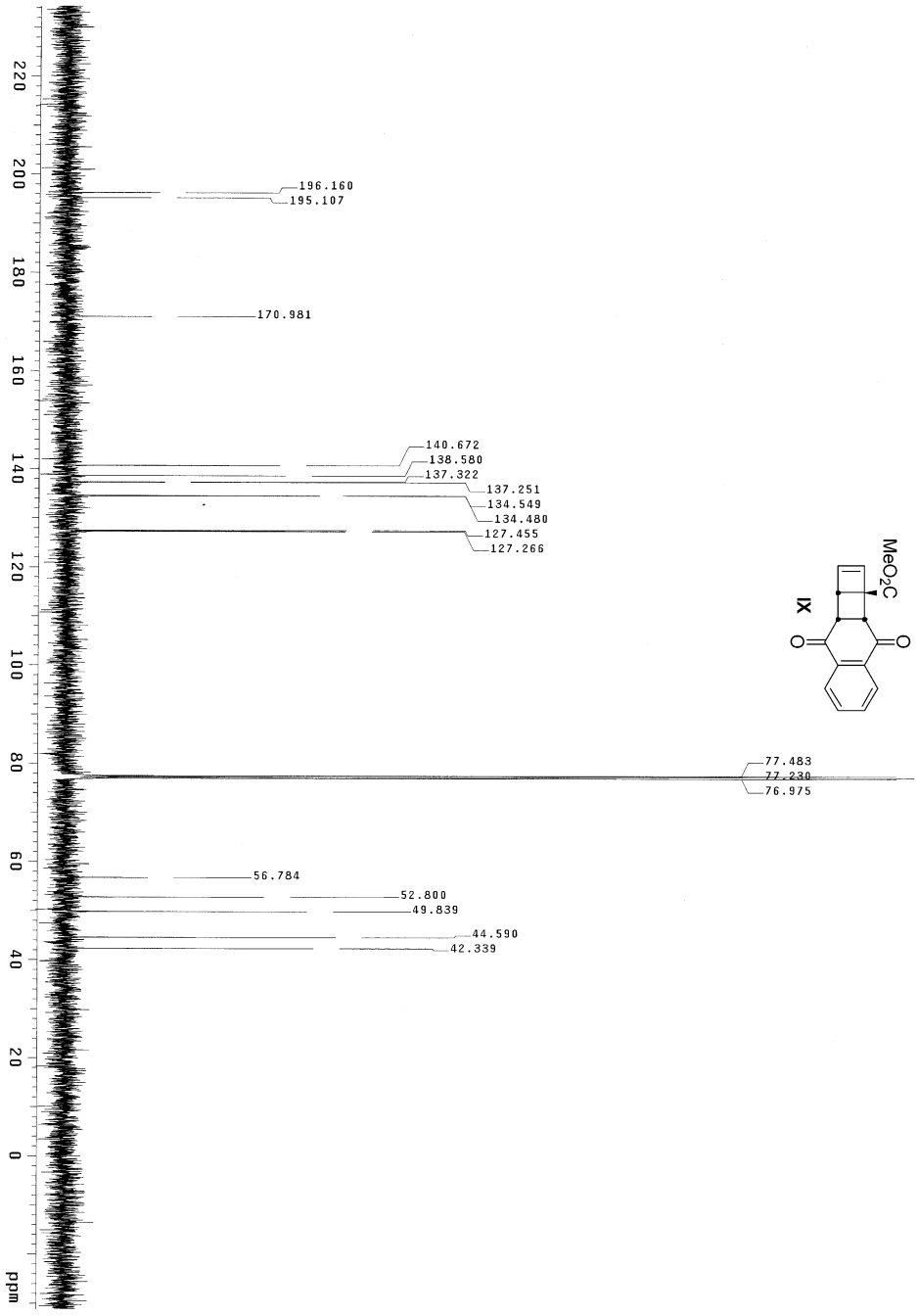
196.160
195.107
170.981
140.672
138.580
137.322
137.251
134.549
134.480
127.455
127.266
77.483
77.230
76.975
56.784
52.800
49.839
44.590
42.339
220
200
180
160
140
120
100
80
60
40
20
0
ppm
IX
MeO2C
O
O

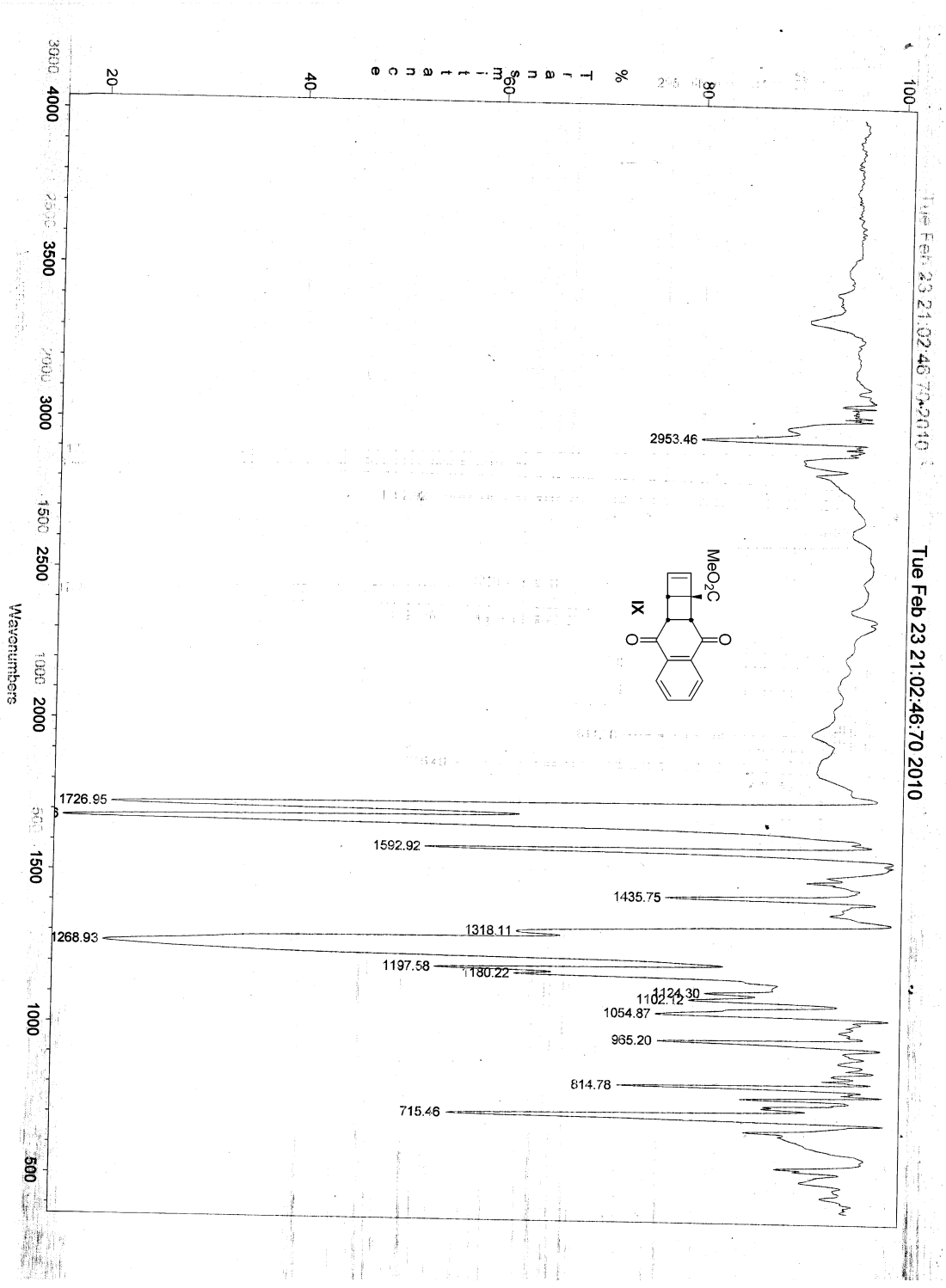
Tue Feb 23 21:02:46 70 2010
Wavenumbers
% Transmittance
4000
3500
3000
2500
2000
1500
1000
500
100
80
60
40
20
2953.46
1726.95
1592.92
1435.75
1318.11
1268.93
1197.58
1180.22
1124.30
1102.12
1054.87
965.20
814.78
715.46
IX
MeO2C
O
O

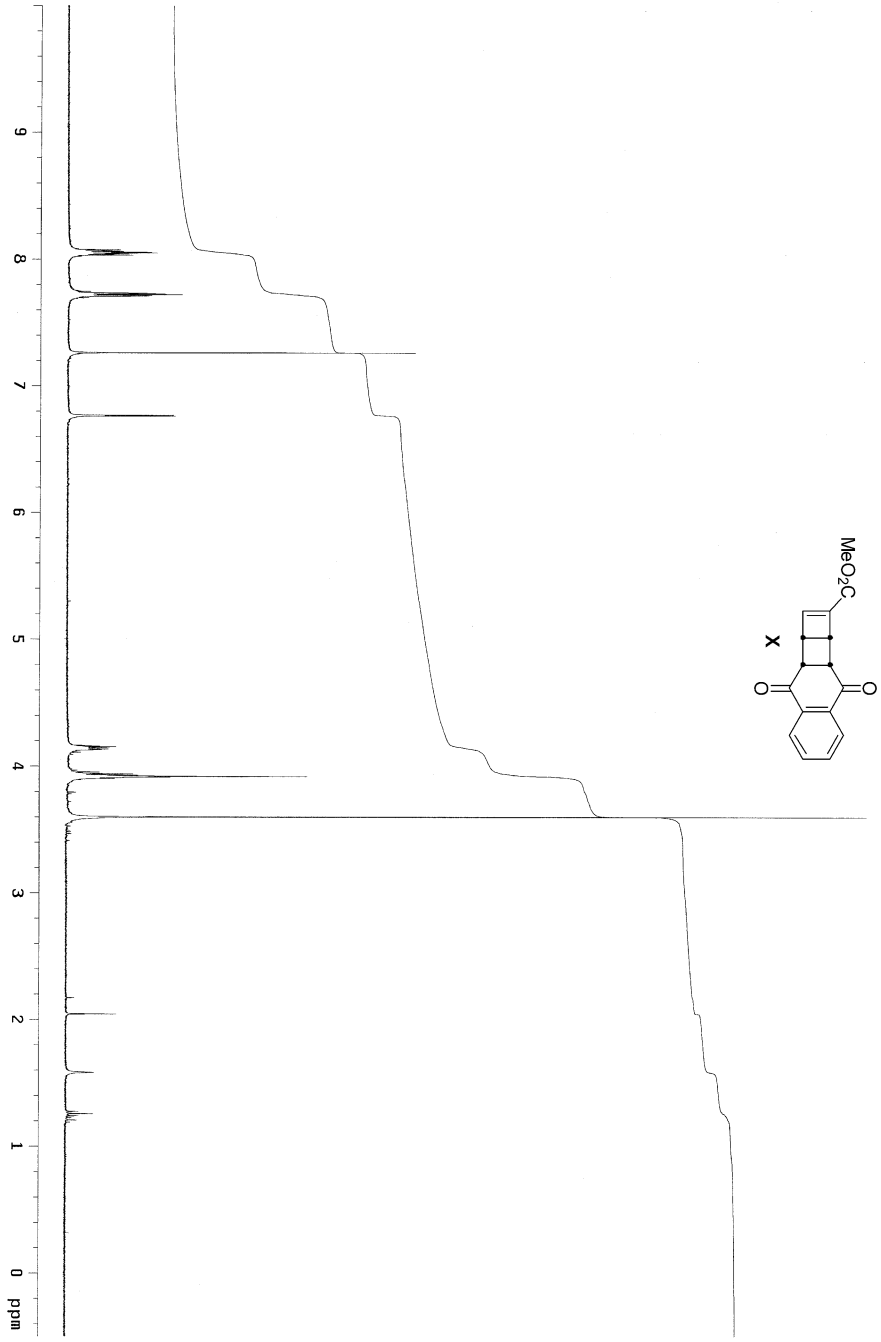
9
8
7
6
5
4
3
2
1
0
ppm
MeO2C
X
O
O

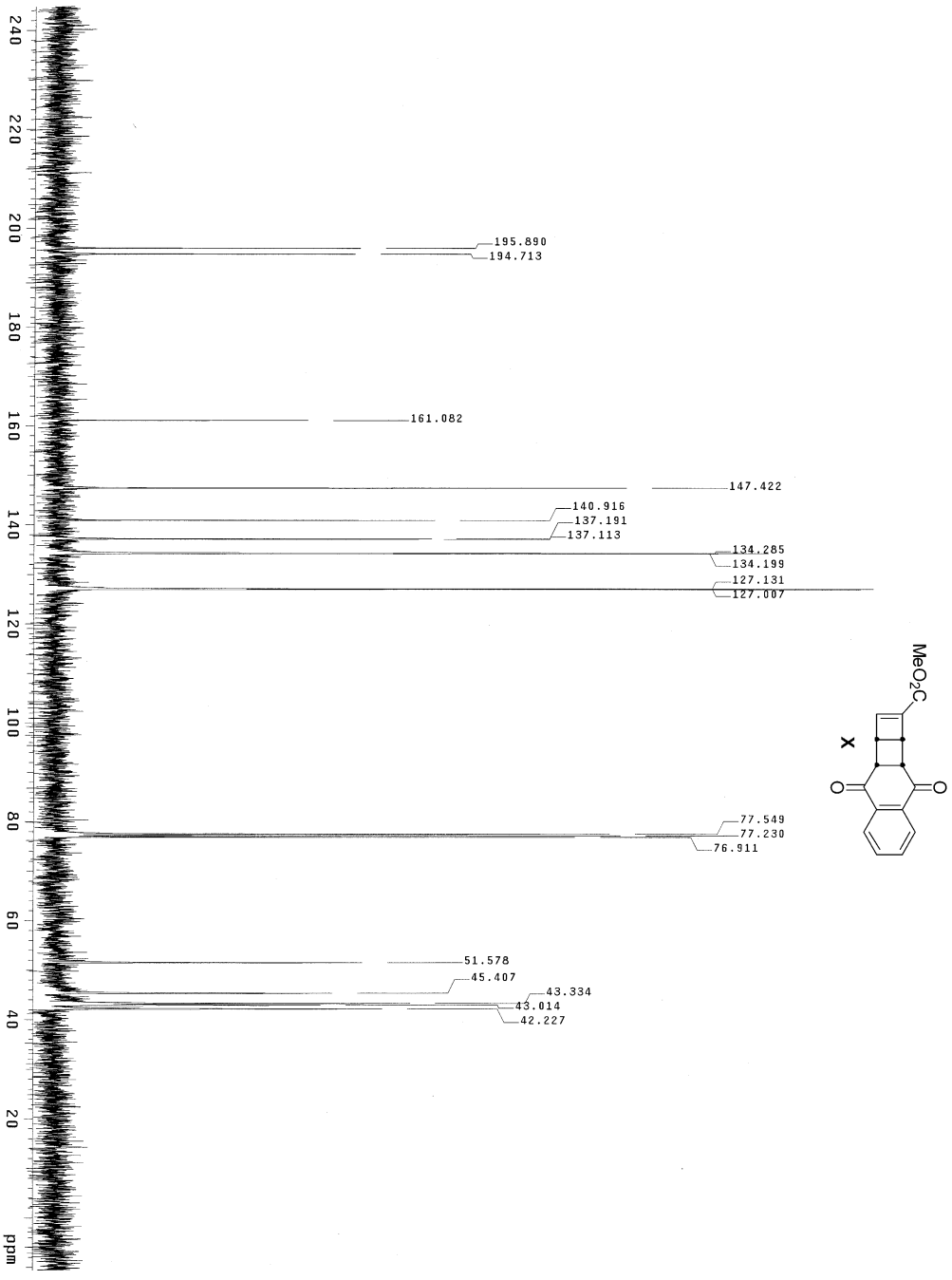
240
220
200
180
160
140
120
100
80
60
40
20
ppm
195.890
194.713
161.082
147.422
140.916
137.191
137.113
134.285
134.199
127.131
127.007
77.549
77.230
76.911
51.578
45.407
43.334
43.014
42.227
MeO2C
X
O
O

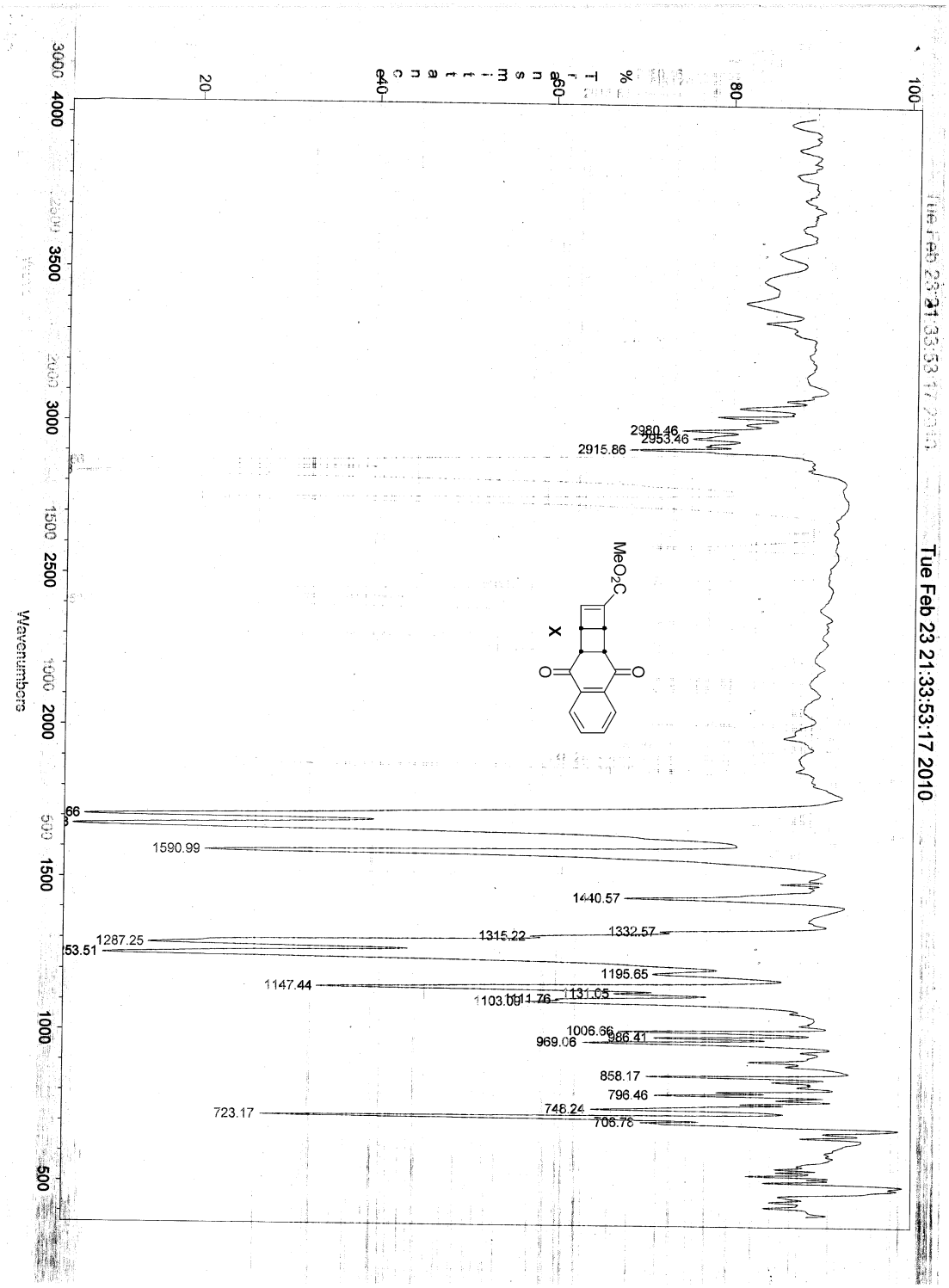
Tue Feb 23 21:33:53:17 2010
Wavenumbers
%
2980.46
2953.46
2915.86
1590.99
1440.57
1315.22
1332.57
1287.25
1195.65
1147.44
1131.05
1006.36
969.06
858.17
796.46
748.24
723.17
706.78
MeO2C
X

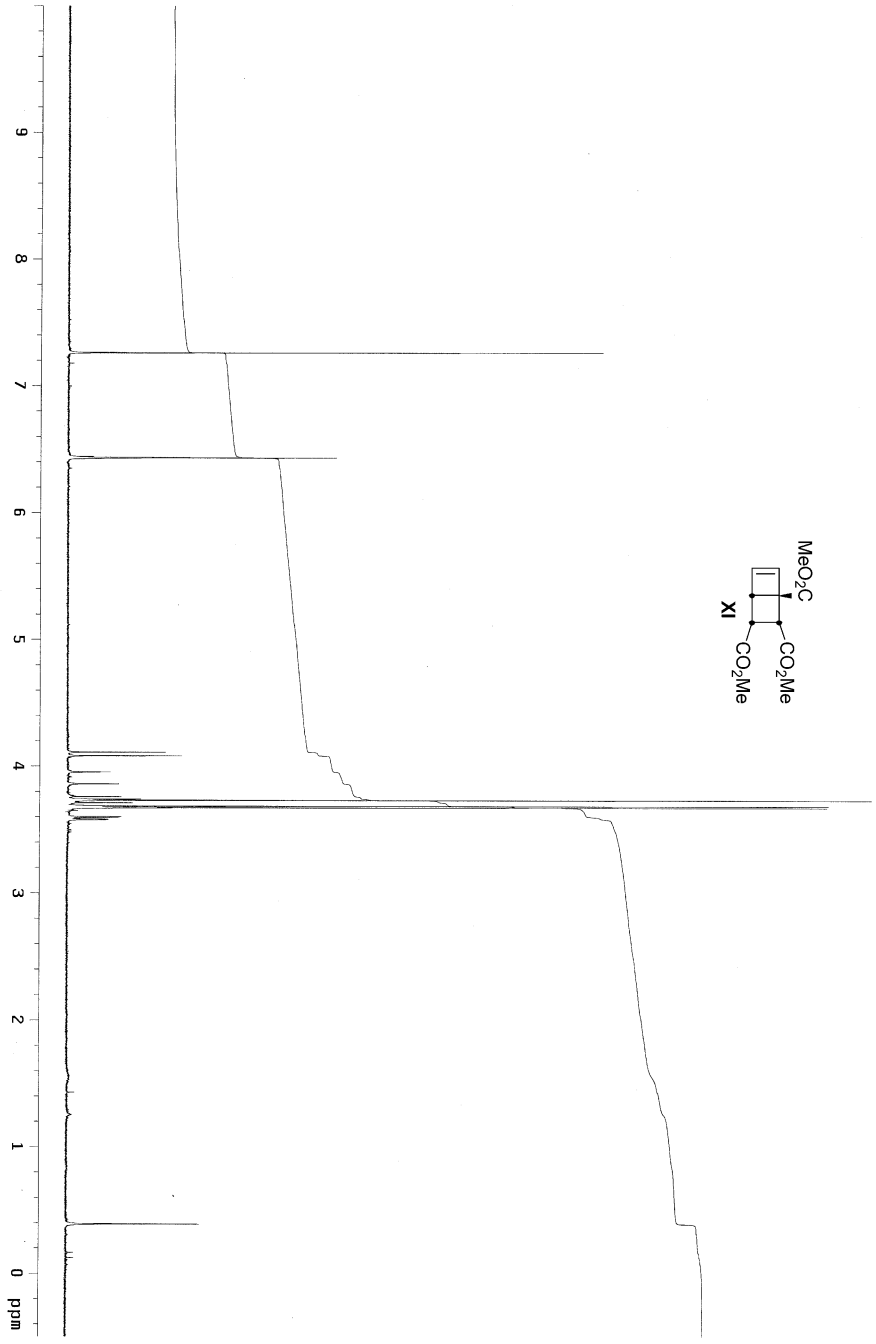
MeO2C
CO2Me
XI
CO2Me
9
8
7
6
5
4
3
2
1
0 ppm

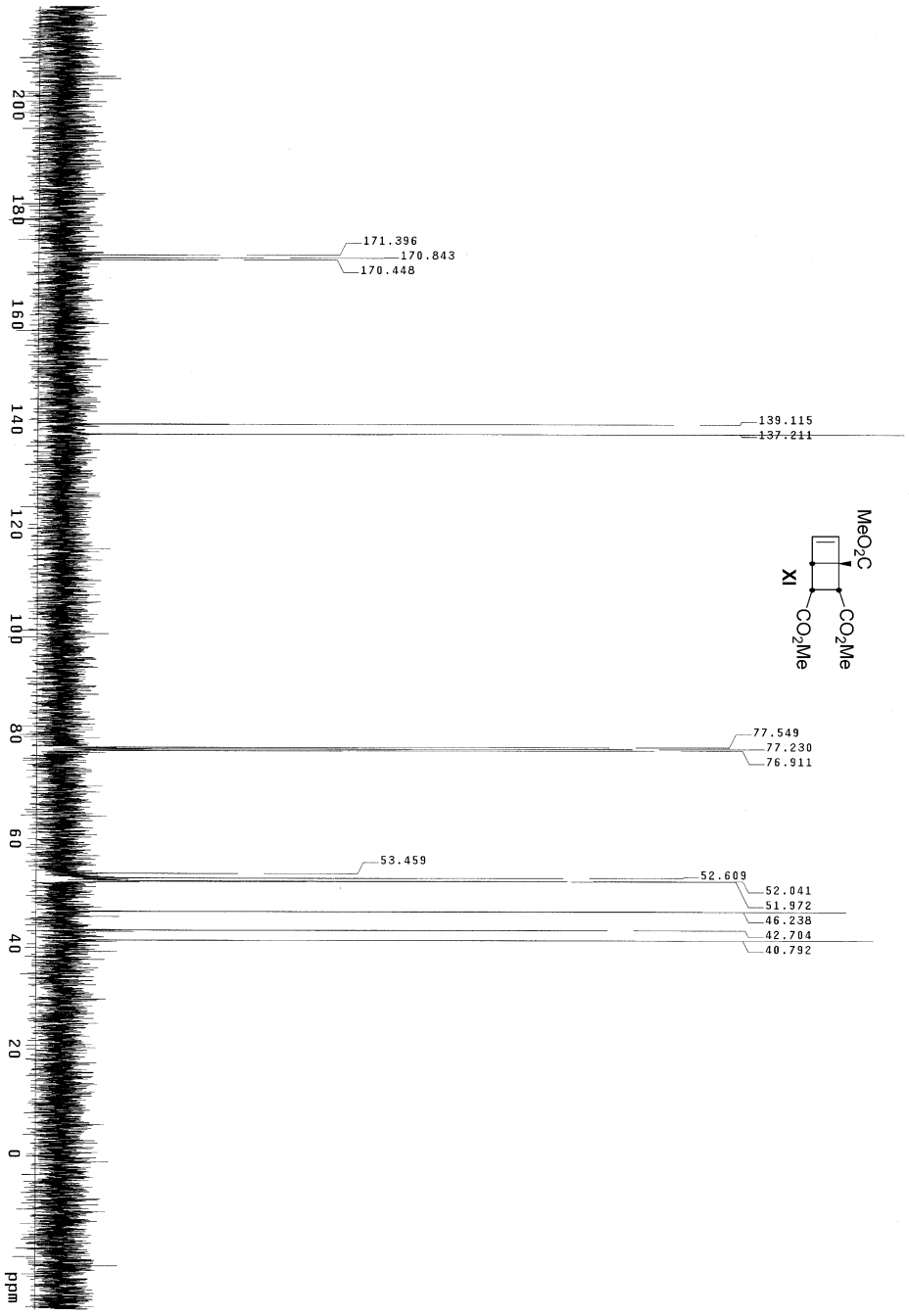
171.396
170.843
170.448
139.115
137.211
77.549
77.230
76.911
53.459
52.609
52.041
51.972
46.238
42.704
40.792
200
180
160
140
120
100
80
60
40
20
0
ppm
XI
MeO2C
CO2Me
CO2Me

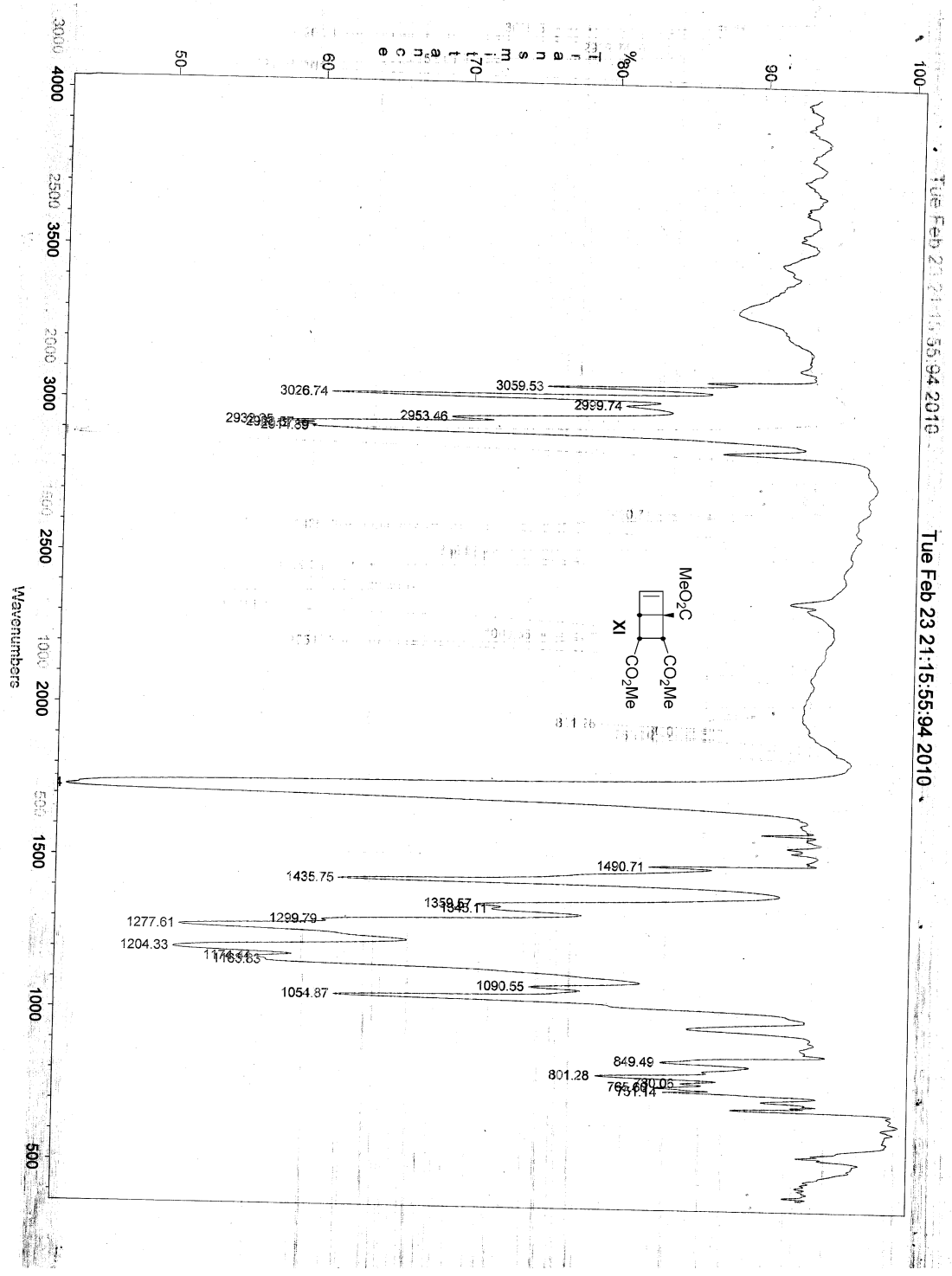
Tue Feb 23 21:15:55:94 2010
Transmittance [%]
Wavenumbers
3026.74
3059.53
2999.74
2953.46
1490.71
1435.75
1277.61
1299.79
1204.33
1090.55
1054.87
849.49
801.28
MeO2C
CO2Me
CO2Me
CO2Me
XI

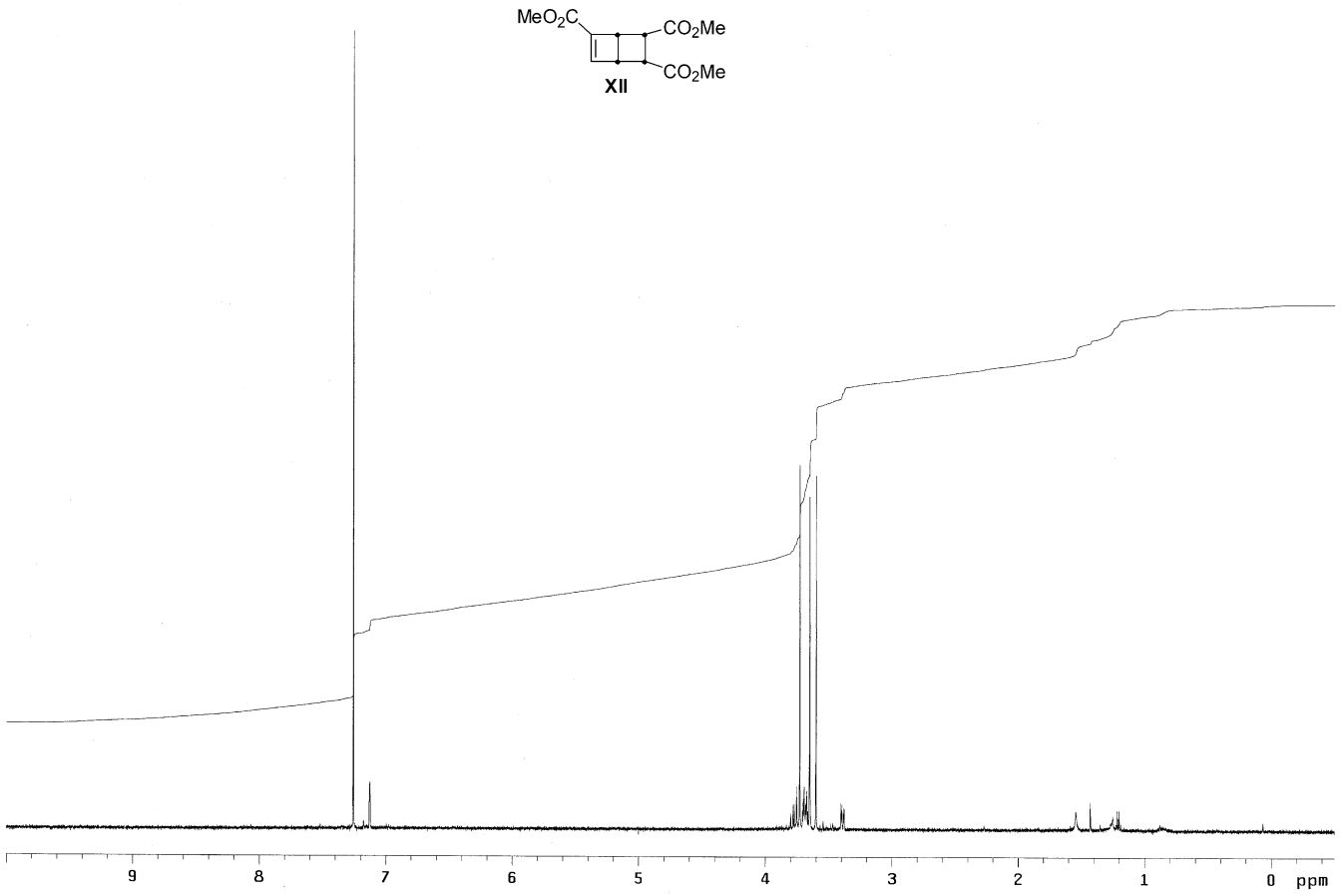
MeO2C
CO2Me
CO2Me
XII
9
8
7
6
5
4
3
2
1
0
ppm

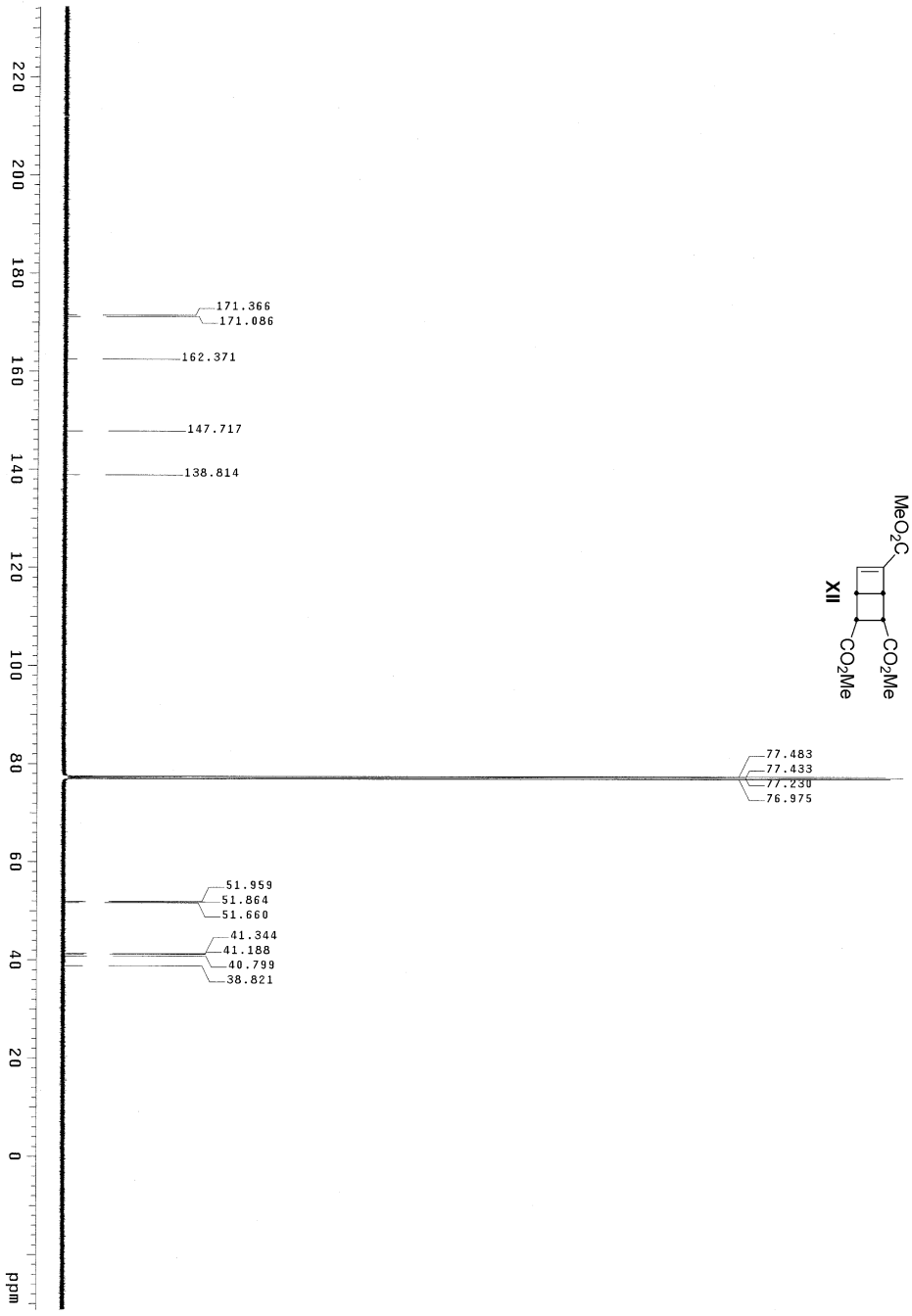
171.366
171.086
162.371
147.717
138.814
77.483
77.433
77.230
76.975
51.959
51.864
51.660
41.344
41.188
40.799
38.821
220
200
180
160
140
120
100
80
60
40
20
0
ppm
XII
MeO2C
CO2Me
CO2Me

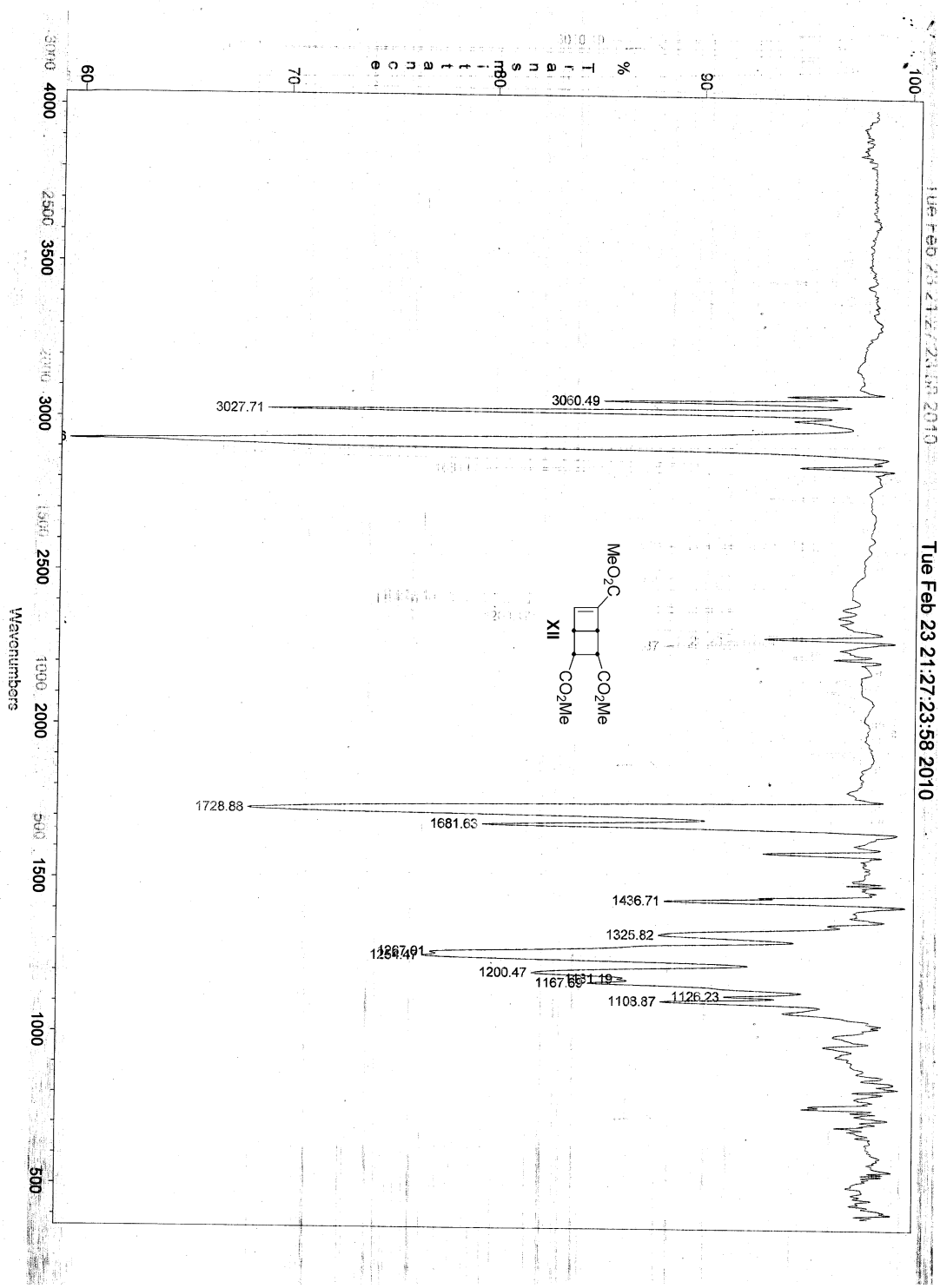
Tue Feb 23 21:27:23:58 2010
% Transmittance
Wavenumbers
4000
3500
3000
2500
2000
1500
1000
500
60
70
80
90
100
3027.71
3060.49
1728.88
1681.68
1436.71
1325.82
1267.91
1254.47
1200.47
1167.69
1131.19
1108.87
1126.23
XII
MeO2C
CO2Me
CO2Me
CO2Me

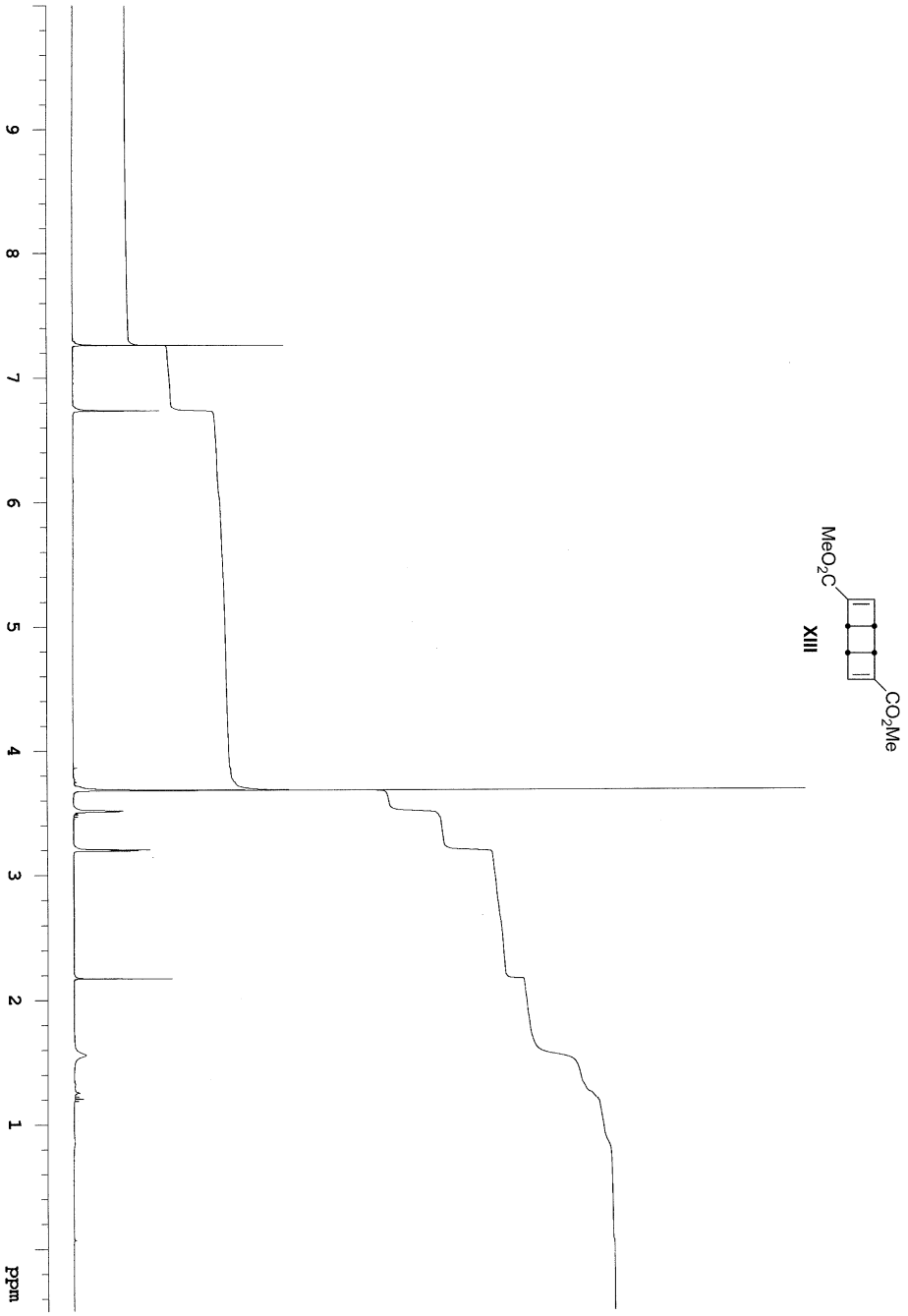
MeO2C
CO2Me
XIII
9
8
7
6
5
4
3
2
1
ppm

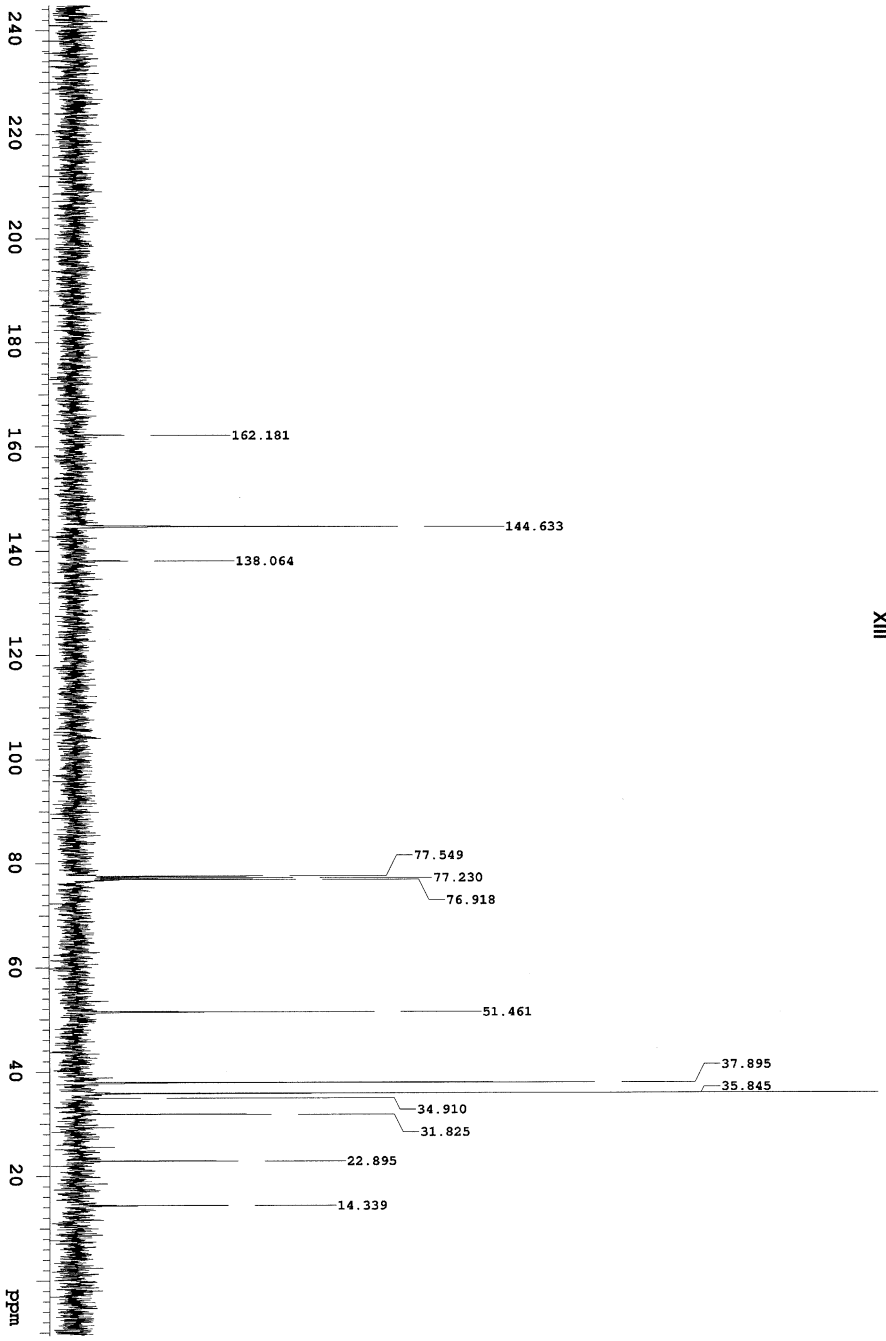
240
220
200
180
160
140
120
100
80
60
40
20
ppm
162.181
144.633
138.064
77.549
77.230
76.918
51.461
37.895
35.845
34.910
31.825
22.895
14.339
MeO2C
CO2Me
XIII

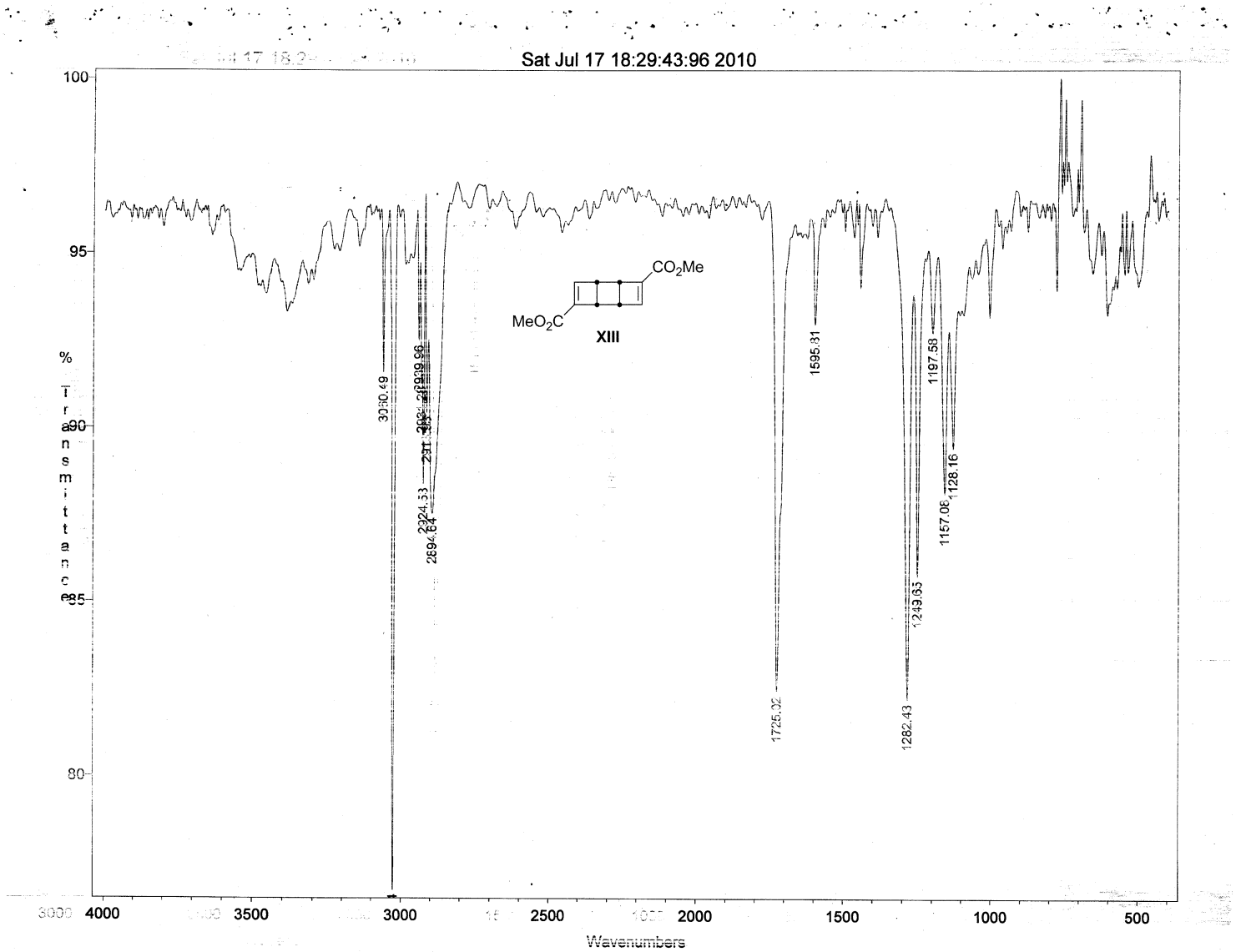
Sat Jul 17 18:29:43:96 2010
100
95
90
85
80
%
Transmittance
3050.49
2924.53
2894.64
1725.02
1595.31
1282.43
1243.63
1197.58
1157.06
1128.16
CO_2Me
MeO_2C
XIII
4000
3500
3000
2500
2000
1500
1000
500
Wavenumbers

Chapter 3: An Approach to the Total Synthesis of Torilin

Introduction

Torilin is a member of the guaiane class of sesquiterpene natural products.[86] This class is distinguished by their bicyclo[5.3.0]decane skeleton, which is commonly referred to as a "5-7" ring system. The core skeleton of the guaianes also includes methyl substitution at the 4 and 10 positions and an isopropyl group at the 7 position of the bicyclic system (using standard guaiane numbering). Within this class, there is a great diversity of chemical functionality and stereochemical relationships (Figure 3.1).[86,87] Many of these natural products also display significant biological activity. This has rendered them attractive targets for chemical synthesis.[88]

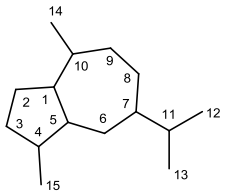

Guaiane skeleton

---

[86] Connoly, J. D.; Hill, R. A. *Dictionary of Terpenoids;* 1st Edition; Chapman & Hall: Cambridge, U. K., 1991; volume 1, 465-476.
[87] Masuda, T.; Jitoe, A.; Nakatani, N. *Chem. Lett.* **1991**, 1625-1628.
[88] For Reviews see: (a) Heathcock, C. H.; Graham, S.L.; Pirrung, M. C.; Plavac, F.; White, C. T. *The Total Synthesis of Natural Products*; ed. ApSimon, I., 1983, volume 5, 333-384.
(b) Zhuzbaev, B. T.; Adekenov, S. M. Veselovsky, V. V. *Uspekhi Khimii*, **1995**, *64*, 198-212.
(c) Foley, D. A.; Maguire, A. R. *Tetrahedron* **2010**, *66*, 1131-1175.

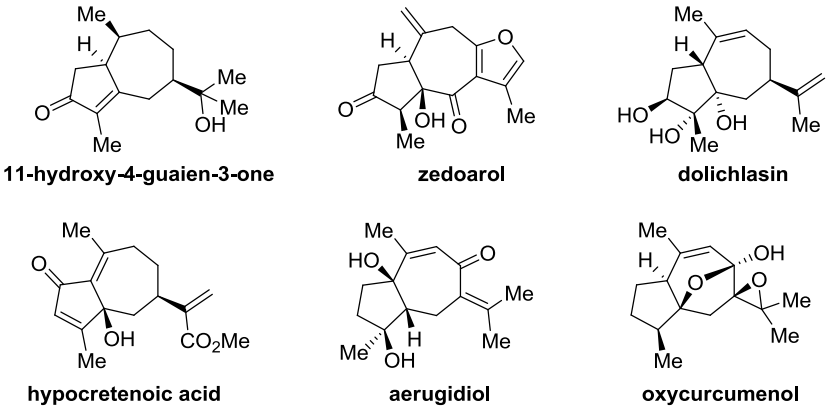

Figure 3.1: Representative Guaiane Natural Products

Guaianes, like other terpenoids, are believed to be formed through cationic cyclization mechanisms[89] and then modified by subsequent transformations to afford the observed functional diversity. The C15 farnesyl pyrophosphate is first enzymatically cyclized to provide a 10-membered cyclic cation. This cation is ultimately quenched by elimination or the trapping of a nucleophile. Protonation or oxidation of an olefin then triggers a transannular bond formation that affords the hydrazulene core of the guaiane natural products (Scheme 3.1[90]).

Scheme 3.1: Guaiane Biosynthesis

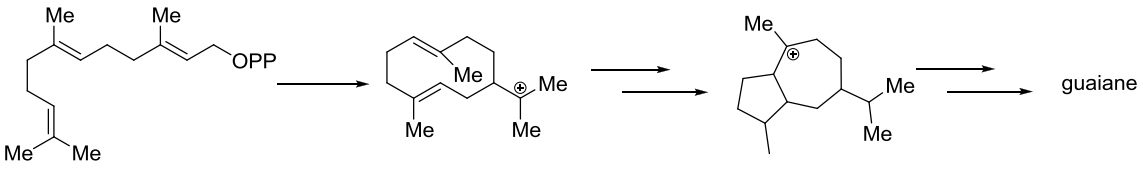

[89] Cane, D. E. *Chem. Rev.* **1990**, *90*, 1089-1103. Also see Reference 88a.
[90] In this generalized depiction, only the carbon skeleton and selected functionality are shown for clarity.

Isolation

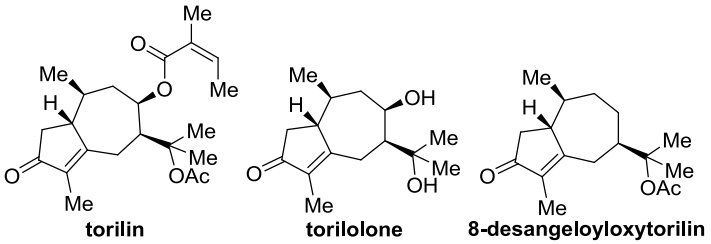

Figure 3.2: Torilin and Related Guaiane Natural Products

The first isolation of torilin was accomplished by Nakazaki and co-workers.[91] They undertook a study aimed at finding the biologically active constituents of seeds from the medicinal herb *Torilis japonica*. The dried seeds were extracted with methanol and chromatographed on alumina. Distillation and crystallization afforded torilin in a 0.4% yield by mass from the seeds. Subsequent studies have also resulted in the isolation of the diol torilolone[92] and the related 8-desangeloyloxytorilin (Figure 3.2).[93]

---

[91] (a) Nakazaki, M.; Chikamatsu, H.; Maeda, M. *Tetrahedron Lett.* **1966**, *37*, 4499-4505. (b) Chikamatsu, H.; Maeda, M.; Nakazaki, M. *Tetrahedron* **1969**, 25, 4751-4765.
[92] Oh, H.; Kim, J. S.; Song, E. K.; Cho, H.; Kim, D. H.; Park, S. E.; Lee, H. S.; Kim, Y. C. *Planta Med.* **2002**, *68*, 748-749.
[93] Ryu, J. H.; Jeong, Y. S. *Arch. Pharm. Res.* **2001**, *24*, 532-535.

Scheme 3.2: Hydrolysis of Torilin

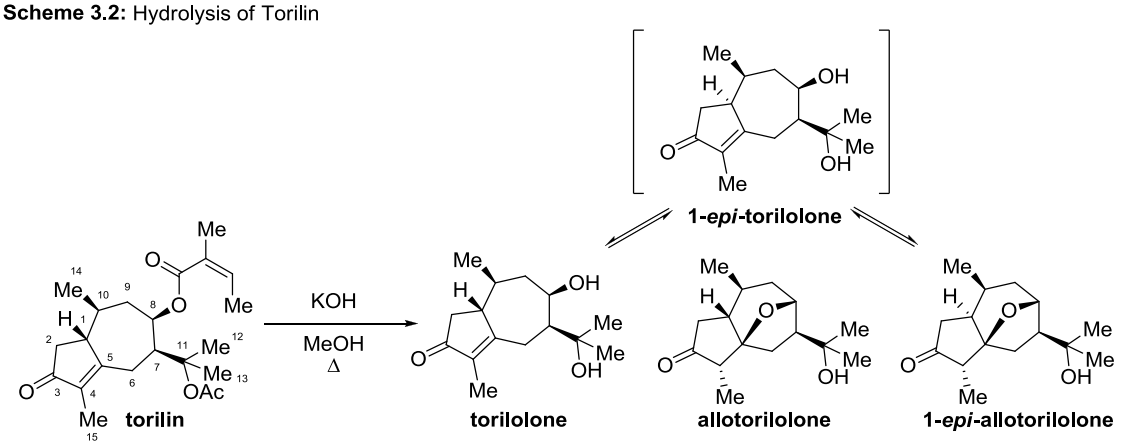

The structure of torilin was elucidated through spectroscopic and chemical methods.[91] Alkaline hydrolysis of torilin produced angelic acid[94], tiglic acid[95] and acetic acid as well as an equilibrium mixture of three keto-alcohols that varied in composition based on the hydrolysis conditions (Scheme 3.2). Specifically, more forcing conditions increased the amount of 1-*epi*-allotorilolone suggesting it was the most stable isomer. The equilibrium likely proceeds via the intermediacy of 1-*epi*-torilolone which, being considerably less stable than its *allo* derivative, is not isolated. This equilibrium was presumed to be similar to that known for conversion of geigerin to allogeigeric acid.[96] This allowed proof of the absolute stereochemistry at C-7, C-8, and C-10 by conversion of 1-*epi*-allotorilolone to (+)-1-*epi*-deoxygeigerin of known absolute configuration (Scheme 3.3).[97] Further correlation studies showed that these degradation products of torilin could be

---

[94] (*Z*)-2-methylbut-2-enoic acid
[95] (*E*)-2-methylbut-2-enoic acid
[96] Barton, D. H. R.; Levisalles, L. E. D. *J. Chem. Soc.* **1958**, 4518.
[97] Barton, D. H. R.; Pinhey, J. T.; and Wells, R. J. *J. Chem. Soc.* ***1964****, 2518.*

interconverted through epimerizations at C-1 or C-4 and, when combined with optical rotatory dispersion measurements, allowed assignment of the absolute configuration at these centers. Distillation of torilin at temperatures above 180 °C resulted in thermal decomposition to afford desacetyltorilin, which confirmed the positions of the acetate and angelate esters (Scheme 3.3).[91]

Scheme 3.3: Selected Chemical Transformations

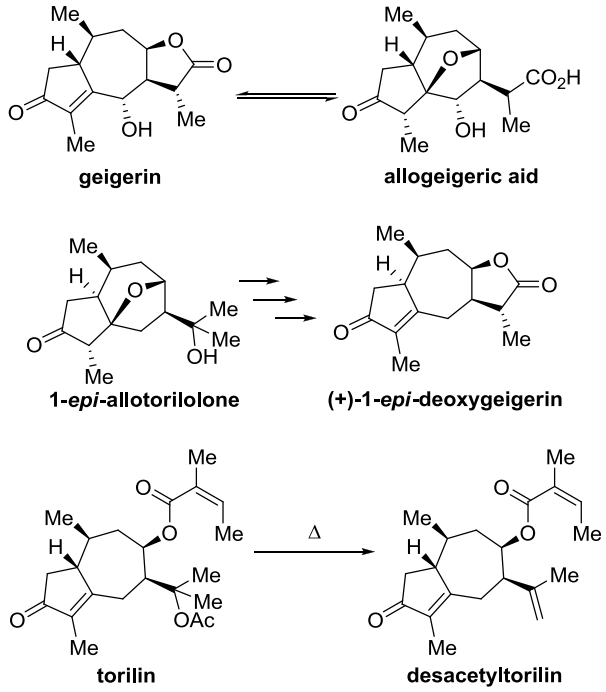

Previous Synthetic Approaches

Torilolone acetate has been prepared once before in the context of a structure proof for guaioxide.[98] The latter sesquiterpene ether can be isolated in

[98] Ishii, H.; Tozyo, T.; Nakamura, M.; Minato, H. *Tetrahedron* **1970**, *26*, 2751-2757.

small quantities from guaiac wood oil or produced by treatment of guaiol with acid (Scheme 3.4). At the time, its structure was unknown, so the authors approached its structure elucidation through chemical correlation. First, a functionalization, which would enable cleavage of the ditetriary ether, was required. Screening of suitable microorganisms[99] showed that guaioxide could be hydroxylated upon incubation with the fungus *Mucor parasiticus* (Scheme 3.4) to afford three compounds (**3.1**, **3.2**, and **3.3**). The structure of these compounds and, by inference, guaioxide, was determined through transformation into torilolone acetate (Scheme 3.5).

Scheme 3.4: Microbial Oxidation of Guaioxide

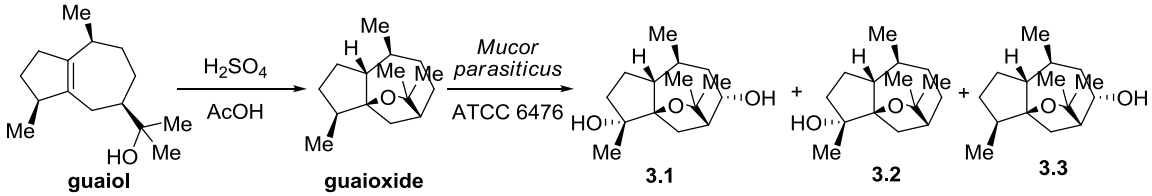

Oxidation product **3.1** was oxidized to keto-alcohol **3.4** with Jones's reagent (Scheme 3.5). This compound could be reduced under Huang-Minlon conditions (a one-pot modification of the Wolff-Kishner reduction) to afford a compound identical to **3.2**, which indicated that the tertiary alcohol in **3.1** and **3.2** were in the same position. Reduction of ketone **3.4** with lithium aluminum hydride proceeded from the least hindered face and provided the β-epimer of the secondary alcohol in **3.1**. Acylation of this alcohol and elimination of the tertiary

[99] Review: Tamm, C. H. *Angew. Chem. Int. Ed.* **1962**, *1*, 178-195.

alcohol with thionyl chloride produced acetate **3.7**. Diol **3.1**, could be treated under similar conditions to afford the α-epimer of this acetate, compound **3.6**. Hydrogenation of **3.6** with Adams's catalyst produced a 1.1:1 mixture of **3.8** and **3.9**. Compound **3.8** was identical to that formed by acylation of **3.3**, indicating that the latter differed from **3.1** only by the presence of the tertiary alcohol. Mesylation and elimination of the secondary alcohol in **3.3** instead afforded **3.10**, which could be hydrogenated to afford guaioxide. This result, based on the lack of trisubstituted olefin formation, indicated that the secondary alcohol was located on C-8 rather than C-9. Identity of the saturated compound with guaioxide also indicated that hydroxylation to afford **3.1** and **3.2** occurred with retention of stereochemistry at C-4 (as expected for microbial oxidation).

Scheme 3.5: Correlation to Guaioxide

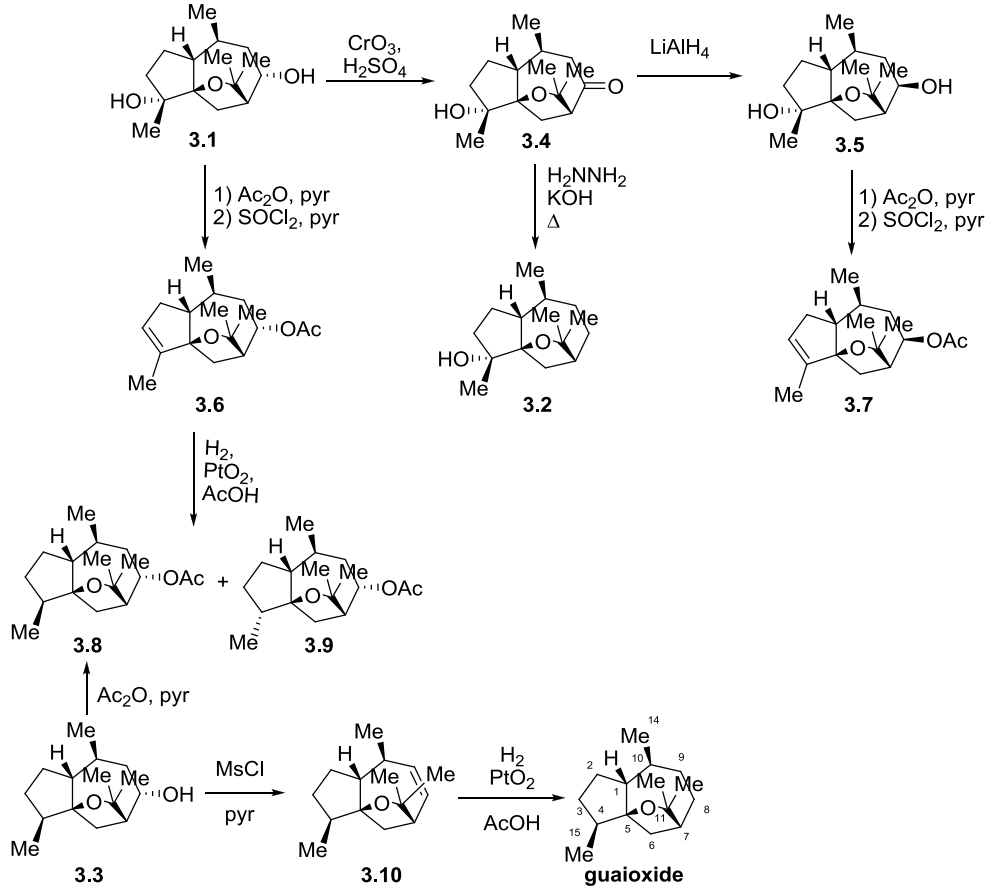

Secondary, unsaturated acetates **3.6** and **3.7** were employed to correlate guaioxide with torilolone (Scheme 3.6). Hydroboration and Jones oxidation of **3.7** afforded a ketone which, upon chromatography on activated alumina, underwent β–elimination of the ether linkage to generate an enone-acetate that was identical to the acetate prepared from an authentic sample of torilolone with pyridine and acetic anhydride. This confirmed the C-5 attachment of the ether in guaioxide and optical rotatory dispersion measurements confirmed that the beta stereochemistry of the hydrogen at the C-1 ring junction was retained from

guaioxide during this sequence. Similar treatment of **3.6** identified it as the C-8 α-epimer of **3.7**. Finally, when the saturated compound **3.11** was functionalized in this manner, it produced 8-desangeloyloxytorilin **3.17** (also referred to as 1-*epi*-hydroxycolorenone), which could be partially epimerized at C-1 by treatment with potassium hydroxide in refluxing methanol. Hydrogenation of enone **3.17**, followed by Huang-Minlon reduction of the carbonyl group provided a mixture of C-4 diastereomers (1.1:1, **3.18**:**3.19**). The minor component (**3.19**) was identical to the product of hydrogenation of guaiol with Raney nickel in ethanol at 100 °C and 120 atm (1β,5β-dihydroguaiol) and the major (**3.18**) was its C-4 α-epimer.

Scheme 3.6: Correlation to Torilolone

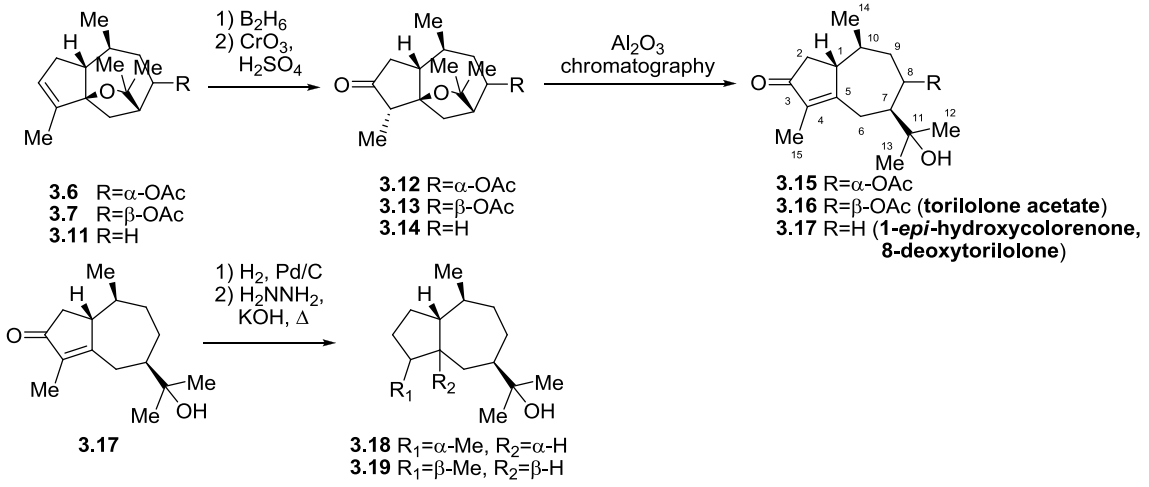

3.6 R=α-OAc
3.7 R=β-OAc
3.11 R=H

3.12 R=α-OAc
3.13 R=β-OAc
3.14 R=H

3.15 R=α-OAc
3.16 R=β-OAc (**torilolone acetate**)
3.17 R=H (**1-*epi*-hydroxycolorenone, 8-deoxytorilolone**)

3.17

3.18 R_1=α-Me, R_2=α-H
3.19 R_1=β-Me, R_2=β-H

While the previous work indeed generated torilolone acetate and related compounds through a combination of biochemical transformations and chemical synthesis (9 steps), the starting material (although inexpensive and readily available) was itself a guaiane natural product. Therefore, the synthetically

challenging medium-ring system and much of the stereochemistry was already in place. As total synthesis was not the implied goal, but rather proof-of-structure, this certainly does not detract from the work. However, total synthesis provides perhaps the ultimate proving ground for synthetic methodology and ideally, the opportunity for methodological discovery.[100] These goals can often be best served by attempting to generate much of the complexity during the synthetic transformations. This requires clever design in the application of the available methodologies. In this vein, Deprés and co-workers provided a rather concise and efficient synthesis (Scheme 3.7)[101] of 8-desangeloyloxytorilin.

Their route[101] began from the commercially available tropylium tetrafluoroborate ($37.44 per gram[102]). This compound was methylated using methyllithium to afford **3.20** in 83% yield. Deprés then employed a dichloroketene cycloaddition-diazoalkane ring expansion methodology to afford key 5-7 enone **3.23** in 44% yield (32:1 dr) over the two steps. This versatile intermediate could undergo a variety of transformations including oxidation, reduction, cycloaddition, and the selective formation of a tricarbonyliron complex of the cycloheptadiene. Of particular note for this synthesis is the regio- and stereoselective conjugate addition. K-selectride, cuprates, and silyl ketene acetals all provided β-1,6 addition products to the chloro-enone. Indeed, addition

---

[100] For a discussion in the context of the ideal synthesis, see Gaich, T., Baran, P. S. *J. Org. Chem.* **2010**, *75*, 4657-4673 and references therein.
[101] Coquerel, Y.; Greene, A. E.; Deprés, J.-P. *Org. Lett.* **2003**, *5*, 4453-4455.
[102] Sigma-Aldrich Catalog pricing, June 12, 2010, $936.00 for 25 grams.

of 2-propenylmagnesium bromide in the presence of copper bromide and chlorotrimethylsilane provided **3.24** in 45% yield. Protection of **3.24** with neopentyl glycol proceeded rather sluggishly to afford dioxane **3.25** in 76% yield at 84% conversion. This protected compound was then metallated and alkylated to afford **3.26** in 93% yield and complete the carbon skeleton of the natural product. Quantitative deprotection of the ketal, followed by oxymercuration of the 1,1-disubstituted olefin and hydrogenation generated the known intermediate **3.17**[98] (8-deoxytorilolone or 1-*epi*-hydroxycolorenone) in 55% yield over two steps. This could be converted, through the known base-catalyzed epimerization of C-1, to hydroxycolorenone and was acylated using acetic anhydride and trimethylsilyltriflate to provide 8-desangeloyloxytorilin in 95% yield. This synthesis required 10 steps in a linear sequence and afforded a 6% overall yield of the natural product. Using key intermediate **3.26**, they were also able to synthesize the guaianolide natural product 6-deoxygeigerin via hydroboration, oxidation, deprotection and iodolactonization.

Scheme 3.7: Deprés's Synthesis of 8-desangeloyloxytorilin

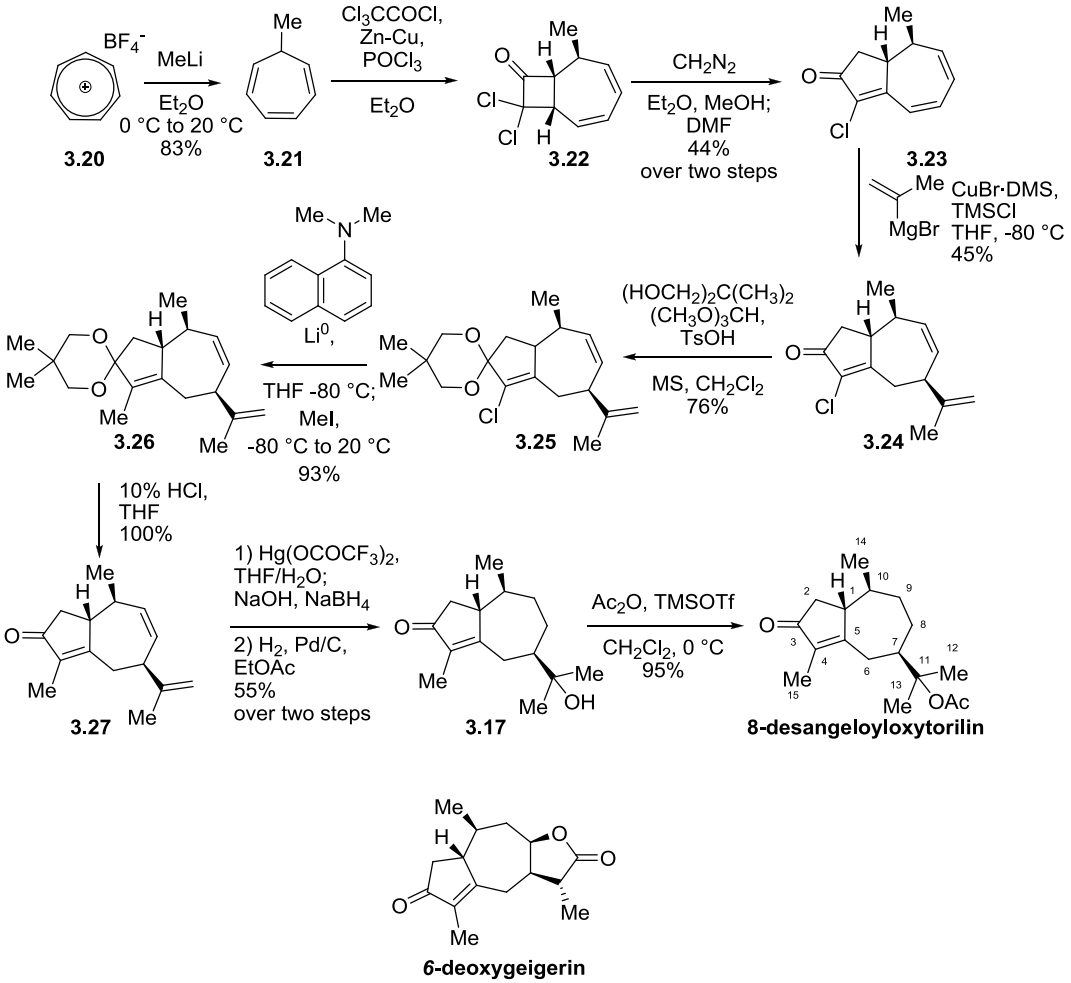

SYNTHETIC PLAN

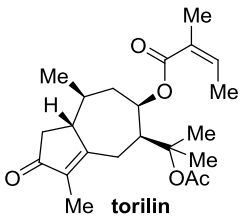
torilin

Torilin represents an intriguing synthetic target for a number of reasons. Its highly oxygenated guaiane skeleton and congested "all *syn*" arrangement of stereogenic centers in the seven-membered ring provide a significant challenge in addition to those posed by formation of the medium ring. While the previous approaches describe routes to some related systems, to the best of our

knowledge, only one approach[103] to torilin itself can be found in the literature, and it does not result in a successful synthesis of the natural product. Highlighting the difficulties in formation of medium-ring systems, routes involving Mukaiyama aldol and metathesis strategies were explored and amidst difficulties with substrate synthesis and ring closure, the project was terminated. The lack of an existing synthetic route to this molecule is of course but one reason to embark on a synthetic expedition.

The relatively unique stereochemistry of torilin presented an intriguing test for our synthetic methodology. Previous research in the Snapper lab has shown that strained cyclobutadiene cycloadducts can be cyclopropanated to generate "housane"-containing tetracyclo[5.3.0.$0^{1,5}$.$0^{2,4}$]decane systems.[104a,c;106a,b] These rigid, highly-strained molecules are susceptible to fragmentation to afford functionalized 7-membered ring products with complete stereochemical control. In fact, two complementary methodologies have been developed (Scheme 3.7).[104] These strategies employ the rapid increase in both strain energy and molecular complexity possible from the cycloaddition of an antiaromatic diene to enable more efficient synthesis of these difficult targets through a strategic "relaxation" to the desired molecular scaffold.

---

[103] Van den Heuvel, A. K. Scope and Limitation of the Non-aldol Aldol Reaction and Progress Toward the Total Synthesis of Torilin. Ph.D. Dissertation, University of California, Los Angeles, Los Angeles, CA, 2004.

[104] (a) Deak, H. L.; Stokes, S. S.; Snapper, M. L. *J. Am. Chem. Soc.* **2001**, *123*, 5152-5153. For helpful discussion, see reference 106b. (b) Deak, H. L.; Williams, M. J.; Snapper, M. L. *Org. Lett.* **2005**, *7*, 5785-5788. (c) Deak, H. L. Cyclopropanation/Isomerization Strategies Toward the Synthesis of bicyclo[5.3.0]decanes (5-7 ring systems) and Applications in Total Synthesis. Ph.D. Dissertation, Boston College, Chestnut Hill, MA, 2004.

As seen in Scheme 3.8, thermal fragmentation[104a] of cyclopropanes **3.28** at temperatures between 180 and 240 °C in a sealed vessel results in fragmentation to afford cycloheptadiene products **3.29** with a stereochemical inversion at the ring-junction (C1 in the guaiane numbering system). This provides an *anti* relationship between this hydrogen and the substituent at C10. However, oxidation of an alcohol at C4 in **3.30**, generates a ketone at this position which is sensitive to treatment with Brönsted or Lewis acids. Acid-mediated activation[104b] of this ketone at 0 °C causes fragmentation of the strained ring system to generate a similar cycloheptadiene-containing compound **3.31**. In this case, the stereochemistry at the C1 ring junction is retained and a *syn* relationship between this hydrogen and the C10 substituent is obtained. As both relative stereochemistries are present in guaiane natural products, these complementary methodologies provide powerful and versatile options for the efficient synthesis of this class of natural products.

Scheme 3.8: Complementary Rearrangements

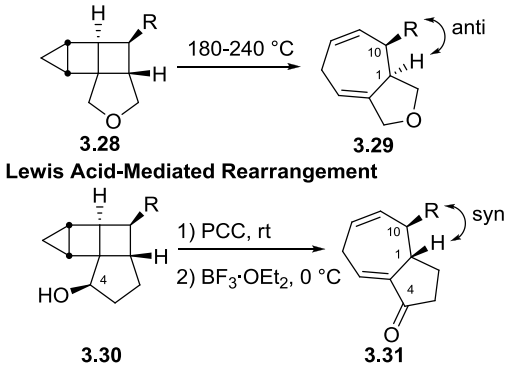

That such varied stereochemical results are obtained from structurally very similar substrates through modification of the reaction conditions suggests

disparate reaction mechanisms. Indeed, one plausible mechanistic scenario for the thermal fragmentation appears in Scheme 3.9.[104a] Thermolysis of cyclopropane **3.32** can result in homolytic cleavage of the highly-strained C5-C9 bond. The newly generated boat diradical **3.33** can then relax to the chair conformation **3.34**. In this conformation, fragmentation of the C1-C10 bond can occur, leading to a divinyl cyclopropane **3.35**. Bond rotation around the C5-C6 bond of this intermediate provides required bis-*endo*-boat conformer **3.37** which has appropriate orbital alignment for a facile Cope rearrangement to afford bicyclo[5.3.0]decane **3.38**. It is this cleavage of the C1-C10 bond and rotation about C5-C6 which likely explains the inversion of stereochemistry at the C1 ring junction. A pair of alternative, concerted $[_{\sigma}2_{s}+_{\sigma}2_{a}]$ cycloreversions also provide a symmetry-allowed[105] pathway to intermediate **3.35**, which cannot be excluded at this point. Cycloreversion of the C5-C9 and C1-C10 bonds of **3.32** would directly produce divinyl cyclopropane **3.35**. On the other hand, cleavage of C6-C8 and C5-C9 generates *cis*,*trans*-cycloheptadiene **3.36**, which due to its strain energy, should undergo Cope rearrangement to divinylcyclopropane **3.35**. This intermediate then proceeds to product **3.38** as previously described.

---

[105] Woodward, R. B.; Hoffmann, R. *Angew. Chem., Int. Ed.* **1969**, *8*, 781-932.

Scheme 3.9: Proposed Mechanism of Thermal Fragmentation

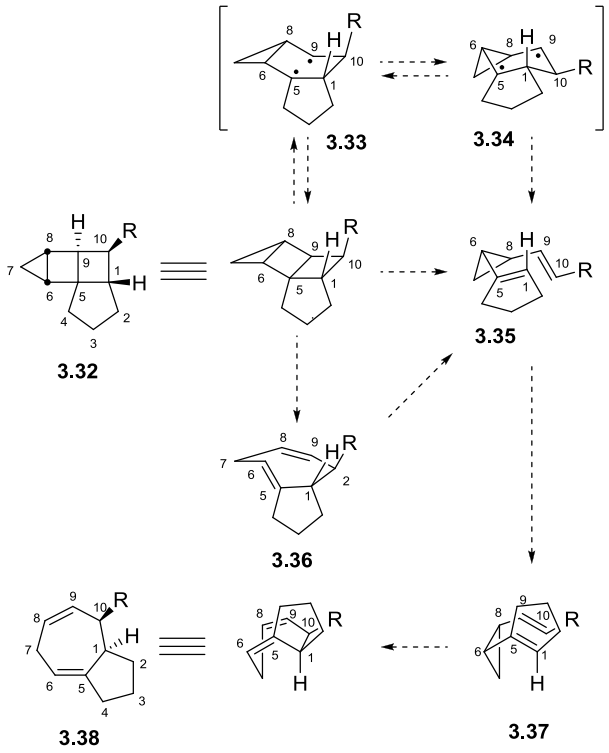

A mechanistic rationale explaining the retention of stereochemistry in the acid-mediated process appears in Scheme 3.10.[104b] Complexation of the C-4 ketone of **3.39** with a Lewis acid activates the carbonyl. The cationic character at C-4 in **3.40** allows fragmentation of the highly-strained C5-C9 bond due to its overlap with the π^* orbital of the carbonyl. This generates a carbocation **3.41**, which, upon relaxation to conformation **3.42**, undergoes cleavage of the C6-C8 cyclopropane bond to afford cycloheptenyl carbocation **3.43**. Collapse of the enolate to quench the cation releases the acid catalyst and affords enone **3.44**. This compound is generated with retention of the *syn* stereochemistry of the C1 hydrogen relative to the C10 substituent since the C1-C10 bond is never broken.

This relative stereochemical arrangement mirrors that found in torilin and its congeners.

Scheme 3.10: Proposed Mechanism of Acid-Mediated Fragmentation

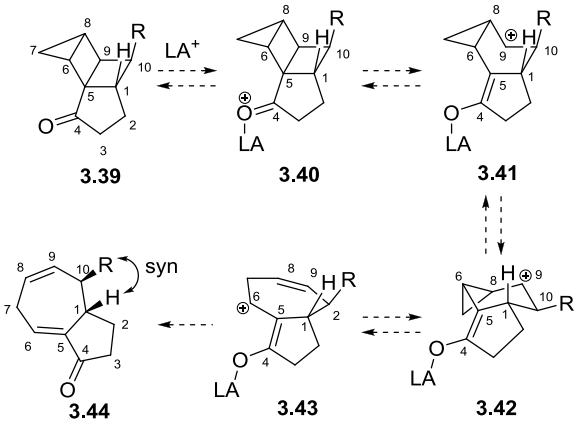

The thermal fragmentation strategy was recently applied to the asymmetric total synthesis of the natural products (+)-pleocarpenene and (-)-pleocarpenone[106a,b] (Scheme 3.11), which highlights its synthetic utility. Functionalized tricarbonylcyclobutadiene iron complex **3.46**, upon oxidation to liberate cyclobutadiene, undergoes [4+2] cycloaddition with the tethered olefin to generate a highly strained, functionalized cyclobutene. When the secondary alcohol in **3.46** is enantiomerically enriched through an oxidation/asymmetric reduction sequence and the cyclobutene diastereomers are separated, each is present as a single enantiomer, the major β-diastereomer being represented by structure **3.47**. This compound can be stereoselectively cyclopropanated and

---

[106] (a) Williams, M. J.; Deak, H. L.; Snapper, M. L. *J. Am. Chem. Soc.* **2007**, *129*, 486-487. (b) Williams, M. J. The Development of New Methods Toward Guaiane Natural Products. Ph.D. Dissertation, Boston College, Chestnut Hill, MA, 2007. (c) Leyhane, A. J. Cyclobutadiene Cycloadditions: Applications toward the Synthesis of Functionalized Oxepines and Guaiane Natural Products. Ph.D. Dissertation, Boston College, Chestnut Hill, MA, 2008.

after some functional group manipulations affords **3.48**, thereby controlling the stereochemistry of the substituent at C7 in the guaiane architecture. Thermal fragmentation generates the highly functionalized cycloheptadiene **3.49** which, after reduction, deprotection and elimination, is converted to the enantiomers of the natural products (+)-pleocarpenene and following ozonolysis and epimerization, (-)-pleocarpenone.

Scheme 3.11: Total Synthesis of (-)-Pleocarpenene and (+)-Pleocarpenone

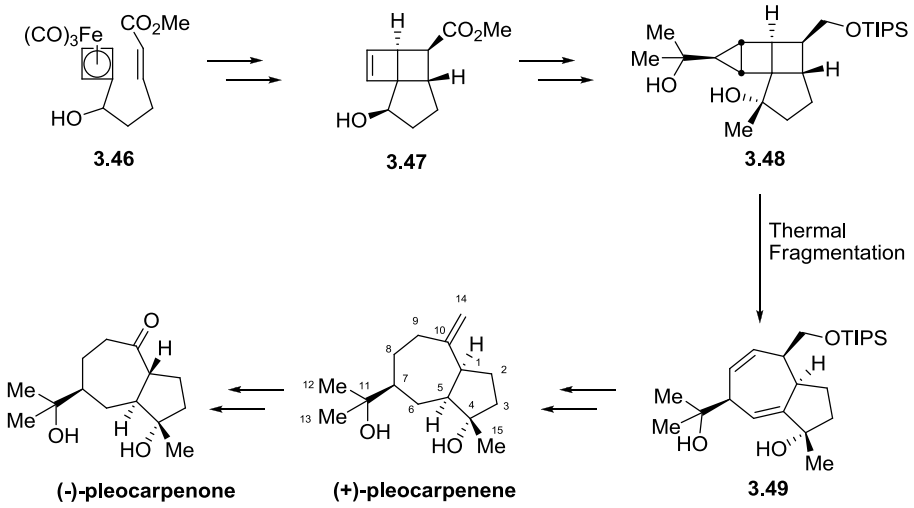

This strategy was expanded to access three additional guaiane natural products, 11-hydroxypogostol, bulnesol, and hanamyol (Scheme 3.12).[106c] In fact, a common intermediate led to these natural products and also provided second generation syntheses of pleocarpenene and pleocarpenone highlighting the versatility of this divergent approach. In a similar sequence to that in Scheme 3.10, iron complex **3.46** underwent oxidation to generate cycloadducts **3.50** which could be transformed into cyclopropane **3.51**. Thermal fragmentation,

hydrogenation and functional group manipulation led to common intermediate **3.52**. This compound could be converted into pleocarpenene and pleocarpenone by epoxidation/reduction to install the tertiary alcohol and application of the final steps from the first generation synthesis.[106a,b] Hydrogenation, deprotection, and elimination then provided intermediate **3.53** from which epoxidation of the exocyclic olefin followed by reduction afforded 11-hydroxypogostol, isomerization provided bulnesol and epoxidation of bulnesol followed by Intramolecular attack on the epoxide completed the synthesis of hanamyol.[106c]

Scheme 3.12: Synthesis of Guaiane Natural Products from Common Intermediate **3.52**

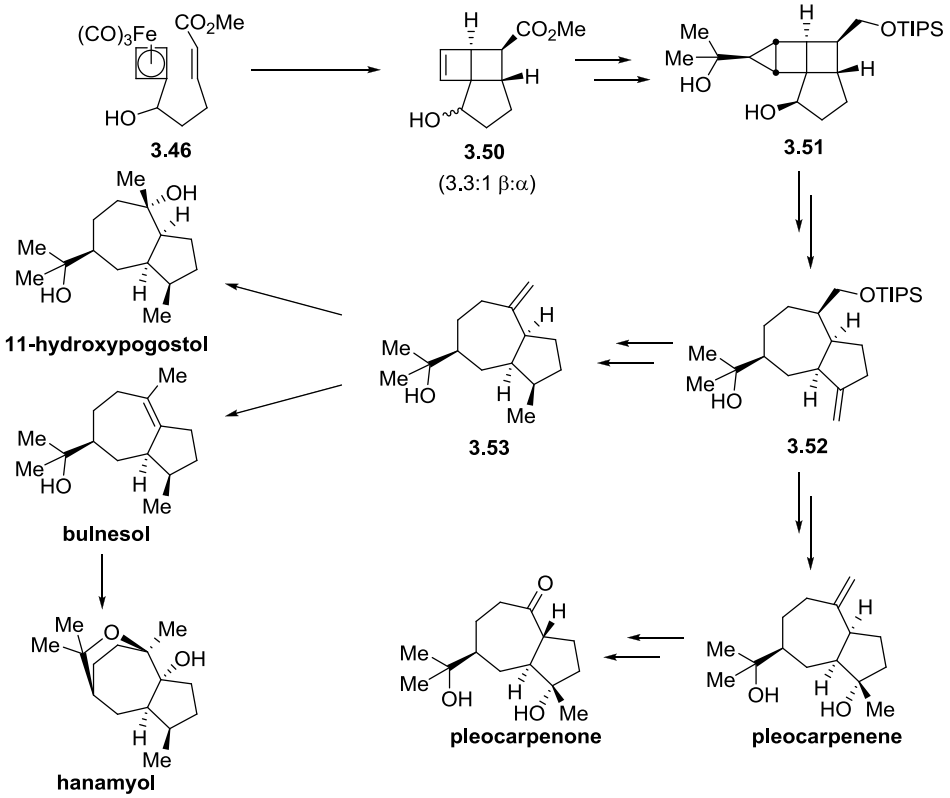

Based on the success of the thermal fragmentation methodology, torilin appeared to be a logical target. It contains an increase in oxygenation and complexity compared to the previous targets. Its relative stereochemistry also provides the opportunity to test the acid-mediated rearrangement developed by the Snapper lab[104b,c] in the context of a natural product total synthesis. In addition to the interesting structural challenges posed by this challenging molecule, it has recently been the subject of much biological study.[107] These motivations prompted the design of a synthetic route to torilin. A route was sought to incorporate much of the functionality in the molecule as quickly as possible while minimizing changes of oxidation state and use of protecting groups.

Retrosynthetically, torilin could most obviously be viewed as a selectively-acylated form of its diol congener torilolone (Scheme 3.13). The secondary alcohol at C8 could likely be introduced by a directed functionalization[108] of the disubstituted olefin in **3.54** with the regio- and stereochemistry controlled by the exocyclic tertiary alcohol. The tetrasubstituted enone present in **3.54** could be generated by a combination of alkylation and reduction along with deprotection of the C3 carbonyl. Compound **3.55** represents the key step in the synthesis and should be accessible *via* oxidation and acid-mediated rearrangement of highly-

---

[107] For a Review, see Chapter 1.
[108] (a) Rarig, R. A. F.; Scheidman, M.; Vedejs, E. *J. Am. Chem. Soc.* **2008**, *130*, 9182-9183. (b) Tamao, K.; Tanaka, T.; Nakajima, T.; Sumiya, R., Arai, H.; Ito, Y. *Tetrahedron Lett.* **1986**, *27*, 3377-3380. c) Evans, D. A.; Muci, A. R.; Stürmer, R. *J. Org. Chem.* **1993**, *58*, 5307-5309. (d) Yadav, J. S.; Sasmal, P. K. *Tetrahedron Lett.* **1997**, *38*, 8769-8772.

functionalized cyclopropane **3.56**. This compound would be formed by stereoselective cyclopropanation of a cyclobutene **3.57**, followed by alkylation, as employed in the previous syntheses of pleocarpenene and pleocarpenone[106a,b,c]. This would allow control of the stereochemistry at C7, however, the increased functionality of this intermediate would also provide a difficult test of the acid-mediated rearrangement methodology in this more complex setting. Cyclobutene **3.57** would be accessible through cyclobutadiene cycloaddition of free cyclobutadiene liberated upon oxidation iron complex **3.58** with the tethered olefin. This cyclobutene (**3.57**) was designed to both include the carbonyl oxidation state at C3 and the methyl group at C10 to obviate the need for oxidation or deoxygenation at a later stage in the synthesis. The dithiane would also likely activate the system toward productive cycloaddition through the Thorpe-Ingold effect despite the electronically unactivated olefin and all-carbon tether, allowing it to out-compete dimerization of the cyclobutadiene.[109] Iron complex **3.58** would be accessible through umpolung addition[110] of the anion generated from the known crotyl dithiane **3.59**[111] into the known iron aldehyde **3.60**[106a] to generate the protected hydroxyl-ketone functionality.

---

[109] Limanto, J.; Tallarico, J. A.; Porter, J. R.; Kuong, K. S.; Houk, K. N.; Snapper, M. L. *J. Am. Chem. Soc.* **2002**, *124*, 14748-14758.
[110] Review: Gröbel, B. T.; Seebach, D. *Synthesis* **1977**, 357-402.
[111] Nicolaou, K. C.; Magolad, R. L.; Sipio, W. J.; Barnette, W. E.; Lysenko, Z.; Joullie, M. M. *J. Am. Chem. Soc.* **1980**, *102*, 3784-3793.

Scheme 3.13: Original Retrosynthetic Analysis for Torilin

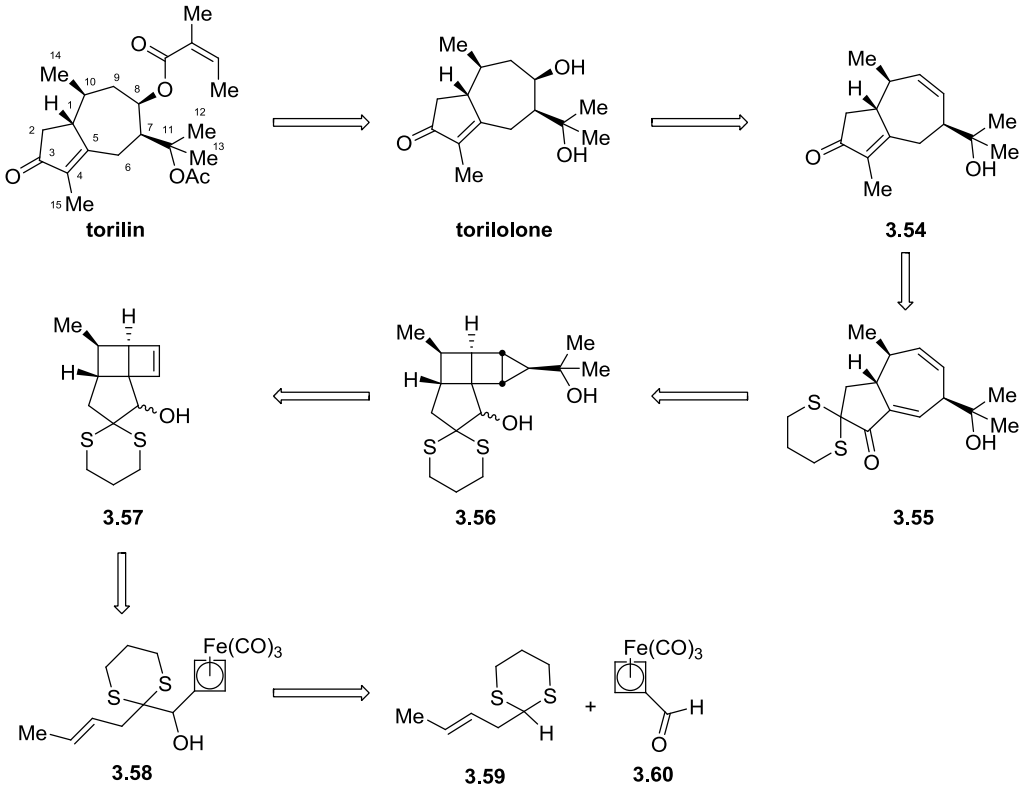

SYNTHETIC STUDIES

Tricarbonylmethylcyclbutadienoate iron (**3.62**) can be prepared conveniently from the commercially available α-pyrone **3.61**. Photochemical irradiation triggers a 4π-electrocyclization and the resulting cyclobutene is complexed using diiron nonacarbonyl with concommitant decarboxylation to afford **3.62**.[112] This stable iron-diene complex can be reduced to alcohol **3.63** with Dibal-H and then re-oxidized with manganese dioxide to provide the known iron aldehyde **3.60**.[106a] In

[112] Limanto, J.; Snapper, M. L. *J. Am. Chem. Soc.* **2000**, *122*, 8071-8072.

order to employ crotyl dithiane **3.59**[113] as an acyl anion equivalent, **3.59** was deprotonated using *tert*-butyllithium[114] and this stabilized anion was allowed to react with iron aldehyde **3.60** at -78 °C.[111] This generated iron complex **3.58** in 79% yield. Iron Dithiane complex **3.58**[115] was also accessible directly from methyl ester **3.62** *via* reduction of the intermediate ketone resulting from mono-addition of the dithianyl anion to the ester.[116] This would effectively shorten the synthesis of **3.58** by one step; however, the overall yield for this process proved slightly lower (Scheme 3.14).

Scheme 3.14: Preparation of Iron Complex **3.58**

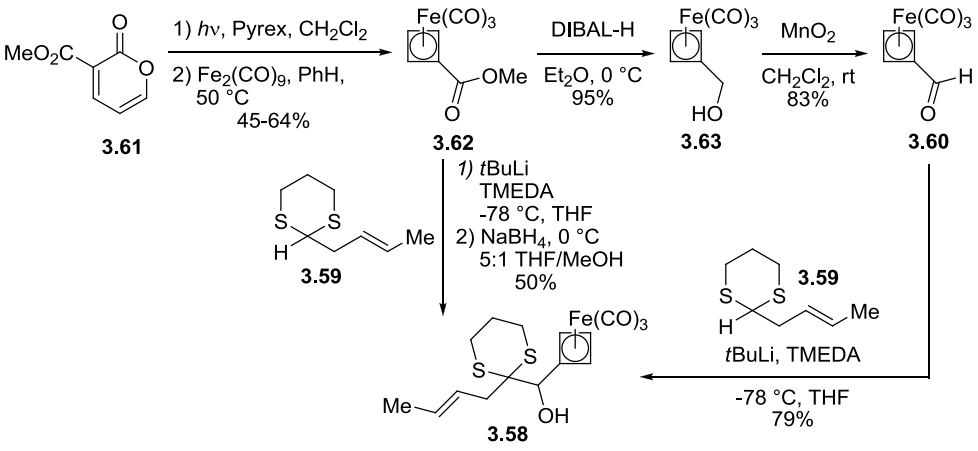

---

[113] Generated from crotyl bromide and 1,3-dithiane according to reference 111. Procedure modified to use technical grade crotyl bromide and final product fractionally distilled according to: Campi, E. M.; Jackson, W. R.; Perlmutter, P.; Tasdelen, E. E. *Aust. J. Chem.* **1993**, *46*, 995-1007. Mixture of olefin isomers were still present (85:15 E:Z).

[114] Any excess *n*-Buli reacted with the carbonyl ligands of iron complex **3.58** resulting in decreased yield and difficult purification.

[115] Complex **3.58** crystallized from hexanes as an ~85:15 E:Z mixture of olefin isomers which were characterized by single crystal X-ray diffraction.

[116] This result is in contrast to that suggested in the literature for substituted methyl benzoates where multiple additions (for 2-methyl-1,3-dithiane) and dithiane ring opening (for substituents larger than methyl) were observed. Valiulin, R. A.; Kottani, R.; Kutateladze, A. G. *J. Org. Chem.* **2006**, *71*, 5047-5049.

Access to **3.58** in enantioenriched form would enable an asymmetric synthesis due to the diastereoselectivity expected in the following transformations. Therefore, the asymmetric umpolung addition to form **3.58** was explored. Based on precedent from the Kang group,[117] (-)-sparteine and (-)-α-isosparteine were selected as ligands. (-)-Sparteine produced higher enantioselectivity than seen in the literature precedent; however, (-)-α-isosparteine resulted in a less selective addition. Due to the low yields and selectivities, the larger tert-butyllithium was also examined and produced essentially no selectivity along with a poor yield. In the end, none of these ligands produced synthetically useful levels of enantioselectivity in this reaction. This is likely caused, at least in part, by the alkyl substitution at the 2-position in the dithiane. The increased steric demands likely prohibit chelation of this lithiated carbanion. Asymmetric reduction of the ketone leading to **3.58** using (*R*)-CBS catalyst[118] also produced the secondary alcohol in low yield and only 5% ee, likely due to the extremely hindered environment around the carbonyl.

---

[117] The most successful ligand for the addition of 2-lithio-1,3-dithiane into benzaldehyde reported to date is (-)-α-isosparteine (70% ee, 73% yield). For comparison, (-)-sparteine provided 3% ee under the same conditions. Kang, J.; Kim, J. I.; Lee. J. H. *Bull. Kor. Chem. Soc.* **1994**, *15*, 865-868.

[118] Corey, E. J.; Helal, C. J. *Angew. Chem. Int. Ed.* **1998**, *37*, 1986-2012.

Table 3.2: Asymmetric Umpolung Addition.

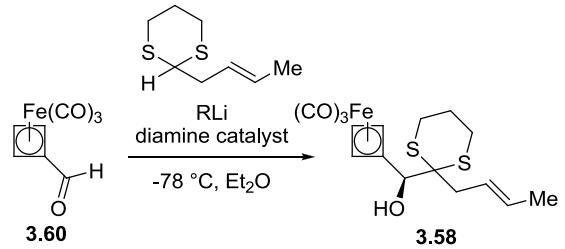

3.60 **3.58**

RLi	Diamine	Yield	ee
*n*BuLi	sparteine	19%	17%
*n*BuLi	isosparteine	35%	10%
*t*BuLi	isosparteine	23%	1%

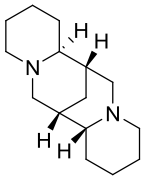

(-)-sparteine

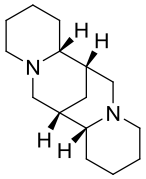

(-)-α-isosparteine

With **3.58** in hand, its oxidation could be explored (Scheme 3.15). After examination of a number of oxidants including trimethylamine N-oxide,[119] lead tetraacetate,[120] and photochemical irradiation,[121] ceric ammonium nitrate (CAN) was found to be superior. Three equivalents of CAN in dilute acetone solution (2 mM) liberated the cyclobutadiene in 5 minutes at ambient temperature to afford cyclobutene **3.57** as an inseperable 2:1 α:β mixture of alcohol diastereomers[122] in 73% yield. This mixture could be homogenized through a cycle of oxidation and reduction to afford α-diastereomer **3.57**α with near complete diastereoselectivity (~95%) owing to the rigid ring system.

---

[119] Shvo, Y.; Hazum, E. *Chem. Commun.* **1974**, 336—337.
[120] Merk, W.; Pettit, R. *J. Am. Chem. Soc.* **1967**, *89*, 4787-4788.
[121] Knölker, H. J.; Goesmann, H.; Klauss, R. *Angew. Chem. Int. Ed.***1999**, *38*, 702-705.
[122] Traces of the product from cycloaddition of the Z-olefin isomer of **3.58** were also detected and were removed through purification during subsequent steps.

Scheme 3.15: Cyclobutadiene Cycloaddition

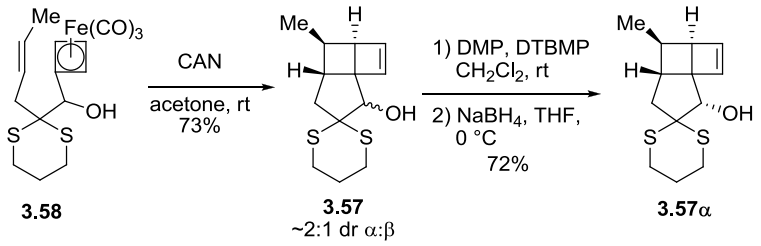

Unfortunately, cyclopropanation of cyclobutene **3.57** proved unsuccessful under the previously developed conditions (ethyl diazoacetate, $Cu(acac)_2$).[106a,b] Attempts to circumvent this problem using other copper or rhodium catalysts also failed. Even cyclopropanation with an acetate protected hydroxyl group and attempts at Simmons-Smith type[123] cyclopropanation using dibromo- and diiodo-acetates only provided traces of desired product among intractable mixtures of dithiane oxidation and various insertion products.

Undeterred, an exchange of carbonyl protecting group was explored (Scheme 3.16). Dithianes can unfortunately be difficult to deprotect, especially in the presence of sensitive functionality. As a result, the best conditions cannot often be predicted *a priori*, but must be determined empirically. Therefore, a multitude of deprotection conditions have been developed.[110,124] Initially, a one-pot procedure for dithiane deprotection and subsequent ketalization using

---

[123] Synthesis of dihalo-acetates: Lee, K.I.; Youn, J. I.; Shim, Y. K.; Kim, W. J. *Bull. Kor. Chem. Soc.* **1992**, *13*, 226-227. Modified Simmons-Smith Cyclopropanation: Charette, A. B.; Lemay, J. *Angew. Chem. Int. Ed. Engl.* **1997**, *36*, 1090-1092. See reference 104 for cyclopropanation of cyclobutenes.

[124] (a) Yus, M.; Najera, C.; Foubelo, F. *Tetrahedron* **2003**, *59*, 6147-6212. (b) Burghardt, T. E. *J. Sulfur Chem.* **2005**, *26*, 411-427.

mercuric chloride[125] appeared successful (**3.57**→**3.64**). Immediate protection of the hydroxyl group crude product was found necessary as the intermediate hydroxyl-ketal proved painfully volatile. The yield for this reaction was capricious, particularly on larger scale and long reaction times approaching three days for the two-step process were necessary. A revision of these conditions would be necessary. The initial success provided small quantities of ketal **3.64**, nonetheless, which enabled development of a successful cyclopropanation to afford **3.65** in excellent yield.

Scheme 3.16: Synthesis of Cyclopropane **3.65**

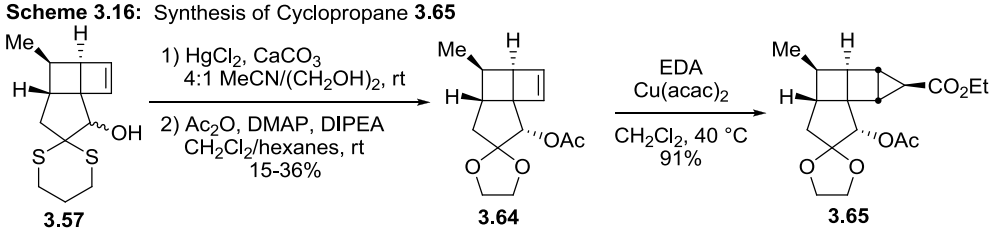

3.57 **3.64** **3.65**

To overcome this roadblock and deliver larger quantities of **3.64**, the protecting group exchange was explored. A wide array of conditions were examined (see selected examples in Table 3.1) with almost unilaterally negative results. Many conditions (Entries 3,8,14,15,19,20) provided limited reactivity, and those that converted the starting material were met with decomposition (Entries 5,6,8,9,10,13,16,20), low yields (Entries 4,7,11,12,13,17,18,21), poor

[125] Nicolaou, K. C.; Frederick, M. O.; Loizidou, E. Z.; Petrovic, G.; Cole, K. P.; Koftis, T. V.; Yamada, Y. M. A. Chem. Asian J. **2006**, 245-263.

purity and the formation of unwanted byproducts. Exchange of the protecting group prior to cycloaddition (iron complex **3.58**, Scheme 3.15) also failed.[126]

[126] Selectfluor and hypervalent iodide reagents appeared to decompose the iron complex and mercuric chloride caused preferential oxymercuration of the olefin with attack of the secondary alcohol.

Table 3.2: Survey of Dithiane Deprotection Conditions (50 mg scale)

Entry	Substrate	Conditions	Result
1	**3.57**	3.5 equiv. $HgCl_2$ portionwise, 4Å MS, 10 equiv. $CaCO_3$, 4:1 MeCN/$(CH_2OH)_2$, rt;[125] 5 equiv. Ac_2O, 6 equiv Et_3N, 25 mol. % DMAP 1:1 CH_2Cl_2/Hexanes[127]	15-36%
2	**3.66**	2.5 equiv. Selectfluor, 4:1 MeCN/$(CH_2OH)_2$, 40 °C[149]	23% (20% over 2 steps)
3	**3.57**	4 equiv. CAN, 4:1 MeCN/$(CH_2OH)_2$, rt[128]	No Conversion[129]
4	**3.57**	2.2 equiv $PhI(O_2CCF_3)_2$, 4:1 MeCN/$(CH_2OH)_2$, rt;[130] acylation	15%,
5	**3.57**	6 equiv. NBS, 6.8 equiv. $AgNO_3$, 2,4,6-collidine 4:1 MeCN/$(CH_2OH)_2$, rt;[131] acylation	Decomposition
6	**3.57**	10 equiv. $NaClO_4$, 5 equiv. NaH_2PO_4, 10 equiv. 2-methyl-2-butene 4:1 MeCN/$(CH_2OH)_2$, rt[132]	Decomposition
7	**3.57**	20 equiv. MeI 4:1 MeCN/$(CH_2OH)_2$, rt[133]	11%
8	**3.57**	2 equiv. HgO-BF_3	Slow Conversion,

[127] These conditions are hereafter abbreviated “acylation”.
[128] Ho, T. L.; Ho, H. C.; Wong, C. M. *Chem. Commun.* **1972**, 791.
[129] Interestingly, excess CAN and extended reaction times in the cycloaddition reaction appeared to deprotect the dithiane to an α-hydroxyketone. However, yields were low and this ketone could not be successfully protected.
[130] (a) Stork, G.; Zhao, K. *Tetrahedron Lett.* **1989**, *30*, 287-290. (b) Matsuura, F.; Peters, R.; Anada, M.; Harried, S. S.; Hao, J.; Kishi, Y. *J. Am. Chem. Soc.* **2006**, *128*, 7463-7465.
[131] Corey, E. J.; Erickson, B. W. *J. Org. Chem.* **1971**, *36*, 3553-3560.
[132] Ichige, T.; Miyake, A.; Kanoh, N.; Nakata, M. *Synthesis* **2004**, 1686-1690.
[133] Tanaka, K.; Fujimori, Y.; Saikawa, Y.; Nakata, M. *J. Org. Chem.* **2008**, *73*, 6292-6298.

Entry	Substrate	Conditions	Result
		15% $(CH_2OH)_2$/THF, rt[134]	Decomposition with excess reagent
9	**3.57**	2 equiv. $Hg(ClO_4)_2$ 1:1 $CH_2Cl_2/(CH_2OH)_2$, 0 °C[135]	Decomposition
10	**3.57**	2 equiv. $AgNO_3$ in 1:1 $CH_2Cl_2/(CH_2OH)_2$, rt[131]	decomposition
11	**3.66**	1.5 equiv. $PhI(O_2CCF_3)_2$, 2:1 MeCN/$(CH_2OH)_2$, rt	Hydrolysis of Sulfoxides slow, even with TFA (7%)[136] or TFAA/DIPEA[137] (19%)
12	**3.57**	$CuCl_2$, CuO, 4:1 Acetone/$(CH_2OH)_2$, 60 °C;[138] acylation	72%* co-elution of copper byproduct
13	**3.57**	$CuCl_2$, CuO, 4Å MS 4:1 THF/$(CH_2OH)_2$, 60 °C;[138] acylation	10% fragmentation to cyclohexadiene
14	**3.66**	3 equiv. DMP 8:1:1 MeCN/$CH_2Cl_2/(CH_2OH)_2$, rt, air[139]	10-38% Slow, variable
15	**3.66**	2 equiv. HgO-BF_3 4:1 THF/$(CH_2OH)_2$, rt[134]	Trace Product
16	**3.66**	4 equiv. CAN	Decomposition

[134] Vedejs, E.; Fuchs, P. L. *J. Org. Chem.* **1971**, *36*, 366-367.
[135] Bao. G.; Zhao, L.; Burnell, D. J. *Org. Biomol. Chem.* **2005**, *3*, 3576-3584.
[136] Krohn, K.; Cludius-Brandt, S. *Synthesis* **2008**, 2369-2372.
[137] Aggarwal,V. K.; Thomas, A.; Franklin, R. J. *Chem. Commun.* **1994**, 1653-1654.
[138] Narasaka, K.; Sakashita, T.; Mukaiyama, T. *Bull. Chem. Soc. Jpn.* **1972**, *45*, 3724.
[139] (a) Langille, N. F.; Dakin, L. A.; Panek, J. S. *Org. Lett.* **2003**, *5*, 575-578. (b) Su, Q.; Dakin, L. A.; Panek, J. S. J. Org. Chem. **2007**, *72*, 2-24.

Entry	Substrate	Conditions	Result
		4:1 MeCN/$(CH_2OH)_2$, rt[128]	
17	**3.57**	4 equiv. $HgCl_2$ portionwise, 3Å MS, 10 equiv. $CaCO_3$, 4:1 MeCN/$(CH_2OH)_2$, rt;[125] 2 equiv. NaH, THF, 66 °C; 2.2 equiv. Ac_2O, 66 °C	13%
18	**3.57**	2 equiv. $HgCl_2$ portionwise, 2.2 equiv. $CdCO_3$, 4:1 MeCN/$(CH_2OH)_2$, rt;[140] acylation	20%
19	**3.66**	4:1:1 MeCN/$(CH_2OH)_2$/Me_2SO_4, 40 °C	Slow Conversion, Trace Product
20	**3.66**	I_2, 4:1 MeCN/$(CH_2OH)_2$, 80 °C [141]	Cyclohexadiene fragmentation[142]
21	**3.66**	2.5 equiv. Me_3OBF_4, CH_2Cl_2, 0 °C;[143] 1:1 CH_2Cl_2/$(CH_2OH)_2$,	10%
22	**3.66**	Selectfluor, 10 equiv. neopentyl glycol MeCN, 40 °C	26% dimethyldioxolane[144] protected carbonyl
23	**3.57**	4 equiv. $HgCl_2$ portionwise, 3Å MS, 10 equiv. $CaCO_3$,	26% Palmitate ester[145]

[140] Jones, J. B.; Grayshan, R. *Chem. Commun.* **1970**, 741-742.
[141] Gaunt, M. J.; Jessiman, A. S.; Orsini, P.; Tanner, H. R.; Hook, D. F.; Ley, S. V. *Org. Lett.* **2003**, *5*, 4819-4822.
[142] No conversion was observed at lower temperatures.
[143] Ueno, A.; Kitawaki, T.; Chida, N. *Org. Lett.* **2008**, *10*, 1999-2002.
[144] No real improvement observed upon switching ketal protection.
[145] Similar yield observed with the lower molecular weight acetate and the C_{16} palmitate. Volatility of the acetate is not an issue.

Entry	Substrate	Conditions	Result
		4:1 MeCN/$(CH_2OH)_2$, rt;[125] 5 equiv. palmitic acid, 6 equiv. DCC, 25 mol. % DMAP, CH_2Cl_2, rt	
24	**3.66**	4 equiv. $HgCl_2$ portionwise, 3Å MS, 10 equiv. Base[146], 4:1 MeCN/$(CH_2OH)_2$, rt;[125]	Deprotection to form **3.57**
25	**3.66**	1.5 equiv. DDQ[147], 4:1 MeCN/$(CH_2OH)_2$, 80 °C	Decomposition

Examination of the X-ray crystal structure of the β-diastereomer of acetate **3.66** (Figure 3.3) may provide some clues to explain this reactivity. The sterically hindered environment around the sulfur atoms is apparent in which S2 is nearly eclipsed by the β-acetate and S1 is tucked under the ring system. Imagining the exchange of O1 of the acetate and H5 to represent the α-diastereomer suggests that the acetate would lie essentially between the two sulfur atoms and in the vicinity of H2A and H4B, the axial protons on the dithiane ring. Inversion of this rigified *spiro* ring system is likely very difficult and the conformation of the dithiane has been apparently fixed by the preferential axial alkylation[148] of the dithianyl anion to form **3.58** as confirmed by X-ray crystallography. This

[146] A screen of bases indicated that $CaCO_3$, $NaHCO_3$, K_3PO_4, KH_2PO_4 and NaOAc all engaged in preferential rapid deprotection the acetate in the presence of ethylene glycol. Amine bases including DTBMP, DIPEA, and pyridine all shut down reactivity with pyridine and DIPEA likely sequestering the mercury salt as a dark precipitate.
[147] Tanemura, K.; Dohya, H.; Imamura, M.; Suzuki, T.; Horaguchi, T. *Chem. Lett.* **1994**, 965-968.
[148] Honda, Y.; Morita, E. Ohshiro, K.I Tsuchihashi, G. *Chem. Lett.* **1988**, 21-24.

arrangement suggests that reagent approach for activation of the sulfur and hydrolysis is likely difficult and suggests an explanation for the slow acylation of the secondary alcohols in **3.57**. Further examination of this structure shows that in this dithiane (and likely the ketal product **3.64** as well) the σ^* of the C5-O1 acetate bond is well aligned with the highly strained C6-C9 bond (ORTEP numbering) which may contribute to fragmentation of this system to form a less-strained cyclohexadiene and possible acetate elimination as pathways (particularly under acidic conditions and at elevated temperatures) accounting for some of the observed decomposition during these ketal exchange reactions. Of course, the requirement of longer reaction times due to the extremely hindered dithiane moiety also provides the opportunity for byproducts stemming from attack on the strained olefin present in these cyclobutenes (**3.57**, **3.66** and **3.64**).

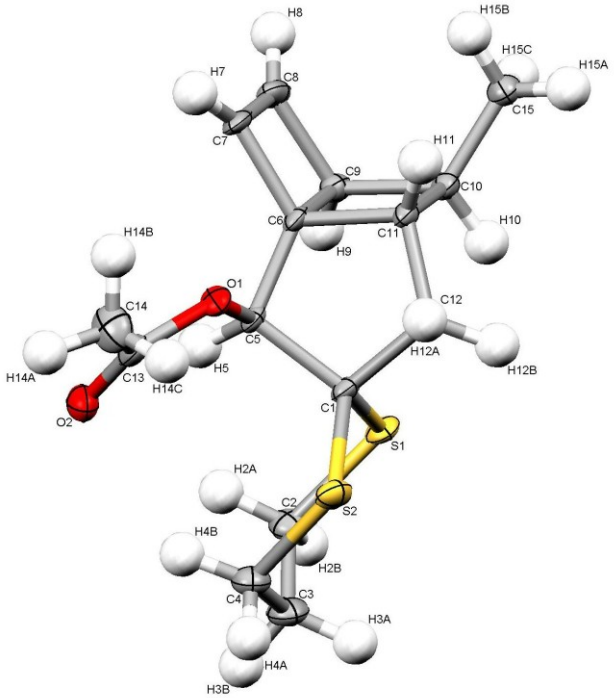

Figure 3.3: ORTEP for β-acetate **3.66**β

Finally, a paper from the Wong group[149] suggested another way forward with deprotection conditions that employ the electrophilic fluorine source Selectfluor. This reagent activates the thioketal toward cleavage and hydrolysis.[150] Gratifyingly, substituting ethylene glycol for water as the nucleophile, allowed development of a new one-pot ketal exchange. In this manner (Scheme 3.17), forcing acylation conditions[151] provided sterically

---

[149] Liu, J.; Wong, C.-H. *Tetrahedron Lett.* **2002**, *43*, 4037-4039.; Review: Nyffler, P. T.; Duron, S. G.; Burkart, M. D.; Vincent, S. P.; Wong, C.-H. *Angew. Chem. Int. Ed.* **2005**, *44*, 192-212.
[150] Mechanism is unclear and may involve either Lewis acid activation or oxidation. See reference 149.
[151] Standard DMAP catalysis in dichloromethane at room temperature resulted in 55% yield of **3.66.**

hindered acetate **3.66**[152] in high yield. Ketal exchange using Selectfluor provided ketal **3.64** in a somewhat disappointing yield of 18%.[153] This was viewed as an improvement, however, when compared to the mercuric chloride reaction as it was very scalable, reproducible and much faster (conversion from **3.57** to **3.64** could be completed in one day), with the added benefit of avoiding the handling and disposal of highly toxic mercury salts.

Scheme 3.17: Revised Protection Sequence

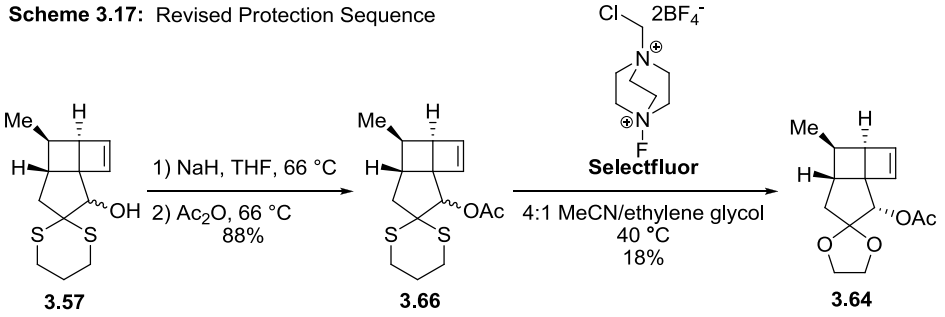

3.57 **3.66** **3.64**

With access to the cyclopropane **3.65** now secured, investigation of the pivotal rearrangement in this synthetic plan could begin (Scheme 3.18). Alkylation with methyllithium in the presence of N,N,N',N'-tetramethylethylenediamine[154] provided diol **3.67**.[155] Screening a

---

[152] β-diastereomer of **3.66** was isolated from the mercuric chloride deprotection (Scheme 3.15, **3.57**→**3.64**) and characterized by single crystal X-ray diffraction.

[153] Decomposition of the minor β-diastereomer is likely occurring, which would account for isolation of only the major α-diastereomer. However, when diastereomerically pure **3.66** was used, the yield did not increase substantially, despite the apparently cleaner reaction. This confusing result suggested beginning with a mixture of diastereomers to be preferable in terms of overall yield.

[154] Reactions proceeded to incomplete conversion (~60%) using methylmagnesium bromide[106a] or methyllithium without the added diamine. In these cases, the product of intermediate acetate deprotection **3.65b** was isolated and could be recycled under the same conditions to provide additional product without reduction of yield. Precedent for this acetate deprotection can be found in Watanabe, Y.; Fujimoto, T.; Shinohara, Ozaki, S. *Chem. Commun.* **1991**, 428-429 and Watanabe, Y.; Fujimoto, T.; Ozaki, S. *Chem. Commun.* **1992**, 681-683.

number of reaction conditions including PCC,[156] Swern,[157] Parrikh-Doering,[158] and Oppenauer[159] failed to provide evidence of the desired product **3.68**. Oxidation of this diol using catalytic tetrapropylammonium perruthenate[160] and subsequent treatment with a Lewis acid, however, produced enone **3.68** in 9% isolated yield. This low yield is likely the result of the highly sensitive nature of **3.68**.[161]

Scheme 3.18: Key Rearrangement

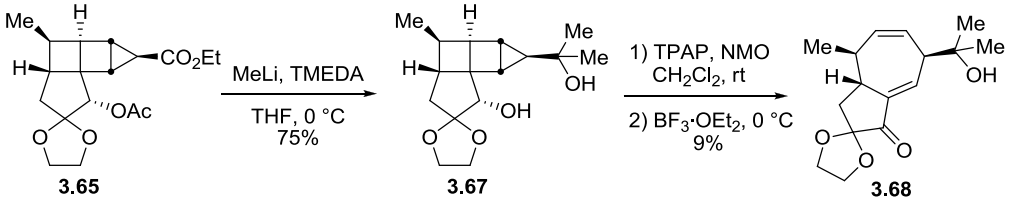

Optimization of this result was attempted through the use of the mild Dess-Martin periodinane.[162] This resulted (Scheme 3.19) in the generation of

---

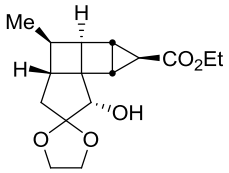

3.65b

[155] **3.67** was characterized as the mono-hydrate by single crystal X-ray diffraction analysis.
[156] Corey, E. J.; Suggs, J. W. *Tetrahedron Lett.* **1975**, *16*, 2647-2650. For an example of tertiary alcohol-substituted cyclopropane fragmentation under these conditions: Wada, E.; Okawara, M.; Nakai, T. *J. Org. Chem.* **1979**, *44*, 2952-2954.
[157] Omura, K.; Swern, D. *Tetrahedron*, *34*, 1651-1660.
[158] Parrikh, J. R.; Doering, W. v. E. *J. Am. Chem. Soc.* **1967**, *89*, 5505-5507.
[159] Neef, G.; Ottow, E.; Ast, G.; Vierhufe, H. *Syn. Commun.* **1993**, *23*, 903-911.
[160] Review: Ley, S. V.; Norman, J.; Griffith, W. P.; Marsden, S. P. *Synthesis*, **1994**, 639-665.
[161] Empirical observations suggest that this skipped dienone is sensitive to acid, base, and oxidation.
[162] Dess, D. B.; Martin, J. C. *J. Am. Chem. Soc.* **1991**, *113*, 7277-7287.

ketone **3.69**, which began to rearrange under the reaction conditions.[163] Completion of the rearrangement was ensured by treatment with Lewis acid[164] to provide **3.68**, which was used directly in the next step in order to minimize material loss through purification. Functionalizations, which would remove the sensitive enone and produce synthetically useful functionalities, were explored. The first transformation attempted was conjugate reduction with L-Selectride[165] followed by triflation of the enolate[166] with Comins's reagent[167] to provide vinyl triflate **3.70**. The tetrasubstituted olefin of the natural product was then formed through Suzuki coupling with potassium methyltrifluoroborate[168] to afford **3.71**. It proved impossible, however, to generate analytically pure material from this sequence. Alternatively, the reduction was quenched with a proton source to afford **3.72**,[169] which could be olefinated[170] in low yield to afford **3.73**. Attempted hydrazone formation[171] from this highly hindered ketone (**3.72**) to prepare for Shapiro reaction[172] also failed. Finally, methyllithium was used to alkylate the

---

[163]Meyer, S. D.; Schreiber, S. L. *J. Org. Chem.* **1994**, *59*, 7549-7552. These conditions result in liberation of one equivalent of acetic acid which is sufficient to trigger the rearrangement. Added pyridine base slows the reaction and does not seem to prevent isomerization.

[164] Treatment of this substrate with $BF_3{\cdot}OEt_2$ at 0 °C under the previously reported[104b] reaction conditions resulted in decomposition.

[165] Fortunato, J. M.; Ganem, B. *J. Org. Chem.* **1976**, *41*, 2194-2200.

[166] Ng, S. M. Investigation of Intramolecular [2+2] Photocycloadditions: Using New Cycloaddition/Fragmentation Strategies Toward Medium Ring-Containing Natural Products. Ph.D. Dissertation. Boston College, Chestnut Hill, MA. 2008.

[167] Comins, D. L.; Dehghani, A. *Tetrahedron Lett.* **1992**, *33*, 6299-6302.

[168] Molander, G. A.; Ellis, N. *Acc. Chem. Res.* **2007**, *40*, 275-286.

[169] The same ketone, **3.72**, could be accessed in 19% yield by reaction of the intermediate ketone **3.69** (produced by Dess-Martin oxidation), with SmI_2 in the presence of HMPA. See Shipe, W. D., Sorensen, E. J. *Org. Lett.* **2002**, 2063-2066 for an example of this type of fragmentation.

[170] Tebbe, F. N.; Parshall, G. W.; Reddy, G. S. *J. Am. Chem. Soc.* **1978**, *100*, 3611-3613.

[171] Both tosyl- and trisylhydrazide were examined as reagents for this transformation.

[172] Lipton, M. F.; Shapiro, R. H. *J. Org. Chem.* **1978**, *43*, 1409-1413.

enone at the carbonyl and generate diol **3.74**. Subsequent deprotection[173] and reduction of the α-hydroxyketone[174] would afford the more stable tetrasubstituted enone **3.75**. Unfortunately, all of these approaches, while producing useful preliminary results, were ultimately unsuccessful. The products from this key sequence were found to be of low purity and consisted of a number of closely related products. Therefore, despite appropriate characteristic peaks in their ^{1}H-NMR spectra, IR spectra indicative of the desired functionality and identification of the expected molecular ions by high-resolution mass spectrometry (HRMS), these intermediates could not be sufficiently purified for complete characterization.

---

[173] Gautier, E. C. L.; Graham, A. E.; McKillop, A.; Standen, S. P.; Taylor, R. J. K. Tetrahedron Lett. **1997**, *38*, *1881-1884.*

[174] (a) Molander, G. A.; Hahn, G. *J. Org. Chem.* **1986**, *51*, 1135-1138. (b) White, J. D.; Somers, T.C. *J. Am. Chem. Soc.* **1987**, *109*, 4424-4426. (c) Holton, R. A.; Williams, A. D. *J. Org. Chem.* **1988**, *53*, 5983-5986. (d) Nicolaou, K. C.; Li, H.; Nold, A. L.; Pappo, D.; Lenzen, A. *J. Am. Chem. Soc.* **2007**, *129*, 10356-10357. (e) Gong, J.; Lin, G.; Li, C. C,; Yang, Z. *Org. Lett.* **2009**, *11*, 4770-4773. (f) Krawczuk, P. J.; Schöne, N., Baran, P. S. *Org. Lett.* **2009**, *11*, 4774-4776.

Scheme 3.19: Preliminary Approaches*

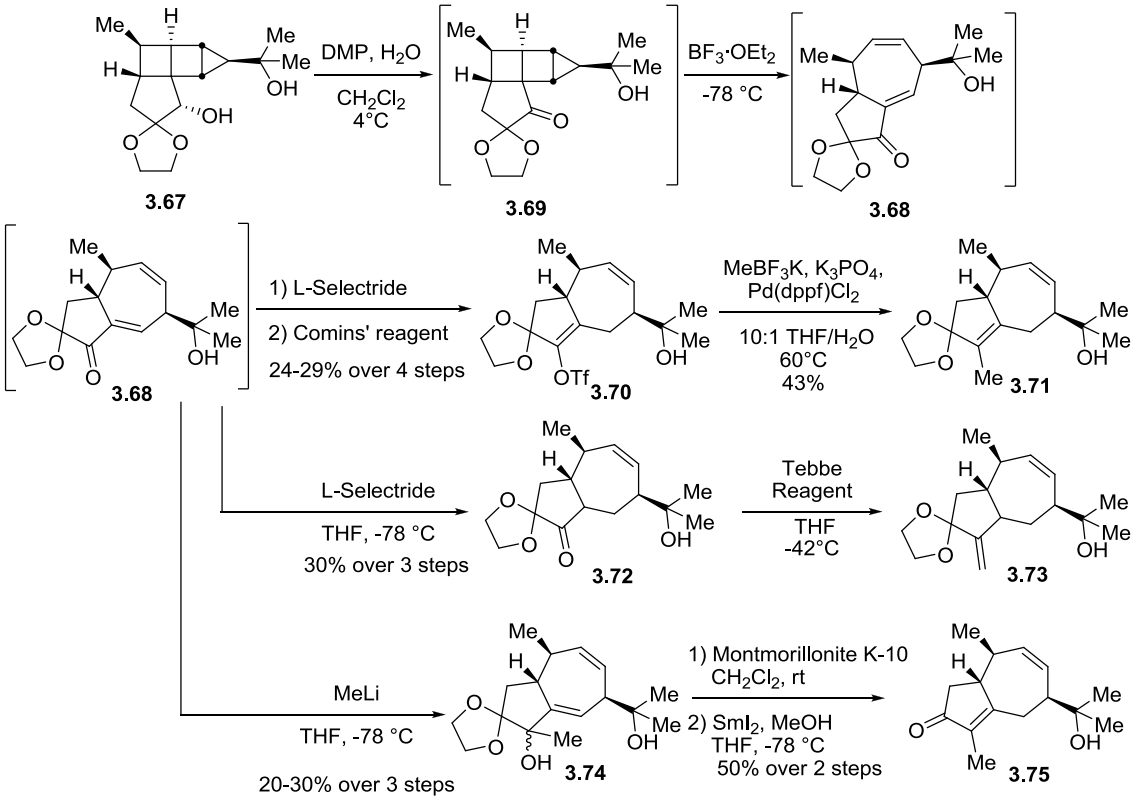

**Yields in this scheme are approximate as compounds could not be obtained analytically pure.*

The prediction of ^{13}C-NMR spectra through *ab-initio* quantum chemical calculations is a powerful tool and has been successfully applied to the confirmation and sometimes revision of the assigned structures of complex, oxygenated terpene natural products (i.e. hexacyclinol).[175] In order to provide support that the intermediates produced by these preliminary reactions were likely represented by the proposed structures, spectral prediction was undertaken. Using a combination of semi-empirical, Hartree–Fock and density functional methods, spectra were predicted through the GIAO method. The predicted

[175] Rychnovsky, S. D.*Org. Lett.* **2006**, *8*, 2895-2898.

^{13}C-NMR spectra[176] (including possible diastereomers) were compared with that recorded for new compound **3.74**.[177] The validity of these predictions was determined by evaluation of the average and maximal deviation between the predicted and experimentally determined chemical shifts.[175] As a benchmark, the spectra predicted for the known compounds torilin, torilolone, **3.17, 3.49** and another guaiane, aerugidiol, were compared with literature values. These results suggest that the α-alcohol diastereomer of **3.74** is the likely major product of this alkylation with an average deviation in the ^{13}C chemical shifts of 2.1 ppm compared to 1.6 ppm for torilin, 1.9 ppm for torilolone 1.9 ppm for **3.17** and 2.0 ppm for **3.49** with greater than 4 ppm deviation observed when this prediction was compared to other terpenoid compounds with reported ^{13}C-NMR data and sharing similar structure and molecular formula. These results are in line with those determined by Rychnovsky[175] in his analysis of hexacyclinol and related compounds. This not only suggested that the desired compound **3.74** is present in these mixtures, it demonstrated the power and applicability of these computational methods when applied to the guaiane class of natural products.

The preliminary investigation of these parallel synthetic routes was extended to the end game (Scheme 3.20). In one approach, the tertiary alcohol was exposed to known conditions for directed hydroboration[178] of the

---

[176] Full computational details and molecular geometries can be found in the experimental section along with comparison tables of predicted and experimental chemical shifts.
[177] For **3.74**, major peaks in the ^{13}C spectrum of the impure product mixture were selected for this study.
[178] See reference 108a for directed hydroboration of primary acyclic homoallylic alcohols.

disubstituted olefin in **3.71** and afforded evidence of diol **3.76**. Alternately, deprotection of the ketal and reduction of the disubstituted olefin of **3.75** in the presence of the enone should provide **3.17**, a precursor to 8-desangeloyloxytorilin in the Deprés synthesis.[101] Again, promising preliminary spectral data could be obtained including HRMS data, but in the end, these compounds could not be obtained in sufficient purity after these late-stage reactions to establish identity with the natural product torilolone[92] or with known intermediate **3.17**[101] or torilolone.[92]

Scheme 3.20: Preliminary End Game*

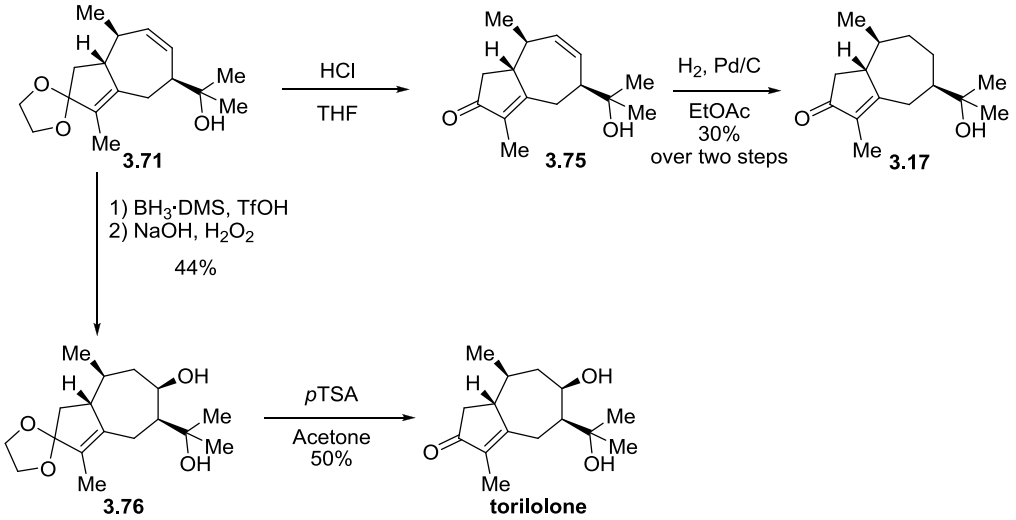

**Yields in this scheme are approximate as compounds could not be obtained analytically pure.*

While this work helped to identify possible conditions for the transformations in Scheme 3.18 and 3.19, no total synthesis could be claimed without material of higher purity. With trepidation, it was noted that the key rearrangement would have to be reevaluated to discover a more efficient reaction

with a better impurity profile.[179] Since TPAP had shown some early success[180] and had been noted in the literature as a mild oxidant for production of hindered ketones in the presence of tertiary alcohols,[181] it was further explored. Indeed, in the presence of N-methylmorpholine-N-oxide, the oxidation proved sluggish but eventually afforded 63% yield of what appeared to be the isomerized and over-oxidized diketone **3.77** over 8 hours at ambient temperature (Scheme 3.21). This indicated that the oxidation was indeed complete, and also, that TPAP was sufficiently Lewis acidic to trigger the rearrangement.[182] Suspecting that base sensitivity of the skipped dienone **3.68** in the presence of NMO was the culprit, the reaction was attempted using stoichiometric TPAP,[183] a solution that has

---

[179] The previous oxidations would often stall prior to complete conversion of the diol and the products would be accompanied by likely products of over-oxidation, olefin isomerization and in the case of reaction with Dess-Martin periodinane at ambient temperature, even apparent acetate transfer (Preferential acylation has been reported for a hindered, heterocyclic secondary alcohol during Dess-Martin oxidation. Biggers, C. K.; Briner, K.; Doeck, C. W.; Fisher, M.J.; Hertel, L. W.; Mancoso, V.; Martinelli, M. J.; Mayer, J. P.; Ornsteine, P. L.; Richardson, T. I.; Shah, J. A.; Shi, Q.; Wu, Z.; Xie, C. Melanocortin Receptor Agonists. International Patent WO 02/059108 A1, January 23, 2002.)

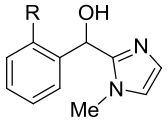

[180] See Scheme 3.17, 9% yield after a slow reaction requiring additional portions of TPAP to reach completion.

[181] Plate, R.; van Wujitswinkel, R. C. A. L; Jans, C. G. J. N; Groen, M. B. *Steroids* **2000**, *65*, 497-504.

[182] The initial failure of the TPAP oxidation/rearrangement was also likely due to treatment of the product with $BF_3 \cdot OEt_2$ at 0 °C, conditions later discovered to cause decomposition.

[183] Acetonitrile is usually considered a good solvent, particularly for sluggish TPAP oxidations.[160] In this case, oxidation of **3.67** with stoichiometric TPAP in acetonitrile afforded 85% yield of an acetonitrile adduct within fifteen minutes. The structure of this adduct is tentatively assigned as **3.67b**.

seen previous application in total synthesis for an unreactive, hindered alcohol.[184] Stoichiometric oxidation in dichloromethane at room temperature provided a near equimolar mixture of the desired **3.68** and the inseparable isomerization byproduct **3.78**. Conducting the reaction in a 4 °C cold room, however, provided the product **3.68** in moderate yield and with only traces of the inseparable **3.78**. Astonishingly, at this point, it was also discovered that these compounds could be purified by chromatography on pyridine-washed silica gel with little loss of material.[185] The slower purification during an initial scale up also provided one final clue. Longer reaction times or allowing the reaction mixture to warm to near ambient temperature in the presence of TPAP, even during the silica gel filtration used for workup of the reaction, produced increased amounts of **3.78**. This indicated that the Lewis acidity of the TPAP could also contribute to isomerization of **3.68**. Ultimately, painstakingly optimized conditions for this key rearrangement were developed in which the reaction was allowed to occur at -15 °C and initial purification to remove TPAP was conducted in a 4 °C cold room. This

---

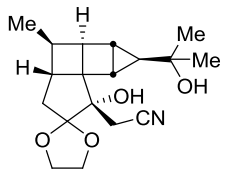

3.67b

Ruthenium-based lewis acids are known to facilitate the addition of acetonitrile to ketones, albeit in the presence of a base. (Kumagai, N.; Matsunaga, S.; Shibasaki, M. *Tetrahedron* **2007**, *63*, 8598-8608.) In this case, it is possible that the 4Å molecular sieves are sufficiently basic (pH=9.4 in acetonitrile, Herr, J. R.; Meckler, H.; Scuderi, F. Jr. *Org. Process Res. Dev.* **2000**, *4*, 43-45.) to afford **3.67b** in the presence of excess acetonitrile before the ketone can rearrange.

[184] Takeda, K.; Kawanishi, E.; Nakamura, H.; Yoshi, E. *Tetrahedron Lett.* **1991**, *32*, 4925-4928.

[185] Previous attempts at purification using triethylamine-washed silica gel or basic alumina resulted in <10% recovery of **3.68**.

suppressed all but traces of the isomerization to **3.78** and allowed **3.68** to be obtained in good purity and 56% yield.

Scheme 3.21: Optimized Key Step Sequence

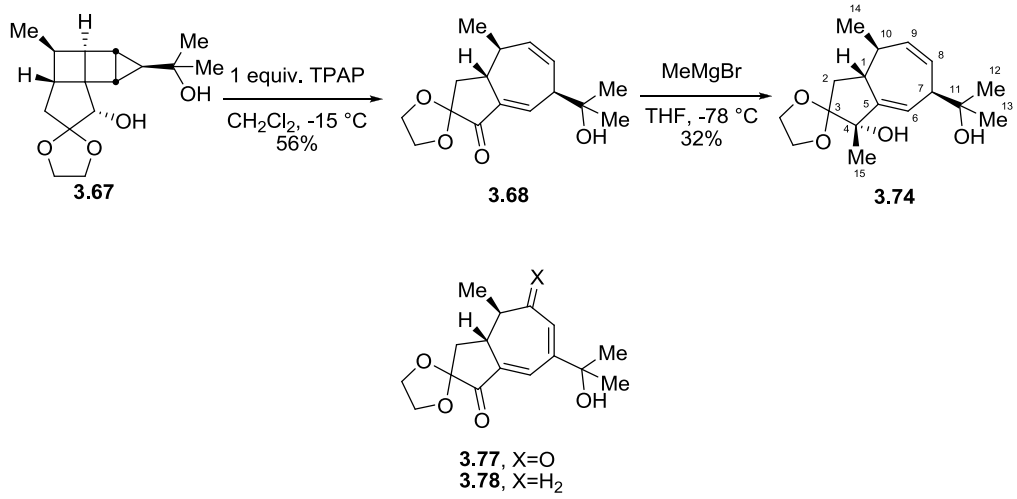

Methylation of the enone carbonyl in **3.68** (Scheme 3.21) was accomplished by dropwise addition of a solution of **3.68** to excess methylmagnesium bromide[186] and afforded diol **3.74** in 32% yield.[187] This intermediate proved difficult to obtain in analytically pure form. Satisfactory ^{13}C-NMR data were obtained, which supported the assigned structure and provided good correlation with the predicted chemical shifts from GIAO calculations.[176] The chemical shift values match those calculated for the C4

[186] Use of methyllithium (even in the presence of TMEDA or $CeCl_3$) or addition of the organometallic reagent to a solution of the substrate produced large amounts of apparently isomerized alkylation products, likely through deprotonation of the doubly-allylic proton at C7 prior to nucleophilic addition by the organometallic reagent itself or the alkoxide formed from the tertiatry alcohol at C11.

[187] **3.74** appears to be produced primarily as one diastereomer of the tertiary allylic alcohol. Due to limitations of scale and purity, the stereochemistry of this addition could not be unequivocally assigned.

β-diastereomer of **3.74** within an average of 2.2 ppm and the C4 α-diastereomer within an average of 2.4 ppm.[188] This supports the structural assignment of **3.74**[189] and is consistent with addition from what appears to be the least hindered face (top face) from examination of a molecular model of enone **3.68** (See Figure 3.4). This intermediate represents completion of the carbon skeleton of torilin and its guaiane congeners.

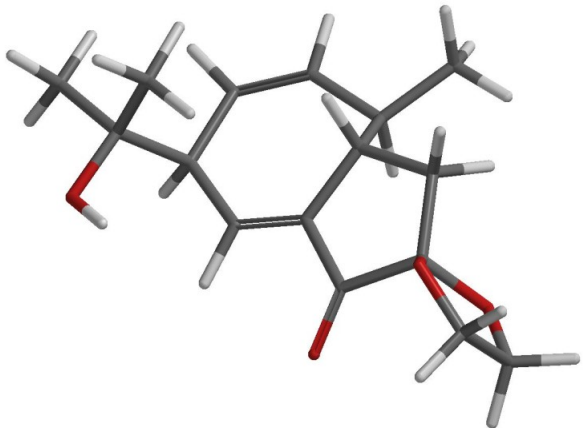

Figure 3.4: Structure of **3.68** at the PM3 level

With the small quantities of **3.74** available, the end-game was explored (Scheme 3.22) and confirmation of the structural assignments through correlation with known intermediate **3.17**[190] was attempted. Deprotection of the ketal under the best previously-discovered conditions afforded a crude α-hydroxy ketone mixture (**3.79**), which was directly reduced using samarium iodide in the

---

[188] Additionally, the spectrum obtained for enone 3.68 showed very good agreement (1.6 ppm average deviation) with that calculated for this structure.
[189] The assignment of C4 stereochemistry is tentative, of course, based on these chemical shift predictions, especially due to the similar average deviation observed for the C4 α- and β-methyl diastereomers.
[190] Isolation of **3.17** would intercept the Deprés synthesis[101] of 8-desangeloyloxytorilin at its penultimate intermediate and represent a formal synthesis of this guaiane natural product.

presence of methanol as a proton source.[191] This provided access to material tentatively representing final key intermediate **3.75**. This intermediate would indeed represent the final branch point in the synthesis of these natural products. As previously described (Scheme 3.20), directed oxygenation[108] should afford torilolone, which could be selectively acylated to afford torilin. Hydrogenation of the disubstituted olefin in **3.75** (Scheme 3.22) afforded **3.17**.[192]

Scheme 3.22: End Game

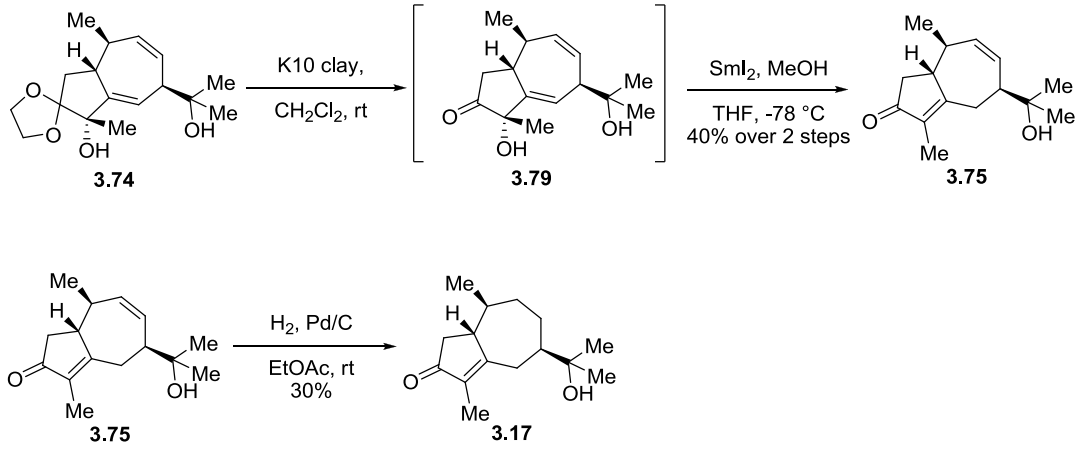

**Yields in this scheme are approximate as compounds could not be obtained analytically pure.*

Unfortunately, these final two intermediates could not be obtained in analytically pure form. Ketone **3.79** was identified based on HRMS, IR and crude ^{1}H-NMR. The reduction product **3.75** was also identified by HRMS and IR,

---

[191] While there is significant precedent for the reduction of α-hydroxy ketones in complex settings,[174] no examples of this transformation for allylic alcohols to provide enones could be found in the literature. Reference 174d demonstrates reduction of an allylic acetate, which upon treatment with triethylamine, isomerizes into a fluorenone en route to the kinamycins. Similar base treatment did not, however, improve yield or purity in the production of **3.75**.

[192] Reference 101 reports a similar transformation in which **3.27** (Scheme 3.6) is transformed into **3.75** through and oxymercuration protocol. Unfortunately, this compound is not isolated, but hydrogenated (using these conditions) to afford **3.17** (1-*epi*-hydroxycolorenone) in 55% yield over two steps.

however, chromatographic purification[193] proved insufficient to remove major impurity peaks at 0.87, 1.25, 1.55, 2.16 and 3.48 ppm in the ^{1}H-NMR.[194] A single olefinic proton resonance at 5.35 ppm seemed consistent with the structure of **3.75** and a partial ^{13}C-NMR spectrum[195] was also obtained, which indicated two olefinic carbon signals at 130.0 and 130.2 ppm in reasonable agreement with GIAO predictions of 131.1 and 129.8 ppm.[196] Hydrogenation then provided **3.17** as observed by disappearance of the olefinic resonance in the ^{1}H-NMR and identification of the molecular ion in HRMS. Subsequent purification of these final intermediates (**3.78** and **3.75**) by mass-directed HPLC on a C18 reverse phase column, eluting with acetonitrile and water, afforded product of slightly improved purity by analytical HPLC. However, even after extensive drying,[197] the same impurity peaks remained in the ^{1}H-NMR making unequivocal comparison with reported spectral data difficult.[198]

---

[193] Purification with either triethylamine-washed silica gel or basic alumina provided only marginal improvements in purity.

[194] While these resonances seemingly correspond to the chemical shifts expected for the common impurities methanol, acetone, water and grease (Gottlieb, H. E.; Kotlyar, V.; Nudelman, A. *J. Org. Chem.* **1997**, *62*, 7512-7515.) drying, varied sources of solvent and further purification did little to reduce their magnitude.

[195] Due to limited quantities of these final intermediates, it proved impossible to obtain a spectrum with sufficient signal-to-noise ratio to resolve the resonances arising from the carbonyl or the tetra-substituted enone.

[196] Excluding the peaks that could not be observed and selecting the major peaks in the partial spectrum, the average deviation between the calculated and observed spectra was 6.0 ppm with a maximum deviation of 11.9 ppm. This indicates a significant discrepancy due to the impurity.

[197] The samples were dried azeotropically and then under high vacuum for 24 hours.

[198] It is certainly possible that **3.17** is present in the final 0.3 mg sample of the natural product. Four resonances were observed having the correct relative chemical shifts and multiplicities for **3.17**. They do appear shifted by approximately 0.15 ppm downfield from the literature values.[101] **Observed ^{1}H NMR** (500 MHz, $CDCl_3$) δ 1.88 (d, *J* = 1.3 Hz, 3H), 1.42 (s, 3H), 1.38 (s, 3H), 1.19 (d, *J* = 6.2 Hz, 3H). **Literature ^{1}H NMR** (500 MHz, $CDCl_3$) δ 1.71 (d, *J* = 1.5 Hz, 3H), 1.25 (s, 3H), 1.23 (s, 3H), 1.04 (d, *J* = 6.8 Hz, 3H)**.**

SUMMARY

This synthetic route to the skeleton of torilin represents a new application of the cyclobutadiene cycloaddition-cyclopropanation acid-mediated rearrangement methodology developed in the Snapper laboratory.[104] A novel umpolung addition provides access to a useful tricarbonylcyclobutadiene iron complex **3.58** with the carbonyl oxidation state in the tether. This complex undergoes a productive cycloaddition despite its highly functionalized all-carbon tether and relatively unactivated olefin. The oxidation proceeds selectively at the iron center despite the sensitive thioether functionality in this substrate. While oxidative deprotection of the hindered dithiane of cyclobutene **3.57** is in need of further development to enable greater material throughput, the resulting cyclobutene can be converted into the densely functionalized cyclopropane diol **3.67**.

This compound provided a difficult test of the acid-mediated rearrangement in generating extremely sensitive cycloheptadieneone **3.68**. Ultimately, a novel use of TPAP as both oxidant and Lewis acid and careful purification succeeded, providing the ring system of the guaiane natural products in 11 steps with the appropriate stereochemistry in place for the carbon skeleton of torilin. Alkylation of **3.68** completed the carbon skeleton, albeit in low yield. With the limited material available, the final steps were explored, providing a promising route which would represent a formal synthesis of 8-desangeloyloxytorilin in 16 steps from commercially available material. This

does not compare favorably to the 10 steps required by the previous synthesis.[101] The 4 linear steps required to synthesize the known iron aldehyde and 2 steps of unfortunate (and low yielding) protecting group manipulations certainly contribute to this fact. This route does, however, represent a demonstration of the ability of this methodology to generate this ring system with most of the functionality and the correct stereochemical relationships in place for an eventual synthesis of torilin and torilolone.

EXPERIMENTAL

General Information

Proton nuclear magnetic resonance spectra (^{1}H-NMR) were measured on either a Gemini-400 instrument (400 MHz) or a Gemini-500 instrument (500 MHz). Chemical shifts are reported in ppm downfield from tetramethylsilane with the solvent reference as the internal standard ($CHCl_3$: δ 7.26 ppm). Data is reported as follows: chemical shift, multiplicity (s = singlet, d = doublet, t = triplet, q = quartet, br = broad, m = multiplet), coupling constants (Hz), and integration. ^{13}C-NMR spectra were recorded on either a Gemini-400 instrument (100 MHz), or a Gemini-500 instrument (125 MHz) with complete proton decoupling. Chemical shifts are reported in ppm downfield from tetramethylsilane with the solvent as the internal reference ($CDCl_3$: δ 77.23 ppm). Infrared spectra (IR) were reported in wave numbers (cm^{-1}). Bands are characterized as broad (br), strong (s), medium (m), or weak (w). Elemental analyses (ICP) were performed by Robertson Microlit Laboratories, Inc., Madison, NJ and are reported in percent atomic abundance. High resolution mass spectral analyses (HRMS) were performed by the Mass Spectrometry Laboratory, University of Illinois at Urbana-Champaign or at Boston College. Melting points (mp) were reported uncorrected.

Starting materials and reagents were purchased from commercial suppliers and used without further purification except the following: Dichloromethane and diethyl ether were used from a solvent purification

system.[199] Methanol was distilled from magnesium methoxide. Hexanes and Et_2O used in chromatography were distilled before use. Molecular sieves were dried in a 250 °C oven overnight before use. (Cyclobutadienal)iron tricarbonyl[106a] was prepared as reported in the literature and displayed satisfactory spectral data. [Please note potential hazards: Iron carbonyls complexes can be a source of carbon monoxide.] All oxygen- or moisture-sensitive reactions were carried out under N_2 atmosphere in oven-dried (140 °C, > 4 h) or flame-dried glassware. Air- or moisture-sensitive liquids were transferred by syringe and were introduced into the reaction flasks through rubber septa or through a stopcock under N_2 positive pressure. Unless otherwise stated, reactions were stirred with a Teflon covered stir bar. Concentration refers to the removal of solvent using a rotary evaporator followed by use of a vacuum pump at approximately 1 torr. Silica gel column chromatography refers to flash chromatography[200] and was performed using 60 Å (230-400 Mesh ASTM) silica gel. Thin layer chromatography was performed on glass backed 60 Å (250 μm thickness) silica gel plates.

X-ray data were collected using a Bruker SMART APEX CCD (charge coupled device) based diffractometer with Mo (λ=0.71073 Å) radiation equipped with an LT-3 low-temperature apparatus operating at 100 K (**V**) or 193 (**VI**). A stable crystal was chosed and mounted on a glass fiber using grease. Data were measured using omega scans of 0.3° per frame for 30 s, such that a hemisphere

---

[199] Pangborn, A. B.; Giardello, M. A.; Grubbs, R. H.; Rosen, R. K.; Timmers. F. J. *Organometallics* **1996**, *15*, 1518.
[200] Still, W.C.; Kahn, M.; Mitra, A. *J. Org. Chem.* **1978**, *43*, 2923.

was collected. A total of 12737 (**V**) or 6730 (**VI**) frames were collected with a maximum resolution of 0.75 Å. Cell parameters were retrieved using SMART[201] software and refined using SAINT on all observed reflections. The structures are solved by the direct method using the SHELXS-97[202] program and refined by least squares method on F2, SHELXTL-97,[203] incorporated in SHELXTL-PC V 5.10.[204] The crystals used for diffraction studies showed no decomposition during data collection. The drawing was displayed at 50% ellipsoids. The structures were solved by Dr. Bo Li at Boston College.

Experimental Procedure

(E)-2-(but-2-enyl)-1,3-dithiane (3.59)

A 1 L round-bottom three-necked flask was fitted with an addition funnel, gas adapter and septum. The flask was charged with 1,3-dithiane (15.0 g, 125 mmol, 1 equiv.) and purged with nitrogen. The dithiane was dissolved in tetrahydrofuran (625 mL, 0.2 M) and the stirring solution was cooled to 0 °C. *n*-Butyllithium (2.3 M in hexanes, 60 mL, 138 mmol, 1.1 equiv.) was transferred into the addition funnel *via* cannula and then added to the dithiane solution dropwise over 30 minutes. The reaction was allowed to stir at 0 °C for 2 hours before

---

[201] SMART V 5.050 (NT) Software for the CCD Detector System; Bruker Analystical X-ray Systems, Madison, WI (1998).
[202] Sheldrick, G. M. SHELXS-90, Program for the Solution of Crystal Structure, University of Gottingen, Germany, 1990.
[203] Sheldrick, G. M. SHELXS-97, Program for the Refinement of Crystal Structure, University of Gottingen, Germany, 1997.
[204] SHELXTL 5.10 (PC-Version), Program Library for Structure Solution and Molecular Graphics, Bruker Analytical X-ray Systems, Madison, WI (1998).

adding crotyl bromide (technical grade (85% trans), 15.4 mL, 150 mmol, 1.2 equiv.) and allowing to stir for 1 hour. The reaction was quenched by slowy pouring into water (500 mL) at 0 °C. The aqueous layer was extracted with diethyl ether (3X500 mL) and the combined organics washed with brine (500 mL), dried over magnesium sulfate, and concentrated to afford a malodorous orange-brown oil. The oil was fractionally distilled through at 15 cm Vigreux column to afford 16.4 g **3.59** (containing 13% of the Z isomer) as a clear colorless oil (75%).

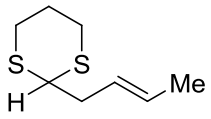

3.59

(**bp** 128-131 °C at 9 torr). **^{1}H NMR** (400 MHz, $CDCl_3$) δ5.72-5.27 (m, 2H), 4.12-3.95 (m, 1H), 3.01-2.70 (m, 4H), 2.61-2.28 (m, 2H), 2.18-1.98 (m, 1H), 1.97-1.69 (m, 1H), 1.69-1.55 (m, 3H). **^{13}C NMR** (101 MHz, $CDCl_3$) δ 128.72, 126.22, 47.76, 38.69, 30.57, 30.54, 25.88, 17.970. **IR** (KBr, thin film) 3026 (m), 2945 (s), 2925 (s), 2896 (s), 2855 (m), 2828 (s), 1687 (m), 1422 (s), 1377 (w), 1276 (m), 1243 (m), 1181 (m), 1037 (m), 965 (s), 908 (m), 755 (s), 702 (m), 541 (m). **DART-HRMS (m/z):** Calc'd for [M+H]+: 175.06152; Found: 175.06186.

(E)-(2-(but-2-enyl)-1,3-dithian-2-yl)-hydroxymethylcyclobutadieneiron tricarbonyl (3.58)

Iron Aldehyde **3.60** (6.45 g, 29.3 mmol, 1 equiv.) and crotyl dithiane **3.59** (7.2 g, 41.3 mmol, 1.4 equiv.) were each added to 500 mL round bottom flasks. The compounds were dissolved in tetrahydrofuran (100 mL and 50 mL respectively) and dried over 3Å mol sieves. A three-necked 500 mL round-

bottom flask fitted with an addition funnel, gas adaptor and septum was purged with nitrogen and charged with the solution of **3.59** *via* cannula (rinsing with 50 mL tetrahydrofuran). N,N,N',N'-tetramethylethylenediamine (6.23 mL, 41.3 mmol, 1.4 equiv) was added and the solution was cooled to -78 °C. *tert*-Butyllithium (1.7 M in pentane, 25 mL. 41.3 mmol, 1.4 equiv) was cannula transferred into the addition funnel and added dropwise to the stirring solution of dithiane over 45 min. The reaction was allowed to stir at -78 °C for an additional 15 minutes and then allowed to warm to 0 °C for 2 hours. The pre-dried aldehyde solution was then cannula transferred into a two-necked 500 mL round bottom flask fitted with a gas adapter and septum and purged with nitrogen. The transfer was completed with an additional 100 mL tetrahydrofuran and the solution cooled to -78 °C. The solution of the dithianyl anion at 0 °C was slowly transferred *via* cannula into the solution of **3.60** at -78 °C (rinsing with 40 mL tetrahyrdofuran). The reaction was allowed to stir at this temperature for 30 min. and then warm to 0 °C for 15 min before quenching by slowly adding 100 mL 1 M aqueous hydrochloric acid at 0 °C. The mixture was then poured into an additional 100 mL 1 M aqueous hydrochloric acid in a 1 L Erlenmyer flask and stirred for 1.5 hours. The layers were separated and the aqueous layer extracted with diethyl ether (3X100 mL). The combined organics were washed with brine (200 mL) and dried over magnesium sulfate. Concentration afforded a deep reddish black oil which was adsorbed onto 25 g silica gel and dry loaded onto a silica gel column for purification. The column was eluted with a step gradient

from hexanes to elute the residual crotyl dithiane, then 2%, 5% and finally 30% *tert*-butyl methyl ether[205] in hexanes. Iron dithiane **3.58** was obtained as a yellow powder (8.75 g, 76%).

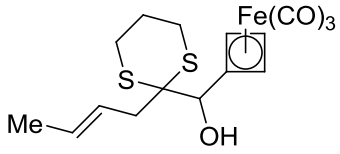

3.58

(**mp** 79-87 °C). **^{1}H NMR** (500 MHz, $CDCl_3$) δ 5.74-5.51 (m, 2H), 4.37 (dd, *J* = 15.5, 1.7 Hz, 1H), 4.30-4.19 (m, 2H), 4.17-4.06 (m, 1H), 3.00-2.85 (m, 2H), 2.78 (dd, *J* = 25.4, 1.7 Hz, 1H), 2.71-2.56 (m, 4H), 2.56-2.45 (m, 1H), 2.13-2.01 (m, 1H), 1.93-1.77 (m, 1H), 1.75-1.71 (m, 3H). **^{13}C NMR** (126 MHz, $CDCl_3$) δ 214.81, 129.84, 125.05, 69.02, 65.34, 64.23, 61.80, 26.36, 25.66, 24.24, 18.209. **IR** (KBr, thin film) 3435 (br), 2958 (w), 2897 (w), 2043 (s), 1965 (s), 1436 (w), 1421 (w), 1073 (w), 964 (w), 613 (m), 590 (m). **DART-HRMS (m/z):** Calc'd for [M+H]+: 395.00742; Found: 395.00576.

5-methyl-spiro[1,3-dithiane-2-8']-tricyclo[4.3.0.0^{1,4}]non-2-en-9-ol (3.57)

Iron complex **3.58** (8.75 g, 22.2 mmol, 1 equiv.) was dissolved in 11.1 L (2mM) of wet acetone in a 5 gallon (approximately 20 L) high-density polyethylene bucket). The bucket was equipped with a mechanical stirrer through a hole in

[205] Dry loading is important to prevent co-elution of **3.58** and residual crotyl dithiane. The use of *tert*-butyl methyl ether for this chromatography prevents cracking of the column during gradient elution. If **3.58** is contaminated with crotyl dithiane, it can be purified by recrystallization from hexanes, which also provided crystals sutiable for x-ray diffraction.

the lid and the solution was stirred vigorously at ambient temperature. Ceric ammonium nitrate (36.5 g, 66.6 mmol, 3 equiv.) was added in one portion. The reaction was judged complete by TLC after 10 minutes and quenched with 150 mL saturated aqueous sodium bicarbonate. Stirring was continued for 20 minutes to allow precipitation of cerium salts and the suspension allowed to settle for 1 hour. Preliminary drying was accomplished by addition of 300 g of sodium sulfate. The solution was filtered in batches using a large Büchner funnel and concentrated. The resulting orange-brown cloudy oil was dissolved in 1 L dichloromethane and dried with magnesium sulfate, filtered and concentrated to afford a red-brown oil which was purified by flash chromatography on silica gel eluted with 30% diethyl ether in hexanes to afford 4.10 g (73%) of cyclobutene **3.57** as a yellow oil.

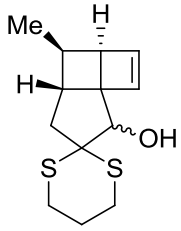

3.57

^{1}H NMR (500 MHz, $CDCl_3$) (2:1 α:β diastereomeric mixture) δ 6.47 (dd, *J* = 2.5, 1.5 Hz, 0.5H), 6.32 (dd, *J* = 2.5, 1.3 Hz, 1H), 6.27 (d, *J* = 2.5 Hz, 0.5H), 6.25 (d, *J* = 2.5 Hz, 1H), 4.35 (d, *J* = 3.6 Hz, 1H), 4.11 (s, 0.5H), 3.37 (d, *J* = 7.5 Hz, 1H), 3.32 (dd, *J* = 7.9, 1.1 Hz, 0.5H), 3.10 – 2.86 (m, 3H), 2.77 – 2.59 (m, 3H), 2.39 (d, *J* = 3.9 Hz, 1H), 2.33 – 2.24 (m, 1H), 2.22 – 1.99 (m, 5H), 1.99 – 1.80 (m, 3H), 0.98 – 0.91 (m, 5H). **^{13}C NMR** (126 MHz, $CDCl_3$) δ 141.53, 140.37, 137.99, 137.93, 77.72, 75.12, 61.61, 60.69, 44.95, 44.68, 44.55, 43.86, 43.75, 34.92, 34.78, 28.81, 28.01, 27.85, 27.33, 25.13, 24.45, 22.84, 17.72, 17.44. **IR** (KBr, thin film) 3446 (br), 3040 (s), 2954 (m), 2924 (w), 1438 (w), 1423 (w), 1371 (w), 1301 (w), 1277

(w), 1234 (w), 1220 (w), 1100 (w), 1071 (w). **DART-HRMS (m/z):** Calc'd for $[M+H-H_2O]+$: 237.07717; Found: 237.07806.

5β-methyl-4α,6β-spiro[1,3-dithiane-2-8']-tricyclo[4.3.0.0^{1,4}]non-2-en-9α-ol (3.57α)

The diastereomeric mixture of cyclobutenes **3.57** (482 mg, 1.89 mmol, 1 equiv.) was dissolved in dichloromethane (38 mL, 0.05 M) in a 100 mL round bottom flask. 2,6-Di-*tert*-butyl-4-methylpyridine (583 mg, 2.84 mmol, 1.5 equiv.) was added to the solution followed by Dess-Martin periodinane (1.20 g, 2.84 mmol, 1.5 equiv.) and the reaction was allowed to stir under a nitrogen atmosphere at ambient temperature for 1 hr until TLC analysis indicated consumption of **3.57**. The reaction was quenched with 30 mL of a 1:1 mixture of saturated aqueous sodium bicarbonate and saturated aqueous sodium thiosulfate. The aqueous layer was extracted with dichloromethane (3X20 mL), combined organics dried over magnesium sulfate, filtered and concentrated to afford a pale yellow oil with some precipitated white solids. This crude residue was dissolved in a 1:1 mixture of tetrahydrofuran and methanol (38 mL, 0.05 M) and cooled to 0 °C under a nitrogen atmoshphere. Sodium borohydride was then added slowly to the stirring solution which became bright yellow with gas evolution. After 15 minutes of stirring, the color had discharged and the reaction was allowed to warm to ambient temperature and stir for an additional 30 minutes. TLC analysis indicated complete consumption of the ketone intermediate so the reaction was again cooled to 0 °C and slowly quenched with 50 mL water. The aqueous layer was extracted with diethyl ether (3X25 mL) and

the combined organics dried over magnesium sulfate, filtered and concentrated to afford a clear, colorless oil which was purified by flash chromatography on silica gel eluted with 30% diethyl ether in hexanes to afford 482 mg **3.57**α (72%) as a clear, colorless oil.

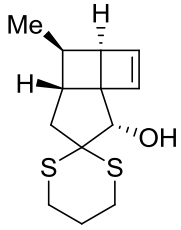

3.64α

^{1}H NMR (500 MHz, $CDCl_3$) δ 6.41–6.31 (m, 1H), 6.27 (d, *J* = 2.4 Hz, 1H), 4.37 (d, *J* = 3.9 Hz, 1H), 3.38 (d, *J* = 7.9 Hz, 1H), 3.02 (tdd, *J* = 14.2, 11.3, 2.7 Hz, 2H), 2.78–2.64 (m, 2H), 2.40 (d, *J* = 3.9 Hz, 1H), 2.29 (dd, *J* = 13.8, 8.4 Hz, 1H), 2.22–2.15 (m, 1H), 2.14–2.04 (m, 2H), 2.00–1.86 (m, 2H), 0.97 (d, *J* = 7.2 Hz, 3H). **^{13}C NMR** (126 MHz, $CDCl_3$) δ 147.55, 138.01, 77.71, 61.63, 60.70, 44.56, 43.88, 43.75, 34.94, 27.87, 27.34, 25.14, 17.45. **IR** (KBr, thin film) 3437 (br), 3059 (m), 3028 (m), 2949 (m), 2927 (s), 2920 (s), 1434 (w), 1422 (w), 1302 (w), 1277 (w), 1233 (w), 1134 (w), 1100 (w), 1069 (w), 765 (w). **DART-HRMS (m/z):** Calc'd for $[M+H-H_2O]+$: 237.07717; Found: 237.07774.

9-acetyloxy-5β-methyl-4α,6β-spiro[1,3-dithiane-2-8']-tricyclo[4.3.0.0^{1,4}]non-2-ene (α/β-3.66)

A 250 mL 3-necked flask was fitted with a gas adapter, reflux condenser, and septum and charged with dry sodium hydride (740 mg, 30.8 mmol, 2 equiv.) which was suspended in 50 mL tetrahydrofuran under a nitrogen atmosphere. Diastereomeric mixture of cyclobutenes **3.57** (3.93 g, 15.4 mmol, 1 equiv.) was dissolved in 50 mL dry THF in a 100 mL round bottom flask and dried with 3Å

molecular sieves (4 g, 100 wt%). The sodium hydride suspension was cooled to 0 °C and this solution of **3.57** was added slowly *via* syringe (slow hydrogen gas evolution). The suspension was allowed to warm to ambient temperature and developed a yellow color. It was then heated to reflux for 1 hour with vigorous gas evolution and a darkening of the color to brown. The reaction was cooled to ambient temperature before addition of acetic anhydride (3.2 mL, 33.9 mmol, 2.2 equiv.). A chunky white precipitate formed with slow gas evolution and the suspension was heated to reflux for 1 hour. The suspension was then cooled to 0 °C and carefully quenched by addition of saturated aqueous sodium bicarbonate. The resulting emulsion of fine white salts was extracted with diethyl ether (3X50 mL) and the combined organics were dried over magnesium sulfate, filtered and concentrated to afford a brown oil which was purified by flash chromatography on a triethylamine-washed silica gel plug eluting with 30% diethyl ether in hexanes to afford 4.02g (88%) of **3.66** as a clear, colorless oil (inseperable 2:1 mixture of α:β acetate diasteromers).

9α-acetyloxy-5β-methyl-4α,6β-spiro[1,3-dithiane-2-8']-tricyclo[4.3.0.0^{1,4}]non-2-ene (α-3.66)

Cyclobutene α-diastereomer **3.64** was acylated as above to afford α-**3.66** as a clear, colorless oil.

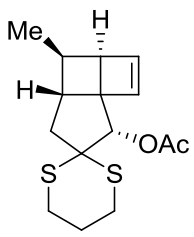

α-**3.66**

^{1}H NMR (500 MHz, $CDCl_3$) δ 6.34 (dd, *J* = 2.5, 1.2 Hz, 1H), 6.18 (dd, *J* = 2.5, 0.5 Hz, 1H), 5.55 (d, *J* = 1.2 Hz, 1H), 3.19 (dd, *J* =

7.9, 0.8 Hz, 1H), 2.99 (dtd, *J* = 14.1, 11.4, 2.7 Hz, 2H), 2.73 – 2.62 (m, 1H), 2.57 (dddd, *J* = 14.1, 5.1, 3.1, 1.1 Hz, 1H), 2.35 (ddd, *J* = 12.5, 7.2, 1.1 Hz, 1H), 2.15 – 2.11 (m, 1H), 2.10 (s, 3H), 2.10 – 1.94 (m, 3H), 1.85 (d, *J* = 13.9 Hz, 1H), 0.97 (d, *J* = 7.2 Hz, 3H). **^{13}C NMR** (126 MHz, $CDCl_3$) δ 170.56, 142.04, 137.04, 60.07, 59.38, 45.10, 44.59, 43.88, 35.21, 28.58, 27.18, 25.30, 25.25, 21.36, 17.22. **IR** (KBr, thin film) 2954 (m), 2932 (m), 2906 (m), 1740 (s), 1436 (w), 1425 (w), 1370 (m), 1278 (w), 1233 (s), 1033 (m), 748 (w). **DART-HRMS (m/z):** Calc'd for [M+H]+: 297.09830; Found: 297.09733.

9β-acetyloxy-5β-methyl-4α,6β-spiro[1,3-dithiane-2-8']-tricyclo[4.3.0.0^{1,4}]non-2-ene (β-3.66)

β-**3.66** was recovered from mercuric chloride deprotection/acylation of diastereomeric mixture **3.57** and formed crystals suitable for x-ray diffraction upon concentration from 30% diethyl ether in hexanes.

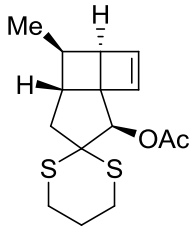

β-**3.66**

(**mp** 106-107 °C). **^{1}H NMR** (300 MHz, $CDCl_3$) δ 6.36–6.19 (m, 2H), 5.49 (s, 1H), 3.43 (dd, *J* = 8.2, 0.9 Hz, 1H), 3.20–2.93 (m, 2H), 2.73–2.47 (m, 2H), 2.43–2.33 (m, 1H), 2.15-2.11 (m, 4H), 2.10–1.98 (m, 3H), 1.93–1.79 (m, 1H), 0.96 (d, *J* = 7.2 Hz, 3H). **^{13}C NMR** (101 MHz, $CDCl_3$) δ 170.46, 139.15, 138.06, 78.33, 60.72, 59.63, 49.05, 45.59, 44.60, 34.37, 29.65, 27.93, 24.76, 21.40, 17.71. **IR** (KBr, thin film) 2952 (m), 2939 (m), 2919 (m), 1737 (s), 1434 (w), 1427 (w), 1369

(m), 1279 (w), 1234 (s), 1065 (w), 1022 (m), 961 (w). **DART-HRMS (m/z):** Calc'd for [M+H]+: 297.09830; Found: 297.09741.

9α-acetyloxy-5β-methyl-4α,6β-spiro[1,3-dioxolane-2-8']-tricyclo[4.3.0.0^{1,4}]non-2-ene (3.64)

A 250 mL 2-neck flask was fitted with a reflux condenser and a septum. The flask was charged with **3.66** (1.95 g, 6.58 mmol, 1 equiv.) and 3Å molecular sieves (5.85 g, 300 wt%). The compound was dissolved in a 4:1 mixture of acetonitrile (132 mL) and ethylene glycol (33 mL). Selectfluor (5.83 g, 16.4 mmol, 2.5 equiv.) was added in one portion and the solution was heated to 40 °C under a nitrogen atmosphere and allowed to stir at that temperature for 5 hours. The reaction was then allowed to cool to ambient temperature filtered into a 500 mL Erlenmeyer flask containing 100 mL saturated aqueous sodium bicarbonate. The aqueous layer was extracted with dichloromethane (3X50 mL), combined organics were washed with brine (50 mL), dried over magnesium sulfate, filtered and concentrated to afford a light orange oil. The crude oil was purified by flash chromatography on triethylamine-washed silica gel eluting with a gradient from 10% diethyl ether in hexanes to 30% diethyl ether in hexanes to afford 284 mg (17%) of a clear, colorless oil which solidified to a white solid upon standing.

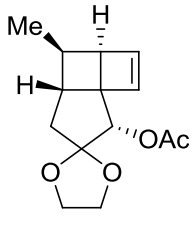

3.64

(**mp** 55-57 °C). **^{1}H NMR** (500 MHz, $CDCl_3$) δ 6.22 (dd, *J* = 2.5, 1.4 Hz, 1H), 6.19 – 6.13 (m, 1H), 5.23 (s, 1H), 4.06 (dt, *J* = 7.3,

6.4 Hz, 1H), 3.99 (td, *J* = 6.9, 5.8 Hz, 1H), 3.95 – 3.87 (m, 2H), 3.32 (d, *J* = 8.0 Hz, 1H), 2.31 – 2.21 (m, 1H), 2.22 – 2.11 (m, 1H), 2.05 (s, 3H), 1.93 – 1.82 (m, 2H), 0.93 (d, *J* = 7.2 Hz, 3H). **^{13}C NMR** (126 MHz, $CDCl_3$) δ 170.82, 140.15, 137.40, 115.14, 76.43, 66.09, 65.12, 55.85, 44.53, 39.85, 38.86, 33.37, 21.27, 17.49. **IR** (KBr, thin film) 3043 (w), 2955 (m), 2893 (w), 1746 (s), 1558 (w), 1541 (w), 1507 (w), 1436 (w), 1436 (w), 1373 (m), 1314 (m), 1238 (s), 1136 (w), 1107 (w), 1088 (m), 1039 (m), 984 (w), 952 (w), 728 (w). **DART-HRMS (m/z):** Calc'd for [M+H]+: 251.12833; Found: 251.12807.

10α-acetyloxy-6β-methyl-2β,4β,5α,7β-spiro[1,3-dioxolane-2-9']tetracyclo[5.3.0.0^{1,5}.0^{2,4}]decane-3β-carboxylic acid ethyl ester (3.65)

A 50 mL round bottom flask was fitted with a Claisen adapter, reflux condenser and septum. The flask was charged with **3.64** (367 mg, 1.46 mmol, 1 equiv.) which was dissolved in dichloromethane (14.6 mL, 0.1 M). Copper (II) acetylacetonate was added and the solution was allowed to stir and heated to reflux under a nitrogen atmosphere. Ethyldiazoacetate (1.54 mL, 14.6 mmol, 10 equiv.) was added to the refluxing solution *via* syringe pump through the Claisen adapter at a rate of 0.5 equiv. per hour. TLC analysis indicated complete consumption of **3.64** so the reaction was allowed to cool to room temperature and quenched by addition of 10 mL saturated aqueous ammonium chloride. The aqueous layer was extracted with dichloromethane (3X10 mL). Combined organics were then washed with brine (20 mL), dried over magnesium sulfate, filtered and concentrated to afford a bright yellow oil. The crude oil was purified

by MPLC using a triethylamine-washed Biotage 40M column and eluted with a gradient from 25% diethyl ether in hexanes to 40% diethyl ether in hexanes to afford 405 mg (82%) of **3.65** as a clear, colorless oil.

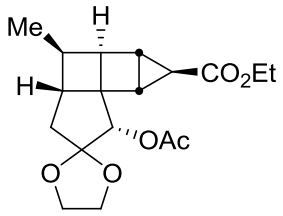

3.65

^{1}H NMR (500 MHz, $CDCl_3$) δ 4.94 (d, *J* = 0.7 Hz, 1H), 4.13-4.05 (m, 2H), 3.96 – 3.89 (m, 2H), 3.89 – 3.84 (m, 2H), 2.59 (dd, *J* = 7.4, 2.6 Hz, 1H), 2.52 – 2.44 (m, 1H), 2.17 – 2.12 (m, 4H), 2.10 (s, 3H), 1.82 – 1.76 (m, 1H), 1.70 (dt, *J* = 6.4, 0.8 Hz, 1H), 1.23 (t, *J* = 7.1 Hz, 3H), 1.20 (d, *J* = 7.2 Hz, 3H). **^{13}C NMR** (126 MHz, $CDCl_3$) δ 172.81, 170.38, 115.33, 76.46, 65.90, 65.01, 60.56, 50.11, 41.81, 41.19, 39.66, 35.67, 29.92, 24.89, 22.54, 21.38, 17.17, 14.52. **IR** (KBr, thin film) 3114 (m), 3094 (m), 3074 (m), 3050 (m), 2956 (m), 2917 (w), 2890 (w), 2871 (w), 1728 (s), 1403 (w), 1382 (m), 1238 (s), 1173 (m), 1131 (m), 1092 (m), 1039 (m), 773 (w), 731 (m), 686 (m), 607 (m), 514 (m). **DART-HRMS (m/z):** Calc'd for [M+H]+: 337.16511; Found: 337.16507.

10α-hydroxy-3β-(1-hydroxy-1-methylethyl)-6β-methyl-2β,4β,5α,7β-spiro[1,3-dioxolane-2-9']tetracyclo[5.3.0.0^{1,5}.0^{2,4}]decane (3.67)

A 50 mL round bottom flask was charged with **3.65** (50 mg, 0.149 mmol, 1 equiv.), N,N,N',N'-tetramethylethylenediamine (225 μL, 1.49 mmol, 10 equiv.) and tetrahydrofuran (3 mL, 0.05 M). The stirring solution was cooled to 0 °C under a nitrogen atmosphere. A solution of methyllithium (1.6 M in diethyl ether) was then added dropwise to the solution causing a bright orange-yellow color to develop. Stirring was continued at 0 °C for 1 hour, at which point, TLC analysis

indicated consumption of **3.65** and production of **3.67** without formation of byproduct **3.65b**. The reaction was quenched by dilution with wet diethyl ether (3 mL) and dropwise addition of saturated aqueous ammonium chloride (3 mL). The aqueous layer was extracted with diethyl ether (3X5 mL), combined organics were dried over magnesium sulfate, filtered and concentrated to afford a clear, colorless oil. The crude oil was purified by MPLC on a triethylamine-washed Biotage 25M column to afford 31.5 mg (75%) **3.67** as a white solid. Recrystallization by slow evaporation from benzene/methanol afforded crystals of the monohydrate suitable for x-ray diffraction.

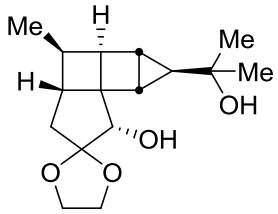

3.67

(**mp** 88-92 °C, monohydrate). **^{1}H NMR** (500 MHz, $CDCl_3$) δ 4.09 – 4.03 (m, 1H), 3.98 – 3.89 (m, 3H), 3.72 (s, 1H), 2.50 (dd, *J* = 7.3, 2.6 Hz, 1H), 2.42 (td, *J* = 7.2, 5.1 Hz, 1H), 2.05 – 1.89 (m, 4H), 1.69 (d, *J* = 13.5 Hz, 1H), 1.65 (d, *J* = 4.2 Hz, 1H), 1.62 (ddd, *J* = 4.1, 2.7, 1.1 Hz, 1H), 1.48 (s, 1H), 1.23 (s, 3H), 1.17 – 1.12 (m, 6H). **^{13}C NMR** (126 MHz, $CDCl_3$) δ 116.27, 77.96, 70.12, 65.61, 65.23, 50.76, 41.52, 39.66, 38.29, 35.32, 33.15, 29.69, 28.37, 23.57, 17.23, 15.28. **IR** (KBr, thin film) 3385 (br), 3068 (m), 3035 (m), 2966 (s), 2925 (m), 2869 (m), 1647 (w), 1382 (m), 1371 (m), 1311 (w), 1300 (w), 1257 (w), 1210 (m), 1143 (m), 1127 (m), 1061 (w), 1041 (m), 1022 (w), 990 (w), 950 (w), 918 (w), 782 (w). **DART-HRMS (m/z):** Calc'd for $[M+H-H_2O]^+$: 263.16472; Found: 263.16494.

10α-hydroxy-6β-methyl-2β,4β,5α,7β-spiro[1,3-dioxolane-2-9']tetracyclo[5.3.0.0^{1,5}.0^{2,4}]decane-3β-carboxylic acid ethyl ester (3.65b)

Cyclopropane **3.65b** is isolated in varying amounts up to 40% from the previous alkylation reaction if the diamine additive is omitted, methyl grignard is substituted, or the reaction is allowed to proceed to incomplete conversion and can be resubmitted to the reaction conditions to afford **3.67**.

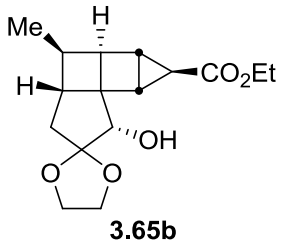

3.65b

(**mp** 113-114 °C). **^{1}H NMR** (500 MHz, $CDCl_3$) δ 4.12 (qd, *J* = 7.1, 1.0 Hz, 3H), 4.09 – 4.04 (m, 1H), 3.98 – 3.92 (m, 3H), 3.80 (d, *J* = 10.0 Hz, 1H), 2.55 (dd, *J* = 7.4, 2.8 Hz, 1H), 2.45 (pd, *J* = 7.2, 5.3 Hz, 1H), 2.17 – 2.14 (m, 1H), 2.14 – 2.10 (m, 1H), 2.10 – 2.07 (m, 1H), 1.98 (ddd, *J* = 14.0, 9.1, 1.1 Hz, 1H), 1.74 (dd, *J* = 14.1, 0.8 Hz, 1H), 1.70 (d, *J* = 10.0 Hz, 1H), 1.30 – 1.23 (m, 3H), 1.19 (d, *J* = 7.2 Hz, 3H). **^{13}C NMR** (126 MHz, $CDCl_3$) δ 173.35, 115.98, 76.91, 65.56, 65.27, 60.46, 51.45, 40.69, 40.00, 38.07, 34.66, 29.85, 24.15, 22.61, 17.18, 14.50. **IR** (KBr, thin film) 3449 (br), 3411 (br), 3069 (m), 3040 (s), 2968 (m), 2955 (m), 2923 (m), 1727 (m), 1257 (s), 1227 (w), 1151 (m), 1123 (w), 1094 (w), 1073 (w), 1049 (m), 1026 (m), 997 (w), 679 (m), 645 (w), 625 (w). **DART-HRMS (m/z):** Calc'd for [M+H]+: 295.15455; Found: 295.15338.

10β-cyanomethyl-10α-hydroxy-3β-(1-hydroxy-1-methylethyl)-6β-methyl-2β,4β,5α,7β-spiro[1,3-dioxolane-2-9']tetracyclo[5.3.0.0^{1,5}.0^{2,4}]decane (3.67b)

A 4-dram vial fitted with a septum was charged with **3.67** (4.8 mg, 0.0171 mmol, 1 equiv.) and powdered 4Å molecular sieves (10 mg, 200 wt%) and dissolved in acetonitrile (340 μL, 0.02M) under a nitrogen atmosphere. Tetra-*n*-propylammonium perruthenate (6 mg, 0.0171 mmol, 1 equiv.) was added to the stirring solution at ambient temperature and the stirring continued for 2.5 hours. TLC analysis indicated complete consumption of **3.67**. The reaction mixture was filtered through Celite and then purified by flash chromatography on pyridine-washed silica gel eluting with hexanes and then ethyl acetate. The ethyl acetate fractions were concentrated to afford 4.1 mg **3.67b** (85%) as a clear, colorless oil.

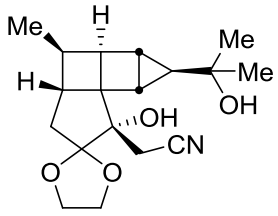

3.67b

^{1}H NMR (400 MHz, $CDCl_3$) δ 4.16 – 4.08 (m, 1H), 4.02 – 3.93 (m, 3H), 2.65 (d, *J* = 16.6 Hz, 1H), 2.56 – 2.44 (m, 2H), 2.40 (dd, *J* = 13.3, 0.9 Hz, 1H), 2.14 – 2.02 (m, 2H), 1.82 (s, 1H), 1.78 – 1.69 (m, 3H), 1.62 (t, *J* = 1.2 Hz, 1H), 1.58 (s, 1H), 1.29 (s, 3H), 1.20 – 1.14 (m, 6H). **^{13}C NMR** (101 MHz, $CDCl_3$) δ 118.34, 116.82, 78.58, 69.95, 65.99, 65.71, 53.05, 41.26, 40.42, 38.42, 34.98, 33.12, 29.85, 28.21, 21.87, 21.27, 17.02, 15.65. **IR** (KBr, thin film) 3502 (br), 3431 (br), 3058 (w), 3035 (s), 2961 (s), 2939 (s), 2923 (m), 2696 (m), 2867 (w), 2251 (w), 1410 (w), 1368 (m), 1313 (m), 1207 (m), 1149 (s), 1122 (m), 1087 (w), 1065 (m), 1035 (m), 951 (m), 916 (m), 779 (w), 765 (w), 731 (m), 702 (w),

678 (w), 568 (w), 533 (m). **DART-HRMS (m/z):** Calc'd for $[M+NH_4]+$: 337.21396; Found: 337.21273.

1,5α,8α,8aβ-tetrahydro-α,α,8β-trimethyl-3-oxo-spiro-[1,3-dioxolane-2-2']-5-azulenemethanol (3.68)

A 4-dram vial fitted with a septum was charged with **3.67** (11 mg, 0.0392 mmol, 1 equiv.) and powdered 4Å molecular sieves under a nitrogen atmosphere. The substrate was dissolved in dichloromethane (800 μL, 0.05 M) and the solution cooled to -15 °C. Tetra-*n*-propylammonium perruthenate (13.8 mg, 0.0392 mmol, 1 equiv.) was added at this temperature and the reaction allowed to stir under a nitrogen atmosphere for 4 hours until TLC analysis indicated complete consumption of **3.67**. The vial was then transferred to a 4 °C cold room for purification. The reaction mixture was filtered through a pyridine-washed silica gel plug with hexanes and then ethyl acetate at 4 °C. The ethyl acetate fractions were concentrated to afford 6.3 mg **3.68** (58%) (with traces of the conjugated isomer by ^{1}H-NMR) as a clear, colorless oil.

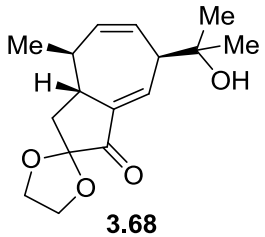

3.68

^{1}H NMR (400 MHz, $CDCl_3$) δ 7.09 (dd, *J* = 4.9, 3.2 Hz, 1H), 5.90 (ddd, *J* = 12.2, 7.5, 2.0 Hz, 1H), 5.60 (ddd, *J* = 12.1, 4.0, 1.3 Hz, 1H), 4.44 – 4.34 (m, 1H), 4.19 – 4.00 (m, 3H), 3.40 – 3.25 (m, 2H), 2.59 (dd, *J* = 11.6, 6.2 Hz, 1H), 2.16 (dt, *J* = 14.2, 5.7 Hz, 1H), 1.92 (dd, *J* = 14.2, 9.5 Hz, 1H), 1.58 (t, *J* = 25.8 Hz, 4H), 1.36 – 1.21 (m, 6H), 0.97 (dd, *J* = 14.9, 7.2 Hz, 3H). **^{13}C NMR** (126 MHz, $CDCl_3$) δ 201.70, 139.60, 137.11, 136.67, 126.48, 108.11, 73.54,

66.21, 65.07, 52.50, 38.78, 35.30, 34.02, 28.38, 27.86, 15.79. **IR** (KBr, thin film) 3502 (br), 3413 (br), 3349 (br), 3041 (s), 2973 (m), 2943 (m), 2920 (w), 2895 (w), 1723 (m), 1640 (s), 1502 (w), 1187 (w), 1083 (m), 1035 (w), 1010 (w), 549 (m), 528 (m). **DART-HRMS (m/z):** Calc'd for $[M+H-H_2O]+$: 261.14907; Found: 261.14978.

1,8α,8aβ-trihydro-α,α,8β-trimethyl-3,7-dioxo-spiro-[1,3-dioxolane-2-2']-5-azulenemethanol (3.77)

A 4-dram vial fitted with a septum was charged with 3.67 (4.3 mg, 0.0153 mmol, 1 equiv.), N-methylmorpholine-N-oxide (3.6 mg, 0.306 mmol, 2 equiv.) and powdered 4Å molecular sieves (1 mg, 25 wt%). The substrate was dissolved in dichloromethane (800 μL, 0.07 M) and tetra-n-propylammonium perruthenate (0.5 mg, 1.53 μmol, 0.1 equiv.) was added at ambient temperature. The solution was allowed to stir at room temperature for 8 hours until TLC analysis indicated complete consumption of 3.67. The reaction mixture was filtered through a pyridine-washed silica gel plug with ethyl acetate to afford 2.7 mg 3.77 (60%) as a yellow oil.

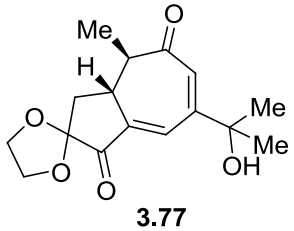

3.77

^{1}H NMR (400 MHz, $CDCl_3$) δ 7.17 (dd, *J* = 2.9, 1.6 Hz, 1H), 6.63 (s, 1H), 4.41 – 4.37 (m, 1H), 4.13 – 4.07 (m, 3H), 2.90 (ddd, *J* = 13.8, 9.8, 5.5 Hz, 1H), 2.67 (dq, *J* = 13.4, 6.7 Hz, 1H), 2.37 (dd, *J* = 13.9, 8.1 Hz, 1H), 2.00 (dd, *J* = 13.9, 10.0 Hz, 1H), 1.51 (s, 3H), 1.46 (s, 3H), 1.20 (d, *J* = 6.7 Hz, 3H).

^{13}C NMR (101 MHz, $CDCl_3$) δ 201.29, 200.87, 153.07, 142.41, 130.12, 129.25, 107.42, 73.49, 66.39, 65.29, 48.16, 36.54, 35.19, 29.75, 29.52, 12.87. **IR** (KBr, thin film) 3426.9 (br), 3060.5 (m), 3022.9 (s), 2974.7 (w), 2919.7 (s), 2904.3 (w), 1727.0 (m), 1640.2 (m), 1383.7 (w), 1188.9 (w), 1160.0 (w), 1135.9 (m), 1086.7 (s), 1049.1 (m), 1029.8 (m), 1013.4 (m), 981.6 (m), 957.5 (m), 764.6 (w), 703.9 (m), 508.9 (w), 560.2 (w), 466.7 (w), 446.4 (w). **DART-HRMS (m/z):** Calc'd for [M+H]+: 293.13890; Found: 293.13988.

3β-hydroxy-1,5α,8α,8aβ-tetrahydro-α,α,3β,8β-tetramethyl-3-oxo-spiro-[1,3-dioxolane-2-2']-5-azulenemethanol (3.74)

A 2-dram vial fitted with a septum was charged with **3.68** (3.9 mg, 0.0140 mmol, 1 equiv) and the substrate dissolved in tetrahydrofuran (280 μL, 0.05 M) under a nitrogen atmosphere. A 4-dram vial fitted with a septum was charged with a solution of methylmagnesium bromide (3.0 M in diethyl ether, 47 μL, 0.140 mmol, 10 equiv.) under a nitrogen atmosphere and the solution cooled to -78 °C. The solution of **3.68** was added dropwise to the stirring solution of methylmagnesium bromide at -78 °C. Once addition was complete, the substrate vial was washed with tetrahydrofuran (2X100 μL) and the solution allowed to stir for 1 hour. The solution was then removed from the cryogenic bath, immediately quenched by dropwise addition of saturated aqueous ammonium chloride (1 mL) and diluted with diethyl ether (1 mL). The aqueous layer was extracted with diethyl ether (3X1 mL) and combined organics were dried over sodium sulfate,

filtered and concentrated to afford 3.7 mg crude oil. The oil was purified by flash chromatography on pyridine-washed silica gel eluting with a gradient from 2.5% methanol in dichloromethane to 5% methanol in dichloromethane to afford 1.3 mg **3.74** (32%) with small inseperable impurities apparent in the ^{1}H-NMR.

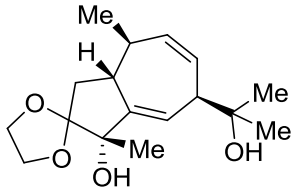

3.74

^{1}H NMR (500 MHz, $CDCl_3$) δ 5.96 (ddd, *J* = 14.1, 5.8, 3.5 Hz, 1H), 5.80 (ddd, *J* = 14.9, 9.1, 2.6 Hz, 1H), 5.60 (ddd, *J* = 14.7, 4.9, 1.0 Hz, 1H), 4.06 – 3.94 (m, 4H), 3.49 (q, *J* = 8.8 Hz, 1H), 3.22 – 2.99 (m, 2H), 2.50 (ddd, *J* = 9.3, 6.0, 1.7 Hz, 1H), 2.41 – 2.30 (m, 1H), 2.29 – 2.15 (m, 1H), 1.95 (dd, *J* = 17.0, 12.1 Hz, 1H), 1.89 – 1.79 (m, 1H), 1.49 – 1.40 (m, 2H), 1.32 – 1.27 (m, 6H), 1.03 (d, *J* = 8.8 Hz, 3H). **^{13}C NMR** (126 MHz, $CDCl_3$) δ 147.09, 136.44, 127.90, 122.28, 115.51, 80.30, 73.74, 69.98, 65.66, 55.04, 51.47, 40.27, 35.57, 29.59, 27.57, 21.80, 16.73. **IR** (KBr, thin film) 3444 (br), 3060 (m), 3026 (s), 2928 (s), 2921 (s), 2910 (m), 1637 (w), 1602 (w), 1492 (w), 1450 (w), 759 (s), 751 (s), 541 (m). **DART-HRMS (m/z):** Calc'd for $[M+NH_4]^+$: 312.21748; Found: 312.21852.

1,4,5α,8α,8aβ-pentahydro-α,α,3,8β-tetramethyl-2-oxo-5-azulenemethanol (3.75)

A 2-dram vial was charged with **3.74** (2.6 mg, 8.83 μmol, 1 equiv.) which was dissolved in dichloromethane (180 μL, 0.05 M). Montmorillonite K10 clay (44 mg, 5000 mg/mmol) was added and the vial capped. The suspension was agetated on a plate shaker for 6 hours at ambient temperature. The reaction mixture was then filtered through Celite with dichloromethane (1 mL) and the

filter cake washed with ethyl acetate (2X1 mL). Concentration of the filtrate afforded 1.1 mg (50% recovery) crude α-hydroxy ketone **3.79** which was used without purification in the next reaction.

The crude **3.79** (1.1 mg, 4.39 μmol, 1 equiv.) was dissolved in tetrahydrofuran (88 μL, 0.05 M). A 2-dram vial was fitted with a septum and charged with a solution of samarium iodide (0.1 M in tetrahydrofuran, 439 μL, 0.0439 mmol, 10 equiv.) and methanol (6 μL, 0.220 mmol, 50 equiv.) under a nitrogen atmosphere. The samarium iodide solution was cooled to -78 °C and substrate solution **3.79** was added dropwise *via* syringe. The substrate vial was rinsed with tetrahydrofuran (2X50 μL) to complete the transfer. The reaction was allowed to warm to ambient temperature and stirred for 30 minutes. The solution was diluted with diethyl ether (1 mL) and quenched with saturated aqueous ammonium chloride (1 mL). The aqueous layer was extracted with diethyl ether (3X1 mL). Combined organics were dried over sodium sulfate, filtered and concentrated to afford 1.8 mg of crude, clear, colorless oil. The oil was purified by flash chromatography on triethylamine-washed silica gel eluting with ethyl acetate to afford 1 mg **3.75** with significant remaining impurities. Mass-directed reverse-phase HPLC purification on a C18 column eluting with 5% to 95% acetonitrile in water afforded a slight improvement in purity and recovery of 0.3 mg **3.75** (23%).

^{1}H NMR (500 MHz, $CDCl_3$) (impure) δ 5.34 (dq, *J* = 8.9, 5.1 Hz, 2H), 2.35 (t, *J* = 7.5 Hz, 1H), 2.22 (t, *J* = 7.7 Hz, 1H), 2.01 (dd, *J* = 11.8, 6.4 Hz, 3H), 1.71 (d, *J* =

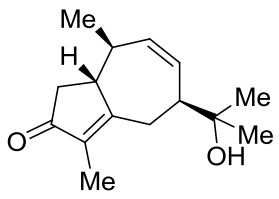

3.75

1.9 Hz, 1H), 1.68 – 1.60 (m, 4H), 1.35 – 1.29 (m, 6H), 1.06 (d, *J* = 8.4 Hz, 3H). **^{13}C NMR** (126 MHz, $CDCl_3$) (partial) δ 130.23, 129.95, 79.30, 36.13, 32.15, 31.18, 29.55, 27.44, 27.39, 25.74, 22.92, 14.33. **IR** (KBr, thin film) 3401 (br), 3034.46 (s), 2956 (s), 2929 (m), 2918 (m), 2885 (m), 2868 (m), 1727 (m), 1464 (m), 1381 (m), 1260 (m), 1091 (br), 754 (m), 737 (m), 549 (m), 527 (m). **DART-HRMS (m/z):** Calc'd for [M+H]+: 235.16980; Found: 235.17098.

1,4,5α,6,7,8α,8aβ-heptahydro-α,α,3,8β-tetramethyl-2-oxo-5-azulenemethanol (3.17)

A 2-dram vial was charged with 10% palladium on activated carbon (2.7 mg, 10% Pd by mass) and ethyl acetate (100 μL) and sparged with hydrogen gas for 5 minutes. A solution of **3.75** (2.7 mg, 0.0115 mmol, 1 equiv.) in ethyl acetate (130 μmol) was added to the catalyst suspension and the substrate vial rinsed with an additional ethyl acetate (100 μL). The suspension was sparged with hydrogen gas for an additional 5 minutes and kept under a hydrogen atmoshphere *via* balloon at ambient temperature vith vigorous stirring. After filtration through celite with ethyl acetate (1 mL) and concentration, the reaction appeared incomplete by ^{1}H-NMR after 5 hours and the crude material was resubjected to the above conditions with a fresh portion of palladium on activated carbon (10 mg, 40 % Pd by mass) for an additional 4 hours. The reaction mixture was filtered through a pad of silica gel eluting with ethyl acetate to afford 2.2 mg white solid. This solid proved to contain significant impurities by ^{1}H-NMR

and was purified by mass-directed reverse-phase HPLC on a C18 column eluting with 5% to 95% acetonitrile in water to afford 0.3 mg (10%) clear oil containing **3.17** of slightly improved purity.

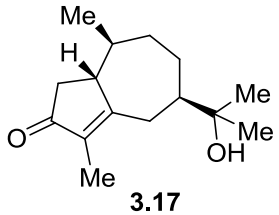

3.17

^{1}H NMR (500 MHz, $CDCl_3$) (partial) δ 1.88 (d, *J* = 1.3 Hz, 3H), 1.42 (s, 3H), 1.38 (s, 3H), 1.19 (d, *J* = 6.2 Hz, 3H) **IR** (KBr, thin film) 3404 (br), 3089 (w), 3071 (m), 3043 (s), 3015 (s), 2960 (m), 2912 (w), 2890 (w), 2881 (w), 2867 (w), 2848 (w), 2842 (w), 1731 (w), 1646 (m), 1468 (w), 1452 (m), 1409 (w), 1384 (w), 1259 (s), 1092 (s), 1051 (s), 1025 (s), 802 (s), 757 (m), 747 (m), 696 (s). **DART-HRMS (m/z):** Calc'd for [M+H]+: 237.18545; Found: 237.18638.

X-ray Crystal Structures

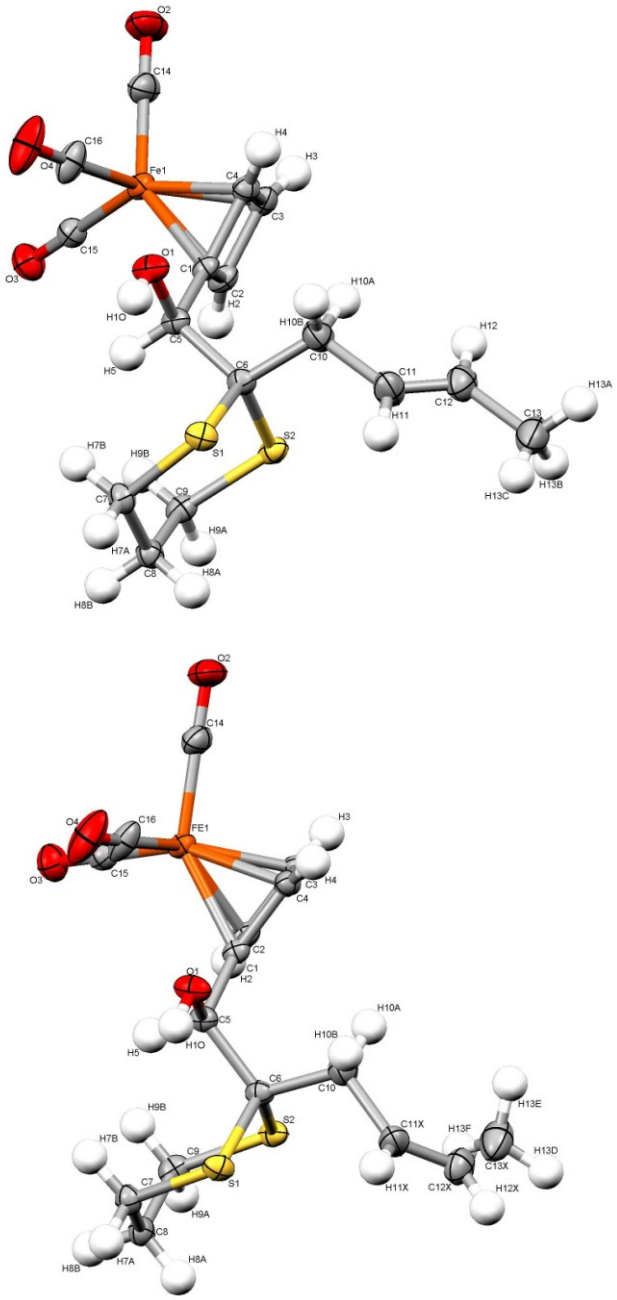

ORTEP for 3.58

Table 1. Crystal data and structure refinement for **3.58**.

Identification code	C16H18FeO4S2	
Empirical formula	C16 H18 Fe O4 S2	
Formula weight	394.27	
Temperature	100(2) K	
Wavelength	0.71073 Å	
Crystal system	Monoclinic	
Space group	P 21/n	
Unit cell dimensions	a = 9.1453(7) Å	α= 90°.
	b = 9.0711(7) Å	β= 95.5030(10)°.
	c = 20.8493(16) Å	γ = 90°.
Volume	1721.6(2) $Å^3$	
Z	4	
Density (calculated)	1.521 Mg/m^3	
Absorption coefficient	1.134 mm^{-1}	
F(000)	816	
Crystal size	0.07 x 0.05 x 0.04 mm^3	
Theta range for data collection	1.96 to 28.31°.	
Index ranges	-12<=h<=12, -12<=k<=12, -27<=l<=27	
Reflections collected	20208	
Independent reflections	4208 [R(int) = 0.0322]	
Completeness to theta = 28.31°	98.2 %	
Absorption correction	Semi-empirical from equivalents	
Max. and min. transmission	0.9561 and 0.9249	
Refinement method	Full-matrix least-squares on F^2	
Data / restraints / parameters	4208 / 260 / 272	
Goodness-of-fit on F^2	1.067	
Final R indices [I>2sigma(I)]	R1 = 0.0346, wR2 = 0.0827	
R indices (all data)	R1 = 0.0418, wR2 = 0.0866	
Extinction coefficient	na	
Largest diff. peak and hole	0.542 and -0.282 $e.Å^{-3}$	

Table 2. Atomic coordinates (x 10^4) and equivalent isotropic displacement parameters ($Å^2$x 10^3) for **3.58**. U(eq) is defined as one third of the trace of the orthogonalized U^{ij} tensor.

	x	y	z	U(eq)
Fe(1)	7462(1)	-7357(1)	254(1)	21(1)
S(1)	7629(1)	-1327(1)	1383(1)	23(1)
S(2)	7628(1)	-4046(1)	2219(1)	23(1)
O(1)	8010(2)	-3496(2)	308(1)	27(1)
C(1)	8100(2)	-5698(2)	886(1)	19(1)
C(2)	7785(2)	-7021(2)	1232(1)	23(1)
C(3)	9028(2)	-7742(2)	1000(1)	24(1)
C(4)	9364(2)	-6429(2)	649(1)	21(1)
C(5)	7570(2)	-4142(2)	879(1)	21(1)
C(6)	8200(2)	-3254(2)	1483(1)	21(1)
C(7)	5665(2)	-1436(2)	1439(1)	24(1)
C(8)	5222(2)	-2143(2)	2052(1)	24(1)
C(9)	5661(2)	-3748(2)	2129(1)	24(1)
C(10)	9891(2)	-3273(2)	1543(1)	31(1)
C(11)	10602(3)	-2635(3)	2153(2)	36(1)
C(12)	11540(3)	-3318(3)	2565(2)	35(1)
C(13)	12264(4)	-2649(4)	3166(2)	48(1)
C(11X)	10652(15)	-2007(15)	1959(7)	36(1)
C(12X)	11420(13)	-2234(15)	2511(5)	35(1)
C(13X)	11679(17)	-3613(17)	2881(8)	48(1)
C(14)	8075(2)	-8919(2)	-172(1)	33(1)
O(2)	8488(2)	-9906(2)	-442(1)	52(1)
C(15)	5648(2)	-8005(2)	332(1)	24(1)
O(3)	4494(2)	-8445(2)	384(1)	34(1)
C(16)	7079(3)	-6153(2)	-420(1)	35(1)
O(4)	6847(2)	-5411(2)	-856(1)	56(1)

Table 3. Bond lengths [Å] and angles [°] for **3.58**.

Fe(1)-C(15)	1.781(2)
Fe(1)-C(16)	1.788(2)
Fe(1)-C(14)	1.792(2)
Fe(1)-C(4)	2.0342(18)
Fe(1)-C(3)	2.0412(19)
Fe(1)-C(1)	2.0467(17)
Fe(1)-C(2)	2.0552(18)
S(1)-C(7)	1.8135(19)
S(1)-C(6)	1.8302(18)
S(2)-C(9)	1.811(2)
S(2)-C(6)	1.8161(18)
O(1)-C(5)	1.420(2)
O(1)-H(1O)	0.820(16)
C(1)-C(2)	1.444(2)
C(1)-C(4)	1.459(2)
C(1)-C(5)	1.493(2)
C(2)-C(3)	1.435(3)
C(2)-H(2)	0.921(15)
C(3)-C(4)	1.447(3)
C(3)-H(3)	0.938(15)
C(4)-H(4)	0.950(15)
C(5)-C(6)	1.558(2)
C(5)-H(5)	1.004(15)
C(6)-C(10)	1.540(3)
C(7)-C(8)	1.519(3)
C(7)-H(7A)	0.972(15)
C(7)-H(7B)	0.974(15)
C(8)-C(9)	1.514(3)
C(8)-H(8A)	0.982(15)
C(8)-H(8B)	0.978(15)
C(9)-H(9A)	0.956(15)
C(9)-H(9B)	0.959(15)

C(10)-C(11)	1.488(3)
C(10)-C(11X)	1.562(11)
C(10)-H(10A)	0.991(16)
C(10)-H(10B)	0.994(16)
C(11)-C(12)	1.310(4)
C(11)-H(11)	0.93(3)
C(12)-C(13)	1.490(4)
C(12)-H(12)	0.95(3)
C(13)-H(13A)	1.007(18)
C(13)-H(13B)	0.994(18)
C(13)-H(13C)	1.003(18)
C(11X)-C(12X)	1.306(14)
C(11X)-H(11)	0.84(3)
C(11X)-H(11X)	0.9500
C(12X)-C(13X)	1.477(14)
C(12X)-H(11)	1.20(3)
C(12X)-H(13C)	1.59(4)
C(12X)-H(12X)	0.9500
C(13X)-H(12)	1.07(3)
C(13X)-H(13B)	1.38(4)
C(13X)-H(13D)	0.9800
C(13X)-H(13E)	0.9800
C(13X)-H(13F)	0.9800
C(14)-O(2)	1.141(3)
C(15)-O(3)	1.144(2)
C(16)-O(4)	1.134(3)

C(15)-Fe(1)-C(16)	99.14(9)
C(15)-Fe(1)-C(14)	97.03(9)
C(16)-Fe(1)-C(14)	98.01(11)
C(15)-Fe(1)-C(4)	150.19(8)
C(16)-Fe(1)-C(4)	99.24(8)
C(14)-Fe(1)-C(4)	103.39(8)
C(15)-Fe(1)-C(3)	117.78(8)

C(16)-Fe(1)-C(3)	140.71(9)
C(14)-Fe(1)-C(3)	90.73(9)
C(4)-Fe(1)-C(3)	41.59(7)
C(15)-Fe(1)-C(1)	113.27(8)
C(16)-Fe(1)-C(1)	94.56(8)
C(14)-Fe(1)-C(1)	144.79(8)
C(4)-Fe(1)-C(1)	41.90(7)
C(3)-Fe(1)-C(1)	59.97(7)
C(15)-Fe(1)-C(2)	90.35(8)
C(16)-Fe(1)-C(2)	133.52(9)
C(14)-Fe(1)-C(2)	126.00(9)
C(4)-Fe(1)-C(2)	60.08(7)
C(3)-Fe(1)-C(2)	41.00(8)
C(1)-Fe(1)-C(2)	41.21(7)
C(7)-S(1)-C(6)	102.38(8)
C(9)-S(2)-C(6)	102.54(8)
C(5)-O(1)-H(1O)	107.2(17)
C(2)-C(1)-C(4)	89.70(14)
C(2)-C(1)-C(5)	135.28(16)
C(4)-C(1)-C(5)	133.90(16)
C(2)-C(1)-Fe(1)	69.71(10)
C(4)-C(1)-Fe(1)	68.59(10)
C(5)-C(1)-Fe(1)	128.10(13)
C(3)-C(2)-C(1)	90.43(15)
C(3)-C(2)-Fe(1)	68.98(10)
C(1)-C(2)-Fe(1)	69.08(10)
C(3)-C(2)-H(2)	135.6(14)
C(1)-C(2)-H(2)	133.7(14)
Fe(1)-C(2)-H(2)	124.3(15)
C(2)-C(3)-C(4)	90.53(15)
C(2)-C(3)-Fe(1)	70.02(11)
C(4)-C(3)-Fe(1)	68.94(10)
C(2)-C(3)-H(3)	134.4(14)
C(4)-C(3)-H(3)	134.6(14)

Fe(1)-C(3)-H(3)	125.0(14)
C(3)-C(4)-C(1)	89.34(15)
C(3)-C(4)-Fe(1)	69.46(10)
C(1)-C(4)-Fe(1)	69.51(10)
C(3)-C(4)-H(4)	133.7(13)
C(1)-C(4)-H(4)	136.3(13)
Fe(1)-C(4)-H(4)	125.5(13)
O(1)-C(5)-C(1)	106.27(14)
O(1)-C(5)-C(6)	110.63(14)
C(1)-C(5)-C(6)	112.77(15)
O(1)-C(5)-H(5)	109.5(12)
C(1)-C(5)-H(5)	108.8(13)
C(6)-C(5)-H(5)	108.9(12)
C(10)-C(6)-C(5)	110.52(15)
C(10)-C(6)-S(2)	107.19(13)
C(5)-C(6)-S(2)	111.36(12)
C(10)-C(6)-S(1)	107.06(13)
C(5)-C(6)-S(1)	108.79(12)
S(2)-C(6)-S(1)	111.83(9)
C(8)-C(7)-S(1)	114.99(13)
C(8)-C(7)-H(7A)	109.4(13)
S(1)-C(7)-H(7A)	105.3(13)
C(8)-C(7)-H(7B)	110.8(13)
S(1)-C(7)-H(7B)	109.5(13)
H(7A)-C(7)-H(7B)	106.3(19)
C(9)-C(8)-C(7)	113.96(16)
C(9)-C(8)-H(8A)	110.4(13)
C(7)-C(8)-H(8A)	108.3(13)
C(9)-C(8)-H(8B)	107.7(13)
C(7)-C(8)-H(8B)	107.0(13)
H(8A)-C(8)-H(8B)	109.3(19)
C(8)-C(9)-S(2)	113.91(13)
C(8)-C(9)-H(9A)	107.8(14)
S(2)-C(9)-H(9A)	103.5(13)

C(8)-C(9)-H(9B)	110.6(13)
S(2)-C(9)-H(9B)	110.5(13)
H(9A)-C(9)-H(9B)	110.3(19)
C(11)-C(10)-C(6)	114.72(19)
C(11)-C(10)-C(11X)	26.5(5)
C(6)-C(10)-C(11X)	115.3(6)
C(11)-C(10)-H(10A)	100.6(14)
C(6)-C(10)-H(10A)	113.7(14)
C(11X)-C(10)-H(10A)	120.0(15)
C(11)-C(10)-H(10B)	104.6(15)
C(6)-C(10)-H(10B)	115.9(15)
C(11X)-C(10)-H(10B)	81.6(16)
H(10A)-C(10)-H(10B)	106(2)
C(12)-C(11)-C(10)	125.5(3)
C(12)-C(11)-H(11)	116(2)
C(10)-C(11)-H(11)	118(2)
C(11)-C(12)-C(13)	124.7(3)
C(11)-C(12)-H(12)	117.0(19)
C(13)-C(12)-H(12)	118.3(19)
C(12)-C(13)-H(13A)	113(2)
C(12)-C(13)-H(13B)	106(2)
H(13A)-C(13)-H(13B)	108(3)
C(12)-C(13)-H(13C)	110(2)
H(13A)-C(13)-H(13C)	105(3)
H(13B)-C(13)-H(13C)	114(3)
C(12X)-C(11X)-C(10)	123.1(12)
C(12X)-C(11X)-H(11)	64(2)
C(10)-C(11X)-H(11)	119(3)
C(12X)-C(11X)-H(11X)	118.4
C(10)-C(11X)-H(11X)	118.4
H(11)-C(11X)-H(11X)	87.4
C(11X)-C(12X)-C(13X)	129.8(13)
C(11X)-C(12X)-H(11)	38.7(16)
C(13X)-C(12X)-H(11)	129(2)

C(11X)-C(12X)-H(13C)	146.5(15)
C(13X)-C(12X)-H(13C)	79.1(12)
H(11)-C(12X)-H(13C)	113(2)
C(11X)-C(12X)-H(12X)	115.1
C(13X)-C(12X)-H(12X)	115.1
H(11)-C(12X)-H(12X)	100.7
H(13C)-C(12X)-H(12X)	40.5
C(12X)-C(13X)-H(12)	97(2)
C(12X)-C(13X)-H(13B)	109.9(18)
H(12)-C(13X)-H(13B)	150(3)
C(12X)-C(13X)-H(13D)	109.5
H(12)-C(13X)-H(13D)	135.1
H(13B)-C(13X)-H(13D)	22.8
C(12X)-C(13X)-H(13E)	109.5
H(12)-C(13X)-H(13E)	25.7
H(13B)-C(13X)-H(13E)	127.3
H(13D)-C(13X)-H(13E)	109.5
C(12X)-C(13X)-H(13F)	109.5
H(12)-C(13X)-H(13F)	94.3
H(13B)-C(13X)-H(13F)	88.6
H(13D)-C(13X)-H(13F)	109.5
H(13E)-C(13X)-H(13F)	109.5
O(2)-C(14)-Fe(1)	178.93(19)
O(3)-C(15)-Fe(1)	178.78(18)
O(4)-C(16)-Fe(1)	178.6(2)

Symmetry transformations used to generate equivalent atoms:

Table 4. Anisotropic displacement parameters ($Å^2 x\ 10^3$)for **3.58**. The anisotropic displacement factor exponent takes the form: $-2\pi^2[\ h^2a^{*2}U^{11} + ... + 2\ h\ k\ a^*\ b^*\ U^{12}\ ]$

	U^{11}	U^{22}	U^{33}	U^{23}	U^{13}	U^{12}
Fe(1)	23(1)	19(1)	20(1)	-1(1)	2(1)	-3(1)
S(1)	26(1)	15(1)	28(1)	1(1)	6(1)	-2(1)
S(2)	32(1)	20(1)	18(1)	1(1)	2(1)	5(1)
O(1)	41(1)	19(1)	23(1)	4(1)	10(1)	5(1)
C(1)	23(1)	18(1)	17(1)	0(1)	2(1)	-1(1)
C(2)	30(1)	21(1)	18(1)	0(1)	3(1)	-4(1)
C(3)	30(1)	18(1)	23(1)	-1(1)	-2(1)	1(1)
C(4)	23(1)	19(1)	22(1)	-2(1)	1(1)	0(1)
C(5)	24(1)	18(1)	20(1)	2(1)	4(1)	0(1)
C(6)	24(1)	17(1)	22(1)	1(1)	3(1)	1(1)
C(7)	23(1)	21(1)	27(1)	3(1)	1(1)	1(1)
C(8)	20(1)	24(1)	27(1)	-1(1)	2(1)	-2(1)
C(9)	28(1)	22(1)	20(1)	1(1)	4(1)	-5(1)
C(10)	24(1)	30(1)	38(1)	-4(1)	2(1)	1(1)
C(11)	29(1)	29(2)	47(2)	-10(1)	-4(1)	2(1)
C(12)	26(1)	42(2)	36(2)	-2(1)	1(1)	-6(1)
C(13)	36(2)	75(2)	32(2)	-4(1)	0(1)	-4(1)
C(11X)	29(1)	29(2)	47(2)	-10(1)	-4(1)	2(1)
C(12X)	26(1)	42(2)	36(2)	-2(1)	1(1)	-6(1)
C(13X)	36(2)	75(2)	32(2)	-4(1)	0(1)	-4(1)
C(14)	26(1)	38(1)	35(1)	-13(1)	2(1)	-6(1)
O(2)	36(1)	58(1)	63(1)	-38(1)	6(1)	-1(1)
C(15)	28(1)	20(1)	24(1)	1(1)	1(1)	1(1)
O(3)	26(1)	36(1)	42(1)	3(1)	4(1)	-3(1)
C(16)	41(1)	34(1)	28(1)	3(1)	-9(1)	-17(1)
O(4)	75(1)	50(1)	36(1)	18(1)	-23(1)	-30(1)

Table 5. Hydrogen coordinates (x 10^4) and isotropic displacement parameters ($Å^2$x 10^3) for **3.58**.

	x	y	z	U(eq)
H(1O)	7740(30)	-2632(19)	303(12)	33
H(2)	7110(20)	-7250(20)	1517(10)	28
H(3)	9500(20)	-8648(19)	1087(10)	29
H(4)	10170(20)	-6140(20)	419(10)	26
H(5)	6469(17)	-4140(20)	861(10)	25
H(7A)	5320(20)	-422(18)	1414(10)	29
H(7B)	5200(20)	-1940(20)	1059(9)	29
H(8A)	5650(20)	-1560(20)	2421(9)	28
H(8B)	4150(17)	-2090(20)	2032(11)	28
H(9A)	5350(20)	-4090(20)	2529(8)	28
H(9B)	5210(20)	-4320(20)	1779(9)	28
H(10A)	10320(30)	-4278(19)	1563(12)	37
H(10B)	10360(30)	-2750(20)	1197(10)	37
H(11)	10280(40)	-1720(40)	2287(16)	43
H(12)	11750(30)	-4330(40)	2476(15)	42
H(13A)	13370(20)	-2590(40)	3170(20)	72
H(13B)	12020(40)	-3290(40)	3527(14)	72
H(13C)	11930(40)	-1600(20)	3210(20)	72
H(11X)	10551	-1024	1803	43
H(12X)	11881	-1384	2704	42
H(13D)	12309	-3410	3278	72
H(13E)	12162	-4332	2621	72
H(13F)	10738	-4014	2989	72

Table 6. Torsion angles [°] for **3.58**.

C(15)-Fe(1)-C(1)-C(2)	61.25(13)
C(16)-Fe(1)-C(1)-C(2)	163.24(13)
C(14)-Fe(1)-C(1)-C(2)	-85.94(18)
C(4)-Fe(1)-C(1)-C(2)	-97.98(14)
C(3)-Fe(1)-C(1)-C(2)	-48.47(11)
C(15)-Fe(1)-C(1)-C(4)	159.24(11)
C(16)-Fe(1)-C(1)-C(4)	-98.77(12)
C(14)-Fe(1)-C(1)-C(4)	12.04(19)
C(3)-Fe(1)-C(1)-C(4)	49.51(11)
C(2)-Fe(1)-C(1)-C(4)	97.98(14)
C(15)-Fe(1)-C(1)-C(5)	-71.04(17)
C(16)-Fe(1)-C(1)-C(5)	30.96(17)
C(14)-Fe(1)-C(1)-C(5)	141.77(18)
C(4)-Fe(1)-C(1)-C(5)	129.7(2)
C(3)-Fe(1)-C(1)-C(5)	179.24(18)
C(2)-Fe(1)-C(1)-C(5)	-132.3(2)
C(4)-C(1)-C(2)-C(3)	0.01(14)
C(5)-C(1)-C(2)-C(3)	-168.6(2)
Fe(1)-C(1)-C(2)-C(3)	67.23(11)
C(4)-C(1)-C(2)-Fe(1)	-67.22(10)
C(5)-C(1)-C(2)-Fe(1)	124.2(2)
C(15)-Fe(1)-C(2)-C(3)	134.70(12)
C(16)-Fe(1)-C(2)-C(3)	-122.30(14)
C(14)-Fe(1)-C(2)-C(3)	35.74(15)
C(4)-Fe(1)-C(2)-C(3)	-49.22(11)
C(1)-Fe(1)-C(2)-C(3)	-98.95(14)
C(15)-Fe(1)-C(2)-C(1)	-126.35(12)
C(16)-Fe(1)-C(2)-C(1)	-23.35(17)
C(14)-Fe(1)-C(2)-C(1)	134.69(12)
C(4)-Fe(1)-C(2)-C(1)	49.74(11)
C(3)-Fe(1)-C(2)-C(1)	98.95(14)
C(1)-C(2)-C(3)-C(4)	-0.01(15)

Fe(1)-C(2)-C(3)-C(4)	67.31(10)
C(1)-C(2)-C(3)-Fe(1)	-67.33(10)
C(15)-Fe(1)-C(3)-C(2)	-53.45(13)
C(16)-Fe(1)-C(3)-C(2)	104.58(17)
C(14)-Fe(1)-C(3)-C(2)	-151.80(12)
C(4)-Fe(1)-C(3)-C(2)	98.66(14)
C(1)-Fe(1)-C(3)-C(2)	48.74(10)
C(15)-Fe(1)-C(3)-C(4)	-152.11(11)
C(16)-Fe(1)-C(3)-C(4)	5.92(19)
C(14)-Fe(1)-C(3)-C(4)	109.55(12)
C(1)-Fe(1)-C(3)-C(4)	-49.92(10)
C(2)-Fe(1)-C(3)-C(4)	-98.66(14)
C(2)-C(3)-C(4)-C(1)	0.01(14)
Fe(1)-C(3)-C(4)-C(1)	68.31(10)
C(2)-C(3)-C(4)-Fe(1)	-68.30(11)
C(2)-C(1)-C(4)-C(3)	-0.01(14)
C(5)-C(1)-C(4)-C(3)	168.9(2)
Fe(1)-C(1)-C(4)-C(3)	-68.27(10)
C(2)-C(1)-C(4)-Fe(1)	68.26(10)
C(5)-C(1)-C(4)-Fe(1)	-122.9(2)
C(15)-Fe(1)-C(4)-C(3)	56.4(2)
C(16)-Fe(1)-C(4)-C(3)	-176.20(12)
C(14)-Fe(1)-C(4)-C(3)	-75.61(13)
C(1)-Fe(1)-C(4)-C(3)	97.29(14)
C(2)-Fe(1)-C(4)-C(3)	48.45(11)
C(15)-Fe(1)-C(4)-C(1)	-40.9(2)
C(16)-Fe(1)-C(4)-C(1)	86.51(12)
C(14)-Fe(1)-C(4)-C(1)	-172.90(12)
C(3)-Fe(1)-C(4)-C(1)	-97.29(14)
C(2)-Fe(1)-C(4)-C(1)	-48.83(10)
C(2)-C(1)-C(5)-O(1)	-164.24(19)
C(4)-C(1)-C(5)-O(1)	31.7(3)
Fe(1)-C(1)-C(5)-O(1)	-64.69(19)
C(2)-C(1)-C(5)-C(6)	74.4(3)

C(4)-C(1)-C(5)-C(6)	-89.7(2)
Fe(1)-C(1)-C(5)-C(6)	173.94(12)
O(1)-C(5)-C(6)-C(10)	-61.81(19)
C(1)-C(5)-C(6)-C(10)	57.1(2)
O(1)-C(5)-C(6)-S(2)	179.17(12)
C(1)-C(5)-C(6)-S(2)	-61.98(17)
O(1)-C(5)-C(6)-S(1)	55.47(16)
C(1)-C(5)-C(6)-S(1)	174.32(12)
C(9)-S(2)-C(6)-C(10)	173.17(13)
C(9)-S(2)-C(6)-C(5)	-65.83(14)
C(9)-S(2)-C(6)-S(1)	56.13(11)
C(7)-S(1)-C(6)-C(10)	-171.92(13)
C(7)-S(1)-C(6)-C(5)	68.62(13)
C(7)-S(1)-C(6)-S(2)	-54.80(12)
C(6)-S(1)-C(7)-C(8)	56.12(16)
S(1)-C(7)-C(8)-C(9)	-63.7(2)
C(7)-C(8)-C(9)-S(2)	64.72(19)
C(6)-S(2)-C(9)-C(8)	-58.72(15)
C(5)-C(6)-C(10)-C(11)	-171.9(2)
S(2)-C(6)-C(10)-C(11)	-50.4(2)
S(1)-C(6)-C(10)-C(11)	69.8(2)
C(5)-C(6)-C(10)-C(11X)	158.8(6)
S(2)-C(6)-C(10)-C(11X)	-79.6(6)
S(1)-C(6)-C(10)-C(11X)	40.5(7)
C(6)-C(10)-C(11)-C(12)	123.2(3)
C(11X)-C(10)-C(11)-C(12)	-139.3(14)
C(10)-C(11)-C(12)-C(13)	178.6(3)
C(11)-C(10)-C(11X)-C(12X)	17.5(8)
C(6)-C(10)-C(11X)-C(12X)	112.6(13)
C(10)-C(11X)-C(12X)-C(13X)	-4(2)
C(15)-Fe(1)-C(14)-O(2)	-167(100)
C(16)-Fe(1)-C(14)-O(2)	93(12)
C(4)-Fe(1)-C(14)-O(2)	-8(12)
C(3)-Fe(1)-C(14)-O(2)	-48(12)

C(1)-Fe(1)-C(14)-O(2)	-17(12)
C(2)-Fe(1)-C(14)-O(2)	-71(12)
C(16)-Fe(1)-C(15)-O(3)	143(8)
C(14)-Fe(1)-C(15)-O(3)	43(8)
C(4)-Fe(1)-C(15)-O(3)	-90(8)
C(3)-Fe(1)-C(15)-O(3)	-51(8)
C(1)-Fe(1)-C(15)-O(3)	-118(8)
C(2)-Fe(1)-C(15)-O(3)	-83(8)
C(15)-Fe(1)-C(16)-O(4)	-104(9)
C(14)-Fe(1)-C(16)-O(4)	-5(9)
C(4)-Fe(1)-C(16)-O(4)	100(9)
C(3)-Fe(1)-C(16)-O(4)	96(9)
C(1)-Fe(1)-C(16)-O(4)	142(9)
C(2)-Fe(1)-C(16)-O(4)	157(9)

Symmetry transformations used to generate equivalent atoms:

Table 7. Hydrogen bonds for **3.58** [Å and °].

D-H...A	d(D-H)	d(H...A)	d(D...A)	<(DHA)
O(1)-H(1O)...S(1)	0.820(16)	2.56(2)	3.0281(14)	118(2)
O(1)-H(1O)...O(3)#1	0.820(16)	2.58(2)	3.129(2)	126(2)

Symmetry transformations used to generate equivalent atoms:

#1 -x+1,-y-1,-z

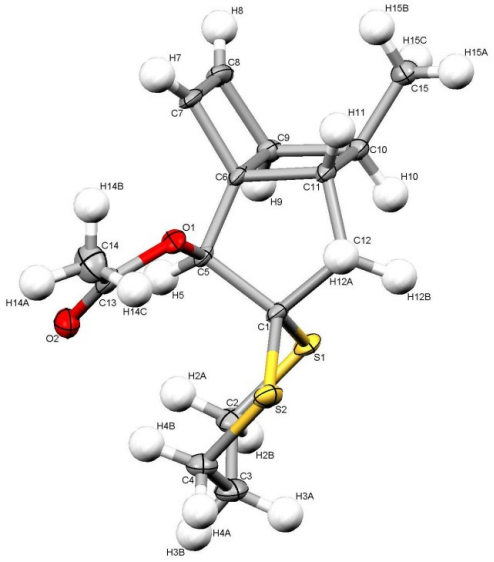

ORTEP for β-3.66

Table 1. Crystal data and structure refinement for **β-3.66**.

Identification code	C15H20O2S2
Empirical formula	C15 H20 O2 S2
Formula weight	296.43
Temperature	100(2) K
Wavelength	0.71073 Å
Crystal system	Monoclinic
Space group	P 21/c

Unit cell dimensions	a = 16.847(5) Å	α= 90°.
	b = 8.264(3) Å	β= 107.583(4)°.
	c = 11.057(4) Å	γ = 90°.
Volume	1467.5(8) $Å^3$	
Z	4	
Density (calculated)	1.342 Mg/m^3	
Absorption coefficient	0.358 mm^{-1}	
F(000)	632	
Crystal size	0.16 x 0.04 x 0.01 mm^3	
Theta range for data collection	2.54 to 28.00°.	
Index ranges	-22<=h<=22, -10<=k<=10, -14<=l<=14	
Reflections collected	19230	
Independent reflections	3530 [R(int) = 0.0764]	
Completeness to theta = 28.00°	99.8 %	
Absorption correction	Semi-empirical from equivalents	
Max. and min. transmission	0.9964 and 0.9449	
Refinement method	Full-matrix least-squares on F^2	
Data / restraints / parameters	3530 / 20 / 232	
Goodness-of-fit on F^2	1.037	
Final R indices [I>2sigma(I)]	R1 = 0.0560, wR2 = 0.1285	
R indices (all data)	R1 = 0.0830, wR2 = 0.1413	
Extinction coefficient	na	
Largest diff. peak and hole	0.738 and -0.346 $e.Å^{-3}$	

Table 2. Atomic coordinates (x 10^4) and equivalent isotropic displacement parameters ($Å^2$x 10^3) for **β-3.66**. U(eq) is defined as one third of the trace of the orthogonalized U^{ij} tensor.

	x	y	z	U(eq)
S(1)	3102(1)	4261(1)	1724(1)	21(1)
S(2)	1444(1)	4608(1)	2215(1)	22(1)
O(1)	1781(1)	8185(2)	2172(2)	19(1)
O(2)	880(1)	8038(2)	206(2)	27(1)
C(1)	2443(2)	5543(3)	2362(2)	16(1)
C(2)	2441(2)	3823(3)	141(3)	25(1)
C(3)	1640(2)	2971(4)	108(3)	28(1)
C(4)	1060(2)	4051(4)	559(3)	25(1)
C(5)	2407(2)	7274(3)	1813(2)	14(1)
C(6)	3209(2)	8042(3)	2567(2)	16(1)
C(7)	3416(2)	9809(3)	2519(2)	21(1)
C(8)	4178(2)	9538(3)	2474(2)	24(1)
C(9)	4103(2)	7718(3)	2457(2)	18(1)
C(10)	4355(2)	6869(3)	3774(2)	18(1)
C(11)	3479(2)	7225(3)	3903(2)	17(1)
C(12)	2888(2)	5793(3)	3792(2)	19(1)
C(13)	1039(2)	8427(3)	1299(2)	22(1)
C(14)	459(2)	9258(4)	1889(3)	35(1)
C(15)	5114(2)	7494(3)	4770(2)	22(1)

Table 3. Bond lengths [Å] and angles [°] for β-**3.66**.

S(1)-C(2)	1.806(3)
S(1)-C(1)	1.824(3)
S(2)-C(4)	1.808(3)
S(2)-C(1)	1.813(3)
O(1)-C(13)	1.343(3)
O(1)-C(5)	1.444(3)
O(2)-C(13)	1.200(3)
C(1)-C(12)	1.545(3)
C(1)-C(5)	1.548(3)
C(2)-C(3)	1.513(4)
C(2)-H(2A)	1.004(17)
C(2)-H(2B)	0.984(17)
C(3)-C(4)	1.515(4)
C(3)-H(3A)	0.985(17)
C(3)-H(3B)	1.002(17)
C(4)-H(4A)	0.974(17)
C(4)-H(4B)	0.981(17)
C(5)-C(6)	1.498(3)
C(5)-H(5)	0.978(16)
C(6)-C(7)	1.506(3)
C(6)-C(11)	1.562(3)
C(6)-C(9)	1.570(4)
C(7)-C(8)	1.319(4)
C(7)-H(7)	0.971(17)
C(8)-C(9)	1.509(4)
C(8)-H(8)	0.944(17)
C(9)-C(10)	1.556(3)
C(9)-H(9)	0.981(17)
C(10)-C(15)	1.504(4)
C(10)-C(11)	1.553(4)
C(10)-H(10)	0.996(17)
C(11)-C(12)	1.527(3)

C(11)-H(11)	0.986(16)
C(12)-H(12A)	0.990(17)
C(12)-H(12B)	0.989(17)
C(13)-C(14)	1.496(4)
C(14)-H(14A)	0.977(18)
C(14)-H(14B)	0.981(18)
C(14)-H(14C)	0.977(18)
C(15)-H(15A)	0.969(17)
C(15)-H(15B)	0.956(17)
C(15)-H(15C)	0.980(17)

C(2)-S(1)-C(1)	102.83(12)
C(4)-S(2)-C(1)	103.79(12)
C(13)-O(1)-C(5)	118.58(19)
C(12)-C(1)-C(5)	103.13(19)
C(12)-C(1)-S(2)	107.40(17)
C(5)-C(1)-S(2)	115.65(17)
C(12)-C(1)-S(1)	108.04(17)
C(5)-C(1)-S(1)	109.96(16)
S(2)-C(1)-S(1)	112.00(13)
C(3)-C(2)-S(1)	113.6(2)
C(3)-C(2)-H(2A)	111.1(17)
S(1)-C(2)-H(2A)	109.2(17)
C(3)-C(2)-H(2B)	113.6(17)
S(1)-C(2)-H(2B)	103.4(16)
H(2A)-C(2)-H(2B)	105(2)
C(2)-C(3)-C(4)	112.2(2)
C(2)-C(3)-H(3A)	109.5(18)
C(4)-C(3)-H(3A)	111.2(18)
C(2)-C(3)-H(3B)	110.1(17)
C(4)-C(3)-H(3B)	107.5(17)
H(3A)-C(3)-H(3B)	106(2)
C(3)-C(4)-S(2)	114.5(2)
C(3)-C(4)-H(4A)	111.7(18)

S(2)-C(4)-H(4A)	102.3(17)
C(3)-C(4)-H(4B)	109.5(17)
S(2)-C(4)-H(4B)	111.6(17)
H(4A)-C(4)-H(4B)	107(2)
O(1)-C(5)-C(6)	103.70(18)
O(1)-C(5)-C(1)	108.63(18)
C(6)-C(5)-C(1)	104.54(18)
O(1)-C(5)-H(5)	110.9(15)
C(6)-C(5)-H(5)	115.6(16)
C(1)-C(5)-H(5)	112.8(16)
C(5)-C(6)-C(7)	124.8(2)
C(5)-C(6)-C(11)	107.42(19)
C(7)-C(6)-C(11)	116.6(2)
C(5)-C(6)-C(9)	127.6(2)
C(7)-C(6)-C(9)	85.68(19)
C(11)-C(6)-C(9)	89.25(17)
C(8)-C(7)-C(6)	94.3(2)
C(8)-C(7)-H(7)	136.7(17)
C(6)-C(7)-H(7)	128.7(18)
C(7)-C(8)-C(9)	95.2(2)
C(7)-C(8)-H(8)	135.2(19)
C(9)-C(8)-H(8)	128.8(19)
C(8)-C(9)-C(10)	116.1(2)
C(8)-C(9)-C(6)	84.71(19)
C(10)-C(9)-C(6)	90.09(17)
C(8)-C(9)-H(9)	118.8(16)
C(10)-C(9)-H(9)	117.7(16)
C(6)-C(9)-H(9)	121.5(16)
C(15)-C(10)-C(11)	119.3(2)
C(15)-C(10)-C(9)	117.5(2)
C(11)-C(10)-C(9)	90.12(18)
C(15)-C(10)-H(10)	108.0(15)
C(11)-C(10)-H(10)	108.3(16)
C(9)-C(10)-H(10)	112.7(16)

C(12)-C(11)-C(10)	117.5(2)
C(12)-C(11)-C(6)	105.19(19)
C(10)-C(11)-C(6)	90.50(18)
C(12)-C(11)-H(11)	112.7(16)
C(10)-C(11)-H(11)	112.4(15)
C(6)-C(11)-H(11)	116.7(16)
C(11)-C(12)-C(1)	106.80(19)
C(11)-C(12)-H(12A)	108.5(17)
C(1)-C(12)-H(12A)	108.1(15)
C(11)-C(12)-H(12B)	114.3(16)
C(1)-C(12)-H(12B)	111.7(16)
H(12A)-C(12)-H(12B)	107(2)
O(2)-C(13)-O(1)	124.0(2)
O(2)-C(13)-C(14)	125.8(3)
O(1)-C(13)-C(14)	110.2(2)
C(13)-C(14)-H(14A)	110(2)
C(13)-C(14)-H(14B)	110(2)
H(14A)-C(14)-H(14B)	106(3)
C(13)-C(14)-H(14C)	106(2)
H(14A)-C(14)-H(14C)	113(3)
H(14B)-C(14)-H(14C)	111(3)
C(10)-C(15)-H(15A)	114.7(18)
C(10)-C(15)-H(15B)	111.9(18)
H(15A)-C(15)-H(15B)	103(2)
C(10)-C(15)-H(15C)	111.5(17)
H(15A)-C(15)-H(15C)	108(2)
H(15B)-C(15)-H(15C)	107(3)

Symmetry transformations used to generate equivalent atoms:

Table 4. Anisotropic displacement parameters ($Å^2 x\ 10^3$) for **β-3.66**. The anisotropic displacement factor exponent takes the form: $-2\pi^2[\ h^2\ a^{*2}U^{11} + ...\ + 2\ h\ k\ a^*\ b^*\ U^{12}\ ]$

	U^{11}	U^{22}	U^{33}	U^{23}	U^{13}	U^{12}
S(1)	26(1)	9(1)	26(1)	-3(1)	7(1)	2(1)
S(2)	27(1)	17(1)	24(1)	0(1)	10(1)	-7(1)
O(1)	22(1)	13(1)	21(1)	-2(1)	5(1)	5(1)
O(2)	28(1)	23(1)	24(1)	1(1)	1(1)	4(1)
C(1)	22(1)	9(1)	19(1)	1(1)	7(1)	-1(1)
C(2)	29(2)	19(1)	26(1)	-8(1)	8(1)	1(1)
C(3)	33(2)	18(2)	31(2)	-9(1)	5(1)	-4(1)
C(4)	28(2)	20(2)	25(1)	-6(1)	4(1)	-4(1)
C(5)	20(1)	8(1)	16(1)	1(1)	7(1)	2(1)
C(6)	22(1)	7(1)	17(1)	2(1)	6(1)	1(1)
C(7)	34(2)	7(1)	20(1)	1(1)	4(1)	-3(1)
C(8)	30(2)	18(1)	22(1)	2(1)	4(1)	-11(1)
C(9)	23(1)	16(1)	18(1)	0(1)	7(1)	-3(1)
C(10)	23(1)	12(1)	18(1)	0(1)	5(1)	0(1)
C(11)	24(1)	10(1)	14(1)	1(1)	4(1)	-1(1)
C(12)	27(1)	15(1)	17(1)	4(1)	8(1)	-2(1)
C(13)	25(1)	12(1)	28(1)	3(1)	6(1)	2(1)
C(14)	29(2)	37(2)	37(2)	-2(1)	10(1)	12(1)
C(15)	26(1)	17(1)	23(1)	-1(1)	4(1)	1(1)

Table 5. Hydrogen coordinates (x 10^4) and isotropic displacement parameters ($Å^2$x 10^3) for **β-3.66**.

	x	y	z	U(eq)
H(2A)	2326(18)	4850(30)	-360(20)	30
H(2B)	2803(15)	3180(30)	-230(20)	30
H(3A)	1770(18)	1970(30)	610(20)	34
H(3B)	1336(16)	2630(40)	-780(18)	34
H(4A)	539(13)	3500(30)	510(30)	30
H(4B)	916(17)	5010(30)	10(20)	30
H(5)	2296(16)	7280(30)	892(16)	17
H(7)	3085(15)	10750(30)	2590(30)	26
H(8)	4655(14)	10180(30)	2560(30)	29
H(9)	4186(16)	7120(30)	1740(20)	22
H(10)	4416(17)	5680(20)	3710(20)	22
H(11)	3503(16)	7930(30)	4630(20)	20
H(12A)	2462(14)	6090(30)	4210(20)	23
H(12B)	3161(16)	4790(30)	4200(20)	23
H(14A)	-36(16)	9640(40)	1230(30)	52
H(14B)	730(20)	10220(30)	2360(30)	52
H(14C)	340(20)	8470(40)	2470(30)	52
H(15A)	5203(18)	7040(40)	5608(19)	34
H(15B)	5076(19)	8630(20)	4910(30)	34
H(15C)	5620(13)	7320(40)	4530(30)	34

Table 6. Torsion angles [°] for **β-3.66**.

C(4)-S(2)-C(1)-C(12)	-170.40(17)
C(4)-S(2)-C(1)-C(5)	75.11(19)
C(4)-S(2)-C(1)-S(1)	-51.94(16)
C(2)-S(1)-C(1)-C(12)	171.45(17)
C(2)-S(1)-C(1)-C(5)	-76.68(19)
C(2)-S(1)-C(1)-S(2)	53.37(16)
C(1)-S(1)-C(2)-C(3)	-59.6(2)
S(1)-C(2)-C(3)-C(4)	68.0(3)
C(2)-C(3)-C(4)-S(2)	-66.0(3)
C(1)-S(2)-C(4)-C(3)	56.2(2)
C(13)-O(1)-C(5)-C(6)	146.4(2)
C(13)-O(1)-C(5)-C(1)	-102.8(2)
C(12)-C(1)-C(5)-O(1)	-74.0(2)
S(2)-C(1)-C(5)-O(1)	42.9(2)
S(1)-C(1)-C(5)-O(1)	171.00(15)
C(12)-C(1)-C(5)-C(6)	36.2(2)
S(2)-C(1)-C(5)-C(6)	153.15(16)
S(1)-C(1)-C(5)-C(6)	-78.79(19)
O(1)-C(5)-C(6)-C(7)	-56.9(3)
C(1)-C(5)-C(6)-C(7)	-170.7(2)
O(1)-C(5)-C(6)-C(11)	85.2(2)
C(1)-C(5)-C(6)-C(11)	-28.5(2)
O(1)-C(5)-C(6)-C(9)	-171.8(2)
C(1)-C(5)-C(6)-C(9)	74.5(3)
C(5)-C(6)-C(7)-C(8)	-136.0(2)
C(11)-C(6)-C(7)-C(8)	84.8(2)
C(9)-C(6)-C(7)-C(8)	-2.15(19)
C(6)-C(7)-C(8)-C(9)	2.2(2)
C(7)-C(8)-C(9)-C(10)	-89.7(2)
C(7)-C(8)-C(9)-C(6)	-2.16(19)
C(5)-C(6)-C(9)-C(8)	133.6(2)
C(7)-C(6)-C(9)-C(8)	1.88(17)

C(11)-C(6)-C(9)-C(8)	-114.85(18)
C(5)-C(6)-C(9)-C(10)	-110.2(2)
C(7)-C(6)-C(9)-C(10)	118.08(18)
C(11)-C(6)-C(9)-C(10)	1.34(18)
C(8)-C(9)-C(10)-C(15)	-40.7(3)
C(6)-C(9)-C(10)-C(15)	-124.9(2)
C(8)-C(9)-C(10)-C(11)	82.8(2)
C(6)-C(9)-C(10)-C(11)	-1.35(18)
C(15)-C(10)-C(11)-C(12)	-129.2(2)
C(9)-C(10)-C(11)-C(12)	108.8(2)
C(15)-C(10)-C(11)-C(6)	123.4(2)
C(9)-C(10)-C(11)-C(6)	1.36(18)
C(5)-C(6)-C(11)-C(12)	9.4(3)
C(7)-C(6)-C(11)-C(12)	155.2(2)
C(9)-C(6)-C(11)-C(12)	-120.0(2)
C(5)-C(6)-C(11)-C(10)	128.13(19)
C(7)-C(6)-C(11)-C(10)	-86.1(2)
C(9)-C(6)-C(11)-C(10)	-1.34(18)
C(10)-C(11)-C(12)-C(1)	-85.2(2)
C(6)-C(11)-C(12)-C(1)	13.5(3)
C(5)-C(1)-C(12)-C(11)	-30.6(2)
S(2)-C(1)-C(12)-C(11)	-153.25(17)
S(1)-C(1)-C(12)-C(11)	85.8(2)
C(5)-O(1)-C(13)-O(2)	-5.8(4)
C(5)-O(1)-C(13)-C(14)	174.9(2)

Symmetry transformations used to generate equivalent atoms:

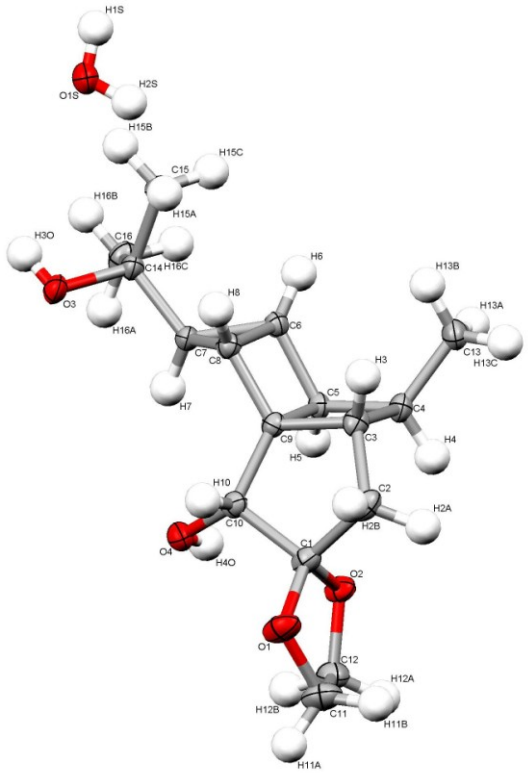

ORTEP for 3.67 · H_2O

Table 1. Crystal data and structure refinement for **3.67**.

Identification code	C16H26O5	
Empirical formula	C16 H26 O5	
Formula weight	298.37	
Temperature	100(2) K	
Wavelength	0.71073 Å	
Crystal system	Monoclinic	
Space group	P 21/c	
Unit cell dimensions	a = 13.207(3) Å	α= 90°.
	b = 8.3846(18) Å	β= 115.673(2)°.
	c = 15.178(4) Å	γ = 90°.
Volume	1514.8(6) $Å^3$	
Z	4	
Density (calculated)	1.308 Mg/m^3	

Absorption coefficient	0.096 mm^{-1}
F(000)	648
Crystal size	0.14 x 0.11 x 0.05 mm^3
Theta range for data collection	2.72 to 27.99°.
Index ranges	-17<=h<=17, -11<=k<=11, -19<=l<=20
Reflections collected	17713
Independent reflections	3639 [R(int) = 0.0315]
Completeness to theta = 27.99°	99.9 %
Absorption correction	Semi-empirical from equivalents
Max. and min. transmission	0.9952 and 0.9867
Refinement method	Full-matrix least-squares on F^2
Data / restraints / parameters	3639 / 27 / 268
Goodness-of-fit on F^2	1.037
Final R indices [I>2sigma(I)]	R1 = 0.0454, wR2 = 0.1141
R indices (all data)	R1 = 0.0509, wR2 = 0.1186
Extinction coefficient	na
Largest diff. peak and hole	0.546 and -0.161 $e.Å^{-3}$

Table 2. Atomic coordinates (x 10^4) and equivalent isotropic displacement parameters ($Å^2$x 10^3) for **3.67**. U(eq) is defined as one third of the trace of the orthogonalized U^{ij} tensor.

	x	y	z	U(eq)
O(1)	2730(1)	-4160(1)	386(1)	34(1)
O(2)	2620(1)	-1921(1)	-502(1)	24(1)
O(3)	886(1)	2288(1)	2490(1)	24(1)
O(4)	1189(1)	-1473(1)	396(1)	24(1)
C(1)	2982(1)	-2515(1)	467(1)	22(1)
C(2)	4220(1)	-2125(2)	1086(1)	25(1)
C(3)	4233(1)	-416(2)	1449(1)	21(1)
C(4)	4142(1)	946(2)	724(1)	20(1)
C(5)	2948(1)	1366(1)	609(1)	18(1)
C(6)	2902(1)	2479(1)	1380(1)	19(1)
C(7)	1876(1)	2110(1)	1525(1)	18(1)
C(8)	2895(1)	1062(1)	2026(1)	19(1)
C(9)	3007(1)	-81(1)	1306(1)	18(1)
C(10)	2363(1)	-1626(1)	977(1)	20(1)
C(11)	2554(2)	-4655(2)	-564(1)	36(1)
C(12)	2103(1)	-3191(2)	-1172(1)	30(1)
C(13)	5026(1)	2250(2)	1078(1)	27(1)
C(14)	1528(1)	3251(1)	2117(1)	21(1)
C(15)	2505(1)	4003(2)	2975(1)	31(1)
C(16)	772(1)	4535(2)	1437(1)	29(1)
O(1S)	-137(1)	9476(1)	1411(1)	30(1)

Table 3. Bond lengths [Å] and angles [°] for **3.67**.

O(1)-C(1)	1.4115(15)
O(1)-C(11)	1.4192(18)
O(2)-C(1)	1.4256(15)
O(2)-C(12)	1.4256(16)
O(3)-C(14)	1.4514(14)
O(3)-H(3O)	0.809(14)
O(4)-C(10)	1.4187(15)
O(4)-H(4O)	0.854(14)
C(1)-C(2)	1.5267(19)
C(1)-C(10)	1.5394(17)
C(2)-C(3)	1.5321(18)
C(2)-H(2A)	1.005(13)
C(2)-H(2B)	0.981(13)
C(3)-C(4)	1.5537(17)
C(3)-C(9)	1.5635(16)
C(3)-H(3)	0.998(12)
C(4)-C(13)	1.5172(18)
C(4)-C(5)	1.5505(16)
C(4)-H(4)	0.991(13)
C(5)-C(6)	1.5183(16)
C(5)-C(9)	1.5893(16)
C(5)-H(5)	0.987(12)
C(6)-C(7)	1.4968(16)
C(6)-C(8)	1.5430(16)
C(6)-H(6)	0.964(13)
C(7)-C(8)	1.5087(17)
C(7)-C(14)	1.5138(16)
C(7)-H(7)	0.986(13)
C(8)-C(9)	1.5075(16)
C(8)-H(8)	0.996(12)
C(9)-C(10)	1.5107(16)
C(10)-H(10)	0.977(12)

C(11)-C(12)	1.496(2)
C(11)-H(11A)	0.979(14)
C(11)-H(11B)	1.012(14)
C(12)-H(12A)	0.990(14)
C(12)-H(12B)	0.965(14)
C(13)-H(13A)	0.987(14)
C(13)-H(13B)	0.990(14)
C(13)-H(13C)	1.008(14)
C(14)-C(15)	1.5179(18)
C(14)-C(16)	1.5254(18)
C(15)-H(15A)	0.999(14)
C(15)-H(15B)	0.980(14)
C(15)-H(15C)	0.977(15)
C(16)-H(16A)	0.991(14)
C(16)-H(16B)	0.968(14)
C(16)-H(16C)	0.978(14)
O(1S)-H(1S)	0.847(15)
O(1S)-H(2S)	0.832(15)

C(1)-O(1)-C(11)	107.67(10)
C(1)-O(2)-C(12)	108.50(10)
C(14)-O(3)-H(3O)	105.7(13)
C(10)-O(4)-H(4O)	108.4(12)
O(1)-C(1)-O(2)	106.88(10)
O(1)-C(1)-C(2)	114.37(11)
O(2)-C(1)-C(2)	110.56(10)
O(1)-C(1)-C(10)	111.14(10)
O(2)-C(1)-C(10)	109.58(10)
C(2)-C(1)-C(10)	104.30(10)
C(1)-C(2)-C(3)	105.32(10)
C(1)-C(2)-H(2A)	111.6(10)
C(3)-C(2)-H(2A)	112.7(9)
C(1)-C(2)-H(2B)	106.6(10)
C(3)-C(2)-H(2B)	110.8(10)

H(2A)-C(2)-H(2B)	109.6(14)
C(2)-C(3)-C(4)	116.61(10)
C(2)-C(3)-C(9)	105.55(10)
C(4)-C(3)-C(9)	90.69(8)
C(2)-C(3)-H(3)	113.3(9)
C(4)-C(3)-H(3)	113.1(9)
C(9)-C(3)-H(3)	115.5(9)
C(13)-C(4)-C(5)	117.72(11)
C(13)-C(4)-C(3)	117.83(10)
C(5)-C(4)-C(3)	90.55(9)
C(13)-C(4)-H(4)	108.9(9)
C(5)-C(4)-H(4)	111.2(9)
C(3)-C(4)-H(4)	109.6(9)
C(6)-C(5)-C(4)	115.52(10)
C(6)-C(5)-C(9)	87.88(8)
C(4)-C(5)-C(9)	89.85(8)
C(6)-C(5)-H(5)	116.3(9)
C(4)-C(5)-H(5)	118.3(9)
C(9)-C(5)-H(5)	122.7(9)
C(7)-C(6)-C(5)	109.07(10)
C(7)-C(6)-C(8)	59.49(8)
C(5)-C(6)-C(8)	91.68(9)
C(7)-C(6)-H(6)	120.4(9)
C(5)-C(6)-H(6)	127.3(9)
C(8)-C(6)-H(6)	127.8(9)
C(6)-C(7)-C(8)	61.78(8)
C(6)-C(7)-C(14)	118.94(10)
C(8)-C(7)-C(14)	120.20(10)
C(6)-C(7)-H(7)	117.7(9)
C(8)-C(7)-H(7)	118.2(9)
C(14)-C(7)-H(7)	111.7(9)
C(9)-C(8)-C(7)	110.58(10)
C(9)-C(8)-C(6)	89.99(9)
C(7)-C(8)-C(6)	58.73(7)

C(9)-C(8)-H(8)	125.4(9)
C(7)-C(8)-H(8)	122.4(9)
C(6)-C(8)-H(8)	127.5(9)
C(8)-C(9)-C(10)	124.52(10)
C(8)-C(9)-C(3)	115.78(10)
C(10)-C(9)-C(3)	107.02(9)
C(8)-C(9)-C(5)	90.30(9)
C(10)-C(9)-C(5)	125.15(10)
C(3)-C(9)-C(5)	88.77(8)
O(4)-C(10)-C(9)	115.79(10)
O(4)-C(10)-C(1)	114.01(10)
C(9)-C(10)-C(1)	103.67(10)
O(4)-C(10)-H(10)	105.2(9)
C(9)-C(10)-H(10)	111.1(9)
C(1)-C(10)-H(10)	106.9(9)
O(1)-C(11)-C(12)	103.43(11)
O(1)-C(11)-H(11A)	108.7(11)
C(12)-C(11)-H(11A)	115.0(11)
O(1)-C(11)-H(11B)	109.0(10)
C(12)-C(11)-H(11B)	111.5(11)
H(11A)-C(11)-H(11B)	109.0(15)
O(2)-C(12)-C(11)	103.52(11)
O(2)-C(12)-H(12A)	108.2(10)
C(11)-C(12)-H(12A)	113.8(10)
O(2)-C(12)-H(12B)	108.7(11)
C(11)-C(12)-H(12B)	112.6(11)
H(12A)-C(12)-H(12B)	109.7(14)
C(4)-C(13)-H(13A)	111.8(11)
C(4)-C(13)-H(13B)	111.5(11)
H(13A)-C(13)-H(13B)	107.2(15)
C(4)-C(13)-H(13C)	110.1(10)
H(13A)-C(13)-H(13C)	107.8(15)
H(13B)-C(13)-H(13C)	108.2(15)
O(3)-C(14)-C(7)	105.02(9)

O(3)-C(14)-C(15)	108.60(10)
C(7)-C(14)-C(15)	114.11(10)
O(3)-C(14)-C(16)	109.59(10)
C(7)-C(14)-C(16)	108.79(10)
C(15)-C(14)-C(16)	110.54(11)
C(14)-C(15)-H(15A)	110.8(11)
C(14)-C(15)-H(15B)	110.3(11)
H(15A)-C(15)-H(15B)	105.7(16)
C(14)-C(15)-H(15C)	110.0(12)
H(15A)-C(15)-H(15C)	111.8(17)
H(15B)-C(15)-H(15C)	108.0(16)
C(14)-C(16)-H(16A)	109.6(11)
C(14)-C(16)-H(16B)	109.0(11)
H(16A)-C(16)-H(16B)	111.7(16)
C(14)-C(16)-H(16C)	107.6(11)
H(16A)-C(16)-H(16C)	110.3(16)
H(16B)-C(16)-H(16C)	108.5(16)
H(1S)-O(1S)-H(2S)	107.6(17)

Symmetry transformations used to generate equivalent atoms:

Table 4. Anisotropic displacement parameters ($Å^2 x\ 10^3$) for **3.67**. The anisotropic displacement factor exponent takes the form: $-2\pi^2[\ h^2\ a^{*2}U^{11} + ...\ + 2\ h\ k\ a^*\ b^*\ U^{12}\ ]$

	U^{11}	U^{22}	U^{33}	U^{23}	U^{13}	U^{12}
O(1)	60(1)	16(1)	34(1)	0(1)	28(1)	-1(1)
O(2)	33(1)	22(1)	19(1)	0(1)	12(1)	-1(1)
O(3)	30(1)	23(1)	29(1)	-1(1)	22(1)	-1(1)
O(4)	23(1)	26(1)	26(1)	-2(1)	13(1)	-4(1)
C(1)	33(1)	16(1)	21(1)	2(1)	15(1)	2(1)
C(2)	28(1)	26(1)	22(1)	4(1)	12(1)	9(1)
C(3)	19(1)	25(1)	19(1)	2(1)	8(1)	3(1)
C(4)	20(1)	24(1)	20(1)	1(1)	11(1)	1(1)
C(5)	18(1)	20(1)	18(1)	2(1)	9(1)	0(1)
C(6)	19(1)	18(1)	21(1)	0(1)	10(1)	-1(1)
C(7)	18(1)	19(1)	20(1)	-3(1)	10(1)	-2(1)
C(8)	21(1)	20(1)	18(1)	0(1)	10(1)	-1(1)
C(9)	19(1)	19(1)	17(1)	1(1)	9(1)	1(1)
C(10)	25(1)	18(1)	20(1)	1(1)	12(1)	-1(1)
C(11)	46(1)	26(1)	35(1)	-8(1)	15(1)	0(1)
C(12)	30(1)	31(1)	26(1)	-6(1)	10(1)	-6(1)
C(13)	23(1)	33(1)	29(1)	-2(1)	14(1)	-4(1)
C(14)	23(1)	20(1)	24(1)	-2(1)	15(1)	-2(1)
C(15)	29(1)	35(1)	32(1)	-16(1)	15(1)	-7(1)
C(16)	34(1)	24(1)	35(1)	3(1)	21(1)	5(1)
O(1S)	28(1)	33(1)	34(1)	-5(1)	19(1)	-7(1)

Table 5. Hydrogen coordinates (x 10^4) and isotropic displacement parameters ($Å^2$x 10^3) for **3.67**.

	x	y	z	U(eq)
H(3O)	644(15)	2900(20)	2762(13)	37
H(4O)	1084(15)	-940(20)	-114(11)	37
H(2A)	4672(13)	-2246(19)	702(12)	30
H(2B)	4493(14)	-2878(18)	1635(11)	30
H(3)	4834(12)	-228(19)	2122(9)	25
H(4)	4116(13)	483(18)	114(10)	25
H(5)	2339(12)	1481(18)	-58(9)	22
H(6)	3280(13)	3489(16)	1589(11)	23
H(7)	1220(12)	1666(18)	965(10)	22
H(8)	3301(12)	975(18)	2751(9)	23
H(10)	2438(13)	-2275(18)	1536(10)	24
H(11A)	2045(14)	-5570(20)	-755(13)	44
H(11B)	3298(13)	-4990(20)	-547(13)	44
H(12A)	2318(15)	-3090(20)	-1719(11)	36
H(12B)	1299(12)	-3090(20)	-1417(12)	36
H(13A)	4818(16)	3160(19)	621(12)	41
H(13B)	5135(15)	2670(20)	1723(11)	41
H(13C)	5768(13)	1820(20)	1142(13)	41
H(15A)	2987(15)	3170(20)	3435(13)	47
H(15B)	2228(15)	4660(20)	3358(13)	47
H(15C)	2933(16)	4690(20)	2740(14)	47
H(16A)	134(14)	4030(20)	885(12)	44
H(16B)	518(15)	5230(20)	1807(13)	44
H(16C)	1226(15)	5160(20)	1195(13)	44
H(1S)	208(15)	10260(20)	1765(13)	44
H(2S)	251(15)	9140(20)	1140(13)	44

Table 6. Torsion angles [°] for **3.67**.

C(11)-O(1)-C(1)-O(2)	17.82(14)
C(11)-O(1)-C(1)-C(2)	-104.89(13)
C(11)-O(1)-C(1)-C(10)	137.34(12)
C(12)-O(2)-C(1)-O(1)	2.58(14)
C(12)-O(2)-C(1)-C(2)	127.63(11)
C(12)-O(2)-C(1)-C(10)	-117.95(11)
O(1)-C(1)-C(2)-C(3)	-155.86(10)
O(2)-C(1)-C(2)-C(3)	83.46(11)
C(10)-C(1)-C(2)-C(3)	-34.25(12)
C(1)-C(2)-C(3)-C(4)	-81.30(12)
C(1)-C(2)-C(3)-C(9)	17.53(12)
C(2)-C(3)-C(4)-C(13)	-127.31(12)
C(9)-C(3)-C(4)-C(13)	124.88(11)
C(2)-C(3)-C(4)-C(5)	110.61(11)
C(9)-C(3)-C(4)-C(5)	2.80(9)
C(13)-C(4)-C(5)-C(6)	-37.34(14)
C(3)-C(4)-C(5)-C(6)	84.82(11)
C(13)-C(4)-C(5)-C(9)	-124.92(11)
C(3)-C(4)-C(5)-C(9)	-2.76(9)
C(4)-C(5)-C(6)-C(7)	-149.91(10)
C(9)-C(5)-C(6)-C(7)	-61.09(10)
C(4)-C(5)-C(6)-C(8)	-91.73(10)
C(9)-C(5)-C(6)-C(8)	-2.91(8)
C(5)-C(6)-C(7)-C(8)	80.35(10)
C(5)-C(6)-C(7)-C(14)	-168.83(10)
C(8)-C(6)-C(7)-C(14)	110.82(12)
C(6)-C(7)-C(8)-C(9)	-76.80(10)
C(14)-C(7)-C(8)-C(9)	174.34(10)
C(14)-C(7)-C(8)-C(6)	-108.85(12)
C(7)-C(6)-C(8)-C(9)	114.29(9)
C(5)-C(6)-C(8)-C(9)	3.06(9)
C(5)-C(6)-C(8)-C(7)	-111.23(9)

C(7)-C(8)-C(9)-C(10)	-81.22(13)
C(6)-C(8)-C(9)-C(10)	-137.54(11)
C(7)-C(8)-C(9)-C(3)	142.18(10)
C(6)-C(8)-C(9)-C(3)	85.86(11)
C(7)-C(8)-C(9)-C(5)	53.40(10)
C(6)-C(8)-C(9)-C(5)	-2.93(8)
C(2)-C(3)-C(9)-C(8)	149.60(10)
C(4)-C(3)-C(9)-C(8)	-92.48(11)
C(2)-C(3)-C(9)-C(10)	5.90(12)
C(4)-C(3)-C(9)-C(10)	123.82(10)
C(2)-C(3)-C(9)-C(5)	-120.66(9)
C(4)-C(3)-C(9)-C(5)	-2.74(9)
C(6)-C(5)-C(9)-C(8)	2.98(8)
C(4)-C(5)-C(9)-C(8)	118.52(9)
C(6)-C(5)-C(9)-C(10)	137.15(11)
C(4)-C(5)-C(9)-C(10)	-107.31(12)
C(6)-C(5)-C(9)-C(3)	-112.80(9)
C(4)-C(5)-C(9)-C(3)	2.74(9)
C(8)-C(9)-C(10)-O(4)	68.01(15)
C(3)-C(9)-C(10)-O(4)	-152.31(9)
C(5)-C(9)-C(10)-O(4)	-51.47(15)
C(8)-C(9)-C(10)-C(1)	-166.36(10)
C(3)-C(9)-C(10)-C(1)	-26.68(12)
C(5)-C(9)-C(10)-C(1)	74.17(13)
O(1)-C(1)-C(10)-O(4)	-71.81(13)
O(2)-C(1)-C(10)-O(4)	46.08(13)
C(2)-C(1)-C(10)-O(4)	164.46(10)
O(1)-C(1)-C(10)-C(9)	161.42(10)
O(2)-C(1)-C(10)-C(9)	-80.68(12)
C(2)-C(1)-C(10)-C(9)	37.70(11)
C(1)-O(1)-C(11)-C(12)	-30.01(15)
C(1)-O(2)-C(12)-C(11)	-20.51(14)
O(1)-C(11)-C(12)-O(2)	30.61(15)
C(6)-C(7)-C(14)-O(3)	-154.96(10)

C(8)-C(7)-C(14)-O(3)	-82.62(13)
C(6)-C(7)-C(14)-C(15)	-36.15(16)
C(8)-C(7)-C(14)-C(15)	36.18(16)
C(6)-C(7)-C(14)-C(16)	87.78(13)
C(8)-C(7)-C(14)-C(16)	160.12(11)

Symmetry transformations used to generate equivalent atoms:

Table 7. Hydrogen bonds for **3.67** [Å and °].

D-H...A	d(D-H)	d(H...A)	d(D...A)	<(DHA)
O(1S)-H(1S)...O(3)#1	0.847(15)	2.011(15)	2.8547(15)	173.3(19)
O(1S)-H(2S)...O(4)#1	0.832(15)	2.071(15)	2.9000(14)	173.9(19)
O(3)-H(3O)...O(1S)#2	0.809(14)	2.120(14)	2.9260(14)	175.0(18)
O(4)-H(4O)...O(1S)#3	0.854(14)	2.191(15)	2.9915(15)	156.1(17)

Symmetry transformations used to generate equivalent atoms:

#1 x,y+1,z #2 -x,y-1/2,-z+1/2 #3 -x,-y+1,-z

Computational Details

In order to evaluate the validity of proposed structures for synthetic intermediates, ^{13}C-NMR chemical shifts were calculated using the GIAO (gauge independent atomic orbital) method[206] and compared to experimentally observed spectral data on the basis of average and maximum deviation of chemical shifts. Given the relatively high levels of oxygenation and unsaturation in these sesquiterpene-like compounds, the method used by Rychnovsky for reassignment of the structure of the complex, oxygenated natural product hexacyclinol was employed. The lowest energy conformation of each structure was obtained through a Monte Carlo search using the MMFF force field. This structure was then optimized at the PM3 semiempirical level.[207] An equilibrium geometry for this structure was then obtained using the HF/3-21G method and the GIAO nuclear magnetic shielding tensors were calculated using the density functional mPW1PW91/6-31G(d,p) method.[208] The calculated isotropic chemical

---

[206] Wolinski, K.; Hinton, J. F.; Pulay, P. *J. Am. Chem. Soc.* **1990**, *112*, 8251-8260.

[207] These optimizations were performed using Spartan '04 (Wavefuntion, Inc. Irvine, CA. as described in Kong, J.; White, C. A.; Krylov, A. I.; Sherrill, C. D.; Adamson, R. D.; Furlani, T. R.; Lee, M. S.; Lee, A. M.; Gwaltney, S. R.; Adams, T. R.; Ochsenfeld, C.; Gilbert, A. T. B.; Kedziora, G. S.; Rassolov, V. A.; Maurice, D. R.; Nair, N.; Shao, Y.; Besley, N. A.; Maslen, P. E.; Dombroski, J. P.; Daschel, H.; Zhang, W.; Korambath, P. P.; Baker, J.; Byrd, E. F. C.; Van Voorhis, T.; Oumi, M.; Hirata, S.; Hsu, C.-P.; Ishikawa, N.; Florian, J.; Warshel, A.; Johnson, B. G.; Gill, P. M. W.; Head-Gordon, M.; Pople, J. A. *J. Computational Chem.*, **2000**, *21*, 1532-1548.).

[208] These calculations were performed using Gaussian 03. (*Gaussian 03, Revision D.01*, Frisch, M. J.; Trucks, G. W.; Schlegel, H. B.; Scuseria, G. E.; Robb, M. A.; Cheeseman, J. R.; Montgomery, J. A., Jr.; Vreven, T.; Kudin, K. N.; Burant, J. C.; Millam, J. M.; Iyengar, S. S.; Tomasi, J.; Barone, V.; Mennucci, B.; Cossi, M.; Scalmani, G.; Rega, N.; Petersson, G. A.; Nakatsuji, H.; Hada, M.; Ehara, M.; Toyota, K.; Fukuda, R.; Hasegawa, J.; Ishida, M.; Nakajima, T.; Honda, Y.; Kitao, O.; Nakai, H.; Klene, M.; Li, X.; Knox; H. P. Hratchian; J. B. Cross; V.

shifts were then referenced by subtraction of the average calculated chemical shift for the carbon atoms in tetramethylsilane (196.5461 ppm). In order to minimize effects from electron correlation or solvent, these values were corrected based on the slope and intercept of a least squares fit line generated from a plot of calculated versus experimental values.[209] The average and maximal absolute deviation between these corrected values and the experimental values provided a key measure of the correctness of the proposed structure.[210] A number of guaiane natural products and synthetic intermediates with structures similar to the compounds of interest were selected for analysis to provide a benchmark for the application of these ^{13}C-NMR predictions. This protocol performed well for this class of natural products and provided useful data to support the structural assignment of newly prepared synthetic intermediates.

Enone 3.68

The first synthetic intermediate evaluated was the cycloheptadienone product of the key rearrangement (**3.68**). The chemical shifts for the major isomer isolated

---

Bakken; C. Adamo; J. Jaramillo; R. Gomperts; R. E. Stratmann, J. E.; Yazyev, O.; Austin, A. J.; Cammi, R.; Pomelli, C.; Ochterski, J. W.; Ayala, P. Y.; Morokuma, K.; Voth, G. A.; Salvador, P.; Dannenberg, J. J.; Zakrzewski, V. G.; Dapprich, S.; Daniels, A. D.; Strain, M. C.; Farkas, O.; Malick, D. K.; Rabuck, A. D.; Raghavachari, K.; Foresman, J. B.; Ortiz; Q. Cui; A. G. Baboul; S. Clifford; J. Cioslowski; B. B. Stefanov; G. Liu; A. Liashenko; P. Piskorz, J. V.; Komaromi, I.; Martin, R. L.; Fox, D. J.; Keith, T.; Al-Laham, M. A.; Peng, C. Y.; Nanayakkara, A.; Challacombe, M.; Gill, P. M. W.; Johnson, B.; Chen, W.; Wong, M. W.; Gonzalez, C.; Pople, J. A. Gaussian, Inc., Wallingford CT, 2004.)

[209] Barone, G.; Gomez-Paloma, L.; Duca, D.; Silvestri, A.; Riccio, R.; Bifulco, G. *Chem. Eur. J.* **2002**, *8*, 3233-3239. The correlation coefficient of this line also gave a measure of the quality of the spectral prediction. The correlation plots are provided along with the comparison tables and atomic Cartesian coordinates for each calculated structure.

[210] Average deviation of approximately 2 ppm is generally considered acceptable and deviations greater than 5 ppm indicate a poor fit with the proposed structure.

from this reaction match the calculated data with an average deviation of 1.6 ppm and maximum deviation of 4.7 ppm indicating that the proposed structure is likely accurate.

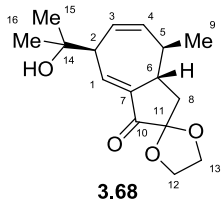

3.68

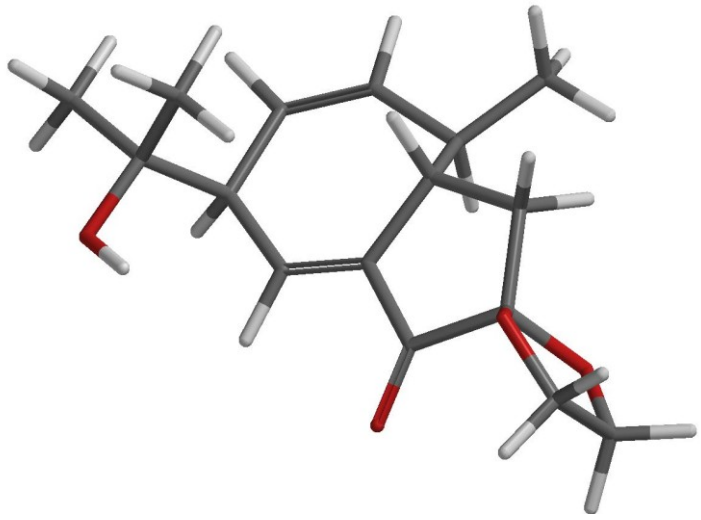

Standard orientation:

Center Number	Atomic Number	Atomic Type	Coordinates (Angstroms) X	Y	Z
1	6	0	-1.044337	-0.634449	-0.393788
2	1	0	-1.082764	-1.661722	-0.702327
3	6	0	-2.400814	0.036474	-0.362208
4	1	0	-2.632070	0.298097	-1.394417
5	6	0	-2.480916	1.283404	0.496268
6	1	0	-3.322373	1.350612	1.158549
7	6	0	-1.630626	2.287719	0.482278
8	1	0	-1.808344	3.118948	1.141928
9	6	0	-0.364842	2.367590	-0.349264
10	1	0	-0.590094	2.149590	-1.389236
11	6	0	0.607960	1.292673	0.163408
12	1	0	0.717777	1.393741	1.237775
13	6	0	0.150595	-0.123494	-0.166881
14	6	0	2.030699	1.337722	-0.462733
15	1	0	2.672304	2.083187	-0.020751
16	1	0	1.967388	1.478620	-1.535161
17	6	0	0.238495	3.782456	-0.253543
18	1	0	-0.490036	4.524132	-0.562869
19	1	0	1.109349	3.884386	-0.888870
20	1	0	0.532241	3.998991	0.768916
21	6	0	1.354705	-0.966350	-0.345420
22	6	0	2.563211	-0.051207	-0.192756
23	8	0	2.977965	-0.167955	1.186740

24	6	0	4.181221	-0.983942	1.242985
25	1	0	4.025195	-1.806452	1.921373
26	1	0	4.998566	-0.366448	1.580807
27	6	0	4.383358	-1.452548	-0.216838
28	1	0	5.412039	-1.441465	-0.533100
29	1	0	3.924861	-2.410004	-0.391912
30	8	0	3.670353	-0.433158	-0.973283
31	8	0	1.400453	-2.156311	-0.567156
32	6	0	-3.478556	-1.007168	0.032247
33	6	0	-4.899936	-0.464686	-0.168164
34	1	0	-5.618463	-1.255722	0.022894
35	1	0	-5.022020	-0.136409	-1.192637
36	1	0	-5.123627	0.356110	0.498653
37	6	0	-3.274233	-1.535663	1.456159
38	1	0	-4.006340	-2.307598	1.675477
39	1	0	-3.391695	-0.746472	2.186376
40	1	0	-2.284684	-1.960963	1.559693
41	8	0	-3.273211	-2.080429	-0.923660
42	1	0	-3.807602	-2.851526	-0.692789

SCF Done: E(RmPW+HF-PW91) = -923.602421378 A.U.

Carbon	Raw GIAO Shift	Relative GIAO Shift (TMS)	Scaled Chemical Shift	Experimental Chemical Shift	Difference	|Difference|
10	0.4016	196.14445	201.7	201.703	0.0	0.0
4	61.7101	134.83595	137.8	139.6	-1.8	1.8
1	62.1508	134.39525	137.4	137.109	0.3	0.3
7	62.4791	134.06695	137.0	136.666	0.4	0.4
3	73.1154	123.43065	126.0	126.476	-0.5	0.5
11	89.3909	107.15515	109.0	108.107	0.9	0.9
14	121.9845	74.56155	75.0	73.538	1.5	1.5
13	127.844	68.70205	68.9	66.209	2.7	2.7
12	131.3192	65.22685	65.3	65.073	0.3	0.3
2	147.7835	48.76255	48.2	52.499	-4.3	4.3
6	155.2275	41.31855	40.4	38.782	1.6	1.6
5	157.7434	38.80265	37.8	35.298	2.5	2.5

8	160.4934	36.05265	34.9	34.016	0.9	0.9
15	167.8867	28.65935	27.2	28.379	-1.2	1.2
16	171.8154	24.73065	23.1	27.859	-4.7	4.7
9	177.5228	19.02325	17.2	15.794	1.4	1.4
					AVG	1.6
					MAX	4.7

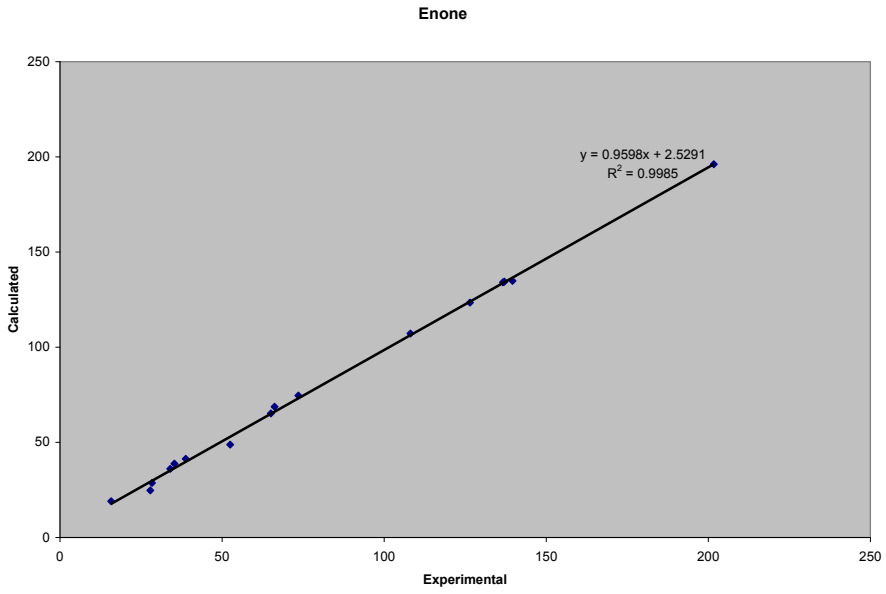

Diol 3.74

The next synthetic intermediate to be evaluated was diol **3.74** from methylation of enone **3.68**. Spectral data was calculated for each of four possible diastereomers of this compound representing retention or inversion of the ring junction stereocenter at C1 and methylation of the carbonyl at C4 to form either the α- or β-methyl tertiary alcohol. The diasteromer with the expected *syn* relationship between the methyl group and ring junction stereocenter and the

β-methyl tertiary alcohol proved to be the best match with the experimental data. The average deviation was 2.2 ppm and the maximum was 5.0 ppm which was the lowest of the group and suggests that this structure is likely correct for synthetic intermediate **3.74**.

αMeSynKetal

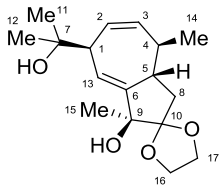

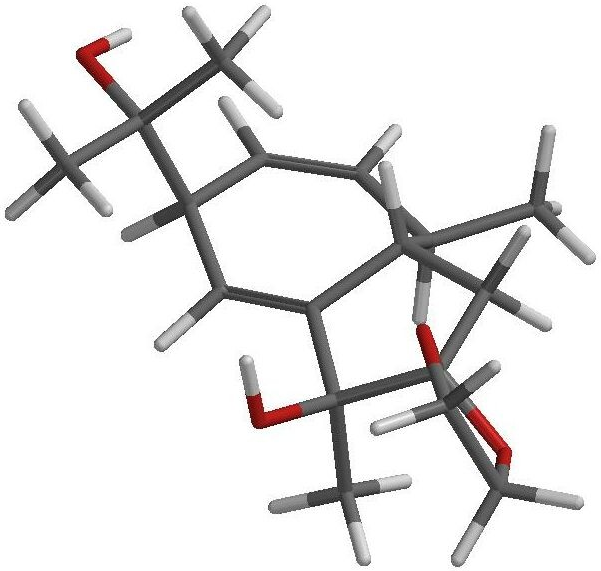

Standard orientation:

Center Number	Atomic Number	Atomic Type	Coordinates (Angstroms) X	Y	Z
1	6	0	2.477875	-0.269059	0.769494
2	1	0	3.049017	-0.504064	1.665150
3	6	0	2.861435	1.155865	0.436503
4	1	0	3.930373	1.270314	0.424579
5	6	0	2.153217	2.249986	0.228043
6	1	0	2.721877	3.152973	0.077164
7	6	0	0.653586	2.481290	0.162251

```
    8          1             0        0.293848    2.737769    1.155555
    9          6             0       -0.114092    1.241418   -0.322648
   10          1             0        0.297094    0.933084   -1.275076
   11          6             0       -0.034717    0.070353    0.651769
   12          6             0        3.046364   -1.253719   -0.303095
   13          6             0       -1.640772    1.477919   -0.504731
   14          1             0       -1.904686    1.769153   -1.510034
   15          1             0       -2.012253    2.217620    0.191226
   16          6             0       -1.437696   -0.379179    1.031261
   17          6             0       -2.256485    0.140588   -0.151093
   18          8             0        4.471903   -0.995003   -0.431191
   19          1             0        4.635580   -0.321789   -1.103731
   20          6             0        2.970535   -2.702495    0.180830
   21          1             0        3.468186   -3.337494   -0.540728
   22          1             0        1.945279   -3.027682    0.294436
   23          1             0        3.487255   -2.800613    1.127680
   24          6             0        2.363991   -1.097813   -1.663974
   25          1             0        2.834422   -1.763553   -2.378691
   26          1             0        2.458278   -0.078966   -2.023279
   27          1             0        1.312692   -1.339697   -1.595388
   28          6             0        1.033783   -0.559350    1.079589
   29          1             0        0.868753   -1.403939    1.724768
   30          6             0        0.396568    3.684020   -0.776938
   31          1             0       -0.654410    3.940814   -0.815971
   32          1             0        0.732831    3.450018   -1.781967
   33          1             0        0.939583    4.557044   -0.431591
   34          6             0       -1.902347    0.231039    2.348987
   35          1             0       -2.946850    0.002154    2.504672
   36          1             0       -1.769287    1.304136    2.354142
   37          1             0       -1.316530   -0.197363    3.150896
   38          8             0       -1.561574   -1.800124    1.171545
   39          1             0       -1.335974   -2.189208    0.314188
   40          8             0       -2.063442   -0.817615   -1.228333
   41          8             0       -3.657287    0.205035    0.064451
   42          6             0       -4.239627   -1.034327   -0.422236
   43          1             0       -4.130667   -1.805100    0.323697
   44          1             0       -5.274018   -0.851065   -0.655898
   45          6             0       -3.361061   -1.321283   -1.647241
   46          1             0       -3.702683   -0.774212   -2.512920
   47          1             0       -3.267849   -2.370198   -1.875273
 -------------------------------------------------------------------
SCF Done:  E(RmPW+HF-PW91) =  -964.124097831     A.U.
```

Carbon	Raw GIAO Shift	Relative GIAO Shift (TMS)	Scaled Chemical Shift	Experimental Chemical Shift	Difference	|Difference|
6	49.8905	146.65555	149.6	147.1	1.9	1.9
3	65.4978	131.04825	133.5	136.4	-3.3	3.3

2	72.8209	123.72515	126.0	127.9	-2.2	2.2
13	76.5313	120.01475	122.1	122.3	-0.4	0.4
10	79.281	117.26505	119.3	115.5	3.6	3.6
9	115.4138	81.13225	82.1	80.3	2.0	2.0
7	119.2079	77.33815	78.2	73.7	4.8	4.8
16	128.3004	68.24565	68.8	70	-0.8	0.8
17	130.6321	65.91395	66.4	65.7	1.1	1.1
1	142.576	53.97005	54.1	55	-0.3	0.3
5	152.3084	44.23765	44.1	51.5	-6.7	6.7
4	158.0935	38.45255	38.1	40.3	-1.4	1.4
8	160.8769	35.66915	35.3	35.6	0.5	0.5
11	169.3226	27.22345	26.6	29.6	-2.1	2.1
12	172.371	24.17505	23.4	27.6	-3.2	3.2
15	173.0566	23.48945	22.7	21.8	1.9	1.9
14	175.0581	21.48795	20.7	16.7	4.9	4.9
					AVG	2.4
					MAX	6.7

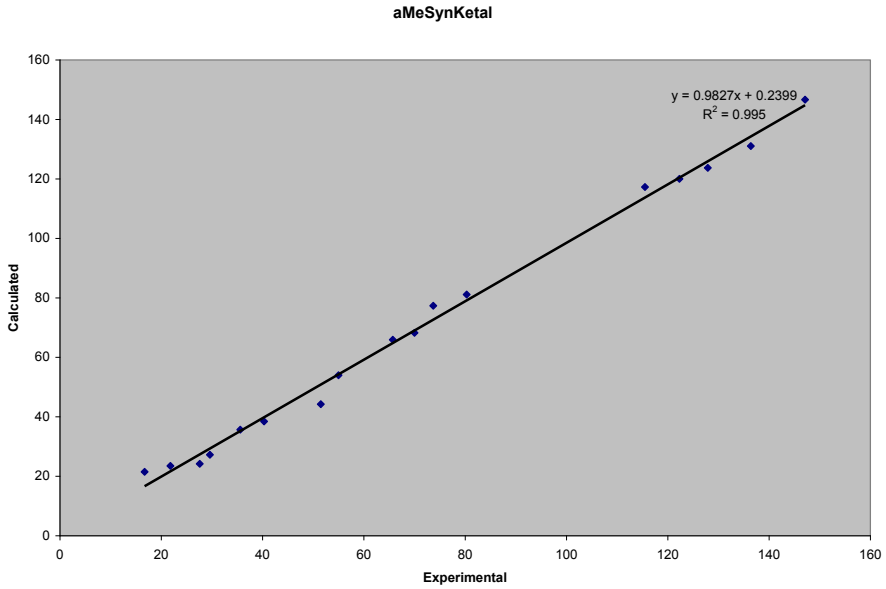

βMeSynKetal (3.74)

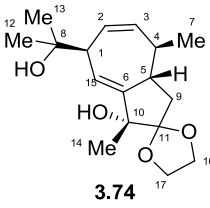

3.74

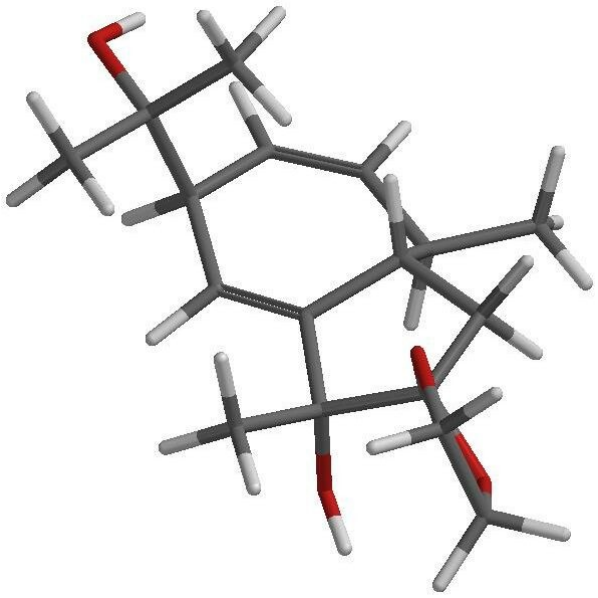

Standard orientation:

Center Number	Atomic Number	Atomic Type	Coordinates (Angstroms) X	Y	Z
1	6	0	2.535271	-0.202847	0.730772
2	1	0	3.143476	-0.404179	1.609835
3	6	0	2.854886	1.229826	0.369373
4	1	0	3.917226	1.386028	0.315048
5	6	0	2.091139	2.289890	0.187180
6	1	0	2.610256	3.217177	0.008426
7	6	0	0.580143	2.441142	0.182111
8	1	0	0.232358	2.630005	1.193447
9	6	0	-0.131294	1.173365	-0.321473
10	1	0	0.289407	0.887171	-1.276025
11	6	0	0.003091	0.012132	0.668044
12	6	0	0.228908	3.660156	-0.703996
13	1	0	0.740783	4.546867	-0.345657
14	1	0	-0.833631	3.865716	-0.695350
15	1	0	0.538710	3.479962	-1.728753
16	6	0	3.101284	-1.186025	-0.344447
17	6	0	-1.666259	1.355914	-0.481983
18	1	0	-1.954868	1.645337	-1.481480
19	1	0	-2.037136	2.067191	0.239615
20	6	0	-1.385015	-0.423101	1.098694
21	6	0	-2.223294	-0.003112	-0.103364
22	8	0	4.513261	-0.884336	-0.520447
23	1	0	4.632084	-0.204720	-1.196015
24	6	0	3.087698	-2.628348	0.163826
25	1	0	3.586636	-3.258084	-0.561427
26	1	0	2.076691	-2.984447	0.308885
27	1	0	3.632829	-2.694090	1.097607
28	6	0	2.374114	-1.076802	-1.686302
29	1	0	2.847423	-1.737928	-2.403449
30	1	0	2.422834	-0.061675	-2.064668
31	1	0	1.334579	-1.354265	-1.582536
32	6	0	-1.565612	-1.884195	1.471432
33	1	0	-1.221036	-2.521942	0.671032
34	1	0	-2.617032	-2.076715	1.655972
35	1	0	-1.021500	-2.106474	2.379666
36	6	0	1.112799	-0.541486	1.097851
37	1	0	1.029975	-1.352192	1.797768
38	8	0	-1.780835	0.449497	2.181971
39	1	0	-2.746518	0.411433	2.261986
40	8	0	-2.070486	-0.929238	-1.190431
41	8	0	-3.611852	-0.016636	0.241226
42	6	0	-4.361784	-0.569799	-0.868565
43	1	0	-5.239143	-1.055528	-0.476368
44	1	0	-4.639189	0.216190	-1.555702
45	6	0	-3.348534	-1.540277	-1.500854
46	1	0	-3.444054	-1.615187	-2.571273
47	1	0	-3.407119	-2.518542	-1.048928

SCF Done: E(RmPW+HF-PW91) = -964.119244225 A.U.

Carbon	Raw GIAO Shift	Relative GIAO Shift (TMS)	Scaled Chemical Shift	Experimental Chemical Shift	Difference	|Difference|
6	53.1795	143.36655	146.2	147.1	-1.6	1.6
3	64.141	132.40505	134.9	136.4	-2.0	2.0
2	74.1724	122.37365	124.6	127.9	-3.7	3.7
15	75.2777	121.26835	123.5	122.3	0.8	0.8
11	77.8653	118.68075	120.8	115.5	5.0	5.0
10	115.6869	80.85915	81.9	80.3	1.8	1.8
8	119.1309	77.41515	78.4	73.7	4.9	4.9
17	128.7954	67.75065	68.4	70	-1.2	1.2
16	129.3283	67.21775	67.9	65.7	2.6	2.6
1	142.2759	54.27015	54.5	55	0.1	0.1
5	150.1745	46.37155	46.4	51.5	-4.4	4.4
4	158.212	38.33405	38.1	40.3	-1.3	1.3
9	159.0909	37.45515	37.2	35.6	2.5	2.5
12	169.2627	27.28335	26.8	29.6	-1.9	1.9
13	172.3086	24.23745	23.6	27.6	-2.9	2.9
7	174.8597	21.68635	21.0	21.8	0.3	0.3
14	179.1592	17.38685	16.6	16.7	1.0	1.0
					AVG	2.2
					MAX	5.0

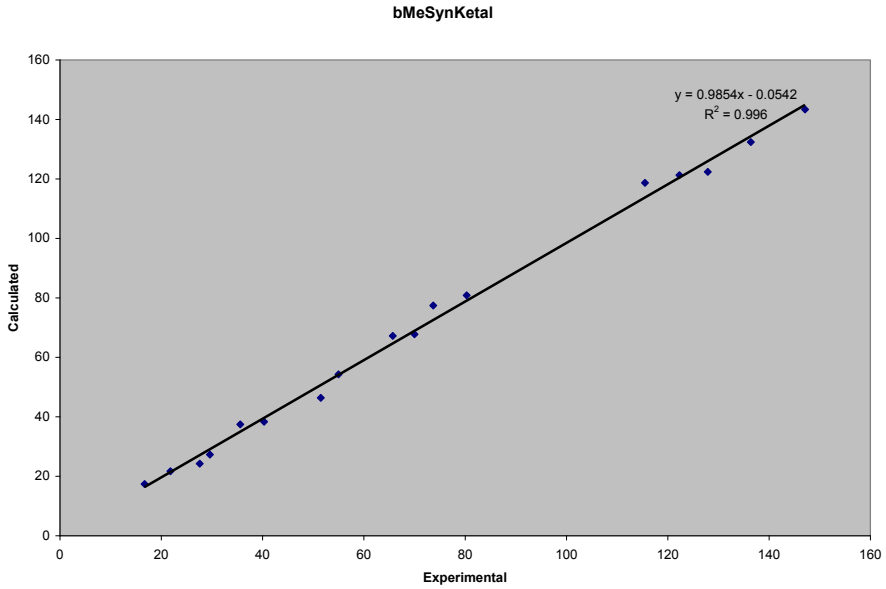

αMeAntiKetal

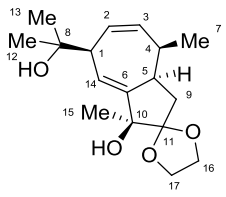

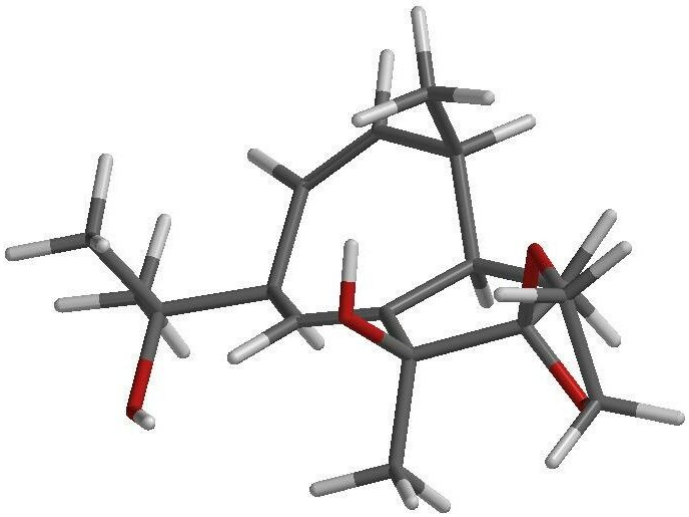

Center Number	Atomic Number	Atomic Type	Coordinates (Angstroms) X	Y	Z
1	6	0	-2.474250	-0.150486	-0.700978
2	1	0	-2.838389	-0.531995	-1.655159
3	6	0	-2.672308	1.348184	-0.717550
4	1	0	-3.683191	1.619638	-0.965399
5	6	0	-1.847594	2.353984	-0.494142
6	1	0	-2.272538	3.341912	-0.556046
7	6	0	-0.370403	2.342334	-0.157618
8	1	0	0.013828	3.326848	-0.412044
9	6	0	0.405523	1.338295	-1.035601
10	6	0	0.086990	-0.116384	-0.729176
11	6	0	-0.160135	2.141285	1.358774
12	1	0	0.887994	2.154057	1.617126
13	1	0	-0.564274	1.189143	1.665312
14	6	0	-3.422818	-0.822091	0.347814
15	6	0	1.955232	1.449708	-0.871687
16	1	0	2.251836	2.297003	-0.271475
17	1	0	2.442556	1.517831	-1.833837
18	6	0	1.385613	-0.907063	-0.659897
19	6	0	2.401712	0.152053	-0.219135
20	8	0	-3.282978	-2.262579	0.188361
21	1	0	-2.711897	-2.634956	0.871240
22	6	0	-3.081036	-0.416337	1.782765
23	1	0	-3.728454	-0.943738	2.474964
24	1	0	-3.214215	0.647480	1.917998
25	1	0	-2.049902	-0.659949	2.013507
26	6	0	-4.900185	-0.554509	0.044628
27	1	0	-5.499145	-1.175100	0.698357
28	1	0	-5.123587	-0.832963	-0.978123
29	1	0	-5.165421	0.481332	0.203791
30	6	0	-1.076185	-0.700850	-0.557897
31	1	0	-1.056540	-1.756839	-0.369836
32	6	0	1.747772	-1.478599	-2.027642
33	1	0	2.727236	-1.931939	-1.987702
34	1	0	1.748302	-0.705489	-2.784655
35	1	0	1.013589	-2.227444	-2.291663
36	8	0	1.342351	-2.008206	0.255198
37	1	0	1.238915	-1.630387	1.140947
38	1	0	0.144328	1.550112	-2.066229
39	1	0	-0.671354	2.926251	1.905892
40	8	0	3.755851	-0.161945	-0.525616
41	8	0	2.341244	0.214171	1.232391
42	6	0	4.324797	-0.844941	0.621784
43	1	0	5.394331	-0.730571	0.586425
44	1	0	4.035491	-1.883800	0.610770
45	6	0	3.652451	-0.097582	1.779608
46	1	0	4.174557	0.817546	2.013805
47	1	0	3.523120	-0.697503	2.665066

SCF Done: E(RmPW+HF-PW91) = -964.119825772 A.U.

Carbon	Raw GIAO Shift	Relative GIAO Shift (TMS)	Scaled Chemical Shift	Experimental Chemical Shift	Difference	|Difference|
6	53.1614	143.38465	146.6	147.1	-0.5	0.5
3	65.1364	131.40965	134.3	136.4	-2.1	2.1
2	73.5666	122.97945	125.6	127.9	-2.3	2.3
14	78.2393	118.30675	120.8	122.3	-1.5	1.5
11	78.568	117.97805	120.5	115.5	5.0	5.0
10	113.1314	83.41465	85.1	80.3	4.8	4.8
8	120.8977	75.64835	77.1	73.7	3.4	3.4
16	129.2213	67.32475	68.6	70	-1.4	1.4
17	130.4097	66.13635	67.4	65.7	1.7	1.7
1	140.7631	55.78295	56.7	55	1.7	1.7
5	155.5755	40.97055	41.6	51.5	-9.9	9.9
4	155.8469	40.69915	41.3	40.3	1.0	1.0
9	159.9516	36.59445	37.1	35.6	1.5	1.5
13	168.9509	27.59515	27.8	29.6	-1.8	1.8
12	171.4212	25.12485	25.3	27.6	-2.3	2.3
15	172.7078	23.83825	24.0	21.8	2.2	2.2
7	179.2544	17.29165	17.3	16.7	0.6	0.6
					AVG	2.6
					MAX	9.9

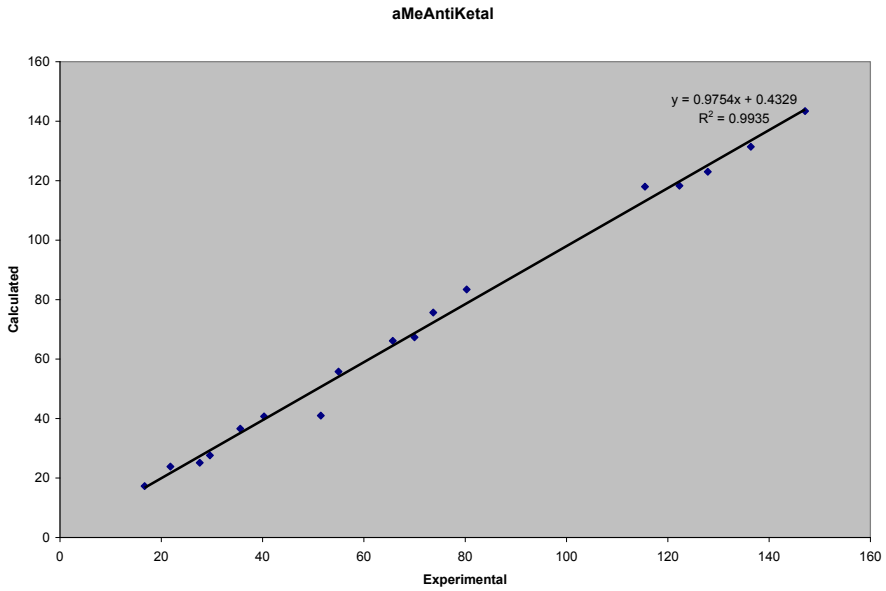

βMeAntiKetal

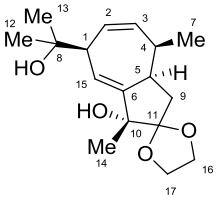

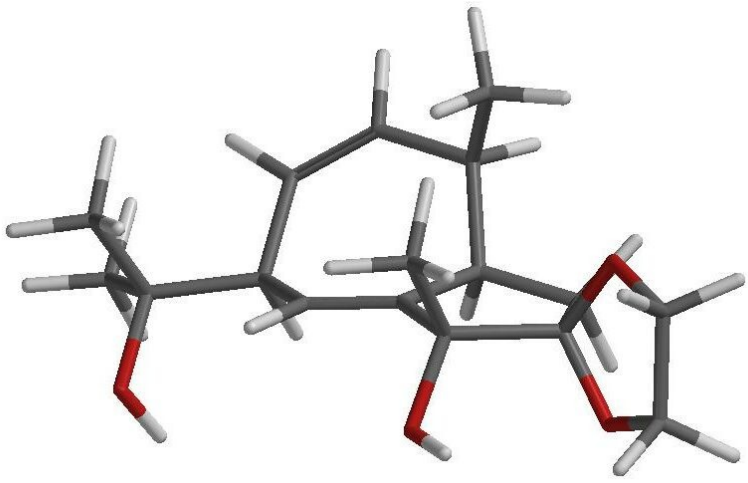

Standard orientation:

Center Number	Atomic Number	Atomic Type	Coordinates (Angstroms) X	Y	Z
1	6	0	-2.511254	-0.090336	-0.668655
2	1	0	-2.844353	-0.434170	-1.652492
3	6	0	-2.641064	1.416459	-0.680900
4	1	0	-3.645276	1.734766	-0.897687
5	6	0	-1.760508	2.379675	-0.491066
6	1	0	-2.137730	3.387618	-0.539717
7	6	0	-0.277116	2.291811	-0.205881
8	1	0	0.155120	3.238494	-0.520278
9	6	0	0.407295	1.200866	-1.055737
10	6	0	0.044241	-0.218899	-0.634293
11	6	0	-0.035912	2.152011	1.313554
12	1	0	-0.472946	2.998626	1.832835
13	1	0	1.017775	2.099606	1.540445
14	1	0	-0.499827	1.247859	1.679138
15	6	0	-3.530421	-0.720725	0.338500
16	6	0	1.964253	1.253791	-0.984127
17	1	0	2.333229	2.153991	-0.514265
18	1	0	2.381346	1.160658	-1.975097
19	6	0	1.320876	-1.034949	-0.545326
20	6	0	2.382091	0.011156	-0.206715
21	8	0	-3.415895	-2.170081	0.258240
22	1	0	-3.710963	-2.480456	-0.609895
23	6	0	-3.187981	-0.387100	1.785978
24	1	0	-3.882862	-0.894261	2.443514
25	1	0	-3.244476	0.679965	1.951788
26	1	0	-2.188578	-0.729159	2.016688
27	6	0	-4.985771	-0.345957	0.019729
28	1	0	-5.633501	-0.976770	0.615530
29	1	0	-5.211216	-0.515460	-1.029853
30	1	0	-5.197923	0.687093	0.255645
31	6	0	1.322756	-2.220643	0.402438
32	1	0	1.076691	-1.902799	1.404561
33	1	0	2.306630	-2.677704	0.400559
34	1	0	0.611105	-2.963157	0.068394
35	6	0	-1.153769	-0.723424	-0.452616
36	1	0	-1.242007	-1.753746	-0.173303
37	8	0	1.610048	-1.444312	-1.903169
38	1	0	2.557162	-1.642783	-1.959109
39	1	0	0.100823	1.348552	-2.083907
40	8	0	2.467332	0.269349	1.202350
41	8	0	3.672783	-0.503354	-0.581810
42	6	0	4.632271	-0.181705	0.452498
43	1	0	5.076935	0.783625	0.258855
44	1	0	5.387663	-0.949182	0.466645
45	6	0	3.756164	-0.155256	1.714473
46	1	0	4.084687	0.561183	2.448541
47	1	0	3.671443	-1.135851	2.156424

SCF Done: E(RmPW+HF-PW91) = -964.115769920 A.U.

Carbon	Raw GIAO Shift	Relative GIAO Shift (TMS)	Scaled Chemical Shift	Experimental Chemical Shift	Difference	|Difference|
6	56.4237	140.12235	142.8	147.1	-4.3	4.3
3	63.6741	132.87195	135.4	136.4	-1.0	1.0
2	75.7357	120.81035	123.1	127.9	-4.8	4.8
15	76.0502	120.49585	122.8	122.3	0.5	0.5
11	76.6598	119.88625	122.2	115.5	6.7	6.7
10	113.1671	83.37895	84.9	80.3	4.6	4.6
8	120.3951	76.15095	77.5	73.7	3.8	3.8
17	128.0983	68.44775	69.6	70	-0.4	0.4
16	130.2476	66.29845	67.4	65.7	1.7	1.7
1	139.6926	56.85345	57.8	55	2.8	2.8
5	152.2542	44.29185	45.0	51.5	-6.5	6.5
4	156.0822	40.46385	41.0	40.3	0.7	0.7
9	156.2921	40.25395	40.8	35.6	5.2	5.2
13	167.6224	28.92365	29.3	29.6	-0.3	0.3
12	174.0957	22.45035	22.6	27.6	-5.0	5.0
7	179.2024	17.34365	17.4	21.8	-4.4	4.4
14	179.3781	17.16795	17.2	16.7	0.5	0.5
					AVG	3.1
					MAX	6.7

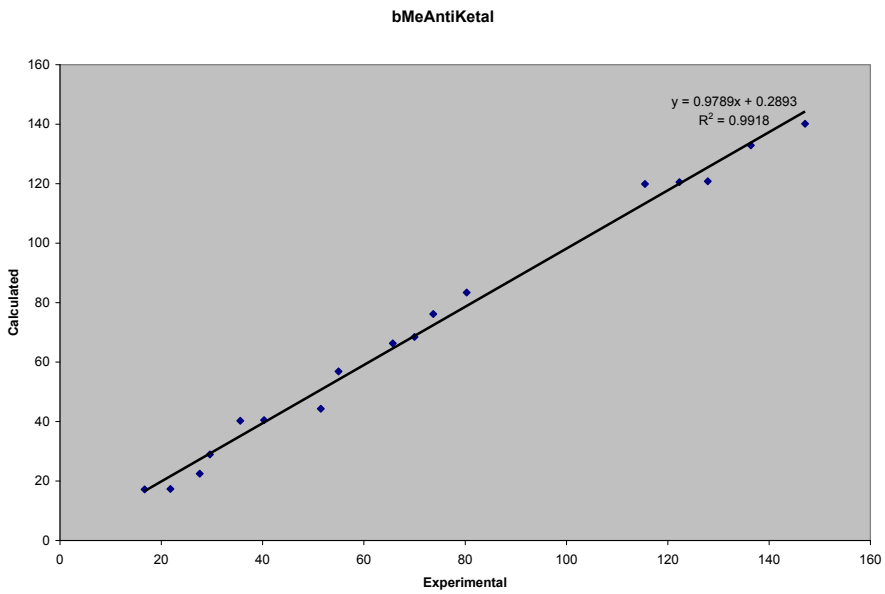

Unsaturated Enone 3.75

Intermediate **3.75** represents an important final branch point in the synthesis and is a precursor to 8-desangeloyloxytorilin, torilolone and torilin. Unfortunately, due to limited material (0.3 mg) of low purity, only a partial carbon spectrum was obtained. Assuming that the peaks with the longest relaxation times (carbonyl and tetrasubstituted enone) were not observed and selecting the major remaining peaks in the spectrum allowed comparison with the calculated data. Unfortunately, while the disubstituted olefin peaks showed good agreement (0.5 ppm average deviation), the overall spectrum deviated by an average of 6.0 ppm and a maximum of 11.9 ppm from the calculated chemical shifts. This poor correlation can likely be attributed to the removal of peaks that were not observed and possible inclusion of peaks from the remaining impurity.

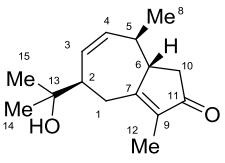

3.75

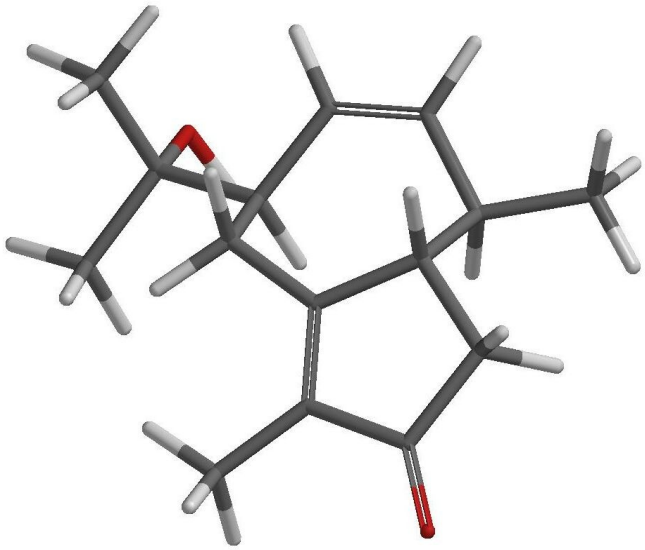

Standard orientation:

Center Number	Atomic Number	Atomic Type	Coordinates (Angstroms) X	Y	Z
1	1	0	-0.747298	-0.222186	1.818442
2	6	0	-0.569633	-0.625588	0.828242
3	1	0	-0.824282	-1.676101	0.843412
4	6	0	-1.477671	0.128853	-0.180693
5	1	0	-1.094566	-0.064530	-1.180741
6	6	0	-1.423408	1.615549	0.094868
7	1	0	-2.358799	2.074000	0.346001
8	6	0	-0.339132	2.361225	0.047251
9	1	0	-0.438546	3.403715	0.293837
10	6	0	1.064031	1.930164	-0.355102
11	1	0	1.040622	1.516933	-1.360651
12	6	0	1.642852	0.835214	0.584431
13	1	0	1.589209	1.207460	1.602036
14	6	0	0.886690	-0.495261	0.486617
15	6	0	1.962024	3.188981	-0.353739
16	1	0	1.527955	3.952727	-0.989585
17	1	0	2.959243	2.984477	-0.717017
18	1	0	2.038356	3.589167	0.652465
19	6	0	1.656863	-1.502152	0.093623
20	6	0	3.096184	0.435899	0.213207
21	1	0	3.791185	0.611763	1.024677
22	1	0	3.462768	0.957988	-0.659008
23	6	0	3.047889	-1.051432	-0.104082
24	6	0	1.301610	-2.946447	-0.126195
25	1	0	0.508877	-3.057867	-0.857810
26	1	0	0.985352	-3.422666	0.796248
27	1	0	2.179419	-3.464629	-0.490292
28	6	0	-2.942684	-0.382745	-0.142812
29	6	0	-3.078660	-1.748866	-0.830042

```
   30          1             0       -4.124147   -2.029415   -0.853257
   31          1             0       -2.523585   -2.517468   -0.309039
   32          1             0       -2.715542   -1.698271   -1.852216
   33          6             0       -3.524905   -0.427811    1.270623
   34          1             0       -4.585891   -0.626365    1.195253
   35          1             0       -3.396573    0.523831    1.769455
   36          1             0       -3.061945   -1.205212    1.863567
   37          8             0       -3.792896    0.568783   -0.837090
   38          1             0       -3.512301    0.665039   -1.758271
   39          8             0        3.978921   -1.743269   -0.454745
 ---------------------------------------------------------------------
SCF Done:  E(RmPW+HF-PW91) =  -735.135219581     A.U.
```

Carbon	Raw GIAO Shift	Relative GIAO Shift (TMS)	Scaled Chemical Shift	Experimental Chemical Shift	Difference	|Difference|
11	-0.0353	196.58135				
7	28.0216	168.52445				
9	64.3321	132.21395	131.0	130.2	0.8	0.8
4	65.5758	130.97025	129.8	130	-0.2	0.2
3	66.2397	130.30635				
13	122.3937	74.15235	71.3	79.3	-8.0	8.0
2	147.2712	49.27485	45.6	36.1	9.5	9.5
6	148.7799	47.76615	44.1	32.2	11.9	11.9
5	157.0384	39.50765	35.6	31.2	4.4	4.4
10	157.3983	39.14775	35.2	29.6	5.6	5.6
1	161.3759	35.17015	31.1	27.4	3.7	3.7
14	167.8686	28.67745	24.4	27.4	-3.0	3.0
8	174.0347	22.51135	18.1	25.7	-7.6	7.6
15	175.0616	21.48445	17.0	22.9	-5.9	5.9
12	188.5149	8.03115	3.2	14.3	-11.1	11.1

					AVG	6.0
					MAX	11.9

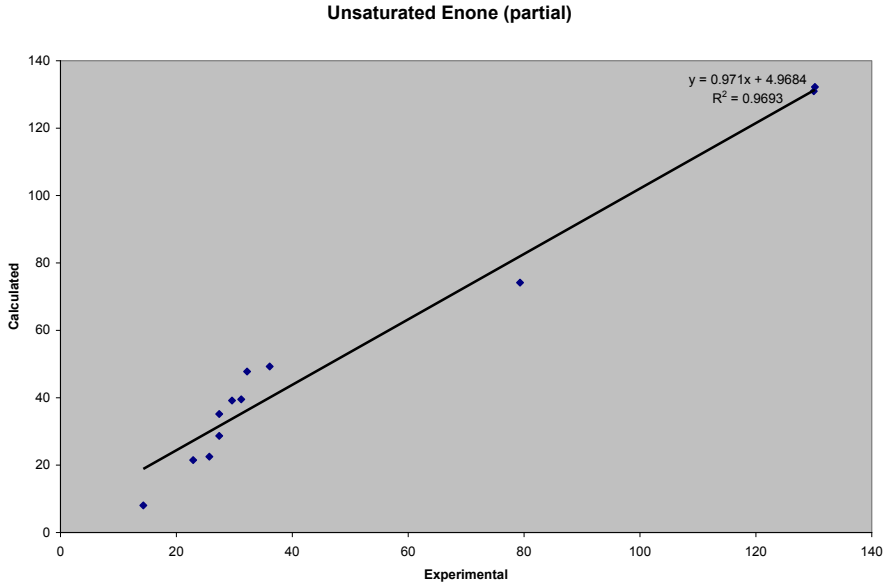

1-*epi*-hydroxycolorenone (Deprés intermediate, 3.17)

Since no carbon spectrum could be obtained, this intermediate was compared to published spectral data[101] to provide a benchmark for these predictions. The average deviation of 1.9 ppm and maximum of 5.4 ppm were both found to be acceptable.

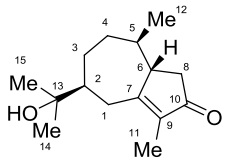

3.17

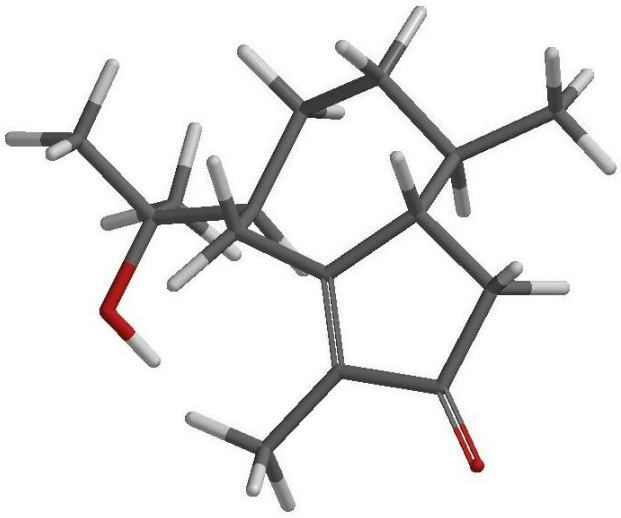

Standard orientation:

Center Number	Atomic Number	Atomic Type	Coordinates (Angstroms) X	Y	Z
1	1	0	0.659385	0.302742	-1.912993
2	6	0	0.572725	-0.326141	-1.034984
3	1	0	0.959345	-1.302968	-1.275322
4	6	0	1.403942	0.256297	0.139509
5	1	0	0.914537	-0.063388	1.055170
6	6	0	1.428920	1.798905	0.128727
7	1	0	1.658701	2.153571	1.127666
8	1	0	2.224708	2.144608	-0.522281
9	6	0	0.121575	2.480679	-0.340254
10	1	0	0.037815	2.421035	-1.420445
11	1	0	0.218629	3.535607	-0.104022
12	6	0	-1.196454	1.956073	0.285378
13	1	0	-1.013509	1.631300	1.305482
14	6	0	-1.781655	0.765801	-0.516463
15	1	0	-1.975062	1.122081	-1.525295
16	6	0	-0.858180	-0.448321	-0.602028
17	6	0	-3.076785	0.179923	0.102190
18	1	0	-3.958975	0.372230	-0.493679
19	1	0	-3.252430	0.565620	1.099433
20	6	0	-1.439339	-1.573613	-0.205705
21	6	0	-2.831633	-1.321820	0.213592
22	6	0	-0.870454	-2.962760	-0.152288
23	1	0	0.196572	-2.949915	0.026363
24	1	0	-1.053342	-3.489127	-1.084548
25	1	0	-1.360655	-3.520479	0.636560
26	6	0	-2.221126	3.112356	0.303368
27	1	0	-2.386911	3.476129	-0.706324
28	1	0	-1.850173	3.936292	0.902902

```
   29          1             0       -3.174456    2.803236    0.712952
   30          6             0        2.812371   -0.384024    0.189020
   31          6             0        3.605542    0.092048    1.414410
   32          1             0        4.513528   -0.492858    1.494810
   33          1             0        3.026939   -0.042997    2.324163
   34          1             0        3.870945    1.137292    1.331702
   35          6             0        3.628937   -0.185765   -1.088106
   36          1             0        4.553050   -0.741841   -0.997158
   37          1             0        3.862027    0.857923   -1.249874
   38          1             0        3.094555   -0.569936   -1.945993
   39          8             0        2.641027   -1.830094    0.278261
   40          1             0        2.315317   -2.073139    1.156111
   41          8             0       -3.624885   -2.151261    0.602543
 ---------------------------------------------------------------------
 SCF Done:  E(RmPW+HF-PW91) =  -736.371607125     A.U.
```

Carbon	Raw GIAO Shift	Relative GIAO Shift (TMS)	Scaled Chemical Shift	Experimental Chemical Shift	Difference	|Difference|
10	-0.861	197.40705	206.6	209.2	-2.6	2.6
7	26.8023	169.74375	177.3	176.9	0.4	0.4
9	65.0908	131.45525	136.8	135.6	1.2	1.2
13	121.5052	75.04085	77.2	73.7	3.5	3.5
6	144.869	51.67705	52.5	51	1.5	1.5
2	145.1927	51.35335	52.1	46.7	5.4	5.4
8	155.8866	40.65945	40.8	42.2	-1.4	1.4
5	158.5124	38.03365	38.0	39.9	-1.9	1.9
4	162.6631	33.88295	33.6	32.5	1.1	1.1
1	167.4862	29.05985	28.5	29.1	-0.6	0.6
3	167.6359	28.91015	28.4	27.9	0.5	0.5
14	168.0569	28.48915	27.9	27.2	0.7	0.7
12	173.0184	23.52765	22.7	25.9	-3.2	3.2
15	176.6629	19.88315	18.8	23.2	-4.4	4.4

11	187.3548	9.19125	7.5	7.8	-0.3	0.3
					AVG	1.9
					MAX	5.4

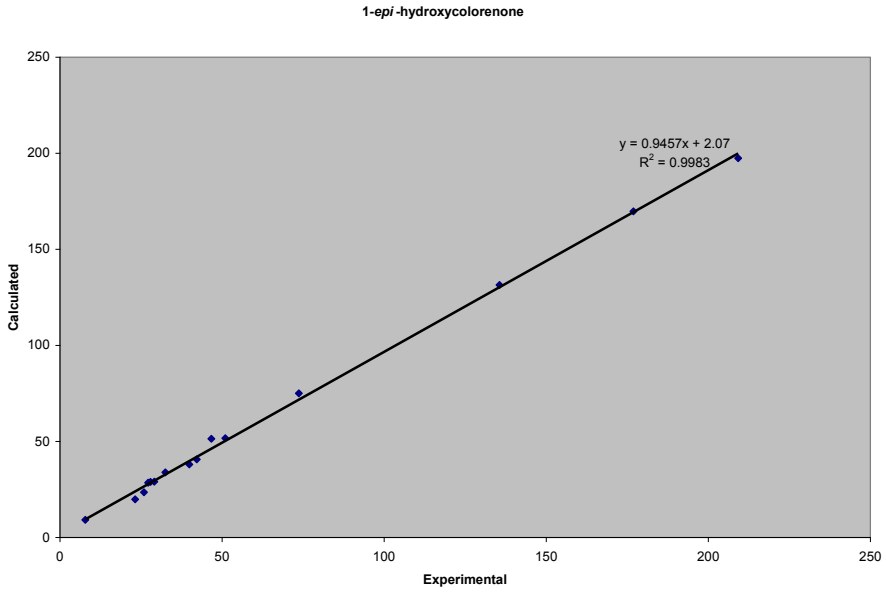

Torilolone

In order to further verify the predictive power of these calculations, NMR prediction for torilolone was found to match the literature values[92] within an average of 1.9 ppm and maximum of 5.0 ppm.

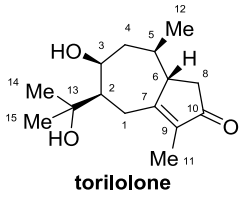

torilolone

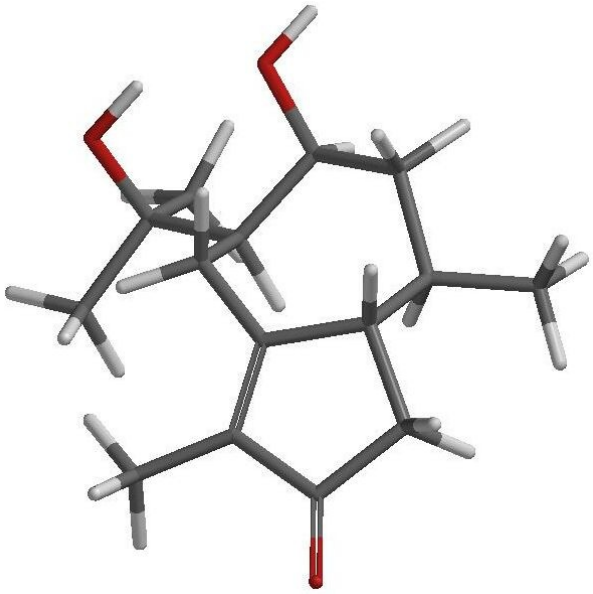

Standard orientation:

Center Number	Atomic Number	Atomic Type	Coordinates (Angstroms) X	Y	Z
1	1	0	0.597191	0.059710	-1.785337
2	6	0	0.377070	-0.538438	-0.910504
3	1	0	0.616880	-1.556998	-1.164670
4	6	0	1.276321	-0.059586	0.262295
5	1	0	0.749482	-0.205052	1.197814
6	6	0	1.560266	1.441539	0.118949
7	1	0	1.980670	1.808450	1.046615
8	6	0	0.354494	2.316567	-0.266693
9	1	0	0.225025	2.249609	-1.340200
10	1	0	0.622479	3.347417	-0.049770
11	6	0	-0.990277	1.989402	0.423664
12	1	0	-0.815038	1.618129	1.428726
13	6	0	-1.771425	0.923670	-0.379349
14	1	0	-1.921972	1.328243	-1.377766
15	6	0	-1.070480	-0.431239	-0.526811
16	6	0	-3.139392	0.548912	0.239874
17	1	0	-3.982282	1.012488	-0.252980
18	1	0	-3.172067	0.809113	1.292644
19	6	0	-1.882258	-1.450888	-0.272258
20	6	0	-3.218620	-0.968653	0.134289
21	6	0	-1.619089	-2.927926	-0.353124
22	1	0	-1.106601	-3.196980	-1.269135
23	1	0	-2.566552	-3.450571	-0.319067
24	1	0	-1.019154	-3.266826	0.485441
25	6	0	-1.827742	3.283796	0.512612
26	1	0	-1.999533	3.685202	-0.481525

```
   27          1             0       -1.305138    4.034117    1.095726
   28          1             0       -2.788831    3.108099    0.978558
   29          6             0        2.585403   -0.899906    0.329543
   30          6             0        2.295435   -2.320723    0.822881
   31          1             0        3.210245   -2.896691    0.768659
   32          1             0        1.560090   -2.812391    0.202947
   33          1             0        1.944023   -2.306730    1.848044
   34          6             0        3.641601   -0.266874    1.253617
   35          1             0        4.497237   -0.928764    1.303448
   36          1             0        3.252160   -0.125725    2.255924
   37          1             0        3.974593    0.681580    0.858449
   38          8             0        3.126646   -1.052527   -0.996260
   39          1             0        3.233641   -0.162400   -1.366429
   40          8             0        2.561043    1.564425   -0.939420
   41          1             0        2.801072    2.486968   -1.095451
   42          8             0       -4.189621   -1.656637    0.361358
 ---------------------------------------------------------------------
SCF Done:  E(RmPW+HF-PW91) =  -811.570045151     A.U.
```

Carbon	Raw GIAO Shift	Relative GIAO Shift (TMS)	Scaled Chemical Shift	Experimental Chemical Shift	Difference	|Difference|
10	0.4046	196.14145	204.9	207.79	-2.9	2.9
7	27.9644	168.58165	175.8	176.78	-1.0	1.0
9	64.7918	131.75425	136.9	133.85	3.0	3.0
3	122.2312	74.31485	76.2	73.05	3.1	3.1
13	123.4748	73.07125	74.9	69.9	5.0	5.0
6	143.7682	52.77785	53.4	51.89	1.5	1.5
2	148.4315	48.11455	48.5	49.5	-1.0	1.0
4	153.2474	43.29865	43.4	44.57	-1.2	1.2
8	155.5384	41.00765	41.0	41.57	-0.6	0.6
5	162.3335	34.21255	33.8	33.6	0.2	0.2
14	168.8791	27.66695	26.9	29.51	-2.6	2.6
1	168.9731	27.57295	26.8	28.91	-2.1	2.1

15	169.7539	26.79215	26.0	24.83	1.1	1.1
12	173.4982	23.04785	22.0	23.06	-1.1	1.1
11	187.9147	8.63135	6.8	8.13	-1.4	1.4
					AVG	1.9
					MAX	5.0

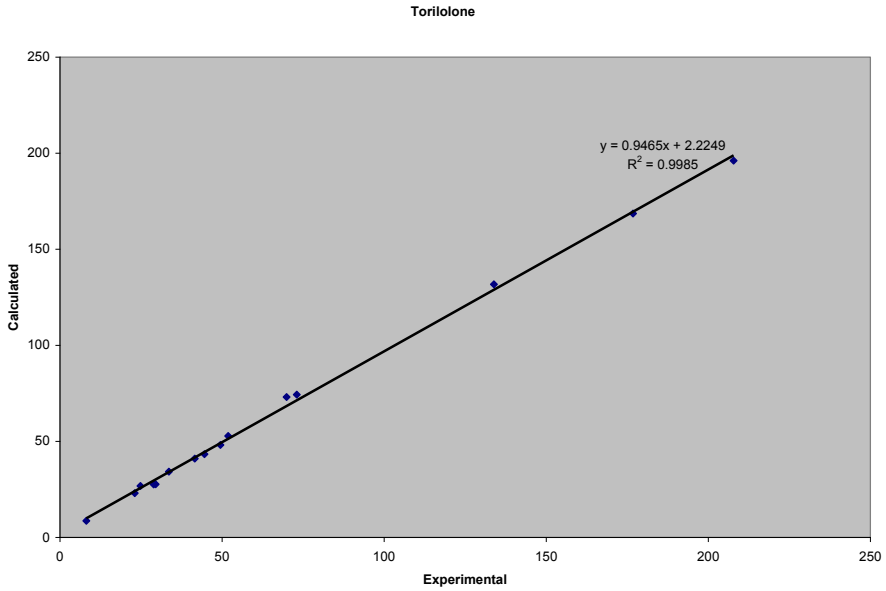

Torilin

The ^{13}C-NMR spectrum of torilin[91] was successfully predicted by this protocol within an average deviation of 1.6 ppm and a maximum of 4.8 ppm.

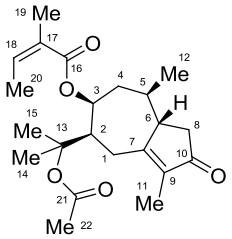

torilin

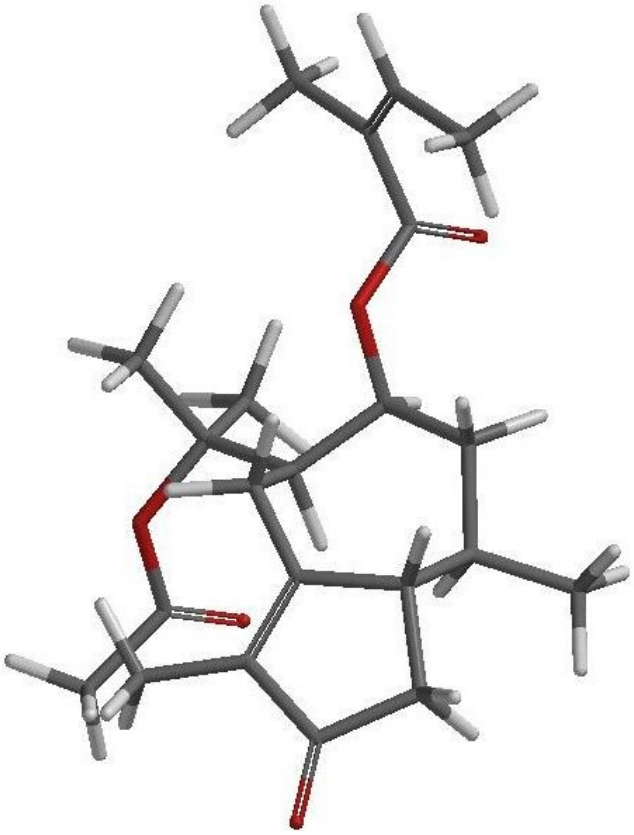

Standard orientation:

Center Number	Atomic Number	Atomic Type	Coordinates (Angstroms) X	Y	Z
1	1	0	-1.021551	0.861122	1.619667
2	6	0	-0.729646	-0.002992	1.044853
3	1	0	-0.031951	-0.581710	1.638590
4	6	0	-0.045604	0.478021	-0.261200
5	1	0	-0.803672	0.537932	-1.027828
6	6	0	0.984406	-0.524961	-0.780227
7	1	0	1.291263	-0.255204	-1.775022
8	6	0	0.534943	-1.993175	-0.753902
9	1	0	0.692361	-2.374567	0.247097
10	1	0	1.211399	-2.537857	-1.403493
11	6	0	-0.925960	-2.273432	-1.175617
12	1	0	-1.247194	-1.561053	-1.928680
13	6	0	-1.873018	-2.184676	0.043278
14	1	0	-1.505019	-2.894222	0.781249
15	6	0	-1.958889	-0.811022	0.725391
16	6	0	-3.350528	-2.506461	-0.287263
17	1	0	-3.646462	-3.513088	-0.028615
18	1	0	-3.549209	-2.348398	-1.342137
19	6	0	-3.212574	-0.462188	0.991392
20	6	0	-4.159686	-1.482493	0.492884
21	6	0	-3.771545	0.739698	1.692055
22	1	0	-4.306234	1.368155	0.986433
23	1	0	-3.006262	1.332128	2.173660
24	1	0	-4.487338	0.419778	2.440856
25	6	0	-0.994473	-3.694126	-1.777818
26	1	0	-0.663106	-4.425702	-1.046956
27	1	0	-0.349334	-3.766246	-2.646144
28	1	0	-1.999615	-3.951652	-2.085866
29	6	0	0.498774	1.928379	-0.146084
30	6	0	1.165851	2.408045	-1.443718
31	1	0	1.381209	3.466077	-1.352180
32	1	0	0.511434	2.260571	-2.289580
33	1	0	2.094335	1.882114	-1.612587
34	6	0	1.400708	2.202364	1.058456
35	1	0	1.591820	3.266412	1.104242
36	1	0	2.330040	1.669305	0.970812
37	1	0	0.913397	1.911532	1.978347
38	8	0	-0.656767	2.812106	0.148077
39	8	0	-5.358755	-1.482003	0.663766
40	8	0	2.187922	-0.488074	0.072736
41	6	0	3.414838	-0.393069	-0.492030
42	8	0	3.549832	-0.217589	-1.682502
43	6	0	4.569291	-0.478921	0.435677
44	6	0	4.531163	-0.762835	1.729135
45	1	0	5.483725	-0.779961	2.231184
46	6	0	5.879531	-0.214574	-0.283632
47	1	0	5.874294	0.769213	-0.737104
48	1	0	6.026068	-0.935214	-1.078516
49	1	0	6.712242	-0.277310	0.403801

```
   50          6           0        3.375670   -1.085950    2.640233
   51          1           0        2.439726   -1.091445    2.118166
   52          1           0        3.335252   -0.354226    3.442768
   53          1           0        3.545125   -2.055117    3.101293
   54          6           0       -1.680808    3.037524   -0.702778
   55          6           0       -2.578911    4.115493   -0.160649
   56          1           0       -3.422781    4.248970   -0.818193
   57          1           0       -2.017017    5.037943   -0.080415
   58          1           0       -2.910785    3.843343    0.832109
   59          8           0       -1.835652    2.450122   -1.745522
 ---------------------------------------------------------------------
E(RmPW+HF-PW91) =  -1233.50972008     A.U.
```

Carbon	Raw GIAO Shift	Relative GIAO Shift (TMS)	Scaled Chemical Shift	Experimental Chemical Shift	Difference	|Difference|
10	-0.6231	197.16915	205.3	207.9	-2.6	2.6
7	32.3234	164.22265	170.5	173.6	-3.1	3.1
21	32.4266	164.11945	170.4	170.2	0.2	0.2
16	35.2874	161.25865	167.4	166.8	0.6	0.6
18	61.0493	135.49675	140.2	138.1	2.1	2.1
9	64.0316	132.51445	137.0	135.2	1.8	1.8
17	73.0884	123.45765	127.5	127.8	-0.3	0.3
13	109.3309	87.21515	89.2	84.4	4.8	4.8
3	123.3223	73.22375	74.4	70.7	3.7	3.7
6	142.5015	54.04455	54.2	51	3.2	3.2
2	153.0444	43.50165	43.1	46.4	-3.3	3.3
4	155.4254	41.12065	40.6	41.2	-0.6	0.6
8	155.6925	40.85355	40.3	40.6	-0.3	0.3
5	162.4319	34.11415	33.2	33.5	-0.3	0.3
1	169.428	27.11805	25.8	25.7	0.1	0.1

15	172.2063	24.33975	22.9	24.5	-1.6	1.6
19	172.6729	23.87315	22.4	23.9	-1.5	1.5
12	173.7469	22.79915	21.2	22.6	-1.4	1.4
14	174.1915	22.35455	20.8	22.5	-1.7	1.7
22	174.8546	21.69145	20.1	20.5	-0.4	0.4
20	178.889	17.65705	15.8	15.7	0.1	0.1
11	185.3935	11.15255	8.9	8	0.9	0.9
					AVG	1.6
					MAX	4.8

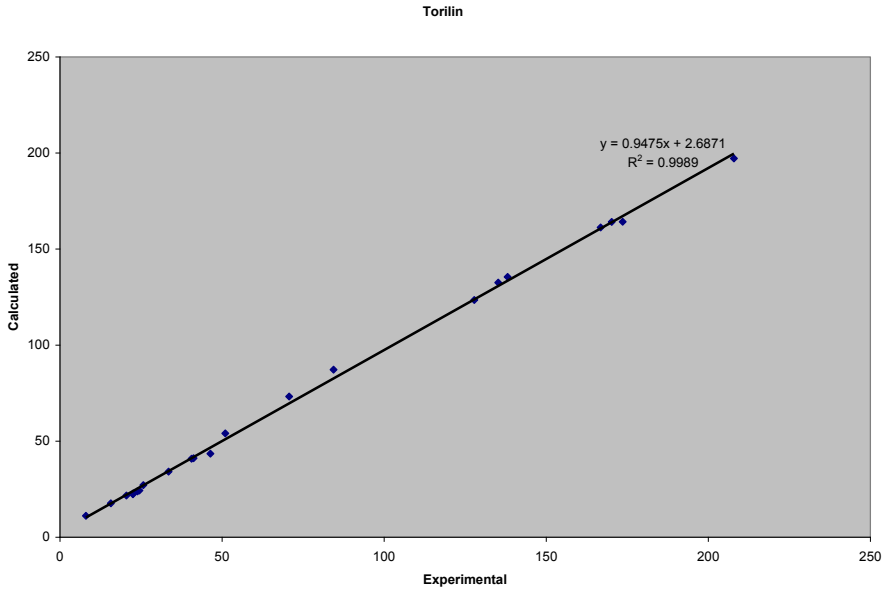

Synthetic Intermediate 3.49 from the Synthesis of Pleocarpenene and Pleocarpenone

A key cycloheptadiene diol intermediate generated by thermal rearrangement of a tetracyclo[5.3.0.$0^{1,5}$.$0^{2,4}$]decane in the previously reported synthesis[106] provided a very similar compound to diol **3.74** in this work. ^{13}C-NMR chemical shifts were calculated for four possible diastereomers in order to test

the ability of this protocol to discriminate among these closely related compounds. The literature data was indeed most closely matched by the prediction for the correct structure of intermediate **3.49** with an average deviation of 2.0 ppm and a maximum of 4.7 ppm while all other diastereomers only matched within 2.3ppm or greater deviation.

αMeAntiTIPS

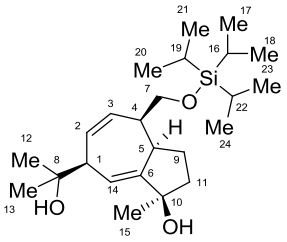

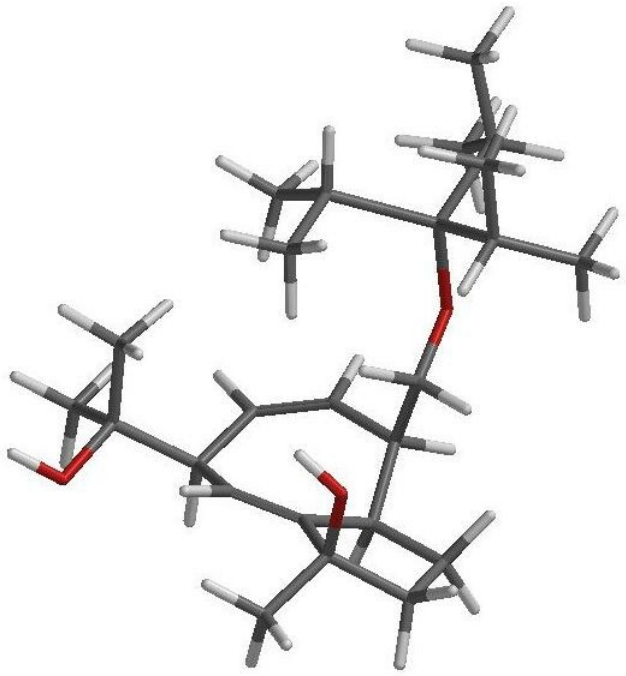

Standard orientation:

Center Number	Atomic Number	Atomic Type	Coordinates (Angstroms) X	Y	Z
1	6	0	3.167764	-1.299338	-0.672861
2	1	0	4.031587	-1.326433	-1.337248
3	6	0	1.926268	-1.574747	-1.505488
4	1	0	1.900012	-2.585735	-1.869488
5	6	0	0.908328	-0.818178	-1.874026
6	1	0	0.136705	-1.294139	-2.450351
7	6	0	0.645857	0.645184	-1.599645
8	1	0	0.048750	1.028451	-2.420592
9	6	0	1.945683	1.458724	-1.524961
10	6	0	2.744733	1.172548	-0.262505

11	6	0	-0.235173	0.770642	-0.348546
12	1	0	-0.361981	1.801174	-0.056080
13	1	0	0.225436	0.237987	0.469699
14	6	0	3.402641	-2.479957	0.320245
15	6	0	1.741377	3.003182	-1.535395
16	1	0	0.770694	3.264948	-1.142397
17	1	0	1.832760	3.406754	-2.535264
18	6	0	2.880227	2.473045	0.520903
19	6	0	2.828859	3.537835	-0.579023
20	8	0	4.628570	-2.113549	1.012810
21	1	0	4.833777	-2.765052	1.696565
22	6	0	2.259604	-2.612220	1.329794
23	1	0	2.140156	-1.689037	1.881742
24	1	0	2.471216	-3.409963	2.036308
25	1	0	1.330736	-2.838991	0.826300
26	6	0	3.661244	-3.814330	-0.395324
27	1	0	2.776910	-4.197324	-0.883356
28	1	0	3.979821	-4.552910	0.334190
29	1	0	4.454167	-3.696094	-1.123507
30	6	0	3.246619	0.011037	0.091702
31	1	0	3.859136	-0.058653	0.966950
32	1	0	2.587348	4.505705	-0.163051
33	1	0	3.789515	3.581566	-1.079676
34	6	0	4.088614	2.583859	1.442256
35	1	0	4.067136	1.818283	2.210892
36	1	0	4.075308	3.550452	1.931079
37	1	0	5.007687	2.477399	0.881409
38	8	0	1.650708	2.691125	1.276832
39	1	0	1.557689	1.997182	1.944325
40	1	0	2.550370	1.185351	-2.383254
41	8	0	-1.503151	0.179218	-0.682047
42	14	0	-2.955606	-0.077008	0.126944
43	6	0	-4.242986	-0.481678	-1.239355
44	1	0	-4.649119	0.473284	-1.565349
45	6	0	-3.599623	-1.149051	-2.479362
46	1	0	-2.768742	-0.563404	-2.848680
47	1	0	-4.336034	-1.252767	-3.271332
48	1	0	-3.229582	-2.139575	-2.237515
49	6	0	-5.426683	-1.344225	-0.737211
50	1	0	-5.086103	-2.327575	-0.432147
51	1	0	-6.153346	-1.478589	-1.533026
52	1	0	-5.938062	-0.890003	0.104475
53	6	0	-3.437020	1.530847	1.060286
54	1	0	-2.642977	1.742005	1.774261
55	6	0	-3.531218	2.745260	0.104682
56	1	0	-4.329840	2.607794	-0.616613
57	1	0	-2.606988	2.895244	-0.441841
58	1	0	-3.742057	3.650915	0.665610
59	6	0	-4.757433	1.387814	1.854870
60	1	0	-4.722392	0.560284	2.556040
61	1	0	-5.595106	1.228022	1.183992
62	1	0	-4.956911	2.293951	2.419222
63	6	0	-2.755533	-1.521624	1.375767
64	1	0	-3.744594	-1.788238	1.741630

```
    65          6           0       -2.142962   -2.769153    0.692079
    66          1           0       -1.176931   -2.529133    0.261768
    67          1           0       -2.778531   -3.142461   -0.102496
    68          1           0       -2.007191   -3.569019    1.414579
    69          6           0       -1.889842   -1.131781    2.599820
    70          1           0       -1.822327   -1.966087    3.291948
    71          1           0       -2.304142   -0.286301    3.137408
    72          1           0       -0.880560   -0.877681    2.292692
 ---------------------------------------------------------------------
 SCF Done:  E(RmPW+HF-PW91) =  -1456.02352599     A.U.
```

Carbon	Raw GIAO Shift	Relative GIAO Shift (TMS)	Scaled Chemical Shift	Experimental Chemical Shift	Difference	|Difference|
6	51.0406	145.50545	149.6	152	-2.4	2.4
3	62.3475	134.19855	137.7	132.6	5.1	5.1
2	76.1304	120.41565	123.4	129.1	-5.7	5.7
14	79.6837	116.86235	119.6	120.9	-1.3	1.3
10	115.8203	80.72575	81.9	80.2	1.7	1.7
8	121.387	75.15905	76.1	73.6	2.5	2.5
7	124.8316	71.71445	72.5	65.5	7.0	7.0
1	145.2218	51.32425	51.2	51.1	0.1	0.1
4	151.2753	45.27075	44.9	44.4	0.5	0.5
5	151.3303	45.21575	44.8	43.3	1.5	1.5
11	156.2349	40.31115	39.7	41.6	-1.9	1.9
13	167.3221	29.22395	28.1	28.2	-0.1	0.1
9	167.8948	28.65125	27.5	27.4	0.1	0.1
12	171.1066	25.43945	24.2	27.3	-3.1	3.1
15	173.4172	23.12885	21.8	26.5	-4.7	4.7
18	177.5753	18.35331	16.8	18.4	-1.6	1.6

24	177.6731	16.31075	14.6	12.3	2.3	2.3
17	177.6846				**AVG**	2.5
23	178.2958				**MAX**	7.0
20	178.8244					
22	179.1032					
21	179.3093					
19	179.9556					
16	181.441					

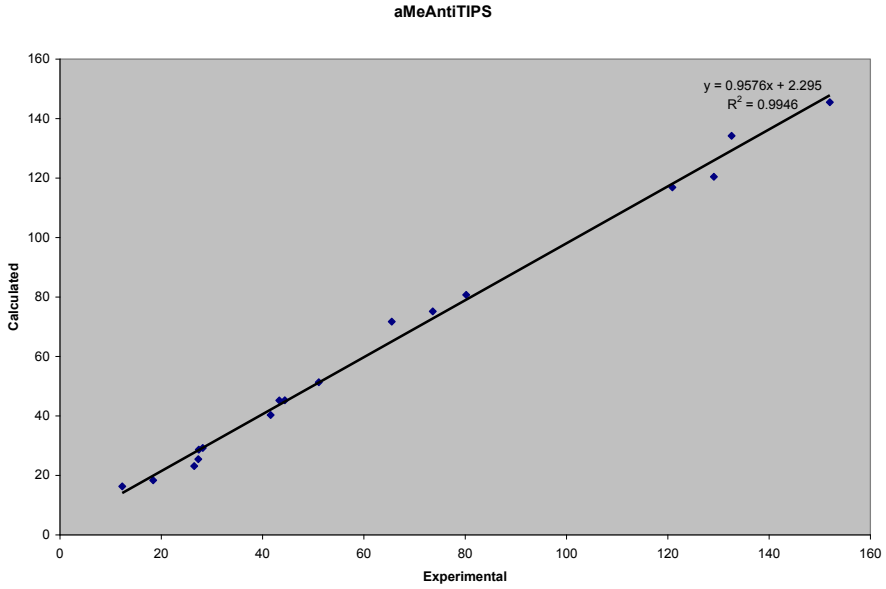

βMeAntiTIPS (3.49)

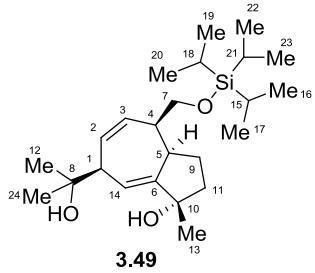

3.49

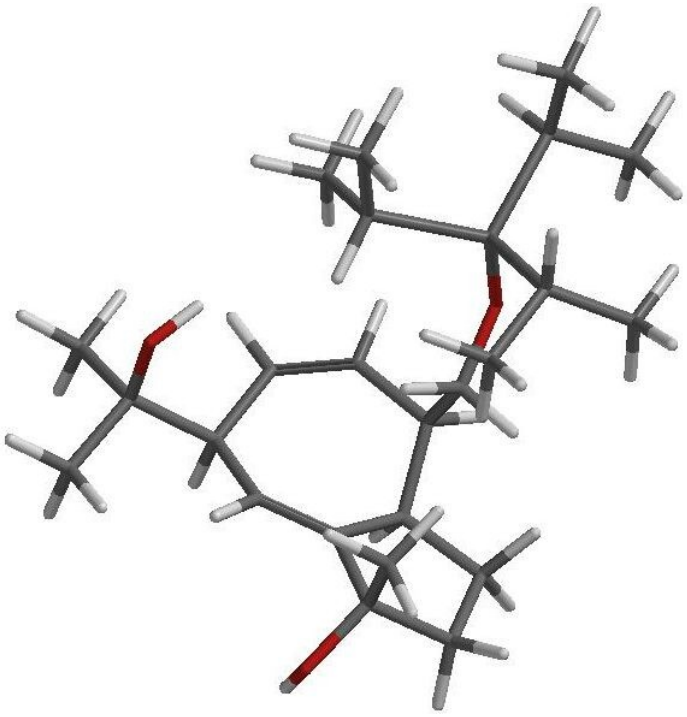

Standard orientation:

Center Number	Atomic Number	Atomic Type	Coordinates (Angstroms) X	Y	Z
1	6	0	-2.938323	1.512787	-0.791809
2	1	0	-3.810805	1.727284	-1.409506
3	6	0	-1.727448	1.523378	-1.704500
4	1	0	-1.617230	2.467734	-2.206939
5	6	0	-0.816755	0.615778	-2.008932
6	1	0	-0.040697	0.923438	-2.685321
7	6	0	-0.681272	-0.818852	-1.546616
8	1	0	-0.124683	-1.352276	-2.310284
9	6	0	-2.047820	-1.501969	-1.389817
10	6	0	-2.889570	-0.978075	-0.240379
11	6	0	0.195894	-0.867332	-0.288933
12	1	0	0.269913	-1.878317	0.087402
13	1	0	-0.228327	-0.239242	0.481411

14	6	0	-2.882984	2.718531	0.198040
15	6	0	-2.005540	-3.043362	-1.173062
16	1	0	-1.141702	-3.332129	-0.589640
17	1	0	-1.965048	-3.574543	-2.114792
18	6	0	-3.407282	-2.149587	0.594574
19	6	0	-3.296570	-3.340578	-0.381001
20	6	0	-2.766288	4.073136	-0.515193
21	1	0	-3.522010	4.155972	-1.287021
22	1	0	-1.787399	4.221800	-0.948331
23	1	0	-2.934497	4.866725	0.206073
24	6	0	-2.560637	-2.370446	1.850298
25	1	0	-2.611235	-1.484574	2.469516
26	1	0	-1.527573	-2.571917	1.603564
27	1	0	-2.964025	-3.205831	2.409691
28	6	0	-3.265587	0.258969	-0.010968
29	1	0	-3.947541	0.435240	0.797443
30	8	0	-4.737753	-1.934783	1.097785
31	1	0	-5.321543	-1.659476	0.377468
32	1	0	-3.280306	-4.292448	0.132734
33	1	0	-4.150054	-3.322722	-1.052668
34	1	0	-2.595134	-1.320754	-2.309923
35	8	0	1.501060	-0.409080	-0.670285
36	14	0	2.919945	0.027689	0.124357
37	6	0	3.395959	-1.294036	1.434870
38	1	0	4.394855	-1.048753	1.789681
39	6	0	3.446527	-2.719439	0.831575
40	1	0	2.476433	-3.007314	0.441033
41	1	0	3.729524	-3.441517	1.591879
42	1	0	4.164157	-2.787839	0.022891
43	6	0	2.451720	-1.287726	2.663582
44	1	0	2.433057	-0.321544	3.154733
45	1	0	2.780093	-2.024250	3.390946
46	1	0	1.435465	-1.540287	2.378319
47	6	0	2.637990	1.717730	0.989728
48	1	0	1.816220	1.583761	1.691298
49	6	0	2.209346	2.810370	-0.019474
50	1	0	1.335983	2.504927	-0.583661
51	1	0	3.009026	3.021651	-0.721631
52	1	0	1.975007	3.734026	0.502185
53	6	0	3.869463	2.200561	1.792508
54	1	0	4.706542	2.398801	1.131319
55	1	0	4.186419	1.471288	2.530719
56	1	0	3.639037	3.124155	2.315384
57	6	0	4.244070	0.177981	-1.258293
58	1	0	4.167911	1.191461	-1.645315
59	6	0	3.973338	-0.781509	-2.442946
60	1	0	2.964222	-0.665797	-2.814206
61	1	0	4.102111	-1.815395	-2.141517
62	1	0	4.670809	-0.581570	-3.251429
63	6	0	5.692986	-0.016909	-0.747747
64	1	0	5.841321	-1.026202	-0.379880
65	1	0	5.943163	0.672087	0.051489
66	1	0	6.397627	0.145850	-1.557810
67	6	0	-1.773933	2.555780	1.239418

```
   68          1             0       -0.807682    2.520090    0.756963
   69          1             0       -1.780074    3.394187    1.930649
   70          1             0       -1.920813    1.643900    1.802706
   71          8             0       -4.184758    2.674307    0.845097
   72          1             0       -4.211856    3.288037    1.591078
 ---------------------------------------------------------------------
SCF Done:  E(RmPW+HF-PW91) =  -1456.02359012     A.U.
```

Carbon	Raw GIAO Shift	Relative GIAO Shift (TMS)	Scaled Chemical Shift	Experimental Chemical Shift	Difference	|Difference|
6	50.9727	145.57335	149.0	152	-3.0	3.0
3	63.8411	132.70495	135.6	132.6	3.0	3.0
2	74.3219	122.22415	124.7	129.1	-4.4	4.4
14	77.4007	119.14535	121.5	120.9	0.6	0.6
10	114.6602	81.88585	82.7	80.2	2.5	2.5
8	120.9447	75.60135	76.2	73.6	2.6	2.6
7	126.6827	69.86335	70.2	65.5	4.7	4.7
1	144.1724	52.37365	52.0	51.1	0.9	0.9
4	151.069	45.47705	44.8	44.4	0.4	0.4
5	153.2898	43.25625	42.5	43.3	-0.8	0.8
11	154.9153	41.63075	40.8	41.6	-0.8	0.8
12	167.1435	29.40255	28.1	28.2	-0.1	0.1
13	168.9286	27.61745	26.2	27.4	-1.2	1.2
9	169.3496	27.19645	25.8	27.3	-1.5	1.5
24	171.9969	24.54915	23.0	26.5	-3.5	3.5
22	177.4578	18.23246667	16.5	18.4	-1.9	1.9
23	177.8505	16.22355	14.4	12.3	2.1	2.1
16	177.9149				**AVG**	2.0

17	178.2656				**MAX**	4.7
19	179.1506					
20	179.2421					
15	179.6033					
18	179.7739					
21	181.5903					

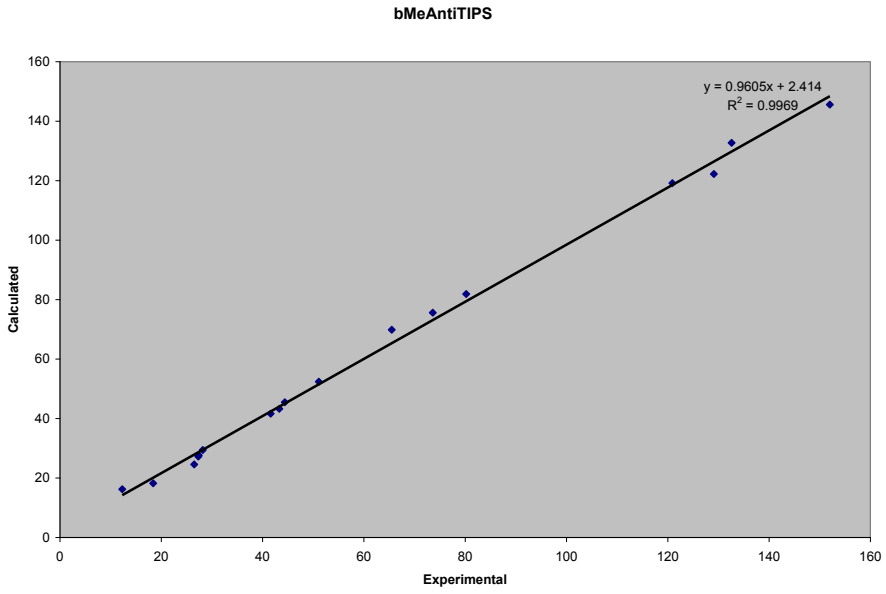

αMeSynTIPS

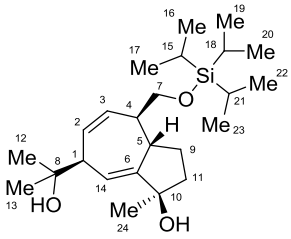

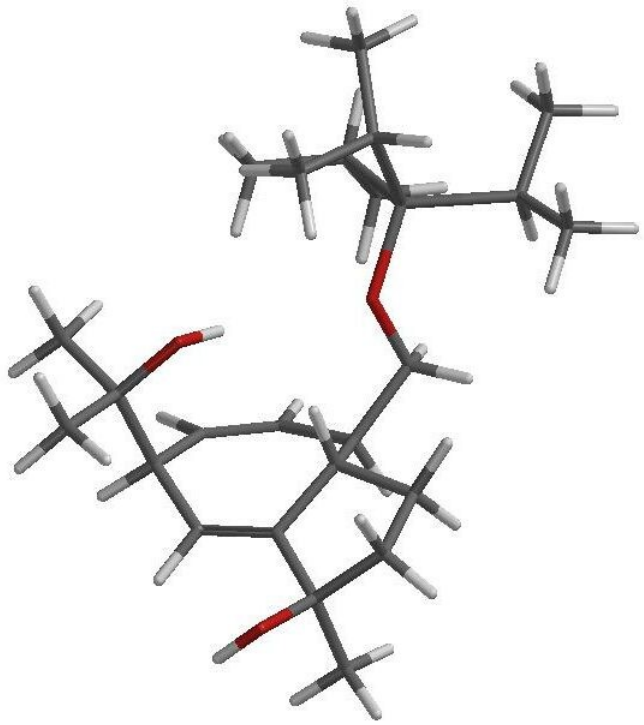

Standard orientation:

Center Number	Atomic Number	Atomic Type	Coordinates (Angstroms) X	Y	Z
1	6	0	-2.603957	1.889839	-0.770577
2	1	0	-3.229835	2.691124	-1.148794
3	6	0	-1.671926	1.499409	-1.900606
4	1	0	-1.495257	2.287502	-2.611630
5	6	0	-1.044803	0.360959	-2.125044
6	1	0	-0.426655	0.326365	-3.008545
7	6	0	-1.028850	-0.958944	-1.381317
8	1	0	-1.454405	-1.702714	-2.053918
9	6	0	-1.784790	-1.027323	-0.044550
10	6	0	-3.196047	-0.465849	-0.094108
11	6	0	0.442652	-1.351113	-1.171854
12	1	0	0.938804	-1.411946	-2.133671
13	1	0	0.501598	-2.323882	-0.702969
14	6	0	-1.790192	2.529698	0.404601
15	6	0	-1.963911	-2.485661	0.477114
16	1	0	-1.159908	-2.779329	1.138649
17	1	0	-1.996215	-3.187365	-0.349372
18	6	0	-4.188240	-1.531455	0.335129
19	6	0	-3.327185	-2.466154	1.204206

20	8	0	-0.785062	1.624274	0.905102
21	1	0	-0.221049	1.253542	0.206866
22	6	0	-1.105471	3.824360	-0.062377
23	1	0	-0.540924	4.238559	0.763787
24	1	0	-1.837710	4.553684	-0.388612
25	1	0	-0.416394	3.631637	-0.875348
26	6	0	-2.692846	2.824406	1.602165
27	1	0	-2.097502	3.263400	2.392962
28	1	0	-3.130680	1.907231	1.968015
29	1	0	-3.481837	3.515058	1.326941
30	6	0	-3.537395	0.776837	-0.336130
31	1	0	-4.570027	1.043935	-0.214558
32	1	0	-3.224663	-2.003402	2.178456
33	1	0	-3.758739	-3.453555	1.320680
34	8	0	1.091519	-0.364406	-0.339625
35	14	0	2.746926	-0.257964	0.072136
36	6	0	2.885717	0.242116	1.919040
37	1	0	2.431435	-0.580247	2.467995
38	6	0	2.136114	1.531307	2.337508
39	1	0	2.158696	1.617112	3.420765
40	1	0	1.104292	1.543991	2.019902
41	1	0	2.630343	2.408954	1.936140
42	6	0	4.363124	0.355773	2.375181
43	1	0	4.879584	1.134698	1.822275
44	1	0	4.908719	-0.570584	2.247365
45	1	0	4.402457	0.619145	3.427750
46	6	0	3.573216	0.964619	-1.155797
47	1	0	4.629927	1.026293	-0.904548
48	6	0	2.977940	2.391837	-1.092122
49	1	0	3.437834	3.021733	-1.848256
50	1	0	3.140268	2.856459	-0.128863
51	1	0	1.910167	2.366293	-1.281716
52	6	0	3.454098	0.448468	-2.613680
53	1	0	3.862322	-0.548263	-2.735850
54	1	0	3.986383	1.111598	-3.288905
55	1	0	2.413820	0.431658	-2.921112
56	6	0	3.496688	-2.017373	-0.194259
57	1	0	3.077778	-2.390596	-1.127112
58	6	0	3.074235	-3.004569	0.923091
59	1	0	3.520725	-2.726953	1.871226
60	1	0	3.405864	-4.010022	0.681685
61	1	0	1.997566	-3.030705	1.056923
62	6	0	5.036848	-2.050435	-0.354809
63	1	0	5.361663	-3.060766	-0.586435
64	1	0	5.535481	-1.748695	0.557697
65	1	0	5.376804	-1.401973	-1.153444
66	1	0	-1.243503	-0.453454	0.685898
67	6	0	-4.751386	-2.259897	-0.894817
68	1	0	-5.322045	-1.558175	-1.489715
69	1	0	-3.958952	-2.667504	-1.506985
70	1	0	-5.402544	-3.076622	-0.591732
71	8	0	-5.262346	-0.902572	1.061090
72	1	0	-5.975321	-1.535226	1.221755

SCF Done: E(RmPW+HF-PW91) = -1456.02539714 A.U.

Carbon	Raw GIAO Shift	Relative GIAO Shift (TMS)	Scaled Chemical Shift	Experimental Chemical Shift	Difference	|Difference|
6	51.0111	145.53495	148.7	152	-3.3	3.3
3	66.5003	130.04575	132.6	132.6	0.0	0.0
2	70.1703	126.37575	128.7	129.1	-0.4	0.4
14	74.5705	121.97555	124.2	120.9	3.3	3.3
10	116.3018	80.24425	80.7	80.2	0.5	0.5
8	118.6417	77.90435	78.2	73.6	4.6	4.6
7	128.1163	68.42975	68.4	65.5	2.9	2.9
1	148.231	48.31505	47.4	51.1	-3.7	3.7
4	148.5344	48.01165	47.1	44.4	2.7	2.7
11	156.3679	40.17815	38.9	43.3	-4.4	4.4
5	157.9998	38.54625	37.2	41.6	-4.4	4.4
12	166.1939	30.35215	28.7	28.2	0.5	0.5
9	166.4094	30.13665	28.5	27.4	1.1	1.1
24	166.9323	29.61375	27.9	27.3	0.6	0.6
13	169.3477	27.19835	25.4	26.5	-1.1	1.1
16	177.7894	18.6195	16.5	18.4	-1.9	1.9
17	177.8222	17.52611667	15.3	12.3	3.0	3.0
15	177.9081				**AVG**	2.3
23	177.9266				**MAX**	4.6
19	178.0492					
20	178.0638					

18	178.4294					
22	178.5705					
21	180.0599					

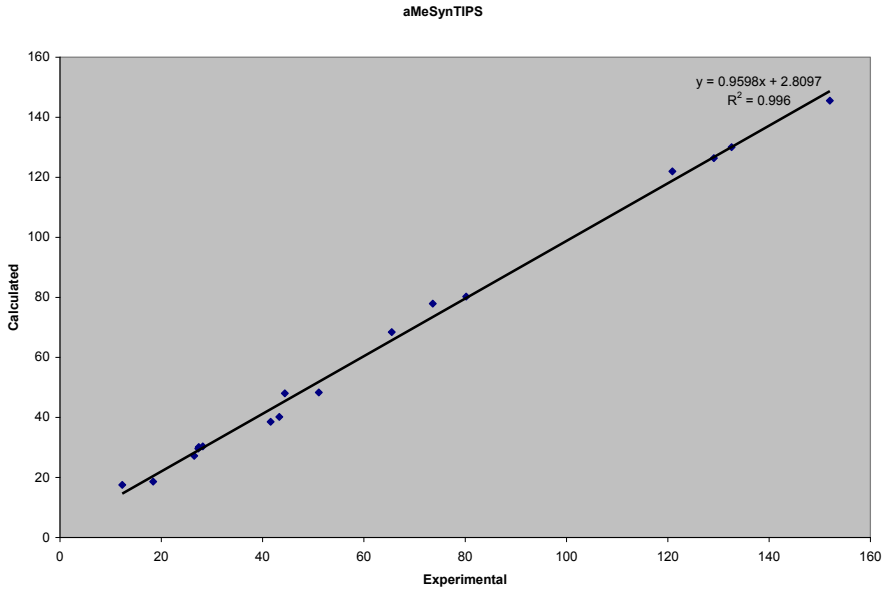

βMeSynTIPS

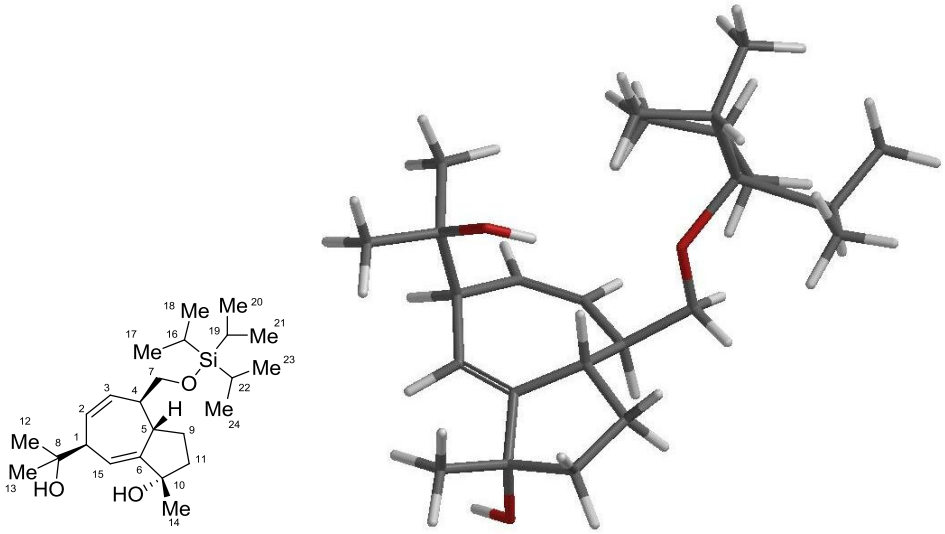

Standard orientation:

Center Number	Atomic Number	Atomic Type	Coordinates (Angstroms) X	Y	Z
1	6	0	-2.590569	1.910927	-0.753106
2	1	0	-3.208247	2.716742	-1.135124
3	6	0	-1.667554	1.501711	-1.883563
4	1	0	-1.486855	2.278933	-2.605167
5	6	0	-1.057598	0.351436	-2.091531
6	1	0	-0.444183	0.293213	-2.976946
7	6	0	-1.057020	-0.953649	-1.322685
8	1	0	-1.507872	-1.703512	-1.970264
9	6	0	-1.800072	-0.993564	0.023135
10	6	0	-3.216237	-0.438476	-0.050452
11	6	0	0.410907	-1.359742	-1.119152
12	1	0	0.897823	-1.449012	-2.083369
13	1	0	0.463073	-2.320469	-0.626627
14	6	0	-1.770371	2.554368	0.415494
15	6	0	-1.977871	-2.449457	0.552129
16	1	0	-1.189502	-2.730607	1.237695
17	1	0	-2.004599	-3.146941	-0.273597
18	6	0	-4.191121	-1.558238	0.287702
19	6	0	-3.367018	-2.445747	1.223457
20	8	0	-0.769063	1.653292	0.926772
21	1	0	-0.211161	1.261508	0.234206
22	6	0	-1.081329	3.840547	-0.069122
23	1	0	-0.511423	4.260666	0.750220
24	1	0	-1.810384	4.570385	-0.401324
25	1	0	-0.396165	3.633883	-0.881696
26	6	0	-2.668959	2.869925	1.610933
27	1	0	-2.071497	3.321910	2.392485
28	1	0	-3.101998	1.958074	1.995551
29	1	0	-3.459945	3.555125	1.327837
30	6	0	-5.545572	-1.140234	0.845971
31	1	0	-5.425868	-0.568239	1.757061
32	1	0	-6.130931	-2.027480	1.053894
33	1	0	-6.095767	-0.539764	0.129005
34	6	0	-3.541751	0.804741	-0.328211
35	1	0	-4.575784	1.096104	-0.282297
36	8	0	-4.369786	-2.375714	-0.905190
37	1	0	-4.664548	-1.816493	-1.637412
38	1	0	-3.318626	-1.988796	2.205347
39	1	0	-3.800487	-3.433240	1.297353
40	8	0	1.079367	-0.358701	-0.316719
41	14	0	2.742009	-0.263555	0.068478
42	6	0	2.915217	0.277170	1.901446
43	1	0	2.463083	-0.528490	2.476248
44	6	0	2.184456	1.582140	2.303445
45	1	0	2.229740	1.694098	3.383626
46	1	0	1.146494	1.594629	2.006877
47	1	0	2.676577	2.445957	1.870759
48	6	0	4.400976	0.387531	2.330488
49	1	0	4.914970	1.149314	1.752003

```
   50          1             0        4.936034   -0.546360    2.214125
   51          1             0        4.460367    0.673445    3.376230
   52          6             0        3.563138    0.923439   -1.197699
   53          1             0        4.623115    0.983156   -0.960193
   54          6             0        2.978685    2.356083   -1.160674
   55          1             0        3.433844    2.964833   -1.936742
   56          1             0        3.155712    2.842020   -0.210567
   57          1             0        1.908544    2.333308   -1.337225
   58          6             0        3.423469    0.374561   -2.641732
   59          1             0        3.822936   -0.627719   -2.745295
   60          1             0        3.952728    1.017825   -3.338241
   61          1             0        2.379689    0.358199   -2.937037
   62          6             0        3.469073   -2.036196   -0.168290
   63          1             0        3.033319   -2.425659   -1.086600
   64          6             0        3.051392   -2.993505    0.976589
   65          1             0        3.513892   -2.699838    1.912174
   66          1             0        3.369009   -4.007524    0.753146
   67          1             0        1.976489   -3.005308    1.125248
   68          6             0        5.006466   -2.090063   -0.348928
   69          1             0        5.316421   -3.108626   -0.564087
   70          1             0        5.520948   -1.775798    0.550442
   71          1             0        5.343011   -1.462066   -1.165184
   72          1             0       -1.258656   -0.406878    0.741995
 -------------------------------------------------------------------
SCF Done:  E(RmPW+HF-PW91) =  -1456.02812974     A.U.
```

Carbon	Raw GIAO Shift	Relative GIAO Shift (TMS)	Scaled Chemical Shift	Experimental Chemical Shift	Difference	|Difference|
6	46.575	149.97105	152.5	152	0.5	0.5
3	65.1072	131.43885	133.4	132.6	0.8	0.8
2	71.809	124.73705	126.5	129.1	-2.6	2.6
15	78.1608	118.38525	119.9	120.9	-1.0	1.0
10	115.7902	80.75585	81.2	80.2	1.0	1.0
8	119.3133	77.23275	77.6	73.6	4.0	4.0
7	127.6294	68.91665	69.0	65.5	3.5	3.5
1	148.1036	48.44245	47.9	51.1	-3.2	3.2
4	148.1188	48.42725	47.9	44.4	3.5	3.5
5	155.8992	40.64685	39.9	43.3	-3.4	3.4

11	157.1521	39.39395	38.6	41.6	-3.0	3.0
9	165.7813	30.76475	29.7	28.2	1.5	1.5
12	166.2172	30.32885	29.3	27.4	1.9	1.9
13	169.1443	27.40175	26.3	27.3	-1.0	1.0
14	173.7808	22.76525	21.5	26.5	-5.0	5.0
17	177.7908	18.62591667	17.2	18.4	-1.2	1.2
18	177.8081	17.48498333	16.1	12.3	3.8	3.8
24	177.9209				**AVG**	2.4
16	177.9223				**MAX**	5.0
21	178.0359					
20	178.0428					
19	178.4641					
23	178.61					
22	180.1091					

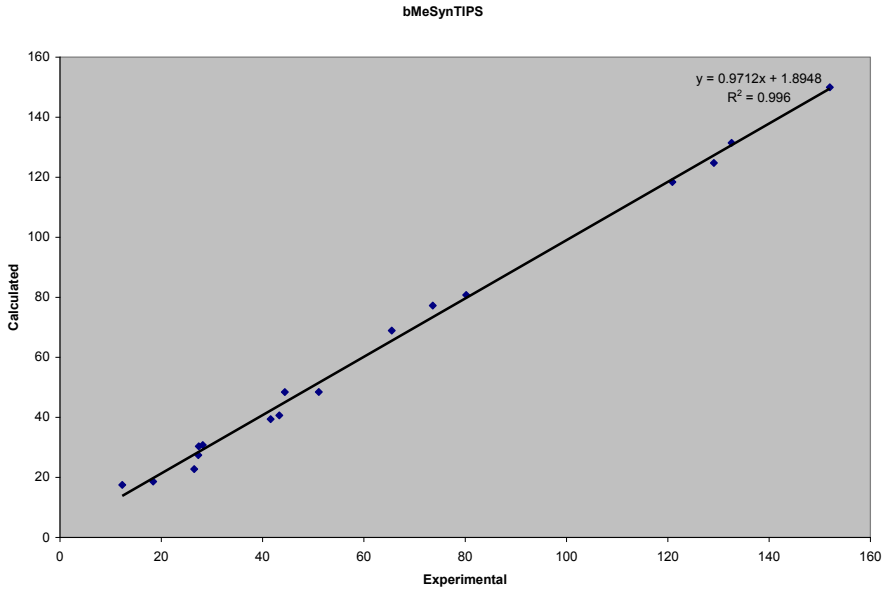

Siol Acetate

The compound siol acetate,[211] a carotane derivative possessing a 5-7 ring system and having the same molecular formula as diol **3.74**, and with a structure defined by x-ray crystallography, was selected to further define the predictive power of this method. The predicted spectral data for this compound matched the literature values very well with an average deviation of 1.6 ppm and a maximum of 3.8 ppm.

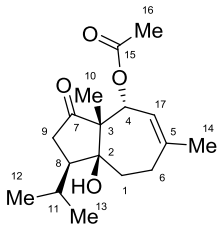

Siol Acetate

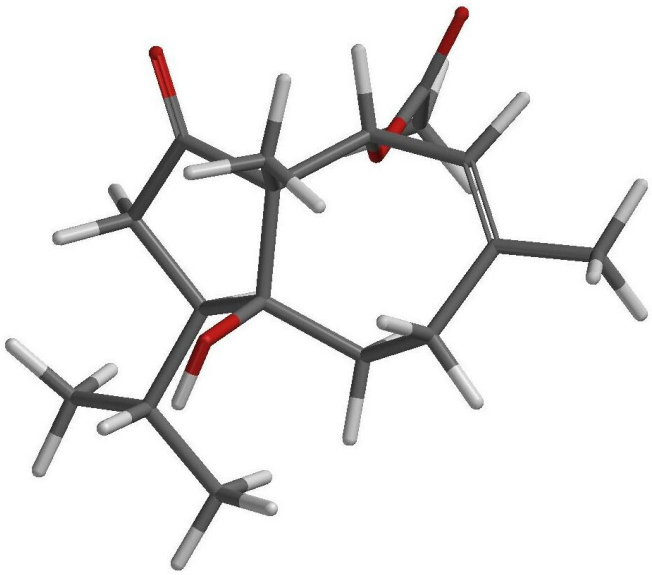

Standard orientation:

Center Number	Atomic Number	Atomic Type	Coordinates (Angstroms) X	Y	Z
1	1	0	0.322536	-0.548534	-1.607276
2	6	0	-0.077863	-1.381719	-1.054186
3	6	0	-0.790380	-0.852978	0.194014
4	6	0	0.177748	-0.159402	1.200857
5	6	0	1.464168	0.408582	0.593664
6	6	0	2.378207	-1.745198	-0.403536

[211] Casinovi, C. G.; Cerrini, S.; Motl, O.; Fardella, G.; Fedeli, W.; Gavuzzo, E.; Lamba, D. *Coll. Czech. Chem. Comm.* **1983**, *48*, 2411-2422.

7	6	0	1.043846	-2.384985	-0.732035
8	1	0	1.193490	-3.026097	-1.595447
9	1	0	0.727498	-3.027646	0.083730
10	6	0	-0.601799	1.046427	1.727106
11	6	0	-1.894501	0.217203	-0.122920
12	1	0	-1.494494	0.874998	-0.884031
13	6	0	-2.008651	0.998106	1.201860
14	1	0	-2.609418	0.421629	1.901029
15	1	0	-2.419294	1.991459	1.111230
16	6	0	0.546431	-1.025415	2.423466
17	1	0	-0.346785	-1.368470	2.919484
18	1	0	1.127757	-0.422327	3.110276
19	1	0	1.127455	-1.886076	2.131043
20	6	0	-3.279410	-0.319879	-0.555282
21	1	0	-3.642806	-0.956896	0.243150
22	6	0	-4.268894	0.857098	-0.725780
23	1	0	-4.408996	1.407554	0.194706
24	1	0	-5.238130	0.486430	-1.040277
25	1	0	-3.906601	1.542756	-1.485613
26	6	0	-3.282539	-1.122792	-1.875970
27	1	0	-4.304423	-1.307005	-2.188283
28	1	0	-2.800279	-2.086813	-1.782520
29	1	0	-2.785003	-0.566634	-2.663144
30	8	0	-0.123160	1.884575	2.453777
31	6	0	3.581123	-2.603131	-0.745055
32	1	0	4.506878	-2.125249	-0.452817
33	1	0	3.513961	-3.561659	-0.237635
34	8	0	1.026339	1.321833	-0.483830
35	6	0	1.883742	2.294270	-0.886675
36	8	0	2.991253	2.407301	-0.432365
37	6	0	1.246292	3.162143	-1.933351
38	1	0	0.944985	2.549992	-2.773915
39	1	0	1.945265	3.918358	-2.252552
40	1	0	0.358340	3.624408	-1.520577
41	6	0	2.532963	-0.548131	0.129001
42	1	0	3.526651	-0.170007	0.275265
43	1	0	3.613984	-2.799120	-1.812813
44	1	0	-0.801678	-1.878558	-1.683880
45	1	0	1.898788	1.040272	1.352503
46	8	0	-1.397862	-1.947462	0.926500
47	1	0	-1.925136	-2.497944	0.334641

SCF Done: E(RmPW+HF-PW91) = -964.175051451 A.U.

Carbon	Raw GIAO Shift	Relative GIAO Shift (TMS)	Scaled Chemical Shift	Experimental Chemical Shift	Difference	|Difference|

7	-15.7887	212.33475	219.8	220.3	-0.5	0.5
15	34.9672	161.57885	166.5	169.2	-2.7	2.7
5	53.9397	142.60635	146.5	146.5	0.0	0.0
17	79.046	117.50005	120.1	119.3	0.8	0.8
2	113.2729	83.27315	84.2	82.3	1.9	1.9
4	118.0761	78.46995	79.1	76	3.1	3.1
3	134.4971	62.04895	61.8	60.3	1.5	1.5
8	143.816	52.73005	52.1	51.7	0.4	0.4
9	153.5181	43.02795	41.9	38.9	3.0	3.0
1	157.7233	38.82275	37.4	37.3	0.1	0.1
11	164.0609	32.48515	30.8	29.2	1.6	1.6
6	167.1616	29.38445	27.5	26.6	0.9	0.9
14	170.2072	26.33885	24.3	26.1	-1.8	1.8
12	172.5373	24.00875	21.9	24.8	-2.9	2.9
13	173.6195	22.92655	20.7	21.3	-0.6	0.6
10	176.8287	19.71735	17.3	21.1	-3.8	3.8
16	177.1104	19.43565	17.1	18.1	-1.0	1.0
					AVG	1.6
					MAX	3.8

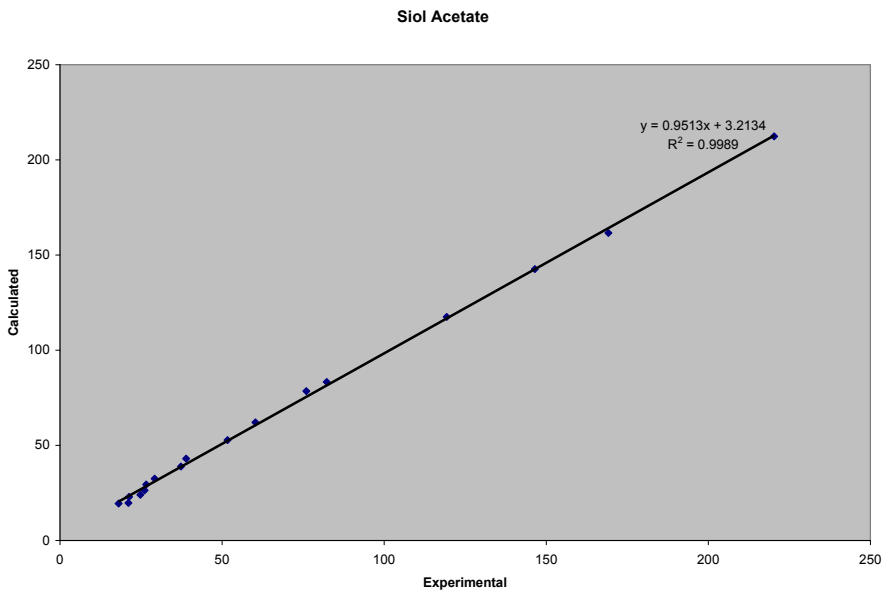

6-*epi*-Siol Acetate

The epimer of Siol acetate is also a natural product[212] and was selected for analysis to test discrimination of the stereochemistry at a tertiary hydroxyl group like that found in diol **3.74**. The predicted spectral data for this compound matched a bit less closely, with an average deviation of 2.2 ppm and a maximum of 6.8 ppm. Comparison of these diastereomers shows the limitation of this method for determination of stereochemistry, as the prediction for siol acetate actually matches the literature data for 6-*epi*-siol acetate better (1.4 ppm average, 3.4 max) than it does the experimental data for siol acetate. NMR chemical shift prediction is a tool which certainly must be used with caution in trying to differentiate these structural nuances. Diol **3.74** differs structurally both in terms

[212] Pandita, K.; Agarwal, S. G.; Thappa, R. K.; Dhar, K. L. *Indian J. Chem.* **1984** *23B*, 956-957.

of functional groups and connectivity, but shares the same molecular formula $C_{17}H_{26}O_4$ with the siol acetate epimers. Comparison of the predicted ^{13}C-NMR data for these compounds with the experimental data for **3.74** shows an average deviation of greater than 15 ppm. This highlights the effect of a grossly incorrect structural prediction in this type of correlation analysis.

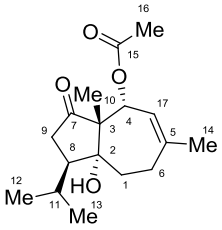

6-*epi*-Siol Acetate

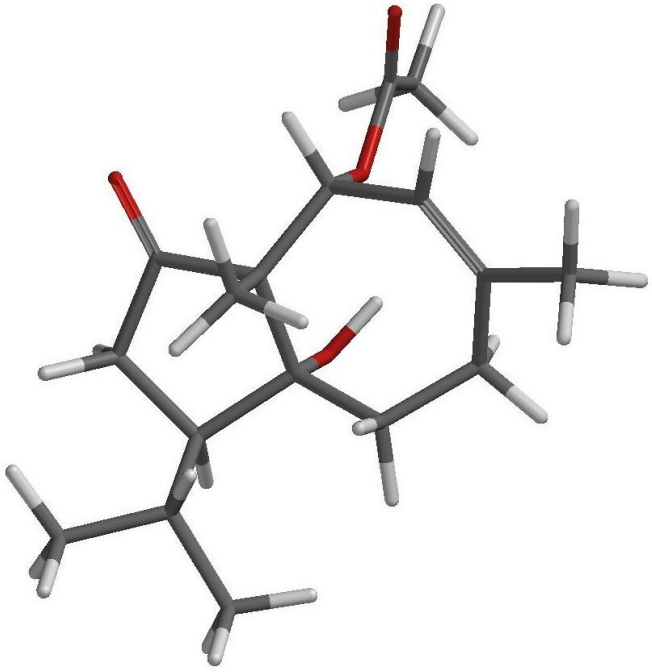

Standard orientation:

Center Number	Atomic Number	Atomic Type	Coordinates (Angstroms) X	Y	Z
1	1	0	1.261644	2.207260	0.048366
2	6	0	0.785665	1.693511	-0.775488
3	1	0	1.335928	1.917935	-1.680364
4	6	0	0.829725	0.178540	-0.591899
5	6	0	0.150951	-0.371053	0.681862
6	6	0	-1.358460	-0.160855	0.818972
7	1	0	-1.701293	-0.787149	1.625746
8	6	0	-1.480078	2.300616	0.309036
9	6	0	-0.658112	2.213182	-0.969439
10	1	0	-1.150887	1.569728	-1.685085

```
    11          1             0       -0.607407    3.201112   -1.411974
    12          6             0        0.508602   -1.842867    0.558414
    13          6             0        2.229143   -0.516180   -0.629565
    14          1             0        2.455561   -0.600936   -1.682059
    15          6             0        1.874086   -1.945052   -0.112151
    16          1             0        2.588177   -2.361834    0.580991
    17          1             0        1.780966   -2.628085   -0.945300
    18          6             0        0.791831    0.101931    2.009368
    19          1             0        1.818734   -0.219202    2.089723
    20          1             0        0.246545   -0.336752    2.837815
    21          1             0        0.750427    1.177037    2.104214
    22          6             0        3.417227    0.244386    0.042363
    23          1             0        3.039864    0.946681    0.772244
    24          6             0        4.430570   -0.675827    0.755214
    25          1             0        4.004994   -1.162593    1.624616
    26          1             0        5.279466   -0.090552    1.091812
    27          1             0        4.796989   -1.440096    0.078011
    28          6             0        4.183360    1.050220   -1.032445
    29          1             0        4.970092    1.641853   -0.576362
    30          1             0        3.529305    1.720294   -1.574460
    31          1             0        4.638929    0.371647   -1.746558
    32          8             0        0.194987   -0.446447   -1.737544
    33          1             0       -0.744283   -0.605602   -1.559815
    34          8             0       -0.169651   -2.758900    0.957146
    35          6             0       -1.971792    3.690577    0.659218
    36          1             0       -2.548139    3.692368    1.575287
    37          1             0       -1.130051    4.367439    0.776975
    38          8             0       -2.012292   -0.680071   -0.399052
    39          6             0       -3.305354   -1.109679   -0.301859
    40          8             0       -3.927755   -1.021662    0.719437
    41          6             0       -3.768867   -1.679225   -1.609801
    42          1             0       -4.797989   -1.989043   -1.525248
    43          1             0       -3.145063   -2.525609   -1.869626
    44          1             0       -3.664706   -0.933433   -2.387690
    45          6             0       -1.776848    1.266304    1.073715
    46          1             0       -2.385062    1.412377    1.946201
    47          1             0       -2.594945    4.080625   -0.140446
 ---------------------------------------------------------------------
SCF Done:  E(RmPW+HF-PW91) =  -964.169470713     A.U.
```

Carbon	Raw GIAO Shift	Relative GIAO Shift (TMS)	Scaled Chemical Shift	Experimental Chemical Shift	Difference	|Difference|
7	-12.5999	209.14595	217.5	219.5	-2.0	2.0
15	36.1742	160.37185	166.5	168.6	-2.1	2.1
5	53.6679	142.87815	148.3	147.2	1.1	1.1

17	78.364	118.18205	122.4	119.5	2.9	2.9
2	111.4829	85.06315	87.8	82.3	5.5	5.5
4	120.7276	75.81845	78.1	76.1	2.0	2.0
3	140.6759	55.87015	57.3	60.4	-3.1	3.1
8	143.6575	52.88855	54.2	52	2.2	2.2
9	159.3911	37.15495	37.7	39.1	-1.4	1.4
1	166.5292	30.01685	30.3	37.1	-6.8	6.8
11	168.3134	28.23265	28.4	29.4	-1.0	1.0
6	168.4158	28.13025	28.3	26.8	1.5	1.5
14	169.1922	27.35385	27.5	25.8	1.7	1.7
13	170.068	26.47805	26.6	24.5	2.1	2.1
12	175.6224	20.92365	20.8	21.1	-0.3	0.3
16	177.5599	18.98615	18.7	20.8	-2.1	2.1
10	178.3722	18.17385	17.9	18	-0.1	0.1
					AVG	2.2
					MAX	6.8

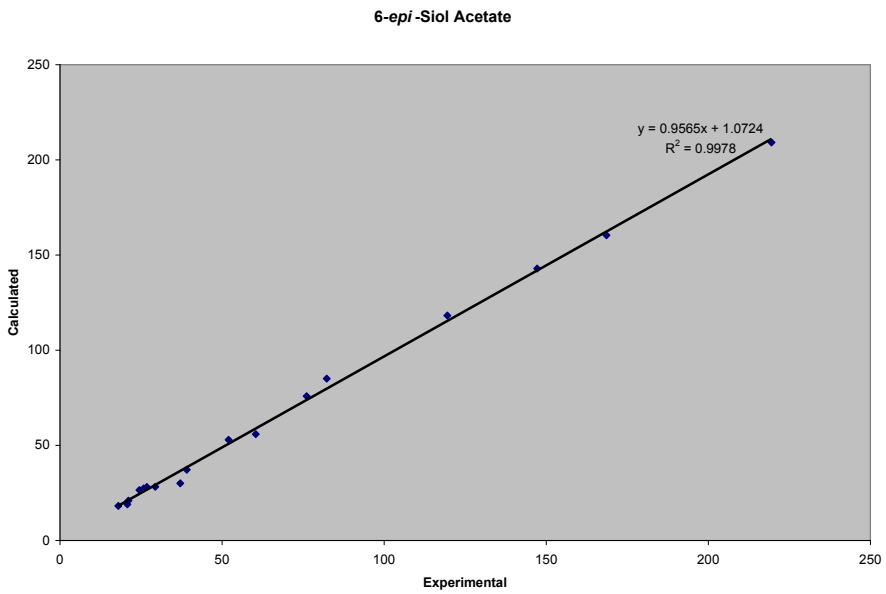

Siol Acetate Diastereomer Comparison

Siol Acetate			6-*epi*-siol acetate		
Raw GIAO Shift	Relative GIAO Shift (TMS)	Scaled Chemical Shift	Experimental Chemical Shift	Difference	|Difference|
-15.7887	212.33475	219.6	219.5	0.1	0.1
34.9672	161.57885	166.3	168.6	-2.3	2.3
53.9397	142.60635	146.4	147.2	-0.8	0.8
79.046	117.50005	120.0	119.5	0.5	0.5
113.2729	83.27315	84.1	82.3	1.8	1.8
118.0761	78.46995	79.0	76.1	2.9	2.9
134.4971	62.04895	61.8	60.4	1.4	1.4
143.816	52.73005	52.0	52	0.0	0.0
153.5181	43.02795	41.8	39.1	2.7	2.7

157.7233	38.82275	37.4	37.1	0.3	0.3
164.0609	32.48515	30.8	29.4	1.4	1.4
167.1616	29.38445	27.5	26.8	0.7	0.7
170.2072	26.33885	24.3	25.8	-1.5	1.5
172.5373	24.00875	21.9	24.5	-2.6	2.6
173.6195	22.92655	20.7	21.1	-0.4	0.4
176.8287	19.71735	17.4	20.8	-3.4	3.4
177.1104	19.43565	17.1	18	-0.9	0.9
				AVG	1.4
				MAX	3.4

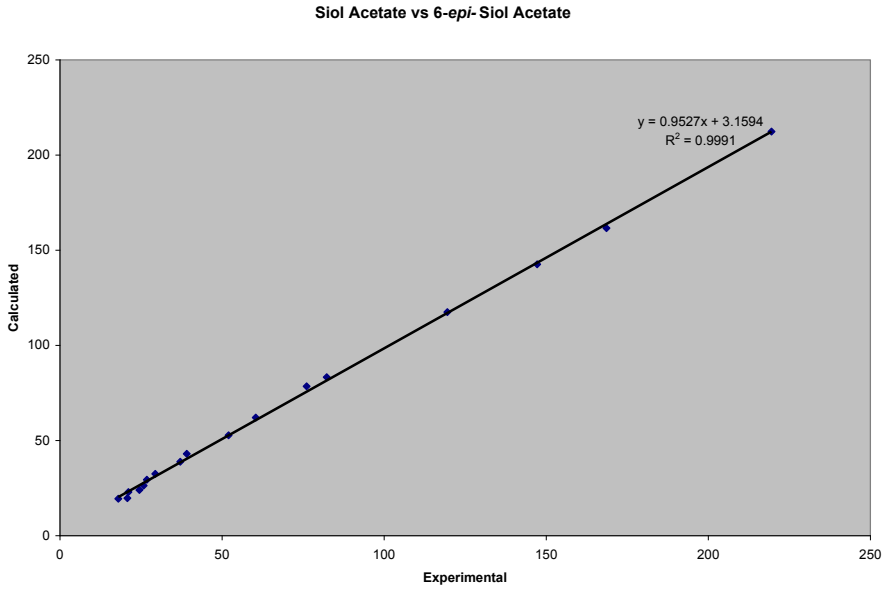

6-*epi*-siol Acetate			**Siol acetate**		
Raw GIAO Shift	**Relative GIAO Shift (TMS)**	**Scaled Chemical Shift**	**Experimental Chemical Shift**	**Difference**	**|Difference|**
-12.5999	209.14595	217.8	220.3	-2.5	2.5

36.1742	160.37185	166.7	169.2	-2.5	2.5
53.6679	142.87815	148.4	146.5	1.9	1.9
78.364	118.18205	122.6	119.3	3.3	3.3
111.4829	85.06315	87.9	82.3	5.6	5.6
120.7276	75.81845	78.2	76	2.2	2.2
140.6759	55.87015	57.3	60.3	-3.0	3.0
143.6575	52.88855	54.2	51.7	2.5	2.5
159.3911	37.15495	37.7	38.9	-1.2	1.2
166.5292	30.01685	30.2	37.3	-7.1	7.1
168.3134	28.23265	28.4	29.2	-0.8	0.8
168.4158	28.13025	28.3	26.6	1.7	1.7
169.1922	27.35385	27.5	26.1	1.4	1.4
170.068	26.47805	26.5	24.8	1.7	1.7
175.6224	20.92365	20.7	21.3	-0.6	0.6
177.5599	18.98615	18.7	21.1	-2.4	2.4
178.3722	18.17385	17.8	18.1	-0.3	0.3
				AVG	2.4
				MAX	7.1

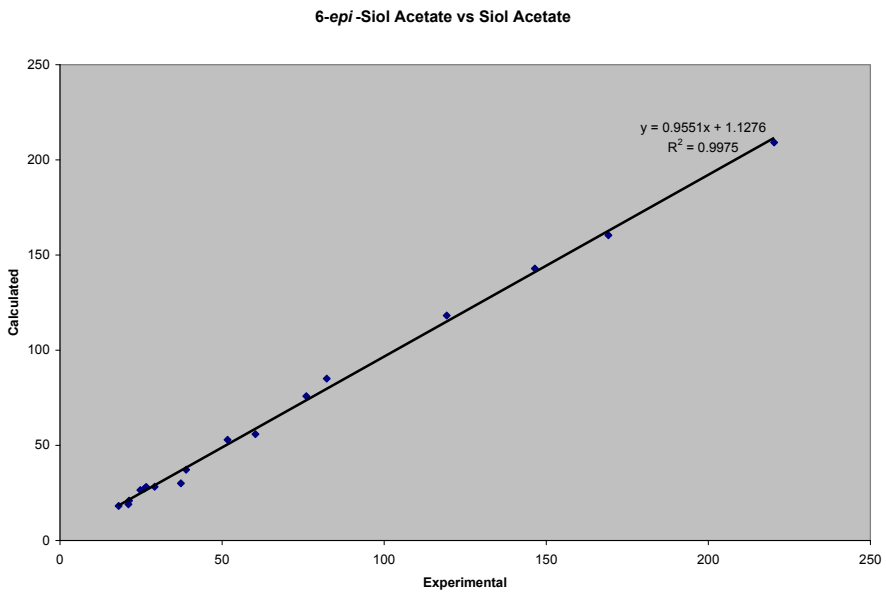

SiOl Acetate, 6-*epi*-SiOl Acetate and 3.74 (Same Molecular Formula)

SiOl Acetate			Ketal Diol		
Raw GIAO Shift	Relative GIAO Shift (TMS)	Scaled Chemical Shift	Experimental Chemical Shift	Difference	|Difference|
-15.7887	212.33475	212.5	147.1	65.4	65.4
34.9672	161.57885	161.8	136.4	25.4	25.4
53.9397	142.60635	142.9	127.9	15.0	15.0
79.046	117.50005	117.8	122.3	-4.5	4.5
113.2729	83.27315	83.6	115.5	-31.9	31.9
118.0761	78.46995	78.8	80.3	-1.5	1.5
134.4971	62.04895	62.4	73.7	-11.3	11.3
143.816	52.73005	53.1	70	-16.9	16.9
153.5181	43.02795	43.4	65.7	-22.3	22.3

157.7233	38.82275	39.2	55	-15.8	15.8
164.0609	32.48515	32.9	51.5	-18.6	18.6
167.1616	29.38445	29.8	40.3	-10.5	10.5
170.2072	26.33885	26.7	35.6	-8.9	8.9
172.5373	24.00875	24.4	29.6	-5.2	5.2
173.6195	22.92655	23.3	27.6	-4.3	4.3
176.8287	19.71735	20.1	21.8	-1.7	1.7
177.1104	19.43565	19.8	16.7	3.1	3.1
				AVG	15.4
				MAX	65.4

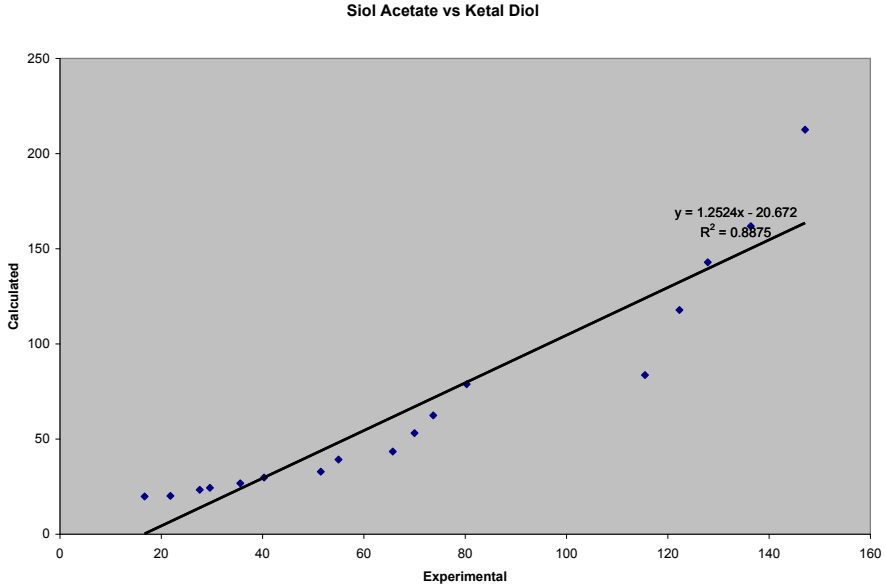

6-*epi*-siol Acetate			**Ketal Diol**		
Raw GIAO Shift	**Relative GIAO Shift (TMS)**	**Scaled Chemical Shift**	**Experimental Chemical Shift**	**Difference**	**|Difference|**
-12.5999	209.14595	209.4	147.1	62.3	62.3

36.1742	160.37185	160.7	136.4	24.3	24.3
53.6679	142.87815	143.2	127.9	15.3	15.3
78.364	118.18205	118.5	122.3	-3.8	3.8
111.4829	85.06315	85.4	115.5	-30.1	30.1
120.7276	75.81845	76.2	80.3	-4.1	4.1
140.6759	55.87015	56.2	73.7	-17.5	17.5
143.6575	52.88855	53.3	70	-16.7	16.7
159.3911	37.15495	37.5	65.7	-28.2	28.2
166.5292	30.01685	30.4	55	-24.6	24.6
168.3134	28.23265	28.6	51.5	-22.9	22.9
168.4158	28.13025	28.5	40.3	-11.8	11.8
169.1922	27.35385	27.7	35.6	-7.9	7.9
170.068	26.47805	26.9	29.6	-2.7	2.7
175.6224	20.92365	21.3	27.6	-6.3	6.3
177.5599	18.98615	19.4	21.8	-2.4	2.4
178.3722	18.17385	18.6	16.7	1.9	1.9
				AVG	16.6
				MAX	62.3

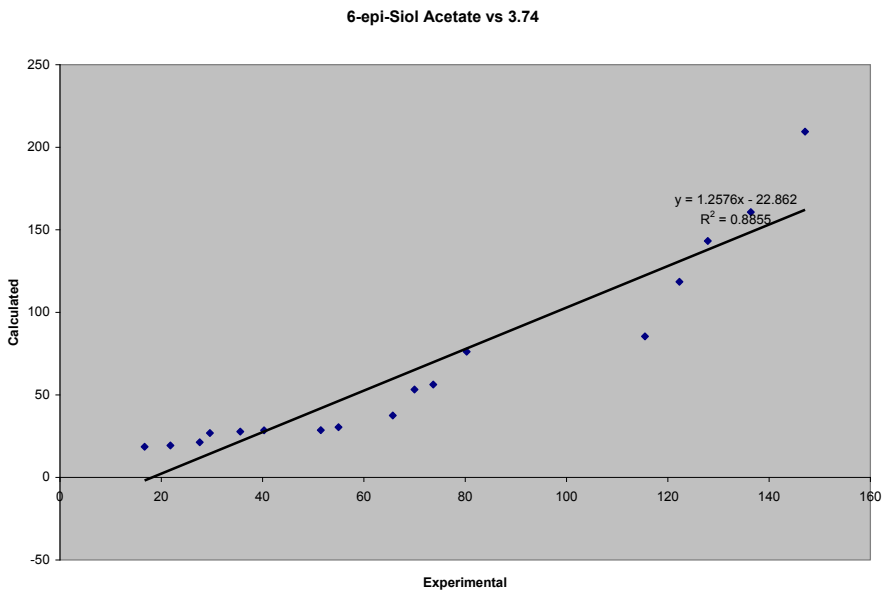

Aerugidiol

Guaiane natural product aerugidiol[87] was selected for prediction since it contains similar functional groups to **3.74**. The predicted values for this compound are an acceptable match for those reported in the literature with an average deviation of 2.3 ppm and a maximum deviation of 5.5 ppm. If the carbonyl resonance in aerugidiol and the ethylene ketal resonances from **3.74** are ignored, the remaining molecular fragments share similar functionality and an identical molecular formula. These selected resonances in the prediction for aerugidiol were compared with the corresponding resonances in the experimental data for **3.74**. They only match with an average deviation of 4.3 ppm and a maximum deviation of 14.0 ppm. This gives an estimate for what is likely the best possible correlation for an incorrect structure in this type of analysis.

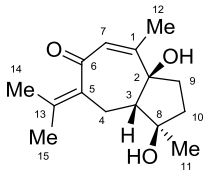

aerugidiol

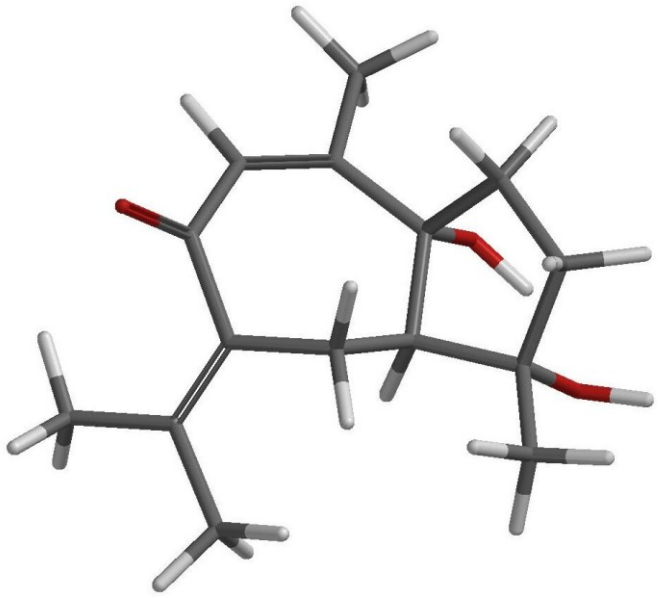

Standard orientation:

Center Number	Atomic Number	Atomic Type	Coordinates (Angstroms) X	Y	Z
1	6	0	-0.352510	2.074899	0.091253
2	6	0	-1.250360	0.858405	0.257695
3	6	0	-0.650355	-0.569905	0.211780
4	6	0	0.445272	-0.693503	-0.860562
5	1	0	0.181187	-0.096192	-1.726196
6	1	0	0.530335	-1.710480	-1.204831
7	6	0	1.790790	-0.237497	-0.330719
8	6	0	2.035200	1.221529	-0.455710
9	6	0	0.926424	2.181636	-0.243757
10	1	0	1.317884	3.176850	-0.335348
11	6	0	-1.891035	-1.436359	-0.111722
12	6	0	-2.314176	0.843787	-0.900059
13	1	0	-3.196835	1.349812	-0.540113
14	1	0	-1.944933	1.364206	-1.772666
15	6	0	-2.594685	-0.648768	-1.226658
16	1	0	-3.653929	-0.874705	-1.257998
17	1	0	-2.165761	-0.918432	-2.182781
18	1	0	-0.259780	-0.835507	1.183100
19	8	0	-1.900746	1.066887	1.526727
20	1	0	-2.402111	0.258988	1.730021
21	8	0	-2.704008	-1.367254	1.106848
22	1	0	-3.544105	-1.830558	0.991160
23	6	0	-1.651380	-2.910832	-0.425363
24	1	0	-2.606502	-3.413893	-0.546653
25	1	0	-1.124298	-3.382986	0.394390
26	1	0	-1.093077	-3.046370	-1.339965
27	6	0	-1.122969	3.357718	0.370584
28	1	0	-1.473993	3.329022	1.391077

```
    29          1           0       -1.989513    3.440467   -0.275569
    30          1           0       -0.497054    4.225930    0.220411
    31          8           0        3.137990    1.696568   -0.688893
    32          6           0        2.684612   -1.070330    0.195133
    33          6           0        4.053541   -0.672565    0.718463
    34          1           0        4.809128   -1.271987    0.217289
    35          1           0        4.112525   -0.896837    1.779789
    36          1           0        4.275164    0.362941    0.545344
    37          6           0        2.436088   -2.560261    0.365101
    38          1           0        2.798623   -2.879097    1.336442
    39          1           0        2.997215   -3.109294   -0.386822
    40          1           0        1.397201   -2.839215    0.289704
 ---------------------------------------------------------------------
SCF Done:  E(RmPW+HF-PW91) =  -810.323119093     A.U.
```

Carbon	Raw GIAO Shift	Relative GIAO Shift (TMS)	Scaled Chemical Shift	Experimental Chemical Shift	Difference	|Difference|
6	10.8896	185.65645	192.3	195.5	-3.2	3.2
1	46.6813	149.86475	154.7	151.3	3.4	3.4
13	57.0262	139.51985	143.9	143.6	0.3	0.3
5	66.9825	129.56355	133.4	133.9	-0.5	0.5
7	74.8977	121.64835	125.1	128.6	-3.5	3.5
8	108.0274	88.51865	90.4	87	3.4	3.4
2	109.3488	87.19725	89.0	83.5	5.5	5.5
3	138.3764	58.16965	58.6	61.2	-2.6	2.6
9	154.8907	41.65535	41.2	37.6	3.6	3.6
10	159.0324	37.51365	36.9	37.5	-0.6	0.6
4	167.4207	29.12535	28.1	27.8	0.3	0.3
12	170.475	26.07105	24.9	24.5	0.4	0.4
11	172.4228	24.12325	22.8	23.5	-0.7	0.7
15	175.0089	21.53715	20.1	22.6	-2.5	2.5

14	176.2101	20.33595	18.9	22.2	-3.3	3.3
					AVG	2.3
					MAX	5.5

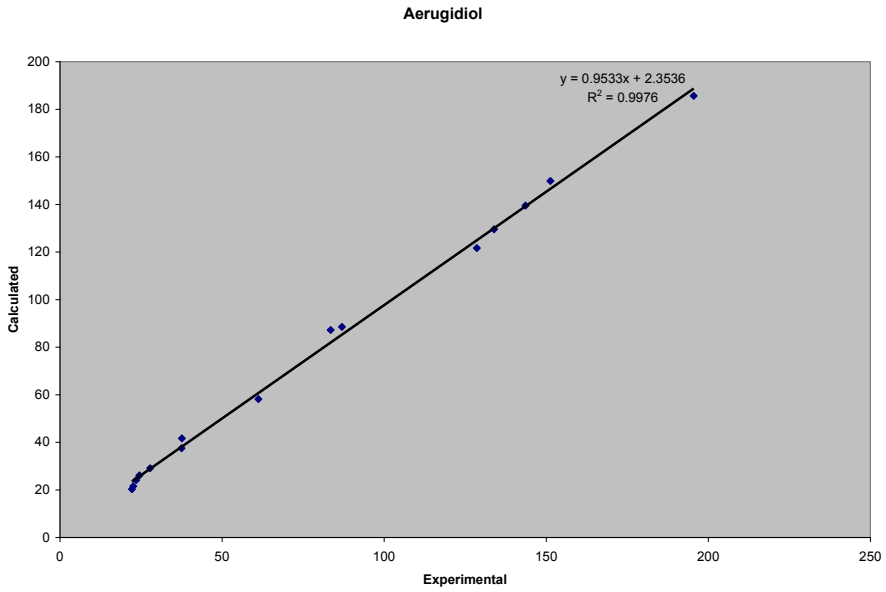

Aerugidiol and 3.74 (Selected Peaks)

Aerugidiol Select			**Ketal Diol**		
Raw GIAO Shift	**Relative GIAO Shift (TMS)**	**Scaled Chemical Shift**	**Experimental Chemical Shift**	**Difference**	**|Difference|**
46.6813	149.86475	146.4	147.1	0.7	0.7
57.0262	139.51985	136.3	136.4	4.9	4.9
66.9825	129.56355	126.6	127.9	5.6	5.6
74.8977	121.64835	118.9	122.3	1.5	1.5
108.0274	88.51865	86.6	80.3	11.5	11.5
109.3488	87.19725	85.3	73.7	14.0	14.0
138.3764	58.16965	57.0	55	8.2	8.2

154.8907	41.65535	41.0	51.5	1.0	1.0
159.0324	37.51365	36.9	40.3	1.5	1.5
167.4207	29.12535	28.7	35.6	-5.9	5.9
170.475	26.07105	25.8	29.6	-0.7	0.7
172.4228	24.12325	23.9	27.6	-2.1	2.1
175.0089	21.53715	21.3	21.8	-2.0	2.0
176.2101	20.33595	20.2	16.7	0.7	0.7
				AVG	4.3
				MAX	14.0

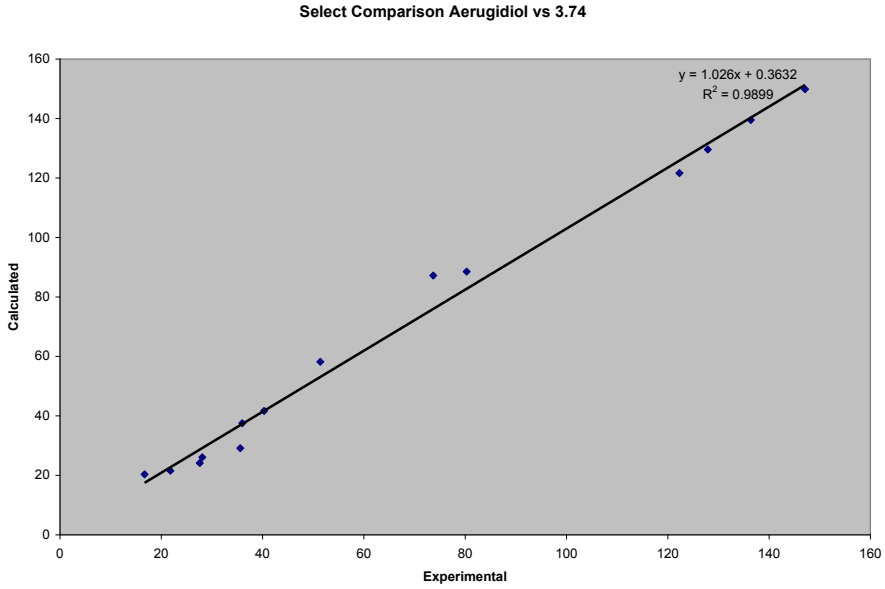

Spectra

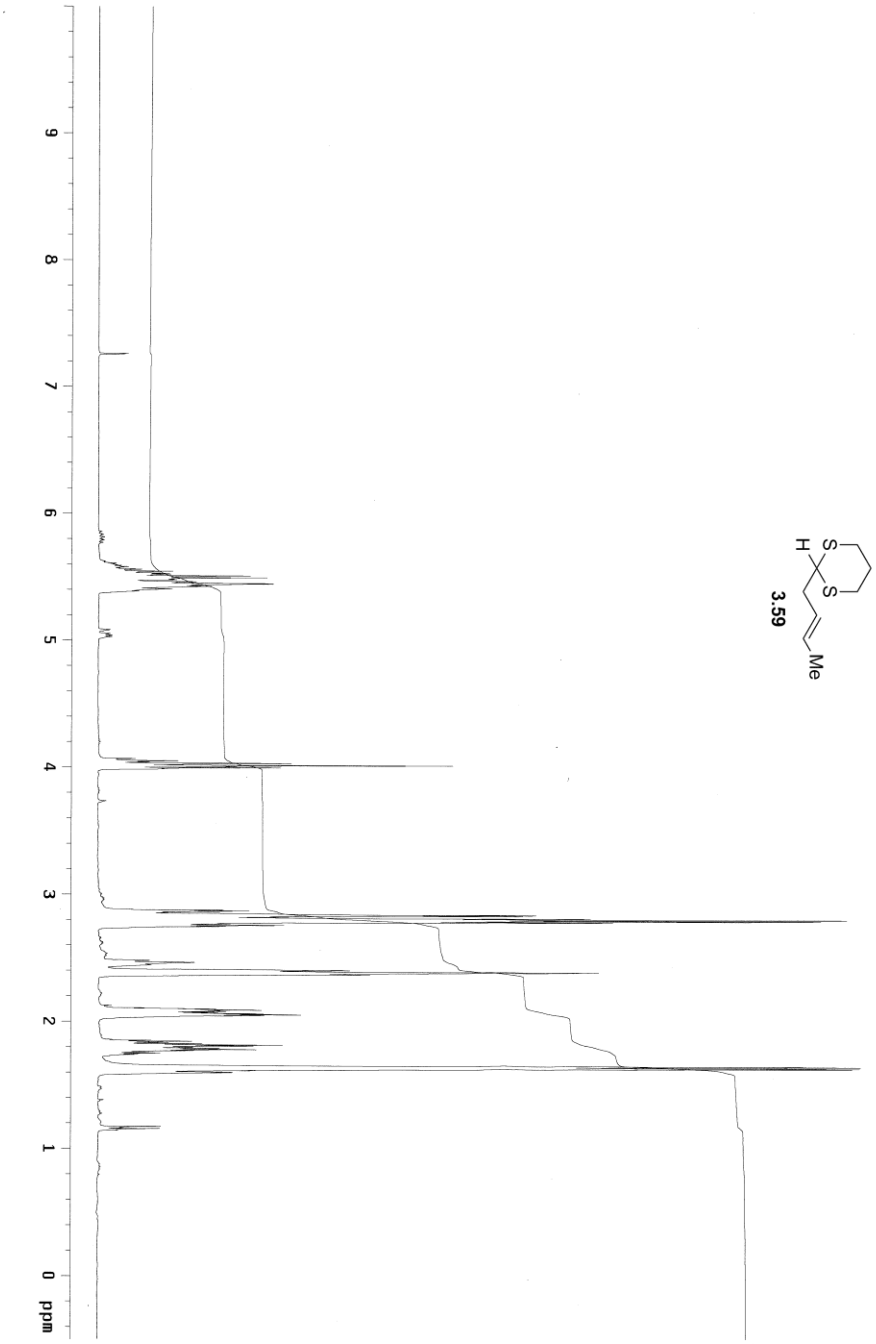
S
H
S
Me
3.59
9
8
7
6
5
4
3
2
1
0
ppm

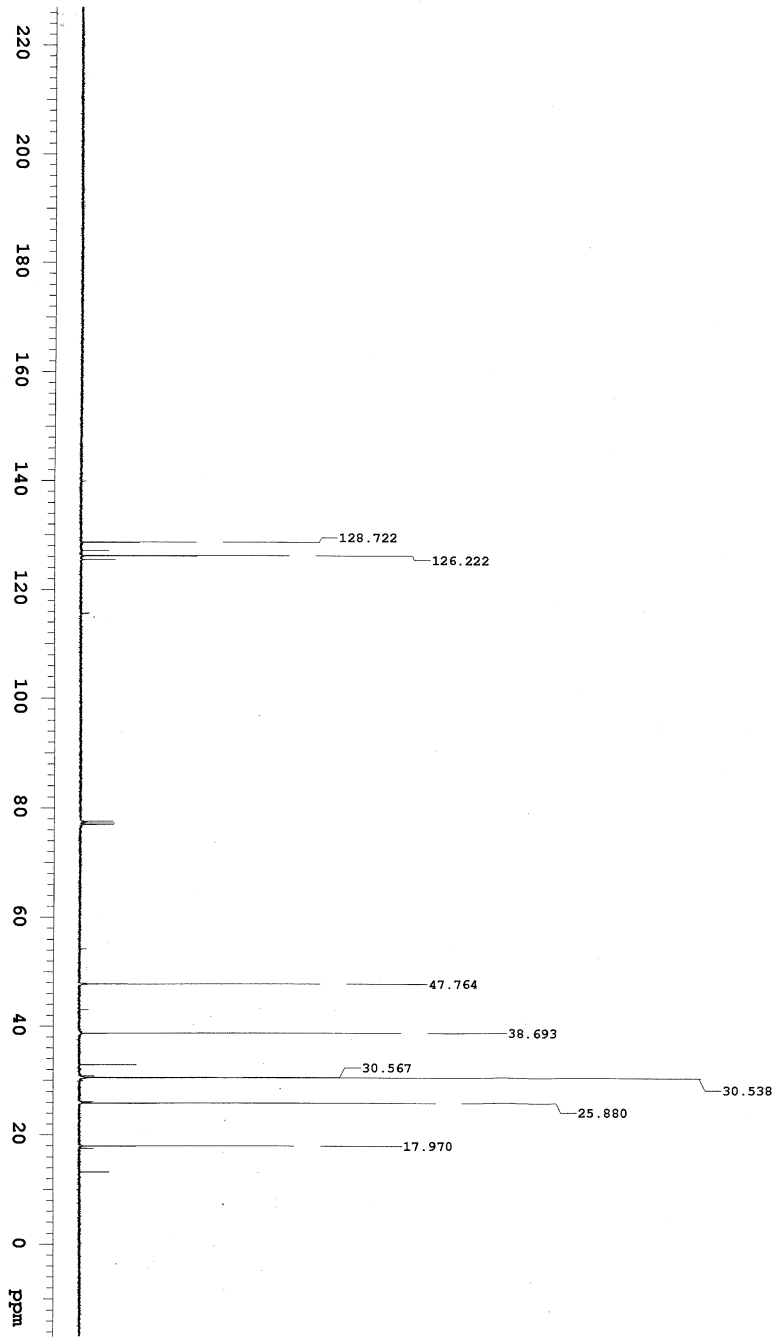
220
200
180
160
140
120
100
80
60
40
20
0
ppm
128.722
126.222
47.764
38.693
30.567
30.538
25.880
17.970

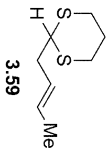
H
S
S
Me

3.59

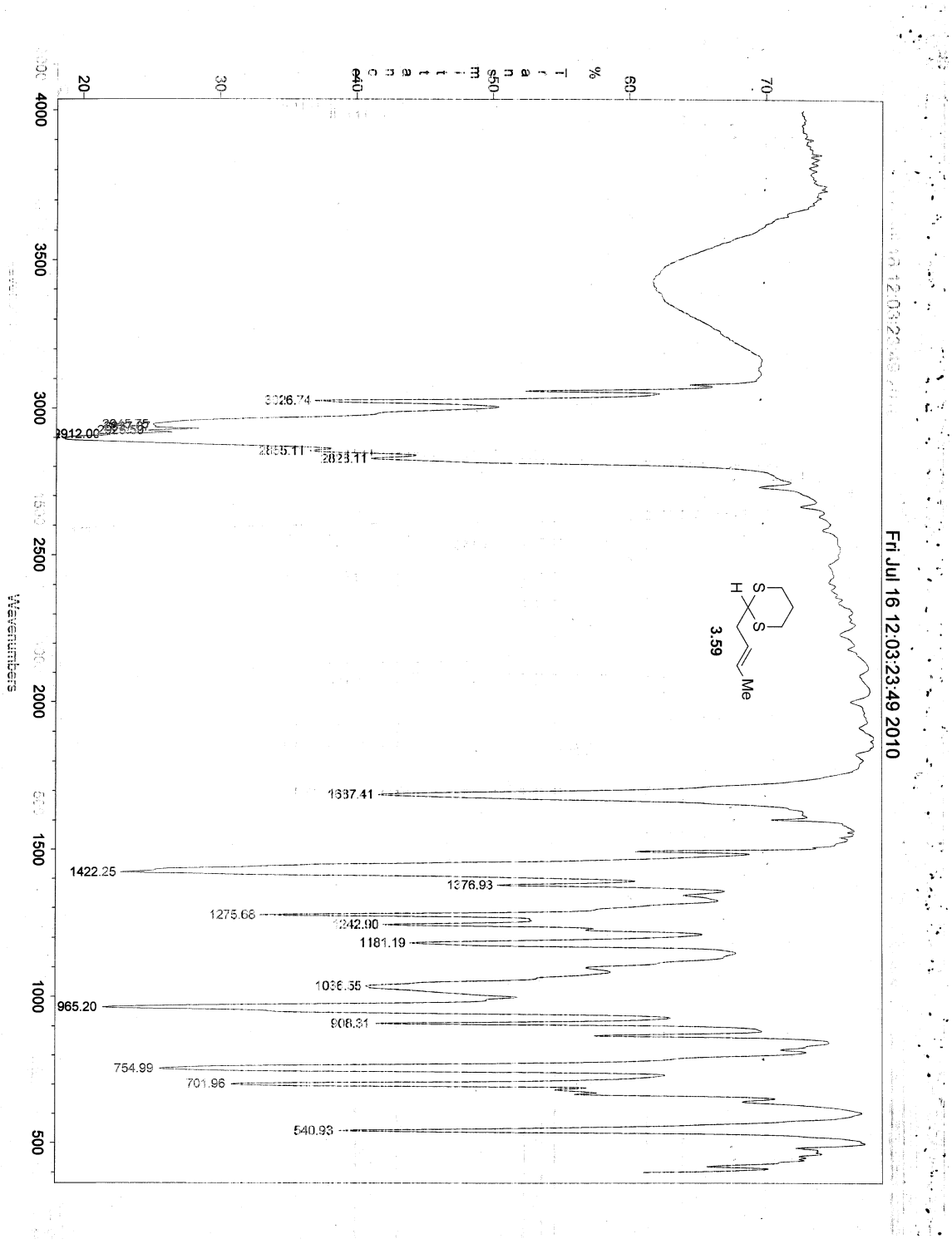
Fri Jul 16 12:03:23.49 2010
Wavenumbers
%Transmittance
4000
3500
3000
2500
2000
1500
1000
500
20
30
40
50
60
70
3026.74
2912.00
2885.11
2023.11
1637.41
1422.25
1376.93
1275.68
1242.90
1181.19
1036.55
965.20
908.31
754.99
701.96
540.93
S
H
S
Me
3.59

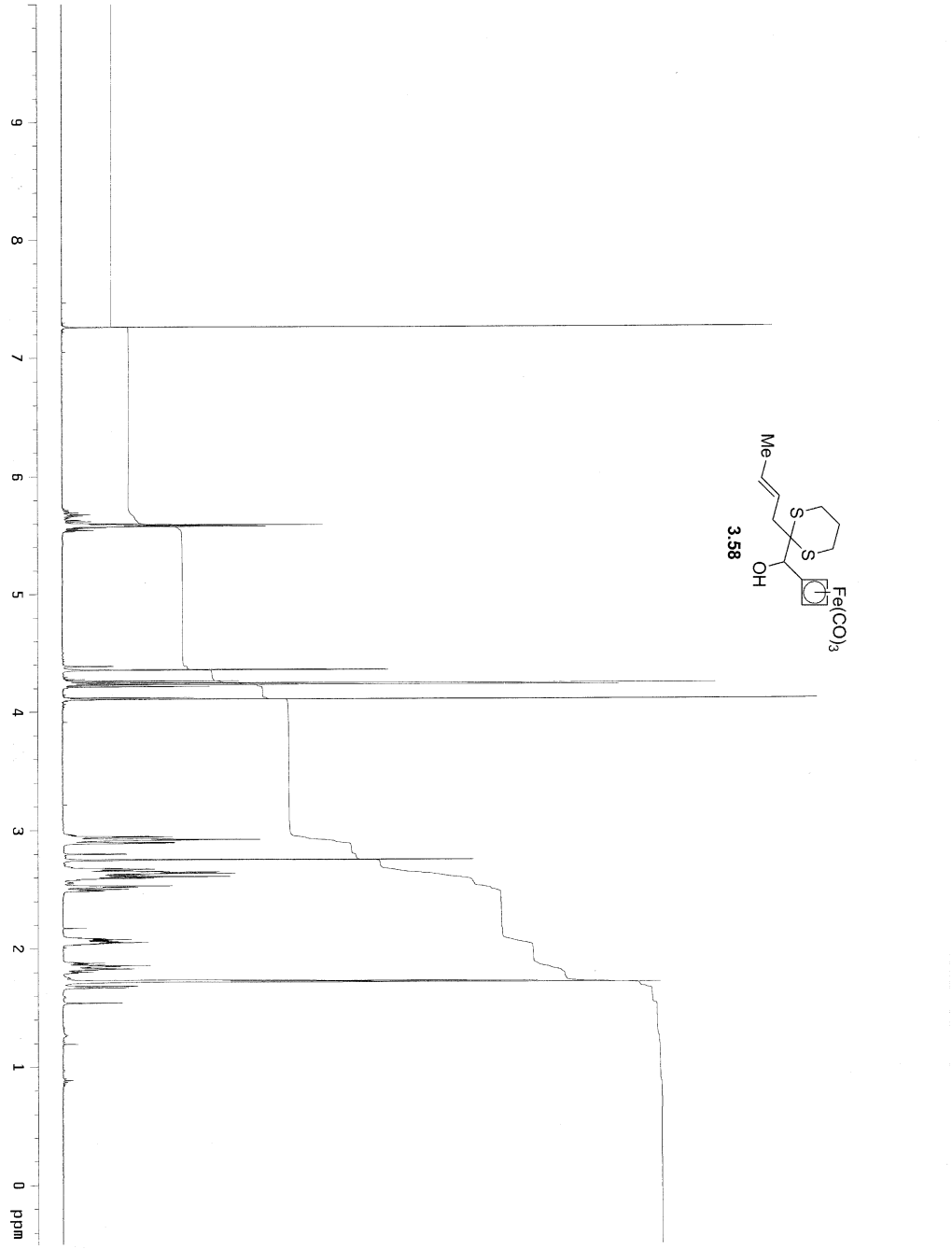
Me
S
S
OH
3.58
Fe(CO)3
9
8
7
6
5
4
3
2
1
0
ppm

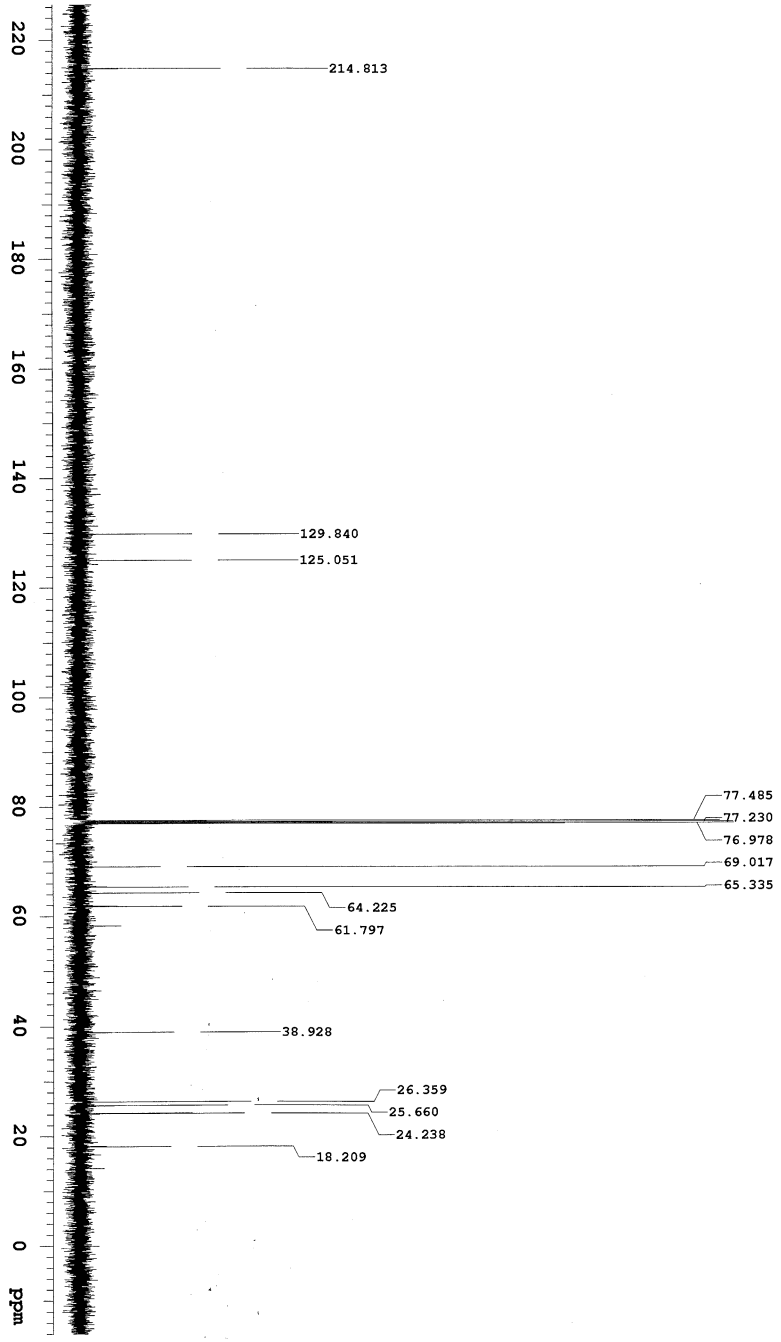
214.813
129.840
125.051
77.485
77.230
76.978
69.017
65.335
64.225
61.797
38.928
26.359
25.660
24.238
18.209
220
200
180
160
140
120
100
80
60
40
20
0
ppm

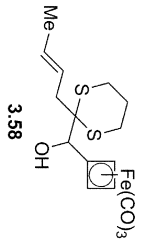
Me
S
S
OH
Fe(CO)3

3.58

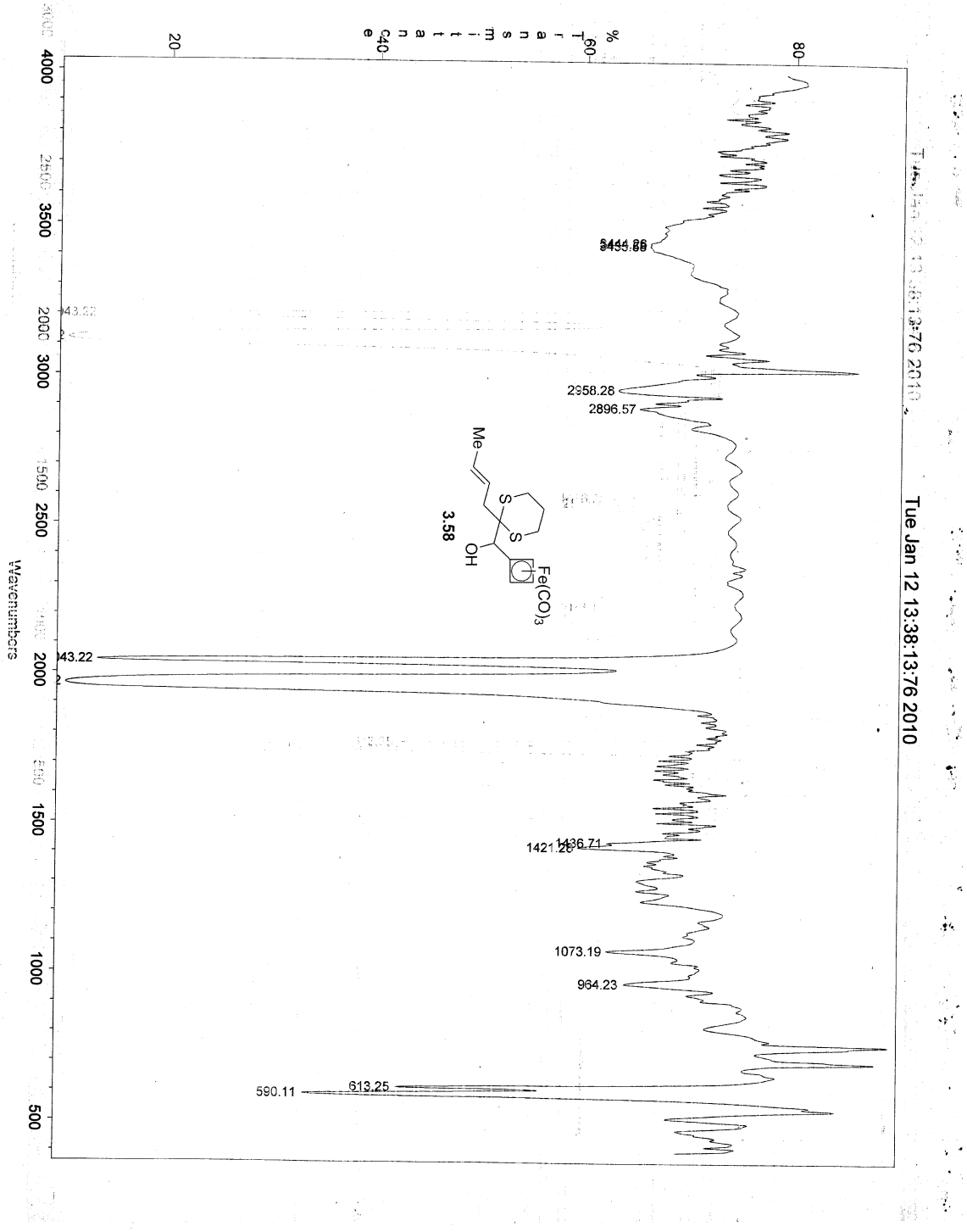
Transmittance %
Wavenumbers
4000
3500
3000
2500
2000
1500
1000
500
20
40
60
80
2958.28
2896.57
2043.22
1421.26
1436.71
1073.19
964.23
613.25
590.11
Me
S
S
OH
Fe(CO)3
3.58
Tue Jan 12 13:38:13:76 2010

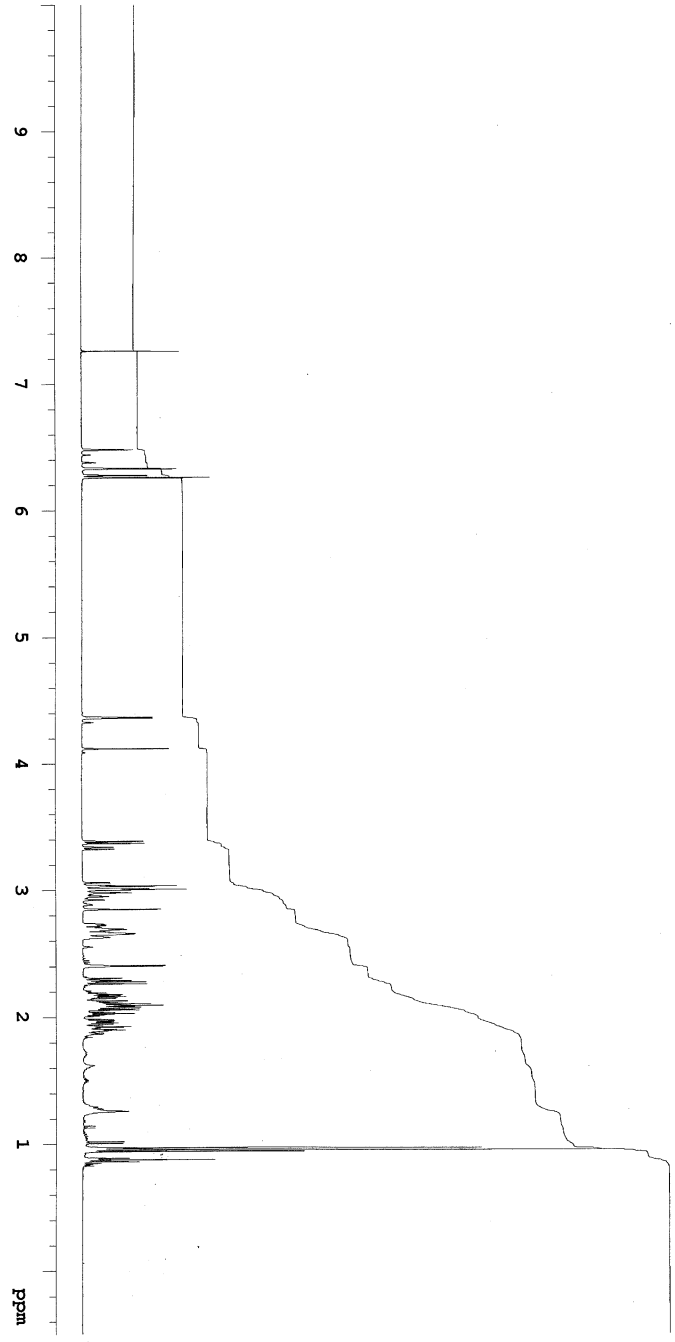

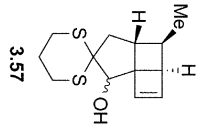

3.57

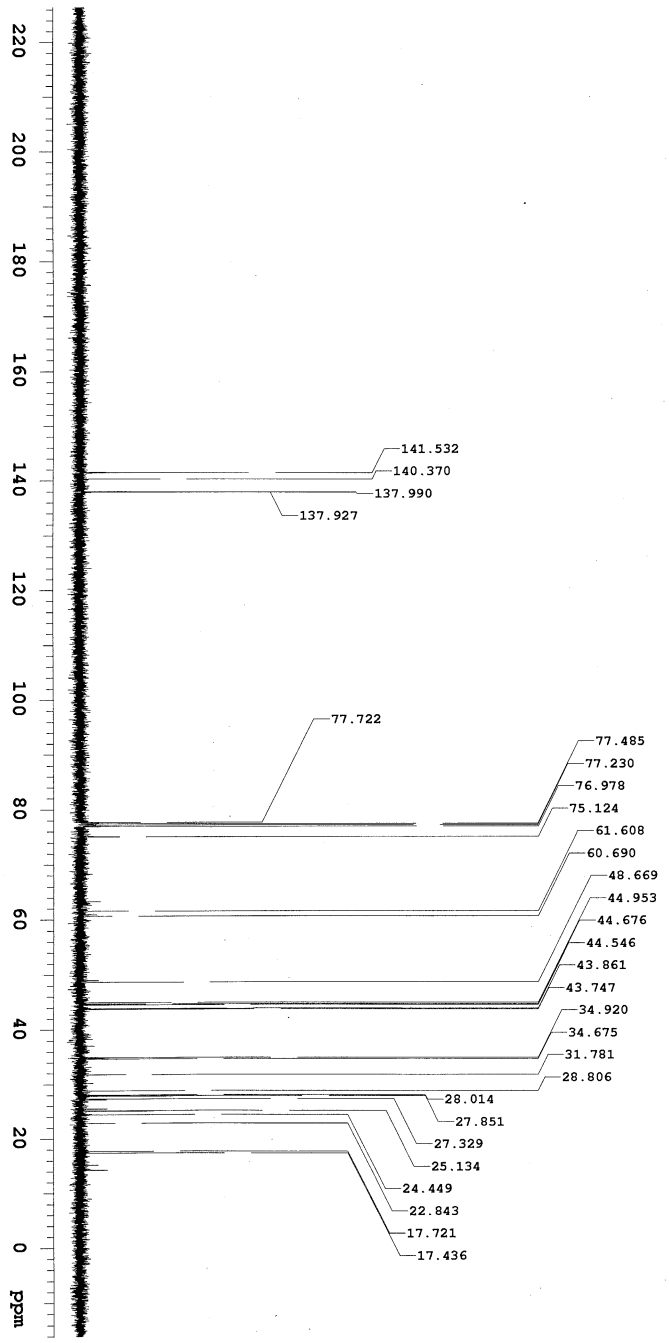
220
200
180
160
140
120
100
80
60
40
20
0
ppm
141.532
140.370
137.990
137.927
77.722
77.485
77.230
76.978
75.124
61.608
60.690
48.669
44.953
44.676
44.546
43.861
43.747
34.920
34.675
31.781
28.806
28.014
27.851
27.329
25.134
24.449
22.843
17.721
17.436

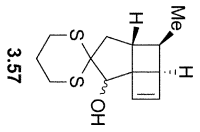
Me
H
S
S
H
OH

3.57

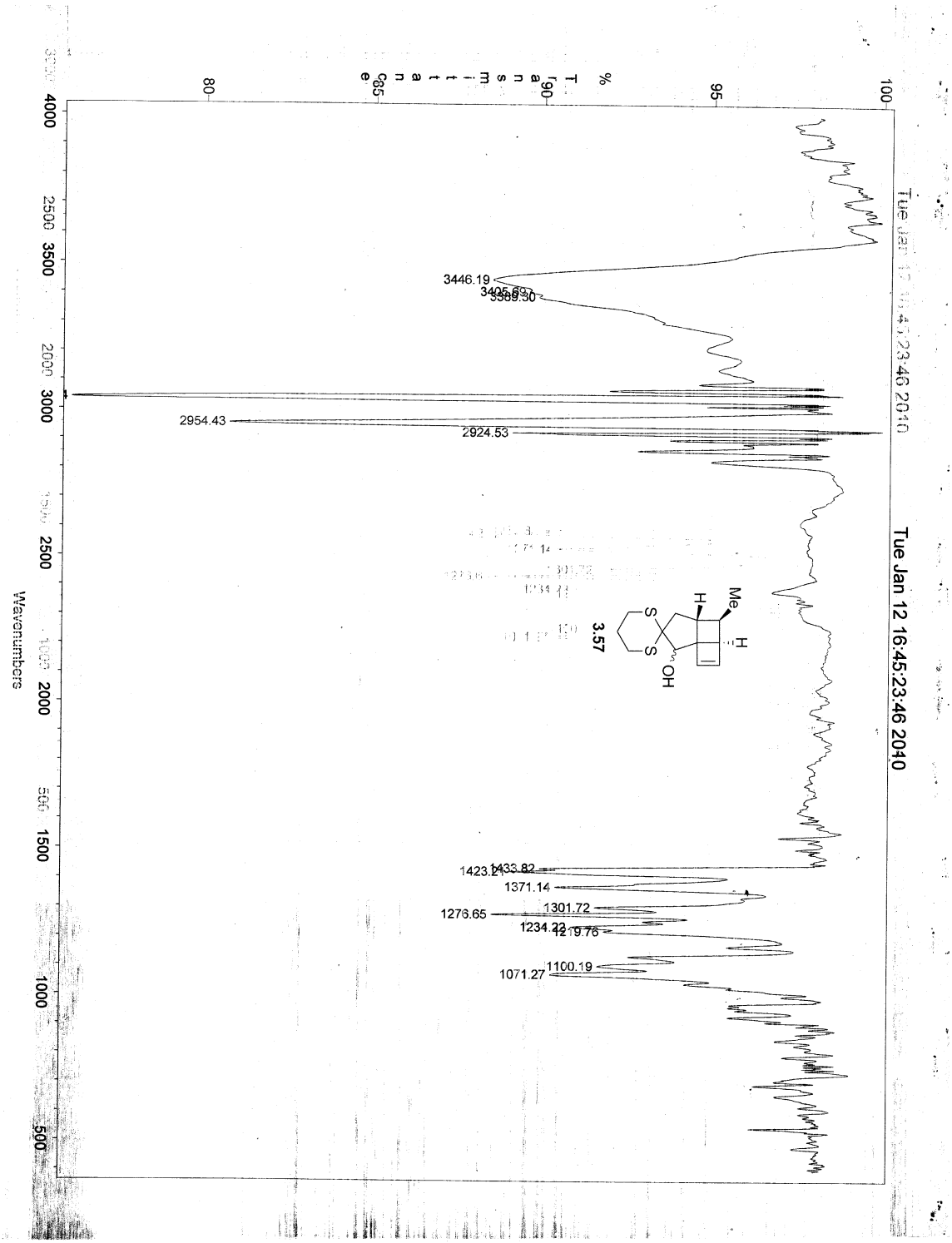
Tue Jan 12 16:45:23:46 2010
Tue Jan 12 16:45:23:46 2010
% Transmittance
Wavenumbers
3446.19
2954.43
2924.53
1423.21
1433.82
1371.14
1301.72
1276.65
1234.22
1219.76
1100.19
1071.27
3.57
Me
H
H
S
S
OH

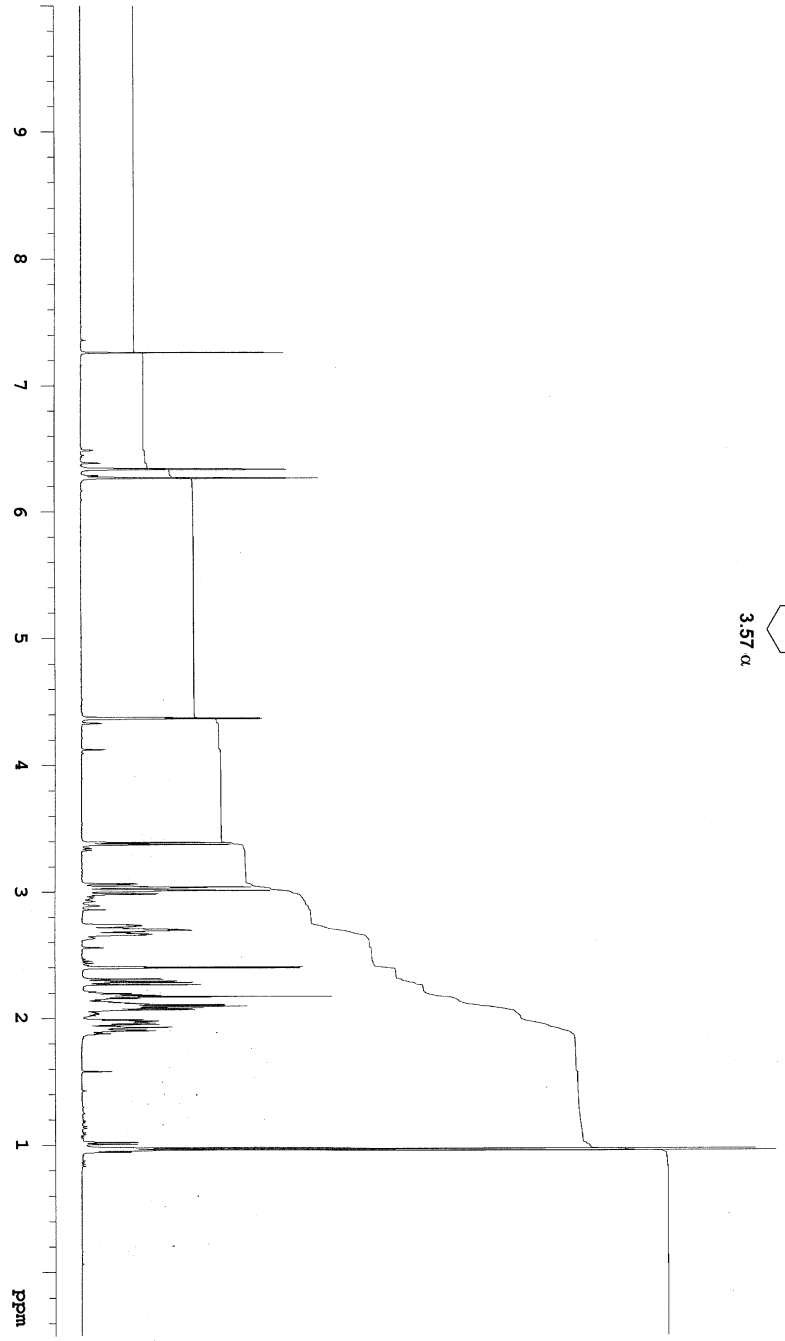
9
8
7
6
5
4
3
2
1
ppm
3.57 α
S
S
OH
H
Me
H

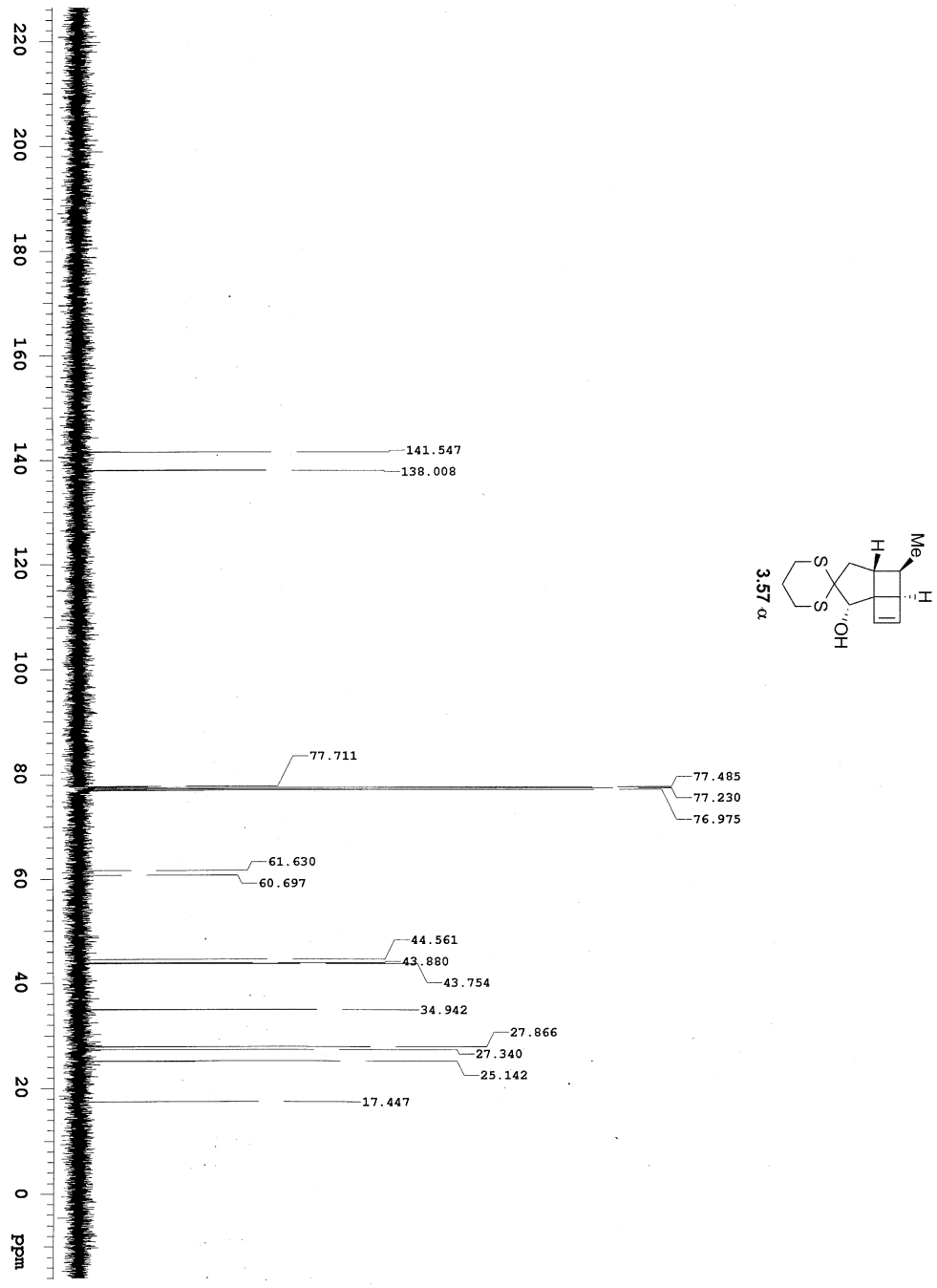
220
200
180
160
140
120
100
80
60
40
20
0
ppm
141.547
138.008
77.711
77.485
77.230
76.975
61.630
60.697
44.561
43.880
43.754
34.942
27.866
27.340
25.142
17.447
3.57 α
S
S
OH
H
Me
H

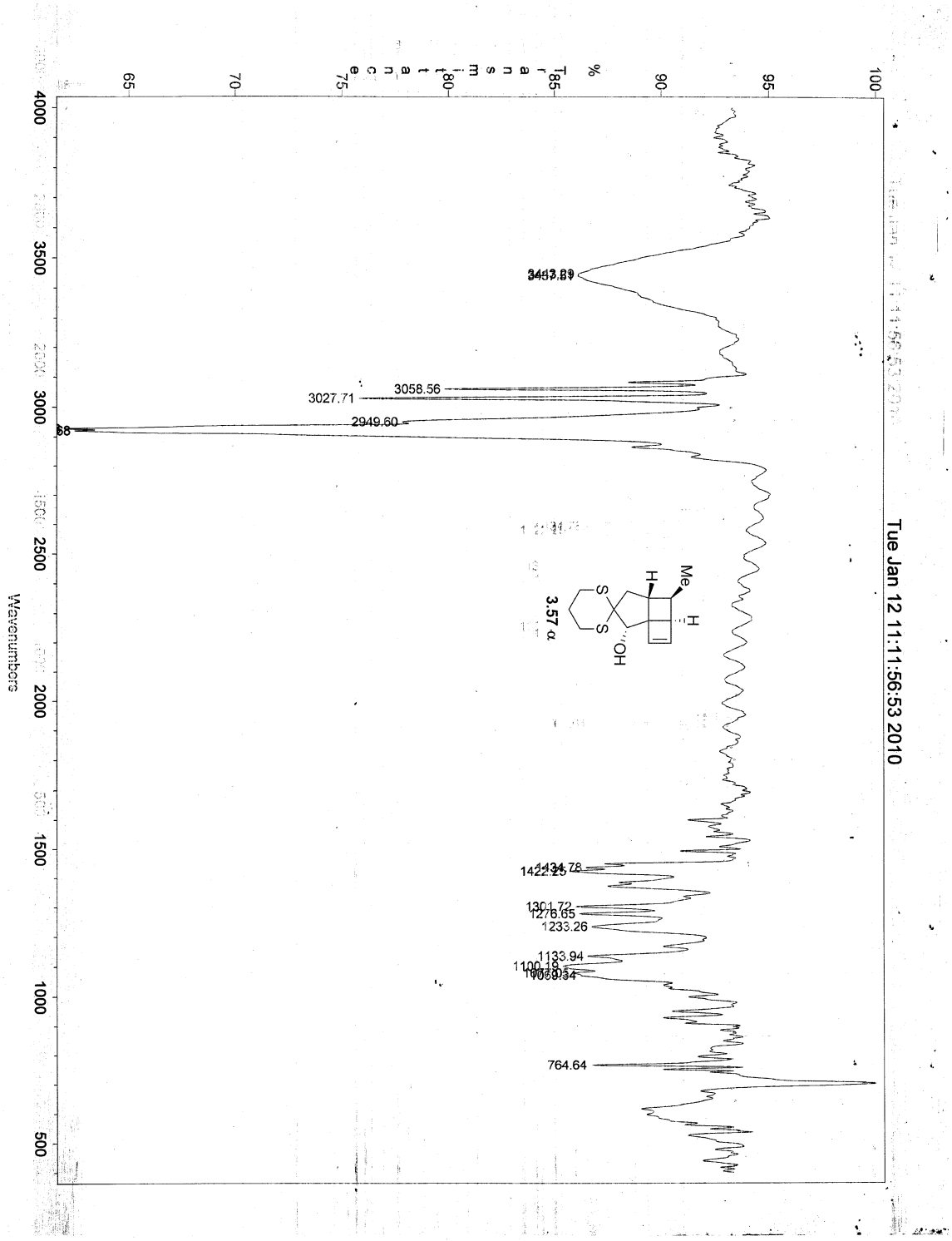
Tue Jan 12 11:11:56:53 2010
% Transmittance
Wavenumbers
3027.71
3058.56
2949.60
1422.25
1301.72
1276.65
1233.26
1133.94
764.64
3.57 α
Me
H
H
S
S
OH

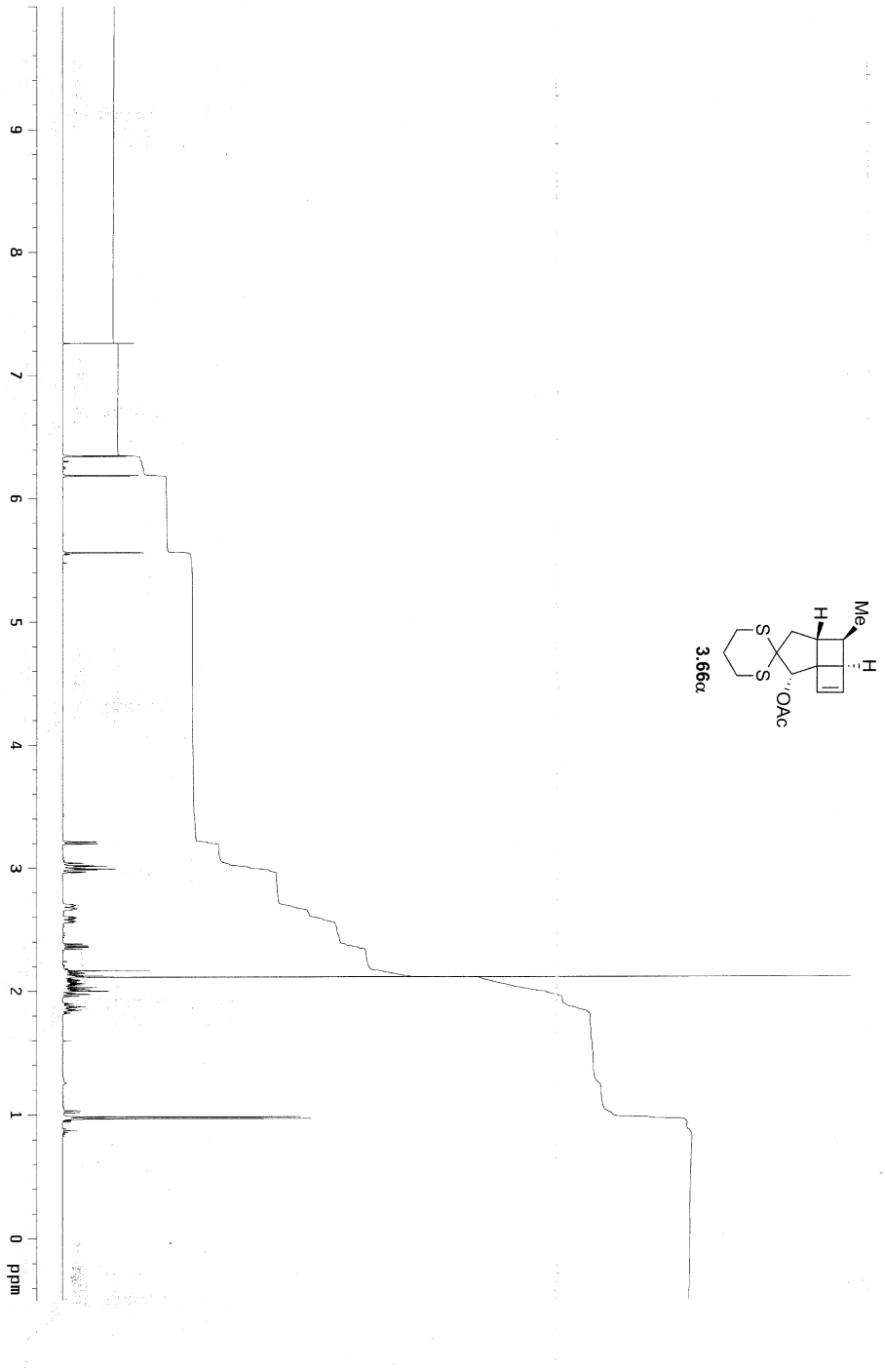
Me
H
H
S
S
OAc
3.66α
9
8
7
6
5
4
3
2
1
0
ppm

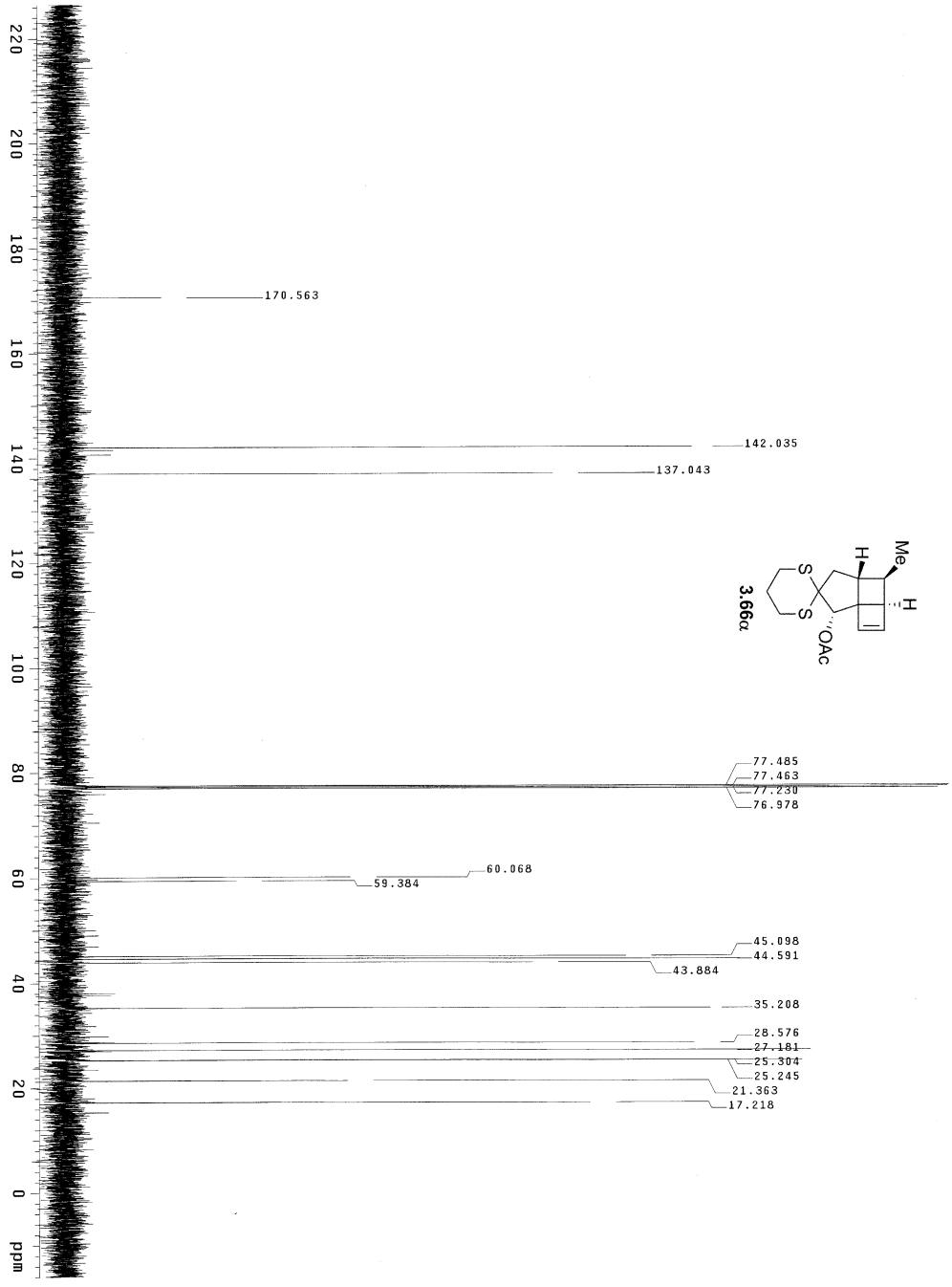
220
200
180
160
140
120
100
80
60
40
20
0
ppm
170.563
142.035
137.043
77.485
77.463
77.230
76.978
60.068
59.384
45.098
44.591
43.884
35.208
28.576
27.181
25.304
25.245
21.363
17.218
S
S
H
Me
H
OAc
3.66α

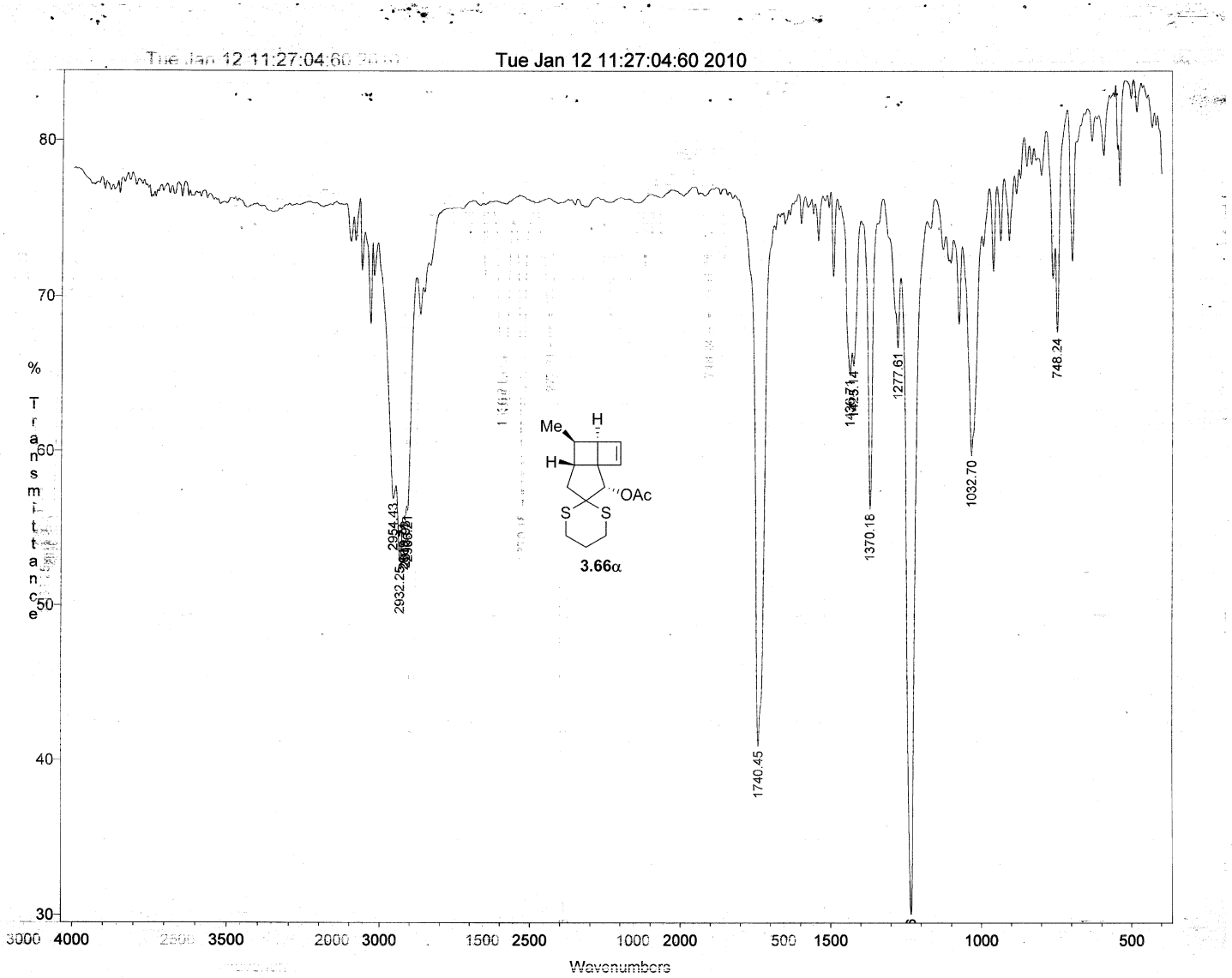
Tue Jan 12 11:27:04:60 2010
% Transmittance
80
70
60
50
40
30
2932.25
2954.43
1740.45
1370.18
1277.61
1032.70
748.24
Me
H
H
OAc
S
S
3.66α
3000
4000
3500
2000
3000
1500
2500
1000
2000
500
1500
1000
500
Wavenumbers

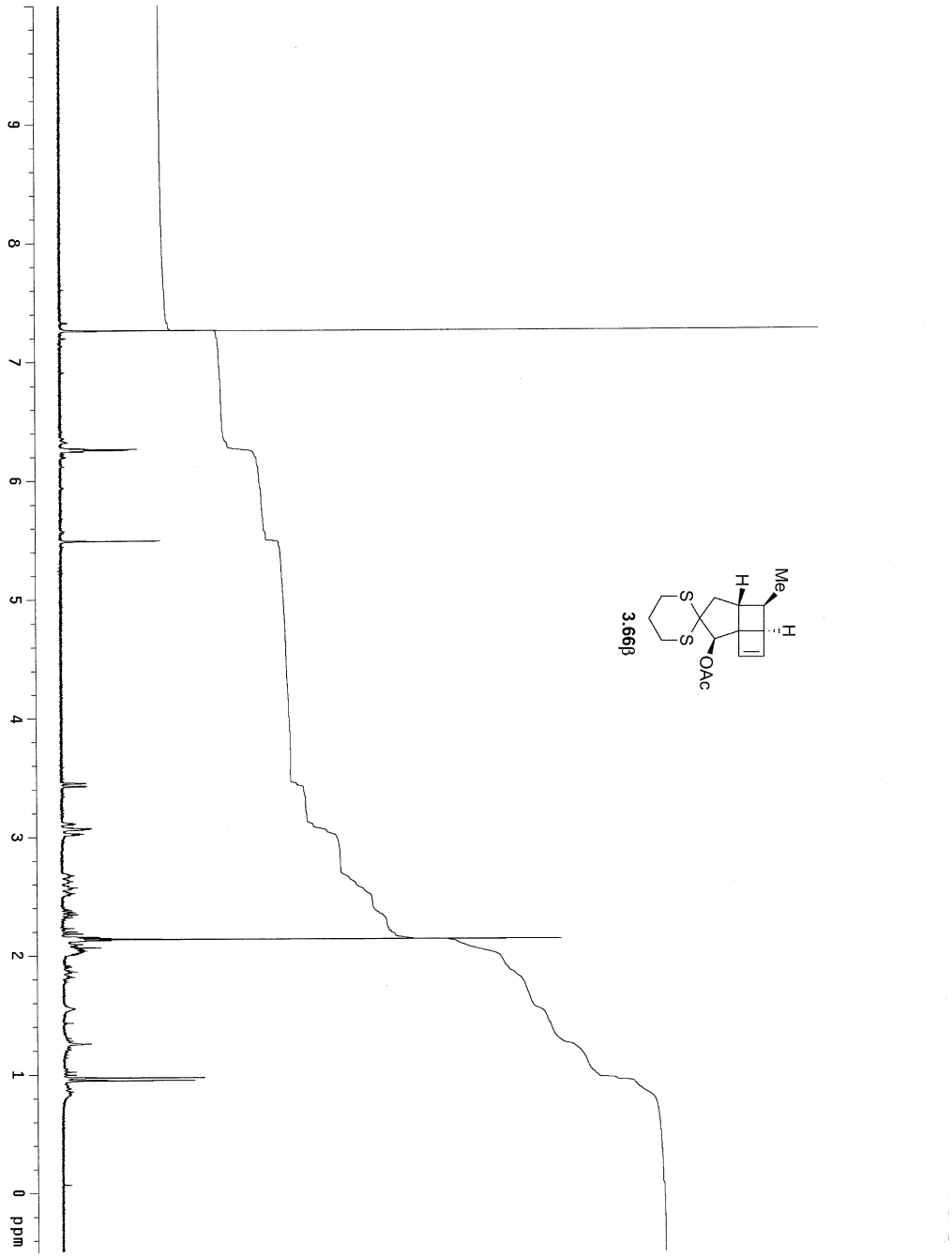
9
8
7
6
5
4
3
2
1
0 ppm
Me
H
H
S
S
OAc
3.66β

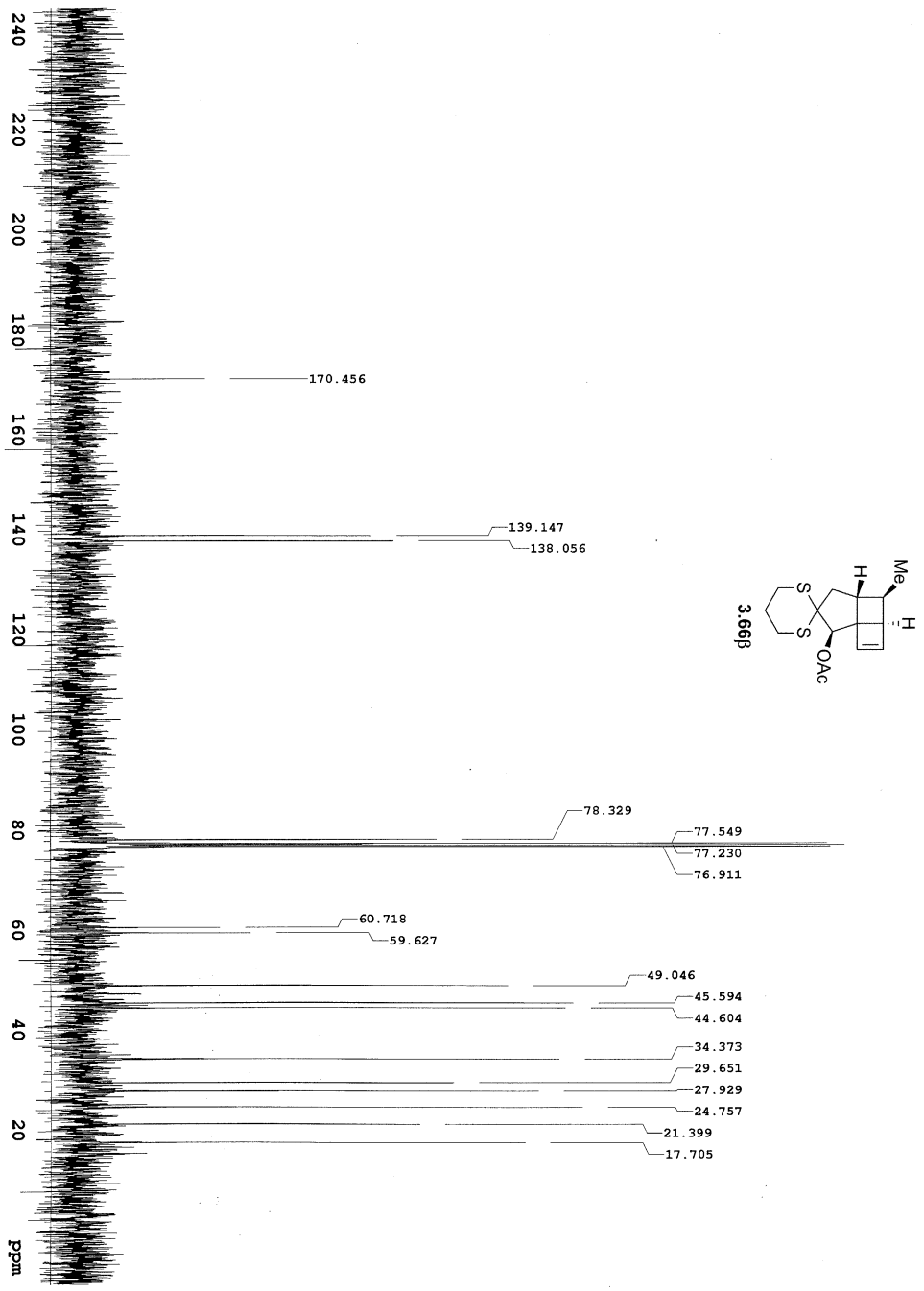
240
220
200
180
160
140
120
100
80
60
40
20
ppm
170.456
139.147
138.056
78.329
77.549
77.230
76.911
60.718
59.627
49.046
45.594
44.604
34.373
29.651
27.929
24.757
21.399
17.705
3.66β
S
S
H
Me
H
OAc

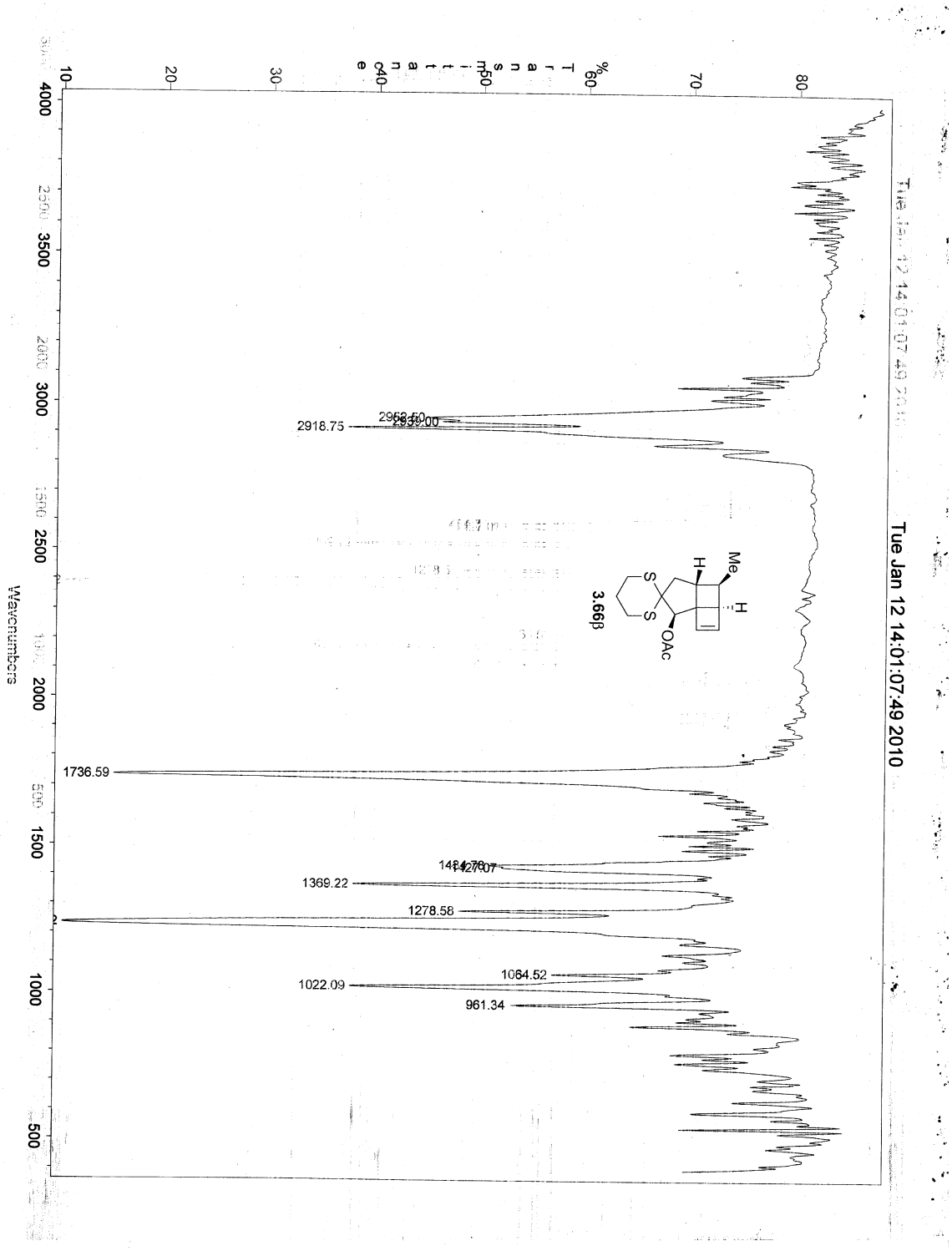
Tue Jan 12 14:01:07:49 2010
Wavenumbers
%Transmittance
2918.75
1736.59
1369.22
1278.58
1022.09
961.34
1064.52
3.66β
Me
H
H
S
S
OAc

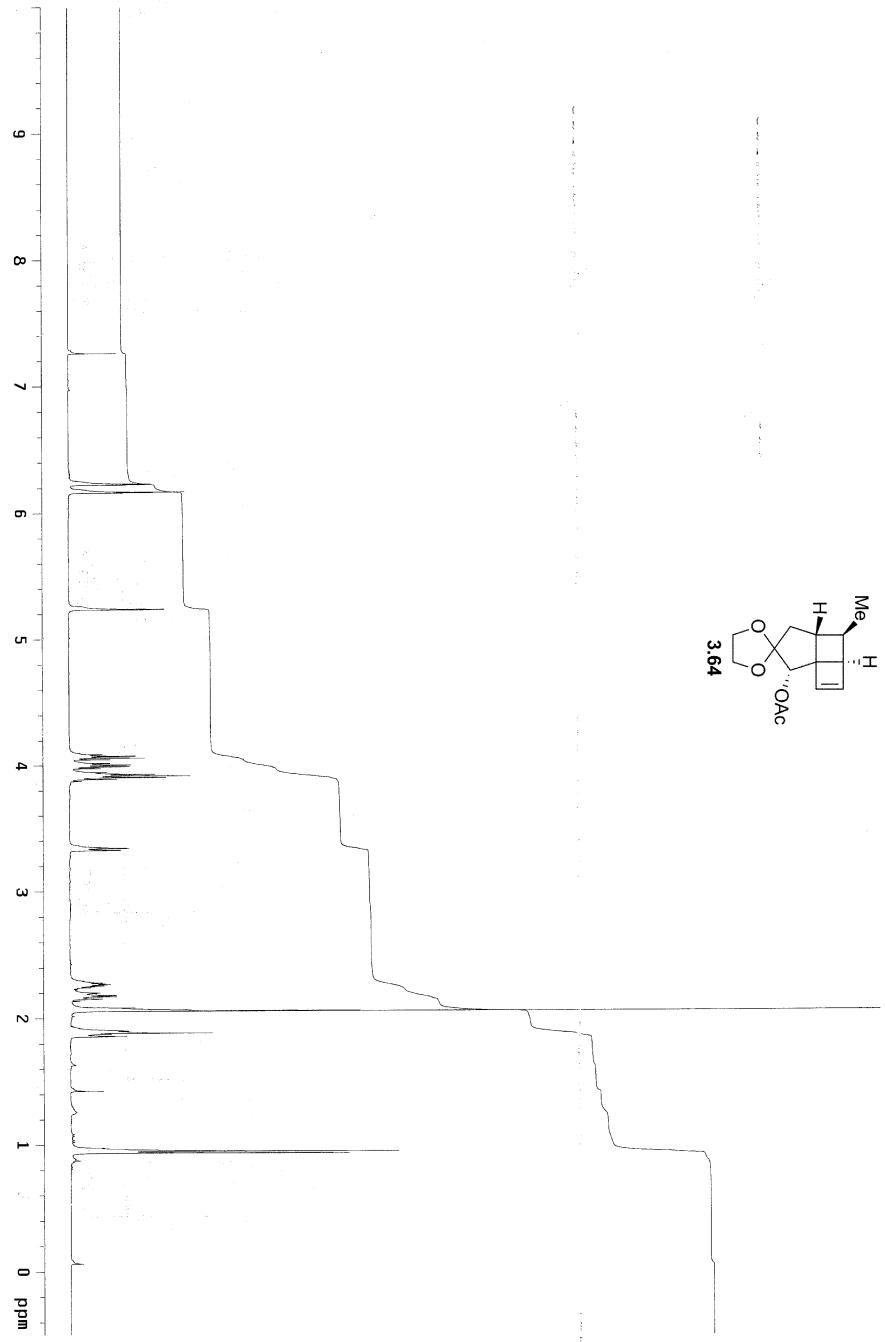
9
8
7
6
5
4
3
2
1
0 ppm
Me
H
H
O
O
OAc
3.64

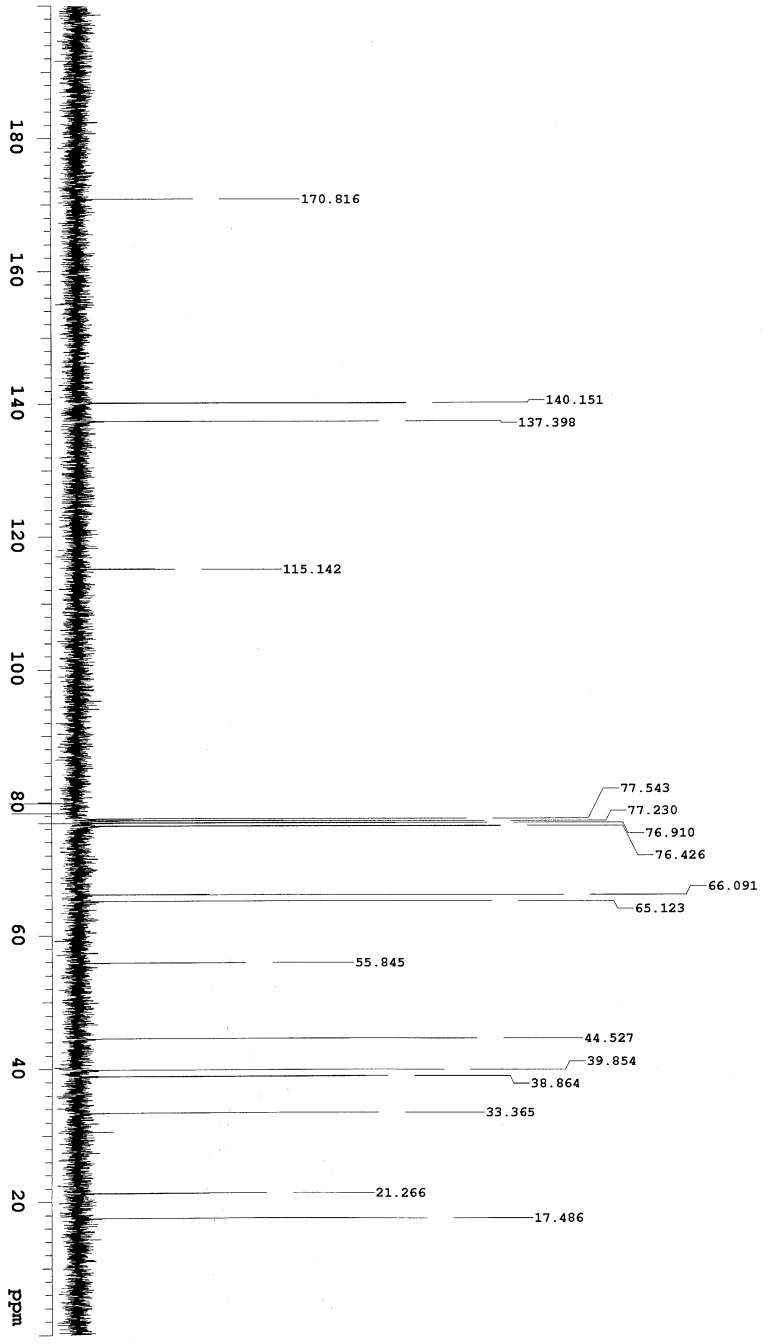
180
160
140
120
100
80
60
40
20
ppm
170.816
140.151
137.398
115.142
77.543
77.230
76.910
76.426
66.091
65.123
55.845
44.527
39.854
38.864
33.365
21.266
17.486
3.64
Me
H
H
OAc

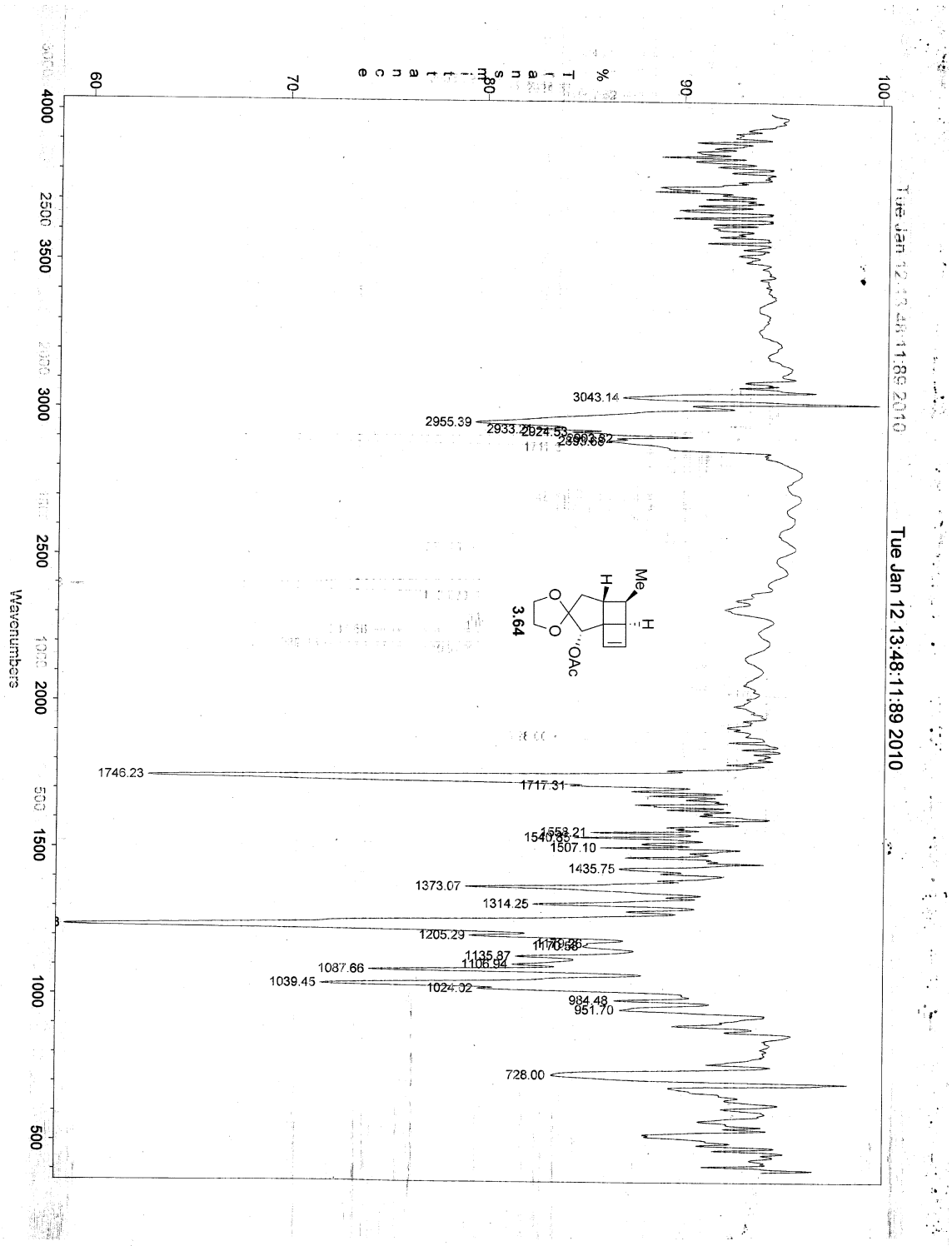
Transmittance %
Wavenumbers
3043.14
2955.39
1746.23
1717.31
1553.21
1507.10
1435.75
1373.07
1314.25
1205.29
1135.87
1087.66
1039.45
984.48
951.70
728.00
3.64
Me
H
H
OAc
Tue Jan 12 13:48:11:89 2010

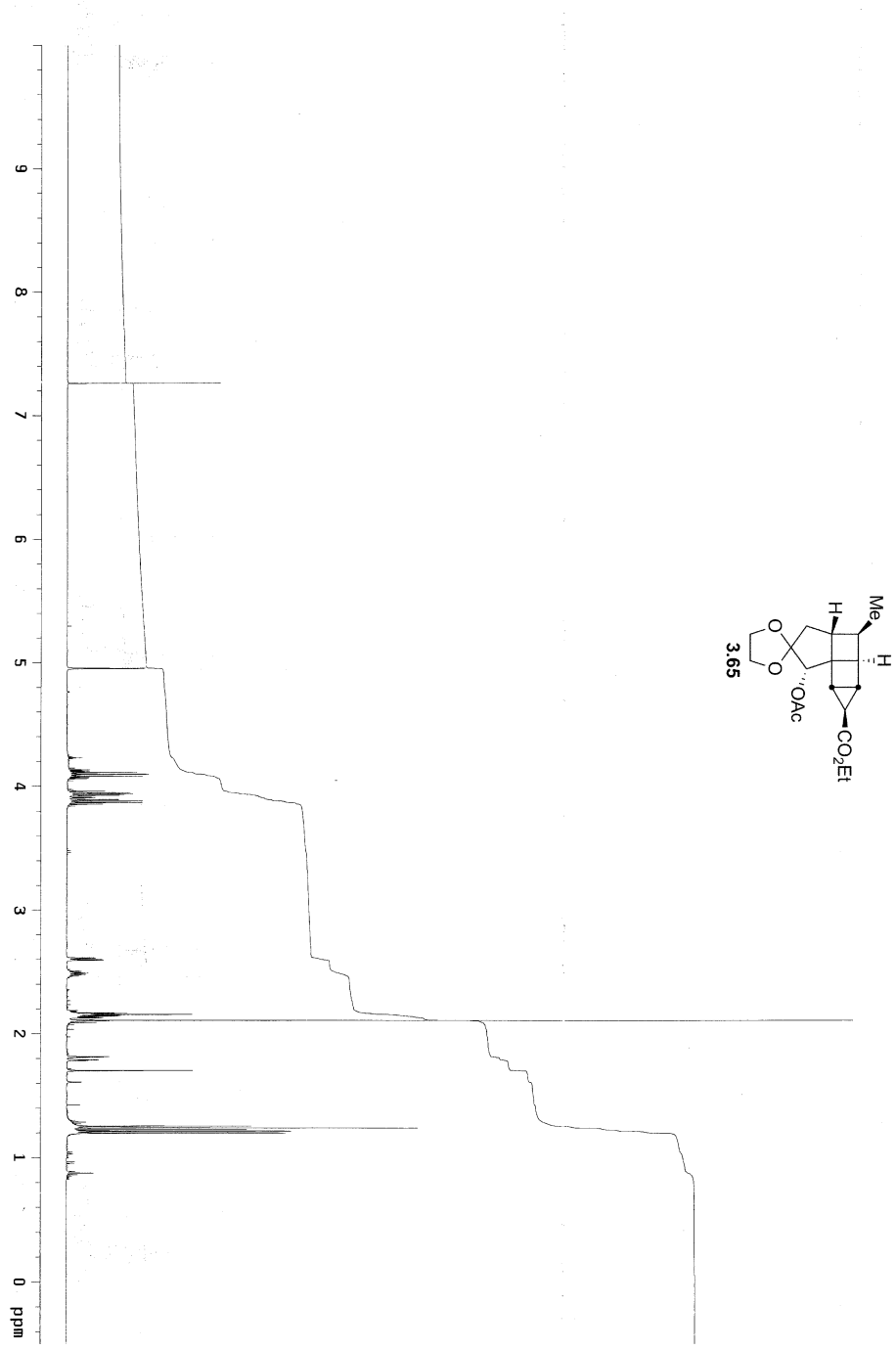
9
8
7
6
5
4
3
2
1
0
ppm
3.65
Me
H
H
O
O
OAc
CO2Et

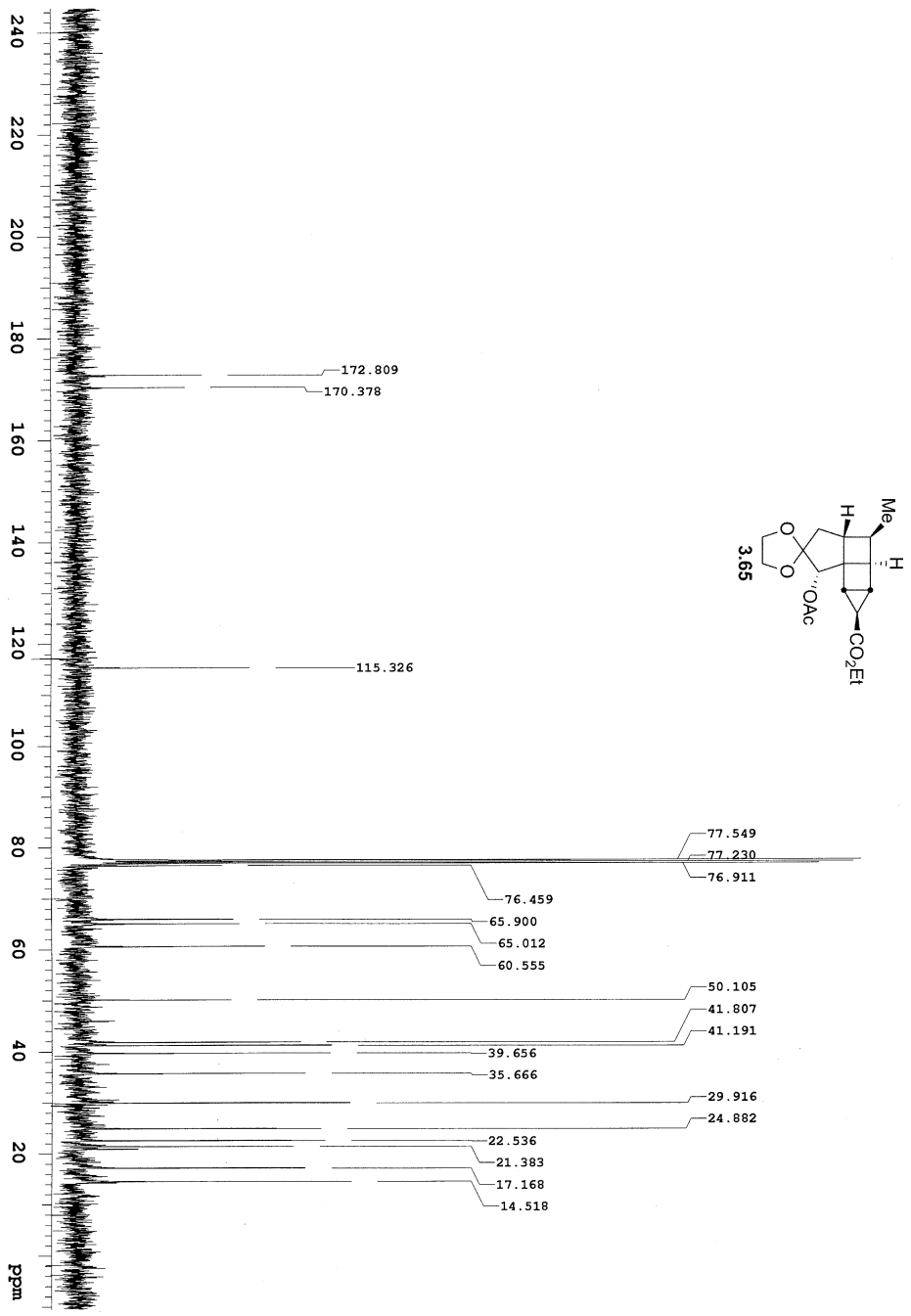
240
220
200
180
160
140
120
100
80
60
40
20
ppm
172.809
170.378
115.326
77.549
77.230
76.911
76.459
65.900
65.012
60.555
50.105
41.807
41.191
39.656
35.666
29.916
24.882
22.536
21.383
17.168
14.518
3.65
Me
H
H
OAc
CO2Et

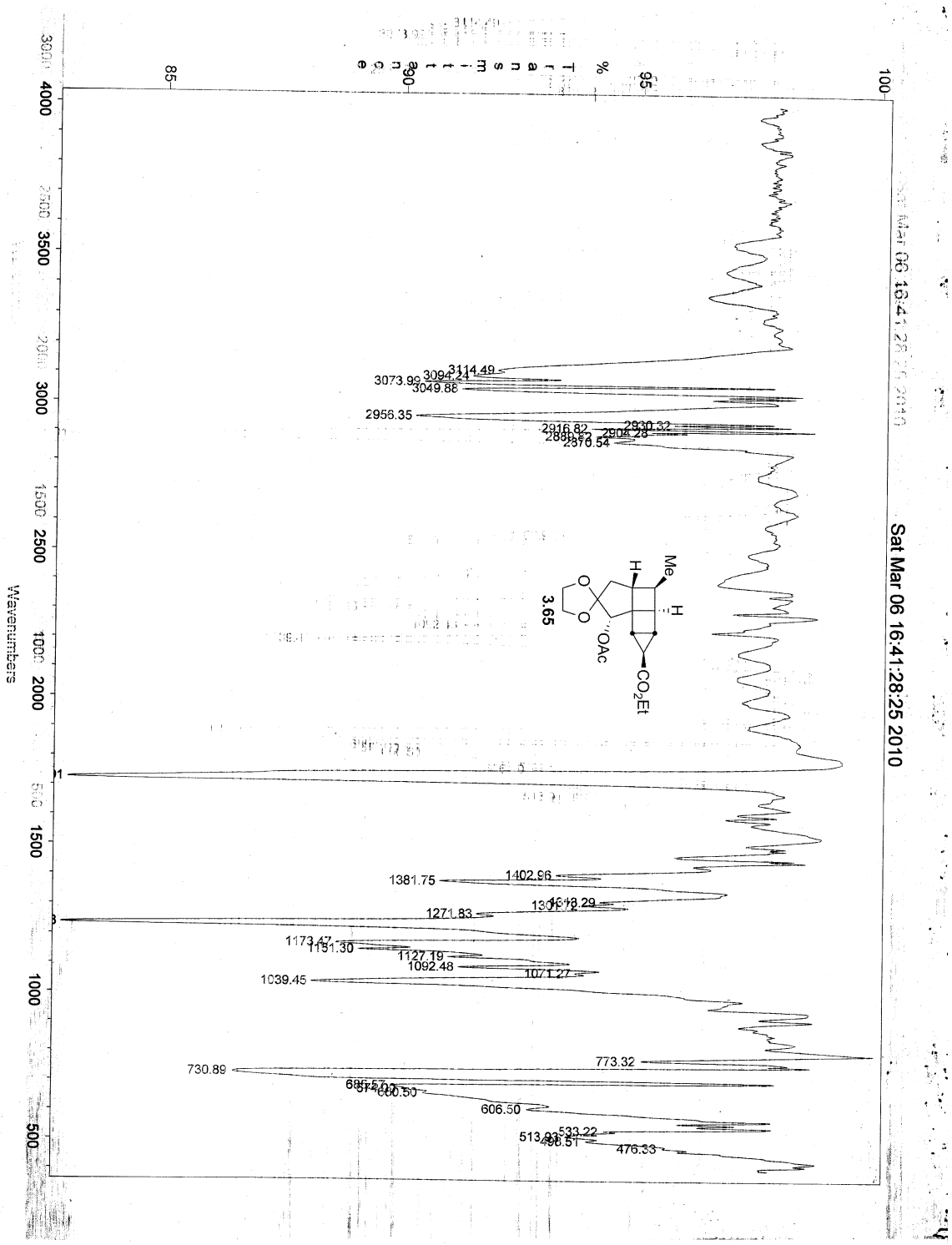
Transmittance %
Wavenumbers
Sat Mar 06 16:41:28:25 2010
3114.49
3073.99
3049.88
2956.35
2930.32
2904.28
2876.54
1402.96
1381.75
1271.83
1173.47
1151.30
1127.19
1092.48
1071.27
1039.45
773.32
730.89
606.50
533.22
476.33
3.65
Me
H
H
OAc
CO2Et

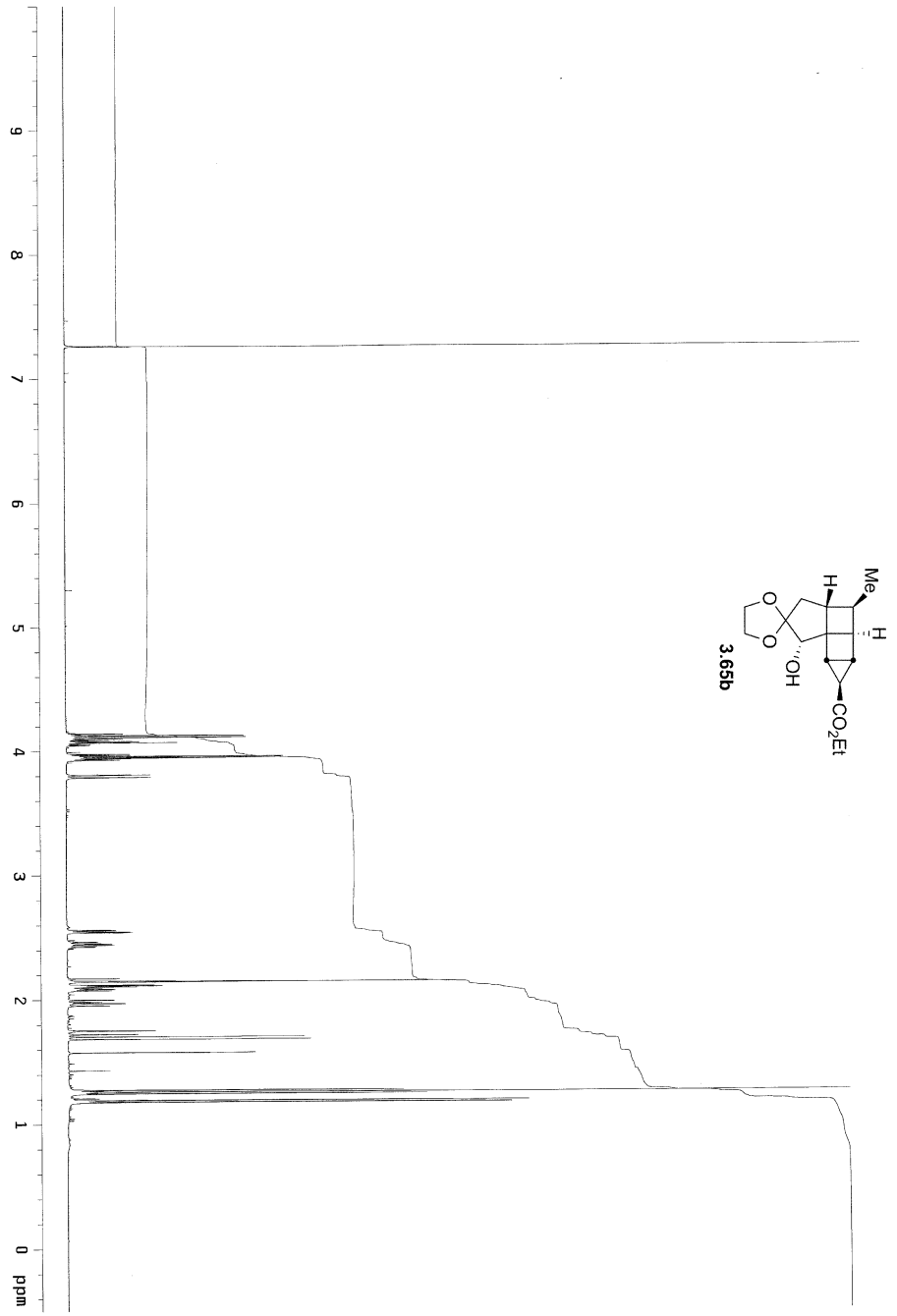
9
8
7
6
5
4
3
2
1
0
ppm
Me
H
H
O
O
OH
CO2Et
3.65b

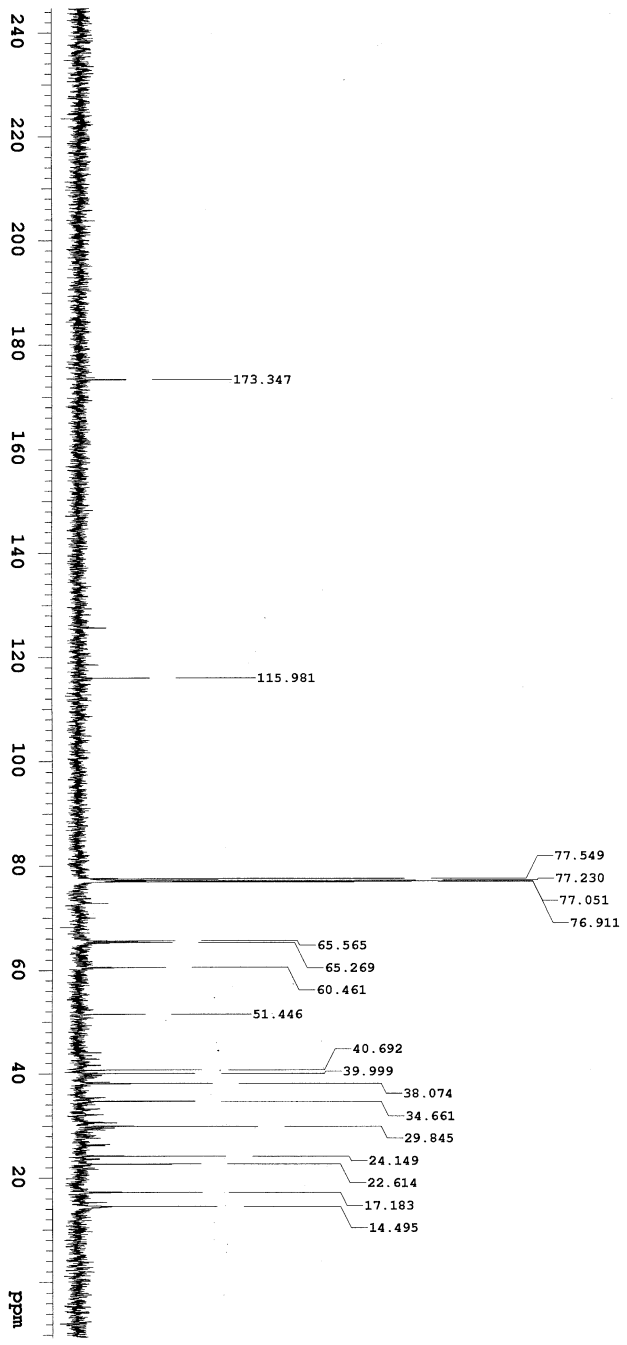
240
220
200
180
160
140
120
100
80
60
40
20
ppm
173.347
115.981
77.549
77.230
77.051
76.911
65.565
65.269
60.461
51.446
40.692
39.999
38.074
34.661
29.845
24.149
22.614
17.183
14.495

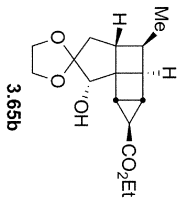
Me
H
H
O
O
OH
CO2Et

3.65b

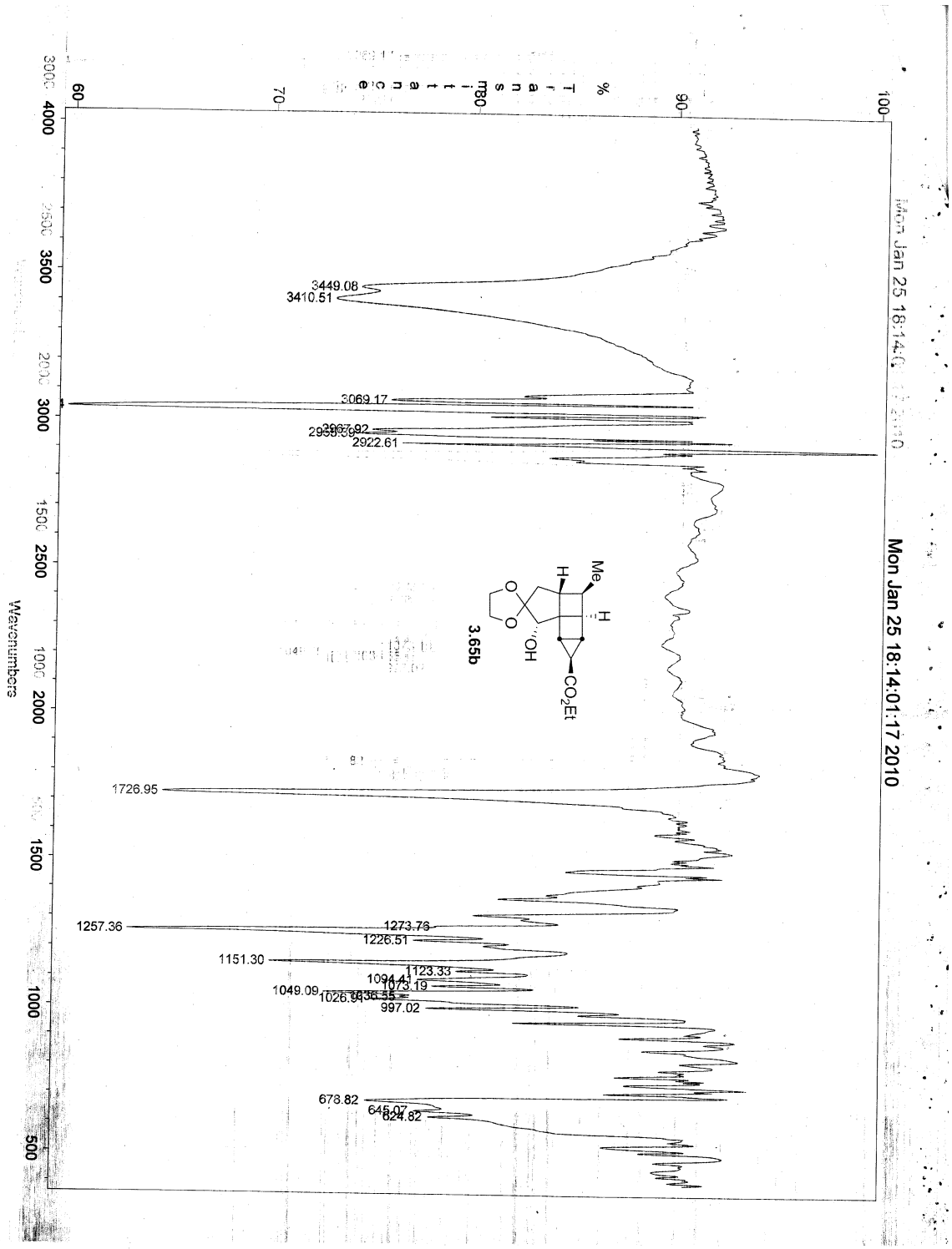
Mon Jan 25 18:14:01:17 2010
Wavenumbers
3449.08
3410.51
3069.17
2922.61
1726.95
1257.36
1273.76
1226.51
1151.30
1123.33
1049.09
997.02
678.82
624.82
Me
H
H
OH
CO2Et
3.65b

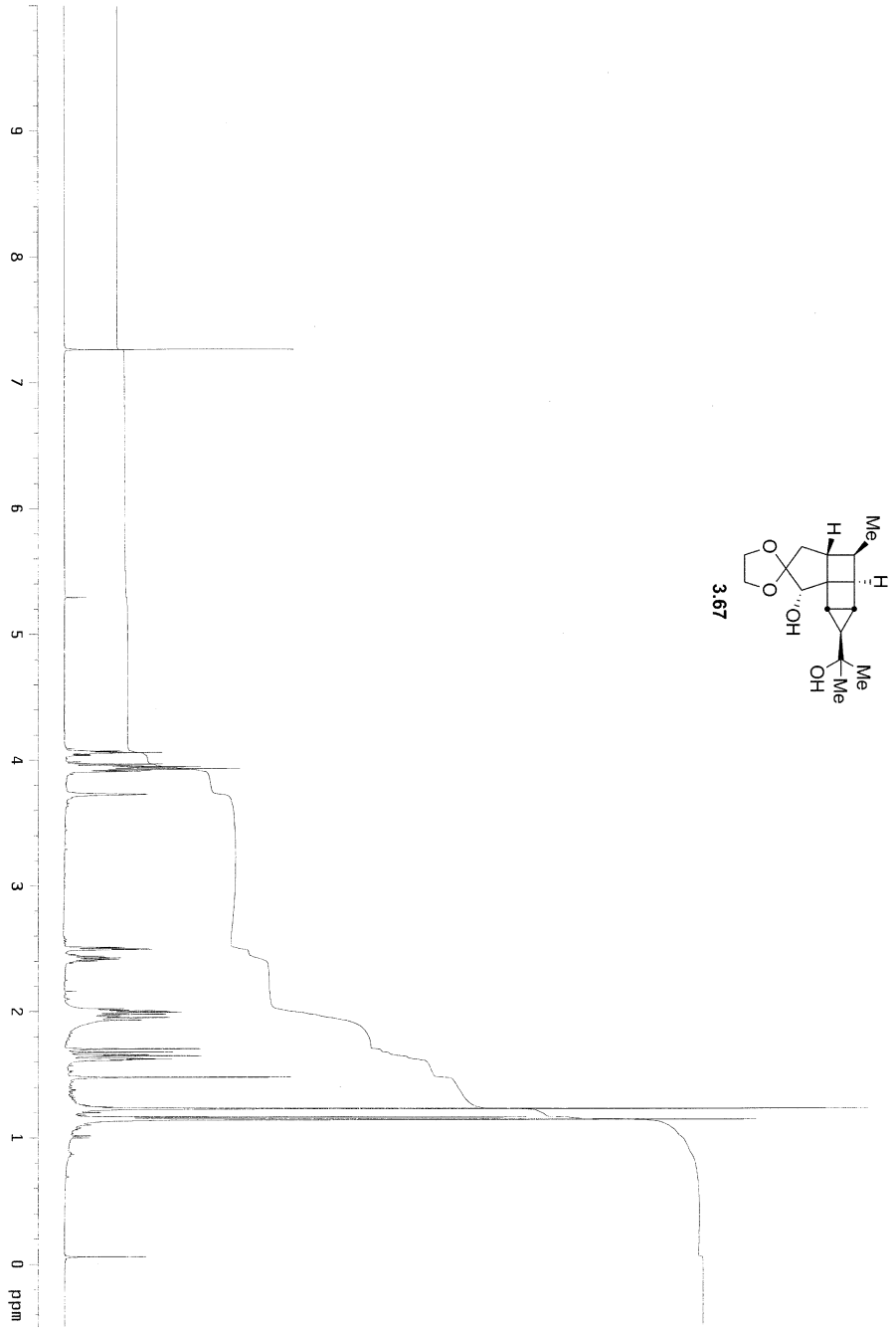

3.67

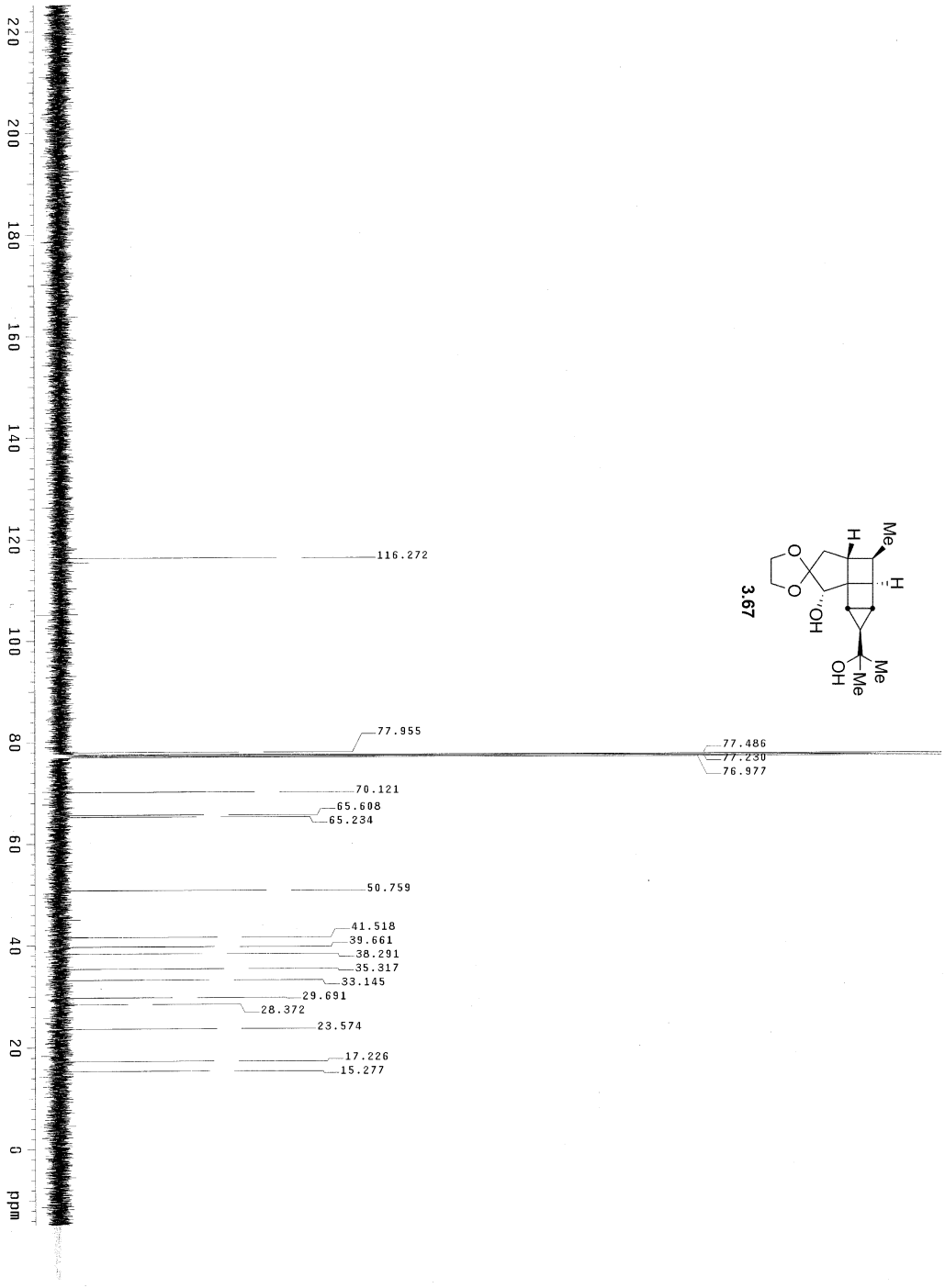
220
200
180
160
140
120
100
80
60
40
20
0
ppm
116.272
77.955
77.486
77.230
76.977
70.121
65.608
65.234
50.759
41.518
39.661
38.291
35.317
33.145
29.691
28.372
23.574
17.226
15.277
3.67
Me
H
OH
Me
OH
Me
H

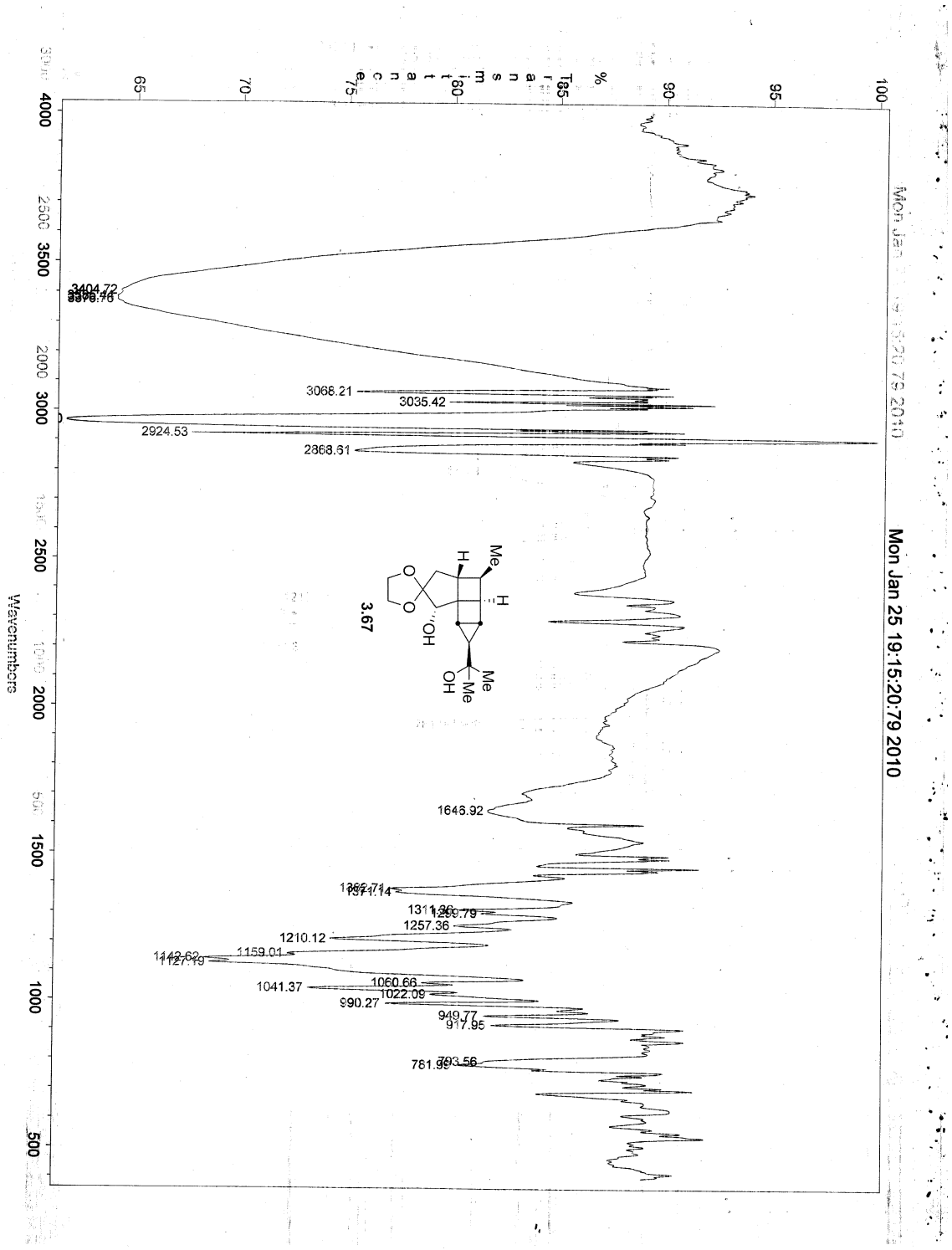
Mon Jan 25 19:15:20:79 2010
Wavenumbers
4000
3500
3000
2500
2000
1500
1000
500
%
Transmittance
65
70
75
80
85
90
95
100
3404.72
3068.21
3035.42
2924.53
2868.51
1646.92
1366.71
1311.36
1299.79
1257.36
1210.12
1159.01
1142.62
1127.19
1060.66
1041.37
1022.09
990.27
949.77
917.95
793.56
781.99
3.67
OH
H
Me
H
Me
OH
Me
OH

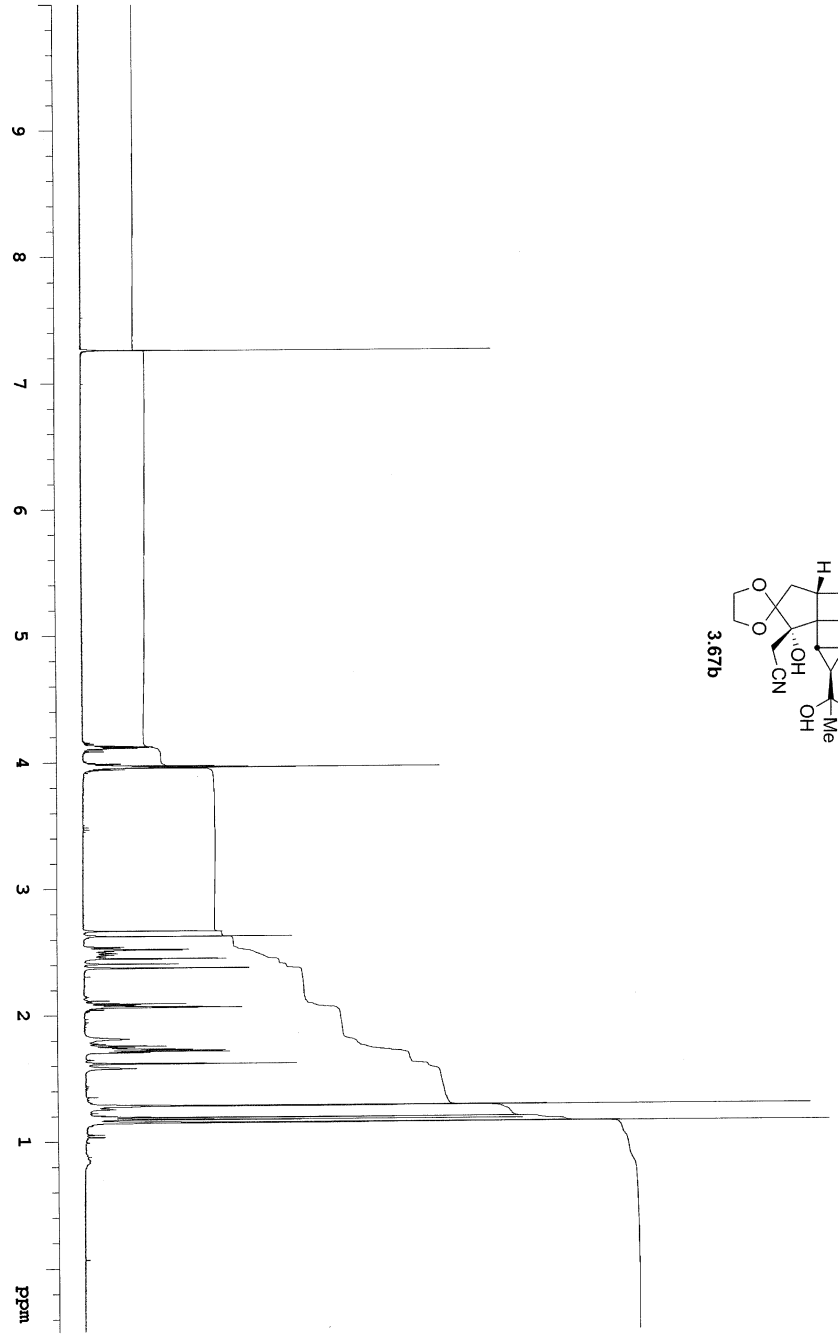

3.67b

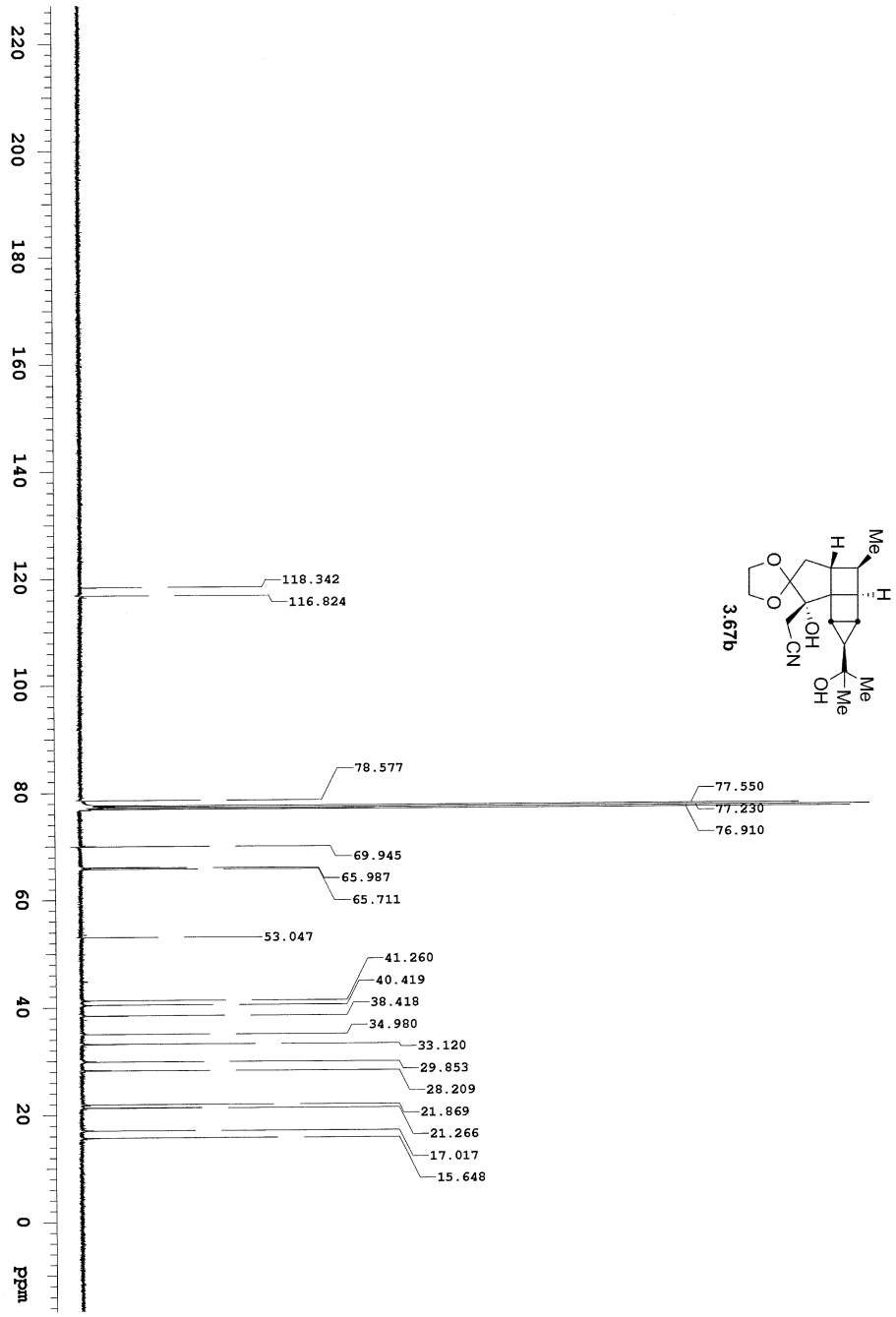
220
200
180
160
140
120
100
80
60
40
20
0
ppm
118.342
116.824
78.577
77.550
77.230
76.910
69.945
65.987
65.711
53.047
41.260
40.419
38.418
34.980
33.120
29.853
28.209
21.869
21.266
17.017
15.648
3.67b
Me
H
H
OH
CN
O
O
OH
Me
Me

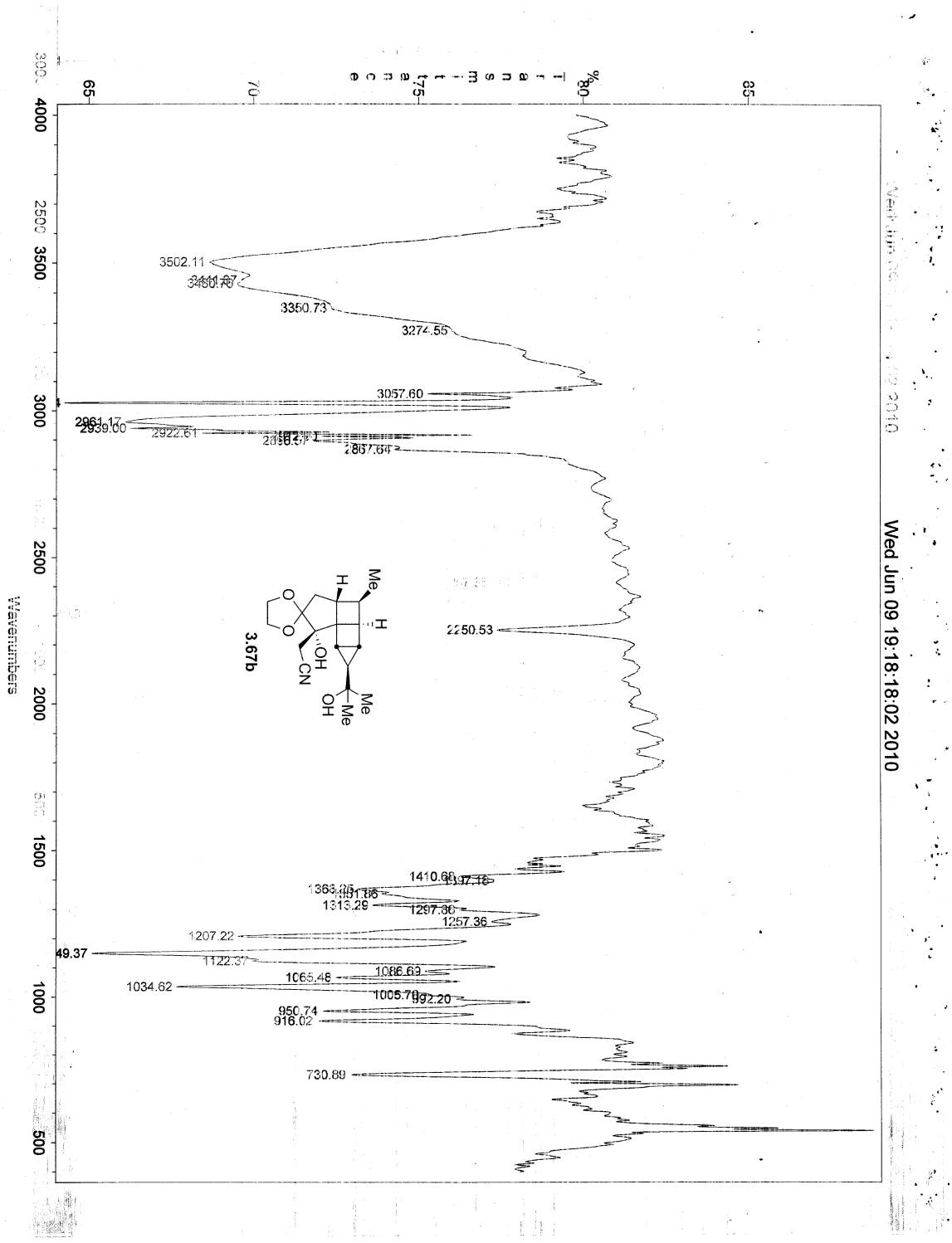
3502.11
3350.73
3274.55
3057.60
2961.17
2939.00
2922.61
2857.64
2250.53
1410.69
1313.29
1297.36
1257.36
1207.22
1122.37
1086.69
1065.48
1034.62
1005.78
992.20
950.74
916.02
730.89
3.67b
Me
H
H
OH
CN
OH
Me
Me
Wavenumbers
%Transmittance
Wed Jun 09 19:18:18:02 2010

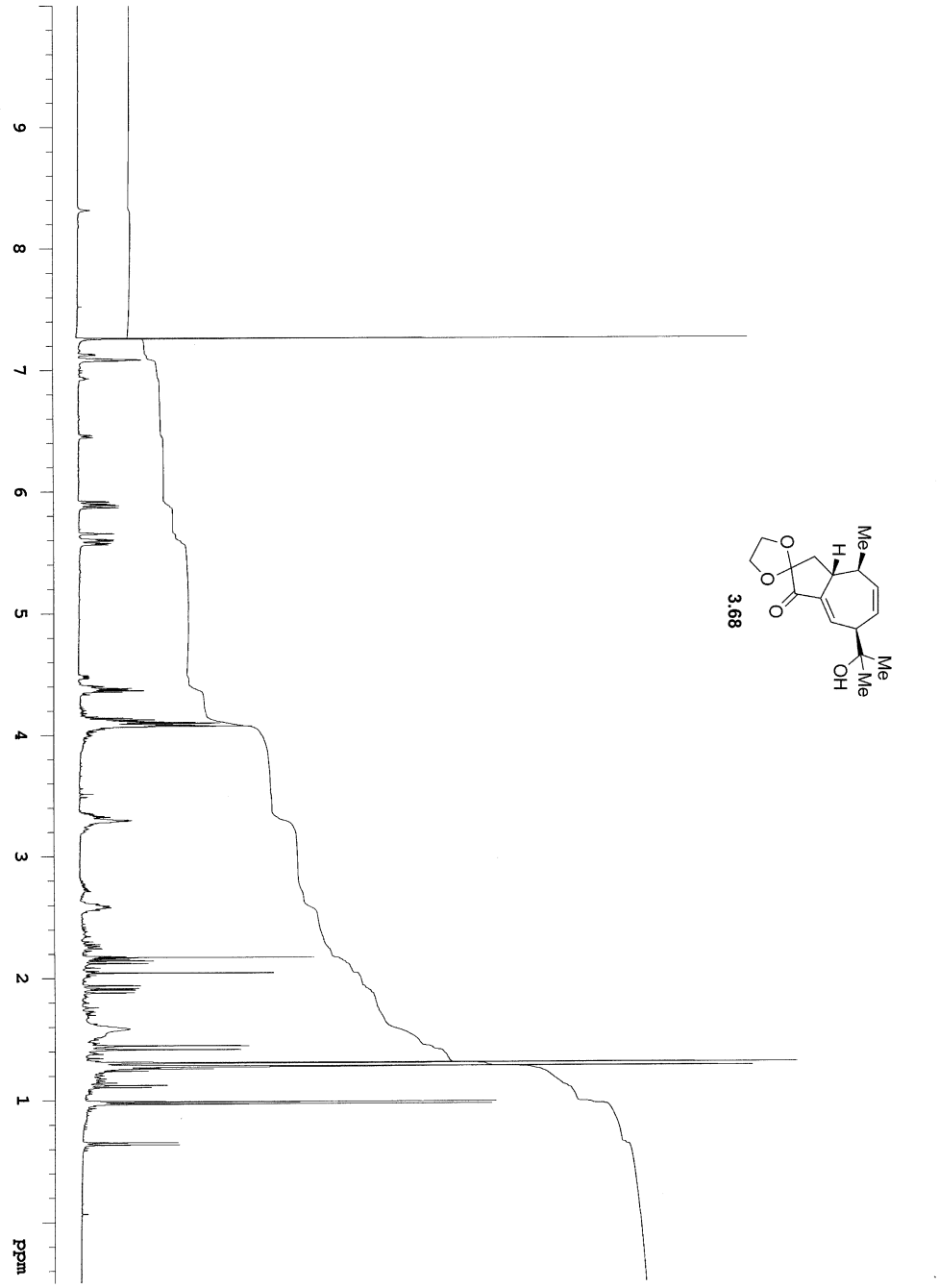
9
8
7
6
5
4
3
2
1
ppm
3.68
Me
H
O
O
O
Me
Me
OH

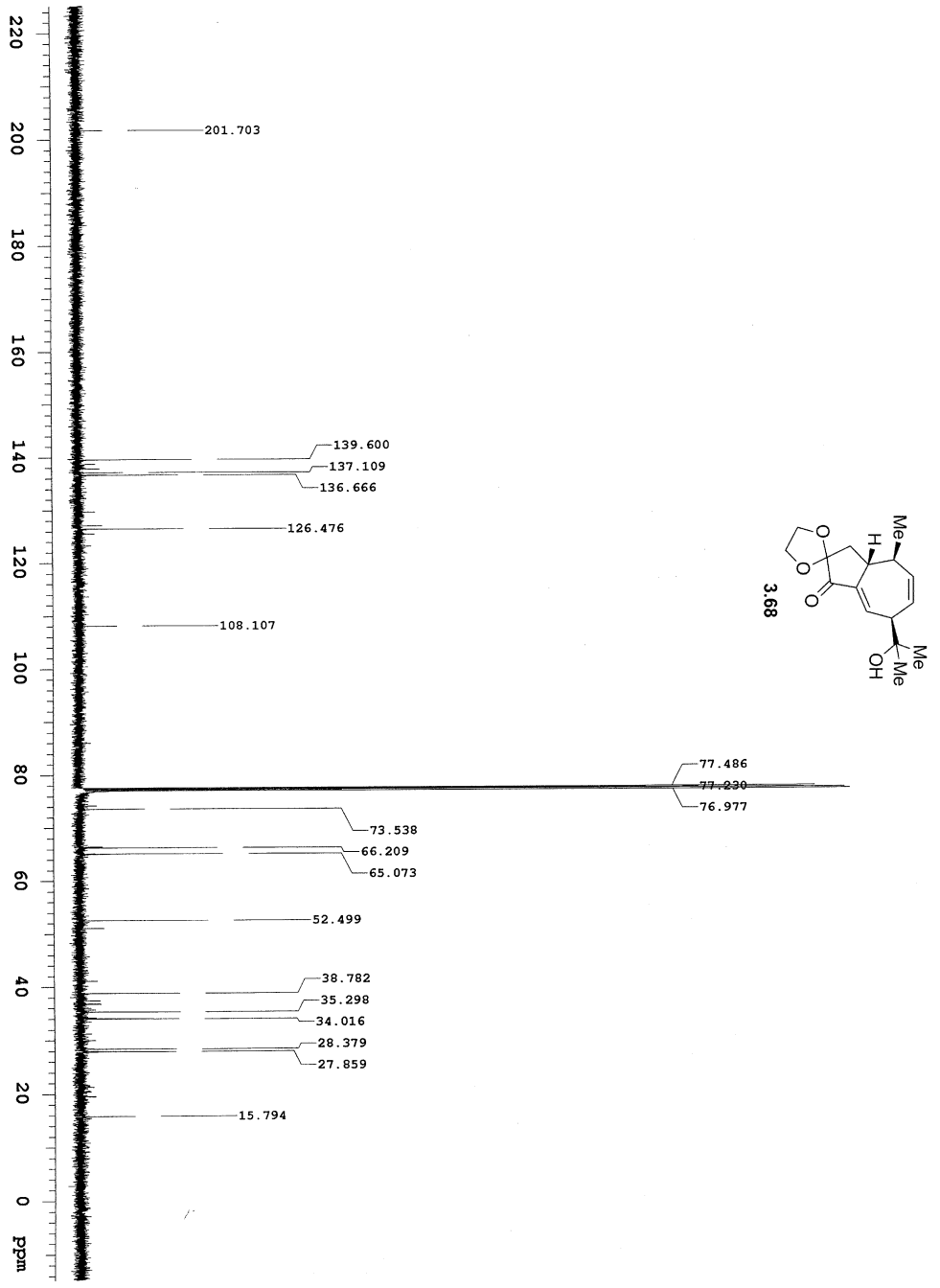
220
200
180
160
140
120
100
80
60
40
20
0
ppm
201.703
139.600
137.109
136.666
126.476
108.107
77.486
77.230
76.977
73.538
66.209
65.073
52.499
38.782
35.298
34.016
28.379
27.859
15.794
3.68
Me
H
O
O
O
Me
Me
OH

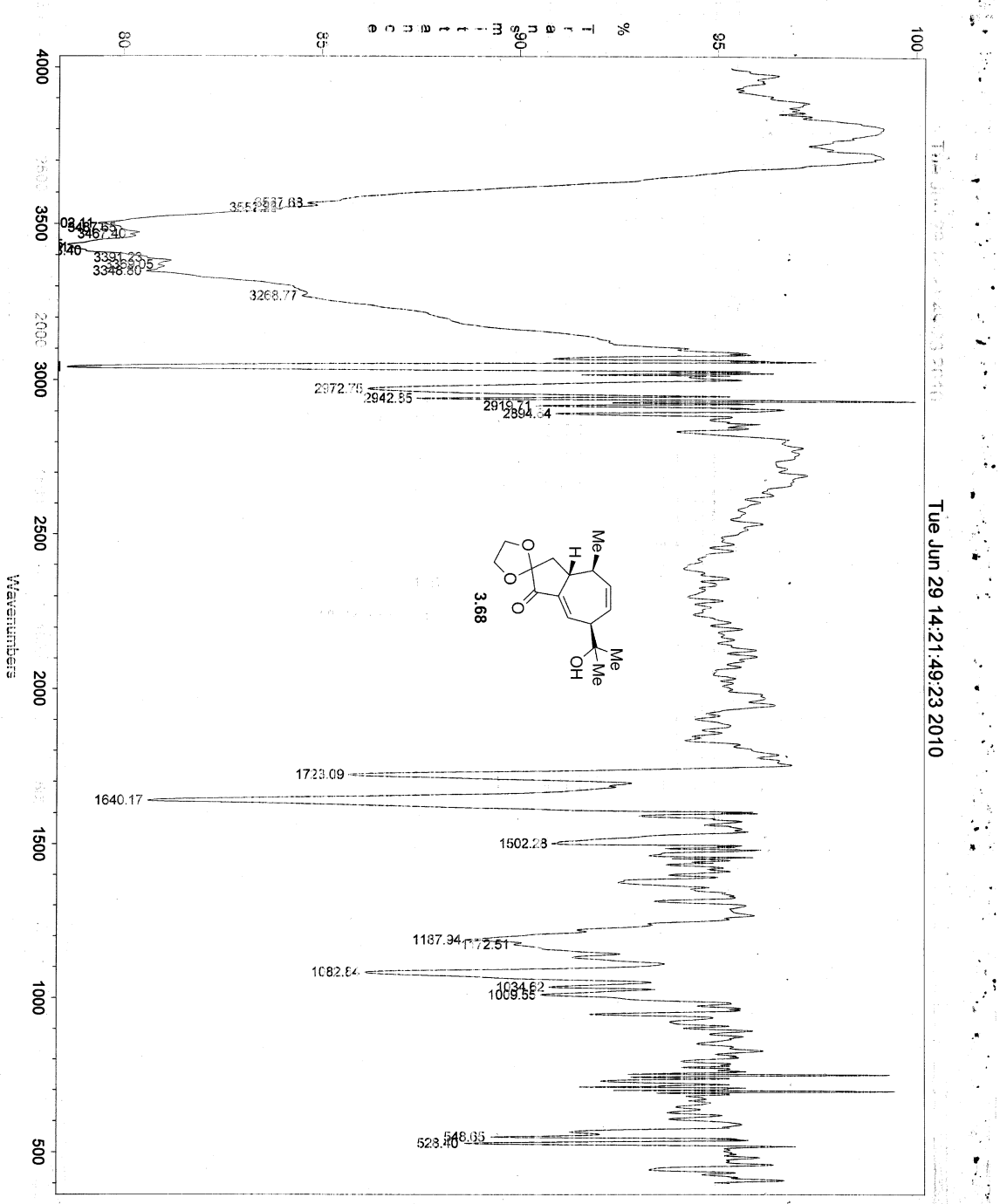
Transmittance %
Wavenumbers
3268.77
2972.76
2942.55
1723.09
1640.17
1502.28
1187.94
1082.84
1009.55
3.68
Me
H
Me
Me
OH
Tue Jun 29 14:21:49:23 2010

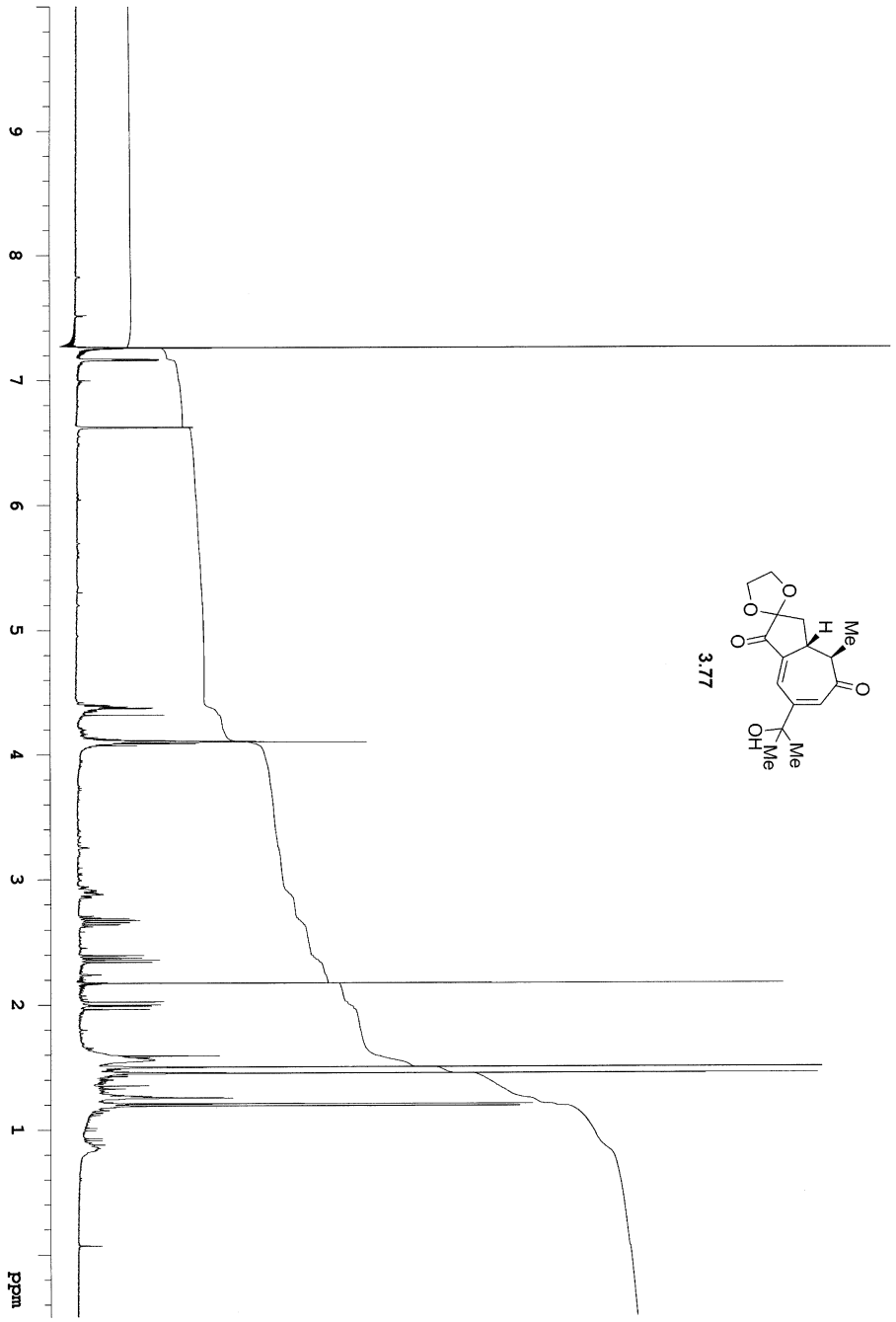
9
8
7
6
5
4
3
2
1
ppm
3.77
O
O
O
H
Me
O
OH
Me
Me

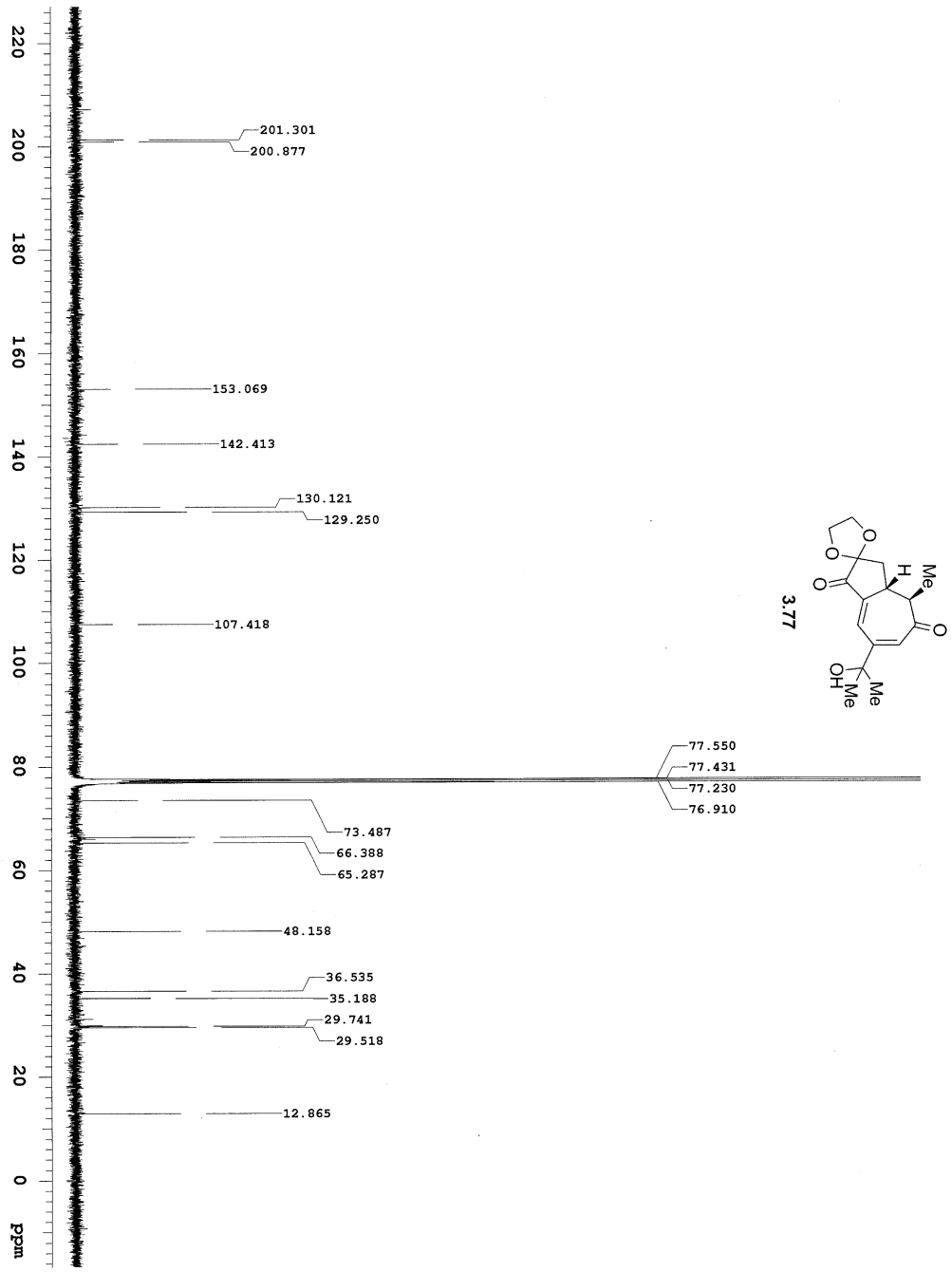
220
200
180
160
140
120
100
80
60
40
20
0
ppm
201.301
200.877
153.069
142.413
130.121
129.250
107.418
77.550
77.431
77.230
76.910
73.487
66.388
65.287
48.158
36.535
35.188
29.741
29.518
12.865
3.77
O
O
O
H
Me
O
OH
Me
Me

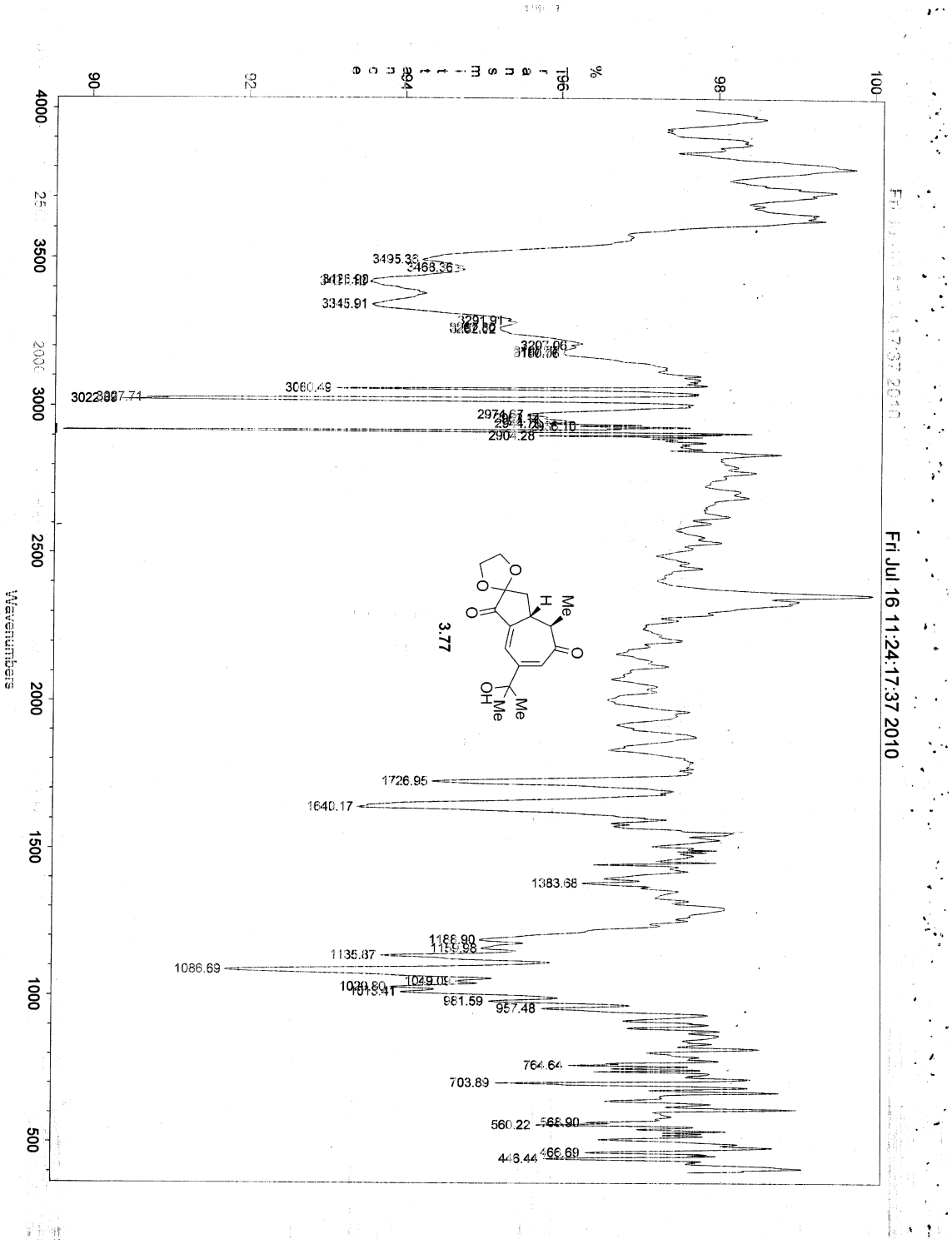
3.77
Fri Jul 16 11:24:17:37 2010
Wavenumbers
% Transmittance
3495.35
3468.36
3345.91
3060.49
2974.67
2904.28
1726.95
1640.17
1383.68
1188.90
1135.87
1086.69
981.59
957.48
764.64
703.89
560.22
446.44

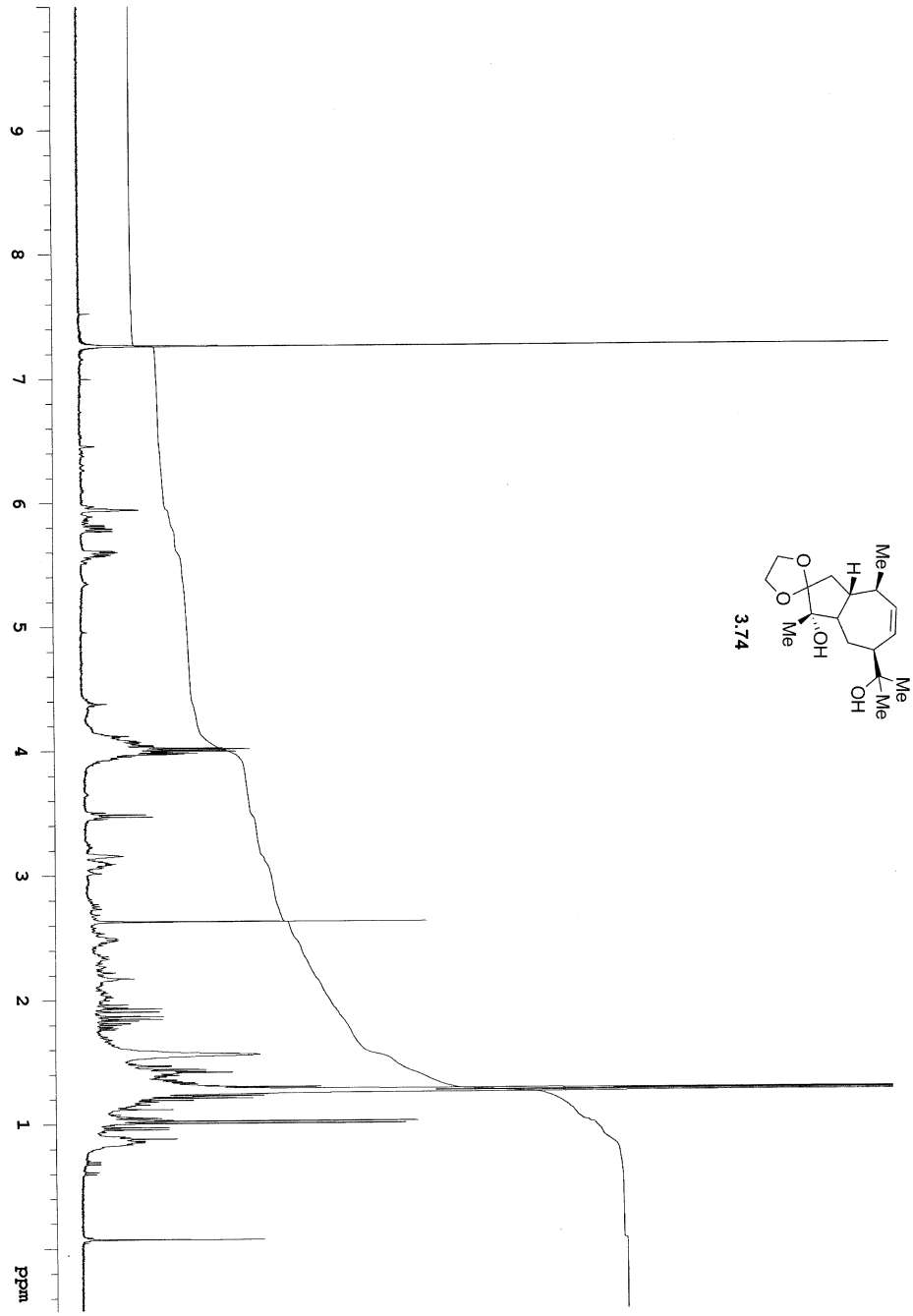
9
8
7
6
5
4
3
2
1
ppm
Me
H
O
O
Me
OH
Me
Me
OH
3.74

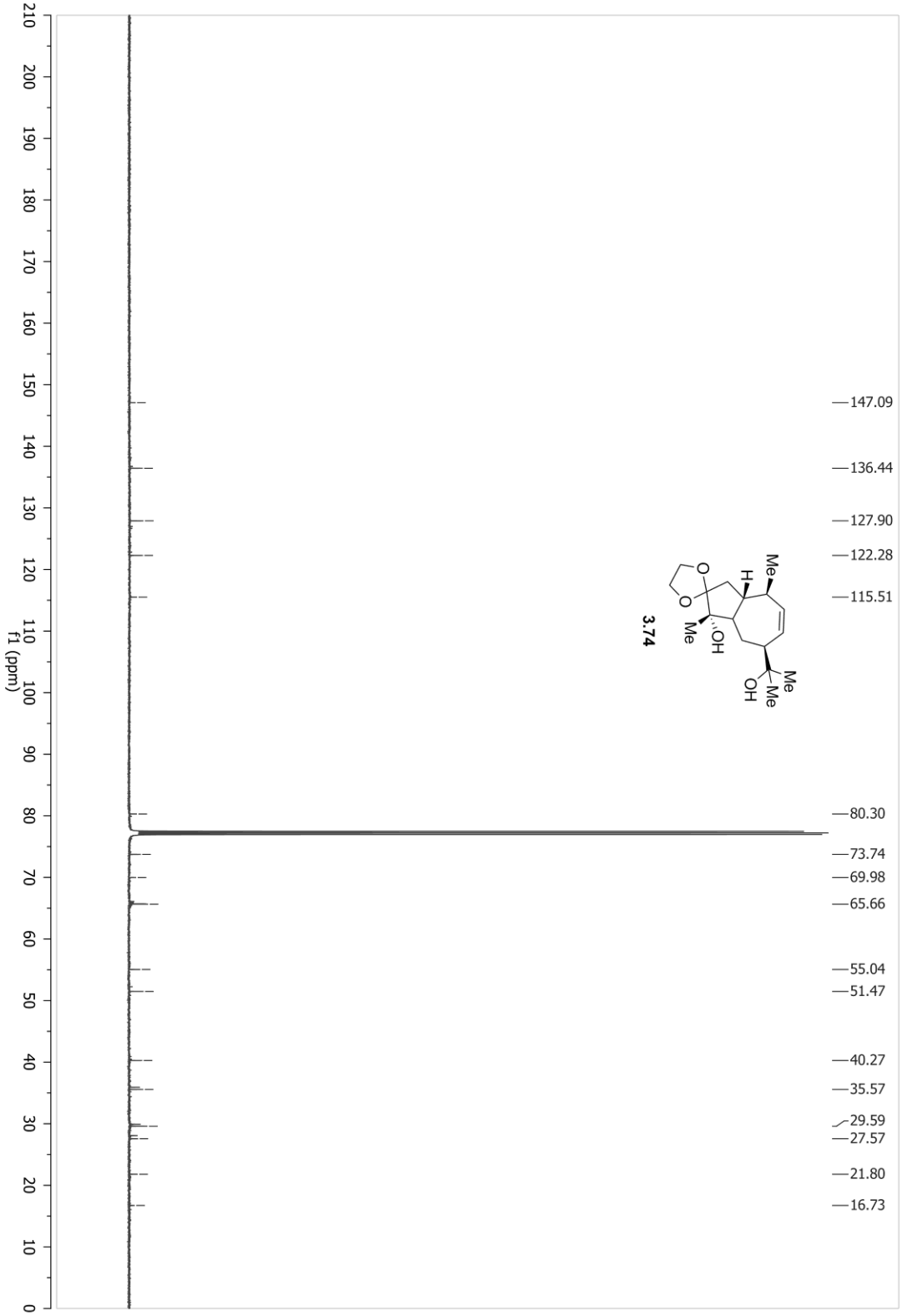
f1 (ppm)
210
200
190
180
170
160
150
140
130
120
110
100
90
80
70
60
50
40
30
20
10
0
147.09
136.44
127.90
122.28
115.51
80.30
73.74
69.98
65.66
55.04
51.47
40.27
35.57
29.59
27.57
21.80
16.73
Me
H
O
O
Me
OH
Me
Me
OH
3.74

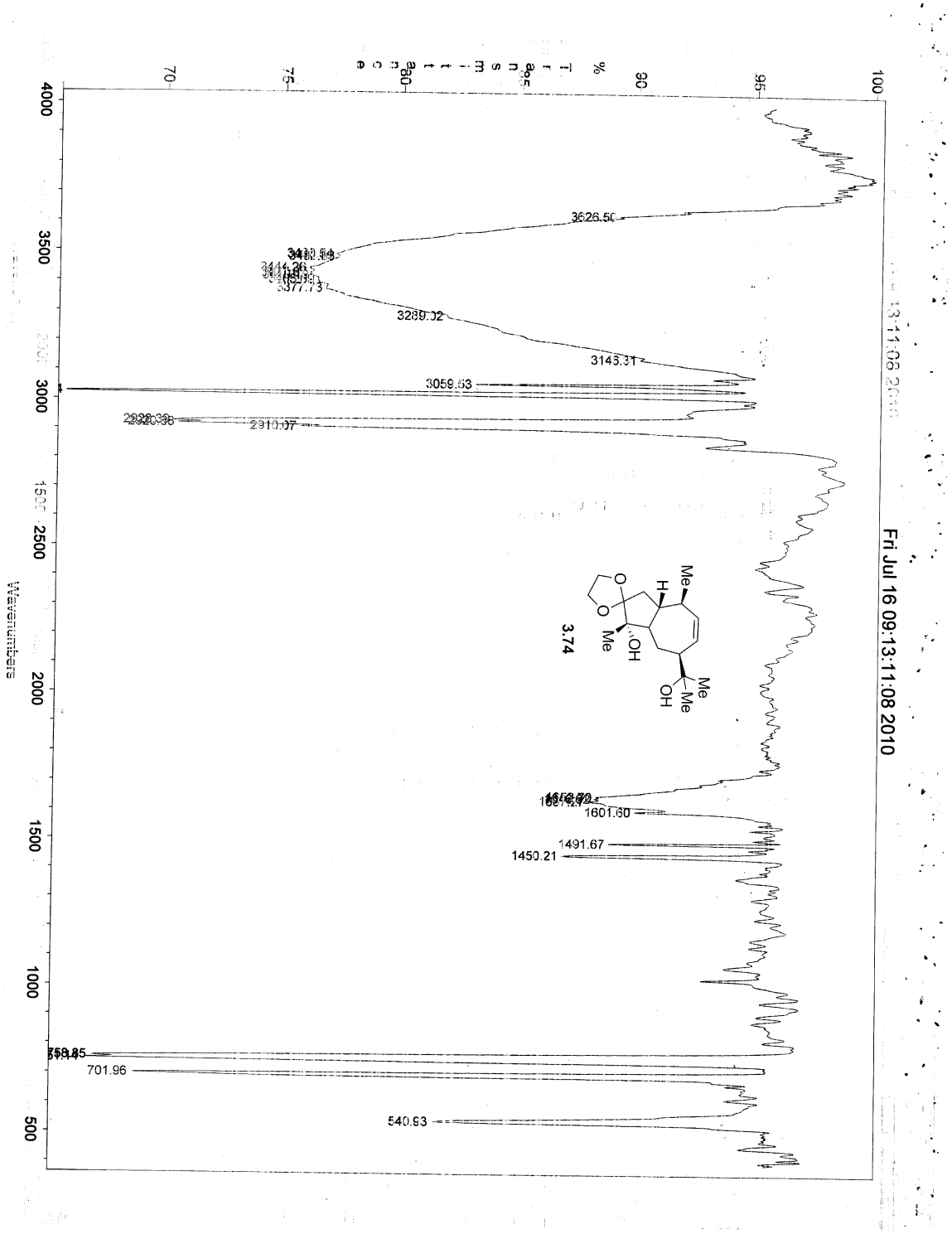
Fri Jul 16 09:13:11:08 2010
Wavenumbers
% Transmittance
3626.50
3289.02
3145.31
3059.53
2910.07
1601.60
1491.67
1450.21
701.96
540.93
3.74
Me
H
O
O
Me
OH
Me
Me
OH

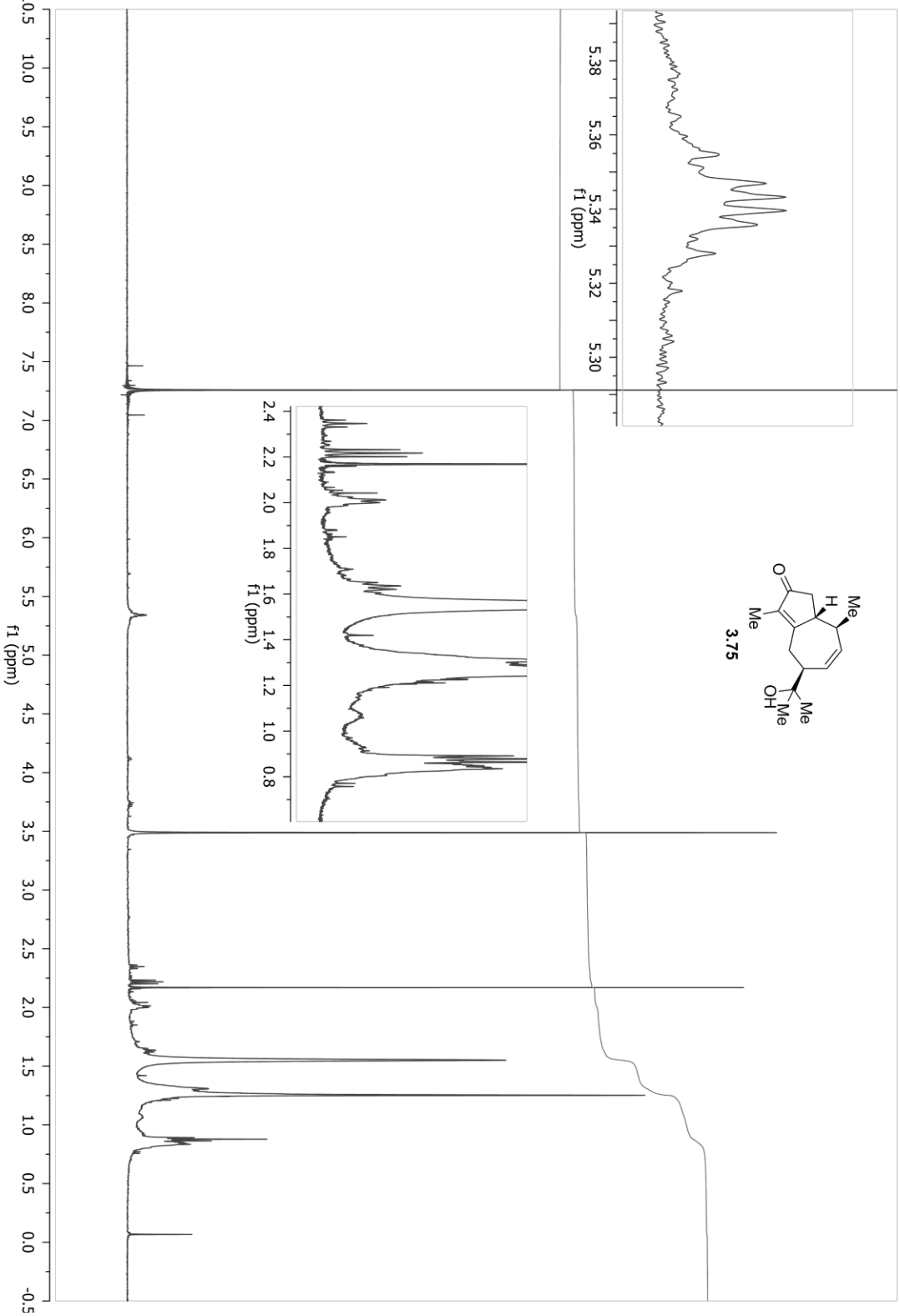
O
Me
H
Me
Me
Me
OH
3.75
f1 (ppm)
f1 (ppm)
f1 (ppm)

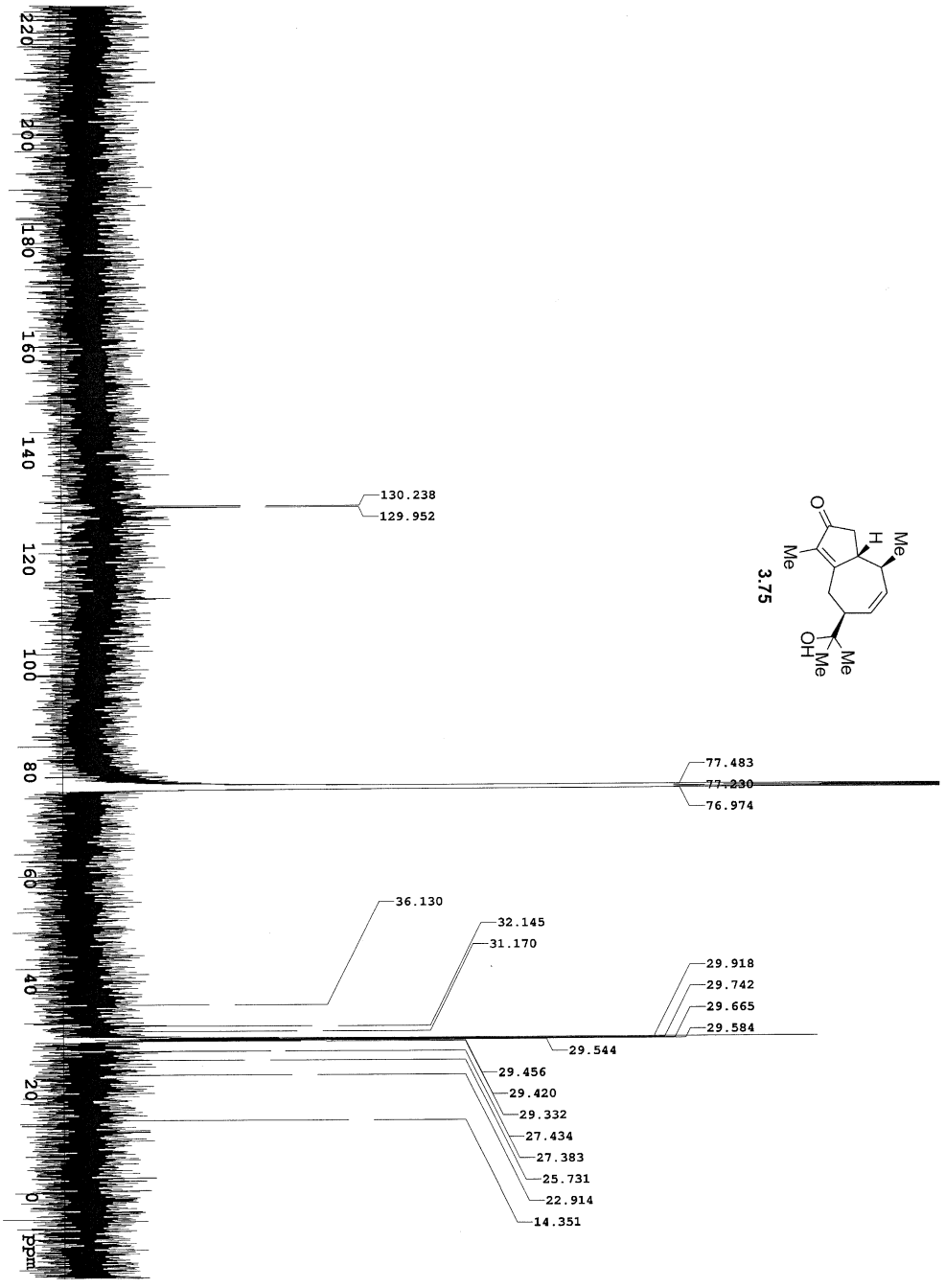
220
200
180
160
140
120
100
80
60
40
20
0
ppm
130.238
129.952
77.483
77.230
76.974
36.130
32.145
31.170
29.918
29.742
29.665
29.584
29.544
29.456
29.420
29.332
27.434
27.383
25.731
22.914
14.351
O
H
Me
Me
OH
Me
Me
3.75

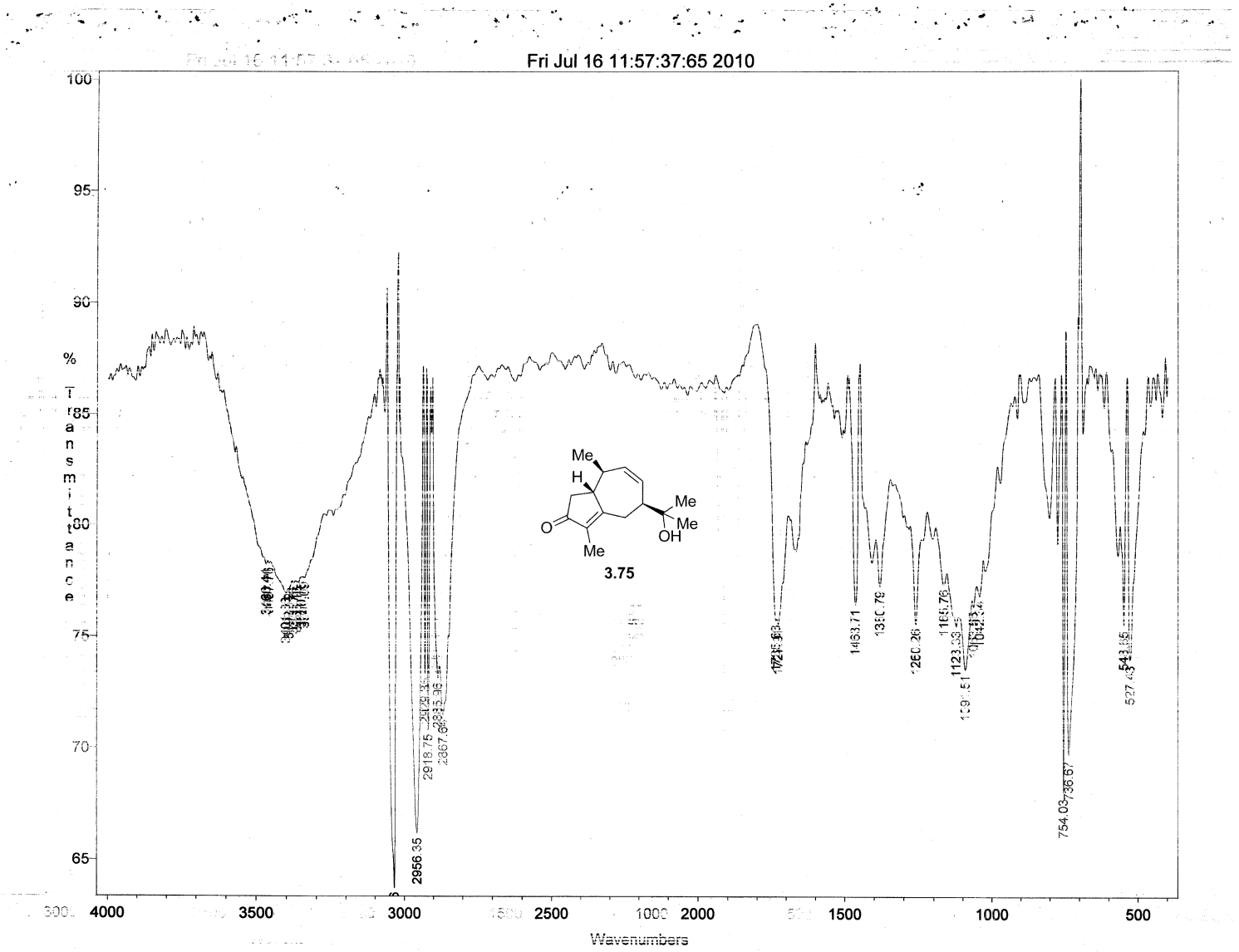
Fri Jul 16 11:57:37:65 2010
100
95
90
85
80
75
70
65
% Transmittance
4000
3500
3000
2500
2000
1500
1000
500
Wavenumbers
2956.35
2918.75
1463.71
1380.79
1165.76
754.03
738.67
Me
H
Me
Me
OH
O
Me
3.75

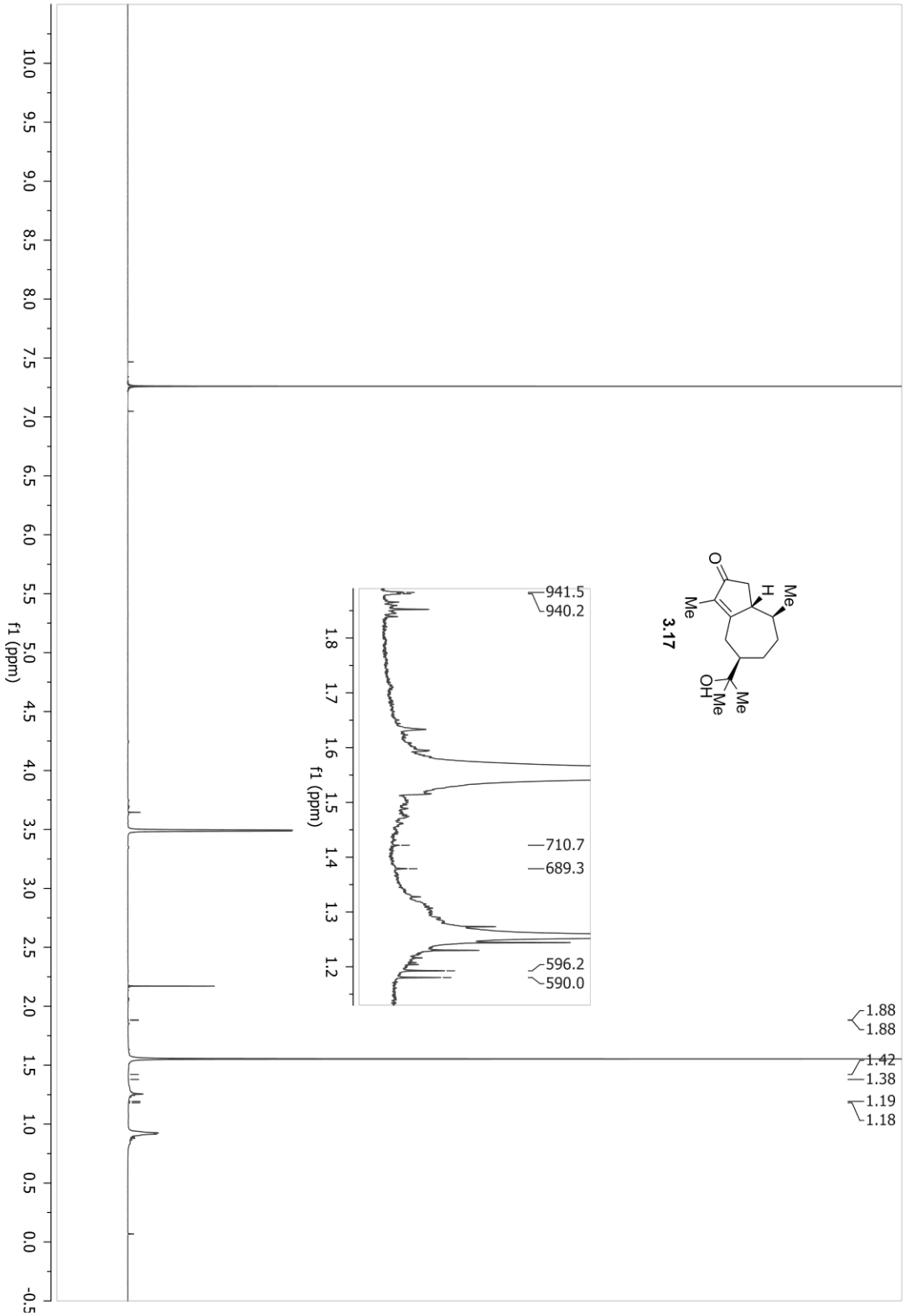
O
Me
H
Me
Me
Me
OH
3.17
941.5
940.2
710.7
689.3
596.2
590.0
1.88
1.88
1.42
1.38
1.19
1.18
f1 (ppm)

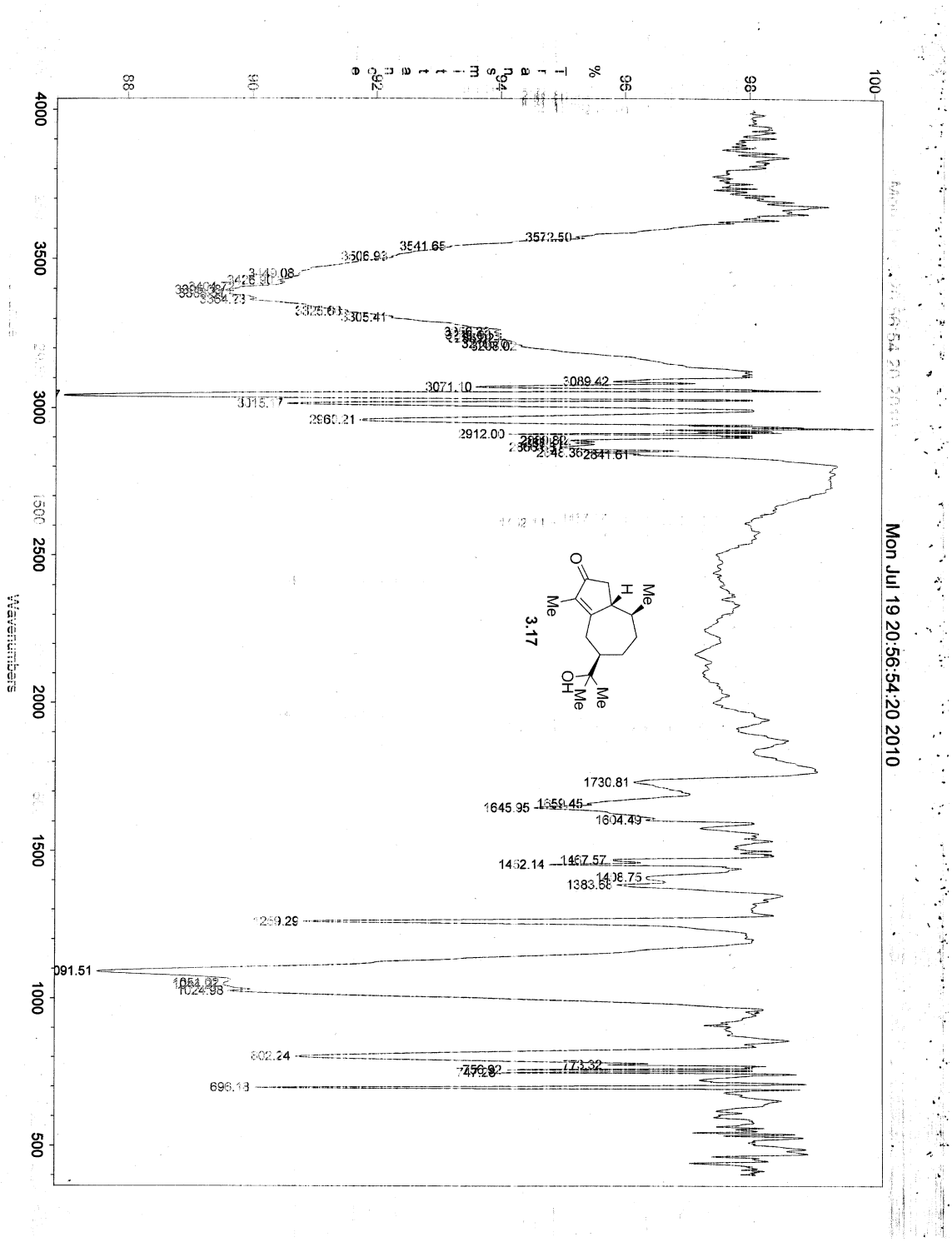
Mon Jul 19 20:56:54:20 2010
Wavenumbers
3.17
3572.50
3541.65
3506.93
3071.10
3089.42
2960.21
2912.00
2841.61
1730.81
1645.95
1604.49
1452.14
1467.57
1383.68
1408.75
1259.29
1091.51
1024.98
902.24
773.32
696.18